Satellite Image Atlas of Glaciers of the World

NORTH AMERICA

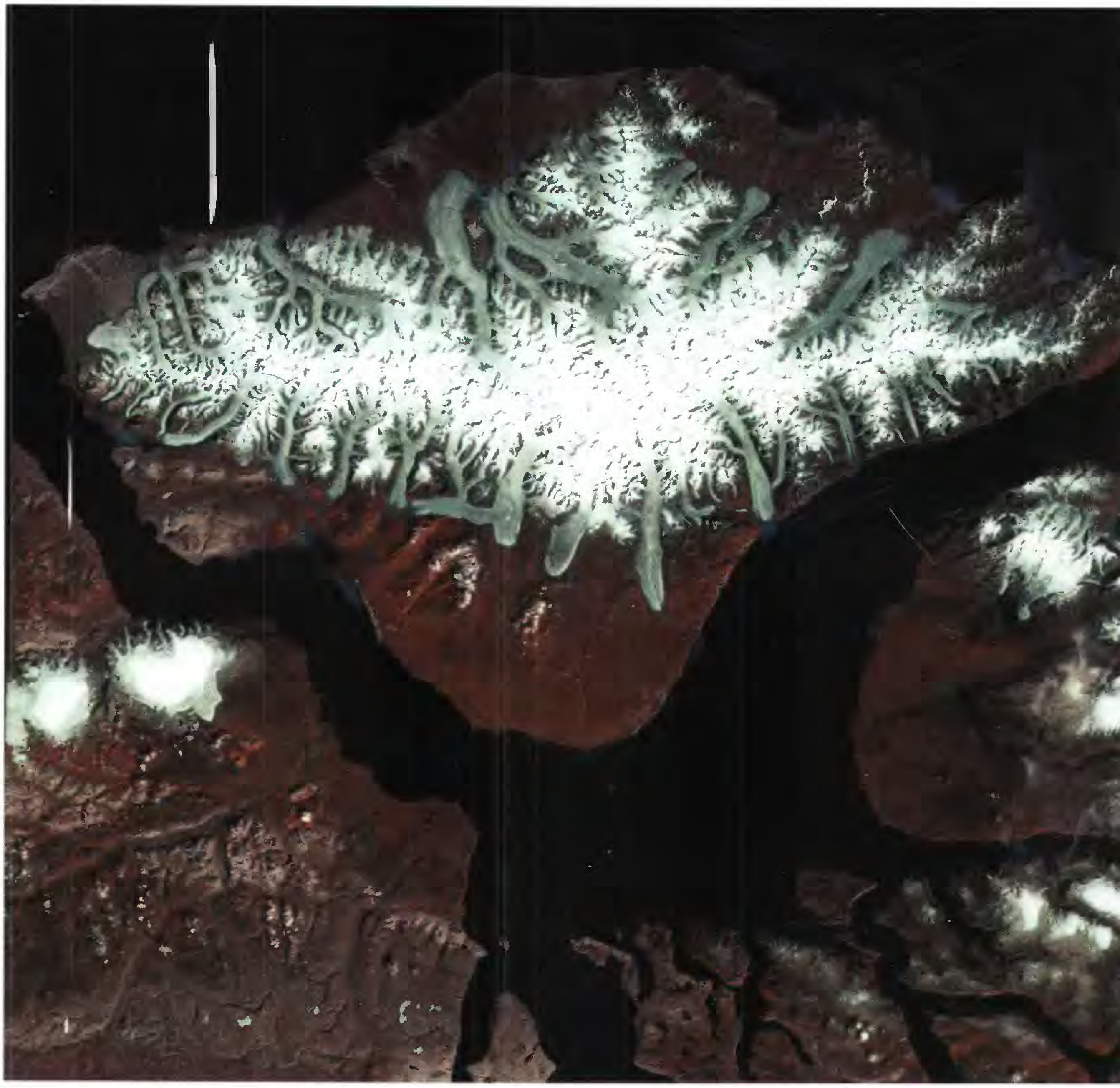

United States Geological Survey
Professional Paper 1386–J

Cover: *Landsat false-color image of ice fields, outlet glaciers, valley glaciers, and cirque glaciers on Bylot Island, as well as ice caps, ice fields, outlet, and valley glaciers on the Borden Peninsula and northern Baffin Island, Nunavut, Canada. Landsat image (20204–16513; 14 August 1975; Path 36, Row 8) from the Canada Centre for Remote Sensing (CCRS), Ottawa, Ontario, Canada*

GLACIERS OF NORTH AMERICA*–

*Excluding Alaska. The Glaciers of Alaska is a separate chapter, 1386-K, in this U.S. Geological Survey Professional Paper series

SATELLITE IMAGE ATLAS OF GLACIERS OF THE WORLD

Edited by RICHARD S. WILLIAMS, Jr., *and* JANE G. FERRIGNO

U.S. GEOLOGICAL SURVEY PROFESSIONAL PAPER 1386-J

Landsat images, together with aerial photographs, selected maps, and other data, have been used to provide a baseline of mid-1970's glacierization in Canada, the conterminous United States, and México

UNITED STATES GOVERNMENT PRINTING OFFICE, WASHINGTON: 2002

U.S. DEPARTMENT OF THE INTERIOR

GALE A. NORTON, *Secretary*

U.S. GEOLOGICAL SURVEY

Charles G. Groat, *Director*

Technical editing by Susan Tufts-Moore

Technical editing by John M. Watson

Design, layout, and illustrations by Kirsten E. Healey

Text review and typesetting by Janice G. Goodell

Layout review by Carolyn H. McQuaig

Library of Congress Cataloging in Publication Data

(Revised for vol. J)
Satellite image atlas of glaciers of the world.
(U.S. Geological Survey professional paper; 1386)
Includes bibliography.
Contents: — Ch. B. Antarctica, by Charles Swithinbank; with sections on The "dry valleys" of Victoria Land, by Trevor J. Chinn, [and] Landsat images of Antarctica, by Richard S. Williams, Jr., and Jane G. Ferrigno — Ch. C. Greenland, by Anker Weidick — Ch. E. Glaciers of Europe — Ch. G. Glaciers of the Middle East and Africa — Ch. H. Glaciers of Irian Jaya, Indonesia, and New Zealand — Ch. I. Glaciers of South America — Ch. J. Glaciers of North America
Supt. of Docs. no.: I 19.16:1386–J
1. Glaciers—Remote sensing. I. Williams, Richard S., Jr. II. Ferrigno, Jane G. III. Series.
GB2401.72.R42S28 1988 551.3'12 87-600497
ISBN 0–607–98290–X

For sale by the U.S. Geological Survey, Information Services
Box 25286, Federal Center,
Denver, CO 80225

Foreword

On 23 July 1972, the first Earth Resources Technology Satellite (ERTS 1 or Landsat 1) was successfully placed in orbit. The success of Landsat inaugurated a new era in satisfying mankind's desire to better understand the dynamic world upon which we live. Space-based observations have become an essential means for monitoring global environmental changes.

The short- and long-term cumulative effects of processes that cause significant changes on the Earth's surface can be documented and studied by repetitive Landsat and other satellite images. Such images provide a permanent historical record of the surface of the planet; they also make possible comparative two- and three-dimensional measurements of change over time. This Professional Paper demonstrates the importance of the application of Landsat images to global studies by using them to determine the 1970's distribution of glaciers on the planet. As images become available from future satellites, the new data will be used to document global changes in glacier extent by reference to the baseline Landsat image record of the 1970's.

Although many geological processes take centuries or even millennia to produce obvious changes on the Earth's surface, other geological phenomena, such as glaciers and volcanoes, cause noticeable changes over shorter periods. Some of these phenomena can have a worldwide impact and often are interrelated. Explosive volcanic eruptions, such as the 1991 Mount Pinatubo, Philippines, eruption, can produce dramatic effects on the global climate. Natural or culturally induced processes can cause global climatic cooling or warming. Glaciers respond to such warming or cooling periods by decreasing or increasing in size, which in turn causes sea level to rise or fall.

As our understanding of the interrelationship of global processes improves and our ability to assess changes caused by these processes develops further, we will learn how to use indicators of global change, such as glacier variation, to manage more wisely the use of our finite land and water resources. This USGS Professional Paper series is an excellent example of the way in which we can use technology to provide needed earth-science information about our planet. The international collaboration represented by this report is also an excellent model for the kind of cooperation that scientists will increasingly find necessary in the future in order to solve important earth-science problems on a global basis.

Charles G. Groat,
Director,
U.S. Geological Survey

Preface

This chapter is the seventh chapter to be released in U.S. Geological Survey Professional Paper 1386, Satellite Image Atlas of Glaciers of the World, a series of 11 chapters. In each chapter, remotely sensed images, primarily from the Landsat 1, 2, and 3 series of spacecraft, are used to study the glacierized regions of our planet and to monitor glacier changes. Landsat images, acquired primarily during the middle to late 1970's, were used by an international team of glaciologists and other scientists to study various geographic regions or to discuss glaciological topics. In each geographic region, the present areal distribution of glaciers is compared, wherever possible, with historical information about their past extent. The atlas provides an accurate regional inventory of the areal extent of glacier ice on our planet during the 1970's as part of a growing international scientific effort to measure global environmental change on the Earth's surface.

The chapter is divided into three parts: Glaciers of Canada (J–1), Glaciers of the Conterminous United States (J–2), and Glaciers of México (J–3). The Glaciers of Alaska is a separate chapter, Chapter 1386–K, of this series.

Glaciers in Canada are located in three principal geographic settings: on several Arctic islands in Nunavut and the Northwest Territories of northern Canada, in the Rocky Mountains and *Interior Ranges* of Alberta, British Columbia, Yukon Territory, and the Northwest Territories, and along the Pacific Coast, where they are sometimes contiguous with glaciers of Alaska. Glaciers are also situated in the Ungava Peninsula of northern Labrador, Newfoundland, and on Vancouver Island, British Columbia. The area covered by glaciers is estimated to be 151,000 km^2 on the Arctic Islands and 50,000 km^2 on the mainland, a total of 201,000 km^2 The types of glaciers in Canada include ice caps and ice fields and associated outlet glaciers, valley glaciers, mountain glaciers, glacierets, and rock glaciers. Landsat images are most useful in the study of large glaciers, ice caps and ice fields and associated outlet glaciers in Arctic Canada, and of ice fields, outlet glaciers, and valley glaciers in western Canada.

Glaciers in the conterminous United States are located in the States of Washington, Oregon, California, Montana, Wyoming, Colorado, Idaho, Utah, and Nevada. They have a total area of about 580 km^2. Only the first five states have glaciers large enough in area to be discernable on Landsat MSS images. Many of the volcanoes in the Cascade Range of the western United States are capped by glaciers, posing a significant hazard in the form of lahars and jökulhlaups in the river basins that originate on the flanks of these volcanoes. In Glacier National Park, Montana, the larger cirque glaciers have been reduced in area and volume during the past 150 years, a reduction rate that accelerated during the 20th century.

Glaciers in México are located on two active stratovolcanoes, Volcán Citlaltépetl (nine named glaciers) and Popocatépetl (three named glaciers), and one dormant stratovolcano, Iztaccíhuatl (12 named glaciers). The total glacier area in the middle 1960's was 11.44 km^2; all glaciers have been receding during the 20th century. Since 1993, intermittent volcanic activity of Popocatépetl has produced changes in its glaciers. The small area of México's glaciers limits the usefulness of Landsat MSS data; Landsat 3 RBV data, however, has sufficient spatial resolution to delineate glacier margins.

Richard S. Williams, Jr.
Jane G. Ferrigno
Editors

About this Volume

U.S. Geological Survey Professional Paper 1386, Satellite Image Atlas of Glaciers of the World, contains 11 chapters designated by the letters A through K. Chapter A is a general chapter containing introductory material on the Earth's cryosphere, including a discussion of the physical characteristics, classification, and global distribution of glaciers. The next 10 chapters, B through K, are arranged geographically and present glaciological information from Landsat and other sources of data on each of the geographic areas. Chapter B covers Antarctica; Chapter C, Greenland; Chapter D, Iceland; Chapter E, Continental Europe (except for the European part of the former Soviet Union), including the Alps, the Pyrenees, Norway, Sweden, Svalbard (Norway), and Jan Mayen (Norway); Chapter F, Asia, including the European part of the former Soviet Union, China (P.R.C.), India, Nepal, Afghanistan, and Pakistan; Chapter G, Turkey, Iran, and Africa; Chapter H, Irian Jaya (Indonesia) and New Zealand; Chapter I, South America; and Chapter J, North America (excluding Alaska); and Chapter K, Alaska.

The realization that one element of the Earth's cryosphere, its glaciers, was amenable to global inventorying and monitoring with Landsat images led to the decision, in late 1979, to prepare this Professional Paper, in which Landsat 1, 2, and 3 multispectral scanner (MSS) and Landsat 2 and 3 return beam vidicon (RBV) images would be used to inventory the areal occurrence of glacier ice on our planet within the boundaries of the spacecraft's coverage (between about 81° north and south latitudes). Through identification and analysis of optimum Landsat images of the glacierized areas of the Earth during the first decade of the Landsat era, a global benchmark or baseline could be established for determining the areal extent of glaciers during a relatively narrow time interval (1972 to 1982). This global "snapshot" of glacier extent could then be used for comparative analysis with previously published maps and aerial photographs and with new maps, satellite images, and aerial photographs in order to determine the areal fluctuation of glaciers in response to natural or culturally induced changes in the Earth's climate.

To accomplish this objective, the editors selected optimum Landsat images of each of the glacierized regions of our planet from the Landsat image data base at the EROS Data Center in Sioux Falls, S. Dak., although some images were also obtained from the Landsat image archives maintained by the Canada Centre for Remote Sensing, Ottawa, Ontario, Canada, and by the European Space Agency in Kiruna, Sweden, and Fucino, Italy. Between 1979 and 1981, these optimum images were distributed to an international team of more than 50 scientists who agreed to write a section of the Professional Paper concerning either a geographic area or a glaciological topic. In addition to analyzing images of a specific geographic area, each author was also asked to summarize up-to-date information about the glaciers within the area and to compare their present areal distribution with historical information (for example, from published maps, reports, and photographs) about their past extent. Completion of this atlas will provide an accurate regional inventory of the areal extent of glaciers on our planet during the 1970's.

Richard S. Williams, Jr.
Jane G. Ferrigno
Editors

CONTENTS

Glaciers of North America—

GLACIERS OF CANADA

INTRODUCTION

By RICHARD S. WILLIAMS, JR. *and* JANE G. FERRIGNO, *Editors*

SATELLITE IMAGE ATLAS OF GLACIERS OF THE WORLD

Edited by RICHARD S. WILLIAMS, Jr., *and* JANE G. FERRIGNO

U.S. GEOLOGICAL SURVEY PROFESSIONAL PAPER 1386–J–1

Glaciers in Canada are situated in three principal locations: on several Arctic islands, in the Rocky Mountains and Interior Ranges, *and along the Pacific Coast. Landsat MSS images are most useful in studying and monitoring changes in ice caps, ice fields, outlet glaciers, and valley glaciers*

CONTENTS

GLACIERS OF NORTH AMERICA–

GLACIERS OF CANADA

INTRODUCTION

By RICHARD S. WILLIAMS, JR. *and* JANE G. FERRIGNO, *Editors*

Glaciers in Canada are located principally in three geographic settings: on several Arctic islands in Nunavut and the Northwest Territories of northern Canada, in the Rocky Mountains and the *Interior Ranges*[1], and along the coast of the Pacific Ocean, where they are sometimes contiguous with glaciers of Alaska (fig. 1, and figs. 1 and 2 in the "History of Glacier Investigations in Canada"). The area covered by glaciers is estimated to be 151,000 km^2 in the Canadian Arctic and 50,000 km^2 in the mountain ranges of Western Canada (table 1). During the Last Glacier Maximum (LGM) during the Pleistocene Epoch, the Laurentide Ice Sheet and the Cordilleran Ice Sheet covered

TABLE 1.—*Estimated glacier area in Canada (from Ommanney, 1970)*

[1, Approximation from previous estimates; 2, Ommanney (1969); 3, Koerner (1968); 4, Measured value from National Topographic System (NTS) 1:250,000-scale maps; 5, Henoch (1967)]

Location of Glaciers		Estimated Glacier Area (square kilometers)
ARCTIC ISLANDS		
Ellesmere		80,000[1]
Ice Shelves (Ellesmere)		500[1]
Axel Heiberg		11,735[2]
Devon		16,200[1]
Coburg		225[1]
Meighen		85[3]
Melville		160[4]
North Kent		152[4]
	Subtotal	109,057
Baffin		37,000[1]
Bylot		5,000[1]
	Subtotal Arctic	151,057
MAINLAND DRAINAGE BASINS		
Pacific		37,659[5]
Nelson		328[5]
Great Slave		626[5]
Yukon		10, 564[5]
Arctic Ocean		840[5]
Labrador		24[5]
	Subtotal Mainland	50,041
	Total Canada	201,098

Figure 1.—*Geographic locations of the currently glacierized regions of Canada (and Greenland and Iceland), by S. Fick and A. Murray (see also Shilts and others, 1998), from the 1998 Canadian Geographic, v. 118, no. 7, Sources: Geomatics Canada, Glacier Atlas of Canada, National Hydrology Research Centre. Used with permission.*

Manuscript approved for publication, 7 March 2002.

[1] The names in this section conform to the usage authorized by the Secretariat of the Canadian Permanent Committee on Geographical Names (CPCGN) and found in the Canadian Geographical Names Data Base (CGNDB). Variant names and names not listed in the CPCGN/CGNDB are shown in italics.

virtually all of Canada (fig. 2), so present-day glaciers in Canada are present only where the regional climates have temperature and (or) accumulation/melt regimes sufficient to maintain these ice masses. Some glaciers may, in fact, be relicts from the late Pleistocene Epoch, or from the late Holocene Epoch "Little Ice Age," and could not re-form under present, regional climatic conditions, if they were to completely melt. Because of the vastness and often inaccessibility of the glacierized regions of Canada, only 176 individual glaciers of the many thousands of glaciers have been studied in the field or with airborne and satellite remote sensing technology during the past 140 years. Between the 1940's and the present, 34 of these 176 glaciers or glacierized areas have been specially mapped one or more times, at scales ranging from 1:5,000 to 1:125,000.

Dunbar and Greenway (1956) published an important book which included numerous trimetrogon aerial photographs of the glaciers of Arctic Canada; their pioneering work with available aerial photographs provided a regional overview of the most glacierized part of Canada and, in a sense, was a forerunner of the use of satellite images to document the areal extent of glacier ice in Canada. More than 120 years ago, the geologist Nathaniel Shaler and the physical geographer William Morris Davis (Shaler and Davis, 1881) pioneered in the use of ground photographs to provide a historical record of glaciers. As soon as new technology becomes available, scientists are quick to apply it to specific research needs. In the examples given, the successive technologies adopted to study glaciers were ground photography, aerial photography, and satellite imagery.

The Glaciers of Canada section of this volume is divided into several sections; two main topical sections and one subsection follow this introduction. Three main sections and two subsections cover the glaciers of the Arctic Islands; three main sections and one subsection cover the glaciers of the Canadian Rockies, Coast Mountains, and St. Elias Mountains. It is obvious that the lack of scientific knowledge about most of the glaciers of Canada precludes a comprehensive discussion of all of the glacierized regions. However, the potential of satellite remote sensing, including the higher spatial and spectral resolution imagery of post-Landsat multispectral scanner (MSS) images to investigate areal changes in Canada's glaciers, is well documented in the following sections. The emphasis on 1970's images in this introduction and the following sections is due to the goal of compiling a global baseline of glacier area (in the 1970's time frame) in this Satellite Image Atlas of Glaciers of the World series.

The first field observations of glaciers in Canada were made in 1861, nine years before Clarence R. King, the first Director of the U.S. Geological Survey (established in 1879), discovered Whitney Glacier on Mt. Shasta, Calif., and three more glaciers on the north slope of the volcano in 1870 (Williams and Ferrigno, 1997). Since that time, 176 glaciers in Canada—13 in the St. Elias Mountains, 63 in the Coast Mountains, 10 in the *Interior Ranges*, 27 in the Rocky Mountains, 41 in the High Arctic, 10 in the Low Arctic, 5 in the Torngat Mountains of Labrador (Newfoundland), and 7 outside these glacierized areas—have been studied. These studies, in the post-World War II to the 1980's period, were driven by scientific, economic, security, and sovereignty concerns, including the impetus from major cooperative international scientific programs, such as the International Geophysical Year and the International Hydrological Decade.

In 1999, the two Federal Departments having responsibilities in glaciology (Natural Resources Canada and Environment Canada) combined their glaciological expertise and resources to form a "National Glaciology Programme" (NGP). The NGP is housed at the Geological Survey of Canada [http://sts.gsc.nrcan.gc.ca] and is responsible, in part, for meeting Canada's glacier-observation commitment to the World Meteorological Organization's (WMO) Global Climate Observing System and the United Nations

Figure 2.*—Glacierization of Canada (and Greenland and Iceland) during the Pleistocene Epoch, by S. Fick and A. Murray (see also Shilts and others, 1998), from the 1998 Canadian Geographic, v. 118, no. 7, Sources: Geomatics Canada, Glacier Atlas of Canada, National Hydrology Research Centre. Used with permission.*

Educational, Scientific, and Cultural Organization's (UNESCO) International Hydrological Programme (IHP). This activity is complemented by participation in the "CRYSYS" program (to study variability and change of the Canadian CRYospheric SYStem) [http://www.crysys.uwaterloo.ca], whose academic and government partners conduct research on the Canadian cryosphere using conventional and remote sensing methods.

As part of the glacier investigations during the past 140 years, especially between the middle 1940's and 1990's, one 1:4,000,000-scale map of the height of the glaciation level in western Canada and southern Alaska (glaciers shown in green) (Anonymous, 1978), one 1:2,000,000-scale map of glaciers and moraines in southern British Columbia and Alberta (glaciers shown in gray) (Østrem and others, 1966), seven 1:1,000,000-scale, 52 1:500,000 scale (Glacier Atlas of Canada), and 114 miscellaneous scale (1:2,500 to 1:125,000) maps of selected glaciers of Canada were published by governmental agencies and academic institutions. Satellite images, combined with digital-elevation models (DEMs) using geographic information systems (GIS) technology, are being used to produce new types of maps of Canada's glaciers. Roger D. Wheate, Robert W. Sidjak, and Garnet T. Whyte provide examples of the application of these technologies to two glaciers in the *Interior Ranges* and Rocky Mountains.

Until the preparation of this volume on the glaciers of Canada, the last effort to carry out a comprehensive review of the glacierized regions of Canada was done by William O. Field and his colleagues at the American Geographical Society (AGS) in the two-volume "Mountain Glaciers of the Northern Hemisphere," which also included an atlas containing 49 plates (Field, 1975c). The two volumes and atlas were produced by the AGS under contract with the Earth Sciences Division of the U.S. Army Engineer Topographic Laboratories and published by the Technical Information Analysis Center, Cold Regions Research and Engineering Laboratory, U.S. Army Corps of Engineers (Hanover, New Hampshire). (An earlier, similar atlas was published in 1958 (Field and Associates, 1958).) They include a comprehensive collation of published reports and maps of the glaciers of Canada (and other glacierized regions of the Northern Hemisphere) and are an excellent source of information from a variety of historical and modern sources. For all of the glacierized regions of Canada, including those regions not addressed in this volume, relevant chapters in the 1975 volumes will be cited.

In 1998, the Royal Canadian Geographical Society published, in the November/December 1998 issue of Canadian Geographic, an article on Canada's glaciers (Anonymous, 1998) and an 8-page color map foldout (Shilts and others, 1998). Several of the maps that appeared in the foldout map are reproduced, with permission and with some minor modifications, in the following sections of the "Glaciers of Canada." Another modern reference map of Canada is the 1:6,000,000-scale "New Century Map of Canada" published by Canadian Geographic in 1999 [http://www.canadiangeographic.ca]. See also the National Atlas (of Canada) Web site at [http://atlas.gc.ca], which will, in the near future, carry maps from the previously noted plates of the Glacier Atlas of Canada and contain links to available glacier-related data bases residing in government and university archives.

Topical Sections

Two topical sections follow this introduction. The two sections, written by C. Simon L. Ommanney, give a comprehensive review of "History of Glacier Investigations in Canada" and "Mapping Canada's Glaciers." The latter review is followed by a subsection on "Mapping Glaciers in the *Interior Ranges* and Rocky Mountains with Landsat Data," by Roger D. Wheate, Robert W. Sidjak, and Garnet T. Whyte.

Glaciers of the Arctic Islands

The glaciers of the Canadian Arctic represent the largest area (151,057 km^2) and volume of glacier ice in Canada and include about 5 percent of the glacierized area of the Northern Hemisphere (fig. 1, and fig. 1 in "Glaciers of the High Arctic Islands"). Ice caps and ice fields and associated outlet glaciers and smaller glaciers are present on several of the Queen Elizabeth Islands (Ellesmere, Axel Heiberg, Meighen, Coburg, Devon, and North Kent Islands, Nunavut, and in the western part of Melville Island, Northwest Territories) (Mercer, 1975b). Roy M. Koerner, in "Glaciers of the High Arctic Islands," describes both dynamic and stagnant ice caps. These ice caps exhibit a very slow response to climate change. Even though the last 150 years have been the warmest in the past millennium, only very slight changes in area and volume of the ice caps can be discerned.

Martin O. Jeffries describes historic and modern changes in the section "Ellesmere Island Ice Shelves and Ice Islands," including the use of Landsat MSS, RADARSAT synthetic aperture radar (SAR) and SPOT haute resolution visible (HRV) images to document changes in the ice shelves and ice plugs (multiyear landfast sea ice) that are located on the northwestern coast of Ellesmere Island. Although the ice shelves have been present since the middle Holocene Epoch, they were much more extensive in the past. The 20th century warming interval has resulted in a significant reduction in their areal extent.

The glaciers of the Canadian Low Arctic are located on Baffin and Bylot Islands (Mercer, 1975a). About 45 percent of Bylot Island (4,859 km^2) is covered by glaciers (see the book's cover). On Baffin Island, glaciers are found on the northern and eastern coasts, from the northeastern part of the Brodeur and Borden Peninsulas to the eastern part of the Hall and Meta Incognita Peninsulas, Nunavut (fig. 1 in "Glaciers of Baffin Island"). John T. Andrews addresses the geographic distribution and types of glaciers (ice caps and ice fields and associated outlet glaciers and smaller glaciers) in "Glaciers of Baffin Island," with specific reference to the two large ice caps, Barnes Ice Cap (5,935 km^2) and Penny Ice Cap (5,960 km^2); he concludes these two ice masses contain ice that represents the last remnants of the Laurentide Ice Sheet (fig. 2). He also concludes that the Barnes Ice Cap is slowly shrinking, a recession that could accelerate if significant regional climate warming were to occur. Gerald Holdsworth, in his discussion entitled "Barnes Ice Cap: Geomorphology and Thermodynamics," confirms that a whitish marginal strip of ice at the ice-cap margin has a $\delta^{18}O$ isotope value that indicates a late Pleistocene Epoch (Wisconsinan) age of the ice. John D. Jacobs examines "Late 20th Century Change of the Barnes Ice Cap Margin," using both Landsat and RADARSAT SAR images to document recession of Lewis Glacier and the calving ice-front in Gee Lake. Figure 3 and table 2 show the optimum Landsat 1, 2, and 3 MSS and RBV images of the glaciers of the Arctic Islands.

The southernmost glaciers in eastern North America are located in the Torngat Mountains, Labrador, Newfoundland (fig. 1), but are not discussed in this chapter. Fahn (1975) states that most of the glaciers are cirque glaciers that form clusters on the slopes of the highest peaks. She further notes that the 1975 climatic conditions in the Torngat Mountains are marginal and that the glaciers have been receding since the end of the "Little Ice Age" (LIA).

Unpublished work by Ommanney (written commun., 2001) summarized the body of knowledge on the distribution of a significant number of rock glaciers in Labrador. Ommanney (written commun., 2001) and his colleagues also mapped one glacieret on the Québec side of the provincial border with Labrador, so there is (or was?) at least one glacier(et) in Québec.

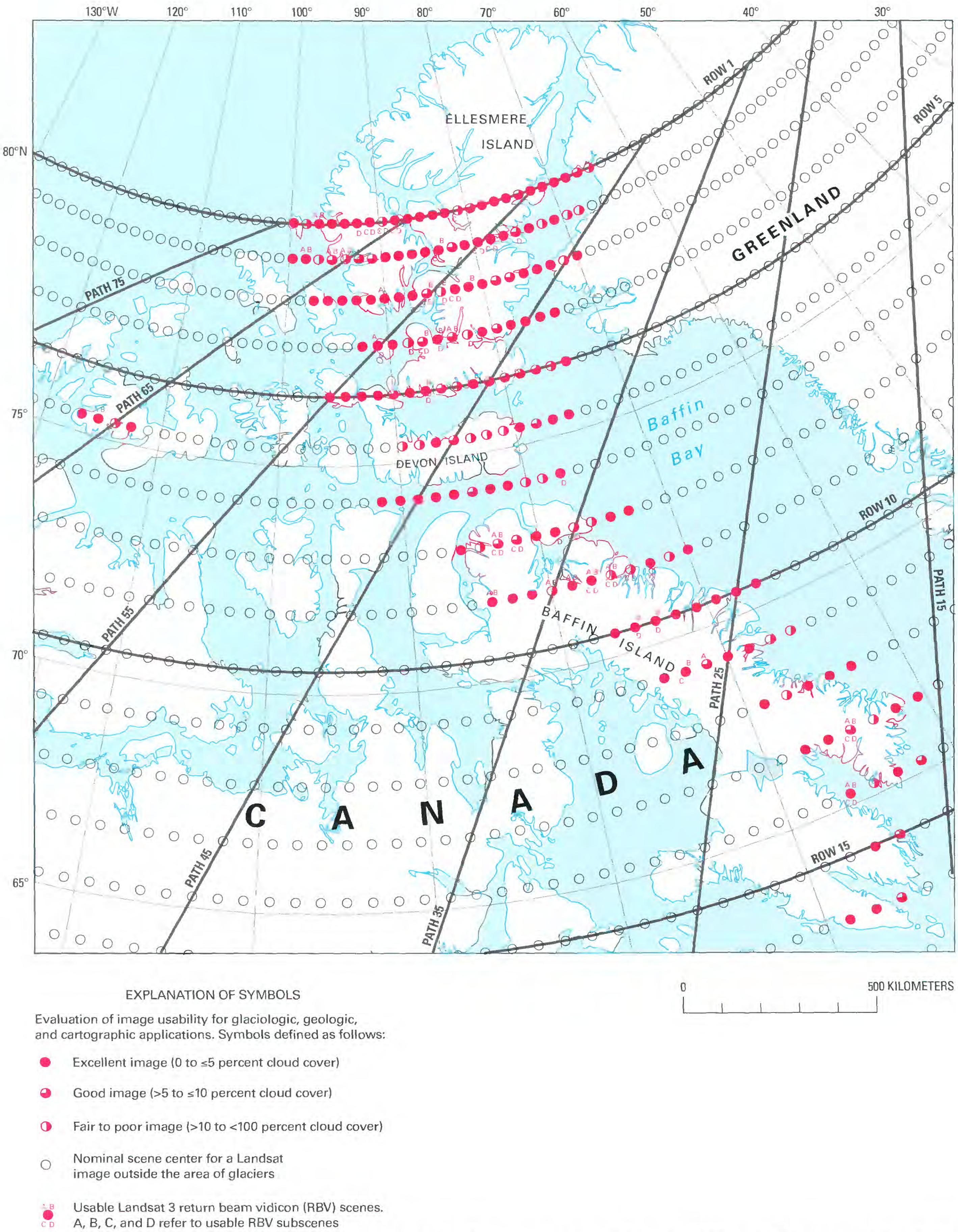

***Figure 3.**—Optimum Landsat 1, 2, and 3 MSS and RBV images of the glaciers of the Arctic Islands of Canada.*

TABLE 2.—*Optimum Landsat 1, 2, and 3 MSS and RBV images of the glaciers of the Arctic Islands of Canada*

[The images archived by the Canada Centre for Remote Sensing (CCRS) are not identified on the CCRS Website (http://www.ccrs.nrcan.gc.ca) by Landsat identification number but can be located by path (track), row (frame), and date. The images archived by the EROS Data Center (EDC) (http://earthexplorer.usgs.gov) are no longer located or ordered by the Landsat identification number on the image but by a different entity number that incorporates satellite number, path, row, and date]

Path-Row	Nominal scene center (lat-long)	Landsat identification number	Date	Solar elevation angle (degrees)	Code	Cloud cover (percent)	Remarks
16–13	66°40'N. 60°28'W.	20202–14590	12 Aug 75	37	●	0	Baffin Island
16–14	65°20'N. 61°57'W.	20202–14592	12 Aug 75	38	●	5	
17–13	66°40'N. 61°55'W.	20185–15051	26 Jul 75	42	●	0	Image used for Andrews' figure 17
17–14	65°20'N. 63°23'W.	20185–15053	26 Jul 75	43	●	0	
17–15	63°59'N. 64°44'W.	1747–15083	09 Aug 74	40	◕	10	EDC[1]; image used for Andrews' figure 18
17–16	62°38'N. 65°58'W.	1747–15090	09 Aug 74	41	◕	10	EDC[1]; Terra Nivea and Grinnell Glacier; image used for Andrews' figure 19
18–13	66°40'N. 63°21'W.	20186–15105	27 Jul 75	42	◑	45	
18–14	65°20'N. 64°49'W.	20186–15112	27 Jul 75	43	◑	15	
18–15	63°59'N. 66°10'W.	20204–15111	14 Aug 75	39	●	0	
18–16	62°38'N. 67°24'W.	1712–15160	05 Jul 74	47	●	0	EDC
19–12	67°59'N. 63°08'W.	21663–15101	12 Aug 79	34	●	0	
19–13	66°40'N. 64°47'W.	21663–15103	12 Aug 79	35	◕	10	Penny Ice Cap; image used for Andrews' figure 16
19–13	66°40'N. 64°47'W.	30156–15172 A, B, C, D	08 Aug 78	38–39	●	5–30	Landsat 3 RBV[1]
19–14	65°20'N. 66°15'W.	21663–15110	12 Aug 79	36	●	0	
19–14	65°20'N. 66°15'W.	30156–15174 A, B, C, D	08 Aug 78	39–40	●	0	
19–16	62°38'N. 68°50'W.	21303–14584	17 Aug 78	~39	●	0	
20–12	67°59'N. 64°34'W.	11488–14431	19 Aug 76	32	●	0	Penny Ice Cap; extensive snow cover
20–13	66°40'N. 66°13'W.	11488–14434	19 Aug 76	33	●	0	Extensive snow cover
21–12	67°59'N. 66°00'W.	11453–14515	15 Jul 76	41	●	0	Penny Ice Cap
21–13	66°40'N. 67°39'W.	11453–14521	15 Jul 76	42	●	0	
22–11	69°17'N. 65°37'W.	11829–14232	26 Jul 77	37	◑	40	
22–12	67°59'N. 67°26'W.	11829–14234	26 Jul 77	37	◑	30	
23–11	69°17'N. 67°03'W.	20911–15163	21 Jul 77	40	◑	30	

TABLE 2.—*Optimum Landsat 1, 2, and 3 MSS and RBV images of the glaciers of the Arctic Islands of Canada*—Continued

Path-Row	Nominal scene center (lat-long)	Landsat identification number	Date	Solar elevation angle (degrees)	Code	Cloud cover (percent)	Remarks
23–12	67°59'N. 68°52'W.	20911–15165	21 Jul 77	41	●	0	
24–10	70°35'N. 66°28'W.	20912–15214	22 Jul 77	39	●	0	
24–11	69°17'N. 68°29'W.	20912–15221	22 Jul 77	40	●	0	
25–10	70°35'N. 67°54'W.	11850–14380	16 Aug 77	30	●	0	
25–11	69°17'N. 69°55'W.	11850–14382	16 Aug 77	31	●	5	Southeastern end of Barnes Ice Cap
26–10	70°35'N. 69°20'W.	21292–15355	06 Aug 78	~36	●	0	
26–11	69°17'N. 71°21'W.	21328–15380	11 Sep 78	22	◕	10	Southeastern end of Barnes Ice Cap
26–11	69°17'N. 71°21'W.	30721–15514 A, B	24 Feb 80	10	◑	30	Landsat 3 RBV; subscene B used for Andrews' figure 15
27–10	70°35'N. 70°46'W.	1379–16124	06 Aug 73	36	●	0	Barnes Ice Cap
27–11	69°17'N. 72°48'W.	1379–16130	06 Aug 73	37	●	0	Barnes Ice Cap
27–11	69°17'N. 72°48'W.	30722–15572 B, C	25 Feb 80	~11	●	0	Barnes Ice Cap; Landsat 3 RBV
28–09	71°50'N. 69°54'W.	10380–16180	07 Aug 73	35	●	0	
28–10	70°35'N. 72°12'W.	10380–16182	07 Aug 73	36	●	0	Barnes Ice Cap; image used for Andrews' figure 5
28–10	70°35'N. 72°12'W.	30525–16065	12 Aug 79	32	●	0	Barnes Ice Cap; image used for Andrews' figure 8A
28–11	69°17'N. 74°14'W.	10380–16185	07 Aug 73	37	●	0	Barnes Ice Cap
28–11	69°17'N. 74°14'W.	30525–16071	12 Aug 79	33	●	0	Barnes Ice Cap
29–09	71°50'N. 71°20'W.	30526–16120	13 Aug 79	31	◑	20	
29–10	70°35'N. 73°38'W.	11119–15585	16 Aug 75	33	●	0	
29–10	70°35'N. 73°38'W.	30526–16122 B, D	13 Aug 79	30	●	0–20	Landsat 3 RBV
30–09	71°50'N. 72°46'W.	11855–15054	21 Aug 77	28	●	0	Extensive snow cover
30–09	71°50'N. 72°46'W.	30491–16174 D	09 Jul 79	41	●	0	Landsat 3 RBV
30–10	70°35'N. 75°04'W.	11855–15060	21 Aug 77	29	●	5	Barnes Ice Cap
30–10	70°35'N. 75°04'W.	30491–16181 B	09 Jul 79	41	●	0	Landsat 3 RBV
30–10	70°35'N. 75°04'W.	30725–16141 D	28 Feb 80	11	◑	20	Landsat 3 RBV

TABLE 2.—*Optimum Landsat 1, 2, and 3 MSS and RBV images of the glaciers of the Arctic Islands of Canada*—Continued

Path-Row	Nominal scene center (lat-long)	Landsat identification number	Date	Solar elevation angle (degrees)	Code	Cloud cover (percent)	Remarks
31–09	71°50'N. 74°13'W.	11463–15471	25 Jul 76	37	◑	15	
31–09	71°50'N. 74°13'W.	30546–16232 C, D	02 Sep 79	26	◑	15–20	Landsat 3 RBV
31–10	70°35'N. 76°30'W.	11463–15473	25 Jul 76	37	●	0	
32–08	73°04'N. 73°03'W.	11464–15522	26 Jul 76	36	●	0	
32–09	71°50'N. 75°39'W.	11857–15170	23 Aug 77	27	◑	40	
32–09	71°50'N. 75°39'W.	30547–16290 A, B, C, D	03 Sep 79	25–26	●	0–10	Landsat 3 RBV
33–08	73°04'N. 74°29'W.	1403–16455	30 Aug 73	26	●	0	
33–09	71°50'N. 77°05'W.	1403–16461	30 Aug 73	27	●	0	Image used for Andrews' figure 4
33–09	71°50'N. 77°05'W.	30548–16345 A, B, C, D	04 Sep 79	25–26	◑	20–30	Landsat 3 RBV
34–08	73°04'N. 75°55'W.	11841–15294	07 Aug 77	32	◑	50	
34–09	71°50'N. 78°31'W.	1404–16515	31 Aug 73	27	●	0	
34–09	71°50'N. 78°31'W.	30549–16403 A, B	05 Sep 79	25	◑	20–50	Landsat 3 RBV
35–08	73°04'N. 77°21'W.	11842–15352	08 Aug 77	31	◑	15	
35–08	73°04'N. 77°21'W.	30586–16445 C, D	12 Oct 79	10	◕	10–20	Landsat 3 RBV
35–09	71°50'N. 79°57'W.	11125–16323	22 Aug 75	30	◑	20	
35–09	71°50'N. 79°57'W.	30586–16452 A, B	12 Oct 79	10	◑	20–40	Landsat 3 RBV
36–08	73°04'N. 78°47'W.	20204–16513	14 Aug 75	31	●	0	Bylot Island
36–08	73°04'N. 78°47'W.	30173–16525 D	25 Aug 78	28	◑	20	Landsat 3 RBV
36–09	71°50'N. 81°23'W.	11468–16152	30 Jul 76	35	●	0	
37–07	74°16'N. 77°14'W.	20943–16332	22 Aug 77	27	●	0	
37–07	74°16'N. 77°14'W.	30516–16572 D	03 Aug 79	33	◑	50	Landsat 3 RBV
37–08	73°04'N. 80°13'W.	20943–16335	22 Aug 77	28	●	0	Image used for Andrews' figure 3
37–09	71°50'N. 82°49'W.	20943–16341	22 Aug 77	29	●	0	
38–06	75°25'N. 75°14'W.	20944–16384	23 Aug 77	26	●	0	

TABLE 2.—*Optimum Landsat 1, 2, and 3 MSS and RBV images of the glaciers of the Arctic Islands of Canada*—Continued

Path-Row	Nominal scene center (lat-long)	Landsat identification number	Date	Solar elevation angle (degrees)	Code	Cloud cover (percent)	Remarks
38–07	74°16'N. 78°40'W.	20926–16400	05 Aug 77	32	◑	50	Eastern end of Devon Island
38–08	73°04'N. 81°39'W.	11827–15540	24 Jul 77	35	◕	10	
38–08	73°04'N. 81°39'W.	30589–17020 C, D	15 Oct 79	9	◕	10–20	Landsat 3 RBV
38–09	71°50'N. 84°15'W.	30589–17023 A, B	15 Oct 79	9	●	0	Landsat 3 RBV
39–06	75°25'N. 76°40'W.	11147–16525	13 Sep 75	19	●	0	
39–07	74°16'N. 80°06'W.	20207–17081	17 Aug 75	29	◑	15	
39–08	73°04'N. 83°05'W.	1733–17123	26 Jul 74	36	◕	10	
39–08	73°04'N. 83°05'W.	30482–17091 A, B, C, D	30 Jun 79	40	●	0	Landsat 3 RBV
40–05	76°31'N. 74°08'W.	11130–16591	27 Aug 75	24	●	0	
40–06	75°25'N. 78°06'W.	11130–16593	27 Aug 75	25	◕	10	Eastern end of Devon Island
40–07	74°16'N. 81°32'W.	11130–17000	27 Aug 75	26	●	0	Eastern end of Devon Island
40–08	73°04'N. 84°31'W.	11130–17002	27 Aug 75	27	◑	15	
41–05	76°31'N. 75°34'W.	20209–17184	19 Aug 75	26	◑	40	Southeastern corner of Ellesmere Island
41–06	75°25'N. 79°33'W.	20551–17124	26 Jul 76	34	●	5	Devon Ice Cap
41–07	74°16'N. 82°58'W.	20551–17130	26 Jul 76	35	●	0	Extensive snow cover
41–08	73°04'N. 85°57'W.	21307–17015	21 Aug 78	~28	●	5	
42–05	76°31'N. 77°00'W.	20948–17010	27 Aug 77	24	◕	10	Southeastern corner of Ellesmere Island
42–06	75°25'N. 80°59'W.	20948–17012	27 Aug 77	25	◑	25	Devon Ice Cap
42–07	74°16'N. 84°24'W.	1376–17372	03 Aug 73	33	◕	10	EDC
43–04	77°33'N. 73°49'W.	20553–17231	28 Jul 76	31	●	5	
43–05	76°31'N. 78°26'W.	20553–17234	28 Jul 76	32	◕	10	
43–06	75°25'N. 82°25'W.	20553–17240	28 Jul 76	34	◑	30	Devon Ice Cap
43–07	74°16'N. 85°50'W.	20553–17243	28 Jul 76	35	●	0	Extensive snow cover

TABLE 2.—*Optimum Landsat 1, 2, and 3 MSS and RBV images of the glaciers of the Arctic Islands of Canada*—Continued

Path-Row	Nominal scene center (lat-long)	Landsat identification number	Date	Solar elevation angle (degrees)	Code	Cloud cover (percent)	Remarks
44–03	78°29'N. 69°53'W.	20554–17283	29 Jul 76	30	●	5	
44–04	77°33'N. 75°15'W.	11458–17000	20 Jul 76	33	●	0	Extensive snow cover
44–05	76°31'N. 79°53'W.	11458–17003	20 Jul 76	34	◕	10	Extensive snow cover
44–06	75°25'N. 83°51'W.	30523–17365	10 Aug 79	28	◑	20	Image used for Koerner's figure 2
44–07	74°16'N. 87°17'W.	1378–17485	05 Aug 73	32	●	0	EDC
45–03	78°29'N. 71°19'W.	20555–17341	30 Jul 76	30	◑	25	
45–04	77°33'N. 76°41'W.	11459–17054	21 Jul 76	33	●	0	Extensive snow cover
45–05	76°31'N. 81°19'W.	11459–17060	21 Jul 76	34	◕	10	Extensive snow cover
45–06	75°25'N. 85°17'W.	20951–17183	30 Aug 77	23	◕	10	Extensive snow cover
45–07	74°16'N. 88°43'W.	30524–17430	11 Aug 79	29	●	0	
46–03	78°29'N. 72°45'W.	11514–17063	14 Sep 76	15	●	0	Eastern side of Ellesmere Island
46–04	77°33'N. 78°07'W.	1758–17500	20 Aug 74	25	●	0	Eastern side of Ellesmere Island; image used for Koerner's figure 5
46–05	76°31'N. 82°45'W.	1758–17503	20 Aug 74	26	●	0	Southeastern corner of Ellesmere Island
46–05	76°31'N. 82°45'W.	30561–17473 A, B, D	17 Sep 79	15–16	◕	10–20	Landsat 3 RBV
46–06	75°25'N. 86°43'W.	1758–17505	20 Aug 74	27	●	0	
46–07	74°16'N. 90°09'W.	1758–17512	20 Aug 74	28	●	0	
47–02	79°19'N. 67°56'W.	2520–17403	25 Jun 76	33	◑	20	EDC; Landsat 2 RBV
47–03	78°29'N. 74°11'W.	11461–17163	23 Jul 76	32	●	0	Extensive snow cover
47–04	77°33'N. 79°33'W.	11854–16411	20 Aug 77	25	◕	10	Southeastern Ellesmere Island
47–05	76°31'N. 84°11'W.	11497–17142	28 Aug 76	23	◑	15	
47–06	75°25'N. 88°09'W.	30184–17552	05 Sep 78	~20	◑	40	Devon Island
47–07	74°16'N. 91°35'W.	1399–18054	26 Aug 73	26	●	0	Extensive snow cover
48–02	79°19'N. 69°22'W.	2558–17505	02 Aug 76	27	◑	30	EDC; Landsat 2 RBV

TABLE 2.—*Optimum Landsat 1, 2, and 3 MSS and RBV images of the glaciers of the Arctic Islands of Canada*—Continued

Path-Row	Nominal scene center (lat-long)	Landsat identification number	Date	Solar elevation angle (degrees)	Code	Cloud cover (percent)	Remarks
48–03	78°29'N. 75°37'W.	1760–18010	22 Aug 74	23	●	0	Ellesmere Island; Prince of Wales Icefield; image used for Koerner's figure 5
48–04	77°33'N. 81°00'W.	1760–18013	22 Aug 74	24	●	0	Ellesmere Island; Prince of Wales Icefield
48–05	76°31'N. 85°37'W.	1760–18015	22 Aug 74	25	◕	10	Ellesmere Island; Sydkap Ice Cap; image used for Koerner's figure 4
48–06	75°25'N. 89°35'W.	1760–18022	22 Aug 74	26	◑	40	
49–02	79°19'N. 70°48'W.	2559–17563	03 Aug 76	27	●	0	EDC
49–03	78°29'N. 77°03'W.	20559–17570	03 Aug 76	29	◕	10	Ellesmere Island; Prince of Wales Icefield
49–04	77°33'N. 82°26'W.	20559–17573	03 Aug 76	30	◑	40	Ellesmere Island; Prince of Wales Icefield
49–04	77°33'N. 82°26'W.	30546–18043 D	02 Sep 79	21	◑	30	Landsat 3 RBV
49–05	76°31'N. 87°03'W.	11463–17284	25 Jul 76	33	●	0	Ellesmere Island; Sydkap Ice Cap
49–05	76°31'N. 87°03'W.	30546–18050 B, D	02 Sep 79	21–22	◕	10	Landsat 3 RBV
50–01	80°01'N. 65°04'W.	2614–18002	27 Sep 76	6	◑	50	EDC
50–02	79°19'N. 72°14'W.	2597–18070	10 Sep 76	14	◑	50	EDC
50–03	78°29'N. 78°29'W.	30511–18100	29 Jul 79	28	◕	10	Ellesmere Island; Prince of Wales Icefield
50–04	77°33'N. 83°52'W.	11839–17000	05 Aug 77	29	◕	10	Ellesmere Island; Sydkap Ice Cap
50–04	77°33'N. 83°52'W.	30187–18114 A, B	08 Sep 78	18	◕	10–50	Landsat 3 RBV
50–05	76°31'N. 88°29'W.	11839–17002	05 Aug 77	30	●	0	
51–01	80°01'N. 66°30'W.	2548–18361	23 Jul 76	27	◕	10	EDC; northeastern Ellesmere Island; Landsat 2 RBV
51–02	79°19'N. 73°40'W.	2543–18083	18 Jul 76	31	●	0	EDC; northeastern Ellesmere Island; Landsat 2 RBV
51–03	78°29'N. 79°55'W.	11465–17391	27 Jul 76	31	●	5	Ellesmere Island; Prince of Wales Icefield
51–04	77°33'N. 85°18'W.	11465–17394	27 Jul 76	32	●	5	
51–04	77°33'N. 85°18'W.	30206–18174 B, D	27 Sep 78	11	◑	20	Landsat 3 RBV
51–05	76°31'N. 89°55'W.	11465–17400	27 Jul 76	33	◕	10	
52–01	80°01'N. 67°56'W.	2544–18135	19 Jul 76	29	●	0	EDC; northeastern Ellesmere Island; Landsat 2 RBV

TABLE 2.—*Optimum Landsat 1, 2, and 3 MSS and RBV images of the glaciers of the Arctic Islands of Canada*—Continued

Path-Row	Nominal scene center (lat-long)	Landsat identification number	Date	Solar elevation angle (degrees)	Code	Cloud cover (percent)	Remarks
52–02	79°19'N. 75°06'W.	20544–18142	19 Jul 76	31	◕	10	
52–02	79°19'N. 75°06'W.	30531–18211 D	18 Aug 79	24	◑	70	Landsat 3 RBV
52–03	78°29'N. 81°21'W.	20904–17595	14 Jul 77	33	●	0	
52–03	78°29'N. 81°21'W.	30521–18213 B	18 Aug 79	24	◑	20	Landsat 3 RBV
52–04	77°33'N. 86°44'W.	20904–18002	14 Jul 77	34	◕	10	
52–04	77°33'N. 86°44'W.	30207–18232 B, D	28 Sep 78	10	◑	20–30	Landsat 3 RBV
52–05	76°31'N. 91°21'W.	20904–18004	14 Jul 77	35	●	0	
53–01	80°01'N. 69°22'W.	2550–18474	25 Jul 76	27	●	5	EDC; Landsat 2 RBV
53–02	79°19'N. 76°32'W.	11860–17141	26 Aug 77	21	●	5	
53–03	78°29'N. 82°47'W.	11860–17144	26 Aug 77	22	●	0	
53–03	78°29'N. 82°47'W.	21265–18063	10 Jul 78	~34	●	0	Ablation area visible
53–03	78°29'N. 82°47'W.	30208–18284 C, D	29 Sep 78	9	◕	10–40	Landsat 3 RBV
53–04	77°33'N. 88°10'W.	30514–18274	01 Aug 79	28	◑	30	
53–04	77°33'N. 88°10'W.	30208–18291 D	29 Sep 78	10	◑	20	Landsat 3 RBV
53–05	76°31'N. 92°47'W.	30514–18280	01 Aug 79	29	●	0	
54–01	80°01'N. 70°48'W.	2583–18295	27 Aug 76	18	●	0	EDC; Ellesmere Island; eastern Agassiz Ice Cap; Landsat 2 RBV
54–02	79°19'N. 77°58'W.	11843–17214	09 Aug 77	26	●	5	
54–02	79°19'N. 77°58'W.	30191–18335 C, D	12 Sep 78	14	◕	10–20	Landsat 3 RBV
54–03	78°29'N. 84°13'W.	21644–18270	24 Jul 79	29	◑	20	
54–03	78°29'N. 84°13'W.	30191–18342 B, D	12 Sep 78	15	◕	10–30	Landsat 3 RBV
54–04	77°33'N. 89°36'W.	20546–18263	21 Jul 76	33	●	0	
54–05	76°31'N. 94°13'W.	20924–18111	03 Aug 77	31	●	0	
55–01	80°01'N. 72°14'W.	2601–18292	14 Sep 76	11	●	0	EDC; Ellesmere Island; Agassiz Ice Cap; Landsat 2 RBV

TABLE 2.—*Optimum Landsat 1, 2, and 3 MSS and RBV images of the glaciers of the Arctic Islands of Canada*—Continued

Path-Row	Nominal scene center (lat-long)	Landsat identification number	Date	Solar elevation angle (degrees)	Code	Cloud cover (percent)	Remarks
55–02	79°19'N. 79°24'W.	11109–18251	06 Aug 75	27	●	0	
55–02	79°19'N. 79°24'W.	30192–18394 C, D	13 Sep 78	14	◑	20–50	Landsat 3 RBV
55–03	78°29'N. 85°39'W.	30516–18384	03 Aug 79	27	◕	10	Southern Axel Heiberg Island
55–03	78°29'N. 85°39'W.	30516–18384 B, C, D	03 Aug 79	27	●	0–5	Southern Axel Heiberg Island; Landsat 3 RBV
55–04	77°33'N. 91°02'W.	30516–18391	03 Aug 79	28	●	0	
55–04	77°33'N. 91°02'W.	30516–18391 A, D	03 Aug 79	28	●	0	Landsat 3 RBV
55–05	76°31'N. 95°39'W.	1371–18511	29 Jul 73	~31	◑	50	EDC
56–01	80°01'N. 73°40'W.	2591–19151	04 Sep 76	14	◕	10	EDC; Ellesmere Island; Agassiz Ice Cap; Landsat 2 RBV
56–02	79°19'N. 80°50'W.	20548–18371	23 Jul 76	30	●	0	
56–03	78°29'N. 87°05'W.	20926–18214	05 Aug 77	28	◑	20	Southern Axel Heiberg Island
56–03	78°29'N. 87°05'W.	20548–18373	23 Jul 76	31	●	0	Southern Axel Heiberg Island
56–04	77°33'N. 92°28'W.	30517–18445	04 Aug 79	27	●	0	
57–01	80°01'N. 75°06'W.	2548–18364	23 Jul 76	29	●	0	EDC; Ellesmere Island; Agassiz Ice Cap; Landsat 2 RBV
57–01	80°01'N. 75°06'W.	2609–19144	22 Sep 76	7	◕	10	EDC; Ellesmere Island; Agassiz Ice Cap; Landsat 2 RBV
57–02	79°19'N. 82°16'W.	11864–17364	30 Aug 77	20	◕	10	
57–03	78°29'N. 88°31'W.	20945–18262	24 Aug 77	22	●	0	Southern Axel Heiberg Island
58–01	80°01'N. 76°32'W.	2550–18480	25 Jul 76	28	●	0	EDC; Ellesmere Island; Agassiz Ice Cap; Landsat 2 RBV; image used for Koerner's figure 8
58–02	79°19'N. 83°42'W.	20550–18483	25 Jul 76	30	●	0	
58–02	79°19'N. 83°42'W.	30123–18560 B, C	06 Jul 78	33	◕	10	Landsat 3 RBV
58–03	78°29'N. 89°57'W.	20154–18563	25 Jun 75	35	●	0	Southern Axel Heiberg Island
58–03	78°29'N. 89°57'W.	30123–18563 A	06 Jul 78	34	◑	20	Landsat 3 RBV
59–01	80°01'N. 77°58'W.	20551–18535	26 Jul 76	28	●	0	Ellesmere Island; Agassiz Ice Cap
59–02	79°19'N. 85°08'W.	20551–18541	26 Jul 76	30	●	0	

TABLE 2.—*Optimum Landsat 1, 2, and 3 MSS and RBV images of the glaciers of the Arctic Islands of Canada*—Continued

Path-Row	Nominal scene center (lat-long)	Landsat identification number	Date	Solar elevation angle (degrees)	Code	Cloud cover (percent)	Remarks
59–03	78°29'N. 91°23'W.	20947–18374	26 Aug 77	22	●	0	Southern Axel Heiberg Island
60–01	80°01'N. 79°24'W.	20552–18593	27 Jul 76	28	◕	10	Ellesmere Island; Agassiz Ice Cap
60–02	79°19'N. 86°34'W.	20948–18430	27 Aug 77	20	●	5	Axel Heiberg Island
60–03	78°29'N. 92°49'W.	20948–18432	27 Aug 77	21	●	0	
61–01	80°01'N. 80°50'W.	2596–19434	09 Sep 76	12	◑	20	EDC; Landsat 2 RBV
61–01	80°01'N. 80°50'W.	30198–19134 C	19 Sep 78	10	◑	20	Landsat 3 RBV
61–02	79°19'N. 88°00'W.	20949–18484	28 Aug 77	20	●	0	Axel Heiberg Island
61–03	78°29'N. 94°15'W.	20949–18490	28 Aug 77	21	●	0	
62–01	80°01'N. 82°16'W.	2559–19390	03 Aug 76	25	●	5	EDC; Landsat 2 RBV
62–02	79°19'N. 89°27'W.	20950–18542	29 Aug 77	20	●	0	Axel Heiberg Island; image used for Koerner's figure 7
62–03	78°29'N. 95°42'W.	20950–18545	29 Aug 77	21	●	0	
63–01	80°01'N. 83°42'W.	2196–19292	06 Aug 75	25	●	0	EDC; Ellesmere Island
63–02	79°19'N. 90°53'W.	2196–19295	06 Aug 75	26	◕	10	EDC; Axel Heiberg Island
63–03	78°29'N. 97°08'W.	30506–19243	24 Jul 79	29	●	0	
64–01	80°01'N. 85°08'W.	1758–19320	20 Aug 74	21	●	0	
64–02	79°19'N. 92°19'W.	20196–19295	06 Aug 75	27	◕	10	Axel Heiberg Island
64–06	75°25'N. 112°32'W.	21654–19254	03 Aug 79	30	●	0	Melville Island
65–01	80°01'N. 86°35'W.	1759–19375	21 Aug 74	21	●	5	
65–02	79°19'N. 93°45'W.	30508–19354	26 Jul 79	27	◑	20	
65–02	79°19'N. 93°45'W.	30202–19365 A, B	23 Sep 78	~9	◑	40–69	Landsat 3 RBV
65–06	75°25'N. 113°58'W.	1723–19411	16 Jul 74	36	◑	20	
66–01	80°01'N. 88°01'W.	1760–19433	22 Aug 74	21	●	5	Axel Heiberg Island
66–01	80°01'N. 88°01'W.	30563–19403 C, D	19 Sep 79	10	●	0	Axel Heiberg Island; Landsat 3 RBV

TABLE 2.—*Optimum Landsat 1, 2, and 3 MSS and RBV images of the glaciers of the Arctic Islands of Canada*—Continued

Path-Row	Nominal scene center (lat-long)	Landsat identification number	Date	Solar elevation angle (degrees)	Code	Cloud cover (percent)	Remarks
66–02	79°19'N. 95°11'W.	11855–18292	21 Aug 77	23	◕	10	Meighen and Axel Heiberg Islands
66–02	79°19'N. 95°11'W.	30563–19405 A, B, C, D	19 Sep 79	11–12	●	0–10	Axel Heiberg Island; Landsat 3 RBV
66–06	75°25'N. 115°24'W.	11855–18310	21 Aug 77	26	●	0	Melville Island; image used for Koerner's figure 16
66–06	75°25'N. 115°24'W.	30527–19431 A, B	14 Aug 79	29	●	0	Melville Island; Landsat 3 RBV
67–01	80°01'N. 89°27'W.	30510–19464	28 Jul 79	28	◑	40	
67–01	80°01'N. 89°27'W.	30204–19481 C, D	25 Sep 78	8	◕	10–20	Landsat 3 RBV
67–02	79°19'N. 96°37'W.	30510–19471	28 Jul 79	27	◑	30	
67–06	75°25'N. 116°50'W.	1725–19523	18 Jul 74	35	●	0	EDC; Melville Island
68–01	80°01'N. 90°53'W.	11857–18401	23 Aug 77	21	●	0	Axel Heiberg Island
68–01	80°01'N. 90°53'W.	30187–19534 C, D	08 Sep 78	15	●	0	Axel Heiberg Island; Landsat 3 RBV
68–02	79°19'N. 98°03'W.	1762–19551	24 Aug 74	20	●	0	EDC; Meighen Island
68–02	79°19'N. 98°03'W.	30187–19534 A, B	08 Sep 78	15	●	0–10	Axel Heiberg Island; Landsat 3 RBV
69–01	80°01'N. 92°19'W.	11858–18455	24 Aug 77	21	●	0	Meighen and Axel Heiberg Islands; image used for Koerner's figures 7 and 9
69–01	80°01'N. 92°19'W.	30188–19593 D	09 Sep 78	14	◕	10	Axel Heiberg Island; Landsat 3 RBV
69–02	79°19'N. 99°29'W.	1763–20005	25 Aug 74	20	●	0	EDC; Meighen Island
70–01	80°01'N. 93°45'W.	11859–18513	25 Aug 77	21	●	5	Meighen and Axel Heiberg Islands
71–01	80°01'N. 95°11'W.	11860–18570	26 Aug 77	20	●	0	Meighen and Axel Heiberg Islands
72–01	80°01'N. 96°37'W.	11861–19024	27 Aug 77	20	●	0	Meighen and Axel Heiberg Islands
72–01	80°01'N. 96°37'W.	30191–20164 A, B	12 Sep 78	12	●	0–40	Axel Heiberg Island; Landsat 3 RBV
73–01	80°01'N. 98°03'W.	11862–19082	28 Aug 77	20	◑	20	Meighen and Axel Heiberg Islands
74–01	80°01'N. 99°29'W.	11863–19140	29 Aug 77	19	●	5	

[1] Most of the images in this table were acquired by the Canada Centre for Remote Sensing (CCRS). Those acquired by the U.S. Geological Survey's EROS Data Center (EDC) are indicated by the EDC acronym. Unfortunately, all of the Return Beam Vidicon (RBV) images acquired by both CCRS and EDC are no longer available from either of the two national Landsat image archives. However, all of the Landsat RBV images listed are archived by the U.S. Geological Survey's Glacier Studies Project.

Glaciers of Western Canada

The glaciers of the Rocky Mountains of Canada were discussed by Denton (1975a) in "Mountain Glaciers of the Northern Hemisphere." In this volume, C. Simon L. Ommanney provides a comprehensive review entitled "Glaciers of the Canadian Rockies." He subdivides the Canadian Rockies into four mountain ranges, Border, Continental, Hart, and Muskwa Ranges, and discusses the extent of glacierization within the many smaller ranges and mountain groups that comprise these ranges. The Continental Ranges are heavily glacierized and include a number of major ice fields and outlet glaciers; the Columbia Icefield, with an area of 325 km^2, is the largest glacier in the Rocky Mountains. In addition to the large ice fields and associated outlet glaciers, many smaller mountain glaciers are distributed throughout the ranges.

The *Interior Ranges* (fig. 4) of British Columbia, situated between the Rocky Mountains on the east and the Coast Mountains on the west, are not

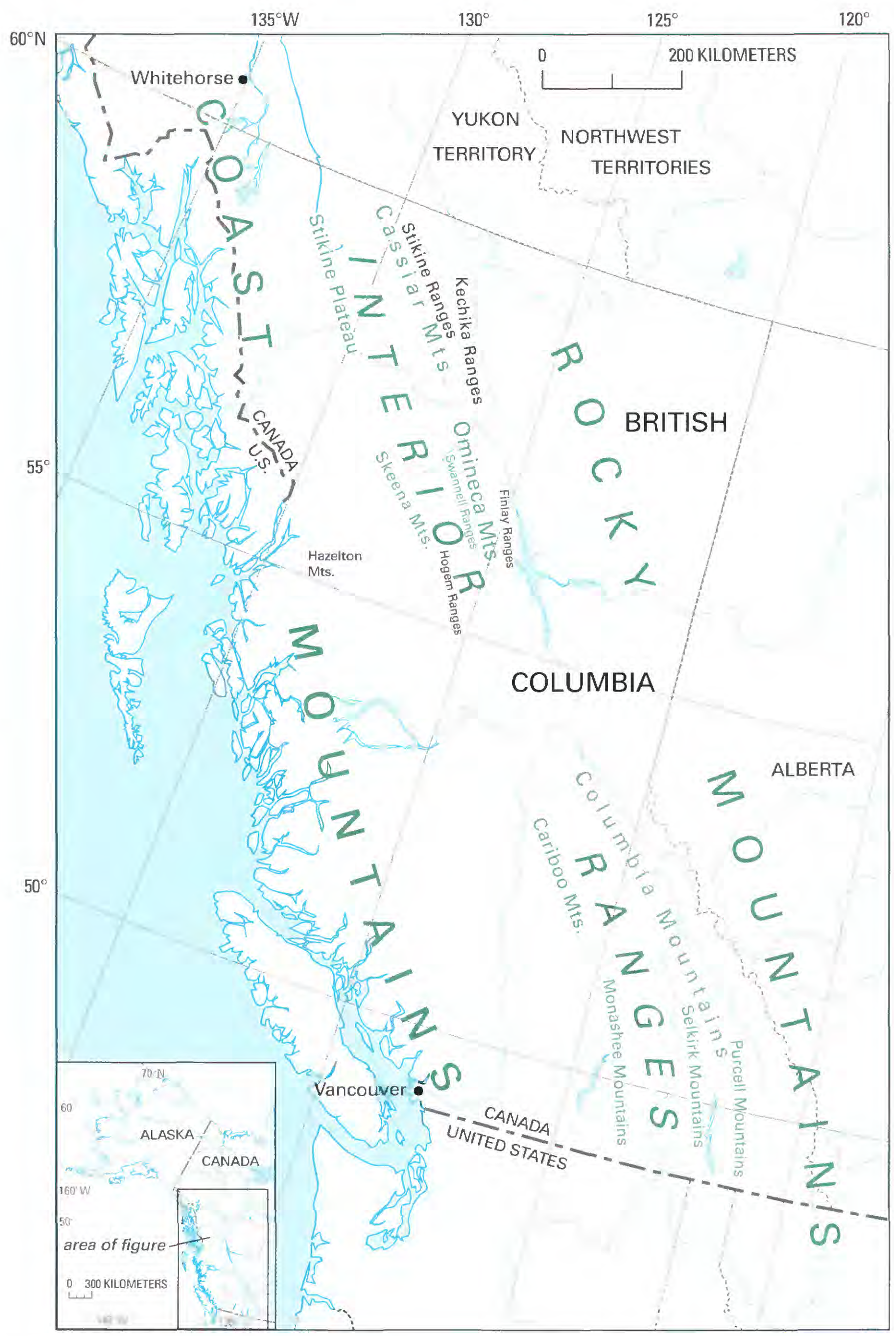

Figure 4.*—Map of the major mountain ranges in the* Interior Ranges *of British Columbia. Glacierized ranges indicated in green, non-glacierized in black.*

discussed in this volume, except with reference to glaciological research and glacier mapping in the "History of Glacier Investigations in Canada" and in "Mapping Canada's Glaciers," by C. Simon L. Ommanney and for an analysis of the Illecillewaet Glacier and Illecillewaet Névé in the Selkirk Mountains within the Columbia Mountains in the section on "Mapping Glaciers in the *Interior Ranges* and Rocky Mountains with Landsat Data," by Roger D. Wheate, Robert W. Sidjak, and Garnet T. Whyte. Figure 5 and table 3 provide a list and assessment of the optimum Landsat 1, 2, and 3 MSS images of the glaciers of the Canadian *Interior Ranges* and Rocky Mountains.

A brief review of the "Interior Ranges of British Columbia" by Denton (1975c) will provide some perspective, however. Denton (1975c) stated that the Selkirk, Purcell, Cariboo, and Monashee Mountains within the Columbia Mountains are glacierized. Part of the Omineca and Cassiar Mountains, including the Swannell Ranges, the Skeena Mountains, and the Stikine Plateau, also contain glaciers (fig. 4). Denton (1975c) concluded that the Finlay, Hogem, Stikine, and Kechika Ranges of the Omineca and Cassiar Mountains and the Hazelton Mountains did not have glaciers (fig. 4).

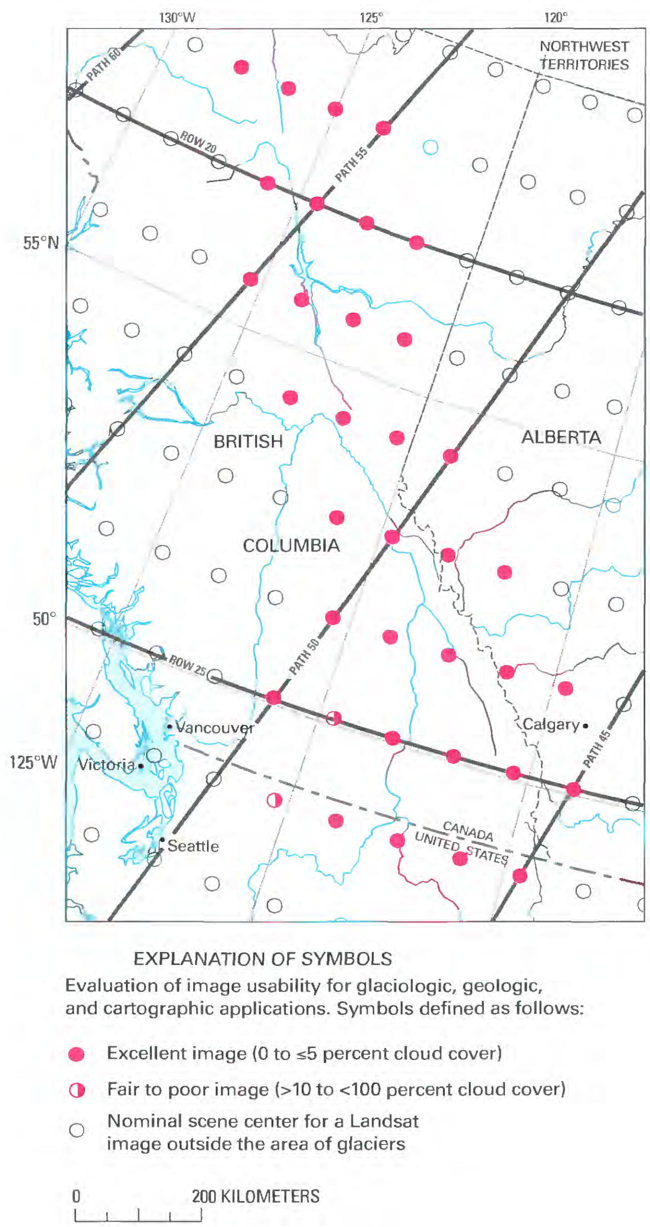

***Figure 5.**—Optimum Landsat 1, 2, and 3 MSS images of the glaciers of the Canadian Rocky Mountains and* Interior *Ranges.*

TABLE 3.—*Optimum Landsat 1, 2, and 3 MSS images of the glaciers of the Canadian Rocky Mountains and* Interior Ranges

[**, The images archived by the Canada Centre for Remote Sensing (CCRS) are not identified on the CCRS Website (http://www.ccrs.nrcan.gc.ca) by Landsat identification number but can be located by path (track), row (frame), and date. The images archived by the EROS Data Center (EDC) (http://earthexplorer.usgs.gov) are no longer located or ordered by the Landsat identification number on the image but by a different entity number that incorporates satellite number, path, row, and date]

Path-Row	Nominal scene center (lat-long)	Landsat identification number	Date	Solar elevation angle (degrees)	Code	Cloud cover (percent)	Remarks
45–25	50°09'N. 113°58'W.	**	14 Sep 81	~38	●	0	Archived by CCRS[1]
45–26	48°44'N. 114°36'W.	22427–17465	14 Sep 81	39	●	0	Archived by EDC
46–24	51°34'N. 114°43'W.	30561–17552	17 Sep 79	36	●	0	Archived by EDC
46–25	50°09'N. 115°24'W.	**	17 Sep 79	37	●	0	Archived by CCRS
46–26	48°44'N. 116°02'W.	30561–17561	17 Sep 79	38	●	0	Archived by EDC
47–24	51°34'N. 116°09'W.	1741–18044	03 Aug 74	49	◑	30	Columbia to Waputik Icefields; archived by EDC
47–24	51°34'N. 116°09'W.	**	11 Aug 81	~46	●	5	Columbia to Waputik Icefields; archived by CCRS
47–25	50°09'N. 116°50'W.	1741–18050	03 Aug 74	50	◑	40	Archived by EDC
47–25	50°09'N. 116°50'W.	**	11 Aug 81	~47	●	0	Archived by CCRS
47–26	48°44'N. 117°28'W.	22393–17584	11 Aug 81	48	●	5	Archived by EDC
48–23	52°58'N. 116°52'W.	**	13 Sep 75	~36	●	0	Archived by CCRS
48–24	51°34'N. 117°35'W.	**	13 Sep 75	~37	●	0	Columbia to Waputik Icefields; archived by CCRS
48–24	51°34'N. 117°35'W.	2252–18062	01 Oct 75	31	●	0	Columbia to Waputik Icefields; image used for figure 7; archived by EDC
48–25	50°09'N. 118°16'W.	2234–18070	13 Sep 75	38	●	0	Archived by EDC
48–26	48°44'N. 118°54'W.	2234–18073	13 Sep 75	39	●	0	Archived by EDC
49–23	52°58'N. 118°18'W.	1419–18233	15 Sep 73	36	●	0	Mount Robson area to Clemenceau Icefield; archived by EDC
49–24	51°34'N. 119°01'W.	1419–18235	15 Sep 73	37	●	0	Archived by EDC
49–25	50°09'N. 119°42'W.	1419–18242	15 Sep 73	39	◑	20	Archived by EDC
49–26	48°44'N. 120°20'W.	1419–18244	15 Sep 73	40	◑	20	Archived by EDC
50–22	54°22'N. 118°59'W.	1420–18285	16 Sep 73	35	●	0	Mount Sir Alexander; archived by EDC
50–23	52°58'N. 119°44'W.	1420–18291	16 Sep 73	36	●	0	Mount Robson area; image used for figure 29; archived by EDC
50–24	51°34'N. 120°27'W.	1420–18294	16 Sep73	37	●	0	Archived by EDC
50–25	50°09'N. 121°08'W.	1420–18300	16 Sep 73	38	●	0	Archived by EDC
51–22	54°22'N. 120°26'W.	1385–18351	12 Aug 73	46	●	0	Mount Sir Alexander; archived by EDC
51–23	52°58'N. 121°11'W.	1385–18353	12 Aug 73	47	●	0	Cariboo Range; archived by EDC
52–21	55°45'N. 121°04'W.	21696–18241	14 Sep 79	34	●	0	Archived by EDC

TABLE 3.—*Optimum Landsat 1, 2, and 3 MSS images of the glaciers of the Canadian Rocky Mountains and* Interior Ranges—Continued

Path-Row	Nominal scene center (lat-long)	Landsat identification number	Date	Solar elevation angle (degrees)	Code	Cloud cover (percent)	Remarks
52–22	54°22'N. 121°52'W.	**	14 Sep 79	~35	●	0	Archived by CCRS
52–22	54°22'N. 121°52'W.	2544–18223	19 Jul 76	50	●	0	Archived by EDC
53–20	57°08'N. 121°39'W.	1783–18355	14 Sep 74	33	●	0	Archived by EDC
53–20	57°08'N. 121°39'W.	**	17 Aug 81	~43	●	0	Archived by CCRS
53–21	55°45'N. 122°30'W.	1783–18361	14 Sep 74	34	◑	40	Archived by EDC
53–21	55°45'N. 122°30'W.	**	17 Aug 81	~44	●	0	Archived by CCRS
53–22	54°22'N. 123°18'W.	1783–18364	14 Sep 74	35	◑	30	Archived by EDC
53–22	54°22'N. 123°18'W.	**	17 Aug 81	~45	●	0	Archived by CCRS
54–20	57°08'N. 123°05'W.	1082–18515	13 Oct 72	23	●	0	Great Snow Mountain; extensive snow cover; archived by EDC
54–20	57°08'N. 123°05'W.	**	14 Aug 75	~44	●	5	Great Snow Mountain; archived by CCRS
54–21	55°45'N. 123°56'W.	1082–18522	13 Oct 72	24	●	0	Extensive snow cover; archived by EDC
54–21	55°45'N. 123°56'W.	**	14 Aug 75	~45	●	5	Archived by CCRS
55–19	58°31'N. 123°37'W.	1767–18473	29 Aug 74	37	◑	30	Mount Roosevelt, Churchill Peak; archived by EDC
55–19	58°31'N. 123°37'W.	**	11 Sep 75	~32	●	5	Mount Roosevelt, Churchill Peak; archived by CCRS
55–20	57°08'N. 124°31'W.	1767–18475	29 Aug 74	39	◑	20	Mount Lloyd George, Great Snow Mountain; archived by EDC
55–20	57°08'N. 124°31'W.	**	11 Sep 75	~33	●	0	Mount Lloyd George, Great Snow Mountain; archived by CCRS
55–21	55°45'N. 125°22'W.	1767–18482	29 Aug 74	39	●	0	Archived by EDC
55–21	55°45'N. 125°22'W.	**	11 Sep 75	~34	●	0	Archived by CCRS
56–19	58°31'N. 125°03'W.	1750–18535	12 Aug 74	43	◕	10	Mount Roosevelt, Mount Lloyd George; image used for figure 33; archived by EDC
56–19	58°31'N. 125°03'W.	**	12 Sep 75	~32	●	5	Mount Roosevelt, Mount Lloyd George; archived by CCRS
56–20	57°08'N. 125°57'W.	1750–18542	12 Aug 74	44	◕	10	Image used for figure 33; archived by EDC
56–20	57°08'N. 125°57'W.	**	12 Sep 75	~33	●	0	Archived by CCRS
57–19	58°31'N. 126°29'W.	1769–18585	31 Aug 74	37	◑	20	Mount Roosevelt; archived by EDC
57–19	58°31'N. 126°29'W.	**	07 Aug 82	~44	●	0	Archived by CCRS
58–19	58°31'N. 127°55'W.	5865–17492	31 Aug 77	30	●	0	Archived by EDC

1 The cloud cover and evaluations of images archived by CCRS are based on the CCRS World Wide Web page listing (http://www.ccrs. nrcan.gc.ca). There is no browse image for these scenes, but the cloud cover evaluation has been reliable when compared with images that have been inspected directly.

The "Glaciers of the Coast Mountains (Pacific Ranges and Cascade Mountains) and Coast Ranges of British Columbia" were previously discussed by Denton (1975b). Ommanney (1972) provided comprehensive information about glaciers on Vancouver Island [Canada: Environment: Inland Waters Branch (1971a, b)], considered to be part of the Coast Ranges (fig. 1). Field (1975a) also addressed the "Glaciers of the Coast Mountains: Boundary Ranges (Alaska, British Columbia, and Yukon Territory.)" In this volume, Garry K.C. Clarke and Gerald Holdsworth discuss some aspects of the "Glaciers of the Coast Mountains," with special emphasis on glaciological hazards, such as jökulhlaups, the use of small glaciers as recreational resources, and the special problems associated with carrying out mining operations in glacierized regions.

The St. Elias Mountains are considered to be the most spectacular series of mountain ranges in North America. They are heavily glacierized and include three of the six highest mountain peaks on the continent. Mt. Logan, Yukon Territory, Canada, at 5,959 m [http://www.ice2001.com], is second only to Mt. McKinley (6,194 m), Alaska, in elevation. The St. Elias Mountains lie along the international border of the United States and Canada, between Alaska and Yukon Territory (fig. 1 in "History of Glacier Investigations in Canada," and fig. 1 in "Glaciers of the St. Elias Mountains"). Field (1975b) described the St. Elias Mountains in his compilation. Garry K.C. Clarke and Gerald Holdsworth, in the "Glaciers of the St. Elias Mountains" section of this volume, describe some of the valley glaciers, plateau glaciers, ice fields and associated outlet glaciers, and piedmont glaciers that characterize the region. The glaciers are classified as temperate, subpolar, and cold; at least 136 of the subpolar glaciers are surge-type glaciers. In a special section, "Quantitative Measurements of Tweedsmuir Glacier and Lowell Glacier Imagery," Gerald Holdworth, Philip J. Howarth, and C. Simon L. Ommanney discuss the application of sequential Landsat images to two surging glaciers. Figure 6 and table 4 provide a list and assessment of the optimum Landsat 1, 2, and 3 MSS and RBV images of the Coast and St. Elias Mountains of Canada.

Several mountain groups in the Yukon and Northwest Territories (fig. 7) have glaciers according to Horvath (1975), including the Hess and Wernecke Mountains in the Selwyn Mountains, the Ogilvie Mountains, and the Backbone and Canyon Ranges of the Mackenzie Mountains. The Logan Mountains, located in the Selwyn Mountains, have glaciers according to provisional (as of 1985) NTS 1:50,000-scale map sheets (Demuth, written commun., 2001). Demuth (written commun., 2001) is evaluating the feasibility of establishing a glacier mass-balance-monitoring site near the Cirque of the Unclimbables in the Logan Mountains. The Yukon Plateau and the Kluane Ranges may also have glaciers (Ommanney, written commun., 2001). None of the these mountains are covered in this volume. Ommanney (1993) reported on an inventory of Yukon glaciers based on hydrologic basins. Glaciers on the Alaska side of the hydrologic divide account for about 7,250 km^2 of ice; those within the Yukon divide, feeding the Yukon River, about 3,000 km^2, and those within the Alsek River basin, draining through the Panhandle into the Pacific Ocean, account for about 3,800 km^2 of ice.

Landsat MSS images are most useful in the study of changes in large glaciers, ice caps and ice fields, and associated outlet glaciers in Arctic Canada, and of ice fields and associated outlet glaciers, and valley glaciers in western Canada. The retreat of glaciers in western Canada can be delineated on Landsat images, time-lapse image coverage that now spans three decades of data acquisition beginning in 1972 with Landsat 1, followed by Landsats 2, 3, 4, 5, and 7. The trend toward an increase in the number of spectral bands and spatial resolution (15 m with the Landsat 7 enhanced thematic mapper (ETM+) and multispectral stereoscopic sensor on the

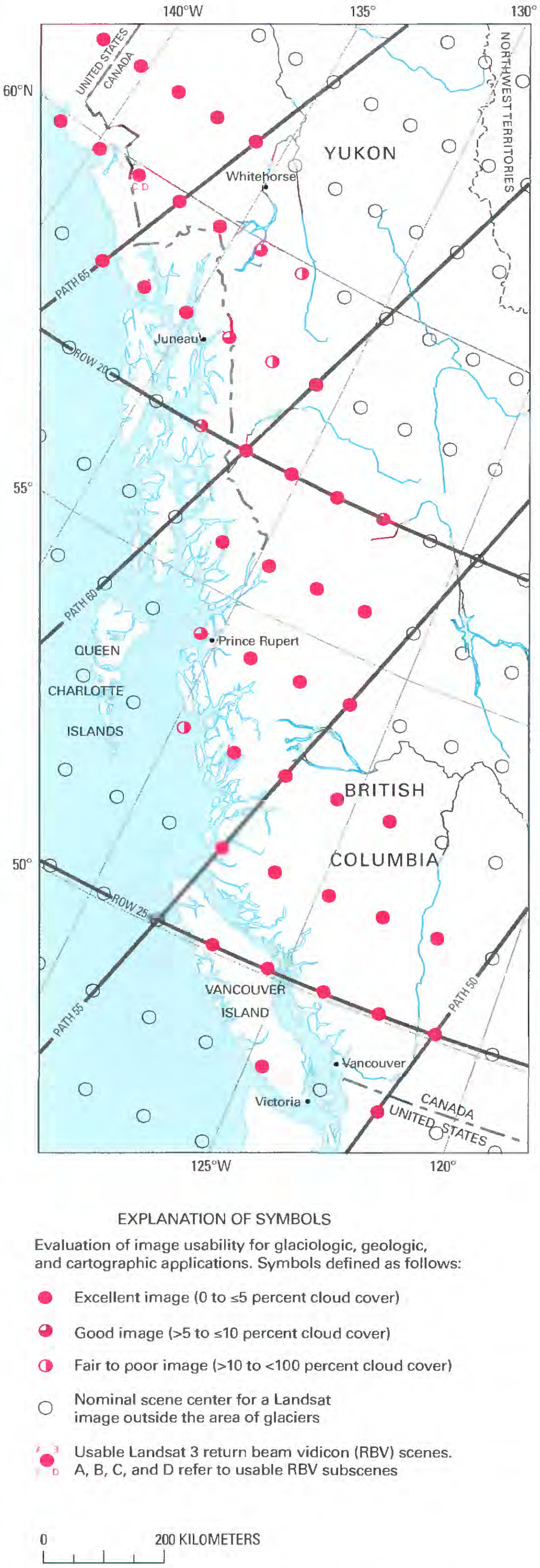

***Figure 6.**—Optimum Landsat 1, 2, and 3 MSS and RBV images of the glaciers of the Coast and St. Elias Mountains of Canada.*

TABLE 4.—*Optimum Landsat 1, 2, and 3 MSS and RBV images of glaciers of the Coast and St. Elias Mountains of Canada*

[The images archived by the Canada Centre for Remote Sensing (CCRS) are not identified on the CCRS Website (http://www.ccrs.nrcan.gc.ca) by Landsat identification number but can be located by path (track), row (frame), and date. The images archived by the EROS Data Center (EDC) (http://earthexplorer.usgs.gov) are no longer located or ordered by the Landsat identification number on the image but by a different entity number that incorporates satellite number, path, row, and date]

Path-Row	Nominal scene center (lat-long)	Landsat identification number	Date	Solar elevation angle (degrees)	Code	Cloud cover (percent)	Remarks
50–25	50°09'N. 121°08'W.	2596–18105	09 Sep 76	39	●	0	
50–26	48°44'N. 121°46'W.	2596–18111	09 Sep 76	40	●	0	Garibaldi Park area
51–24	51°34'N. 121°53'W.	1385–18360	12 Aug 73	48	●	0	
51–25	50°09'N. 122°34'W.	1385–18362	12 Aug 73	49	●	0	Pemberton Icefield
52–24	51°34'N. 123°19'W.	5877–17154	12 Sep 77	30	●	0	
52–25	50°09'N. 124°00'W.	5841–17195	07 Aug 77	40	●	0	Pemberton and Homathko Icefields
52–26	48°44'N. 124°38'W.	1764–18332	26 Aug 74	45	●	0	Vancouver Island
53–23	52°58'N. 124°03'W.	1027–18472	19 Aug 72	46	●	0	
53–24	51°34'N. 124°45'W.	1027–18475	19 Aug 72	43	●	0	Klinaklini Glacier, Mount Waddington, Homathko Icefield
53–25	50°09'N. 125°26'W.	2203–18360	13 Aug 75	48	●	0	
54–23	52°58'N. 125°29'W.	1766–18433	28 Aug 74	42	●	0	
54–24	51°34'N. 126°11'W.	1766–18435	28 Aug 74	43	●	0	Monarch Icefield, Klinaklini Glacier, Mount Waddington
54–25	50°09'N. 126°52'W.	1766–18442	28 Aug 74	44	●	0	Vancouver Island
55–22	54°22'N. 126°10'W.	1767–18484	29 Aug 74	40	●	0	
55–23	52°58'N. 126°55'W.	1767–18491	29 Aug 74	41	●	0	
55–24	51°34'N. 127°37'W.	1767–18493	29 Aug 74	42	●	0	
56–21	55°45'N. 126°48'W.	1768–18540	30 Aug 74	39	●	0	
56–22	54°22'N. 127°36'W.	1768–18543	30 Aug 74	40	●	0	
56–23	52°58'N. 128°21'W.	1768–18545	30 Aug 74	41	●	0	
57–20	57°08'N. 127°23'W.	1769–18592	31 Aug 74	38	◕	10	
57–21	55°45'N. 128°14'W.	1769–18594	31 Aug 74	39	●	0	Cambria Icefield
57–22	54°22'N. 129°02'W.	1769–19001	31 Aug 74	40	●	0	
57–23	52°58'N. 129°47'W.	1049–19101	10 Sep 72	38	◑	50	

TABLE 4.—*Optimum Landsat 1, 2, and 3 MSS and RBV images of glaciers of the Coast and St. Elias Mountains of Canada*—Continued

Path-Row	Nominal scene center (lat-long)	Landsat identification number	Date	Solar elevation angle (degrees)	Code	Cloud cover (percent)	Remarks
58–20	57°08'N. 128°49'W.	1770–19050	01 Sep 74	38	●	0	
58–21	55°45'N. 129°40'W.	21288–18435	02 Aug 78	45	●	0	Cambria Icefield; image used for Coast Mountains, figure 2
58–22	54°22'N. 130°28'W.	1788–19050	19 Sep 74	33	◕	10	
59–20	57°08'N. 130°15'W.	5848–17571	14 Aug 77	36	●	5	
59–21	55°45'N. 131°06'W.	5848–17574	14 Aug 77	36	●	0	
60–19	58°31'N. 130°47'W.	1772–19160	03 Sep 74	36	●	0	
60–20	57°08'N. 131°41'W.	1722–19162	03 Sep 74	37	●	0	Stikine Icefield; image used for Coast Mountains, figure 3
61–19	58°31'N. 132°13'W.	5850–18080	16 Aug 77	35	◑	25	Juneau Ice Field, Canadian glaciers cloudfree
61–20	57°08'N. 133°07'W.	2931–18571	10 Aug 77	42	◑	15	Stikine Icefield, Canadian glaciers cloudfree
62–18	59°54'N. 132°41'W.	21670–19193	19 Aug 79	39	◑	20	Archived by CCRS[1]
62–19	58°31'N. 133°39'W.	21670–19195	19 Aug 79	40	◕	10	
63–18	59°54'N. 134°07'W.	1775–19324	06 Sep 74	34	◕	10	
63–19	58°31'N. 135°05'W.	1775–19330	06 Sep 74	35	●	0	Juneau Ice Field
64–18	59°54'N. 135°33'W.	30147–19373	30 Jul 78	45	●	0	
64–18	59°54'N. 135°33'W.	1416–19473	12 Sep 73	32	●	0	Band 6 evaluated, Band 7 missing
64–19	58°31'N. 136°31'W.	30147–19375	30 Jul 78	46	●	0	Glacier Bay
64–19	58°31'N. 136°31'W.	1416–19480	12 Sep 73	33	●	0	Glacier Bay
65–17	61°16'N. 135°56'W.	1417–19525	13 Sep 73	30	●	0	
65–18	59°54'N. 136°59'W.	1417–19531	13 Sep 73	32	●	0	Image used for St. Elias Mountains, figures 9 and 12
65–19	58°31'N. 137°57'W.	1417–19534	13 Sep 73	33	●	0	
66–17	61°16'N. 137°22'W.	21314–19293	28 Aug 78	35	●	0	Archived by CCRS
66–18	59°54'N. 138°25'W.	21314–19295	28 Aug 78	36	●	0	Image used for St. Elias Mountains, figures 1, 9, and 12
66–18	59°54'N. 138°25'W.	30167–19491 A, C, D	19 Aug 78	39	◕	10	Landsat 3 RBV; subscene A used for St. Elias Mountains, figure 6; archived by USGS Glacier Studies Project
67–17	61°16'N. 138°48'W.	2955–19285	03 Sep 77	32	●	0	Image used for St. Elias Mountains, figures 2 and 4

TABLE 4.—*Optimum Landsat 1, 2, and 3 MSS and RBV images of glaciers of the Coast and St. Elias Mountains of Canada*—Continued

Path-Row	Nominal scene center (lat-long)	Landsat identification number	Date	Solar elevation angle (degrees)	Code	Cloud cover (percent)	Remarks
67–18	59°54'N. 139°51'W.	2955–19292	03 Sep 77	33	●	0	Seward Glacier; image used for St. Elias Mountains, figure 2
68–17	61°16'N. 140°14'W.	2956–19343	04 Sep 77	32	●	0	Image used for St. Elias Mountains, figure 1
68–18	59°54'N. 141°17'W.	2956–19350	04 Sep 77	33	●	5	Seward Glacier; image used for St. Elias Mountains, figure 1
69–17	61°16'N. 141°40'W.	21677–19593	26 Aug 79	36	●	5	

[1] The cloud cover and evaluations of images archived by CCRS are based on the CCRS World Wide Web page (http://www.ccrs.nrcan.gc.ca) listing. There is no browse image for these scenes, but the cloud cover evaluation has been reliable when compared with images that have been directly inspected.

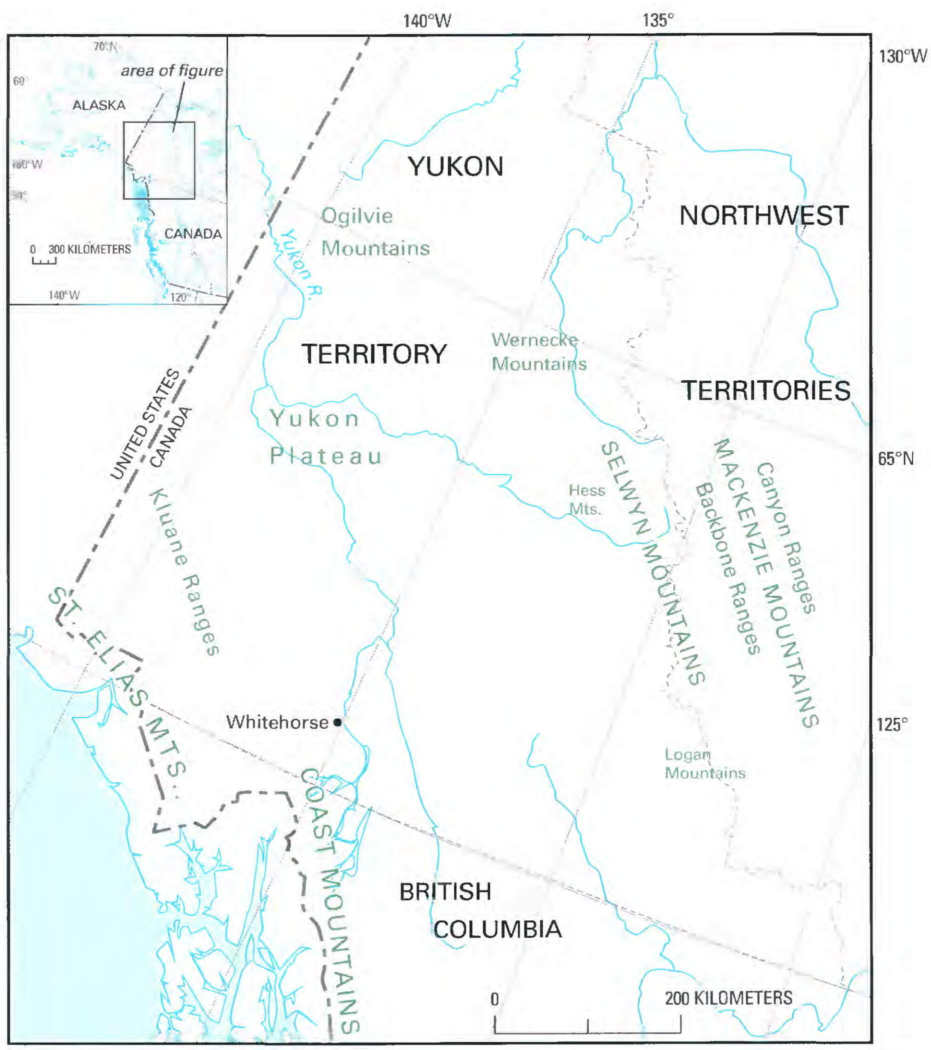

Figure 7.—*Map of the major mountain ranges in the Yukon and Northwest Territories of Canada. Glacierized ranges indicated in green.*

advanced thermal emission and reflectance radiometer (ASTER) on the Terra Spacecraft); the surface-elevation profile capability of the Ice, Cloud, and land Elevation Satellite (ICESat), estimated to be ±1 m; the all-weather radar sensors, such as the Canadian RADARSAT; and high-resolution panchromatic IKONOS and QuickBird-2 images [1-m picture elements (pixels) and 61-cm pixels, respectively) will provide new opportunities for glaciologists to use satellite remote sensing and GIS technologies to monitor changes in the area and volume of glaciers in the future (Williams and others, 1997; Williams and Hall, 1998). The following sections are directed primarily at an analysis and evaluation of Landsat MSS (and RBV) images of selected Canadian glaciers, in the context of the history of glacier investigations and glacier mapping in Canada, as a contribution to the objective of establishing a global baseline of glacier area during the 1970's. Although the pixel resolution of Landsat MSS images (79 m) generally precluded analysis of changes in small glaciers, the MSS images do provide an objective historical, time-precise record of the areal extent of large glaciers (that comprise most of the glacier area in Canada) during the 1970's.

References Cited

Anonymous, 1978, Height of the glaciation level in western Canada and southern Alaska: Oslo, 1:4,000,000-scale map, *in* Height of the glaciation level in northern British Columbia and southeastern Alaska: Geografiska Annaler, v. 54A, p. 76–84.

———1998, Rivers of ice: Canadian Geographic, v. 118, no. 7, p. 34–39.

Canada: Environment: Inland Waters Branch, 1971a, 8.8.1—South Vancouver Island, glacier inventory, area 4*8H: Ottawa, Ontario, produced by the Inland Waters Branch, Department of the Environment; printed by the Surveys and Mapping Branch, Department of Energy, Mines and Resources, map. (Glacier Atlas of Canada IWB 1137, scale 1:500,000.)

Canada: Environment: Inland Waters Branch, 1971b, 8.8.2—Northern Vancouver Island, glacier inventory, area 4*8H: Ottawa, Ontario, produced by the Inland Waters Branch, Department of the Environment; printed by the Surveys and Mapping Branch, Department of Energy, Mines and Resources, map. (Glacier Atlas of Canada IWB 1139, scale 1:500,000.)

Denton, G.H., 1975a, Glaciers of the Canadian Rocky Mountains, *in* Field, W.O., ed., Mountain glaciers of the Northern Hemisphere, v. 1: Hanover, N.H., U.S. Army Cold Regions Research and Engineering Lab., p. 603–653.

———1975b, Glaciers of the Coast Mountains (Pacific Ranges and Cascade Mountains) and Coast Ranges of British Columbia, *in* Field, W.O., ed., Mountain glaciers of the Northern Hemisphere, v. 1: Hanover, N.H., U.S. Army Cold Regions Research and Engineering Lab., p. 671–687.

———1975c, Glaciers of the Interior Ranges of British Columbia, *in* Field, W.O., ed., Mountain glaciers of the Northern Hemisphere, v. 1: Hanover, N.H., U.S. Army Cold Regions Research and Engineering Lab., p. 655–670.

Dunbar, M., and Greenway, K.R., 1956, Arctic Canada from the air: Ottawa, Queen's Printer, 541 p.

Fahn, C., 1975, Glaciers of northern Labrador, *in* Field, W.O., ed., Mountain glaciers of the Northern Hemisphere, v. 2: Hanover, N.H., U.S. Army Cold Regions Research and Engineering Lab., p. 673–682.

Field, W.O., Jr., 1975a, Glaciers of the Coast Mountains—Boundary Ranges (Alaska, British Columbia, and Yukon Territory), *in* Field, W.O., ed., Mountain glaciers of the Northern Hemisphere, v. 2: Hanover, N.H., U.S. Army Cold Regions Research and Engineering Lab., p. 11–141.

———1975b, Glaciers of the St. Elias Mountains, *in* Field, W.O., ed., Mountain glaciers of the Northern Hemisphere, v. 2: Hanover, N.H., U.S. Army Cold Regions Research and Engineering Lab., p. 143–297.

———1975c, Mountain glaciers of the Northern Hemisphere: Hanover, N.H., U.S. Army Cold Regions Research and Engineering Lab., v. 1, 698 p., v. 2, 932 p., atlas, 49 plates.

Field, W.O and Associates, 1958, Atlas of mountain glaciers in the Northern Hemisphere: Natick, Mass., Headquarters Quartermaster Research and Engineering Command, U.S. Army Research and Engineering Center, Environmental Protection Research Division, Technical Report EP–92, unpaginated, various plates.

Henoch, W.E.S., 1967, Surface measurements of glacierized area in Canada: Ottawa, Department of Energy, Mines and Resources, Water Research Branch, Glaciology Section, unpublished manuscript, 4 p.

Horvath, Eva, 1975, Glaciers of the Yukon and Northwest Territories (excluding the Queen Elizabeth Islands and St. Elias Mountains), *in* Field, W.O., ed., Mountain glaciers of the Northern Hemisphere, v. 1: Hanover, N.H., U.S. Army Cold Regions Research and Engineering Lab., p. 689–698.

Koerner, R.M., 1968, Fabric analysis of a core from the Meighen Ice Cap, Northwest Territories, Canada: Journal of Glaciology, v. 7, no. 51, p. 421–430.

Mercer, J.H., 1975a, Glaciers of Baffin and Bylot Islands, *in* Field, W.O., ed., Mountain glaciers of the Northern Hemisphere, v. 2: Hanover, N.H., U.S. Army Cold Regions Research and Engineering Lab., p. 683–721.

———1975b, Glaciers of the Queen Elizabeth Islands, N.W.T., Canada, *in* Field, W.O., ed., Mountain glaciers of the Northern Hemisphere, v. 2: Hanover, N.H., U.S. Army Cold Regions Research and Engineering Lab., p. 723–752.

Ommanney, C.S.L., 1969, Glacier inventory of Canada-Axel Heiberg Island, Northwest Territories: Ottawa, Department of Energy, Mines and Resources, Inland Waters Branch Technical Bulletin No. 37, 97 p.

Ommanney, Simon, 1970, The Canadian glacier inventory, *in* Glaciers, Proceedings of Workshop Seminar, 1970; Ottawa Canadian National Committee, the International Hydrological Decade, p. 23–30.

Ommanney, C.S.L., 1972, Application of the Canadian glacier inventory to studies of the static water balance. 1. The glaciers of Vancouver Island, *in* Adams, W.P., and Helleiner, F.M., eds., International Geography 1972, v. 2: Toronto, University of Toronto Press, p. 1266–1268.

———1993, Yukon glaciers, *in* Prowse, T.D., Ommanney, C.S.L., and Ulmer, K.E., eds., International Northern Research Basins Symposium/Workshop, 9th, Whitehorse, Dawson City, Eagle Plains, Yukon; Inuvik, Northwest Territories, 1992, Proceedings: Saskatoon, Saskatchewan, National Hydrology Research Institute, Environment Canada, v. 1, p. 373–382. (NHRI Symposium 10.)

Østrem, Gunnar, Arnold, K.C., and Simpson, K., compilers, 1966, Glaciers and moraines in southern British Columbia and Alberta, 1:2,000,000-scale map, *in* Østrem, G., and Arnold, K., 1970, Ice-cored moraines in southern British Columbia and Alberta, Canada: Geografiska Annaler, v. 52A, p. 120–128.

Shaler, N.S., and Davis, W.M., 1881, Illustrations of the Earth's surface: Glaciers: Boston, J.R. Osgood and Co., 198 p.

Shilts, Elizabeth, Fick, Steven, Murray, Andrew, and McLean, Janice, 1998, The glaciers of Canada: Canadian Geographic, v. 118, no. 7, p. 51–52 (8-page foldout, color map).

Williams, R.S., Jr., and Ferrigno, J.G., workshop coordinators, 1997, Final Report of the Workshop on Long-Term Monitoring of Glaciers of North America and Northwestern Europe: U.S. Geological Survey Open-File Report 98–31, 144 p.

Williams, R.S., Jr., Garvin, J.B., Sigurðsson, O., Hall, D.K., and Ferrigno, J.G., 1997, Measurement of changes in the area and volume of the Earth's large glaciers with satellite sensors, *in* Williams, R.S., Jr., and Ferrigno, J.G., workshop coordinators, Final Report of the Workshop on Long-Term Monitoring of Glaciers of North America and Northwestern Europe: U.S. Geological Survey Open-File Report 98–31, p. 74–76.

Williams, R.S., Jr., and Hall, D.K., 1998, Use of remote sensing techniques, *in* Haeberli, W., Hoelzle, M., and Suter, S., eds., Into the 2nd century of world glacier monitoring: Prospects and strategies: A contribution to the International Hydrological Programme (IHP), and the Global Environmental Monitoring System (GEMS), World Glacier Monitoring Service: Paris, UNESCO Publishing, Studies and Reports in Hydrology, Publication 56, p. 97–111.

Glaciers of North America—

GLACIERS OF CANADA

HISTORY OF GLACIER INVESTIGATIONS IN CANADA

By C. SIMON L. OMMANNEY

SATELLITE IMAGE ATLAS OF GLACIERS OF THE WORLD

Edited by RICHARD S. WILLIAMS, Jr., *and* JANE G. FERRIGNO

U.S. GEOLOGICAL SURVEY PROFESSIONAL PAPER 1386–J–1

The earliest recorded description of a Canadian glacier was in 1861. Since that time, various glaciological investigations have been conducted in the several glacierized regions of Canada (for example, Coast Mountains, Interior Ranges, *Rocky Mountains, and Arctic Islands), including mass balance, modeling, dendrochronology, climatology, ice chemistry and physics, ice-core analyses, glacier-surge mechanics, and airborne and satellite remote sensing*

CONTENTS

GLACIERS OF NORTH AMERICA–

GLACIERS OF CANADA

HISTORY OF GLACIER INVESTIGATIONS IN CANADA

By C. SIMON L. OMMANNEY[1]

Abstract

Because of extensive high mountain ranges (peaks nearly 6,000 meters above sea level in western Canada) and high latitude (latitude 83° North in the High Arctic Islands), Canada has a large number of glacierized regions; the area covered by glaciers increases from south to north along the border with Alaska in the west and from Labrador to Ellesmere Island in the east. Glaciers cover an estimated 150,000 square kilometers of the Arctic Islands, three times the glacier cover in western Canada (about 50,000 square kilometers), for an approximate total area of 200,000 square kilometers. The principal glacierized regions of Canada are the mountain groups of the Coast Mountains: St. Elias Mountains, Boundary Ranges, and Pacific Ranges; *Interior Ranges*; Rocky Mountains; and Arctic Islands: Baffin Island, Devon Island, Ellesmere Island, Axel Heiberg Island, Meighen Island, and Melville Island. The first field observations of Canadian glaciers were made in 1861. During the past 140 years, various types of glaciological measurements, from observations in the field to airborne and satellite remote sensing, have been made, for varying periods of time, of 176 individual glaciers, including 13 glaciers in Yukon Territory (St. Elias Mountains), 63 glaciers in the Coast Mountains, 10 glaciers in the *Interior Ranges*, 27 glaciers in the Rocky Mountains, 41 glaciers in the High Arctic, 10 glaciers in the Low Arctic, and 5 glaciers in Labrador (Torngat Mountains). Seven other glaciers have been studied but are outside these mountain ranges and are not discussed. Most of the studies of mass-balance, modeling, dendrochronology, climatology, ice chemistry and physics, ice-core analysis, glacier-surge mechanics, and airborne and satellite remote sensing were carried out during the past 50 years, stimulated by the need for increased knowledge of water resources in the western glacierized basins and to support scientific work during the International Geophysical Year (1945 to middle 1950's), increased knowledge of Arctic Canada, a response to security and sovereignty concerns (middle 1950's to the middle 1960's), and by the International Hydrological Decade (middle 1960's to the 1970's). During the 1990's governmental support of glacier research in Canada waned, but by the beginning of the 21st century, the Geological Survey of Canada initiated a National Glaciology Programme, including a Cryospheric Systems Research Initiative (CRYSYS), motivated by achieving a better scientific understanding of the potential impact of climate change on Canada's water resources and the Arctic region. With the increased availability of the higher spatial and spectral resolution in satellite imagery (including stereoscopic imagery), radar imagery (including InSAR), and laser altimetry, glaciologists will increasingly rely on satellite remote sensing to acquire some of the data needed to monitor changes in area and volume and glacier velocity.

Occurrence of Glaciers

The Canadian landmass, extending from long 53°W. to 141°W. and from lat 42°N. to 83°N., has an area of almost 10 million km^2. The mountains range up to a height of nearly 6,000 m above sea level and contain a variety of environments suitable for the development and maintenance of glaciers.

Manuscript approved for publication 7 March 2002.

[1] International Glaciological Society, Lensfield Road, Cambridge CB2 1ER, England (formerly with the National Hydrology Research Institute [now the National Hydrology Research Centre], Environment Canada, Saskatoon, Saskatchewan S7N 3H5, Canada).

Field, in his memorable study of mountain glaciers, described the glacier distribution and reported on much of the work done on them (Field, 1975c); work on the glaciers was last updated by Ommanney (1996). Small glaciers are found on both continental margins, in the Torngats of Labrador (Fahn, 1975), and in the central mountains of Vancouver Island (Ommanney, 1972a). Larger glacier masses are found in the Rocky Mountains (Denton, 1975a), the *Interior Ranges* (Coleman, 1921; Denton, 1975c), and the Coast Mountains (Denton, 1975b). The glaciers get progressively larger as one moves north along the "Panhandle" (Field, 1975a), the boundary between British Columbia and Alaska. The size continues to increase through the Juneau Icefield region up to the Yukon Territory (Ommanney, 1993) and the Icefield Ranges (Field, 1975b, 1990), which contain large glacier systems such as the Seward Glacier [11],[2] (Post and LaChapelle, 1971) (table 1, fig. 1). Some smaller outliers are found in the eastern Yukon Territory and western District of Mackenzie (Northwest Territories) (Horvath, 1975). The variety of the landscapes encountered can be seen in Dunbar and Greenaway (1956), Post and LaChapelle (1971), Slaney (1981), Prest (1983), and Mollard and Janes (1984).

The mean height of the equilibrium line of the glaciers rises steadily as one crosses the mountains from west to east, from about 1,700 m in the Coast Mountains to more than 2,700 m in the Rockies, reflecting a continentality effect. Moving northward, the glaciers increase in size and reach to lower elevations, demonstrating a latitudinal effect due to the lowering of mean annual temperature as one moves toward the North Pole. This effect is best seen in the eastern Arctic, where the mean height of the equilibrium line declines from some 700 m on Baffin Island virtually to sea level at the Ward Hunt Ice Shelf [120] (table 2, fig. 2). Glaciers in the eastern Arctic are distributed along the mountain and fjord coast of Baffin Island (Ives, 1967c), with bigger concentrations of ice in the Barnes [164] and Penny [168] Ice Caps (Mercer, 1975a). Such concentrations become larger and more common farther north. Axel Heiberg Island, Ellesmere Island, and Devon Island are partially covered by large ice fields and ice caps several thousand square kilometers in size (Mercer, 1975b). The regional characteristics of glaciation levels, snowlines, and equilibrium lines throughout Canada have been described by Østrem (1966a, 1972, 1973b), Andrews and Miller (1972), Bradley (1975) and Miller and others (1975).

Figure 1 shows the distribution of glaciers in western Canada. The numbers in this figure refer to those in table 1 and identify the locations of specific glaciers mentioned in the text or for which some historical information is summarized in the table. The numbers are given in the text in square brackets after the glacier names to aid the reader in identifying their geographic location. Figure 2 and table 2 provides the same information for the glaciers of arctic and eastern Canada.

To aid in the management of its glacier resources, the Canadian government initiated a comprehensive inventory of all Canadian glaciers in the 1960's. The inventory was a contribution to the International Hydrological Decade (IHD) and also to the International Hydrological Programme (IHP) (Ommanney, 1980). However, no recent measurement of the total area of Canada's glaciers has been made. A summary of the best available information (Ommanney, 1971a) shows that about three-quarters of Canada's permanent ice masses, some 150,000 km^2, is found in the eastern Arctic, with the balance lying on the mainland, chiefly in the Yukon Territory and British Columbia (Ommanney, 1989) (table 3).

***Figure 1.**—(opposite page) The glaciers of western Canada. Numbers on the map correlate to the numbered glaciers in table 1. The areas shown in darker green are national parks and other protected areas; the areas shown in purple are glaciers. Modified from map in Canadian Geographic (Shilts and others, 1998). Used with permission.*

[2] Numbers in brackets refer to tables 1 and 2 and to figures 1 and 2.


CANADA
ALASKA
YUKON TERRITORY
Whitehorse
Skagway
Juneau
PACIFIC OCEAN
COAST MOUNTAINS
BRITISH COLUMBIA
Queen Charlotte Islands
Queen Charlotte Sound
VANCOUVER ISLAND
Vancouver
Victoria
WASHINGTON
CANADA U.S.A.
ST. ELIAS MOUNTAINS
Stikine River
Skeena River
Fraser River
Columbia River
Kootenay River
COLUMBIA MOUNTAINS
ROCKY MOUNTAINS
Jasper
Banff
ALBERTA
60°N
55°
140°W
135°
130°
125°
50°
0 100 km
N

TABLE 1.—*Summary of historical information on glaciers of western Canada (see also fig. 1)*

[x, variations; o, mass balance; *, variations and mass balance; z, other studies; s, other, some mass balance; m, other, some variations; ?, missing glacier area and location data; italicized place-names are variant names and names not listed in the CPCGN/CGNDB[3]]

YUKON TERRITORY	Latitude North	Longitude West	km²	1890	1900	1910	1920	1930	1940	1950	1960	1970	1980	1990	2000
1. Klutlan Glacier	61°30.0'	140°37.0'	1091.								....zz..	.....z...			
2. Hazard Glacier	61°15.7'	140°21.9'	16.									.....zz..z			
3. Steele Glacier	61°14.6'	140°10.6'	99.								......zzzz	..zzzzz..z	z.......		
4. Trapridge Glacier (*Hyena*)	61°13.6'	140°20.0'	5.5								.......zz	zzzzz.z...	zzzzzzzzzz	zzzzzzzzz.	
5. Backe Glacier (*Jackal*)	61°12.8'	140°17.9'	3.4								........z.	.x........			
6. Rusty Glacier (*Fox*)	61°12.4'	140°17.9'	4.9								..zoo	zzzzzzz..			
7. Donjek Glacier	61°03.6'	139°42.8'	290.									....z....z			
8. Walsh Glacier	60°53.0'	140°45.0'								.xx.......	...xxx...				
9. Kaskawulsh Glacier	60°45.0'	139°06.0'	700.					x			.zzzzzzzzz	z..zz.....			
10. Mount Logan	60°34.0'	140°23.0'	?								........z.	....zzz.z.	zz....z.zz		
11. Seward Glacier	60°25.0'	140°30.0'	?						xx	...o....	...zz....	.z........			
12. Hubbard Glacier	60°22.6'	139°22.5'	?		....			....	....	....	....	....	.z.z.z....	....	
13. Lowell Glacier	60°17.8'	138°17.2'	530.		....	....			....	....	....	xxxxx	xxxxx.....	....	

COAST MOUNTAINS	Latitude North	Longitude West	km²	1890	1900	1910	1920	1930	1940	1950	1960	1970	1980	1990	2000
14. Tweedsmuir Glacier	59°52.0'	138°19.3'	497.			....						....xx....			
15. Nadahini Glacier	59°44.0'	136°41.0'	6.1								...x.x.x.	x.x.x.....			
16. *East Arm Glacier*	59°43.2'	137°35.6'	102.										.x.x.....		
17. Tats Glacier	59°41.4'	137°46.2'	16.1										........oo		
18. Cathedral Glacier	59°20.3'	134° 06.3'	2.0									.ooo.o....			
19. Grand Pacific Glacier	59°07.5'	137°08.0'	565.			....	.....x...		......x..	x.......x.	...x.....	....x.....			
20. Tulsequah Glacier	58°50.0'	133°45.6'	~200.					..z.......							
21. Flood Glacier	57°10.7'	131°55.0'	11.									.........z	zzzzzz....		
22. Alexander Glacier	57°06.4'	130°49.1'	5.8							....		.........o	oooooo..oo	o.........	
23. Natavas Glacier	57°03.6'	130°49.6'	3.1										zo........		
24. Yuri Glacier	56°58.0'	130°42.2'	3.6			....				....		........oo	oooooo..oo	o.........	
25. Andrei Glacier	56°55.7'	130°55.6'	92.									........oo	oooooo..oo	o.........	
26. *Forrest Kerr Glacier*	56°54.1'	130°05.6'	99.				......x..	.x..x.....	.....xxxx.			........oo	ooo.......		
27. Great Glacier	56°50.9'	131°52.0'	~175.											....	
28. *Ridge Icefield Glacier*	?	?	?	....										.z.......	
29. *Tim Williams Glacier*	56°33.4'	130°00.0'	8.							......z...			.........z		
30. Leduc Glacier	56°14.0'	130°22.0'	12.3								.....z....				
31. Frank Mackie Glacier	56°19.5'	130°10.0'	153.								.....z....				
32. Berendon Glacier	56°14.8'	130°05.0'	33.4								.....z.ooo	oooooo....			
33. Salmon Glacier	56°08.6'	130°04.0'	35.	....	....					......zz.z	.....z.zzz	z.........			
34. New Moon Glacier	53°55.3'	127°46.5'	1.0						......x..	....x.....	.......x..	.x...x..x.	...x......		
35. UTEM Glacier	53°54.5'	127°46.7'	1.2								....		...x......		
36. Purgatory Glacier	52°09.0'	126°22.0'	13.9		x.........				.......x..	....x.....	....x.....	........x.	....x.....		
37. Atavist Glacier	52°09.0'	126°09.0'	5.5	....	x.........					.x..x.....	....x.....	........x.	....x.....		
38. Noeick Glacier	52°06.5'	126°16.7'	8.9	....	x.........					....x.....	....x.....	........x.			
39. Fyles Glacier	52°06.0'	126°13.6'	15.9		x.........				......x..	....x.....	....x.....	...x....x.	...mmm..		
40. Ape Glacier	52°04.3'	126°12.2'	8.1		x.........				......x..	.x..x.....	....x.....	...x....x.	....x.x..		
41. *Deer Lake Glacier*	52°04.0'	126°10.0'	4.6									...x......			
42. Bench Glacier	51°27.0'	124°56.0'	10.			....	....				....	....	.ooooo..oo	o.........	
43. *Tsoloss Glacier*	51°23.5'	123°52.0'	1.1		x.........	....				.x........			..x.......		
44. *Elkin Glacier*	51°22.5'	123°51.0'	1.5							.x........			..x.......		
45. Tiedemann Glacier	51°19.5'	125°00.0'	63.										.ooooo..oo	o.........	
46. Franklin Glacier	51°14.5'	125°28.0'	132.				.......x..	.x..x.....	.....xxxx.						
47. Cumberland Glacier	51°12.0'	124°23.3'	2.8	....									...z.....		
48. Miserable Glacier	51°04.2'	123°52.0'	3.3		x.........	....	....	....	....	.x........	....	.....x...	....	....	

TABLE 1.—*Summary of historical information on glaciers of western Canada (see also fig. 1)*—Continued

[x, variations; o, mass balance; *, variations and mass balance; z, other studies; s, other, some mass balance; m, other, some variations; ?, missing glacier area and location data; italicized place-names are variant names and names not listed in the CPCGN/CGNDB[3]]

COAST MOUNTAINS	Latitude North	Longitude West	km²		1890	1900	1910	1920	1930	1940	1950	1960	1970	1980	1990	2000
49. Pathetic Glacier	51°03.4'	123°47.5'	0.1	..	....	x	... .	... .	.. ...	.. ...	x.... ...	....	.... x...	. ...	....	
50. Friendly Glacier	51°03.0'	123°51.4'	4.4	..	....	x.... ...	. ... ..	....	....	.. ....	.x...	 x	... x...	.x.	....	
51. Hourglass Glacier	51°01.6'	123°46.0'	4.2	.	....	x....	. ...	.. ..	....	... .	x.... ...	....	... .x.. .	....	... .	
52. Tchaikazan Glacier	51°01.2'	123°47.3'	21.4	. .	.. . .	x...	....	. ...	... .	. . ..	.x..	....x.	.. ..xx...	..x	....	
53. *Sykora Glacier*	50°52.7'	123°33.8'	25.	..	....	....	....	. ...	... .	....	....	....	00000	000000....	... .	
54. Bridge Glacier	50°49.4'	123°33.0'	83.5	...	.. ..	... .	....	....	. ...	....	.. ..	... .	00000	000000 ...	. ...	
55. *Zavisha Glacier*	50°48.4'	123°25.3'	6.5	...	. ...	.. ..	....	....	. ...	.. . .	....	.. ..	00000	000000....	....	
56. Berm Glacier	50°33.0'	123°59.0'	1.1	...	....	. ...	. ... ..	... .	....	.. ...xx.	.x... ...	... .	x.. ...x.x	....	....	
57. Havoc Glacier	50°30.3'	123°52.3'	9.5	..	..x.	. ...	....	... .	....	.. ....x.	x....... .	. ..x.....	x. ....x x	....	....	
58. Wave Glacier	50°30.0'	123°59.0'	4.4	. .	....	....	....	.. ..	....	. ..... xx.	.x.	...x.....	x .....x.x	... .	....	
59. Surf Glacier	50°29.7'	123°58.1'	1.0	...	.. x... ..	....	.. . .	....	.. ..	. .... .x..	x.	... x.....	x..... .x.x	.. ..	.. ..	
60. Terrific Glacier	50°26.4'	123°57.8'	4.6	...	....	....	... .	....	. ...	.......x.	.x..... ..	... x.....	x.......x.x	. ...	. ...	
61. Clendenning Glacier	50°25.2'	123°54.1'	26.5	...	. .x......	. ...	... .	....	....	x	.x..... ...	.. .x.. .	x.. ...x x	....	... . .	
62. Place Glacier	50°25.3'	122°36.0'	3.8	..	... ...	. ...	... .	... .	....	....	.. ..	00000	0000000000	0000000000	0000000000	
63. Wedgemount Glacier	50°09.2'	122°47.8'	2.6	. .	....	x.....	... ...	x	....	.. ..x.x	x...	. .x ..x	..xx.xzxxx	x* *xxx.. .	x...xx. ..	
64. *Caltha Lake Glacier*	50°08.7'	122°17.0'	0.1	. .	....	... .	....	. ...	... .	. ...	.x.	x	....	x..x.x ...	... .	
65. Boomerang Glacier	50°07.2'	123°15.8'	4.0	...	.. ..	... .	... .	....	.. ..	....	.. ..	... .	.z.. ..	....	.. ..	
66. *Brandy Bowl Glacier*	50°07.1'	123°14.7'	1.5	...	.. ..	.. ..	. . ..	....	. ...	....	.. ..	....	..z.	. . ..	....	
67. Horstman Glacier	50°05.8'	122°53.0'		...	. ...	. ...	. ...	....	....	... ...	. ...	....	.. ..	....	....	
68. Overlord Glacier	50°01.2'	122°50.0'	2.6	..	....	x....	. ...	... .x.	... .. .	.. ..	x........	. ... ..	..x. .. .	....	x.xx x....	
69. Helm Glacier	49°57.8'	123°00.0'	3.1	. .	....	....	.x.	.. ..x.	... xxx..	xxxxx	x.x x.x.x.	x.........	00000	0000000000	000000....	
70. Sphinx Glacier	49°55.0'	122°57.5'	4.7	..	....	... .	.x..	....	... .xxx..	xxxxx	x.x.x.x.x.	x.. x.x.x.	x.x.. 0000	000... ...	... .	
71. Sentinel Glacier	49°53.6'	122°58.9'	1.8	...	. ...	.. ..	.. ..	....	..xxx.	 xxxxx	x.x.x x.x	x. .xo*o*o	*o*0000000	0000000000	... .	
72. Thunderclap Glacier	45°51.0'	122°39.0'	2.7	...	. ...	. ...	.. ..	....	x.... ...	... .	.xx..	... ..x x	..x ...x .	....	....	
73. Griffin Glacier	49°51.0'	122°38.0'	2.1	..	....	. ...	. ...	... ...	.x..	.. ..	xx.	. .....x .x	..x.....xx.	....	....	
74. Staircase Glacier	49°51.0'	122°37.0'	1.6	. .	....	....	....	. ...	.x	.. ..	.xx........	......x..x	..x.....xx.	....	....	
75. Gl. de Fleur des Neiges	49°51.0'	122°36.0'	0.4	..	....	....	....	. ...	.x	. ...	.xx........	...... x..x	. x... xx.	....	....	
76. Moving Glacier	49°33.0'	125°23.2'	1.2	...	... .	... .	....	....	.x	....	... .	..x	....	.x...... ..	.. ..	

INTERIOR RANGES	Latitude North	Longitude West	km²		1890	1900	1910	1920	1930	1940	1950	1960	1970	1980	1990	2000
77. Silvertip Glacier	51°42.2'	117°54.2'	3.5	.	....	... ..	x.x.	.. ..	....	 x	x...x...	. ....x...	... .x.x..	....	....	
78. Haworth Glacier	51°41.6'	117°54.3'	4.1	.	....	....	x.x.	.. ..	....	 x	.x...x. .	......x...	.. ..x.x..	....	....	
79. Sir Sandford Glacier	51°40.3'	117°54.0'	10.4	...	.. ..	....	x.x	. ...	... .	x	.x ..x. ..	.x ...x...	. ....x.x..	... .	... .	
80. Illecillewaet Glacier	51°14.2'	117°26.5'	6.4	xx	x. xx	xxxxxxxxxx	xxx... ..	....	.x...... ..	xxxxx	x.x.x.x.x	x.........	....	... .	.. ..	
81. Asulkan Glacier	51°12.4'	117°27.3'	1.2	...	 xx	xx.xxxxx x	xxx..	....	.x.... ...	... .	.. ..	... .	....	. .. ...	....	
82. Woolsey Glacier	51°07.5'	118°02.5'	3.9	...	... .	....	. ...	... .	....	.. ..	....	00000	000000...	....	....	
83. Bugaboo Glacier	50°43.8'	116°46.5'	5.	.	....	....	....	.. ..	... .	. ...	....	....x x.x.	x.x.x. ...	....	....	
84. Commander Glacier	50°25.7'	116°32.5'	6.0	..	... .	... .	... . . .	x....... ..	... .	. ...	.....x......	x..... . ..	.. ..	... .	....	
85. Toby Glacier	50°13.7'	116°32.0'	8.	...	.. ..	... .	... x.. .	x..x ..xx	.. ..	....	....	....	. ...	.. ..	... .	
86. Kokanee Glacier	49°45.0'	117°08.5'	3.1	...	. ...	.. ..	....	...x. . ..	. ...	 xxxxx	x x.x.x.x.	x. x.x.x.	x.x...... .	....	.. ..	

ROCKY MOUNTAINS	Latitude North	Longitude West	km²		1890	1900	1910	1920	1930	1940	1950	1960	1970	1980	1990	2000
87. Robson Glacier	53°08.5'	119°06.0'	13.		... .	....x.	.x.x..... .	. x..... ..	.x.	. ...	...x.	... ...	.. ..	... .	...., ...	
88. *Small River Glacier*	53°06.0'	119°17.0'	5.8		. ...	... .	... .	....	. ...	....	.. ..	....	. ...	... .	...z.z....	
89. Angel Glacier	52°41.0'	118°04.0'	0.9		....	.. . .	....	....	.. ..	... .xx..	z.	... .	....	.. ..	. ...	
90. Scott Glacier	52°26.0'	118°05.0'	16.		....	. ...	.. ..	....x......	....	.. ..	...x.. ...	....	....	....	.. ..	
91. *East Chaba Glacier*	52°12.5'	117°40.8'	1.7		....	....	. ...	... ...x .	.... x..	....	. ...	. ...x...	x..	....	....	
92. Saskatachewan Glacier	52°12.5'	117°08.2'	30.	(1824–62)		....	..x.	. ...x. ..	....	...xxxxx	x.xxx.x.x.	x.xxxxxxxx	xxxxxxxxxx	... .	.mmmmmmmm.	
93. Athabasca Glacier	52°11.7'	117°15.0'	15.	(1843–44)		... .	....	.x... ...	.. ..	xxxxx	x.xxx.x.xm	mmmmxzmmmm	xxxxxxxxxx	.x .xx ...	.mmmmmmmm.	
94. Columbia Icefield	52°10.0'	117°20.0'	285.		....	... .	... .	....	. ...	. ...	... .	... .	....z	zz..... .	... .	
95. Columbia Glacier	52°09.5'	117°23.0'	16.	(1698–1739)	. ...		x	....x......	. ...	x	...x.. ...	.. ...x..	x.x.	....	.. ..	

TABLE 1.—*Summary of historical information on glaciers of western Canada (see also fig. 1)*—Continued

[x, variations; o, mass balance; *, variations and mass balance; z, other studies; s, other, some mass balance; m, other, some variations; ?, missing glacier area and location data; italicized place-names are variant names and names not listed in the CPCGN/CGNDB[3]]

ROCKY MOUNTAINS	Latitude North	Longitude West	km²	1890	1900	1910	1920	1930	1940	1950	1960	1970	1980	1990	2000
96. *Boundary Glacier*	52°11.5'	117°11.4'	1.5	....	..x.... .	... .	. ...	. ...	x	......x...	......x. .	x.x..... .	...xxx....	x	
97. Dome Glacier	52°12.1'	117°18.1'	5.92	(1846).	....	....	....	.. ..	. ...	...x... ..	....	.......m.	x..xx..zz	zxzzzzzzz.	
98. *Hilda Glacier*	52°11.0'	117°10.0'	1.35	... .	....	... .	.. ..	... .	. ...	.. ..	....	. .... .z.	....	. ...z.	
99. *Cline Glacier*	52°05.0'	116°41.0'	?	....	. ...	....	... .	....	... .	....	. ... ..	.. ..	.. ....zzz	zz.... .	
100. Southeast Lyell Glacier	51°54.5'	117°01.6'	16.	(1858)...	.. ..	x	......x...	x...	... .	...x.... .	.. ..	... ...m..	.x .xx..zz	zxzzzzzzz.	
101. Ram River Glacier	51°51.0'	116°11.5'	1.8	....	.. ..	....	... .	. ...	....	....	00000	000000...	... .	....	
102. Freshfield Glacier	51°45.8'	116°54.2'	40.	....	.x.	....	. x.. x ..	x...x. x..	 xxx	x.x.x.....	....	... .	....	....	
103. Peyto Glacier	51°40.6'	116°32.8'	13.	... .x.	. ...	....	... .	.. x..x .x	..x..xxxxx	x.x.x.x.x.	x.x.o*oooo	ooooooooos	oosososooo	. ooooooo.	
104. Bow Glacier	51°38.9'	116°30.4'	5.1	. .... x.	.. ..	.. ..	..x	...x......	... .x. ..	..xx.... .	. ....x...	....	....	.. ...zzz	
105. Yoho Glacier	51°36.0'	116°32.5'	23.	. ... .x..	.x xxxxxxx	x xxx.xxxx	....	x.x.....	....	....	.. ..	... .	... .	... .	
106. Hector Glacier	51°35.7'	116°15.5'	2.5	....	... x.....	.. ..	. ...	. .... .x.	....	. x..	.....x. ..	....	....	....	
107. Drummond Glacier	51°35.5'	116°02.0'	1.3	... .	......x.	.. ....	x....	x x	....	..x.......	..****xx..	....	....	....	
108. Emerald Glacier	51°30.0'	116°32.0'	1.9	.. ..	. ...	....	.. ... .	... .	. ...	....	....	xx	xxx.......	....	
109. *Cathedral Glacier*	51°24.3'	116°23.4'	0.9	....	. ...	... .	.. ..	....	.. ..	....	. ...	.... zx	..z.z. ...	....	
110. Victoria Glacier	51°22.8'	116°17.2'	3.5	 xx	.. x. x.x	x.x..	....	x..	xxxxx	x.x.. . .	.. ...x...	... ..x ..	....	....	
111. Wenkchemna Glacier	51°18.7'	116°14.2'	4.3	.. ..	xxx.x ...	.. ..	....	....	....	..x. ...	.. ..z.z.z	.... ..z z	....	....	
112. *Robertson Glacier*	50°44.0'	115°20.0'	0.8	... .	....	.. ..	....	. ...	....	....	....	....	....	.....zz. .	
113. *Rae Glacier*	50°37.4'	114°59.1'	?	....	.. . .	.. . .	. ...	.. ..	. ...	....	....	....	....	...z......	

TABLE 2.—*Summary of historical information on glaciers of arctic and eastern Canada (see also fig. 2)*

[x, variations; o, mass balance; *, variations and mass balance; z, other studies; s, other, some mass balance; m, other, some variations; ?, missing glacier area data; italicized place-names are variant names and names not listed in the CPCGN/CGNDB[3]]

HIGH ARCTIC	Latitude North	Longitude West	km²	1890	1900	1910	1920	1930	1940	1950	1960	1970	1980	1990	2000
120. Ward Hunt Ice Shelf (Elles)	83°07.2'	73°30.3'	660.	... .	.. ..	.. .. ..	....	. . ..	... .	...zz....z	ozzzzooooo	ooooooo..	oooooo....	....	
121. *Ward Hunt Ice Rise* (Elles)	83°07.0'	74°10.0'	32.	....	... .	. ...	....	....	....	....oo	oooooooooo	ooooooo...	oooooo.. .	....	
122. Milne Glacier (Elles)	82°24.0'	80°00.0'	900.	....	....	.. ..	....	....	....	x	.... x...	....	...x.....	....	
123. Gilman Glacier (Elles)	82°05.8'	70°36.9'	480.	. ...	....	... .	....	....	... .	. .... ooo	oooooooooo	....	.o.......	... .	
124. *Muskox Glacier* (Elles)	82°05.0'	86°10.0'	?	... .	. ...	....	. ...	. .... .	.. ..	.. ..	....	....	. ....z...	....	
125. *Unnamed Ice Cap* (Elles)	81°57.3'	64°12.0'	7.5	....	... .	. ...	... .	....	....	....	......oo..	ooooooo...	....	.. ..	
126. Per Ardua Glacier (Elles)	81°31.0'	76°27.0'	4.3	....	....	.. ..	....	....	....	... .	...oooooo	oo.... ...	....	. ...	
127. Otto Glacier (Elles)	81°20.0'	84°15.0'	1018.	. ...	....	... .	....	....	. ...	. ...	...x..z...	....	....	....	
128. Hare Fiord Glacier (Elles)	81°08.5'	82°20.0'	?	....	. ...	. ...	. ...	.. ..	.. ..	........x.	....	....x.	.. ..	....	
129. Webber Glacier (Elles)	80°55.0'	82°10.0'	123.	....	.. ... .	....	....	. . ..	....	... .	... .	..... .z.	.. ..	. ...	
130. Gnome Glacier (Elles)	80°54.5'	82°23.5'	3.1	....	....	.. ..	....	....	. .. .	....	....	.. ..x.	....	... .	
131. Dwarf Glacier (Elles)	80°54.0'	82°30.3'	4.3	. ...	....	....	....	....	. ...	....	. ...	........x.	. ...	....	
132. Midget Glacier (Elles)	80°53.7'	82°37.3'	3.0	....	.. ..	. ...	. ...	.. ..	....	... .	....	....x.	.. ..	....	
133. Arklio Glacier (Elles)	80°53.6'	82°44.0'	7.2	....	.. ..	....	... .	.. ....	....	....	....	. ...x.	... .	. ...	
134. Okpuddyshao Glacier (Elles)	80°53.1'	82°50.9'	5.6	....	... .	. ...	....	....	....	....	....	........x.	....	....	
135. Nukapingwa Glacier (Elles)	80°52.9'	82°58.1'	4.8	. ...	... .	....	....	. ...	. ...	. ...	.. ..	x	. ...	....	
136. Van Royen Glacier (Elles)	80°53.2'	83°10.5'	111.	. ...	. ...	....	. ...	.. ..	. . ..	... .	....	.... .x.	....	....z.....	
137. *Shirley Glacier* (Elles)	80°50.0'	83°25.0'	?	.. ..	.. ..	....	... .	... .	.... ..	....	....	. ...	....	.. .z. ...	
138. *Blackwelder Ice Cap* (Elles)	80°38.0'	85°00.0'	117.	....	... .	. ...	....	....	....	... .	....	... .	....	... z....	
139. Agassiz Ice Cap (Elles)	80°25.0'	75°00.0'	17326.	.... ..	....	.. ..	....	....	....	. ...	....	.. . .ssss	ssssssssss	sssssssss.	

TABLE 2.—*Summary of historical information on glaciers of arctic and eastern Canada (see also fig. 2)*—Continued

[x, variations; o, mass balance; *, variations and mass balance; z, other studies; s, other, some mass balance; m, other, some variations; ?, missing glacier area data; italicized place-names are variant names and names not listed in the CPCGN/CGNDB[3]]

HIGH ARCTIC	Latitude North	Longitude West	km²	1890	1900	1910	1920	1930	1940	1950	1960	1970	1980	1990	2000
140. d'Iberville Glacier (Elles)	80°25.6'	77°33.0'	1609.	—	—	—	—	—	—	—	—	...zz....	—	—	
141. John Evans Glacier (Elles)	79°38.5'	74°30.0'	220.	—	—	—	—	—	—	—	—	—	—	....ossss.	
142. *Quviagivaa Glacier* (Elles)	79°34.0'	83°15.0'	?	—	—	—	—	—	—	—	—	—	—	.ooo......	
143. Leffert Glacier (Elles)	78°41.3'	75°01.4'	593.	—	—	—	—	—	—	—	—	.........o	o........	—	
144. *Unnamed Glacier* (Elles)	78°39.1'	74°55.0'	50.	—	—	—	—	—	—	—	—	.........o	o.........	—	
145. Prince of Wales Icefield (Elles)	78°15.0'	80°00.0'	?	—	—	....	—	—	—	—	—	..zzz......	—	—	
146. *Laika Glacier* (Coburg)	75°53.5'	79°05.2'	4.3	—	—	—	—	—	—	—	—	...oo....o	o.........	—	
147. *Laika Ice Cap* (Coburg)	75°53.0'	79°09.1'	10.	....	....	—	—	....	....	—	—	....ooo..o	o........	—	
148. *Wolf Glacier* (Coburg)	75°54.2'	79°12.2'	2.0	—	—	—	—	—	—	—	—	.........o	o.........	—	
149. Baby Glacier (Axel)	79°26.4'	90°58.0'	0.6	—	—	—	—	—	—	.........o	oooooooooo	oooooooooo	ooo..... o	oo........	
150. Crusoe Glacier (Axel)	79°25.7'	91°10.0'	44.	—	—	—	—	—	—	x	xxxxxxxxxxx	xxxxxxxxxx	xxx.......	....	
151. Müller Ice Cap (Axel)	79°54.0'	90°59.0'	6300.	—	—	—	—	—	—	.........z	zzzz......	......o..	—	—	
152. Thompson Glacier (Axel)	79°28.0'	90°30.0'	230.	—	—	—	—	—	—	x	xxxxxxxxxx	xxxxxxxxxx	xxx.......	z.........	
153. White Glacier (Axel)	79°26.7'	90°40.0'	39.	—	—	—	—	—	—	..........o	oooooooooo	oooooooooo	oooooooooo	ooooooooo	
154. *Good Friday Bay Glacier* (Axel)	78°37.0'	91°10.0	641.	—	—	—	—	—	—	..x......x	—	—	—	—	
155. Meighen Ice Cap (Meighen)	79°57.2'	99°08.0'	90.	—	—	—	—	—	—	........o	oooooSSSoo	oo.ooooooo	.ooooooooo	o....o....	
156. *South Ice Cap* (Melville)	75°25.4'	115°01.1	66	—	—	—	—	—	—	—	...oooo.oo	oo.oo.....	.oo.......	.ooooo....	
157. *West Ice Cap* (Melville)	75°37.8'	114°45.0'	36.4	—	—	....	—	—	—	—	...oooo.oo	oo.o......	—	.ooooo...	
158. *East Ice Cap* (Melville)	75°39.3'	114°28.6'	16.0	—	—	—	—	—	—	—	...oooo.oo	oo.o......	—	.ooooo....	
159. Leopold Glacier (Melville)	75°49.0'	114°45.0'	27.7	—	—	—	—	—	....	....	...oooo.oo	oo.o.....	—	.ooooo....	
160. Devon Ice Cap (Devon)	75°20.0'	82°30.0'	12825.	—	—	—	—	—	—	—	.ooooooooo	ssssssosooo	oooooooooo	oooooo....	
161. Sverdrup Glacier (Devon)	75°40.6'	83°15.5'	672.	—	—	—	—	—	—	—	.ooo......	—	....	....	
LOW ARCTIC	**Latitude North**	**Longitude West**	**km²**	**1890**	**1900**	**1910**	**1920**	**1930**	**1940**	**1950**	**1960**	**1970**	**1980**	**1990**	**2000**
162. Aktineq Glacier (Bylot)	72°54.9'	78°51.8'		—	—	—	—	—	—	—	—	—	—	—	
163. Lewis Glacier (Baffin)	70°25.9'	74°46.0'	182.	—	—	—	—	—	—	—	..zooo....	—	—	—	
164. Barnes Ice Cap (Baffin)	70°10.0'	73°30.0'	6200.	—	—	—	—	—	—	s.........	..zooooooo	ssssssssss	sssss....z	zzzzzz.z..	
165. Decade Glacier (Baffin)	69°38.2'	69°49.5'	8.7	—	—	—	—	—	—	—	.....ooooo	oo.o......	—	—	
166. *Akudnirmuit Glacier* (Baffin)	67°34.6'	65°14.5'	0.6	—	—	—	—	—	—	—	—	.oo.......	—	—	
167. *Boas Glacier* (Baffin)	67°34.1'	65°15.6'	1.4	—	—	—	—	—	—	—	.......o	oooooo....	—	—	
168. Penny Ice Cap (Baffin)	67°10.0'	66°13.0'	6000.	—	—	—	—	—	—	...z......	..z.zz...z	—	........z	zzzzzz. ..	
169. Turner Glacier (Baffin)	66°41.2'	65°14.1'	26.2	—	—	—	—	—	—	...z......	—	—	....	—	
170. Virginia Glacier (Baffin)	66°36.5'	62°18.5'		—	—	—	—	—	—	—	—	—	—	—	
171. Grinnell Glacier (Baffin)	62°32.4	66°51.4'	126.	—	—	—	—	—	—	..x.......	.....x....	—	.z........	—	
LABRADOR	**Latitude North**	**Longitude West**	**km²**	**1890**	**1900**	**1910**	**1920**	**1930**	**1940**	**1950**	**1960**	**1970**	**1980**	**1990**	**2000**
172. *Bryant's Glacier*	59°19.0	63°55.7	1.3	—	........x.	—	—	.x........	—	—	—	—	—	—	
173. Superguksoak Glacier	58°57.0	63°47.0	1.8	—	—	—	—	—	—	—	—	—	.oooo.....	—	
174. Abraham Glacier	58°56.2	63°31.9	0.8	—	—	—	—	—	—	—	—	....	.****.....	—	
175. Hidden Glacier	58°55.7	63°32.7	0.7	—	—	—	—	—	—	—	—	—	.oooo.....	—	
176. Minaret Glacier	58°53.1	63°41.2	0.9	....	....	....	....	....	....	....	....	....	.oooo.....	....	

[3] The names in this section conform to the usage authorized by the Secretariat of the Canadian Permanent Committee on Geographic Names (CPCGN); URL address: [http://GeoNames.NRCan.gc.ca/]. The website is maintained by the Secretariat through Geomatics Canada, Natural Resources Canada, and combines the CPCGN server with the Canadian Geographical Names Data Base (CGNDB). Variant names and names not listed in the CPCGN/CGNDB are shown in italics.

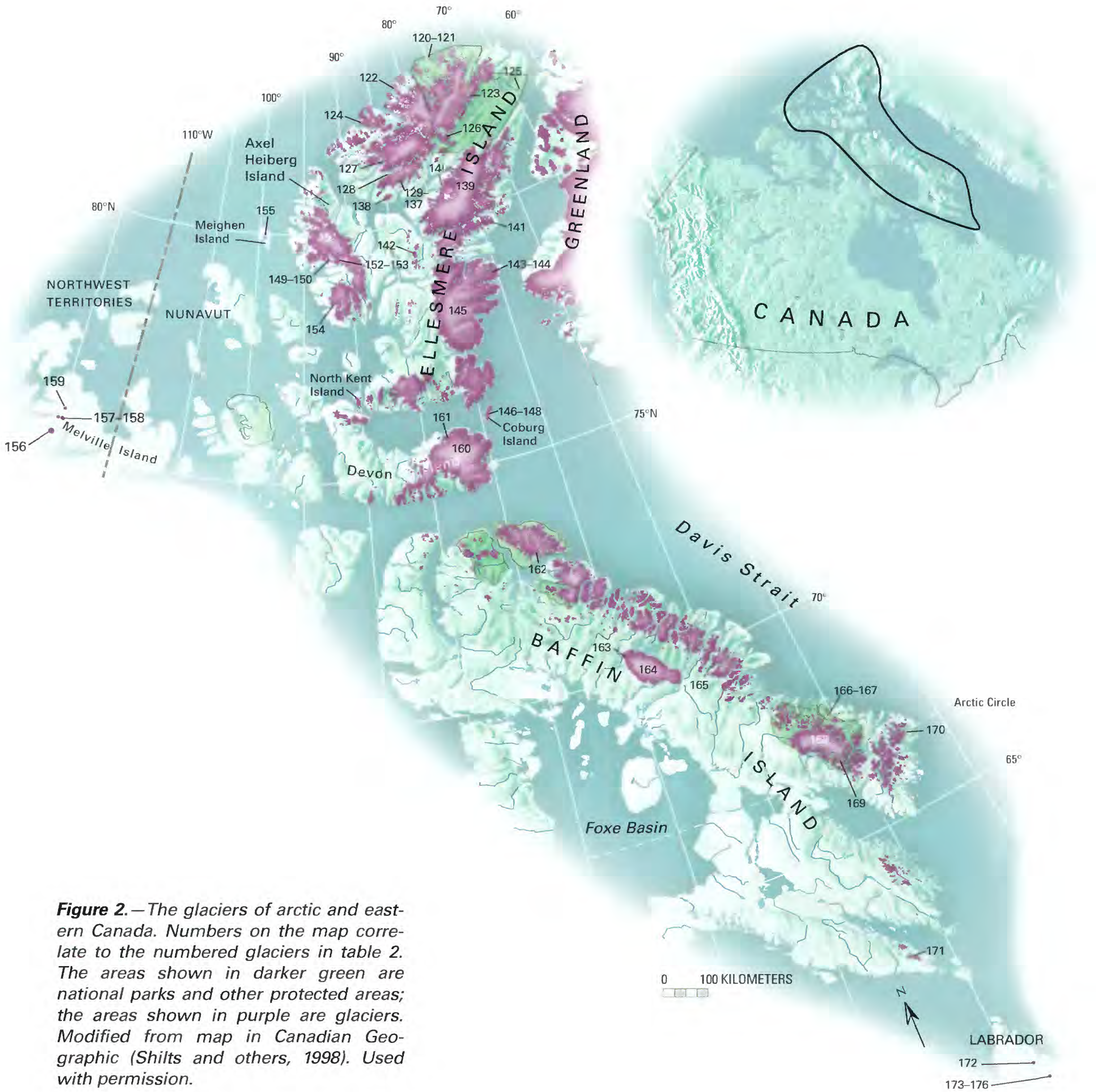

Figure 2.—*The glaciers of arctic and eastern Canada. Numbers on the map correlate to the numbered glaciers in table 2. The areas shown in darker green are national parks and other protected areas; the areas shown in purple are glaciers. Modified from map in Canadian Geographic (Shilts and others, 1998). Used with permission.*

TABLE 3.—*The Glacierized Areas of Canada* (km^2) *(Ommanney, 1971a)*

ARCTIC ISLANDS	
Ellesmere Island	80,000
ice shelves	500
Axel Heiberg Island	11,735
Devon Island	16,200
Coburg Island	225
Meighen Island	85
Melville Island	160
North Kent Island	152
Baffin Island	37,000
Bylot Island	5,000
Subtotal	151,057
MAINLAND	
Pacific drainage	37,659
Nelson River drainage	328
Great Slave Lake drainage	626
Yukon River drainage	10,564
Arctic Ocean drainage	840
Labrador	24
Subtotal	50,041
Total Glacierized Area	201,098

Observation of Glaciers

Historic (Prior to World War II)

Penetration of the western mountains by the Canadian voyageurs, by European traders, and by settlers took place only comparatively recently. Although some aboriginal legends refer to glaciers (Morey, 1971), the earliest recorded description of a Canadian glacier was probably that made by James Hector (1861), a geologist on the Palliser Expedition who visited Southeast Lyell Glacier [100] in 1858. Another early observation of note was that of the Great Glacier [27] by W.P. Blake (1867), a member of a scientific party on a Russian naval squadron ship, in 1863. Developments since then have largely been linked to technological innovations or to the stimulation provided by international initiatives.

One major influence on the settlement of southern Canada, and an element that is deeply etched in the Canadian psyche, has been the railroad. The crossing of the cordillera by the Canadian Pacific Railroad (CPR) was the first technological development that impacted the study of glaciers. The opening up of the west by the CPR and the linking of British Columbia with the rest of Canada gave everyone access to the Rocky Mountains and *Interior Ranges* (fig. 3), creating an opportunity for the first systematic glacier observations. New facilities such as Chateau Lake Louise and Glacier House provided bases from which the early amateur and professional scientists could work. Guides, imported from Switzerland, were made available to those wishing to climb or do glacier research. It was the CPR, responding to pressure from A.O. Wheeler, a prominent Canadian surveyor, and his

***Figure 3.**—Oblique aerial photograph of the Columbia Mountains,* Interior Ranges, *British Columbia, Canada, in late summer of 1970, showing the rugged topography and several mountain glaciers. Photograph by C. Simon L. Ommanney, National Hydrology Research Institute. [NTS Map: 082L16]*

influential friends, that provided the free passes that enabled the founders of the Alpine Club of Canada (ACC) to meet and establish that organization.

Glacier House was built by the CPR at Rogers Pass, in what is now Glacier National Park, because the grade was too steep to permit the inclusion of a restaurant car on the train. Passengers were required to disembark, and many took the opportunity of this enforced stop to take the trail to the Illecillewaet Glacier (or "Great Glacier") [80]. It is hardly surprising then that this, and the neighbouring Asulkan Glacier [81], became the object of the first investigations. Although the earliest observations in Glacier National Park were made by the Rev. Spotswood Green (1890), the subsequent systematic studies were made mainly by members of the Vaux family of Philadelphia (Vaux, G., Jr., and Vaux, W.S., Jr., 1900a, b, 1901, 1908; Vaux, W.S., Jr., 1907, 1909; Vaux, G., 1910; Vaux, M.M., 1911, 1913) (fig. 4). Their activities and contributions were reviewed by Edward Cavell (1983). Other studies of note in this area were those by A.O. Wheeler (1905, 1920; Wheeler and Parker, 1912) and Howard Palmer (1914). In the 1970's, the Canadian Exploration Group visited Palmer's field area and resurveyed the Silvertip, Haworth, and Sir Sandford Glaciers [77–79] (Marsh, 1976, 1978).

The Victoria Glacier [110], visible and easily accessible from Chateau Lake Louise, also received early attention. Studies here and on the Wenkchemna [111] and Yoho [105] Glaciers were conducted by W.H. Sherzer of the Smithsonian Institution (Sherzer, 1907, 1908; Gardner, 1977, 1978). The Yoho Glacier was also included in the set of observations undertaken by the Vaux family (Vaux, G., Jr., and Vaux, W.S., Jr., 1907a, b, 1908; Vaux, G., 1910; Vaux, M.M., 1911, 1913; Vaux, M.M., and Vaux, G., Jr., 1911). These studies were extended by A.O. Wheeler and members of the ACC who held a number of field camps near this glacier (Wheeler, 1911, 1913, 1932, 1934).

Table 1 summarizes the available information on glacier observations during this period. The early records for the Illecillewaet [80], Asulkan [81], and Yoho [105] Glaciers are evident, as is the comparative lack of similar studies in the Coast Mountains. Some of the apparent observations there [36–40, 43, 48–52, 57, 59, 61, 63, 68] reflect modern reconstructions of glacier snout positions using air-photo interpretation and dendrochronological techniques rather than field observations at the dates indicated.

The First World War caused a hiatus in the recording of glacier variations that continued until after the Second World War. However, a few observations were made in the interwar years by members of the ACC (Palmer, 1924; Munday, 1931; McCoubrey, 1938; Thorington, 1938), and snout positions for many other glaciers have been reconstructed.

An interesting development at this time was the 1931 aerial survey of glaciers in Labrador, completed under the auspices of the American Geographical Society (AGS) by Forbes and others (1938). Some ground observations of *Bryant's Glacier* [172][3] were made by Odell (1933), who compared the snout position with that recorded by Bryant and Forbes in 1908.

Compared to many more highly populated mountain areas, such as the Alps, the early record of Canadian glacier variations is fairly sparse. However, at least for the three glaciers discussed above (the Illecillewaet, Asulkan, and Yoho Glaciers), we do have fairly complete records of their retreat during an extended period of glacier recession.

---

[3] The names in this section conform to the usage authorized by the Secretariat of the Canadian Permanent Committee on Geographic Names (CPCGN); URL address: [http://GeoNames.NRCan.gc.ca/]. The website is maintained by the Secretariat through Geomatics Canada, Natural Resources Canada, and combines the CPCGN server with the Canadian Geographical Names Data Base (CGNDB). Variant names and names not listed in the CPCGN/CGNDB are shown in italics.

***Figure 4.**—Photograph of the Illecillewaet Glacier ("Great Glacier"),* Interior Ranges, *British Columbia, taken 19 August 1898. The successful crossing of the western mountains by the Canadian Pacific Railroad in the late 1880's gave access to the Rocky Mountains and* Interior Ranges *and made systematic glacier observations possible. The Vaux family was among the earliest to take an interest in the glaciers. According to George, Jr., and W.S. Vaux, Jr., the Illecillewaet Glacier was the most accessible and one of the most remarkable in the area. It was notable for the lack of debris at its foot and the rapidity of the ice fall. They concluded that photography offered the most satisfactory means of permanently recording the position of the ice from year to year. Photograph is a reproduction of Plate 5 from Vaux and Vaux (1900b). (Glacier 80 in table 1; see also section in this volume by Wheate and others on Mapping Glaciers in the* Interior Ranges *and Rocky Mountains with Landsat Data.)*

1945 to the Middle 1950's

The immediate postwar period saw a significant increase in the number of glacier studies. This was largely due to the commencement of an annual survey of specific glaciers in the cordillera. The survey was initiated by the Dominion Water and Power Bureau (DWPB), forerunner of the Water Survey of Canada (WSC), as part of its studies of the water resources of mountain rivers. In 1945, seven glaciers in Alberta—Angel [89], Athabasca [93], Freshfield [102], Peyto [103], Saskatchewan [92], Southeast Lyell [100], and Victoria [110] Glaciers—were investigated by the DWPB Calgary office. Eight glaciers in British Columbia were observed by the DWPB Vancouver office—Bugaboo [83], Franklin [46], Helm [69], Illecillewaet [80], Kokanee [86] (fig. 5), Nadahini [15] (fig. 6), Sentinel [71], and Sphinx [70] (fig. 7) Glaciers. The position of the glacier termini and changes in their areal extent were measured, and a set of plaques were placed on the ice surface to determine velocity. Some surveys were abandoned after a few years, but table 1 shows that many continued every year until 1950, when they became biennial. Detailed reports were prepared by the DWPB as internal documents, but some results were published (Lang, 1943; McFarlane, 1946; Meek, 1948a, b; Webb, 1948; McFarlane and others, 1950; Collier, 1958; Strilaeff, 1961). Summaries of the reports for Peyto Glacier and the Victoria Glacier have been published by Ommanney (1971b, 1972b).

During this period, photographs of many cordilleran glaciers appeared in mountaineering journals, and some specific photographic recording of glaciers was carried out (Field, 1949). Following on the WSC initiatives, the next significant development was by the American Geographical Society (AGS), which established the Juneau Icefield Research Project in 1948 in conjunction with the U.S. Office of Naval Research (ONR). This project concentrated on glaciers in Alaska but laid the groundwork for the subsequent Summer Institute of Glaciological and Arctic Sciences that, from its subsidiary base in Atlin, B.C., has contributed to our knowledge of Canadian glaciers in the area, particularly the Cathedral Glacier [18] (Field and Miller, 1950; Eagan, 1963; Miller, 1963; Marcus, 1964; Miller and Anderson, 1974). Another AGS expedition visited a number of glaciers in the Rockies in 1953. Glacier surface areas and variations for the Robson [87], Columbia [95], Southeast Lyell [100], Peyto [103], Freshfield [102], Athabasca [93], and Saskatchewan [92] Glaciers were documented using photographic and botanical techniques (Field and Heusser, 1954; Heusser, 1954, 1956, 1960). In the Yukon Territory, the Arctic Institute of North America (AINA)

***Figure 5.**—Photograph of the terminus of the Kokanee Glacier,* Interior Ranges, *British Columbia, Canada, showing the transient snowline in September 1972. Photograph by I.A. Reid, Water Survey of Canada. (Glacier 86 in table 1) [NTS Map: 082F11]*

***Figure 6.**—Photograph of Nadahini Glacier in August 1974 at Photo Station No. 5, Coast Mountains, British Columbia. Studies of the glacier terminus and changes in its areal extent were begun in 1945 by the Dominion Water and Power Bureau, forerunner of the Water Survey of Canada. Studies continued in the 1960's and 1970's. Photograph by I.A. Reid, Water Survey of Canada. (Glacier 15 in table 1)*

***Figure 7.**—Photograph of the terminus of Sphinx Glacier, Coast Mountains, British Columbia, Canada, in September 1968. Photograph by Oleg Mokievsky-Zubok, National Hydrology Research Institute. (Glacier 70 in table 1) [NTS Map: 092G15]*

sponsored Project Snow Cornice. This airborne expedition established a semipermanent research station on Seward Glacier [11] (Wood, 1948, 1949; Baird and Salt, 1949; Sharp, 1950).

Advances in transportation technology made a significant impact on postwar field research in Canada. Previously inaccessible areas were opened up to scientists. Thus Baird, through the Arctic Institute of North America, was able to mount major expeditions on Baffin Island to study the Barnes Ice Cap [164] in 1950 (Baird and others, 1950; Baird, 1952a) and the Penny Ice Cap [168] in 1953 (Baird and others, 1953). These expeditions provided the first substantial information on glaciers in this region (Orvig, 1951, 1953, 1954; Baird, 1952b; Baird and others, 1953; Ward and Orvig, 1953; Ward, 1954, 1955; Ward and Baird, 1954). Other scientists also found it easier to work independently in such areas—for example, Mercer's (1956) study of Grinnell Glacier [171].

Meanwhile, in the High Arctic, a group sponsored by the United States government was attempting to understand the nature and origin of ice islands, such as Fletcher's Ice Island or T–3, by studies on Ward Hunt Ice Shelf [120] in 1953 and 1954 (Crary, 1956).

Mention was made earlier of the influence of international programs on Canadian glaciological studies. Although the International Geophysical Year (IGY) (1957–58) did not focus any particular emphasis on such studies, it did prompt some organizations to undertake new programs or to extend existing ones. Canadian participation in the IGY led to a University of Toronto Expedition (1956–57) to study Salmon Glacier [33] (Adkins, 1958, 1959; Jacobs, 1958; Haumann, 1960; Russell and others, 1960; Doell, 1963). On Ellesmere Island, the Defence Research Board (DRB) started a program on Gilman Glacier [123] and continued studies on the Ward Hunt Ice Shelf (Hattersley-Smith, 1954, 1959, 1961; Hattersley-Smith and others, 1961; Weber, 1961; Weber and others, 1961; Lister, 1962; Lyons and Ragle, 1962; Ragle and others, 1964; Lyons and others, 1972).

Middle 1950's to the Middle 1960's

In the period immediately following the IGY, concern in Canadian government circles about security and sovereignty in the Arctic, and a lack of knowledge about that region, translated into funding for major projects. The Geological Survey of Canada (GSC) mounted Operation Franklin to map the geology of the Queen Elizabeth Islands. A consortium of McGill University professors, in conjunction with George Jacobsen, an entrepreneur, obtained a major expedition grant from the National Research Council of Canada (NRCC) to launch the Jacobsen-McGill Arctic Research Expedition to Axel Heiberg Island under the direction of the Swiss glaciologist Fritz Müller. The Department of Mines and Technical Surveys organized Arctic logistics through the Polar Continental Shelf Project (PCSP), which was also charged with a multidisciplinary investigation of the continental shelf region, and appointed geologist Fred Roots as its first coordinator. The Arctic Institute of North America mounted an expedition to Devon Island, and the Department of National Defence continued and expanded its studies on Ellesmere Island. This Defence Research Board (DRB) expedition, led by Geoffrey Hattersley-Smith, and named Operation Hazen after the lake on which its base camp was located, later became Operation Tanquary when the camp was moved to the head of Tanquary Fiord (Hattersley-Smith, 1974). All these activities combined to raise glaciological research in Canada to a new level and helped establish Canada's reputation in the international scientific community during that period.

The McGill University expedition started with a small reconnaissance party in 1959; this was followed in 1960 and 1961 by large multidisciplinary parties working on Crusoe [150], Baby [149], White [153], and Thompson [152] Glaciers and on the Müller Ice Cap (renamed; previously Akaioa Ice Cap or informally *McGill Ice Cap*) [151] (Müller, 1961; Müller 1962a, b, 1963; Müller and others, 1963; Andrews, R.H.G., 1964; Havens, 1964; Havens and others, 1965; Redpath, 1965; Adams, 1966; Müller and Keeler, 1969) (fig. 8). A comprehensive list of publications arising out of this early work was included in a glacier inventory of Axel Heiberg Island (Ommanney, 1969).

Within the terms of reference establishing the PCSP, provision was made for the hiring of staff scientists to cover disciplines not contributed by the participating government departments. Stan Paterson joined the PCSP and started working on Meighen Ice Cap [155]. By the middle 1960's, his program on that ice cap had been expanded to include the Melville Island ice caps [156–159] and Devon Ice Cap [160], taking over in the latter case from the AINA, whose studies there were winding down.

The AINA program involved mass balance and meteorological studies on Devon Ice Cap and some detailed investigations of Sverdrup Glacier [161] (Apollonio, 1962; Keeler, 1964; Hyndman, 1965; Koerner, 1966; Vögtli, 1967; Holmgren, 1971).

Figure 8.—*Photographs of the Müller Ice Cap* **A**, *and Crusoe Glacier* **B**, *on Axel Heiberg Island, Nunavut, High Arctic. In 1960 and 1961, large multidisciplinary parties of the Jacobsen-McGill Arctic Research Expedition carried out a number of glaciological studies, including measurements of mass balance and glacier variation under the direction of the Swiss glaciologist Fritz Müller on Müller Ice Cap, and Crusoe, White, Baby, and Thompson Glaciers on Axel Heiberg Island. Some studies continued in following years.* **A**, *Photograph of Müller Ice Cap (Glacier 151 in table 2) and "White Crown" in 1962 by C. Simon L. Ommanney, McGill University.* **B**, *Photograph of Crusoe Glacier in August 1962, looking to the northeast. Note that the termini abuts the terminal moraine, implying a mass balance in relative equilibrium. Photograph by C. Simon L. Ommanney, McGill University. (Glacier 150 in table 2)*

Operation Hazen, on Ellesmere Island, was a large multidisciplinary investigation, similar to the one underway on neighbouring Axel Heiberg Island. The glaciological part of the program was concentrated on Gilman Glacier [123], the Ward Hunt Ice Shelf [120] and *Ward Hunt Ice Rise* [121]. It resulted in reports on glacier surveying (Faig, 1966; Konecny and Faig, 1966; Dorrer, 1971), mass balance (Hattersley-Smith, 1960a, 1961; Hattersley-Smith and others, 1961; Sagar, 1964; Hattersley-Smith and Serson, 1970; Serson, 1979), temperatures (Hattersley-Smith, 1960b; Lyons and Ragle, 1962), radio-echo sounding (Evans and Robin, 1966; Hattersley-Smith, 1969b), and a popular account of the work done (Hattersley-Smith, 1974). A comprehensive bibliography covering this and other work on Ellesmere Island was published by Ommanney (1982).

Farther south, the Geographical Branch, Department of Mines and Technical Surveys, was continuing the work begun by the Baird (AINA) expedition on Barnes Ice Cap [164]. Geomorphologists were intrigued by this remnant of the last "Ice Age" and started a major investigation to map and study evidence of Wisconsinan glaciation in the area. Included were studies of the Barnes Ice Cap itself and the small Lewis Glacier [163] at its northern margin (Ives, 1966, 1967a, b; Løken, 1966; Løken and Andrews, 1966; Sagar, 1966; Anonymous, 1967) and regional variations of glaciers in northern Baffin Island and Bylot Island (Falconer, 1962). Some additional observations were also made on Penny Ice Cap [168] (Andrieux, 1970; Weber and Andrieux, 1970).

Many of the pilots who returned or emigrated to Canada after the war brought with them skills that were invaluable in the north. Most of the expeditions described above owed much to the use of small fixed-wing aircraft equipped with low-pressure balloon tires that were able to land on unprepared ground. The successful deployment of innumerable field camps was made possible by pilots who were willing to accede to the scientists' often unreasonable demands.

There was also much activity on the mainland at this time. In 1961, the AGS, in conjunction with the AINA, established the Icefield Ranges Research Project (IRRP) (Wood, 1963; Ragle, 1964, 1973). This was similar in scope and intent to the McGill and DRB expeditions. It was centered on what is now Kluane National Park and included detailed glaciological and climatological studies (Taylor-Barge, 1969), particularly on the Kaskawulsh Glacier [9] and around Mount Logan (Holdsworth, 1965, 1969; Shimizu and Wakahama, 1965; Brecher, 1966; Clarke, 1967; MacPherson and Krouse, 1967; Dewart, 1968; Keeler, 1969; Collins, 1970; Loomis and others, 1970; Anderton, 1973; Cameron, 1976). It was an incarnation of the earlier Project Snow Cornice. Many glaciologists received their early training in the Icefield Ranges, and some, such as Garry Clarke and Gerald Holdsworth, have continued to work in the area. The results of the scientific investigations were published in four volumes by the AGS (Bushnell and Ragle, 1969, 1970, 1972; Bushnell and Marcus, 1974).

Elsewhere, in the Coast Mountains, a study in connection with a mining development was initiated on the Leduc, Frank Mackie, Berendon, and Salmon Glaciers [30–33] by Bill Mathews of the University of British Columbia (Mathews, 1964c). Of particular concern was the activity of the Berendon Glacier [32] (fig. 9) (Untersteiner and Nye, 1968; Fisher and Jones, 1971). A more detailed report on this work is included in two separate sections of this volume, Glaciers of the Coast Mountains and Glaciers of the St. Elias Mountains. Other work here has focused on the provenance of material within and on the glacier (Eyles and Rogerson, 1977a, b, c, 1978a, b; Rogerson and Eyles, 1979; Eyles and others, 1982). Research was also being carried out on a number of other glaciers in the Rocky Mountains (West and Maki, 1961), but most of this will be reviewed in the following section.

Figure 9.—*Photograph of the Berendon Glacier showing its prominent medial moraines, Coast Mountains, British Columbia, Canada, on 27 August 1974. Photograph by A.D. Stanley, National Hydrology Research Institute. (Glacier 32 in table 1) [NTS Map: 104B01]*

Middle 1960's to the 1990's

The most important next stimulus was provided by the International Hydrological Decade (IHD) program (1965–74), which led to a major expansion of glaciological investigations in Canada. The nature of some of these developments has been reviewed by various authors (Meier and Post, 1962; Løken, 1971; Ommanney, 1975; Roots, 1984; Ommanney and Young, 1988). In the Cordillera, five glaciers—Place [62], Sentinel [71], Woolsey [82], Peyto [103] and Ram River [101] Glaciers—were selected for an east-west transect, and Berendon Glacier [32] was added to provide a link in the north-south chain. The program was run by the Glacier Section of the Geographical Branch, Department of Mines and Technical Surveys, the forerunner of the Snow and Ice Division, later known as the Hydrology Division (Glaciology Subdivision) of the National Hydrology Research Institute (NHRI), Department of the Environment (Østrem, 1966b, 1973a, b; Mokievsky-Zubok, 1973a, b, 1974; Stanley, 1975; Zubok, 1975; Mokievsky-Zubok and Stanley, 1976a, b; Young and Stanley, 1976a, b; Fogarasi and Mokievsky-Zubok, 1978; Young, 1981; Mokievsky-Zubok and others, 1985). It followed a set of standardized measurements for mass balance and hydrological observations outlined in the manual by Østrem and Stanley (1966), which was subsequently revised (Østrem and Brugman, 1991) (fig. 10). Data were deposited with the World Glacier Monitoring Service (WGMS) in Zürich.

Decade Glacier on Baffin Island [165] was selected as a contribution to the north-south chain in the eastern Arctic (Østrem and others, 1967; Løken, 1972), which included the DRB studies on Per Ardua Glacier [126] and the McGill University studies on White [153] and Baby [149] Glaciers (Young, 1972). However, the effective network was much larger than the official "representative glacier basins" because existing research investigations continued or were expanded to include a larger hydrological component. Thus, in the Arctic, data continued to be collected and analyzed for the Ward Hunt Ice Shelf and *Ward Hunt Ice Rise* [120, 121] (Hattersley-Smith and Serson, 1970; Holdsworth, 1971; Williams and Hutter, 1983; Hattersley-Smith, 1985; Holdsworth, 1986b, 1987; MacAyeal and Holdsworth, 1986; Narod and others, 1988), Gilman Glacier [123], Meighen Ice Cap [155] (Arnold, 1965; Paterson, 1969; Alt, 1979), the Melville Island ice caps [156–159] (Spector, 1966; Paterson and Koerner, 1974), the Devon Ice Cap [160] (Koerner, 1970a, b, 1973, 1979, 1985, 1986; Koerner and others, 1973; Alt, 1978, 1985, 1987; Koerner and Russell, 1979) and

Figure 10.—*Photographs of the Place Glacier, Coast Mountains, British Columbia.* **A,** *Dr. Gunnar Østrem and members of the 1980 Field Glaciology Course making mass-balance measurements on Place Glacier. In 1965, as part of a major expansion of glaciological studies during the International Hydrological Decade, Place Glacier was selected to be part of an east-west transect of glaciers to be monitored in western Canada. The mass-balance measurements begun here in 1965 have continued to the present day.* **B,** *Terminus of the Place Glacier and its proglacial lake in October 1975. Photograph by Oleg Mokievsky-Zubok, National Hydrology Research Institute. (Glacier 62 in table 1) [NTS Map: 092J07]*

the Barnes Ice Cap [164] (Løken and Sagar, 1968; Parker, 1975). New studies included those on an unnamed ice cap near St. Patrick Bay [125] (Hattersley-Smith and Serson, 1973), which was continued by Bradley (Bradley and England, 1977, 1978a, b; Bradley and Serreze, 1987a, b; Serreze and Bradley, 1987) and ones on *Boas* [167] and *Akudnirmuit* [166] *Glaciers* by the University of Colorado (Andrews and Webber, 1969; Andrews and others, 1970; Andrews and Barry, 1972; Jacobs and others, 1973; Williams, 1974, 1975; Weaver, 1975).

Similarly, on the mainland, new studies began on Rusty (*Fox*) [6] (Crossley and Clarke, 1970; Clarke, 1971; Collins, S.G., 1972; Faber, 1973), Cathedral [18] (Jones, 1974; Guigné, 1975; Miller, 1975; Cialek, 1977) and Drummond [107] (Nelson and others, 1966; Brunger and others, 1967) Glaciers. Many of these did not continue throughout the IHD, and, of the representative basins, the investigations on Woolsey, Ram River, Berendon, Decade, and Per Ardua Glaciers were terminated during or at the end of the IHD, but various studies did continue on the other glaciers.

The availability of semipermanent facilities at most of these glaciers, and core staff to maintain a measurement program throughout the summer melt season, led to the development of many other complementary glaciological investigations. The case of Peyto Glacier [103] exemplifies this situation. Studies here, during and after the IHD, included the following: **mapping** (Sedgwick and Henoch, 1975; Henoch and Croizet, 1976; Young and Arnold, 1978; Glenday, 1991; Wallace, 1995), **dendrochronology** (Parker and Henoch, 1971; Reynolds, 1992), **depth sounding** (Goodman, 1970; Goodman and Terroux, 1973; Hobson and Jobin, 1975; (Holdsworth and others, in press), **instrumentation** (Young, 1976), **hydrochemistry** (Collins and Young, 1979, 1981; Binda, 1984; Collins and Power, 1985; Binda and others, 1985; Bradley, 1990), **hydrological modeling** (Derikx and Loijens, 1971; Henoch, 1971; Derikx, 1973, 1975; Loijens, 1974; Munro, 1976; Power and Young, 1979; Gottlieb, 1980; Young, 1982, 1990; Johnson and Power, 1985; Power, 1985; Johnson and David, 1987), **mass balance and techniques, including remote sensing** (Young, 1971, 1974, 1975, 1976, 1981; Pietroniro and Demuth, 1999) and **meteorology** (Goodison, 1971, 1972a, b; Föhn, 1973; Munro, 1976, 1989, 1990, 1991a, b; Munro and Davies, 1976, 1977, 1978; Young, 1978; Munro and Young, 1980, 1982; Stenning and others, 1981; Nakawo and Young, 1982; Cutler and Munro, 1996) (fig. 11). The need to place these single-site observations within the larger regional context was recognized, so a study was made on Yoho Glacier [105] (David, 1989) and the

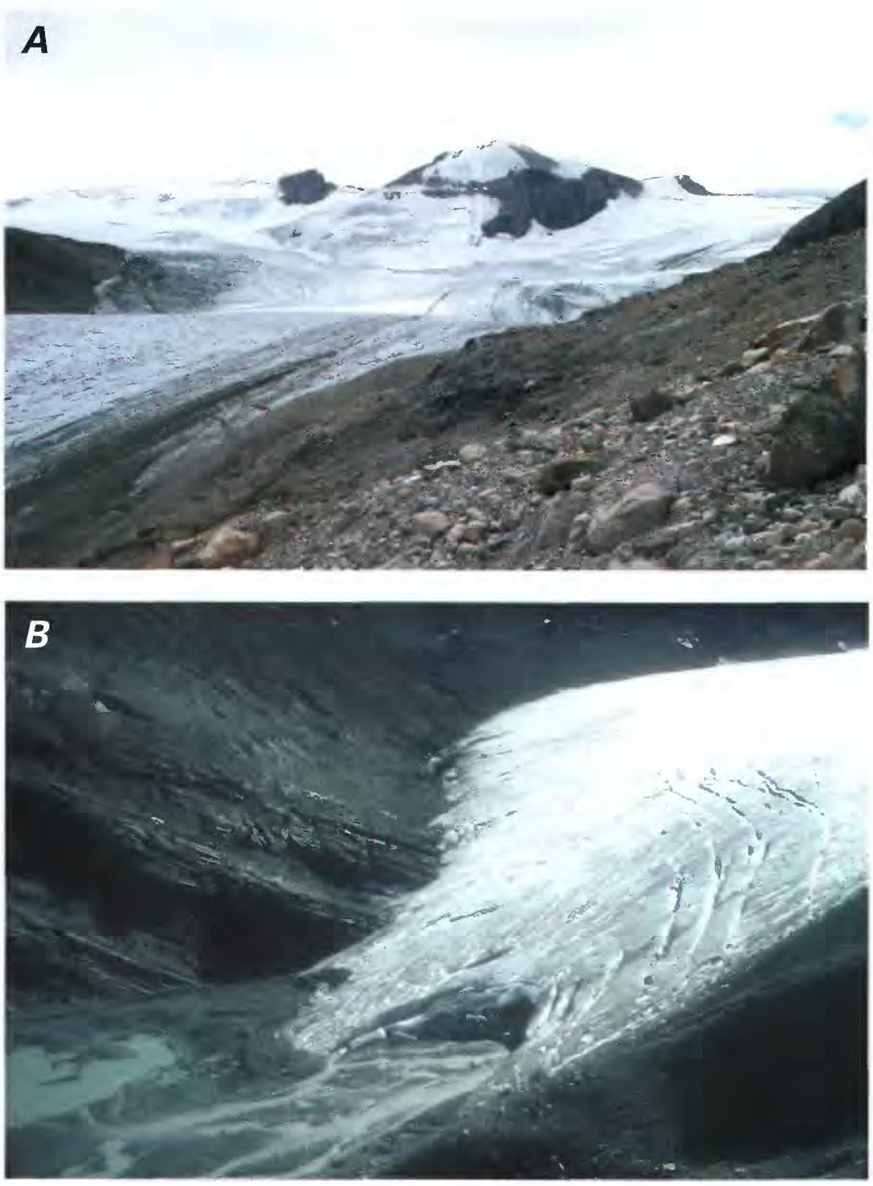

Figure 11.—**A**, *Photograph of Peyto Glacier, Rocky Mountains, Alberta, in late summer 1967. Peyto Glacier has been the site of numerous glacier studies since the early 1900's, including glacier variation, dendrochronology, hydrochemistry, meteorology, and mass-balance measurements and techniques. During the International Hydrological Decade, Peyto Glacier was one of the glaciers monitored in the east-west transect of western Canada. Mass-balance measurements begun here in 1964 are continuing. Photograph by C. Simon L. Ommanney, National Hydrology Research Institute. (Glacier 103 in table 1)* **B**, *Photograph of the terminal lobe of Peyto Glacier, Rocky Mountains, Alberta, on 25 September 1991. Photograph by Gerald Holdsworth, Arctic Institute of North America.*

Figure 12.—*Photographs of Bugaboo Glacier,* Interior Ranges, *British Columbia, Canada, in* **A**, *August 1970, and* **B**, *July 1970. Photographs by I.A. Reid, Water Survey of Canada. (Glacier 83 in table 1) [NTS Map: 082K10]*

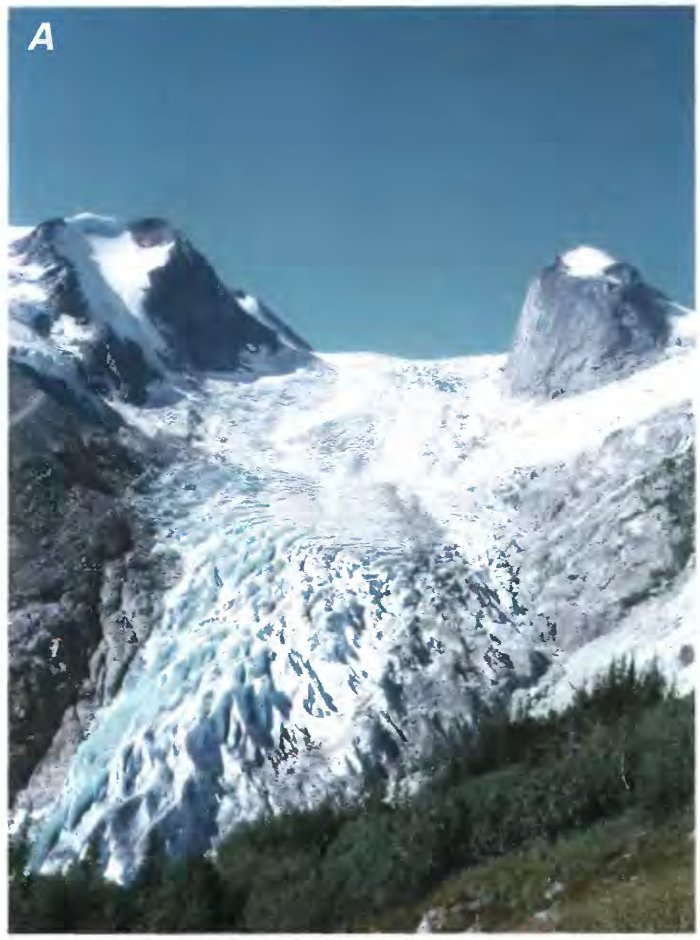

Yoho Valley on the other side of the Continental Divide, as well as the intervening Waputik Icefield from which both glaciers flow.

Although the IHD studies within the Columbia River basin had been terminated, some studies were initiated in Glacier National Park for the Canadian Parks Service (Champoux and Ommanney, 1986a, b), on Bugaboo Glacier [83] (fig. 12) (Osborn, 1986; Osborn and Karlstrom, 1988), and elsewhere (Power, 1985; Rogerson, 1985; Luckman and others, 1987; Duchemin and Seguin, 1998).

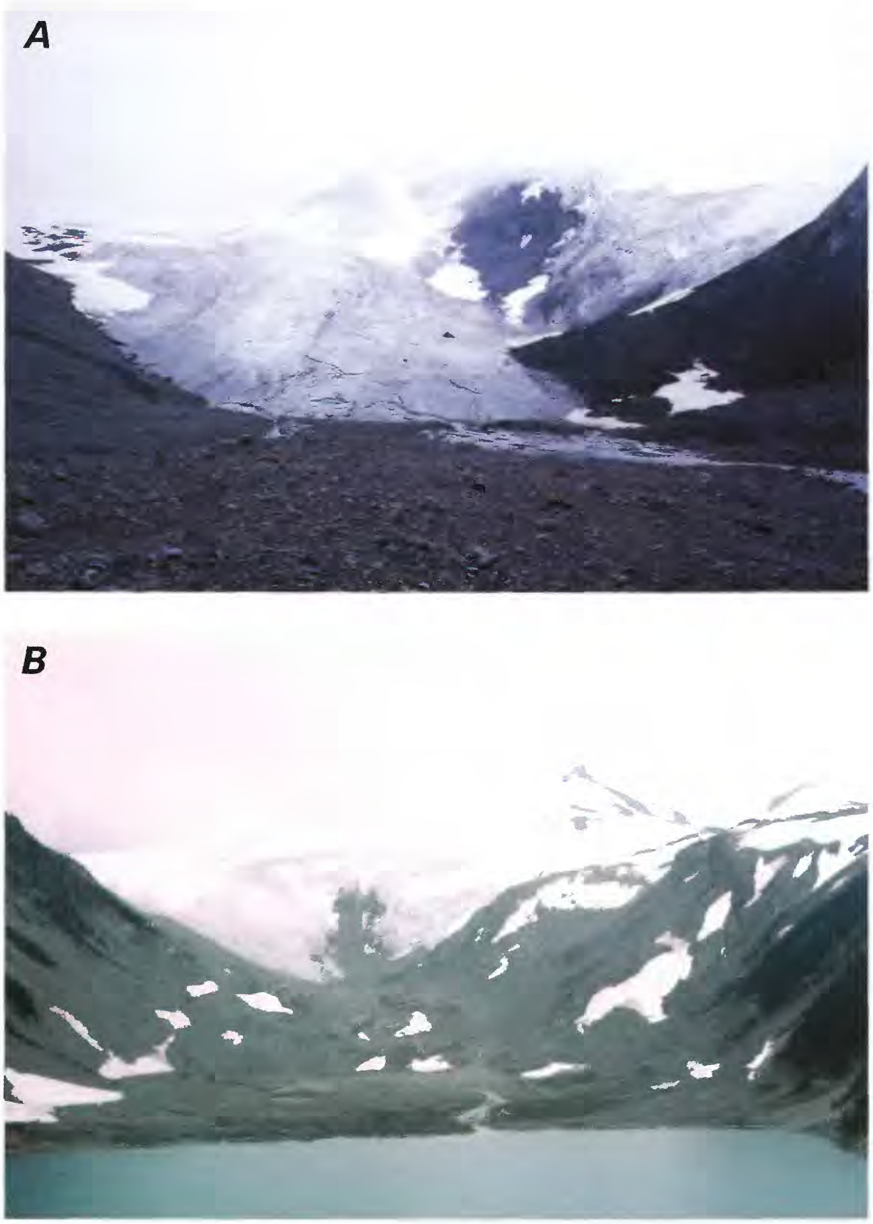

Figure 13.—*Photographs of Sentinel Glacier, Coast Mountains, British Columbia, Canada, showing the transient snowline in* **A**, *September 1968 and* **B**, *25 September 1973. Photographs by Oleg Mokievsky-Zubok, National Hydrology Research Institute. (Glacier 71 in table 1) [NTS Map: 092G15]*

In the Coast Mountains, continuous records were maintained on Sentinel [71] (fig. 13) and Place [62] Glaciers (Mokievsky-Zubok, 1987; Schmok, 1990), which served as bases for local studies (Yarnal, 1984b; Fogarasi and Mokievsky-Zubok, 1987; Brugman, 1991) and as benchmarks for comparison with shorter term mass-balance investigations elsewhere. The studies were closely related to the operational needs of the various governmental water-management agencies. Thus the program on the Bridge River glaciers, *Sykora Glacier* [53] (fig. 14), Bridge Glacier [54] (fig. 15), and *Zavisha Glacier* [55], aided in the management of the Downton Reservoir (Mokievsky-Zubok, 1980a; Mokievsky-Zubok, 1985). On the basis of data from Andrei [25], Alexander [22], *Forrest Kerr* [26], Natavas [23], and Yuri [24] Glaciers, the feasibility of a hydroelectric development in the Stikine and Iskut River basins was being assessed (Fogarasi, 1981; Mokievsky-Zubok, 1983b; Mokievsky-Zubok, 1992b). A similar study was started in the Homathko basin, on the Bench [42] and Tiedemann [45] (fig. 16) Glaciers (Mokievsky-Zubok, 1983a; Mokievsky-Zubok, 1992a). Data from all these studies were compiled in annual reports by NHRI and deposited with the WGMS. In the early 1990's, following a review of future hydroelectric needs for British Columbia, support for operational programs was withdrawn by BC Hydro.

Figure 14.—Photograph of the terminus of the Sykora Glacier, Coast Mountains, British Columbia, Canada, on 19 August 1975. Photograph by Oleg Mokievsky-Zubok, National Hydrology Research Institute. (Glacier 53 in table 1)

Figure 15.—Photograph of the terminus of the Bridge Glacier, Coast Mountains, British Columbia, Canada, on 19 August 1975, showing icebergs which have calved into the proglacial lake. Photograph by Oleg Mokievsky-Zubok, National Hydrology Research Institute. (Glacier 54 in table 1) [NTS Map: 092J13]

Figure 16.—Photograph of the terminus of the Tiedemann Glacier, Coast Mountains, British Columbia, Canada, in August 1982, showing prominent trim lines on the valley wall, prominent medial moraines, and the morainic-debris-covered lower part of the glacier. The difference in elevation of the trimline and the present surface of the glacier in its lower part indicates significant reduction in glacier volume and a prolonged period of negative mass balance. Photograph by Oleg Mokievsky-Zubok, National Hydrology Research Institute. (Glacier 45 in table 1) [NTS Map: 092N06]

Data from these transects and supplementary studies have been used in a number of regional analyses of the spatial distribution of glaciers, their variations, and the relationship between glacier mass balance and climate (Henoch, 1972; Yarnal, 1984a; Osborn and Luckman, 1988; Letréguilly, 1988; Letréguilly and Reynaud, 1989, 1990; Luckman and others, 1993; Demuth, in press).

The Juneau Icefield Research Project, partly working from a base in Atlin, British Columbia, continued to introduce students to glaciology and mountain environments. Some results from work on the Juneau Icefield and Cathedral Glacier [18] are available (Johnson, R.F., 1983; Marston, 1983; Hasenauer, 1984; Mauelshagen, 1984; Mauelshagen and Slupetzky, 1985; Yao Tandong, 1987; Rentsch and others, 1990; Marcus and others, 1992).

On Barnes Ice Cap [164] the mass-balance program soon changed to one emphasizing glacier physics (Jones, 1972; Hooke, 1973a, b, 1976a, b, 1981; Holdsworth, 1973a, b, 1975, 1977c; Barnett and Holdsworth, 1974; Hudleston, 1976, 1980; Classen, 1977; Hooke and others, 1979, 1980, 1983, 1987; Hooke and Hudleston, 1980, 1981; Hudleston and Hooke, 1980; Hooke and Clausen, 1982; Hudleston, 1983; Hooke and Hanson, 1986; Stolle, 1986, 1988; Hanson, 1987, 1990). The mass-balance program maintained by R. Hooke (Hooke and others, 1987) lapsed. New studies subsequently began here, using remote sensing to assess changes in the ice cap (Lodwick and Paine, 1985; Moisan and Dubois, 1993; Jacobs and others, 1997). Work was also done on the subglacial characteristics of Aktineq Glacier [162] on Bylot Island (Souchez and De Groote, 1985; Souchez and others, 1988; Tison and others, 1989; Zdanowicz and others, 1996). In the south, Grinnell Glacier [171] was revisited in connection with a sediment study (Dowdeswell, 1986) and became the subject of an educational project that included mapping, directed by Gunnar Østrem (Norwegian Water Resources and Energy Administration, 1991). Nearby, a climbing expedition measured the fluctuations of Virginia Glacier [170] (Cochran, 1978).

Interest in reconstructing past climates in the High Arctic led to deep ice-coring projects on Meighen Ice Cap [155], Devon Ice Cap [160] and Agassiz Ice Cap [139] (fig. 17). Although mass-balance investigations were an integral part of the initial surface observations, the focus subsequently changed to analysis of the core constituents and their interpretation. Reports have covered the following: **climate at different time scales** (Koerner and Paterson, 1974; Koerner, 1977a, 1989, 1992; Fisher and Koerner, 1981; Koerner and Fisher, 1981, 1985, 1990; Alt and others, 1985, 1992; Harvey, 1988; Reeh, 1991; Fisher, 1992); **snow and ice properties** (Koerner, 1968, 1973; Fisher and Koerner, 1986; Goto-Azuma and others, 1997); **englacial temperatures, precipitation and isotope analysis** (Paterson, 1968, 1976a; Krouse and others, 1977; Paterson and others, 1977; Paterson and Clarke, 1978; Fisher, 1979, 1991; Paterson and Waddington, 1984; Fisher and Koerner, 1988, 1994; Fisher and others, 1996); **core particles and gases** (Lichti-Federovich, 1975; Koerner and Taniguchi, 1976; Koerner, 1977b; Koerner and Fisher, 1982; McAndrews, 1984; Barrie and others, 1985; Raisbeck and Yiou, 1985; Bourgeois, 1986, 1990; Cresswell and Herd, 1991; Koerner and others, 1991, 1998; Gregor, 1992; Nriagu and others, 1994; Sturges and others, 1998); **glacier flow** (Doake and others, 1976; Paterson, 1976b, 1977, 1985; Koerner and Fisher, 1979; Waddington and others, 1986; Reeh and others, 1987; Reeh and Paterson, 1988); **thickness and topographic measurements** (Oswald, 1975; Koerner, 1977c; Walford and others, 1977; Koerner and others, 1987; Haythornthwaite, 1988); **basal conditions** (Koerner, 1983; Gemmell and others, 1986; Fisher, 1987); and the **interpretation of records** (Fisher and others, 1983, 1985; Koerner and others, 1988; Illangasekare and others, 1990; Pfeffer and others, 1990; Clarke and Waddington, 1991). Attention was later directed to the Penny Ice Cap [168] on Baffin Island, where cores were taken and analyses made (Holdsworth, 1984; Short and Holdsworth, 1985; Fisher and others, 1998; Grumet and others, 1998).

Figure 17.—*Photograph of the electro-mechanical ice-core drill being lowered into the borehole on top of the Devon Ice Cap in April 1998. The drill was used in a partially fluid-filled borehole to minimize core fracturing. Lamp oil was used as a fluid and is filtered and re-used during drilling operations. On ice caps where the ice at the top of the flow line is often about 300-m thick, core fracturing usually begins at a depth of about 150 m and consists of microfractures that obscure the stratigraphy. Geological Survey of Canada personnel working in the shelter tent are as follows: D.A. Fisher is at the control box on the right; C. Zdanovicz has his hand on the torque springs on the left; and R. M. Koerner is in the left foreground. The torque springs prevent the outer sonde casing and the cable from turning in the borehole. Geological Survey of Canada photograph.*

McGill University continued the Axel Heiberg Island investigations after the end of the Jacobsen-McGill phase in 1962. Following the move of Fritz Müller to the Geographisches Institut, Eidgenössische Technische Hochschule in Zürich, the work was largely directed from Switzerland. Many excellent research reports and papers were written by expedition members (Maag, 1969; Iken, 1972, 1974; Müller and Iken, 1973; Müller, 1976; Alean and Müller, 1977; Hambrey and Müller, 1978; Arnold, 1981; Braithwaite, 1981; Weiss, 1984; Blatter, 1987a, b; Blatter and Hutter, 1991). Recently the work has been continued by Trent University on Baby [149] (Adams and Ecclestone, 1991; Tolland and others, 1991; Dicks and others, 1992; Adams and others, 1998) and White [153] (Jung-Rothenhäusler and others, 1992; Adams and others, 1995; Cogley and others, 1996b; Robertson, 1997) Glaciers, with some continuing involvement by McGill University on Thompson Glacier [152] (Parent, 1991; Lehmann, 1992; Moisan and Pollard, 1992). Earlier results have been compiled and carefully analysed (Glenday, 1989; Cogley and others, 1995, 1996a)

Changing priorities and reduced resources eventually led to the abandonment of the Arctic glacier program of the Snow and Ice Division. Study of Per Ardua Glacier [126], which had been handed over to this group on the termination of the DRB Operation Tanquary, was given up, as was a new project on Leffert Glacier [143] (Holdsworth, 1978), and a shorter term study of d'Iberville Glacier [140] (Holdsworth, 1975, 1977b). However, support subsequently became available for continuation of studies on the Ward Hunt Ice Shelf and new studies along the northern Ellesmere Island coast (Jeffries, 1982, 1984, 1986a, b, 1991, 1992; Jeffries and Serson, 1983, 1986;

Jeffries and Krouse, 1985; Jeffries and Sackinger, 1990; Jeffries and others, 1988, 1991; Lemmen, 1988; Sackinger and others, 1985; Stewart, 1991). [See section in this volume on Ellesmere Island Ice Shelves and Ice Islands.] The University of Heidelberg later mounted a small multidisciplinary expedition to investigate the Webber, Gnome, Dwarf, Midget, Arklio, Van Royen, Okpuddyshao, and Nukapingwa Glaciers at the head of Oobloyah Bay [129–136] (Barsch and King, 1981; King, 1983) and a glacier tongue in the neighboring Hare Fiord [128] (Römmer and Hell, 1986; Hell and King, 1988). Meanwhile, studies of some other glaciers on Ellesmere Island (fig. 18) had been initiated: on *Quviagivaa Glacier* [142] (Wolfe, 1995; Wolfe and English, 1996); around *Blackwelder Ice Cap* [138], on *Shirley Glacier* [137] and a revisit to Van Royen Glacier [136] (Smith, 1997); at the head of Phillips Inlet on *Muskox Glacier* [124] (Evans and Fisher, 1987; Evans, 1989, 1993; Evans and England, 1992); and the University of Alberta commenced regular visits to John Evans Glacier [141] (Woodward, 1996; Arendt, 1997; Woodward and others, 1997).

In the middle 1960's, following the Glacier Mapping Symposium held in Ottawa and from recommendations made by the NRCC's Subcommittee on Glaciers, the WSC switched to a program of terrestrial photogrammetry that involved mapping the ablation areas of their glaciers every 2 years (Campbell and others, 1969a, b; Reid and Shastal, 1970; Reid and Charbonneau, 1972, 1975, 1979a, b; Reid, 1973; Reid and others, 1978). Terminus and plaque surveys of the Saskatchewan and Athabasca Glaciers [92–93] were continued in the intermediate years by the Calgary office of the WSC (Warner and others, 1972; Canada, 1976, 1982).

The accessibility of the Columbia Icefield [94] (Harmon and Robinson, 1981), particularly the Athabasca (Kucera, 1972) and Saskatchewan Glaciers, and the availability of a fairly good historical sequence of observations, probably favored its selection as the site for a wide variety of glaciological studies. These included investigations of **glacier chemistry** (Sharp and Epstein, 1958; Epstein and Sharp, 1959; Hallet, 1976; Mayewski and others, 1979), **glacier flow** (Meier and others, 1954; Meier, 1958a, b, 1960; Rigsby, 1958, 1960; Paterson, 1960, 1961, 1962, 1964, 1970; Paterson and Savage, 1963a, b; Savage and Paterson, 1963, 1965; Clee and others, 1969; Raymond, 1971a, b, 1973), **depth measurement** (Kanasewich, 1963; Neave and Savage, 1970; Goodman, 1973, 1975; Rossiter and others, 1973; Trombley, 1986), **glacial history** (Luckman, 1986, 1988, 1993), **photogrammetry** (Reid, 1961; Konecny, 1966; Paterson, 1966; Reid and Paterson, 1973; Kite and Reid, 1977; Reynolds, and Young, 1997), **remote sensing** (Østrem, 1973b; Gratton and others, 1990, 1993; Vachon and others, 1996); **resistivity** (Keller and Frischknecht, 1960, 1961), **sediment transport and erosion** (Mathews, 1964a, b; Iverson, 1991) and **temperature** (Paterson, 1971, 1972). Nearby studies have included the **hydrology** of the *Small River Glacier* [88] (Smart, 1992, 1998) and **glacierized alpine karst** (Smart, 1984, 1986, 1988; Smart and Ford, 1983, 1986; Worthington, 1991), **erosion and hydrological characteristics** of Decade Glacier [165] (Østrem and others, 1967), *Hilda Glacier* [98] (Hammer and Smith, 1983; Gardner and Bajewsky, 1987; Bajewsky and Gardner, 1989), *Boundary Glacier* [96] (Gardner and Jones, 1985; Jones, 1987; Sloan, 1987; Mattson, 1990; Mattson and Gardner, 1991) and Dome Glacier [97] (Gardner, 1992). A welcome development was the construction of a new Icefields Interpretative Centre in the middle 1990's (Waskasoo Design Group Limited, 1991)

The fortunate conjunction of a climbing camp in the St. Elias Range and the surge of the Steele Glacier [3] (Roots, 1967) led to studies of its cause (Bayrock, 1967; Nielsen, 1969; Stanley, 1969), spawned an influential symposium which outlined directions for future research (Ambrose, 1969), and helped generate grants for further work (Jarvis and Clarke, 1974; Clarke and Jarvis, 1976). Garry Clarke has focused much of his research effort on the elucidation of the problem of **surging glaciers**. Extremely detailed studies have been carried out on the Trapridge (*Hyena*), Backe (*Jackal*), Rusty (*Fox*), and Donjek Glaciers [4–7] (Classen and Clarke, 1971; Johnson, 1971, 1972; Hoffmann and Clarke, 1973; Clarke and Goodman, 1975; Jarvis and Clarke, 1975; Clarke, 1976, 1991, 1996; Collins and Clarke, 1977; Collins, 1980; Narod and Clarke, 1980; Clarke and Collins, 1984; Clarke and others, 1984, 1986b; Maxwell, 1986; Clarke and Blake, 1991; Blake and Clarke, 1992; Stone and Clarke, 1993, 1998; Fischer and Clarke, 1994, 1997; Murray and Clarke, 1995; Waddington and Clarke, 1988;

Figure 18.—Ice field adjoining ice cap, Victoria, and Albert Mountains, east coast Ellesmere Island, Queen Elizabeth Islands, Nunavut (80°18'N., 74°21'W.); view to the east; John Richardson Bay is at top right and Kane Basin and Greenland in the background. NAPL T400L–201. From figure 2 in Prest, 1983, p. 13.

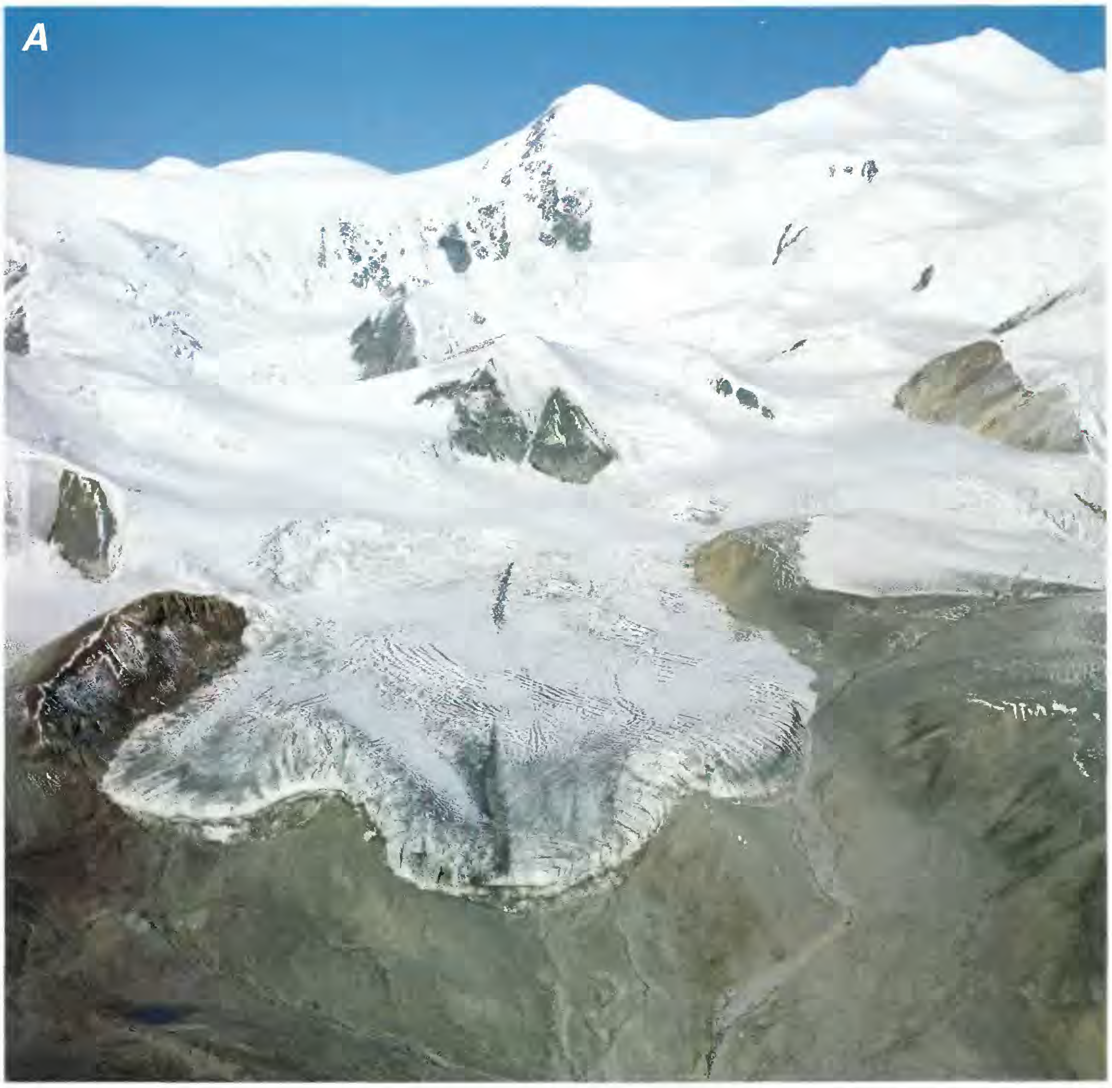

Flowers and Clarke, 1999) (fig. 19). Other surging-glacier studies of have been made of the Tweedsmuir [14], Lowell [13] and Walsh Glaciers [8] (Post, 1966; Krimmel and Meier, 1975; Post and others, 1976), of Otto Glacier [127] (Hattersley-Smith, 1964, 1969a), Milne Glacier [122] (Jeffries, 1984), *Good Friday Bay Glacier* [154] (Müller, 1969), of the Barnes Ice Cap [164] (Holdsworth, 1973a, 1977c; Løken, 1969), and of the distribution of such features (Post, 1969). The most recent surge to attract substantial public attention was that of Hubbard Glacier [12] (Begley and White, 1986; Mayo, 1989; Trabant and others, 1991; Krimmel and Trabant, 1992).

Curiosity about the environmental effects of the large polynya known as the North Water, located at the head of Baffin Bay between Greenland and Ellesmere Island, prompted Fritz Müller to launch a major scientific program there. Although the focus was primarily on energy exchanges, sea ice, and atmospheric effects, mass-balance studies on Coburg Island, on *Wolf Glacier*, *Laika Glacier*, and *Laika Ice Cap* [146–148] (Berger and Müller, 1977; Blatter and Kappenberger, 1988), on Leffert Glacier, and on a neighboring unnamed glacier [143, 144] were started (Müller and others, 1974–80, 1977). A popular account of this work, and that on Axel Heiberg Island, was also published (Müller, 1981). Unfortunately, the unexpected death of Fritz Müller led to the premature termination of this project before all the analyses had been completed.

A later initiative by Karl Ricker, a private consultant, in conjunction with Bill Tupper of the British Columbia Institute of Technology, added

Figure 19.—**A**, *Oblique aerial photograph of Trapridge Glacier, Yukon, Canada, in August 1999. The peak in the background (top right) is Mount Wood. Photograph by Garry K.C. Clarke.* **B**, *(opposite page) Graduate students from the University of British Columbia connecting sensors to one of more than 20 data loggers operating year-round at Trapridge Glacier. Photograph by Garry K.C. Clarke, University of British Columbia. (Glacier 4 in table 1)*

significantly to our knowledge of recent glacier variations in the Coast Mountains. Studies of glaciers (glacier numbers in table 1 shown in brackets for each mountain range) ranged from the St. Elias Mountains [16], through the Hazelton Mountains [34, 35], the Pacific Ranges [36–41], the Chilcotin Ranges [43, 44, 48–52], the Elaho Range [56–58], the Clendenning Range [59–61], and the Lillooet Ranges [64] to Garibaldi Provincial Park [63, 72–75] and Overlord Glacier [68] (Ricker, 1976, 1977, 1979, 1980, 1990; Tupper and Ricker, 1982; Ricker and others, 1983; Ricker and Jozsa, 1984; Ricker and Parke, 1984; Tupper and others, 1984, 1985, 1986; Ricker and Tupper, 1988, 1992, 1996). The extensive ice cover of parts of British Columbia means that geophysical surveys for mineral exploration are often conducted on and through glaciers; these have included *Ridge Icefield Glacier* [28] at McLymont Creek and Horstman Glacier [67] (J.P. Schmok, oral commun., 1991–93).

A valuable study was that begun by Robert Rogerson of Memorial University in 1981 on four glaciers in Labrador—Superguksoak, Abraham, Hidden, and Minaret Glaciers [173–176]. As small glaciers are expected to respond quite rapidly to changes in climate, and climatologists are predicting global warming as a result of the "greenhouse effect," the results, at the southeastern limits of glacier cover in Canada, would have been most interesting. Unfortunately, the program was concluded after only a few years (McCoy, 1983; Branson, 1984; Rogerson, 1986; Rogerson and others, 1986). However, Dan Smith of the University of Victoria started investigating the behavior of Moving Glacier [76] on Vancouver Island (Smith, 1994), which would be representative of the southwestern limits. While at the University of Saskatchewan, he had initiated a study of *Rae Glacier* [113] (Lawby and others, 1994), the most southerly of any glacier investigated in the Canadian Rocky Mountains.

In the Yukon Territory, Gerald Holdsworth, in conjunction with the AINA and their considerably reduced program in the Icefield Ranges, has been establishing the recent climate history of the southwest Yukon through the analysis of an ice core obtained from the 5,340-m-high plateau of Mount Logan [10] (fig. 20), (De la Barre, 1977; Holdsworth, 1977a, 1983, 1986a, 1990; Holdsworth and Jones, 1979; Holdsworth and others, 1984, 1989, 1991, 1992; Holdsworth and Peake, 1985; Pourchet and others, 1988; Monaghan and Holdsworth, 1990; Dibb and others, 1993; Holdsworth and Sawyer, 1993; Mayewski and others, 1993; Yang and others, 1995). Peter Johnson, together with staff and students from the University of Ottawa, has studied the glacier hydrology of the Grizzly Creek region and debris- and moraine-covered ice masses (Johnson, 1976, 1980a, b, 1981, 1983, 1984, 1985, 1991a, b, 1992, 1998; Lacasse, 1985; Johnson and David, 1987; Johnson and Lacasse, 1988; Kruszynski and Johnson, 1993).

Observations that cannot readily be subjected to either a systematic regional or chronological review are those on ice-dammed lakes and associated hazards. Their regional distribution on the mainland has been discussed by Post and Mayo (1971) and other general aspects reviewed by several authors (VanDine, 1985; Young, 1985; Evans, 1986; Shoemaker, 1991; Clague and Evans, 1994). The catastrophic drainage (jökulhlaup) of Summit Lake, dammed by Salmon Glacier [33], caused severe flooding downstream and washed out the access road to the Granduc Mine at Berendon Glacier [32] (Mathews, 1965, 1973; Gilbert, 1971; Fisher, 1973; Mathews and Clague, 1993). That of Ape Lake removed trees from a substantial area of forest downstream of Fyles Glacier [39] (Jones and others, 1985; Desloges and others, 1989; Desloges and Church, 1992). Other catastrophic events noted in British Columbia include those on Klattasine Creek associated with Cumberland Glacier [47] (Blown and Church, 1985; Clague and others, 1985) and on *Tim Williams Glacier* [29] (Evans and Clague, 1990). Detailed studies have been made on lakes associated with the surge-type Steele [3], Donjek [7] and Kaskawulsh [9] Glaciers (Collins and Clarke, 1977; Clarke and Mathews, 1981; Clarke, 1982; Liverman, 1987; Kasper and Johnson, 1991; Johnson and Kasper, 1992). To the south, the Tulsequah Glacier [20] flood was investigated by Marcus (1960). Hydropower feasibility investigations in the Stikine and Iskut River basins have included similar studies (Perchanok, 1980), particularly of the Flood Glacier [21] jökulhlaup (Mokievsky-Zubok, 1980b; Clarke and Waldron, 1984) (fig. 21). An interesting case study was that of the

Figure 20.*—Photograph of Mount Logan (5,959 m), St. Elias Mountains, Yukon Territory, Canada, from the ice-core drill site at Eclipse (3,017m) in June 1990. Photograph by Gerald Holdsworth, Arctic Institute of North America.*

Figure 21.*—Photograph of Flood Glacier, Coast Mountains, British Columbia, on 13 July 1979 showing the iceberg-filled lake dammed by the glacier. In August 1979, the lake drained catastrophically, causing severe flooding downstream. Photograph by Oleg Mokievsky-Zubok, National Hydrology Research Institute. (Glacier 21 in table 1)*

Figure 22.—Bed instruments developed for studying the subglacial mechanical processes of Trapridge Glacier. A, Slidometer used to measure basal sliding rate. B, Ploughmeter used to measure the ploughing interaction between a glacier and a soft sedimentary bed. C, Tilt cell to measure the deformation of subglacial sediment. D, Schematic diagram (not to scale) showing the foregoing instruments installed near the ice-bed contact. Detail: Progressive tilting of a tilt cell in response to shear deformation of subglacial sediment. Diagram from Garry K.C. Clarke, University of British Columbia.

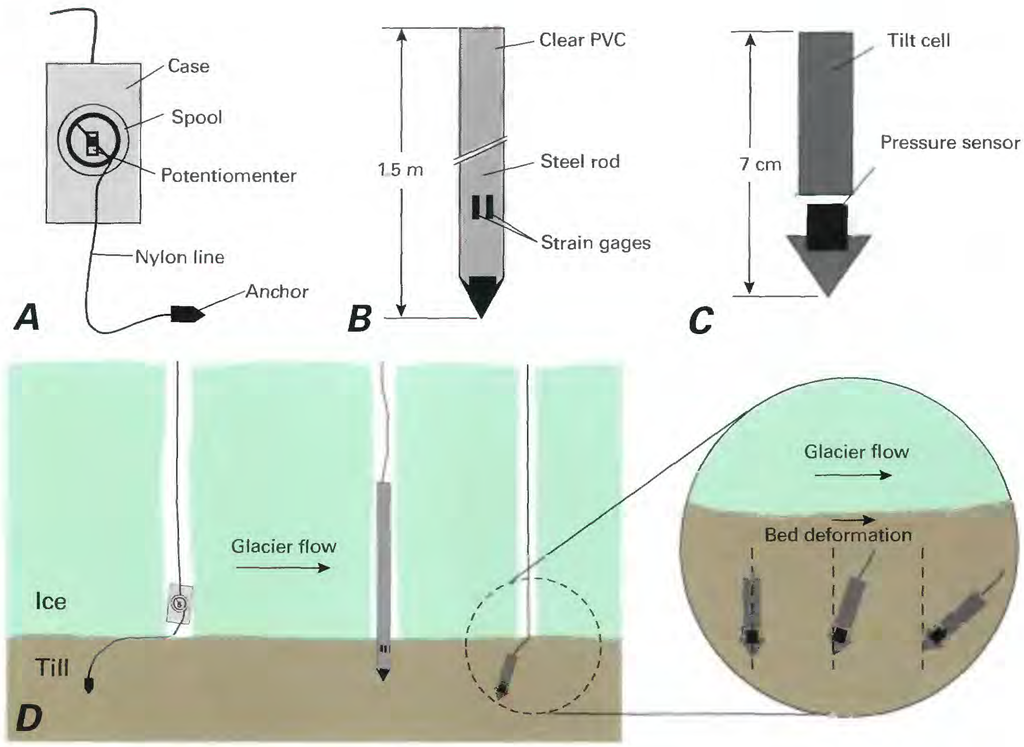

Cathedral Glacier [109] jökulhlaup, whose debris flows periodically block the CPR railway and Trans-Canada Highway in Kicking Horse Pass (Jackson, 1979, 1980; Jackson and others, 1989). Such studies have not been limited to the mainland. Maag (1969) completed a comprehensive report on ice-dammed lakes and associated jökulhlaups in the expedition area of Axel Heiberg Island. Ricker (1962) has also reported on this area, and a later study was made by a McMaster University group along the margin of the Prince of Wales Icefield [145] on Ellesmere Island (McCann and Cogley, 1977; Blachut and McCann, 1981). Some environmental-impact studies have had a glaciological component that, carried out in connection with the proposed Alcan pipeline route in the Yukon, included a general study of glacier-dammed lakes in the St. Elias Mountains (Canada, 1977; Young, 1980). Studies on Tats Glacier [17] (J.P. Schmok, oral commun.,1990) were in connection with an impact assessment of the Windy Craggy development (Canada, 1990). In Alberta, a small glacier on Mount Cline [99] was assessed in response to a license application to mine the glacier for "pure" water and ice cubes (The Ice Age Co., 1989; Rains, 1990).

To complete this review, it is worth mentioning briefly that some of the field programs described above have prompted the development of new glaciological instruments and techniques. The geophysical group at the University of British Columbia, driven by the desire to measure Trapridge Glacier in even more detail, has been a leader in this area. Radars and ancillary equipment have been constructed (Narod and Clarke, 1983; Prager, 1983; Jones and others, 1989; Cross and Clarke, 1990), as well as devices for recording activity at the glacier bed (Blake and Clarke, 1991; Blake, 1992; Blake and others, 1992; Stone and others, 1993; Waddington and Clarke, 1995; Kavanaugh and Clarke, 1996) (fig. 22) and on the surface (Clarke and others, 1986a). One member of the group has gone on to develop instrumentation for use elsewhere (Blake and others, 1998). The current techniques used for mass-balance measurement in mainland Canada have been documented (Østrem and Brugman, 1991) and a conductivity measurement system automated for use in the Columbia River basin (Kite, 1994). A major contribution to the glaciological community has been Paterson's outstanding book on glacier physics (Paterson, 1994), now in its third edition.

The 21st Century

In the decade or so leading up to the end of the 20th century, there was a significant decline in governmental support of glacier research in Canada. At the end of the 20th century, systematic long-term mass-balance observations were being continued at Peyto Glacier [103] in the Rocky Mountains, Place Glacier [62] and Helm Glacier [69] in the Coast Mountains, and White Glacier [153] on Axel Heiberg Island, Canadian High Arctic, Nunavut (Haeberli and others, 1999), by the GSC under its new National Glaciology Programme. Three of the sites, one in the Rockies and two in the Coast Mountains, are low latitude and are unlikely to be representative of the full extent of these ranges. Old glacier sites may be revisited from time to time and additional glaciers added to the record as opportunities present themselves (for example, Bow [104] and *Robertson* [112] Glaciers (M. Sharp, oral commun., 2000). Airborne and satellite remote sensing and geographic information system (GIS) technology will be used increasingly in glaciological studies, such as the use of synthetic aperture radar (SAR) imagery in glacier-hydrology investigations of Place Glacier [62], Coast Mountains (Adam and others, 1997); Landsat Thematic Mapper (TM) and SAR imagery of Wapta Icefield and Peyto Glacier [103] (Brugman and others, 1996); airborne laser altimetry and interferometric SAR (InSAR) mapping of the Wapta Icefield (Demuth and others, 2001); areal and volumetric changes of the Prince of Wales Icefield and Devon Ice Cap using historical aerial photographs and Landsat 7 imagery (Burgess and others, 2001); studies of fluctuations of glacier termini on Axel Heiberg Island, using historical aerial photographs and satellite imagery (Cogley, 2001); and the Illecillewaet Icefield and Illecillewaet Glacier [80], *Interior Ranges* (see section on Mapping Glaciers in the *Interior Ranges* and Rocky Mountains with Landsat Data, by Roger D. Wheate, Robert W. Sidjak, and Garnet T. Whyte, in this volume). Improvements in spatial [reduction in size of picture elements (pixels)] and spectral (increase in the number and/or smaller band width) resolution of satellite sensors [for example Landsat 7 Enhanced Thematic Mapper (ETM+) (15-m pixels), Advanced Spaceborne Thermal Emission and Reflection Radiometer (ASTER) (15-m pixels, stereoscopic capability; and 14 spectral bands on three sensors), and IKONOS (1-m pixels)] and the surface profile and elevation data to be acquired by ICESat (±1 m) after its planned launch in December 2002, will provide glaciologists with additional remote sensing datasets. The Global Land Ice Measurements from Space (GLIMS) is using ASTER and other satellite images to foster increased cooperation between regional centers.

The work in the Yukon Territory, by teams from the University of British Columbia and Ottawa University, will likely continue, but continued research may well be in doubt when the principal investigators retire. In the Arctic, the continuation of some of the smaller expeditions, on Axel Heiberg and Ellesmere Islands, is also in doubt. The Polar Continental Shelf Project provided the logistical support that has enabled scientists to work in remote areas of Nunavut for the last 40 years. Fortunately, the GSC's ice-coring project has been receiving sufficient support to continue acquiring data from existing core sites and even to obtain a new core from the Penny Ice Cap [168]. In 1998 and 1999, new ice cores to bedrock were obtained from Devon Island.

Looking to the future, it seems likely that water will return to the national agenda early in the 21st century. Recently there has been renewed public discussion in Canada about water exports. The gradual depletion of mountain reservoirs as the climate warms will alter not only the amount but also the timing of discharges. The switch from a glacial to a nival regime in some prairie rivers may adversely affect agriculture. The depletion of resources in central British Columbia potentially could lead to water-transfer disputes with the United States as flow in the Columbia River declines. If a warming climate creates more demand for energy, the hydroelectric-generating companies may be obliged to revisit some of their earlier proposals. All of these situations involve glaciers and may lead to the restoration of some previous studies and the initiation of new ones. However, as qualified and experienced scientists retire, a new generation of glaciologists will need to be trained.

Interest in past and present climates is expected to continue and even increase. Impact and adaptation studies funded by the Government of Canada's Climate Change Action Fund indicate renewed interest in water resources, including glacier hydrology. The Canadian CRYSYS (Cryospheric Systems Research Initiative), a Canadian contribution to the National Aeronautics and Space Administration Earth Observing System (EOS) Program, includes a glacier/ice cap theme as part of a government/university partnership. In the first decade of the 21st century, we will probably see a redrilling on the Agassiz Ice Cap [139]. Additional drilling programs are in the planning stage for Barnes Ice Cap, Baffin Island, and on Mt. Oxford, Ellesmere Island, Nunavat. After a long and patient wait we can also expect Trapridge Glacier [4] to surge and, thanks to all the preparatory work that has been done by Garry Clarke and his colleagues, to provide valuable new insights into the mechanism of surging glaciers, perhaps finally answering the question "why do some glaciers surge and what are the process(es) that cause some glaciers to surge?"

A promising recent development has been the establishment of a National Glaciology Programme (NGP) in the Terrain Sciences Division, Geological Survey of Canada (GSC), Natural Resources Canada. In 2001, a new ice core from a glacier on Mount Logan was obtained as part of this program. The NGP of the GSC also provides a national correspondent (Canada) to the World Glacier Monitoring Service, Zürich, Switzerland, who is responsible for the annual submission of glaciological data, including fluctuation of glaciers in Canada, and mass-balance data from the Place, Peyto, Helm, and White Glaciers. Glaciologists with the NGP (GSC) and the International Glaciological Society (Cambridge, England, U.K.) also provided information for the special issue of Canadian Geographic on Canada's glaciers (Anonymous, 1998), including a fold-out map on the Glaciers of Canada (Shilts and others, 1998).

References Cited

Adam, S., Toutin, T., Pietroniro, Alain, and Brugman, Melinda, 1997, Using ortho-rectified SAR imagery acquired over rugged terrain for thematic applications in glacier hydrology: Canadian Journal of Remote Sensing, v. 23, no. 1, p. 76–80.

Adams, W.P., 1966, Ablation and run-off on the White Glacier, Axel Heiberg Island, Canadian Arctic Archipelago: Montréal, Québec, McGill University, Axel Heiberg Island Research Reports, Glaciology No. 1, 77 p.

Adams, W.P., and Ecclestone, M.A., 1991, Mass balance measurements on Baby Glacier, Axel Heiberg Island, NWT, Canada, 1959–present, for the record: Eastern Snow Conference, 48th Annual Meeting, Guelph, Ontario, 5–7 June 1991, Proceedings, p. 317–324.

Adams, W.P., Cogley, J.G., and Ecclestone, M.A., 1995, The equilibrium zone on polar glaciers: Eastern Snow Conference, 52nd Annual Meeting, Toronto, Ontario, 6–8 June 1995, Proceedings, p. 211–219.

Adams, W.P., Cogley, J.G., Ecclestone, M.A., and Demuth, M.N., 1998, A small glacier as an index of regional mass balance—Baby Glacier, Axel Heiberg Island, 1959–1992: Geografiska Annaler, v. 80A, no. 1, p. 37–50.

Adkins, C.J., 1958, The summer climate in the accumulation area of the Salmon Glacier: Journal of Glaciology, v. 3, no. 23, p. 195–206.

———1959, Measurement of the atmospheric potential gradient on a Canadian glacier: Quarterly Journal of the Royal Meteorological Society, v. 85, no. 363, p. 60–67.

Alean, Jürg, and Müller, Fritz, 1977, Zum Massenhaushalt des Baby Glacier, Axel Heiberg Island, kanadische Hocharktis: Geographica Helvetica, v. 32, no. 4, p. 203–208.

Alt, B.T., 1978, Synoptic climate controls of mass-balance variations on Devon Island Ice Cap: Arctic and Alpine Research, v. 10, no. 1, p. 61–80.

———1979, Investigation of summer synoptic climate controls on the mass balance of Meighen Ice Cap: Atmosphere-Ocean, v. 17, no. 3, p. 181–199.

———1985, 1550–1620: A period of summer accumulation in the Queen Elizabeth Islands: Ottawa, Ont., National Museums of Canada, National Museum of Natural Sciences, Syllogeus No. 55, p. 461–479.

———1987, Developing synoptic analogs for extreme mass balance conditions on Queen Elizabeth Island ice caps: Journal of Climate and Applied Meteorology, v. 26, no. 12, p. 1605–1623.

Alt, B.T., Fisher, D.A. and Koerner, R.M., 1992, Climatic conditions for the period surrounding the Tambora signal in ice cores from the Canadian High Arctic islands, *in* Harington, C.R., ed., The year without a Summer? World climate in 1816: Ottawa, Ont., Canadian Museum of Nature, p. 309–327.

Alt, B.T., Koerner, R.M., Fisher, D.A., and Bourgeois, J.C., 1985, Arctic climate during the Franklin era, as deduced from ice cores, *in* Sutherland, P.D., ed., The Franklin Era in Canadian Arctic history, 1845–1859: Ottawa, Ont., National Museum of Man, Archaeological Survey of Canada, Mercury Series Paper No. 131, p. 69–92.

Ambrose, J.W., ed., 1969, Papers presented at the Seminar on the Causes and Mechanics of Glacier Surges, St. Hilaire, Québec, Canada, September 10–11, 1968, and the Symposium on Surging Glaciers, Banff, Alberta, Canada, June 6–8, 1968: Canadian Journal of Earth Sciences, v. 6, no. 4, pt. 2, p. 807–1018.

Anderton, P.W., 1973, Structural glaciology of a glacier confluence, Kaskawulsh Glacier, Yukon Territory, Canada: Columbus, Ohio, Ohio State University, Institute of Polar Studies Report No. 26, 109 p.

Andrews, J.T., and Barry, R.G., 1972, Present and paleo-climatic influences on the glacierization and deglacierization of Cumberland Peninsula, Baffin Island, N.W.T., Canada: Durham, NC, U.S. Army Research Office, Final Report, Grant No. DA-AR0-D-31-124-70-G80, 220 p.

Andrews, J.T., and Miller, G.H., 1972, Quaternary history of northern Cumberland Peninsula, Baffin Island, N.W.T., Canada—Part IV. Maps of the present glaciation limits and lowest equilibrium line altitude for north and south Baffin Island: Arctic and Alpine Research, v. 4, no. 1, p. 45–59.

Andrews, J.T., and Webber, P.J., 1969, Lichenometry to evaluate changes in glacial mass budgets, as illustrated from north-central Baffin Island, N.W.T: Arctic and Alpine Research, v. 1, no. 3, p. 181–194.

Andrews, J.T., Barry, R.G., and Drapier, Lyn, 1970, An inventory of the present and past glacierization of Home Bay and Okoa Bay, east Baffin Island, N.W.T., Canada, and some climatic and paleoclimatic considerations: Journal of Glaciology, v. 9, no. 57, p. 337–362.

Andrews, R.H.G., 1964, Meteorology and heat balance of the ablation area, White Glacier, Canadian Arctic Archipelago—summer 1960 (Lower Ice Station: 79°26' N., 90°39' W., 208 m): Montréal, Québec, McGill University, Axel Heiberg Island Research Reports, Meteorology No. 1, 107 p.

Andrieux, Pierre, 1970, Les méthodes électriques de prospection, appliquées à l'étude de la glace et des glaciers—résultats obtenus de 1962 à 1965: Paris, Comité National Français des Recherches Antarctiques, Institut Géographique National, Rapport No. 24, 62 p.

Anonymous, 1967, Hydrology of the Lewis Glacier, north-central Baffin Island, N.W.T., and discussion of reliability of the measurements: Geographical Bulletin, v. 9, no. 3, p. 232–261.

Anonymous, 1998, Rivers of ice: Canadian Geographic, v. 118, no. 7, p. 34–39.

Apollonio, Spencer, 1962, The Devon Island Expedition, 1960–64: Arctic, v. 15, no. 4, p. 317–321.

Arendt, Anthony, 1997, Mass balance modelling of an Arctic glacier: M.Sc. thesis, Edmonton, Alberta, University of Alberta., 222 p.

Arnold, K.C., 1965, Aspects of the glaciology of Meighen Island, Northwest Territories, Canada: Journal of Glaciology, v. 5, no. 40, p. 399–410.

———1981, Ice ablation measured by stakes and terrestrial photogrammetry—A comparison on the lower part of the White Glacier, Axel Heiberg Island, Canadian Arctic Archipelago: Montréal, Québec, McGill University, Axel Heiberg Island Research Reports, Glaciology No. 2, 98 p. and maps.

Baird, P.D., 1952a, The Baffin Island Expedition, 1950: Geographical Journal, v. 118, pt. 3, p. 267–279.

———1952b, The glaciological studies of the Baffin Island Expedition, 1950. Part I, Method of nourishment of the Barnes Ice Cap: Journal of Glaciology, v. 2, no. 11, p. 2–9, 17–19.

Baird, P.D., and Salt, D.J., 1949, Report on Expedition Snow Cornice: Ottawa, Ont., National Research Council of Canada (NRCC 2034), Associate Committee on Soil and Snow Mechanics, Technical Memorandum No. 14, p. 1–13.

Baird, P.D., and others, 1950, Baffin Island Expedition, 1950—A preliminary report: Arctic, v. 3, no. 3, p. 131–149.

———1953, Baffin Island expedition 1953—A preliminary field report: Arctic, v. 6, no. 4, p. 226–251.

Bajewsky, Ingrid, and Gardner, J.S., 1989, Discharge and sediment-load characteristics of the Hilda Rock-Glacier stream, Canadian Rocky Mountains, Alberta: Physical Geography, v. 10, no. 4, p. 295–306.

Barnett, D.M., and Holdsworth, Gerald, 1974, Origin, morphology, and chronology of sublacustrine moraines, Generator Lake, Baffin Island, Northwest Territories, Canada: Canadian Journal of Earth Sciences, v. 11, no. 3, p. 380–408.

Barrie, L.A., Fisher, D.[A.], and Koerner, R.M., 1985, Twentieth century trends in Arctic air pollution revealed by conductivity and acidity observations in snow and ice in the Canadian High Arctic: Atmospheric Environment, v. 19, no. 12, p. 2055–2063.

Barsch, Dietrich, and King, Lorenz, 1981, Ergebnisse der Heidelberg-Ellesmere Island Expedition (Results of the Heidelberg Ellesmere Island Expedition): Heidelberger Geographische Arbeiten, v. 69, 573 p. and map.

Bayrock, L.A., 1967, Catastrophic advance of the Steele Glacier, Yukon, Canada: Edmonton, Alberta, University of Alberta, Boreal Inst., Occasional Paper No. 3, 35 p.

Begley, S., and White, B., 1986, Alaska's runaway glacier: Newsweek, v. 108, no. 8, p. 52–53.

Berger, Peter, and Müller, Fritz, 1977, Massenhaushalt des Laika Glacier, Coburg Island, kanadischer arktischer Archipel: Geographica Helvetica, v. 32, no. 4, p. 209–212.

Binda, G.G., 1984, Fluvioglacial sediment and hydrochemical dynamics, Peyto Glacier, Alberta: M.A. thesis, Ottawa, Ont., University of Ottawa, Department of Geography, 139 p.

Binda, G.G., Johnson, P.G., and Power, J.M., 1985, Glacier control of suspended-sediment and solute loads in a Rocky Mountain basin, *in* Water quality evolution within the hydrological cycle of watersheds, Québec, Québec, 10–12 June 1984, Proceedings of the Canadian Hydrology Symposium No. 15, v. 1: Ottawa, Ont., National Research Council of Canada (NRCC 24633), Associate Committee on Hydrology, p. 309–327.

Blachut, S.P., and McCann, S.B., 1981, The behaviour of a polar ice-dammed lake, Ellesmere Island, N.W.T., Canada: Arctic and Alpine Research, v. 13, no. 1, p. 63–74.

Blake, E.W., 1992, The deforming bed beneath a surge-type glacier—Measurement of mechanical and electrical properties: Ph.D. thesis, Vancouver, B.C., University of British Columbia, 179 p.

Blake, E.W., and Clarke, G.K.C., 1991, Correspondence. Subglacial water and sediment samplers: Journal of Glaciology, v. 37, no. 125, p. 188–190.

———1992, Interpretation of borehole-inclinometer data—A general theory applied to a new instrument: Journal of Glaciology, v. 38, no. 128, p. 113–124.

Blake, E.[W.], Clarke, G.K.C., and Gérin, M.C., 1992, Tools for examining subglacial bed deformation: Journal of Glaciology, v. 38, no. 130, p. 388–396.

Blake, E.W., Wake, C.P., and Gerasimoff, M.D., 1998, The ECLIPSE drill—A field-portable intermediate-depth ice-coring drill: Journal of Glaciology, v. 44, no. 146, p. 175–178.

Blake, W.P., 1867, The glaciers of Alaska, Russian America: American Journal of Science, 2nd Series, no. 44, p. 96–101.

Blatter, Heinz, 1987a, On the thermal regime of an Arctic valley glacier—A study of White Glacier, Axel Heiberg Island, N.W.T., Canada: Journal of Glaciology, v. 33, no. 114, p. 200–211.

———1987b, Stagnant ice at the bed of White Glacier, Axel Heiberg Island, N.W.T., Canada: Annals of Glaciology, v. 9, p. 35–38.

Blatter, Heinz, and Hutter, Kolumban, 1991, Polythermal conditions in Arctic glaciers: Journal of Glaciology, v. 37, no. 126, p. 261–269.

Blatter, Heinz, and Kappenberger, Giovanni, 1988, Mass balance and thermal regime of Laika ice cap, Coburg Island, N.W.T., Canada: Journal of Glaciology, v. 34, no. 116, p. 102–110.

Blown, Iain, and Church, Michael, 1985, Catastrophic lake drainage within the Homathko River basin, British Columbia: Canadian Geotechnical Journal, v. 22, no. 4, p. 551–563.

Bourgeois, J.C., 1986, A pollen record from the Agassiz Ice Cap, northern Ellesmere Island, Canada: Boreas, v. 15, no. 4, p. 345–354.

———1990, Seasonal and annual variation of pollen content in the snow of a Canadian High Arctic ice cap: Boreas, v. 19, no. 4, p. 313–322.

Bradley, C., 1990, Water quality dynamics in meltwaters draining Peyto Glacier, Alberta: M.A. thesis, Waterloo, Ont., Wilfrid Laurier University, Department of Geography, 133 p.

Bradley, R.S., 1975, Equilibrium-line altitudes, mass balance, and July freezing-level heights in the Canadian High Arctic: Journal of Glaciology, v. 14, no. 71, p. 267–274.

Bradley, R.S., and England, John, 1977, Past glacial activity in the High Arctic: Amherst, MA, University of Massachusetts, Department of Geology and Geography, Contribution No. 31, 184 p.

Bradley, R.S., and England, John, 1978a, Recent climatic fluctuations of the Canadian High Arctic and their significance for glaciology: Arctic and Alpine Research, v. 10, no. 4, p. 715–731.

———1978b, Volcanic dust influence on glacier mass balance at high latitudes: Nature, v. 271, no. 5647, p. 736–738.

Bradley, R.S., and Serreze, M.C., 1987a, Mass balance of two High Arctic plateau ice caps: Journal of Glaciology, v. 33, no. 113, p. 123–128.

———1987b, Topoclimatic studies of a High Arctic plateau ice cap: Journal of Glaciology, v. 33, no. 114, p. 149–158.

Braithwaite, R.J., 1981, On glacier energy balance, ablation, and air temperature: Journal of Glaciology, v. 27, no. 97, p. 381–391.

Branson, D., 1984., Magnitude and characteristics of ablation on four Torngat glaciers: B.A. honours thesis, St. John's, Newfoundland, Memorial University of Newfoundland, Department of Geography.

Brecher, H.H., 1966, Surface velocity measurements on the Kaskawulsh Glacier, Yukon Territory, Canada: Columbus, Ohio, Ohio State University, Institute of Polar Studies Report No. 21, 73 p.

Brugman, M.M., 1991, Scale dependent albedo variations and runoff from a glacierized Alpine basin, *in* Snow, hydrology and forests in high alpine areas, Proceedings of the Vienna Symposium, 11–24 August 1991: IAHS Publication No. 205, p. 61–71.

Brugman, M.M., Pietroniro, Alain, and Shi, Jiancheng, 1996, Mapping alpine snow and ice using Landsat TM and SAR imagery at Wapta Icefield: Canadian Journal of Remote Sensing, v. 22, no. 1, p. 127–129.

Brunger, A.G., Nelson, J.G., and Ashwell, I.Y., 1967, Recession of the Hector and Peyto Glaciers—Further studies in the Drummond Glacier, Red Deer River valley area, Alberta: Canadian Geographer, v. 11, no. 1, p. 35–48.

Burgess, D., Sharp, M., and Mair, D., 2001, Dynamics and volumetric changes of ice caps: Ice, no. 125, p. 15.

Bushnell, V.C., and Marcus, M.G., 1974, Icefield Ranges Research Project scientific results, v. 4: Montréal, Québec, Arctic Institute of North America and American Geographical Society, New York, 385 p.

Bushnell, V.C., and Ragle, R.H., 1969, Icefield Ranges Research Project scientific results, v. 1: Montréal, Québec, Arctic Institute of North America and American Geographical Society, New York, 224 p.

———1970, Icefield Ranges Research Project scientific results, v. 2: Montréal, Québec, Arctic Institute of North America and American Geographical Society, New York, 138 p.

———1972, Icefield Ranges Research Project scientific results, v. 3: Montréal, Québec, Arctic Institute of North America and American Geographical Society, New York, 259 p.

Cameron, R.L., 1976, Glaciological studies in the St. Elias Mountains, Alaska—Yukon Territory, 1968: Washington, D.C., National Geographic Society Research Reports 1968, v. 9, p. 57–59.

Campbell, P.I., Reid, I.A., and Shastal, John, 1969a, Glacier surveys in Alberta: Ottawa, Ont., Department of Energy, Mines and Resources, Water Survey of Canada, Inland Waters Branch Report Series No. 4, 16 p.

———1969b, Glacier surveys in British Columbia: Ottawa, Ont., Department of Energy, Mines and Resources, Water Survey of Canada, Inland Waters Branch Report Series No. 5, 18 p.

Canada, 1976, 1974–1976 survey of the Athabasca and Saskatchewan glaciers: Calgary, Alberta, Environment Canada, Western Region, Inland Waters Directorate, Calgary District Office, Water Survey of Canada, Internal report, 36 p.

———1977, Report on the influence of glaciers on the hydrology of streams affecting the proposed Alcan pipeline route: Vancouver, B.C., Fisheries and Environment Canada, Pacific Region, Inland Waters Directorate submitted by Glaciology Division, Unpublished report, pt. 1, 38 p., appendices, map and bibliography, 54 p.

———1982, 1978–1980 Survey of the Athabasca and Saskatchewan glaciers: Calgary, Alberta, Environment Canada, Western and Northern Region, Inland Waters Directorate, Calgary District Office, Water Survey of Canada, Internal report, 36 p.

———1990, Detailed review comments on the Windy Craggy Stage I environmental and socioeconomic impact assessment (January 1990): Vancouver, B.C., Environment Canada, Environmental Protection, Conservation and Protection, 114 p.

Cavell, Edward, 1983, Legacy in ice—The Vaux family and the Canadian Alps: Banff, Alberta, Altitude Publishing, Peter and Catharine Whyte Foundation, 98 p.

Champoux, André, and Ommanney, C.S.L., 1986a, Evolution of the Illecillewaet Glacier, Glacier National Park, B.C., using historical data, aerial photography and satellite image analysis: Annals of Glaciology, v. 8, p. 31–33.

———1986b, Photo-interpretation, digital mapping, and the evolution of glaciers in Glacier National Park, B.C: Annals of Glaciology, v. 8, p. 27–30.

Cialek, C.J., 1977, The Cathedral Massif, Atlin Provincial Park, British Columbia: Department of Geography, Michigan State University, sponsored by the Foundation for Glacier and Environmental Research, Pacific Science Center, Seattle, Washington, map, scale 1:20,000, contour interval 100 feet.

Clague, J.J., and Evans, S.G., 1994, Formation and failure of natural dams in the Canadian Cordillera: Geological Survey of Canada Bulletin No. 464, 35 p.

Clague, J.J., Evans, S.G., and Blown, I.G., 1985, A debris flow triggered by the breaching of a moraine-dammed lake, Klattasine Creek, British Columbia: Canadian Journal of Earth Sciences, v. 22, no. 10, p. 1492–1502.

Clarke, G.K.C., 1967, Geophysical measurements on the Kaskawulsh and Hubbard Glaciers, Yukon Territory: Montréal, Québec, Arctic Institute of North America, Technical Paper No. 20, 36 p.

———[1971], Temperature measurements in Fox Glacier, Yukon Territory, *in* Glaciers, Proceedings of IHD Workshop Seminar 1970, Vancouver, B.C., 24–25 September 1970: Ottawa, Ont., Canadian National Committee for the I.H.D., p. 47–48.

———1976, Thermal regulation of glacier surging: Journal of Glaciology, v. 16, no. 74, p. 231–250.

———1982, Glacier outburst floods from "Hazard Lake," Yukon Territory, and the problem of flood magnitude prediction: Journal of Glaciology, v. 28, no. 98, p. 3–21.

———1991, Length, width and slope influences on glacier surging: Journal of Glaciology, v. 37, no. 126, p. 236–246.

———1996, Lumped-element analysis of subglacial hydraulic circuits: Journal of Geophysical Research, v. 101, no. B8, p. 17,547–17,559.

Clarke, G.K.C., and Blake, E.W., 1991, Geometric and thermal evolution of a surge-type glacier in its quiescent state—Trapridge Glacier, Yukon Territory, Canada, 1969–89: Journal of Glaciology, v. 37, no. 125, p. 158–169.

Clarke, G.K.C., and Collins, S.G., 1984, The 1981–1982 surge of Hazard Glacier, Yukon Territory: Canadian Journal of Earth Sciences, v. 21, no. 3, p. 297–304.

Clarke, G.K.C., and Goodman, R.H., 1975, Radio echo soundings and ice-temperature measurements in a surge-type glacier: Journal of Glaciology, v. 14, no. 70, p. 71–78.

Clarke, G.K.C., and Jarvis, G.T., 1976, Post-surge temperatures in Steele Glacier, Yukon Territory, Canada: Journal of Glaciology, v. 16, no. 74, p. 261–268.

Clarke, G.K.C., and Mathews, W.H., 1981, Estimates of the magnitude of glacier outburst floods from Lake Donjek, Yukon Territory, Canada: Canadian Journal of Earth Sciences, v. 18, no. 9, p. 1452–1463.

Clarke, G.K.C., and Waddington, E.D., 1991, A three-dimensional theory of wind pumping: Journal of Glaciology, v. 37, no. 125, p. 89–96.

Clarke, G.K.C., and Waldron, D.A., 1984, Simulation of the August 1979 sudden discharge of glacier-dammed Flood Lake, British Columbia: Canadian Journal of Earth Sciences, v. 21, no. 4, p. 502–504.

Clarke, G.K.C., Collins, S.G., and Thompson, D.E., 1984, Flow, thermal structure, and subglacial conditions of a surge-type glacier: Canadian Journal of Earth Sciences, v. 21, no. 2, p. 232–240.

Clarke, G.K.C., Meldrum, R.D., and Collins, S.G., 1986a, Measuring glacier-motion fluctuations using a computer-controlled survey system: Canadian Journal of Earth Sciences, v. 23, no. 5, p. 727–733.

Clarke, G.K.C., Schmok, J.P., Ommanney, C.S.L., and Collins, S.G., 1986b, Characteristics of surge-type glaciers: Journal of Geophysical Research, v. 91, no. B7, p. 7165–7180.

Classen, D.F., 1977, Temperature profiles for the Barnes Ice Cap surge zone: Journal of Glaciology, v. 18, no. 80, p. 391–405.

Classen, D.F., and Clarke, G.K.C., 1971, Basal hot spot on a surge type glacier: Nature, v. 229, no. 5285, p. 481–483.

Clee, T.E., Savage, J.C., and Neave, K.G., 1969, Internal friction in ice near its melting point: Journal of Geophysical Research, v. 74, no. 4, p. 973–980.

Cochran, G. van B., 1978, Virginia Glacier Expedition 1977: Canadian Alpine Journal, v. 61, p. 36–38.

Cogley, J.G., 2001, Glaciers of the Canadian High Arctic: Ice, no. 125, p. 15.

Cogley, J.G., Adams, W.P., Ecclestone, M.A., Jung-Rothenhäusler, Friedrich, and Ommanney, C.S.L., 1995, Mass balance of Axel Heiberg Island glaciers, 1960–1991—A reassessment and discussion: Saskatoon, Sask., Environment Canada, National Hydrology Research Institute, NHRI Science Report No. 6, 168 p.

———1996a, Mass balance of White Glacier, Axel Heiberg Island, N.W.T., Canada, 1960–1991: Journal of Glaciology, v. 42, no. 142, p. 548–563.

Cogley, J.G., Ecclestone, M.A., and Adams, W.P., 1996b, Fluctuations of the terminuses of White and Thompson Glaciers, Axel Heiberg Island, N.W.T., Canada: Eastern Snow Conference, 53rd Annual Meeting, Williamsburg, Virginia, 1–3 May 1996, Proceedings, p. 83–94.

Coleman, A.P., 1921, Glaciers of the Rockies and Selkirks (2d ed.): Ottawa, Ont., Department of the Interior, Dominion Parks Branch, 36 p.

Collier, E.P., 1958, Glacier variation and trends in run-off in the Canadian Cordillera, *in* General Assembly of Toronto, v. 4, September 3–14, 1957: Association Internationale d'Hydrologie Scientifique Publication No. 46, p. 344–357.

Collins, D.N., and Power, J.M., 1985, Meltwater provenance, hydrological pathways and hydrochemical processes in an alpine glacierised basin, *in* Water quality evolution within the hydrological cycle of watersheds, Québec, Québec, 10–12 June 1984, Proceedings of the Canadian Hydrology Symposium No. 15, v. 1: National Research Council of Canada (NRCC 24633), Associate Committee on Hydrology, p. 307–308.

Collins, D.N., and Young, G.J., 1979, Separation of runoff components in glacierized alpine watersheds by hydrochemical analysis, *in* Canadian Hydrology Symposium: 79—Cold Climate Hydrology, Vancouver, B.C., 10–11 May 1979, Proceedings: Ottawa, Ont., National Research Council of Canada (NRCC 17834), Associate Committee on Hydrology, p. 570–581.

———1981, Meltwater hydrology and hydrochemistry in snow- and ice-covered mountain catchments: Nordic Hydrology, v. 12, no. 4–5, p. 319–334.

Collins, I.F., 1970, A slip-line field analysis of the deformation at the confluence of two glacier streams: Journal of Glaciology, v. 9, no. 56, p. 169–193.

Collins, S.G., 1972, Survey of the Rusty Glacier area, Yukon Territory, Canada, 1967–70: Journal of Glaciology, v. 11, no. 62, p. 235–253.

———1980, Three surging glaciers, St. Elias Mountains, Canada: Washington, D.C., National Geographic Society Research Reports 1971, v. 12, p. 103–115.

Collins, S.G., and Clarke, G.K.C., 1977, History and bathymetry of a surge-dammed lake: Arctic, v. 30, no. 4, p. 217–224.

Crary, A.P., 1956, Geophysical studies along northern Ellesmere Island: Arctic, v. 9, no. 3, p. 155–165.

Cresswell, R.G., and Herd, R.K., 1991, Concentrations of cosmic spherules from the Devon Island ice cap, Devon Island, Northwest Territories [abs.], *in* Program with Abstracts, Geological Association of Canada and Mineralogical Association of Canada Joint Annual Meeting with Society of Economic Geologists, Toronto, Ontario, 27–29 May 1991, 16th: p. A27.

Cross, G.M., and Clarke, G.K.C., 1990, A waveform alignment approach to positioning airborne radar-sounding data: IEEE Transactions on Geoscience and Remote Sensing, v. 28, no. 1, p. 123–126.

Crossley, D.J., and Clarke, G.K.C., 1970, Gravity measurements on "Fox Glacier," Yukon Territory, Canada: Journal of Glaciology, v. 9, no. 57, p. 363–374.

Cutler, P.M., and Munro, D.S., 1996, Visible and near-infrared reflectivity during the ablation period on Peyto Glacier, Alberta, Canada: Journal of Glaciology, v. 42, no. 141, p. 333–340.

David, C.R., 1989, Hydrological regimes of nival and glacierized mountain basins, Yoho National Park, British Columbia: M.A. thesis, Ottawa, Ont., Ottawa University, Department of Geography, 127 p.

De la Barre, Kenneth, 1977, The Icefield Ranges Research Project, 1975 and 1976: Arctic, v. 30, no. 2, p. 130–132.

Demuth, M.N., ed., in press, Peyto Glacier—One century of science: Saskatoon, National Water Research Institute.

Demuth, M.N., Pietroniro, Alain, Hopkinson, C., and Sitar, M., 2001, Airborne LASER mapping of Wapta Icefield: Ice, no. 125, p. 14.

Denton, G.H., 1975a, Glaciers of the Canadian Rocky Mountains, *in* Field, W.O., ed., Mountain glaciers of the Northern Hemisphere, v. 1: Hanover, N.H., U.S. Army Cold Regions Research and Engineering Lab., p. 603–653.

———1975b, Glaciers of the Coast Mountains (Pacific Ranges and Cascade Mountains) and Coast Ranges of British Columbia, *in* Field, W.O., ed., Mountain glaciers of the Northern Hemisphere, v. 1: Hanover, N.H., U.S. Army Cold Regions Research and Engineering Lab., p. 671–687.

———1975c, Glaciers of the Interior Ranges of British Columbia, *in* Field, W.O., ed., Mountain glaciers of the Northern Hemisphere, v. 1: Hanover, N.H., U.S. Army Cold Regions Research and Engineering Lab., p. 655–670.

Derikx, Leo, 1973, Glacier discharge simulation by ground-water analogue, *in* Symposium on the Hydrology of Glaciers, Cambridge, 7–13 September, 1969: Association Internationale d'Hydrologie Scientifique Publication No. 95, p. 29–40.

———1975, The heat balance and associated runoff from an experimental site on a glacier tongue, *in* Snow and Ice Symposium, Moscow, August 1971, Proceedings: IAHS-AISH Publication No. 104, p. 59–69.

Derikx, Leo, and Loijens, H.[S.], 1971, Model of runoff from glaciers, *in* Runoff from snow and ice, Québec, 26–27 May 1971: National Research Council, Associate Committee on Geodesy and Geophysics, Subcommittee on Hydrology, Hydrology Symposium No. 8, v. 1, p. 153–199.

Desloges, J.R., and Church, Michael, 1992, Geomorphic implications of glacier outburst flooding—Noeick River valley, British Columbia: Canadian Journal of Earth Sciences, v. 29, no. 3, p. 551–564.

Desloges, J.R., Jones, D.P., and Ricker, K.E., 1989, Estimates of peak discharge from the drainage of ice-dammed Ape Lake, British Columbia, Canada: Journal of Glaciology, v. 35, no. 121, p. 349–354.

Dewart, Gilbert, 1968, Seismic investigation of ice properties and bedrock topography at the confluence of two glaciers, Kaskawulsh Glacier, Yukon Territory, Canada: Columbus, Ohio, Ohio State University, Institute of Polar Studies Report No. 27, 207 p.

Dibb, J.E., Rasmussen, R.A., Mayewski, P.A., and Holdsworth, Gerald, 1993, Northern Hemisphere concentrations of methane and nitrous oxide since 1800—Results from the Mt. Logan and 20D ice cores: Chemosphere, v. 27, no. 12, p. 2413–2423.

Dicks, W., Adams, W.P., and Ecclestone, M.[A.], 1992, Mass balance and ablation season processes, Baby Glacier, Axel Heiberg Island, N.W.T: Musk-ox, v. 39, p. 15–23.

Doake, C.S.M., Gorman, M.[R.], and Paterson, W.S.B., 1976, A further comparison of glacier velocities measured by radio-echo and survey methods: Journal of Glaciology, v. 17, no. 75, p. 35–38.

Doell, R.R., 1963, Seismic depth study of the Salmon Glacier, British Columbia: Journal of Glaciology, v. 4, no. 34, p. 425–437.

Dorrer, Egon, 1971, Movement of the Ward Hunt Ice Shelf, Ellesmere Island, N.W.T., Canada: Journal of Glaciology, v. 10, no. 59, p. 211–225.

Dowdeswell, J.A., 1986, The distribution and character of sediments in a tidewater glacier, southern Baffin Island, N.W.T., Canada: Arctic and Alpine Research, v. 18, no. 1, p. 45–56.

Duchemin, Marc, and Seguin, M.K., 1998, Modeling and simulation of Illecillewaet watershed, southeastern British Columbia, Canada [abs.]: EOS, Transactions, American Geophysical Union, v. 79, no. 45, Fall Meeting Supplement, p. F353.

Dunbar, Moira, and Greenaway, K.R., 1956, Arctic Canada from the air: Ottawa, Ont., Queen's Printer, Defence Research Board, 541 p.

Eagan, C.P., 1963, Résumé of the 1962 field season of the Michigan State University Glaciological Institute, Juneau Icefield, Alaska: Compass of Sigma Gamma Epsilon, v. 41, no. 1, p. 61–69.

Epstein, Samuel, and Sharp, R.P., 1959, Oxygen-isotope variations in the Malaspina and Saskatchewan Glaciers: Journal of Geology, v. 67, no. 1, p. 88–102.

Evans, D.J.A., 1989, The nature of glacitectonic structure and sediments at sub-polar glacier margins, northwest Ellesmere Island, Canada: Geografiska Annaler, v. 71A, no. 3–4, p. 113–123.

———1993, High-latitude rock glaciers—A case study of forms and processes in the Canadian Arctic: Permafrost and Periglacial Processes, v. 4, no. 1, p. 17–35.

Evans, D.J.A., and England, John, 1992, Geomorphological evidence of Holocene climatic change from northwest Ellesmere Island, Canadian High Arctic: Holocene, v. 2, no. 2, p. 148–158.

Evans, D.J.A., and Fisher, T.G., 1987, Evidence of a periodic ice-cliff avalanche on north-west Ellesmere Island, N.W.T., Canadian High Arctic: Journal of Glaciology, v. 33, no. 113, p. 68–71.

Evans, S.G., 1986, The maximum discharge of outburst floods caused by breaching of man-made and natural dams: Canadian Geotechnical Journal, v. 23, no. 3, p. 385–387.

Evans, S.G., and Clague, J.J., 1990, Reconnaissance observations on the Tim Williams Glacier rock avalanche, near Stewart, British Columbia: Geological Survey of Canada Paper No. 90–1E, p. 351–354.

Evans, Stanley, and Robin, G. de Q., 1966, Glacier depth-sounding from the air: Nature, v. 210, no. 5039, p. 883–885.

Eyles, Nicholas, and Rogerson, R.J., 1977a, Artificially induced thermokarst in active glacier ice—An example from northwest British Columbia, Canada: Journal of Glaciology, v. 18, no. 80, p. 437–444.

———1977b, Glacier movement, ice structures, and medial moraine form at a glacier confluence, Berendon Glacier, British Columbia: Canadian Journal of Earth Sciences, v. 14, no. 12, p. 2807–2816.

———1977c, How to save your mine from a glacier: Canadian Mining Journal, v. 98, no. 7, p. 32.

———1978a, A framework for the investigation of medial moraine formation—Austerdalsbreen, Norway, and Berendon Glacier, British Columbia, Canada: Journal of Glaciology, v. 20, no. 82, p. 99–113.

———1978b, Sedimentology of medial moraines on Berendon Glacier, British Columbia, Canada—Implications for debris transport in a glacierized basin: Geological Society of America Bulletin, v. 89, no. 11, p. 1688–1693.

Eyles, Nicholas, Sasseville, D.R., Slatt, R.M., and Rogerson, R.J., 1982, Geochemical denudation rates and solute transport mechanisms in a maritime temperate glacier basin: Canadian Journal of Earth Sciences, v. 19, no. 8, p. 1570–1581.

Faber, Th., 1973, Rusty Glacier basin, Yukon Territory, Canada—Results of the 1968 hydrological field work [abs.], *in* Symposium on the Hydrology of Glaciers, Cambridge, 7–13 September, 1969: Association Internationale d'Hydrologie Scientifique Publication No. 95, p. 197.

Fahn, C., 1975, Glaciers of northern Labrador, *in* Field, W.O., ed., Mountain glaciers of the Northern Hemisphere, v. 2: Hanover, N.H., U.S. Army Cold Regions Research and Engineering Lab., p. 673–682.

Faig, Wolfgang, 1966, Photogrammetry applied to Arctic glacier surveys: Ottawa, Ont., Department of National Defence, Defence Research Board, Operation Hazen Report D Phys R(G) Hazen 27, 56 p.

Falconer, G., 1962, Glaciers of northern Baffin and Bylot Islands, N.W.T.: Ottawa, Canada Department of Energy, Mines and Resources, Technical Surveys, Geographical Branch, Geographical Paper 33, 31 p.

Field, W.O., Jr., 1949, Glacier observations in the Canadian Rockies, 1948: Canadian Alpine Journal, v. 32, p. 99–114.

———1975a, Glaciers of the Coast Mountains—Boundary Ranges (Alaska, British Columbia, and Yukon Territory), *in* Field, W.O., ed., Mountain glaciers of the Northern Hemisphere, v. 2: Hanover, N.H., U.S, Army Cold Regions Research and Engineering Lab., p. 11–141.

———1975b, Glaciers of the St. Elias Mountains, *in* Field, W.O., ed., Mountain glaciers of the Northern Hemisphere, v. 2: Hanover, N.H., U.S. Army Cold Regions Research and Engineering Lab., p. 143–297.

———1975c, Mountain glaciers of the Northern Hemisphere: Hanover, N.H., American Geographical Society. U.S. Army Cold Regions Research and Engineering Lab., v. 1, 698 p., v. 2, 932 p., atlas, 49 plates.

———1990, Glaciers of Alaska and adjacent Yukon Territory and British Columbia: American Alpine Journal, v. 32, no. 64, p. 79–149.

Field, W.O., Jr., and Heusser, C.J., 1954, Glacier and botanical studies in the Canadian Rockies, 1953: Canadian Alpine Journal, v. 37, p. 128–140.

Field, W.O., Jr., and Miller, M.M., 1950, The Juneau Ice Field research project: Geographical Review, v. 40, no. 2, p. 179–190.

Fischer, U.H., and Clarke, G.K.C., 1994, Ploughing of subglacial sediment: Journal of Glaciology, v. 40, no. 134, p. 97–106.

———1997, Stick-slip sliding behaviour at the base of a glacier: Annals of Glaciology, v. 24, p. 390–396.

Fisher, D.[A.], 1973, Subglacial leakage of Summit Lake, British Columbia, by dye determinations, *in* Symposium on the Hydrology of Glaciers, Cambridge, 7–13 September, 1969: Association Internationale d'Hydrologie Scientifique Publication No. 95, p. 111–116.

———1979, Comparison of 105 years of oxygen isotope and insoluble impurity profiles from the Devon Island and Camp Century ice cores: Quaternary Research, v. 11, no. 3, p. 299–305.

———1987, Enhanced flow of Wisconsin ice related to solid conductivity through strain history and recrystallization, *in* Symposium on the Physical Basis of Ice Sheet Modelling, Vancouver, British Columbia, Canada, 9–22 August, 1987, Proceedings: IASH Publication No. 170, p. 45–51.

Fisher, D.[A.], 1991, Remarks on the deuterium excess in precipitation in cold regions: Tellus, Series B., Chemical and Physical Meteorology, v. 43B, no. 5, p. 401–407.

———1992, Possible ice-core evidence for a fresh melt water cap over the Atlantic Ocean in the Early Holocene, *in* Bard, Edouard, and Broecker, W.S., eds., The last deglaciation—Absolute and radiocarbon chronologies: Berlin, Springer-Verlag, NATO ASI Series I: Global Environmental Change No. 2, p. 267–293.

Fisher, D.A., and Jones, S.J., 1971, The possible future behaviour of Berendon Glacier, Canada—A further study: Journal of Glaciology, v. 10, no. 58, p. 85–92.

Fisher, D.A., and Koerner, R.M., 1981, Some aspects of climatic change in the High Arctic during the Holocene as deduced from ice cores, *in* Mahaney, W.C., ed., Quaternary paleoclimate, Proceedings of Fourth Conference on Quaternary Research, Toronto, Ontario, 18–20 May 1979: Norwich, U.K., Geo Abstracts Ltd., p. 249–271.

———1986, On the special rheological properties of ancient microparticle-laden Northern Hemisphere ice as derived from bore-hole and core measurements: Journal of Glaciology, v. 32, no. 112, p. 501–510.

———1988, The effects of wind on $\delta(^{18}O)$ and accumulation give an inferred record of seasonal δ amplitude from the Agassiz Ice Cap, Ellesmere Island, Canada: Annals of Glaciology, v. 10, p. 34–37.

———1994, Signal and noise in four ice-core records from the Agassiz Ice Cap, Ellesmere Island, Canada—Details of the last millennium for stable isotopes, melt and solid conductivity: Holocene, v. 4, no. 2, p. 113–120.

Fisher, D.A., Koerner, R.M., Paterson, W.S.B., Dansgaard, Willi, Gundestrup, N.[S.], and Reeh, Niels, 1983, Effect of wind scouring on climatic records from ice-core oxygen-isotope profiles: Nature, v. 301, no. 5897, p. 205–209.

Fisher, D.A., Koerner, R.M., Kuivinen, K.C., Clausen, H.B., Johnsen, S.J., Steffensen, J.P., Gundestrup, N.S., and Hammer, C.U., 1996, Inter-comparison of $\delta^{18}O$ and precipitation records from sites in Canada and Greenland over the last 3500 years and over the last few centuries in detail using EOF techniques, *in* Jones, P.D., Bradley, R.S., and Jouzel, Jean, eds., Climatic variations and forcing mechanisms of the last 2000 years: Berlin, Springer-Verlag, NATO ASI Series I: Global Environmental Change No. 41, p. 297–328.

Fisher, D.A., Koerner, R.M., Bourgeois, J.C., Zielinski, G., Wake, C.[P.], Hammer, C.U., Clausen, H.B., Gundestrup, N.[S.], Johnsen, S.[J.], Goto-Azuma, Kumiko, Hondoh, Takeo, Blake, E.[W.], and Gerasimoff, M.[D.], 1998, Penny Ice Cap cores, Baffin island, Canada, and the Wisconsinan Foxe Dome connection—Two states of Hudson Bay ice cover: Science, v. 279, no. 5351, p. 692–695.

Fisher, D.A., Reeh, Niels, and Clausen, H.B., 1985, Stratigraphic noise in time series derived from ice cores: Annals of Glaciology, v. 7, p. 76–83.

Flowers, G.E., and Clarke, G.K.C., 1999, Surface and bed topography of Trapridge Glacier, Yukon Territory, Canada—Digital elevation models and derived hydraulic geometry: Journal of Glaciology, v. 45, no. 149, p. 165–174.

Fogarasi, Stephen, 1981, Albedo survey on Andrei Glacier, Iskut River basin, B.C., midsummer, 1980: Ottawa, Ont., Environment Canada, Inland Waters Directorate, National Hydrology Research Institute Paper No. 15, 13 p.

Fogarasi, Stephen, and Mokievsky-Zubok, Oleg, 1978, Principal components analysis on glacier-climatological data for Sentinel Glacier, British Columbia: Ottawa, Ont., Fisheries and Environment Canada, Water Resources Branch, Inland Waters Directorate Scientific Series No. 95, 9 p.

———1987, An analysis of flow data from Sentinel Creek, British Columbia—Part 1: Saskatoon, Sask., Environment Canada, Surface Water Division, National Hydrology Research Institute Contribution No. 87012, 43 p.

Föhn, P.M.B., 1973, Short-term snow melt and ablation derived from heat- and mass-balance measurements: Journal of Glaciology, v. 12, no. 65, p. 275–289.

Forbes, Alexander, Miller, O.M., Odell, N.E., and Abbe, E.C., 1938, Northernmost Labrador mapped from the air: New York, N.Y., American Geographical Society, Special Publication No. 22, 255 p. and maps.

Gardner, J.S., 1977, The Wenkchemna Glacier: Canadian Alpine Journal, v. 60, p. 58–59.

———1978, Wenkchemna Glacier—Ablation complex and rock glacier in the Canadian Rocky Mountains: Canadian Journal of Earth Sciences, v. 15, no. 7, p. 1200–1204.

———1992, The zonation of freeze-thaw temperatures at a glacier headwall, Dome Glacier, Canadian Rockies, *in* Dixon, J.C., and Abrahams, A.D., eds., Periglacial geomorphology: Chichester, John Wiley and Sons, p. 89–102.

Gardner, J.S., and Bajewsky, Ingrid, 1987, Hilda rock glacier stream discharge and sediment load characteristics, Sunwapta Pass area, Canadian Rocky Mountains, *in* Giardino, J.R., Shroder, J.F., Jr., and Vitek, J.D., eds., Rock glaciers: London, Allen and Unwin, p. 161–174.

Gardner, J.S., and Jones, N.K., 1985, Evidence for a Neoglacial advance of the Boundary Glacier, Banff National Park, Alberta: Canadian Journal of Earth Sciences, v. 22, no. 11, p. 1753–1755.

Gemmell, A.M.D., Sharp, M.J., and Sugden, D.E., 1986, Debris from the basal ice of the Agassiz Ice Cap, Ellesmere Island, Arctic Canada: Earth Surface Processes and Landforms, v. 11, no. 2, p. 123–130.

Gilbert, Robert, 1971, Observations on ice-dammed Summit Lake, British Columbia, Canada: Journal of Glaciology, v. 10, no. 60, p. 351–356.

Glenday, P.J., 1989, Mass balance parameterization, White Glacier, Axel Heiberg Island, N.W.T., 1970–80: B.A. thesis, Peterborough, Ont., Trent University, Department of Geography, 120 p.

———1991, Determination of morphologic and volumetric change, Peyto Glacier, Alberta, 1966–1989: M.A. thesis, Waterloo, Ont., Wilfrid Laurier University, Department of Geography, 130 p.

Goodison, B.E., [1971], The relation between ablation and global radiation over Peyto Glacier, Alberta, *in* Glaciers, Proceedings of IHD Workshop Seminar 1970, Vancouver, B.C., 24–25 September 1970: Ottawa, Ont., Canadian National Committee for the I.H.D., p. 39–42.

Goodison, B.E., [1971], 1972a, An analysis of climate and runoff events for Peyto Glacier, Alberta: Ottawa, Ont., Environment Canada, Water Resources Branch, Inland Waters Directorate Scientific Series No. 21, 29 p.

———1972b, The distribution of global radiation over Peyto Glacier, Alberta: Ottawa, Ont., Environment Canada, Water Resources Branch, Inland Waters Directorate Scientific Series No. 22, 22 p.

Goodman, R.H., 1970, Radio-echo sounding on temperate glaciers—A Canadian view, *in* Gudmandsen, P., ed., Proceedings of the International Meeting on Radio Glaciology, May 1970: Lyngby, Technical University of Denmark, Lab. of Electromagnetic Theory, p. 135–146.

———1973, Time-dependent intraglacier structures: Journal of Glaciology, v. 12, no. 66, p. 512–513.

———1975, Radio echo sounding on temperate glaciers: Journal of Glaciology, v. 14, no. 70, p. 57–69.

Goodman, R.H., and Terroux, A.C.D., 1973, Use of radio-echo sounder techniques in the study of glacial hydrology [abs.], *in* Symposium on the Hydrology of Glaciers, Cambridge, 7–13 September 1969: Association Internationale d'Hydrologie Scientifique Publication No. 95, p. 149.

Goto-Azuma, Kumiko, Koerner, R.M., Nakawo, Masayoshi, and Kudo, Akira, 1997, Snow chemistry of Agassiz Ice Cap, Ellesmere Island, Northwest Territories, Canada: Journal of Glaciology, v. 43, no. 144, p. 199–206.

Gottlieb, Lars, 1980, Development and applications of a runoff model for snowcovered and glacierized basins: Nordic Hydrology, v. 11, no. 5, p. 255–272.

Gratton, D.J., Howarth, P.J., and Marceau, D.J., 1990, Combining DEM parameters with Landsat MSS and TM imagery in a GIS for mountain glacier characterization: IEEE Transactions on Geoscience and Remote Sensing, v. 28, no. 4, p. 766–769.

———1993, Using Landsat-5 Thematic Mapper and digital elevation data to determine the net radiation field of a mountain glacier: Remote Sensing of Environment, v. 43, no. 3, p. 315–331.

Green, W.S., 1890, Among the Selkirk glaciers—Being the account of a rough survey in the Rocky Mountain regions of British Columbia: London, Macmillan and Co., 251 p.

Gregor, D.J., 1992, Organic micropollutants in arctic snow and firn, *in* Woo, M.-k., and Gregor, D.J., eds., Arctic environment—Past, present and future, Proceedings of Symposium, Hamilton, Ontario, 14–15 November 1991: Hamilton, Ont., Department of Geography, McMaster University, p. 79–90.

Grumet, N.S., Wake, C.P., Zielinski, G.A., Fisher, D.[A.], Koerner, R.[M.], and Jacobs, J.D., 1998, Preservation of glaciochemical time series in snow and ice from the Penny Ice Cap, Baffin Island: Geophysical Research Letters, v. 25, no. 3, p. 357–360.

Guigné, J.-Y., 1975, Glacio-hydrological mass balance study of the Cathedral Massif Glacier system, 1975, Atlin, British Columbia, Canada: Seattle, WA, Foundation for Glacier and Environmental Research, Juneau Icefield Research Program, Internal Report, 69 p.

Haeberli, Wilfried, Hoelzle, Martin, and Frauenfelder, Regula, eds., 1999, Glacier mass balance bulletin: Zürich, World Glacier Monitoring Service, Bulletin No. 5 (1996–1997), p. 8.

Hallet, Bernard, 1976, The effect of subglacial chemical processes on glacier sliding: Journal of Glaciology, v. 17, no. 76, p. 209–221.

Hambrey, M.J., and Müller, Fritz, 1978, Structures and ice deformation in the White Glacier, Axel Heiberg Island, Northwest Territories, Canada: Journal of Glaciology, v. 20, no. 82, p. 41–66.

Hammer, K.M., and Smith, N.D., 1983, Sediment production and transport in a proglacial stream—Hilda Glacier, Alberta, Canada: Boreas, v. 12, no. 2, p. 91–106.

Hanson, Brian, 1987, Reconstructing mass-balance profiles from climate for an Arctic ice cap, *in* Symposium on The Physical Basis of Ice Sheet Modelling, Vancouver, British Columbia, Canada, 9–22 August 1987, Proceedings: IAHS Publication No. 170, p. 181–189.

———1990, Thermal response of a small ice cap to climatic forcing: Journal of Glaciology, v. 36, no. 122, p. 49–56.

Harmon, Don, and Robinson, Bart, 1981, Columbia Icefield—A solitude of ice: Banff, Alberta, Altitude Publishing Ltd., 103 p.

Harvey, L.D.D., 1988, Climatic impact of ice-age aerosols: Nature, v. 334, no. 6180, p. 333–335.

Hasenauer, R., 1984, Die Berechnung der Massenbilanz des Cathedral Glacier (Atlin region, B.C., Kanada) für die Jahre 1976/77 und 1977/78: Hausarbeit aus Geographie, Institut für Geographie, Universität Salzburg, Salzburg, Austria, 38 p.

Hattersley-Smith, Geoffrey, 1954, Glaciological reconnaissance in northern Ellesmere Island, *in* General Assembly of Rome, v. 4, 1954: Association Internationale d'Hydrologie Scientifique Publication No. 39, p. 229–235.

———1959, Research in the Lake Hazen region of northern Ellesmere Island in the International Geophysical Year: The Arctic Circular, v. 12, no. 1, p. 2–12.

———1960a, Glaciological studies—Snow cover, accumulation and ablation: Ottawa, Ont., Department of National Defence, Defence Research Board, Operation Hazen D Phys R(G) Hazen 10, 13 p.

———1960b, Studies of englacial profiles in the Lake Hazen area of northern Ellesmere Island: Journal of Glaciology, v. 3, no. 27, p. 610–625.

———1961, Glaciological studies on Gilman Glacier, progress report 1960: Ottawa, Ont., Department of National Defence, Defence Research Board, Operation Hazen D Phys R(G) Hazen 16, 13 p.

———1964, Rapid advance of glacier in northern Ellesmere Island: Nature, v. 201, no. 4915, p. 176.

———1969a, Recent observations on the surging Otto Glacier, Ellesmere Island: Canadian Journal of Earth Sciences, pt. 2, v. 6, no. 4, p. 883–889.

———1969b, Results of radio echo soundings in northern Ellesmere Island, 1966: The Geographical Journal, v. 135, no. 4, p. 553–557.

Hattersley-Smith, Geoffrey, 1974, North of Latitude Eighty—The Defence Research Board in Ellesmere Island: Ottawa, Ont., Information Canada Cat. No. DR3-1774, Defence Research Board, 121 p.

———1985, Spreading rate of an Arctic ice shelf: Nature, v. 315, no. 6019, p. 462.

Hattersley-Smith, Geoffrey, and Serson, H.[V.], 1970, Mass balance of the Ward Hunt Ice Rise and Ice Shelf—A 10 year record: Journal of Glaciology, v. 9, no. 56, p. 247–252.

———1973, Reconnaissance of a small ice cap near St. Patrick Bay, Robeson Channel, northern Ellesmere Island, Canada: Journal of Glaciology, v. 12, no. 66, p. 417–421.

Hattersley-Smith, Geoffrey, Lotz, J.R., and Sagar, R.B., 1961, The ablation season on Gilman Glacier, northern Ellesmere Island, *in* General Assembly of Helsinki, 25 July–6 August 1960: Association Internationale d'Hydrologie Scientifique Publication No. 54, p. 152–168.

Haumann, Dieter, 1960, Photogrammetric and glaciological studies of Salmon Glacier: Arctic, v. 13, no. 2, p. 75–110 and map.

Havens, J.M., 1964, Meteorology and heat balance of the accumulation area, McGill Ice Cap, Canadian Arctic Archipelago—Summer 1960 (Upper Ice Station I, 79°41' N., 90°27' W., 1530 m): Montréal, Québec, McGill University, Axel Heiberg Island Research Reports, Meteorology No. 2, 87 p.

Havens, J.M., Müller, Fritz, and Wilmot, G.C., 1965, Comparative meteorological survey and a short-term heat balance study of the White Glacier, Canadian Arctic Archipelago—summer 1962: Montréal, Québec, McGill University, Axel Heiberg Island Research Reports, Meteorology No. 4, 68 p.

Haythornthwaite, T.W., 1988, Topographic change of the Meighen Ice Cap, Meighen Island, N.W.T., *in* Adams, W.P., and Johnson, P.G., eds., Student research in Canada's North: National Student Conference on Northern Studies, Proceedings, Ottawa, Ontario, 18–19 November 1986, p. 87–92.

Hector, James, 1861, On the geology of the country between Lake Superior and the Pacific Ocean between the 48th and 54th parallels: Quarterly Journal of the Geological Society of London, v. 17, no. 68, p. 388–445.

Hell, Günther, and King, Lorenz, 1988, Fluctuations of a glacier tongue 1958–1978 at Hare Fjord, N.W.T., Canada, 1:20,000, *in* Haeberli, W. and Müller, P., eds., Fluctuations of glaciers 1980–1985, v. V: Wallingford, Oxfordshire, U.K., IAHS Press; Nairobi, UNEP; Paris, UNESCO, p. 66–67 and map.

Henoch, W.E.S., 1971, Estimate of glaciers' secular (1948–1966) volumetric change and its contribution to the discharge in the upper North Saskatchewan River basin: Journal of Hydrology, v. 12, no. 2, p. 145–160.

———1972, Glacier variations, *in* Guidebook to the International Symposium on the Role of Snow and Ice in Hydrology, 1972, Banff, Alberta: Ottawa, Ont., Canadian National Committee for I.H.D., p. 91–96.

Henoch, W.E.S., and Croizet, J.L., 1976, The Peyto Glacier map/A three-dimensional depiction of mountain relief: Canadian Cartographer, v. 13, no. 1, p. 69–86.

Heusser, C.J., 1954, Glacier fluctuations in the Canadian Rockies, *in* General Assembly of Rome, v. 4, 1954: Association Internationale d'Hydrologie Scientifique Publication No. 39, p. 493–497.

———1956, Postglacial environments in the Canadian Rocky Mountains: Ecological Monographs, v. 26, no. 4, p. 263–302.

———1960, Late-Pleistocene environments of North Pacific North America—An elaboration of Late-Glacial and Postglacial climatic, physiographic and biotic changes: New York, American Geographical Society, Special Publication No. 35, 308 p.

Hobson, G.D., and Jobin, Claude, 1975, A seismic investigation—Peyto Glacier, Banff National Park and Woolsey Glacier, Mount Revelstoke National Park: Geoexploration, v. 13, no. 2, p. 117–127.

Hoffmann, J.W., and Clarke, G.K.C., 1973, Periodic temperature instabilities in sub-polar glaciers, *in* The role of snow and ice in hydrology, Proceedings of the Banff Symposium, September 1972: IAHS-AISH Publication No. 107, v. 1, p. 445–453.

Holdsworth, Gerald, 1965, An examination and analysis of the formation of transverse crevasses, Kaskawulsh Glacier, Yukon Territory, Canada: Columbus, Ohio, Ohio State University, Institute of Polar Studies Report No. 16, p. 91.

———1969, Primary transverse crevasses: Journal of Glaciology, v. 8, no. 52, p. 107–129.

———1971, Calving from Ward-Hunt Ice Shelf 1961–62: Canadian Journal of Earth Sciences, v. 8, no. 2, p. 299–305.

———1973a, Evidence of a surge on Barnes Ice Cap, Baffin Island: Canadian Journal of Earth Sciences, v. 10, no. 10, p. 1565–1574.

———1973b, Ice calving into the proglacial Generator Lake, Baffin Island, N.W.T., Canada: Journal of Glaciology, v. 12, no. 65, p. 235–250.

———1975, Deformation and flow of Barnes Ice Cap, Baffin Island: Ottawa, Ont., Environment Canada, Water Resources Branch, Inland Waters Directorate Scientific Series No. 52, 19 p.

———1977a, Glaciological studies on Mt. Logan: Canadian Alpine Journal, v. 60, p. 57–58.

———1977b, Ice flow and related measurements of d'Iberville Glacier, Ellesmere Island, N.W.T., Canada: Ottawa, Ont., Environment Canada, Inland Waters Directorate, Glaciology Division, Internal report, 28 p.

———1977c, Surge activity on the Barnes Ice Cap: Nature, v. 269, no. 5629, p. 588–590.

———1978, Some mechanisms for the calving of icebergs; *in* Husseiny, A.A., ed., Iceberg utilization: New York, Pergamon Press, p. 160–165.

———1983, A 100 year ice core record of volcanic pollution, topospheric [sic] chemistry and climate change in the Yukon [abs.], *in* Neighbours in science, Alaska Science Conference, 34th Alaska/Canada North, Whitehorse, Yukon, 28 September–1 October 1983, Proceedings: American Association for the Advancement of Science, Arctic Division, p. 132.

———1984, Glaciological reconnaissance of an ice core drilling site, Penny Ice Cap, Baffin Island: Journal of Glaciology, v. 30, no. 104, p. 3–15.

———1986a, Evidence of a link between atmospheric thermonuclear detonations and nitric acid: Nature, v. 324, no. 6097, p. 551–553.

———1986b, Ice shelf creep rates and the flow law of ice: Nature, v. 319, no. 6056, p. 727.

———1987, The surface wave forms on the Ellesmere Island ice shelves and ice islands, *in* Pilkington, G.R., and Danielwicz, B.W., eds., Workshop on Extreme Ice Features, Banff, Alberta, 3–5 November 1986: Ottawa, Ont., National Research Council of Canada (NRCC 28003), Snow and Ice Subcommittee, Associate Committee on Geotechnical Research Technical Memorandum No. 141, p. 385–403.

———1990, Scientific correspondence—Sunspot cycles and climate: Nature, v. 346, no. 6286, p. 705–706.

Holdsworth, Gerald, and Jones, D.P., 1979, Glaciological studies on Mt. Logan, 1978: Canadian Alpine Journal, v. 62, p. 67.

Holdsworth, Gerald, and Peake, E., 1985, Acid content of snow from a mid-troposphere sampling site on Mount Logan, Yukon Territory, Canada: Annals of Glaciology, v. 7, p. 153–160.

Holdsworth, Gerald, and Sawyer, B., 1993, Mount Logan map, research and reference folio: Calgary, Alberta, Arctic Institute of North America, two map sheets.

Holdsworth, Gerald, Demuth, M.N., and Beck, T.M.H., in press, Radar measurements of ice thickness on Peyto Glacier, Alberta, *in* Demuth, M.N., ed., Peyto Glacier—One century of science: Saskatoon, National Water Research Institute.

Holdsworth, Gerald, Fogarasi, Stephen, and Krouse, H.R., 1991, Variation of the stable isotopes of water with altitude in the St. Elias Mountains of Canada: Journal of Geophysical Research, v. 96, no. D4, p. 7483–7494.

Holdsworth, Gerald, Krouse, H.R., and Nosal, M., 1992, Ice core climate signals from Mount Logan, Yukon A.D. 1700–1987, *in* Bradley, R.S., and Jones, P.D., eds., Climate since A.D. 1500: London, Routledge, p. 483–504.

Holdsworth, Gerald, Krouse, H.R., Nosal, M., Spencer, M.J., and Mayewski, P.A., 1989, Analysis of a 290-year net accumulation time series from Mt. Logan, Yukon, *in* Snow cover and glacier variations, Proceedings of the Baltimore Symposium, 10–19 May, 1989: IAHS-AISH Publication No. 183, p. 71–79.

Holdsworth, Gerald, Pourchet, Michel, Prantl, F.A., and Meyerhof, D.P., 1984, Radioactivity levels in a firn core from the Yukon Territory, Canada: Atmospheric Environment, v. 18, no. 2, p. 461–466.

Holmgren, Björn, 1971, Climate and energy exchange on a subpolar ice cap in summer; Arctic Institute of North America Devon Island Expedition 1961–1963, 5 Parts: Uppsala, Uppsala Universitet, Meteorologiska Institutionen, Meddelande Nr. 107–112, 83 p., 47 p., 43 p., 29 p., 111 p., and 53 p.

Hooke, R. LeB., 1973a, Flow near the margin of the Barnes Ice Cap, and the development of ice-cored moraines: Geological Society of America Bulletin, v. 84, no. 12, p. 3929–3948.

———1973b, Structure and flow in the margin of the Barnes Ice Cap, Baffin Island, N.W.T., Canada: Journal of Glaciology, v. 12, no. 66, p. 423–438.

———1976a, Near-surface temperatures in the superimposed ice zone and lower part of the soaked zone of polar ice sheets [abs.]: Journal of Glaciology, v. 16, no. 74, p. 302–304.

———1976b, Pleistocene ice at the base of the Barnes Ice Cap, Baffin Island, N.W.T., Canada: Journal of Glaciology, v. 17, no. 75, p. 49–59.

———1981, Flow law for polycrystalline ice in glaciers—Comparison of theoretical predictions, laboratory data, and field measurements: Reviews of Geophysics and Space Physics, v. 19, no. 4, p. 664–672.

Hooke, R. LeB., and Clausen, H.B., 1982, Wisconsin and Holocene $\delta^{18}O$ variations, Barnes Ice Cap, Canada: Geological Society of America Bulletin, v. 93, no. 8, p. 784–789.

Hooke, R. LeB., and Hanson, Brian, 1986, Borehole deformation experiments, Barnes Ice Cap, Canada: Cold Regions Science and Technology, v. 12, no. 3, p. 261–276.

Hooke, R. LeB., and Hudleston, P.J., 1980, Ice fabrics in a vertical flow plane, Barnes Ice Cap, Canada: Journal of Glaciology, v. 25, no. 92, p. 195–214.

———1981, Ice fabrics from a borehole at the top of the south dome, Barnes Ice Cap, Baffin Island: Geological Society of America Bulletin, pt. 1, v. 92, no. 5, p. 274–281.

Hooke, R. LeB., Alexander, E.C., Jr., and Gustafson, R.J., 1980, Temperature profiles in the Barnes Ice Cap, Baffin Island, Canada, and heat flux from the subglacial terrane: Canadian Journal of Earth Sciences, v. 17, no. 9, p. 1174–1188.

Hooke, R. LeB., Gould, J.E., and Brzozowski, Jerzy, 1983, Near-surface temperatures near and below the equilibrium line on polar and subpolar glaciers: Zeitschrift für Gletscherkunde und Glazialgeologie, v. 19, no. 1, p. 1–25.

Hooke, R. LeB., Johnson, G.W., Brugger, K.A., Hanson, Brian, and Holdsworth, Gerald, 1987, Changes in mass balance, velocity, and surface profile along a flow line on Barnes Ice Cap, 1970–1984: Canadian Journal of Earth Sciences, v. 24, no. 8, p. 1550–1561.

Hooke, R. LeB., Raymond, C.F., Hotchkiss, R.L., and Gustafson, R.J., 1979, Calculations of velocity and temperature in a polar glacier using the finite-element method: Journal of Glaciology, v. 24, no. 90, p. 131–146.

Horvath, Eva, 1975, Glaciers of the Yukon and Northwest Territories (excluding the Queen Elizabeth Islands and St. Elias Mountains), *in* Field, W.O., ed., Mountain glaciers of the Northern Hemisphere, v. 1: Hanover, N.H., U.S. Army Cold Regions Research and Engineering Lab., p. 689–698.

Hudleston, P.J., 1976, Recumbent folding in the base of the Barnes Ice Cap, Baffin Island, Northwest Territories, Canada: Geological Society of America Bulletin, v. 87, no. 12, p. 1684–1692.

Hudleston, P.J., 1980, The progressive development of inhomogeneous shear and crystallographic fabric in glacial ice: Journal of Structural Geology, v. 2, no. 1–2, p. 189–196.

———1983, Strain patterns in an ice cap and implications for strain variations in shear zones: Journal of Structural Geology, v. 5, no. 3–4, p. 455–463.

Hudleston, P.J., and Hooke, R. LeB., 1980, Cumulative deformation in the Barnes Ice Cap and implications for the development of foliation: Tectonophysics, v. 66, no. 1–3, p. 127–146.

Hyndman, R.D., 1965, Gravity measurements on the Devon Island ice cap and an adjoining glacier: Journal of Glaciology, v. 5, no. 40, p. 489–496.

Iken, Almut, 1972, Measurements of water pressure in moulins as part of a movement study of the White Glacier, Axel Heiberg Island, Northwest Territories, Canada: Journal of Glaciology, v. 11, no. 61, p. 53–58.

———1974, Velocity fluctuations of an Arctic valley glacier; a study of the White Glacier, Axel Heiberg Island, Canadian Arctic Archipelago: Montréal, Québec, McGill University, Axel Heiberg Island Research Reports, Glaciology No. 5, 116 p.

Illangasekare, T.H., Walter, R.J., Jr., Meier, M.F., and Pfeffer, W.T., 1990, Modeling of meltwater infiltration in subfreezing snow: Water Resources Research, v. 26, no. 5, p. 1001–1012.

Iverson, N.R., 1991, Morphology of glacial striae: Implications for abrasion of glacier beds and fault surfaces: Geological Society of America Bulletin, v. 103, no. 10, p. 1308–1316.

Ives, J.D., 1966, Glaciology in the Geographical Branch, 1961–1965: Geographical Bulletin, v. 8, no. 1, p. 1–2.

———1967a, Glacier terminal and lateral features in northeast Baffin Island—Illustrations with descriptive notes: Geographical Bulletin, v. 9, no. 2, p. 106–114.

———1967b, Glacier terminal features in northeast Baffin Island—Illustrations with descriptive notes: Geographical Bulletin, v. 9, no. 1, p. 62–70.

———1967c, Glaciers: Canadian Geographical Journal, v. 74, no. 4, p. 110–117.

Jackson, L.E., Jr., 1979, A catastrophic glacial outburst flood (jökulhlaup) mechanism for debris flow generation at the Spiral Tunnels, Kicking Horse River basin, British Columbia: Canadian Geotechnical Journal, v. 16, no. 4, p. 806–813.

———1980, New evidence on the origin of the September 6, 1978 jökulhlaup from Cathedral Glacier, British Columbia: Geological Survey of Canada Paper No. 80–1B, p. 292–294.

Jackson, L.E., Jr., Hungr, O., Gardner, J.S., and Mackay, C., 1989, Cathedral Mountain debris flows: Bulletin of the International Association of Engineering Geology, v. 40, p. 35–54.

Jacobs, J.A., 1958, Geophysical investigations on the Salmon Glacier, British Columbia, *in* Symposium on Physics of the Movement of the Ice, Symposium of Chamonix, September 16–24, 1958: Association Internationale d'Hydrologie Scientifique Publication No. 47, p. 43–44.

Jacobs, J.D., Andrews, J.T., Barry, R.G., Bradley, R.S., Weaver, Ronald, and Williams, L.D., 1973, Glaciological and meteorological studies on the Boas Glacier, Baffin Island, for two contrasting seasons (1969–70 and 1970–71), *in* The role of snow and ice in hydrology, Proceedings of the Banff Symposium, September 1972: IAHS-AISH Publication No. 107, v. 1, p. 371–382.

Jacobs, J.D., Simms, É.L., and Simms, A.[E.], 1997, Recession of the southern part of Barnes Ice Cap, Baffin Island, Canada, between 1961 and 1993, determined from digital mapping of Landsat TM: Journal of Glaciology, v. 43, no. 143, p. 98–102.

Jarvis, G.T., and Clarke, G.K.C., 1974, Thermal effects of crevassing on Steele Glacier, Yukon Territory, Canada: Journal of Glaciology, v. 13, no. 68, p. 243–254.

———1975, The thermal regime of Trapridge Glacier and its relevance to glacier surging: Journal of Glaciology, v. 14, no. 71, p. 235–250.

Jeffries, M.[O.], 1982, The Ward Hunt Ice Shelf, Spring 1982: Arctic, v. 35, no. 4, p. 542–544.

———1984, Milne Glacier, northern Ellesmere Island, N.W.T., Canada—A surging glacier?: Journal of Glaciology, v. 30, no. 105, p. 251–253.

———1986a, Glaciers and the morphology and structure of Milne Ice Shelf, Ellesmere Island, N.W.T., Canada: Arctic and Alpine Research, v. 18, no. 4, p. 397–405.

———1986b, Ice island calvings and ice shelf changes, Milne Ice Shelf and Ayles Ice Shelf, Ellesmere Island, N.W.T.: Arctic, v. 39, no. 1, p. 15–19.

———1991, Perennial water stratification and the role of basal freshwater flow in the mass balance of the Ward Hunt Ice Shelf, Canadian High Arctic, *in* Weller, Gunter, Wilson, C.L., and Severin, B.A.B., eds., International Conference on the Role of the Polar Regions in Global Change, Proceedings of a conference held 11–15 June 1990 at the University of Alaska Fairbanks, v. 1: Fairbanks, AK, University of Alaska, Geophysical Institute/Center for Global Change and Arctic System Research, p. 332–337.

———1992, Arctic ice shelves and ice islands—Origin, growth and disintegration, physical characteristics, structural-stratigraphic variability, and dynamics: Reviews of Geophysics, v. 30, no. 3, p. 245–267.

Jeffries, M.O., and Krouse, H.R., 1985, Arctic ice shelf growth, fiord oceanography and climate: Zeitschrift für Gletscherkunde und Glazialgeologie, 1984, v. 20, p. 147–153.

Jeffries, M.O., and Sackinger, W.M., 1990, Ice island detection and characterization with airborne synthetic aperture radar: Journal of Geophysical Research, v. 95, no. C 4, p. 5371–5377.

Jeffries, M.O., and Serson, H.[V.], 1983, Recent changes at the front of Ward Hunt Ice Shelf, Ellesmere Island, N.W.T.: Arctic, v. 36, no. 3, p. 289–290.

Jeffries, M.O., and Serson, H.V., 1986, Survey and mapping of recent ice shelf changes and landfast sea ice growth along the north coast of Ellesmere Island, NWT, Canada: Annals of Glaciology, v. 8, p. 96–99.

Jeffries, M.O., Sackinger, W.M., Krouse, H.R., and Serson, H.V., 1988, Water circulation and ice accretion beneath Ward Hunt Ice Shelf (northern Ellesmere Island, Canada), deduced from salinity and isotope analysis of ice cores: Annals of Glaciology, v. 10, p. 68–72.

Jeffries, M.O., Serson, H.V., Krouse, H.R., and Sackinger, W.M., 1991, Ice physical properties, structural characteristics and stratigraphy in Hobson's Choice Ice Island and implications for the growth history of East Ward Hunt Ice Shelf, Canadian High Arctic: Journal of Glaciology, v. 37, no. 126, p. 247–260.

Johnson, P.G., 1971, Ice-cored moraine formation and degradation, Donjek Glacier, Yukon Territory, Canada: Geografiska Annaler, v. 53A, no. 3–4, p. 198–202.

———1972, The morphological effects of surges of the Donjek Glacier, St. Elias Mountains, Yukon Territory, Canada: Journal of Glaciology, v. 11, no. 62, p. 227–234.

———1976, Environmental controls on geomorphic processes, Grizzly Creek, south-west Yukon Territory: Ottawa, Ont., University of Ottawa, Department of Geography and Regional Planning Research Note No. 9, 108 p.

———1980a, Glacier-rock glacier transition in the southwest Yukon Territory, Canada: Arctic and Alpine Research, v. 12, no. 2, p. 195–204.

———1980b, Rock glaciers—Glacial and non-glacial origin, *in* World Glacier Inventory Workshop, Riederalp, Switzerland, 17–22 September, 1978: IAHS-AISH Publication No. 126, p. 285–293.

———1981, The structure of a talus-derived rock glacier deduced from its hydrology: Canadian Journal of Earth Sciences, v. 18, no. 9, p. 1422–1430.

———1983, Rock glaciers—a case for a change in nomenclature: Geografiska Annaler, v. 65A, no. 1–2, p. 27–34.

———1984, Rock glacier formation by high-magnitude low-frequency slope processes in the southwest Yukon: Annals of the Association of American Geographers, v. 74, no. 3, p. 408–419.

———1985, Implications of Holocene palaeoclimatic changes for the glacier hydrology of the southwest Yukon: Zeitschrift für Gletscherkunde und Glazialgeologie, v. 21, p. 165–174.

———1991a, Discharge regimes of a glacierized basin, Slims River, Yukon, *in* Prowse, T.D., and Ommanney, C.S.L., eds., Northern hydrology—Selected perspectives, Proceedings of the Northern Hydrology Symposium, Saskatoon, 10–12 July 1990: Saskatoon, Sask., Environment Canada, National Hydrology Research Institute Symposium No. 6, p. 151–164.

———1991b, Pulses in glacier discharge:—Indicators of the internal drainage system of glaciers, *in* Prowse, T.D., and Ommanney, C.S.L., eds., Northern hydrology—Selected perspectives, Proceedings of the Northern Hydrology Symposium, Saskatoon, 10–12 July 1990: Saskatoon, Sask., Environment Canada, National Hydrology Research Institute Symposium No. 6, p. 165–175.

———1992, Stagnant glacier ice, St. Elias Mountains, Yukon: Geografiska Annaler, v. 74A, no. 1, p. 13–19.

Johnson, P.G., 1998, Morphology and surface structures of Maxwell Creek rock glaciers, St. Elias Mountains, Yukon—Rheological implications: Permafrost and Periglacial Processes, v. 9, no. 1, p. 57–70.

Johnson, P.G., and David, C.R., 1987, Impacts on river discharge of changes in glacierized components of mountain basins: Water Pollution Research Journal of Canada, v. 22, no. 4, p. 518–529.

Johnson, P.G., and Kasper, J.N., 1992, The development of an ice-dammed lake—The contemporary and older sedimentary record: Arctic and Alpine Research, v. 24, no. 4, p. 304–313.

Johnson, P.G., and Lacasse, Diane, 1988, Rock glaciers of the Dalton Range, Kluane Ranges, south-west Yukon Territory, Canada: Journal of Glaciology, v. 34, no. 118, p. 327–332.

Johnson, P.G., and Power, J.M., 1985, Flood and landslide events, Peyto Glacier terminus, Alberta, Canada, 11–14 July 1983: Journal of Glaciology, v. 31, no. 108, p. 86–91.

Johnson, R.F., 1983, Ice movement and structural characteristics of the Cathedral Glacier system, Atlin Provincial Park, British Columbia: M.Sc. thesis, Bozeman, MT, Montana State University, 65 p.

Jones, D.P., Ricker, K.E., Desloges, J.R., and Maxwell, M.G., 1985, Glacier outburst flood on the Noeick River—The draining of Ape Lake, British Columbia, October 20, 1984: Geological Survey of Canada Open File Report No. 1139, p. 107 and maps.

Jones, F.H.M., Narod, B.B., and Clarke, G.K.C., 1989, Design and operation of a portable, digital impulse radar: Journal of Glaciology, v. 35, no. 119, p. 143–148.

Jones, N.K., 1987, Debris transport and deposition at Boundary Glacier, Banff National Park, Alberta: Ph.D. thesis, Waterloo, Ont., University of Waterloo, Department of Geography.

Jones, S.J., 1972, Radio depth-sounding on Meighen and Barnes Ice Caps, Arctic Canada: Ottawa, Ont., Environment Canada, Inland Waters Directorate Scientific Series No. 25, 13 p.

Jones, V.K., 1974, Late-Neoglacial regimes of an inland cirque glacier and their paleoclimatic implications, *in* Quaternary environments, York University Symposium on Quaternary Research, 1st: Toronto, Ont., York University, Atkinson College, Geographical Monographs No. 5, p. 293–294.

Jung-Rothenhäusler, Friedrich, Cogley, J.G., and Adams, [W.]P., 1992, Preparations for a glacier study using Landsat imagery and a digital elevation model: Musk-ox, v. 39, p. 31–38.

Kanasewich, E.R., 1963, Gravity measurements on the Athabaska Glacier, Alberta, Canada: Journal of Glaciology, v. 4, no. 35, p. 617–631.

Kasper, J.N., and Johnson, P.G., 1991, Drainage of an ice-dammed lake, Kaskawulsh Glacier basin, Yukon, *in* Prowse, T.D., and Ommanney, C.S.L., eds., Northern hydrology—Selected perspectives, Proceedings of the Northern Hydrology Symposium, Saskatoon, 10–12 July 1990: Saskatoon, Sask., Environment Canada, National Hydrology Research Institute Symposium No. 6, p. 177–188.

Kavanaugh, J.L., and Clarke, G.K.C., 1996, An instrument for detecting seasonal changes in sliding rate [abs.]: EOS, Transactions, American Geophysical Union, v. 77, no. 46, Fall Meeting Supplement, p. F218.

Keeler, C.M., 1964, Relationship between climate, ablation, and run-off on the Sverdrup Glacier, 1963, Devon Island, N.W.T: Montréal, Québec, Arctic Institute of North America Research Paper No. 27, 125 p.

———1969, Snow accumulation on Mount Logan, Yukon Territory, Canada: Water Resources Research, v. 5, no. 3, p. 719–723.

Keller, G.V., and Frischknecht, F.C., 1960, Electrical resistivity studies on the Athabasca Glacier, Alberta, Canada: Journal of Research of the National Bureau of Standards, Washington, D.C., v. 64D, no. 5, p. 439–448.

———1961, Induction and galvanic resistivity studies on the Athabasca Glacier, Alberta, Canada, *in* Raasch, G.O., ed., Geology of the Arctic, v. 2: Toronto, Ont., University of Toronto Press, p. 809–832.

King, Lorenz, 1983, Contribution to the glacial history of the Borup Fiord area, northern Ellesmere Island, N.W.T., Canada, *in* Schroeder-Lanz, H., ed., Late-and postglacial oscillations of glaciers—Glacial and periglacial forms, Colloquium, Trier, Germany, 15–17 May 1980: Rotterdam, A.A. Balkema, p. 305–323.

Kite, G.[W.], 1994, Measuring glacier outflows using a computerized conductivity system: Journal of Glaciology, v. 40, no. 134, p. 93–96.

Kite, G.W., and Reid, I.A., 1977, Volumetric change of the Athabasca Glacier over the last 100 years: Journal of Hydrology, v. 32, no. 3–4, p. 279–294.

Koerner, R.M., 1966, Accumulation on the Devon Island ice cap, Northwest Territories, Canada: Journal of Glaciology, v. 6, no. 45, p. 383–392.

———1968, Fabric analysis of a core from the Meighen Ice Cap, Northwest Territories, Canada: Journal of Glaciology, v. 7, no. 51, p. 421–430.

———1970a, The mass balance of the Devon Island ice cap, Northwest Territories, Canada, 1961–66: Journal of Glaciology, v. 9, no. 57, p. 325–336.

———1970b, Some observations on superimposition of ice on the Devon Island ice cap, N.W.T. Canada: Geografiska Annaler, v. 52A, no. 1, p. 57–67.

———1973, Specific electrolytic conductivity of snow and deep core samples, Canadian Arctic Archipelago, *in* The role of snow and ice in hydrology, Proceedings of the Banff Symposium, September 1972: IAHS-AISH Publication No. 107, v. 1, p. 51–63.

———1977a, Devon Island ice cap—Core stratigraphy and paleoclimate: Science, v. 196, no. 4285, p. 15–18.

———1977b, Distribution of microparticles in a 299-m core through the Devon Island ice cap, Northwest Territories, Canada, *in* Isotopes and impurities in snow and ice, Proceedings of the Grenoble Symposium, August/September 1975: IAHS-AISH Publication No. 118, p. 371–376.

———1977c, Ice thickness measurements and their implications with respect to past and present ice volumes in the Canadian High Arctic ice caps: Canadian Journal of Earth Sciences, v. 14, no. 12, p. 2697–2705.

———1979, Accumulation, ablation, and oxygen isotope variations on the Queen Elizabeth Islands ice caps, Canada: Journal of Glaciology, v. 22, no. 86, p. 25–41.

Koerner, R.M., 1983, Conditions at the ice/rock interface of large ice sheets, *in* Heinrich, W., ed., Workshop on Transitional Processes, 4–5 November 1982, Ottawa, Ontario: Pinewa, Manitoba, Whiteshell Nuclear Research Establishment, Atomic Energy of Canada Ltd., p. 200–211.

———1985, The Canadian Arctic Islands—Glacier mass balance and global sea level, *in* Glaciers, ice sheets, and sea level: effect of a CO_2-induced climatic change, Report of a workshop held in Seattle, Washington, September 13–15, 1984: Washington, D.C., U.S. Department of Energy, Office of Energy Research, Attachment 7, Report DOE/ER/60235-1, p. 145–154.

———1986, Novyy metod ispol'zovaniya lednikov dlya monitoringa izmeneniy klimata / A new method for using glaciers as monitors of climate: Materialy Glyatsiologicheskikh Issledovaniy, Khronika, Obsuzhdeniya (Data of Glaciological Studies, Chronicle, Discussion), v. 57, p. 47–52 (Russian), 175–179 (English).

———1989, Ice core evidence for extensive melting of the Greenland ice sheet in the last interglacial: Science, v. 244, no. 4907, p. 964–968.

———1992, Past climate changes as deduced from Canadian ice cores, *in* Woo, Ming-k., and Gregor, D.J., eds., Arctic environment—Past, present and future, Proceedings of Symposium, Hamilton, 14–15 November 1991: Hamilton, Ont., McMaster University, Department of Geography, p. 61–70.

Koerner, R.M., and Fisher, D.A., 1979, Discontinuous flow, ice texture, and dirt content in the basal layers of the Devon Island ice cap: Journal of Glaciology, v. 23, no. 89, p. 209–222.

———1981, Studying climatic change from Canadian High Arctic ice cores: Syllogeus, National Museum of Natural Sciences, National Museums of Canada, Ottawa, Ont., v. 33, p. 195–218.

———1982, Acid snow in the Canadian High Arctic: Nature, v. 295, no. 5845, p. 137–140.

———1985, The Devon Island ice core and the glacial record, *in* Andrews, J.T., ed., Quaternary environments: Eastern Canadian Arctic, Baffin Bay and western Greenland: Boston, MA, Allen and Unwin, p. 309–327.

———1990, A record of Holocene summer climate from a Canadian high-Arctic ice core: Nature, v. 343, no. 6259, p. 630–631.

Koerner, R.M., and Paterson, W.S.B., 1974, Analysis of a core through the Meighen Ice Cap, Arctic Canada, and its paleoclimatic implications: Quaternary Research, v. 4, no. 3, p. 253–263.

Koerner, R.M., and Russell, R.D., 1979, $\delta^{18}O$ variations in snow on the Devon Island ice cap, Northwest Territories, Canada: Canadian Journal of Earth Sciences, v. 16, no. 7, p. 1419–1427.

Koerner, R.M., and Taniguchi, Hiroshi, 1976, Artificial radioactivity layers in the Devon Island Ice Cap, Northwest Territories: Canadian Journal of Earth Sciences, v. 13, no. 9, p. 1251–1255.

Koerner, R.M., Alt, B.T., Bourgeois, J.C., and Fisher, D.A., 1991, Canadian ice caps as sources of environmental data, *in* Weller, Gunter, Wilson, C.L., and Severin, B.A.B., eds., International Conference on the Role of the Polar Regions in Global Change, Proceedings of a conference held June 11–15, 1990 at the University of Alaska-Fairbanks, v. 2: Fairbanks, AK, University of Alaska, Geophysical Institute/Center for Global Change and Arctic System Research, p. 576–581.

Koerner, R.M., Bourgeois, J.C., and Fisher, D.A., 1988, Pollen analysis and discussion of time-scales in Canadian ice cores: Annals of Glaciology, v. 10, p. 85–91.

Koerner, R.M., Fisher, D.[A.], and Goto-Azuma, Kumiko, 1998, A 100 year record of ion chemistry from Agassiz Ice Cap, northern Ellesmere Island, N.W.T., Canada: Atmospheric Environment, v. 33, no. 3, p. 347–357.

Koerner, R.M., Fisher, D.A., and Paterson, W.S.B., 1987, Wisconsinan and pre-Wisconsinan ice thicknesses on Ellesmere Island, Canada—Inferences from ice cores: Canadian Journal of Earth Sciences, v. 24, no. 2, p. 296–301.

Koerner, R.M., Paterson, W.S.B., and Krouse, H.R., 1973, $\delta^{18}O$ profile in ice formed between the equilibrium and firn lines: Nature, Physical Science, v. 245, no. 148, p. 137–140.

Konecny, Gottfried, 1966, Applications of photogrammetry to surveys of glaciers in Canada and Alaska: Canadian Journal of Earth Sciences, v. 3, no. 6, p. 783–798.

Konecny, Gottfried, and Faig, W., 1966, Studies of ice movements on the Ward Hunt Ice Shelf by means of triangulation-trilateration: Arctic, v. 19, no. 4, p. 337–342.

Krimmel, R.M., and Meier, M.F., 1975, Glacier applications of ERTS images: Journal of Glaciology, v. 15, no. 73, p. 391–402.

Krimmel, R.M., and Trabant, D.C., 1992, The terminus of Hubbard Glacier, Alaska: Annals of Glaciology, v. 16, p. 151–157.

Krouse, H.R., Hislop, R.[W.P.], Brown, H.M., West, K.[E.], and Smith, J.L., 1977, Climatic and spatial dependence of the retention of D/H and O^{18}/O^{16} abundances in snow and ice of North America, *in* Isotopes and impurities in snow and ice, Proceedings of the Grenoble Symposium, August/September 1975: IAHS-AISH Publication No. 118, p. 242–247.

Kruszynski, G.A., and Johnson, P.G., 1993, Glacierized basin hydrological variability and climate change trends, *in* Prowse, T.D., Ommanney, C.S.L., and Ulmer, K.E., eds., Proceedings of the 9th International Northern Research Basins Symposium/Workshop, 14–22 August 1992, Whitehorse, Dawson City, Eagle Plains, Yukon; Inuvik, Northwest Territories, v. 1: Saskatoon, Saskatchewan, Environment Canada, National Hydrology Research Institute Symposium No. 10, p. 269–284.

Kucera, R.E., 1972, Probing the Athabasca Glacier: Vancouver, British Columbia, Evergreen Press, 32 p.

Lacasse, Diane, 1985, État des connaissances actuelles sur la chronologie des fluctuations glaciaire de l'Holocène, sud-ouest du Yukon: Geoscope, v. 15, no. 2, p. 80–93.

Lang, A.H., 1943, Glaciers of the Rockies and Selkirks: Canadian Geographical Journal, v. 26, no. 2, p. 56–67.

Lawby, C.P., Smith, D.J. Laroque, C.P., and Brugman, M.M., 1994, Glaciological studies at Rae Glacier, Canadian Rocky Mountains: Physical Geography, v. 15, no. 5, p. 425–441.

Lehmann, Rainer, 1992, Arctic push moraines, a case study of the Thompson Glacier moraine, Axel Heiberg Island, N.W.T., Canada: Zeitschrift für Geomorphologie, Supplementband 86, p. 161–171.

Lemmen, D.S., 1988, The glacial history of Marvin Peninsula, northern Ellesmere Island, and Ward Hunt Island, High Arctic Canada: Ph.D. thesis, Edmonton, Alberta, University of Alberta, Department of Geography, 176 p.

Letréguilly, Anne, 1988, Relation between the mass balance of western Canadian mountain glaciers and meteorological data: Journal of Glaciology, v. 34, no. 116, p. 11–18.

Letréguilly, Anne, and Reynaud, Louis, 1989, Spatial patterns of mass-balance fluctuations of North American glaciers: Journal of Glaciology, v. 35, no. 120, p. 163–168.

———1990, Space and time distribution of glacier mass-balance in the Northern Hemisphere: Arctic and Alpine Research, v. 22, no. 1, p. 43–50.

Lichti-Federovich, Sigrid, 1975, Pollen analysis of ice core samples from the Devon Island Ice Cap: Canada Geological Survey Paper No. 75-1A, p. 441–444.

Lister, Hal, 1962, Heat and mass balance at the surface of the Ward Hunt Ice Shelf, 1960: Montréal, Québec, Arctic Institute of North America Research Paper No. 19, 54 p.

Liverman, D.G.E., 1987, Sedimentation in ice-dammed Hazard Lake, Yukon: Canadian Journal of Earth Sciences, v. 24, no. 9, p. 1797–1806.

Lodwick, G.D., and Paine, S.H., 1985, A digital elevation model of the Barnes Ice Cap derived from Landsat MSS data: Photogrammetric Engineering and Remote Sensing, v. 51, no. 12, p. 1937–1944.

Løken, O.H., 1966, Science on Baffin Island—Field research in physical geography: Canadian Geographical Journal, v. 72, no. 2, p. 38–47.

———1969, Evidence of surges on the Barnes Ice Cap, Baffin Island: Canadian Journal of Earth Sciences, v. 6, no. 4, pt. 2, p. 899–901.

———1971, Glacier studies in the Canadian IHD program, *in* Glaciers, Proceedings of the IHD Workshop Seminar 1970, Vancouver, B.C., 24–25 September 1970: Ottawa, Ont., Canadian National Committee for the I.H.D., p. 1–4.

———1972, Growth and decay of glaciers as an indicator of long-term environmental changes, *in* Environmental conditions in the Northwest Atlantic, Proceedings of symposium in Dartmouth, Nova Scotia: International Commission for Northwest Atlantic Fisheries, Special Publication No. 8, p. 71–87.

Løken, O.H., and Andrews, J.T., 1966, Glaciology and chronology of fluctuations of the ice margin at the south end of the Barnes Ice Cap, Baffin Island, N.W.T.: Geographical Bulletin, v. 8, no. 4, p. 341–359.

Løken, O.H., and Sagar, R.B., 1968, Mass balance observations on the Barnes Ice Cap, Baffin Island, Canada, *in* General Assembly of Bern 1967—Snow and Ice: Association Internationale d'Hydrologie Scientifique Publication No. 79, p. 282–291.

Loijens, H.S., 1974, Streamflow formation in the Mistaya River basin, Rocky Mountains, Canada: Western Snow Conference, 42nd Annual Meeting, Anchorage, Alaska, 16–20 April 1974, Proceedings, p. 86–95.

Loomis, S.R., Dozier, J., and Ewing, K.J., 1970, Studies of morphology and stream action on ablating ice: Montréal, Québec, Arctic Institute of North America Research Paper No. 57, 167 p.

Luckman, B.H., 1986, Reconstruction of Little Ice Age events in the Canadian Rocky Mountains: Géographie Physique et Quaternaire, v. 40, no. 1, p. 17–28.

———1988, 8000 year old wood from the Athabasca Glacier, Alberta: Canadian Journal of Earth Sciences, v. 25, no. 1, p. 148–151.

———1993, Glacier fluctuation and tree-ring records for the last millenium in the Canadian Rockies: Quaternary Science Reviews, v. 12, no. 6, p. 441–450.

Luckman, B.H., Harding, K.A., and Hamilton, J.P., 1987, Recent glacier advances in the Premier Range, British Columbia: Canadian Journal of Earth Sciences, v. 24, no. 6, p. 1149–1161.

Luckman, B.H., Holdsworth, Gerald, and Osborn, G.D., 1993, Neoglacial glacier fluctuations in the Canadian Rockies: Quaternary Research, v. 39, no. 2, p. 144–153.

Lyons, J.B., and Ragle, R.H., 1962, Thermal history and growth of the Hard Hunt Ice Shelf, *in* Variations of the Regime of Existing Glaciers, Symposium at Obergurgl, 10–18 September, 1962: Association Internationale d'Hydrologie Scientifique Publication No. 58, p. 88–97.

Lyons, J.B., Ragle, R.H., and Tamburi, A.J., 1972, Growth and grounding of the Ellesmere Island ice rises: Journal of Glaciology, v. 11, no. 61, p. 43–52.

Maag, Hans, 1969, Ice-dammed lakes and marginal glacial drainage on Axel Heiberg Island, Canadian Arctic Archipelago: Montréal, Québec, McGill University, Axel Heiberg Island Research Reports, 147 p.

MacAyeal, D.R., and Holdsworth, Gerald, 1986, An investigation of low-stress ice rheology on the Ward-Hunt Ice Shelf: Journal of Geophysical Research, v. 91, no. B6, p. 6347–6358.

MacPherson, D.S., and Krouse, H.R., 1967, O^{18}/O^{16} ratios in snow and ice of the Hubbard and Kaskawulsh Glaciers, *in* Stout, G.E., ed., Isotope techniques in the hydrologic cycle: Washington, D.C., American Geophysical Union, Geophysical Monograph No. 11, p. 180–194.

Marcus, M.G., 1960, Periodic drainage of glacier-dammed Tulsequah Lake, British Columbia: Geographical Review, v. 50, no. 1, p. 89–106.

———1964, Climate-glacier studies in the Juneau Ice Field region, Alaska: Chicago, Ill., University of Chicago, Department of Geography Research Paper No. 88, 128 p.

Marcus, W.A., Roberts, Keith, Harvey, Leslie, and Tackman, Gary, 1992, An evaluation of methods for estimating Manning's n in small mountain streams: Mountain Research and Development, v. 12, no. 3, p. 227–239.

Marsh, J.S., 1976, The Mt. Sir Sandford area, Selkirk Mountains, British Columbia, a scientific report of the Canadian Exploration Group's 1975 Selkirk Mountain expedition: Peterborough, Ont., Canadian Exploration Group, 133 p.

Marsh, J.[S.], 1978, Glacier and microclimate research in Mount Sir Sandford area, British Columbia: Canadian Alpine Journal, v. 61, p. 70–73.

Marston, R.A., 1983, Supraglacial stream dynamics on the Juneau Icefield: Annals of the Association of American Geographers, v. 73, no. 4, p. 597–608.

Mathews, W.H., 1964a, Discharge of a glacial stream, *in* Symposium on Surface Water, General Assembly of Berkeley, 19–31 August 1963: Association Internationale d'Hydrologie Scientifique Publication No. 63, p. 290–300.

Mathews, W.H., 1964b, Sediment transport from Athabasca Glacier, Alberta, *in* Symposium on Land Erosion, Precipitations, Hydrometry, Soil Moisture, General Assembly of Berkeley, 19–31 August 1963: Association Internationale d'Hydrologie Scientifique Publication No. 65, p. 155–165.

———1964c, Water pressure under a glacier: Journal of Glaciology, v. 5, no. 38, p. 235–240.

———1965, Two self-dumping ice-dammed lakes in British Columbia: Geographical Review, v. 55, no. 1, p. 46–52.

———1973, Record of two jökullhlaups, *in* Symposium on the hydrology of glaciers, Cambridge, 7–13 September 1969: Association Internationale d'Hydrologie Scientifique Publication No. 95, p. 99–110.

Mathews, W.H., and Clague, J.J., 1993, The record of jökulhlaups from Summit Lake, northwestern British Columbia: Canadian Journal of Earth Sciences, v. 30, no. 3, p. 499–508.

Mattson, L.E., 1990, A comparison of meltwater discharge from a debris-free and a debris-covered glacier, Canadian Rocky Mountains: Eastern Snow Conference, 47th Annual Meeting, Bangor, Maine, 7–8 June 1990, Proceedings, p. 237–242.

Mattson, L.E., and Gardner, J.S., 1991, Mass wasting on valley-side ice-cored moraines, Boundary Glacier, Alberta, Canada: Geografiska Annaler, v. 73A, no. 3–4, p. 123–128.

Mauelshagen, L., 1984, Zur Entstehungsgeschichte und Herstellung der Karte des Cathedral Gletscher Vorfeldes in British Kolumbien (Kanada), *in* Festschrift zum 60, Geburtstag von Prof. Dr. Ing. G. Kupfer: Bonn, Germany: p. 90–99.

Mauelshagen, L., and Slupetzky, H., 1985, Cathedral Massif Glacier and forefield (Atlin Provincial Wildernes Park, B.C., Canada): Salzburg, Austria, Universität Salzburg, Institut für Geographie, map, scale 1:5,000.

Maxwell, M.G., 1986, Isotopic identification of subglacial processes: Ph.D. thesis, Vancouver, B.C., University of British Columbia, Department of Geophysics and Astronomy, 130 p.

Mayewski, P.A., Holdsworth, Gerald, Spencer, M.J., Whitlow, S.[I.], Twickler, M.[S.], Morrison, M.C., Ferland, K.K., and Meeker, L.D., 1993, Ice core sulfate from three Northern Hemisphere sites—Source and temperature forcing implications: Atmospheric Environment, ser. A, v. 27, no. 17–18, p. 2915–2919.

Mayewski, P.A., Pregent, G., Armstrong, T., Brown, P., Butler, D., Hassinger, J.[M.], Jeschke, P.[A.], Palais, J.[M.], and Trombley, T.[J.], 1979, Results of the 1978 Athabasca Glacier Expedition: Durham, N.H., University of New Hampshire, Department of Earth Science, Glaciology Report Series, 56 p.

Mayo, L.R., 1989, Advance of Hubbard Glacier and 1986 outburst of Russell Fiord, Alaska, U.S.A.: Annals of Glaciology, v. 13, p. 189–194.

McAndrews, J.H., 1984, Pollen analysis of the 1973 ice core from Devon Island glacier, Canada: Quaternary Research, v. 22, no. 1, p. 68–76.

McCann, S.B., and Cogley, J.G., 1977, Floods associated with glacier margin drainage in Ellesmere Island, N.W.T., *in* Canadian Hydrology Symposium 77, Edmonton, Alberta, 29–31 August 1977, Proceedings: Ottawa, Ont., National Research Council of Canada (NRCC 16428), Associate Committee on Hydrology, p. 14–23.

McCoubrey, A.A., 1938, Glacier observations, 1936 and 1937: Canadian Alpine Journal, v. 25, p. 113–116.

McCoy, W.D., 1983, Holocene glacier fluctuations in the Torngat Mountains, northern Labrador: Géographie Physique et Quaternaire, v. 37, no. 2, p. 211–216.

McFarlane, W.T., 1946, Glacier investigations in Banff, Yoho and Jasper National Parks: Canadian Alpine Journal, v. 29, no. 2, p. 265–273.

McFarlane, W.T., Blair, R.V., and Ozga, W.J., 1950, Glacier survey in Banff and Jasper National Parks, 1949: Canadian Alpine Journal, v. 33, p. 120–126.

Meek, Victor, 1948a, Glacier obervations in the Canadian Cordillera: Canadian Geographical Journal, v. 37, no. 5, p. 190–209.

———1948b, Glacier observations in the Canadian Cordillera, *in* General Assembly of Oslo, 19–28 August 1948, v. 2: Association Internationale d'Hydrologie Scientifique Publication No. 30, p. 264–275.

Meier, M.F., 1958a, The mechanics of crevasse formation, *in* General Assembly of Toronto, v. 4, 3–14 September 1957: Association Internationale d'Hydrologie Scientifique Publication No. 46, p. 500–508.

———1958b, Vertical profiles of velocity and the flow law of glacier ice, *in* Symposium on Physics of the Movement of the Ice, Symposium of Chamonix, 16–24 September 1958: Association Internationale d'Hydrologie Scientifique Publication No. 47, p. 169–170.

———1960, Mode of flow of Saskatchewan Glacier, Alberta, Canada: U.S. Geological Survey Professional Paper 351, p. 70.

Meier, M.F., and Post, A.S., 1962, Recent variations in mass net budgets of glaciers in western North America, *in* Variations of the Regime of Existing Glaciers, Symposium at Obergurgl, 10–18 September 1962: Association Internationale d'Hydrologie Scientifique Publication No. 58, p. 63–77.

Meier, M.F., Rigsby, G.P., and Sharp, R.P., 1954, Preliminary data from Saskatchewan Glacier, Alberta, Canada: Arctic, v. 7, no. 1, p. 3–26.

Mercer, J.H., 1956, The Grinnell and Terra Nivea Ice Caps, Baffin Island: Journal of Glaciology, v. 2, no. 19, p. 652–656.

———1975a, Glaciers of Baffin and Bylot Islands, *in* Field, W.O., ed., Mountain glaciers of the Northern Hemisphere, v. 2: Hanover, N.H., U.S. Army Cold Regions Research and Engineering Lab., p. 683–721.

———1975b, Glaciers of the Queen Elizabeth Islands, N.W.T., Canada, *in* Field, W.O., ed., Mountain glaciers of the Northern Hemisphere, v. 2: Hanover, N.H., U.S. Army Cold Regions Research and Engineering Lab., p. 723–752.

Miller, G.H., Bradley, R.S., and Andrews, J.T., 1975, The glaciation level and lowest equilibrium line altitude in the High Canadian Arctic—Maps and climatic interpretation: Arctic and Alpine Research, v. 7, no. 2, p. 155–168.

Miller, M.M., 1963, A field institute of glaciological and expeditionary sciences in Alaska: Appalachia, v. 34, no. 136, p. 499–508.

Miller, M.M., 1975, Mountain and glacier terrain study and related investigations in the Juneau Icefield region, Alaska-Canada—Final Report 1971–1973 by Maynard M. Miller and Research Associates of the Juneau Icefield Research Program: Seattle, WA, Pacific Science Center, Foundation for Glacier and Environmental Research, 326 p.

Miller, M.M., and Anderson, J.H., 1974, The Alaskan Glacier Commemorative Project, Phase IV—Pleistocene-Holocene sequences in the Alaska-Canada Boundary Ranges: National Geographic Society Research Reports 1967, p. 197–223.

Moisan, Yves, and Dubois, J.-M.M., 1993, Estimation des variations spatiales de l'aire occupée par la calotte glaciaire de Barnes (Terre de Baffin, Territoire du Nord-Ouest) entre 1979 et 1990 à l'aide de données MSS de Landsat: 16e Symposium canadien sur la télédétection et 8e Congrès de l'Association Québécoise de télédétection, Sherbrooke, Québec, 7–10 juin 1993, Compte rendu, p. 221–226.

Moisan, Yves, and Pollard, W.H., 1992, Changes at the snout and proglacial zone of the White-Thompson Glacier complex, Axel Heiberg Island, Northwest Territories: Musk-ox, v. 39, p. 1–8.

Mokievsky-Zubok, Oleg, 1973a, Determination of mass balance on Sentinel Glacier, British Columbia, Canada: Ottawa, Ont., Department of the Environment, Water Resources Branch, Inland Waters Directorate Scientific Series No. 30, 39 p.

———1973b, Study of Sentinel Glacier, British Columbia, Canada, within the International Hydrological Decade (IHD) program—Procedures and techniques: Ottawa, Ont., Department of the Environment, Water Resources Branch, Inland Waters Directorate Technical Bulletin No. 77, 31 p.

———1974, Analysis of mass balance values and their accuracy at Sentinel Glacier, B.C., Canada: Ottawa, Ont., Department of the Environment, Water Resources Branch, Inland Waters Directorate Scientific Series No. 31, 4 p.

———1980a, Selected information on some West Coast glaciers studied in 1979: Ottawa, Ont., Environment Canada, National Hydrology Research Institute, Snow and Ice Division, Unpublished report to B.C. Hydro, Hydroelectric Design Division, Hydrology Section, Burnaby Mountain SCS, Vancouver, B.C., 11 p.

———1980b, Sudden discharge of glacier-dammed Flood Lake, August 1979: Ottawa, Ont., Environment Canada, National Hydrology Research Institute, Snow and Ice Division, Summary report, 17 p.

———1983a, Glaciological studies in Homathko River basin in 1982: Ottawa, Ont., Environment Canada, National Hydrology Research Institute, Internal report, 18 p.

———1983b, Glaciological studies in Iskut River basin in 1982: Ottawa, Ont., Environment Canada, National Hydrology Research Institute, Internal report, 25 p.

———1985, Glaciological studies in Bridge River basin in 1984: Ottawa, Ont., National Hydrology Research Institute, Environment Canada, Internal report, 22 p.

———1987, Glacier mass balance for 1986 on Sentinel, Helm and Place Glaciers, British Columbia: Saskatoon, Sask., Environment Canada, Surface Water Division, National Hydrology Research Institute Contribution No. 87061, 16 p.

———1992a, Glaciological studies in the Homathko River basin in 1991: Ottawa, Ont., Glacier Consulting Services, Contract report to B.C. Hydro, Vancouver, B.C., 19 p.

———1992b, Glaciological studies in the Iskut River basin in 1991: Ottawa, Ont., Glacier Consulting Services, Contract report to B.C. Hydro, Vancouver, B.C., 27 p.

Mokievsky-Zubok, Oleg, and Stanley, A.D., 1976a, Canadian glaciers in the International Hydrological Decade program, 1965–1974. No. 1. Sentinel Glacier, British Columbia—Summary of measurements: Ottawa, Ont., Fisheries and Environment Canada, Water Resources Branch, Inland Waters Directorate Scientific Series No. 68, 75 p.

———1976b, Canadian glaciers in the International Hydrological Decade program, 1965–1974. No. 2. Place Glacier, British Columbia—Summary of measurements: Ottawa, Ont., Fisheries and Environment Canada, Water Resources Branch, Inland Waters Directorate Scientific Series No. 69, 77 p.

Mokievsky-Zubok, Oleg, Ommanney, C.S.L., and Power, J.[M.], 1985, NHRI glacier mass balance, 1964–1984 (Cordillera and Arctic): Ottawa, Ont., Environment Canada, Surface Water Division, National Hydrology Research Institute, Internal report, 59 p.

Mollard, J.D., and Janes, J.R., 1984, Airphoto interpretation and the Canadian landscape: Ottawa, Ont., Department of Energy, Mines and Resources, 415 p.

Monaghan, M.C., and Holdsworth, Gerald, 1990, The origin of non-sea-salt sulphate in the Mount Logan ice core: Nature, v. 343, no. 6255, p. 245–248.

Morey, Anton, 1971, The legend of the Great Glacier battle: North/Nord, v. 18, no. 5, p. 20–23.

Müller, B.S., 1961, Jacobsen-McGill Arctic Research Expedition to Axel Heiberg Island, Queen Elizabeth Islands—Preliminary report of 1959–1960: Montréal, Québec, McGill University, 219 p.

Müller, Fritz, 1962a, Glacier mass-budget studies on Axel Heiberg Island, Canadian Arctic Archipelago, *in* Variations of the Regime of Existing Glaciers, Symposium at Obergurgl, 10–18 September 1962: Association Internationale d'Hydrologie Scientifique Publication No. 58, p. 131–142.

———1962b, Zonation in the accumulation area of the glaciers of Axel Heiberg Island, N.W.T., Canada: Journal of Glaciology, v. 4, no. 33, p. 302–311.

———1963, Englacial temperature measurements on Axel Heiberg Island, Canadian Arctic Archipelago, *in* Symposium on Snow and Ice, General Assembly of Berkeley, 19–31 August 1963: Association Internationale d'Hydrologie Scientifique Publication No. 61, p. 168–180.

———1969, Was the Good Friday glacier on Axel Heiberg Island surging?: Canadian Journal of Earth Sciences, v. 6, no. 4, pt. 2, p. 891–894.

———1976, On the thermal regime of a high-Arctic valley glacier: Journal of Glaciology, v. 16, no. 74, p. 119–133.

———1981, The living Arctic: Agincourt, Ont., Methuen Publications, 233 p.

Müller, Fritz, and Iken, Almut, 1973, Velocity fluctuations and water regime of Arctic valley glaciers, *in* Symposium on the Hydrology of Glaciers, Cambridge, 7–13 September 1969: Association Internationale d'Hydrologie Scientifique Publication No. 95, p. 165–182.

Müller, Fritz, and Keeler, C.M., 1969, Errors in short-term ablation measurements on melting ice surfaces: Journal of Glaciology, v. 8, no. 52, p. 91–105.

Müller, Fritz, and others, 1963, Jacobsen-McGill Arctic Research Expedition 1959–1962; preliminary report 1961–1962 and map supplement: Montréal, Québec, McGill University, Axel Heiberg Island Research Reports, p. 241 and 6 maps.

Müller, Fritz and others, 1974–80, North Water project—Progress reports I–CI—Glaciological and climatological investigations of the North Water polynya in northern Baffin Bay: Zürich, ETH, Geographisches Institut, and Montréal, Québec, McGill University, Unpublished progress reports.

Müller, Fritz, Stauffer, Bernhard, and Schriber, G., 1977, Isotope measurements and firn stratigraphy on ice caps surrounding the North Water polynya, *in* Isotopes and impurities in snow and ice, Proceedings of the Grenoble Symposium, August/September 1975: IAHS-AISH Publication No. 118, p. 188–196.

Munday, W.A.D., 1931, Retreat of Coast Range glaciers: Canadian Alpine Journal, v. 20, p. 140–142.

Munro, D.S., 1976, On estimating the roughness lengths of glacier ice, *in* Davies, J.A., ed., Papers in climatology—the CAM Allen memorial volume: Hamilton, Ont., McMaster University, Department of Geography Discussion Paper No. 7, p. 129–141.

———1989, Surface roughness and bulk heat transfer on a glacier—Comparison with eddy correlation: Journal of Glaciology, v. 35, no. 121, p. 343–348.

———1990, Comparison of melt energy computations and ablatometer measurements on melting ice and snow: Arctic and Alpine Research, v. 22, no. 2, p. 153–162.

———1991a, On modelling surface meltwater discharge from arctic and alpine glaciers, *in* Prowse, T.D., and Ommanney, C.S.L., eds., Northern hydrology—Selected perspectives, Proceedings of the Northern Hydrology Symposium, Saskatoon, 10–12 July 1990: Saskatoon, Sask., Environment Canada, National Hydrology Research Institute Symposium No. 6, p. 253–262.

———1991b, A surface energy exchange model of glacier melt and net mass balance: International Journal of Climatology, v. 11, no. 6, p. 689–700.

Munro, D.S., and Davies, J.A., 1976, Diurnal energy flux variations and glacier surface hydrology, *in* Lvovitch, M.I., Kotlyakov, V.M., and Rauner, Yu.L., eds., International Geography '76, Section 2—Climatology, Hydrology, Glaciology: Moscow, International Geographical Congress, 23rd, Moscow, 22–26 July 1976, Proceedings, p. 75–77.

———1977, An experimental study of the glacier boundary layer over melting ice: Journal of Glaciology, v. 18, no. 80, p. 425–436.

———1978, On fitting the log-linear model to wind speed and temperature profiles over a melting glacier: Boundary-Layer Meteorology, v. 15, no. 4, p. 423–437.

Munro, D.S., and Young, G.J., 1980, A net shortwave radiation model for glacierized basins: 37th Annual Meeting, Eastern Snow Conference, Peterborough, Ontario, 5–6 June 1980, Proceedings, p. 159–169.

———1982, An operational net shortwave radiation model for glacier basins: Water Resources Research, v. 18, no. 2, p. 220–230.

Murray, Tavi, and Clarke, G.K.C., 1995, Black-box modeling of the subglacial water system: Journal of Geophysical Research, v. 100, no. B6, p. 10,231–10,245.

Nakawo, Masayoshi, and Young, G.J., 1982, Estimate of glacier ablation under a debris layer from surface temperature and meteorological variables: Journal of Glaciology, v. 28, no. 98, p. 29–34.

Narod, B.B., and Clarke, G.K.C., 1980, Airborne UHF radio echo-sounding of three Yukon glaciers: Journal of Glaciology, v. 25, no. 91, p. 23–31.

———1983, UHF radar system for airborne surveys of ice thickness: Canadian Journal of Earth Sciences, v. 20, no. 7, p. 1073–1086.

Narod, B.B., Clarke, G.K.C., and Prager, B.T., 1988, Airborne UHF radar sounding of glaciers and ice shelves, northern Ellesmere Island, Arctic Canada: Canadian Journal of Earth Sciences, v. 25, no. 1, p. 95–105.

Neave, K.G., and Savage, J.C., 1970, Icequakes on the Athabasca Glacier: Journal of Geophysical Research, v. 75, no. 8, p. 1351–1362.

Nelson, J.G., Ashwell, I.Y., and Brunger, A.G., 1966, Recession of the Drummond Glacier, Alberta: Canadian Geographer, v. 10, no. 2, p. 71–81.

Nielsen, L.E., 1969, The ice-dam, powder-flow theory of glacier surges: Canadian Journal of Earth Sciences, v. 6, no. 4, pt. 2, p. 955–961.

Norwegian Water Resources and Energy Administration, 1991, Part of Grinnell Glacier, Baffin Island, N.W.T.: Oslo, Norway, Norwegian Water Resources and Energy Administration map, scale 1:20,000, contour interval—10 m on glacier, 20 m elsewhere.

Nriagu, J.O., Lawson, G.S., and Gregor, D.J., 1994, Cadmium concentrations in recent snow and firn layers in the Canadian Arctic: Bulletin of Environmental Contamination and Toxicology, v. 52, no. 5, p. 756–759.

Odell, N.E., 1933, The mountains of northern Labrador: Geographical Journal, v. 82, no. 3, p. 193–210, v. 82, no. 4, p. 315–325.

Ommanney, C.S.L., 1969, Glacier inventory of Canada—Axel Heiberg Island, Northwest Territories: Ottawa, Ont., Department of Energy, Mines and Resources, Inland Waters Branch Technical Bulletin No. 37, 97 p. and maps.

———[1971]a, Canadian glacier inventory, *in* Glaciers, Proceedings of Workshop Seminar 1970, Vancouver, B.C., 24–25 September 1970: Ottawa, Ont., Canadian National Committee for the I.H.D., p. 23–30.

———1971b, Glacier surveys by District personnel of the Water Survey of Canada—1. The Victoria Glacier: Ottawa, Ont., Department of the Environment, Inland Waters Branch, Glacier Inventory Note No. 6, 18 p.

———1972a, Application of the Canadian glacier inventory to studies of the static water balance—1. The glaciers of Vancouver Island, *in* Adams, W.P., and Helleiner, F.M., eds., International geography 1972, v. 2: Toronto, Ont., University of Toronto Press, p. 1266–1268.

———1972b, Glacier surveys by District personnel of the Water Survey of Canada: 2. Peyto Glacier: Ottawa, Ont., Department of the Environment, Inland Waters Branch, Glacier Inventory Note No. 7, 20 p.

———1975, Canadian glacier studies 1960–1975, retrospect and prospect, *in* Canadian Hydrology Symposium—75, Winnipeg, Manitoba, 11–14 August 1975, Proceedings: Ottawa, Ont., National Research Council of Canada (NRCC 15195), Associate Committee on Hydrology, p. 262–281.

———1980, The inventory of Canadian glaciers: Procedures, techniques, progress and applications, *in* World Glacier Inventory Workshop, Riederalp, Switzerland, 17–22 September 1978: IAHS-AISH Publication No. 126, p. 35–44.

———1982, Bibliography of Canadian Glaciology, 1982—Bibliography No. 2, Ellesmere Island glaciers and ice shelves: Ottawa, Ont., Environment Canada, National Hydrology Research Institute, Glacier Inventory Note No. 9, NHRI Paper No. 20, IWD Report Series No. 58, 53 p.

———1989, Glacier Atlas of Canada: Saskatoon, Sask., Environment Canada, National Hydrology Research Institute, Scientific Information Division, Limited edition, 2 p. and 52 maps.

———1993, Yukon Glaciers, *in* Prowse, T.D., Ommanney, C.S.L., and Ulmer, K.E., eds., Proceedings of the 9th International Northern Research Basins Symposium/Workshop, Whitehorse, Dawson City, Eagle Plains, Yukon; Inuvik, Northwest Territories, 14–22 August 1992: Saskatoon, Saskatchewan, Environment Canada, National Hydrology Research Institute Symposium No. 10, v. 1, p. 373–382.

———1996, 100 years of glacier observations in Canada (1890–1990): Geografía Física e Dinámica Quaternaria, 1995, v. 18, no. 2, p. 321–330.

Ommanney, C.S.L., and Young, G.J., 1988, Research on Canadian glaciers within the IHD/IHP, in CHS–88 Canadian research basins—Successes, failures and future, Banff, Alberta, 9–11 May 1988, Proceedings: National Research Council of Canada (NRCC 30416), Associate Committee on Hydrology, Canadian Hydrology Symposium No. 17, p. 21–28.

Orvig, Svenn, 1951, The climate of the ablation period on the Barnes Ice-Cap in 1950: Geografiska Annaler, v. 33, p. 166–209.

———1953, The glaciological studies of the Baffin Island Expedition, 1950. Part V—On the variation of the shear stress on the bed of an ice cap: Journal of Glaciology, v. 2, no. 14, p. 242–247.

———1954, Glacial-meteorological observations on icecaps in Baffin Island: Geografiska Annaler, v. 36, no. 3–4, p. 193–318.

Osborn, G.[D.], 1986, Lateral-moraine stratigraphy and neoglacial history of Bugaboo Glacier, British Columbia: Quaternary Research, v. 26, no. 2, p. 171–178.

Osborn, G.[D.], and Karlstrom, E.T., 1988, Holocene history of the Bugaboo Glacier, British Columbia: Geology (Boulder), v. 16, no. 11, p. 1015–1017.

Osborn, G.[D.], and Luckman, B.H., 1988, Holocene glacier fluctuations in the Canadian Cordillera (Alberta and British Columbia): Quaternary Science Reviews, v. 7, no. 2, p. 115–128.

Østrem, Gunnar, 1966a, The height of the glaciation limit in southern British Columbia and Alberta: Geografiska Annaler, v. 48A, no. 3, p. 126–138.

———1966b, Mass balance studies on glaciers in western Canada, 1965: Geographical Bulletin, v. 8, no. 1, p. 81–107.

———1972, Height of the glaciation level in northern British Columbia and southeastern Alaska: Geografiska Annaler, v. 54A, no. 2, p. 76–84 and map.

———1973a, Runoff forecasts for highly glacierized basins, *in* The role of snow and ice in hydrology, Proceedings of the Banff Symposium, September 1972: IAHS-AISH Publication No. 107, v. 2, p. 1111–1132.

———1973b, The transient snowline and glacier mass balance in southern British Columbia and Alberta, Canada: Geografiska Annaler, v. 55A, no. 2, p. 93–106.

Østrem, Gunnar, and Brugman, M.[M.], 1991, Glacier mass-balance measurements—A manual for field and office work: Saskatoon, Sask., Environment Canada, National Hydrology Research Institute NHRI Science Report No. 4, 224 p.

Østrem, Gunnar, and Stanley, A.D., 1966, Glacier mass balance measurements—A manual for field work: Ottawa, Ont., Department of Energy, Mines and Resources, Glaciology Section, 81 p. and tables.

Østrem, Gunnar, Bridge, C.W., and Rannie, W.F., 1967, Glaciohydrology, discharge and sediment transport in the Decade Glacier, Baffin Island, N.W.T.: Geografiska Annaler, v. 49A, no. 2–4, p. 268–282.

Oswald, G.K.A., 1975, Investigation of sub-ice bedrock characteristics by radio-echo sounding: Journal of Glaciology, v. 15, no. 73, p. 75–87.

Palmer, Howard, 1914, Mountaineering and exploration in the Selkirks—A record of pioneer work among the Canadian Alps, 1908–1912: New York and London, Knickerbocker Press, G.P. Putnam's Sons, 439 p.

———1924, Observations on the Freshfield Glacier, Canadian Rockies: Journal of Geology, v. 32, no. 5, p. 432–441.

Parent, Michel, 1991, La zone frontale des glaciers Thompson et White dans l'île Axel Heiberg du Haut Arctique canadien—Quelques observations préliminaires: Geological Survey of Canada Paper No. 91-1E, p. 203–210.

Parker, G., 1975, Meandering of supraglacial melt streams: Water Resources Research, v. 11, no. 4, p. 551–552.

Parker, M.L., and Henoch, W.E.S., 1971, The use of Engelmann spruce latewood density for dendrochronological purposes: Canadian Journal of Forest Research, v. 1, no. 2, p. 90–98.

Paterson, W.S.B., 1960, Glaciological research in western Canada in 1959—Expedition to Athabasca Glacier: Canadian Alpine Journal, v. 43, p. 99–102.

———1961, Glaciological research on Athabasca Glacier in 1960: Canadian Alpine Journal, v. 44, p. 110–111.

———1962, Glaciological research on Athabaska Glacier in 1961: Canadian Alpine Journal, v. 45, p. 148.

———1964, Variations in velocity of Athabasca Glacier with time: Journal of Glaciology, v. 5, no. 39, p. 277–285.

Paterson, W.S.B., 1966, Test of contour accuracy on a photogrammetric map of Athabasca Glacier: Canadian Journal of Earth Sciences, v. 3, no. 6, p. 909–915.

———1968, A temperature profile through the Meighen Ice Cap, Arctic Canada, *in* General Assembly of Bern 1967—Snow and Ice: Association Internationale d'Hydrologie Scientifique Publication No. 79, p. 440–449.

———1969, The Meighen Ice Cap, Arctic Canada—Accumulation, ablation and flow: Journal of Glaciology, v. 8, no. 54, p. 341–352.

Paterson, W.S.B., 1970, The sliding velocity of Athabasca Glacier, Canada: Journal of Glaciology, v. 9, no. 55, p. 55–63.

———1971, Temperature measurements in Athabasca Glacier, Alberta, Canada: Journal of Glaciology, v. 10, no. 60, p. 339–349.

———1972, Temperature distribution in the upper layers of the ablation area of Athabasca Glacier, Alberta, Canada: Journal of Glaciology, v. 11, no. 61, p. 31–41.

———1976a, Temperatures in the Devon Island ice cap, Arctic Canada: Journal of Glaciology, v. 16, no. 74, p. 277.

———1976b, Vertical strain-rate measurements in an Arctic ice cap and deductions from them: Journal of Glaciology, v. 17, no. 75, p. 3–12.

———1977, Secondary and teritiary creep of glacier ice as measured by borehole closure rates: Reviews of Geophysics and Space Physics, v. 15, no. 1, p. 47–55.

———1985, Flow law for ice in polar ice sheets: Nature, v. 318, no. 6041, p. 82–83.

———1994, The physics of glaciers (3d ed.): Oxford, Elsevier, 480 p.

Paterson, W.S.B., and Clarke, G.K.C., 1978, Comparison of theoretical and observed temperature profiles in Devon Island ice cap, Canada: Geophysical Journal of the Royal Astronomical Society, v. 55, no. 3, p. 615–632.

Paterson, W.S.B., and Koerner, R.M., 1974, Radio echo sounding on four ice caps in Arctic Canada: Arctic, v. 27, no. 3, p. 225–233.

Paterson, W.S.B., and Savage, J.C., 1963a, Geometry and movement of the Athabasca Glacier: Journal of Geophysical Research, v. 68, no. 15, p. 4513–4520.

———1963b, Measurements on Athabasca Glacier relating to the flow law of ice: Journal of Geophysical Research, v. 68, no. 15, p. 4537–4543.

Paterson, W.S.B., and Waddington, E.D., 1984, Past precipitation rates derived from ice-core measurements—Methods and data analysis: Reviews of Geophysics and Space Physics, v. 22, no. 2, p. 123–130.

Paterson, W.S.B., Koerner, R.M., Fisher, D.A., Johnsen, S.J., Clausen, H.B., Dansgaard, Willi, Bucher, Peter, and Oeschger, Hans, 1977, An oxygen-isotope climatic record from the Devon Island ice cap, Arctic Canada: Nature, v. 266, no. 5602, p. 508–511.

Perchanok, M.S., 1980, Reconnaissance of glacier-dammed lakes in the Stikine and Iskut River basins, British Columbia: Ottawa, Ont., Environment Canada, Inland Waters Directorate, National Hydrology Research Institute, Contract No. KL229-0-4292, Unpublished report, 38 p. and maps.

Pfeffer, W.T., Illangasekare, T.H., and Meier, M.F., 1990, Analysis and modeling of melt-water refreezing in dry snow: Journal of Glaciology, v. 36, no. 123, p. 238–246.

Pietroniro, Alain, and Demuth, Michael, 1999, Inferring glacier mass balance using Radarsat: Results from Peyto Glacier, Canada: Geografiska Annaler, v. 81A, no. 4, p. 521–540.

Post, A.[S.], 1966, The recent surge of Walsh Glacier, Yukon and Alaska: Journal of Glaciology, v. 6, no. 45, p. 375–381.

———1969, Distribution of surging glaciers in North America: Journal of Glaciology, v. 8, no. 53, p. 229–240.

Post, A.S., and LaChapelle, E.R., 1971, Glacier ice: Seattle, WA, Toronto, Ont., University of Toronto Press, 110 p.

Post, A.[S.], and Mayo, L.R., 1971, Glacier dammed lakes and outburst floods in Alaska: U.S. Geological Survey Hydrological Investigations Atlas HA-455, 10 p. and 3 maps.

Post, A.[S.], Meier, M.F., and Mayo, L.R., 1976, Measuring the motion of the Lowell and Tweedsmuir surging glaciers of British Columbia, Canada: U.S. Geological Survey Professional Paper 929, p. 180–184.

Pourchet, Michel, Pinglot, J.F., Reynaud, Louis, and Holdsworth, Gerald, 1988, Identification of Chernobyl fall-out as a new reference level in Northern Hemisphere glaciers: Journal of Glaciology, v. 34, no. 117, p. 183–187.

Power, J.M., 1985, Canada case study—Water supply, *in* Young, G.J., ed., Techniques for prediction of runoff from glacierized areas: International Association of Hydrological Sciences Publication No. 149, p. 59–71.

Power, J.M., and Young, G.J., 1979, Application of the UBC watershed model to Peyto Glacier basin, *in* Canadian Hydrology Symposium 79, Cold Climate Hydrology, Vancouver, B.C., 10–11 May 1979, Proceedings: Ottawa, Ont., National Research Council of Canada (NRCC 17834), Associate Committee on Hydrology, p. 217–228.

Prager, B.T., 1983, Digital signal processing of UHF radio echo sounding data: M.Sc. thesis, Vancouver, B.C., University of British Columbia, Department of Geophysics and Astronomy, 88 p.

Prest, V.K., 1983, Canada's heritage of glacial features/l'héritage glaciaire du Canada: Geological Survey of Canada Miscellaneous Report No. 28, 119 p.

Ragle, R.H., 1964, The Icefield Ranges research project, 1963: Arctic, v. 17, no. 1, p. 55–57.

———1973, The Icefield Ranges research project, 1972: Arctic, v. 26, no. 3, p. 258–263.

Ragle, R.H., Blair, R.G., and Persson, L.E., 1964, Ice core studies of Ward Hunt Ice Shelf, 1960: Journal of Glaciology, v. 5, no. 37, p. 39–59.

Rains, R.B., 1990, Cline Glacier and Shoe Leather Creek, Alberta—Morphology and hydrology: Edmonton, Alberta, University of Alberta, Department of Geography, 20 p.

Raisbeck, G.M., and Yiou, F., 1985, ^{10}Be in polar ice and atmospheres: Annals of Glaciology, v. 7, p. 138–140.

Raymond, C.F., 1971a, Determination of the three-dimensional velocity field in a glacier: Journal of Glaciology, v. 10, no. 58, p. 39–53.

——1971b, Flow in a transverse section of Athabasca Glacier, Alberta, Canada: Journal of Glaciology, v. 10, no. 58, p. 55–84.

Raymond, C.F., 1973, Inversion of flow measurements for stress and rheological parameters in a valley glacier: Journal of Glaciology, v. 12, no. 64, p. 19–44.

Redpath, B.B., 1965, Seismic investigation of glaciers on Axel Heiberg Island, Canadian Arctic Archipelago: Montréal, Québec, McGill University, Axel Heiberg Island Research Reports, Geophysics No. 1, 26 p.

Reeh, Niels, 1991, The last interglacial as recorded in the Greenland ice sheet and Canadian Arctic ice caps: Quaternary International, v. 10–12, p. 123–142.

Reeh, Niels, and Paterson, W.S.B., 1988, Application of a flow model to the ice-divide region of Devon Island Ice Cap, Canada: Journal of Glaciology, v. 34, no. 116, p. 55–63.

Reeh, Niels, Hammer, C.U., Thomsen, H.H., and Fisher, D.A., 1987, Use of trace constituents to test flow models for ice sheets and ice caps, *in* Symposium on the Physical Basis of Ice Sheet Modelling, Vancouver, British Columbia, Canada, 9–22 August 1987, Proceedings: IASH Publication No. 170, p. 299–310.

Reid, I.A., 1961, Triangulation survey of the Athabasca Glacier, July 1959: Ottawa, Ont., Department of Northern Affairs and National Resources, Water Resources Branch, Internal report, p. 20 and 2 maps.

———1973, Glacier surveys by the Water Survey of Canada, *in* The role of snow and ice in hydrology, Proceedings of the Banff Symposium, September 1972: IAHS-AISH Publication No. 107, v. 2, p. 1133–1143.

Reid, I.A., and Charbonneau, J.O.G., 1972, Glacier surveys in Alberta: Ottawa, Ont., Environment Canada, Water Resources Branch, Inland Waters Directorate Report Series No. 22, 17 p. and maps.

———1975, Glacier surveys in British Columbia—1970: Ottawa, Ont., Environment Canada, Water Resources Branch, Inland Waters Directorate Report Series No. 32, 23 p. and 5 maps.

———1979a, Glaciers surveys in Alberta—1977: Ottawa, Ont., Environment Canada, Water Resources Branch, Inland Waters Directorate Report Series No. 65, 17 p. and maps.

———1979b, Glaciers surveys in British Columbia—1976: Ottawa, Ont., Environment Canada, Water Resources Branch, Inland Waters Directorate Report Series No. 63, 21 p. and maps.

Reid, I.A., and Paterson, W.S.B., 1973, Simple method for measuring the average amount of water produced annually by melting of ice on a glacier, *in* Symposium on the Hydrology of Glaciers, Cambridge, 7–13 September 1969: Association Internationale d'Hydrologie Scientifique Publication No. 95, p. 215–218.

Reid, I.A., and Shastal, John, 1970, Glaciers surveys in British Columbia—1968: Ottawa, Ont., Department of Energy, Mines and Resources, Inland Waters Branch Report Series No. 10, 26 p. and maps.

Reid, I.A., Charbonneau, J.O.G., and Warner, L.A., 1978, Glacier surveys in Alberta—1975: Ottawa, Ont., Fisheries and Environment Canada, Water Resources Branch, Inland Waters Directorate Report Series No. 60, 17 p. and maps.

Rentsch, Hermann, Welsch, Walter, Heipke, Christian, and Miller, M.M., 1990, Digital terrain models as a tool for glacier studies: Journal of Glaciology, v. 36, no. 124, p. 273–278.

Reynolds, J.R., 1992, Dendrochronology and glacier fluctuations at Peyto Glacier, Banff National Park: B.A. thesis, London, Ont., University of Western Ontario, Department of Geography, 73 p.

Reynolds, J.R., and Young, G.J., 1997, Changes in areal extent, elevation and volume of Athabasca Glacier, Alberta, Canada, as estimated from a series of maps produced between 1919 and 1979: Annals of Glaciology, v. 24, p. 60–65.

Ricker, K.[E.], 1962, Polar ice-dammed lakes: Canadian Alpine Journal, v. 45, p. 149–151.

———1976, Tchaikazan Valley earth science notes: Canadian Alpine Journal, v. 59, p. 16–19.

———1977, Wedgemount Lake and lower Glacier basin: Vancouver, B.C., Mountain Equipment Coop., map-scale 1:5,000. [Map drawn by K. Ricker with additional contour information provided by K. Bracewell, W. Tupper, and the British Columbia Institute of Technology].

———1979, Earth Science Studies—Snowcap Lakes—a dramatic record of diachronous glacier movement, drainage reversals, and fluctuating water levels: Canadian Alpine Journal, v. 62, p. 59–65.

———1980, Earth science features and glacier regimen of the Clendenning and Elaho Ranges, Coast Mtns., British Columbia: Canadian Alpine Journal, v. 63, p. 57–65.

———1990, Overlord Glacier—A 1989 update: The British Columbia Mountaineer, v. 60, p. 108.

Ricker, K.E., and Jozsa, L., 1984, Retreat of the New Moon Glacier, Buckley Ranges, Hazelton Mountains, western British Columbia: Canadian Alpine Journal, v. 67, p. 66–69.

Ricker, K.E., and Parke, B.[A.], 1984, Caltha Lake moraines and other natural history matters, Stein River Divide in the Lillooet Ranges of the Coast Mountains: Canadian Alpine Journal, v. 67, p. 62–65.

Ricker, K.[E.], and Tupper, W.A., 1988, A recent advance of the Overlord Glacier: British Columbia Mountaineer, v. 59, p. 84–86.

———1992, Glacier variations in northern Garibaldi Park—1991 update: British Columbia Mountaineer, v. 61, p. 104–105.

———1996, Overlord and Wedgemount Glaciers—a century of shrinkage: British Columbia Mountaineer, v. 63, p. 99–104.

Ricker, K.[E.], Tupper, W.A., Lyon, R.D., and Fairley, J., 1983, Wedgemount Lake and Glacier studies, northern Garibaldi Park—1982 progress report: Canadian Alpine Journal, v. 66, p. 58–61.

Rigsby, G.P., 1958, Fabrics of glacier and laboratory deformed ice, *in* Symposium on Physics of the Movement of the Ice, Symposium of Chamonix, 16–24 September 1958: Association Internationale d'Hydrologie Scientifique Publication No. 47, p. 351–358.

———1960, Crystal orientation in glacier and experimentally deformed ice: Journal of Glaciology, v. 3, no. 27, p. 589–606.

Robertson, B., 1997, Mass balance methods in the accumulation zone of the White Glacier, Axel Heiberg Island, N.W.T., Canada: B.Sc. thesis, Peterborough, Ont., Trent University, Department of Geography.

Rogerson, R.J., 1985, Measured re-advance of a debris-covered glacier terminus in the President Range, Yoho National Park, British Columbia, Canada: Journal of Glaciology, v. 31, no. 107, p. 13–17.

Rogerson, R.J., 1986, Mass balance of four cirque glaciers in the Torngat Mountains of northern Labrador, Canada: Journal of Glaciology, v. 32, no. 111, p. 208–218.

Rogerson, R.J., and Eyles, Nicholas, 1979, Subglacial, englacial, and supraglacial sediment differentiation and erosion in glacial basins [abs.]: Journal of Glaciology, v. 23, no. 89, p. 413.

Rogerson, R.J., Olson, M.E., and Branson, D., 1986, Medial moraines and surface melt on glaciers of the Torngat Mountains, northern Labrador, Canada: Journal of Glaciology, v. 32, no. 112, p. 350–354.

Römmer, S., and Hell, Günther, 1986, Veräungen der Zunge eines Gletschers am Harefjord (NWT, Kanada) zwischen 1958 und 1978: Diplomarbeit im Studiengang Kartographie, FH Karlsruhe, FRG, map.

Roots, E.F., 1967, Yukon Centennial projects—A variety of survey problems: Canadian Surveyor, v. 21, no. 3, p. 250–259.

———1984, Glacier mass balance measurements—An honourable past, an important future: Geografiska Annaler, v. 66A, no. 3, p. 165–167.

Rossiter, J.R., LaTorraca, G.A., Annan, A.P., Strangway, D.W., and Simmons, Gene, 1973, Radio interferometry depth sounding—Part II. Experimental results: Geophysics, v. 38, no. 3, p. 581–599.

Russell, R.D., Jacobs, J.A., and Grant, F.S., 1960, Gravity measurements on the Salmon Glacier and adjoining snowfield, British Columbia: Geological Society of America Bulletin, v. 71, no. 8, p. 1223–1229.

Sackinger, W.M., Serson, H.V., Jeffries, M.O., Shoemaker, H.D., and Yan, M.-H., 1985, Ice island generation and trajectories north of Ellesmere Island, Canada: POAC85, International Conference on Port and Ocean Engineering under Arctic Conditions, 8th, Narssarssuaq, Greenland, 7–14 September 1985, Proceedings, v. 2: Hørsholm, Danish Hydraulic Institute, p. 1009–1040.

Sagar, R.B., 1964, Meteorological and glaciological observations on the Gilman Glacier, northern Ellesmere Island, 1961: Geographical Bulletin, v. 22, p. 13–56.

———1966, Glaciological and climatological studies on the Barnes Ice Cap, 1962–64: Geographical Bulletin, v. 8, no. 1, p. 3–47.

Savage, J.C., and Paterson, W.S.B., 1963, Borehole measurements in the Athabasca Glacier: Journal of Geophysical Research, v. 68, no. 15, p. 4521–4536.

———1965, Additional borehole measurements in the Athabasca Glacier: Journal of Geophysical Research, v. 70, no. 14, p. 3511–3513.

Schmok, J.P., 1990, 1989 mass balance determination and geodetic survey of Sentinel, Place and Helm Glaciers, British Columbia: Saskatoon, Sask., Environment Canada, Physical Hydrology Division, National Hydrology Research Institute Contract Report No. 90001, 29 p.

Sedgwick, J.K., and Henoch, W.E.S., 1975, Peyto Glacier, general information: Ottawa, Ont., Department of the Environment, Inland Waters Directorate, Water Resources Branch, Glaciology Division, 30 p. and map.

Serreze, M.C., and Bradley, R.S., 1987, Radiation and cloud observations on a High Arctic plateau ice cap: Journal of Glaciology, v. 33, no. 114, p. 162–168.

Serson, H.V., 1979, Mass balance of the Ward Hunt Ice Rise and Ice Shelf—An 18-year record: Victoria, B.C., Department of National Defence, Research and Development Branch, Defence Research Establishment Pacific Technical Memorandum No. 79–4, 14 p.

Sharp, R.P., 1950, Report of glaciological work on Project Snow Cornice in 1949: American Alpine Journal, v. 7, no. 4, p. 432–435.

Sharp, R.P., and Epstein, Samuel, 1958, Oxygen-isotope ratios and glacier movement, *in* Symposium on Physics of the Movement of the Ice, Symposium of Chamonix, 16–24 September 1958: Association Internationale d'Hydrologie Scientifique Publication No. 47, p. 359–369.

Sherzer, W.H., 1907, Glaciers of the Canadian Rockies and Selkirks (Smithsonian Expedition of 1904): Washington, D.C., Smithsonian Institution, Smithsonian Contributions to Knowledge, v. 34, art. 4 (1692), 135 p.

———1908, The nature and activity of Canadian glaciers: Canadian Alpine Journal, v. 1, no. 2, p. 249–263.

Shilts, Elizabeth, Fick, Steven, Murray, Andrew, and McLean, Janice 1998, The glaciers of Canada: Canadian Geographic, v. 118, no. 7, p. 51–52 (8-page foldout, color map).

Shimizu, Hiromu, and Wakahama, Gorow, 1965, Kasukaurushu hyoga (Kanada) genryuiki ni okeru sekisetsu chosa (On the firn study in the accumulation area of Kaskawulsh Glacier, Canada): Teion Kagaku (Low Temperature Science), Series A, v. 23, p. 137–156.

Shoemaker, E.M., 1991, On the formation of large subglacial lakes: Canadian Journal of Earth Sciences, v. 28, no. 12, p. 1975–1981.

Short, S.K., and Holdsworth, Gerald, 1985, Pollen, oxygen isotope content and seasonality in an ice core from the Penny Ice Cap, Baffin Island: Arctic, v. 38, no. 3, p. 214–218.

Slaney, V.R., 1981, Landsat images of Canada—A geological appraisal: Canada Geological Survey Paper No. 80–15, 102 p.

Sloan, V.F., 1987, Relationships between glacier terminus melt processes and climatic conditions, Boundary Glacier, Alberta: Eastern Snow Conference, 43rd Annual Meeting, Hanover, New Hampshire, 5–6 June 1986, Proceedings, p. 222–227.

Smart, C.C., 1984, Glacier hydrology and the potential for subglacial karstification: Norsk Geografisk Tidsskrift, v. 38, no. 3–4, p. 157–161.

———1986, Some observations on subglacial ground-water flow: Journal of Glaciology, v. 32, no. 111, p. 232–234.

———1988, Exceedance probability distributions of steady conduit flow in karst aquifers: Hydrological Processes, v. 2, no. 1, p. 31–41.

———1992, Temperature compensation of electrical conductivity in glacial meltwaters: Journal of Glaciology, v. 38, no. 128, p. 9–12.

———1998, Statistical evaluation of glacier boreholes as indicators of basal drainage systems, *in* Sharp, M.J., Richards, K.S., and Tranter, Martyn, eds., Glacier hydrology and hydrochemistry: Chichester, Wiley, p. 175–189.

Smart, C.C., and Ford, D.C., 1983, The Castleguard karst, Main Ranges, Canadian Rocky Mountains: Journal of Hydrology, v. 61, no. 1–3, p. 193–197.

Smart, C.C., 1986, Structure and function of a conduit aquifer: Canadian Journal of Earth Sciences, v. 23, no. 7, p. 919–929.

Smith, D.J., 1994, Field investigations in Strathcona Provincial Park—1993: Victoria, Ministry of Environment, Lands and Parks, British Columbia Parks Branch, Strathcona District.

Smith, R.F., 1997, Final report of the Joint Services Expedition to the Blue Mountains, Ellesmere Island, High Arctic Canada, 1994: Elmwood Avenue, Feltham, Middlesex TW13 7AH, U.K., Military Survey, 174 p.

Souchez, R.A., and De Groote, J.M., 1985, δD–$\delta^{18}O$ relationships in ice formed by subglacial freezing—Paleoclimatic implications: Journal of Glaciology, v. 31, no. 109, p. 229–232.

Souchez, R.[A.], Lorrain, R.[D.], Tison, J.L., and Jouzel, Jean, 1988, Co-isotopic signature of two mechanisms of basal-ice formation in Arctic outlet glaciers: Annals of Glaciology, v. 10, p. 163–166.

Spector, Allan, 1966, A gravity survey of the Melville Island ice caps: Journal of Glaciology, v. 6, no. 45, p. 393–400.

Stanley, A.D., 1969, Observations on the surge of the Steele Glacier, Yukon Territory, Canada: Canadian Journal of Earth Sciences, v. 6, no. 4, pt. 2, p. 819–830.

———1975, Mass and water balance studies at selected glacier basins in western Canada, *in* Snow and Ice Symposium, Moscow, August 1971, Proceedings: IAHS-AISH Publication No. 104, p. 181–184.

Stenning, A.J., Banfield, C.E., and Young, G.J., 1981, Synoptic controls over katabatic layer characteristics above a melting glacier: Journal of Climatology, v. 1, no. 4, p. 309–324.

Stewart, T.G., 1991, Glacial marine sedimentation from tidewater glaciers in the Canadian High Arctic, *in* Anderson, J.B., and Ashley, G.M., eds., Glacial marine sedimentation; paleoclimatic significance: Boulder, Colo., Geological Society of America Special Paper No. 261, p. 95–105.

Stolle, D.F.E., 1986, Two-dimensional line element for glacier flow problems: Engineering Analysis, v. 3, no. 3, p. 161–165.

———1988, A one-dimensional finite-element model for two-dimensional glacier flow: Journal of Glaciology, v. 34, no. 117, p. 236–241.

Stone, D.B., and Clarke, G.K.C., 1993, Estimation of subglacial hydraulic properties from induced changes in basal water pressure: A theoretical framework for borehole-response tests: Journal of Glaciology, v. 39, no. 132, p. 327–340.

———1998, In situ measurements of basal water quality and pressure as an indicator of the character of subglacial drainage systems, *in* Sharp, M.J., Richards, K.S., and Tranter, Martyn, eds., Glacier hydrology and hydrochemistry: Chichester, Wiley, p. 205–218.

Stone, D.B., Clarke, G.K.C., and Blake, E.W., 1993, Subglacial measurement of turbidity and electrical conductivity: Journal of Glaciology, v. 39, no. 132, p. 415–420.

Strilaeff, P.W., 1961, Glacier surveys in British Columbia: Western Snow Conference, 29th Annual Meeting, Spokane, Washington, 11–13 April 1961, Proceedings, p. 1–5.

Sturges, W.T., Penkett, S.A., Atlas, E.L., and Chappellaz, J.[A.], 1998, Evidence from trace gas profiles of biogenic activity in deep firn layers from Devon Island, Canada [abs.]: EOS, Transactions, American Geophysical Union, v. 79, no. 45, Fall Meeting Supplement, p. F58.

Taylor-Barge, Bea, 1969, The summer climate of the St. Elias Mountains Region, *in* Icefield Ranges Research Project: Scientific Results, v. 1: American Geographical Society and Arctic Institute of North America, p. 33–49.

The Ice Age Co., 1989, Cline Glacier ice mining project—Environmental impact assessment: Edmonton, Alberta, The Ice Age Co. Inc., 62 p.

Thorington, J.M., 1938, Notes on Saskatchewan and Freshfield Glaciers: American Alpine Journal, v. 3, no. 2, p. 219–220.

Tison, J.L., Souchez, Roland, and Lorrain, Reginald, 1989, On the incorporation of unconsolidated sediments in basal ice—Present-day examples: Zeitschrift für Geomorphologie, Supplementband 72, p. 173–183.

Tolland, L., Dicks, W., Buttle, J.[M.], Ecclestone, M.[A.], and Adams, W.P., 1991, Observations of discharge from the Baby Glacier, Axel Heiberg Island, N.W.T, *in* Third National Student Conference on Northern Studies, Ottawa, Ontario, 23–24 October 1991, Abstracts of Papers: Ottawa, Ont., Association of Canadian Universities for Northern Studies, p. 205–206.

Trabant, D.C., Krimmel, R.M., and Post, A.[S.], 1991, A preliminary forecast of the advance of Hubbard Glacier and its influence on Russell Fiord, Alaska: U.S. Geological Survey Water-Resources Investigations Report No. 90–4172, 34 p.

Trombley, T.J., 1986, A radio echo-sounding survey of Athabasca Glacier, Alberta, Canada: M.Sc. thesis, Manchester, N.H., University of New Hampshire, Department of Earth Science, 64 p.

Tupper, W.A., and Ricker, K.E., 1982, Wedgemount Lake and Glacier studies, northern Garibaldi Park—1981 progress report: Canadian Alpine Journal, v. 65, p. 51–52.

Tupper, B.[W.A.], Ricker, K.E., Bremner, R., Frankich, K., and Fairley, J., 1984, Wedgemount Lake and Glacier studies, northern Garibaldi Park—1983 progress report: Canadian Alpine Journal, v. 67, p. 61–62.

Tupper, B.[W.A.], Ricker, K.[E.], Fairley, J., and Lyon, R.D., 1986, Wedgemount Lake and Glacier, northern Garibaldi Park—1985 progress report: Canadian Alpine Journal, v. 69, p. 44–45.

Tupper, W.A., Ricker, K.E., and McKnight, B., 1985, Wedgemount Lake and Glacier, northern Garibaldi Park—1984 progress report: Canadian Alpine Journal, v. 68, p. 41.

Untersteiner, Norbert, and Nye, J.F., 1968, Computations of the possible future behaviour of Berendon Glacier, Canada: Journal of Glaciology, v. 7, no. 50, p. 205–213.

Vachon, P.W., Geudtner, D., Mattar, K.[E.], Gray, A.L., Brugman, M.[M.], and Cumming, I., 1996, Differential SAR interferometry measurements of Athabasca and Saskatchewan Glacier flow rate: Canadian Journal of Remote Sensing, v. 22, no. 3, p. 287–296.

VanDine, D.F., 1985, Debris flows and debris torrents in the southern Canadian Cordillera: Canadian Geotechnical Journal, v. 22, no. 1, p. 44–68.

Vaux, George, 1910, Observations on glaciers in 1909: Canadian Alpine Journal, v. 2, no. 2, p. 126–129.

Vaux, George, [Jr.] and Vaux, W.S., Jr., 1900a, Additional observations on glaciers in British Columbia: Proceedings of the Academy of Natural Sciences of Philadelphia, p. 501–511.

———1900b, Some observations on the Illecillewaet and Asulkan Glaciers of British Columbia: Proceedings of the Academy of Natural Sciences of Philadelphia, p. 121–124.

———1901, Observations made in 1900 on glaciers in British Columbia: Proceedings of the Academy of Natural Sciences of Philadelphia, p. 213–215.

———1907a, Glacier observations: Canadian Alpine Journal, v. 1, no. 1, p. 138–148.

———1907b, Observations made in 1906 on glaciers in Alberta and British Columbia: Proceedings of the Academy of Natural Sciences of Philadelphia, p. 568–579.

———1908, Observations made in 1907 on glaciers in Alberta and British Columbia: Proceedings of the Academy of Natural Sciences of Philadelphia, p. 560–563.

Vaux, M.M., 1911, Observations on glaciers in 1910: Canadian Alpine Journal, v. 3, p. 127–129.

———1913, Observations on glaciers: Canadian Alpine Journal, v. 5, p. 59–61.

Vaux, M.M., and Vaux, George, Jr., 1911, The glaciers of the Canadian Rockies and Selkirks (2d ed.): Bryn Mawr, Pennsylvania, privately printed, 20 p.

Vaux, W.S., [Jr.] 1907, Modern glaciers: their movements and the methods of observing them: Proceedings of the Engineers Club of Philadelphia, v. 24, no. 3, p. 1–25.

———1909, Modern glaciers: Canadian Alpine Journal, v. 2, no. 1, p. 56–78.

Vögtli, Kurt, 1967, D.C. resistivity soundings on Devon Island, N.W.T., Canada: Journal of Glaciology, v. 6, no. 47, p. 635–642.

Waddington, B.S., and Clarke, G.K.C., 1995, Hydraulic properties of subglacial sediment determined from the mechanical response of water-filled boreholes: Journal of Glaciology, v. 41, no. 137, p. 112–124.

Waddington, E.D., and Clarke, G.K.C., 1988, Stable-isotope pattern predicted in surge-type glaciers: Canadian Journal of Earth Sciences, v. 25, no. 5, p. 657–668.

Waddington, E.D., Fisher, D.A., Koerner, R.M., and Paterson, W.S.B., 1986, Flow near an ice divide—Analysis problems and data requirements: Annals of Glaciology, v. 8, p. 171–174.

Walford, M.E.R., Holdorf, P.C., and Oakberg, R.G., 1977, Phase-sensitive radio-echo sounding at the Devon Island ice cap, Canada: Journal of Glaciology, v. 18, no. 79, p. 217–229.

Wallace, A.L., 1995, The volumetric change of the Peyto Glacier, Alberta, Canada 1896–1966: M.A. thesis, Waterloo, Ont., Wilfred Laurier University, 110 p.

Ward, W.H., 1954, Glaciological studies in the Penny Highland, Baffin Island, 1953, *in* General Assembly of Rome, v. 4: Association Internationale d'Hydrologie Scientifique Publication No. 39, p. 297–308.

———1955, Studies in glacier physics on the Penny Ice Cap, Baffin Island, 1953. Part IV—The flow of Highway Glacier: Journal of Glaciology, v. 2, no. 18, p. 592–599.

Ward, W.H., and Baird, P.D., 1954, Studies in glacier physics on the Penny Ice Cap, Baffin Island, 1953. Part I—A description of the Penny Ice Cap, its accumulation and ablation: Journal of Glaciology, v. 2, no. 15, p. 342–355.

Ward, W.H., and Orvig, Svenn, 1953, The glaciological studies of the Baffin Island Expedition, 1950. Part IV—The heat exchange at the surface of the Barnes Ice Cap during the ablation period: Journal of Glaciology, v. 2, no. 13, p. 158–168.

Warner, L.A., Anderson, J.E., Kerber, R.E., and Robinson, C.P., 1972, 1972 survey of the Athabasca and Saskatchewan Glaciers: Calgary, Alberta, Department of the Environment, Water Survey of Canada, Internal Report, 34 p.

Waskasoo Design Group Limited, 1991, Columbia Icefield visitor centre interpretation media concepts: Jasper, Alberta, Canadian Parks Service, Interpretive Service, Jasper National Park, 171 p.

Weaver, R.L., 1975, "Boas" Glacier (Baffin Island, N.W.T., Canada) mass balance for the five years 1969 to 1974: Arctic and Alpine Research, v. 7, no. 3, p. 279–284.

Webb, C.E., 1948, Glacier studies in British Columbia: Western Snow Conference, Annual Meeting, Reno, Nevada, 15–17 April 1948, Proceedings, p. 46–54.

Weber, J.R., 1961, Comparison of gravitational and seismic depth determinations on the Gilman Glacier and adjoining ice-cap in northern Ellesmere Island, *in* Raasch, G.O., ed., Geology of the Arctic, v. 2: Toronto, Ont., University of Toronto Press, p. 781–790.

Weber, J.R., and Andrieux, Pierre, 1970, Radar soundings on the Penny Ice Cap, Baffin Island: Journal of Glaciology, v. 9, no. 55, p. 49–54.

Weber, J.R., Sandstrom, N., and Arnold, K.C., 1961, Geophysical surveys on Gilman Glacier, northern Ellesmere Island, *in* General Assembly of Helsinki, 25 July–6 August 1960: Association Internationale d'Hydrologie Scientifique Publication No. 54, p. 500–511.

Weiss, Jakob, 1984, Massenhaushalt eines Gletschers, Fragen an glaziologische Untersuchungen und die Resultate der Messreihe am White Glacier in der kanadischen Arktis: Diplomarbeit, Geographisches Institut, University of Zürich and ETH, Zürich, Switzerland, 149 p.

West, Robert, and Maki, Arthur, 1961, An advancing glacier in Canada: Science, v. 133, no. 3461, p. 1361.

Wheeler, A.O., 1905, The Selkirk Range: Ottawa, Ont., Government Printing Bureau, Department of the Interior, v. 1: 459 p., v. 2: maps.

———1911, Motion of the Yoho Glacier: Canadian Alpine Journal, v. 3, p. 123–126.

———1913, Motion of the Yoho Glacier: Canadian Alpine Journal, v. 5, p. 53–58.

———1920, Notes on the glaciers of the Main and Selkirk Ranges of the Canadian Rocky Mountains: Canadian Alpine Journal, v. 11, p. 121–146.

———1932, Glacial change in the Canadian Cordillera, the 1931 expedition: Canadian Alpine Journal, v. 20, p. 120–137.

Wheeler, A.O., 1934, Records of glacial observations in the Canadian Cordillera, 1933 and 1934: Canadian Alpine Journal, v. 22, p. 172–187.

Wheeler, A.O., and Parker, E., 1912, The Selkirk Mountains—A guide for mountain climbers and pilgrims: Winnipeg, Manitoba, Stovel Co., 191 p.

Williams, F.M., and Hutter, Kolumban, 1983, Thermal response of unconfined ice shelves to climatic conditions: Acta Mechanica, v. 48, no. 3–4, p. 131–146.

Williams, L.D., 1974, Computer simulation of glacier mass balance throughout an ablation season: Western Snow Conference, 42nd Annual Meeting, Anchorage, Alaska, 16–20 April 1974, Proceedings, p. 23–28.

———1975, The variation of corrie elevation and equilibrium line altitude with aspect in eastern Baffin Island, N.W.T., Canada: Arctic and Alpine Research, v. 7, no. 2, p. 169–181.

Wolfe, P.M., 1995, Hydrometeorological investigations on a small valley glacier in the Sawtooth Range, Ellesmere Island, Northwest Territories: M.A. thesis, Waterloo, Ont., Wilfrid Laurier University, Department of Geography, 225 p.

Wolfe, P.M., and English, M.C., 1996, Mass balance of a small valley glacier in the Canadian High Arctic, Ellesmere Island, Northwest Territories: Zeitschrift für Gletscherkunde und Glazialgeologie, 1995, v. 31, pt. 1, p. 93–103.

Wood, W.A., 1948, Project Snow Cornice: Arctic, v. 1, no. 2, p. 107.

———1949, Snow Cornice 1949: A preliminary report: Arctic, v. 2, no. 2, p. 118.

———1963, The Icefield Ranges Research Project: Geographical Review, v. 50, no. 2, p. 163–184.

Woodward, John, 1996, The influence of superimposed ice formation on the sensitivity of glacier mass balance to climate change: M.Sc. thesis, Edmonton, Alberta, University of Alberta, Department of Geography.

Woodward, John, Sharp, M.[J.], and Arendt, Anthony, 1997, The influence of superimposed-ice formation on the sensitivity of glacier mass balance to climate change: Annals of Glaciology, v. 24, p. 186–190.

Worthington, S.R.H., 1991, Karst hydrology of the Canadian Rocky Mountains: Ph.D. thesis, Hamilton, Ont., McMaster University, Department of Geography, 408 p.

Yang, Qinzhao, Mayewski, P.A., Whitlow, S.[I.], Twickler, M.[S.], Morrison, M.[C.], Talbot, R.[W.], Dibb, J.[E.], and Linder, Ernst, 1995, Global perspective of nitrate flux in ice cores: Journal of Geophysical Research, v. 100, no. D3, p. 5113–5121.

Yao Tandong, 1987, The primary investigation of the Juneau Icefield, U.S.A.: Bingchuan Dongtu (Journal of Glaciology and Geocryology), v. 9, no. 2, p. 183–186. (In Chinese with English abstract.)

Yarnal, B.[M.], 1984a, Relationships between synoptic-scale atmospheric circulation and glacier mass balance in south-western Canada during the International Hydrological Decade, 1965–74: Journal of Glaciology, v. 30, no. 105, p. 188–198.

———1984b, Synoptic-scale atmospheric circulation over British Columbia in relation to the mass balance of Sentinel Glacier: Annals of the Association of American Geographers, v. 74, no. 3, p. 375–392.

Young, G.J., [1971], Mass balance measurements related to surface geometry on Peyto Glacier, Alberta, *in* Glaciers, Proceedings of Workshop Seminar 1970, Vancouver, B.C., 24–25 September 1970: Ottawa, Ont., Canadian National Committee for the I.H.D., p. 11–20.

———1972, White Glacier mass balance, *in* Müller, Fritz, and others, eds., International Geographical Union, Field Tour Ea 2, Arctic Archipelago I, 22nd International Geographical Congress: Montréal, Québec, McGill University, Axel Heiberg Island Research Reports, Miscellaneous Papers, p. 25–30.

———1974, A data collection and reduction system for snow accumulation studies, *in* Santeford, H.S., and Smith, J.L., eds., Advanced concepts and techniques in the study of snow and ice resources: Washington, D.C., National Academy of Sciences, p. 304–313.

———1975, Accumulation and ablation patterns as functions of the surface geometry of a glacier, *in* Snow and Ice Symposium, Moscow, August 1971, Proceedings: IAHS-AISH Publication No. 104, p. 134–138.

———1976, An approach to glacier mass-balance analysis utilizing terrain characterization: Ottawa, Ont., Environment Canada, Water Resources Branch, Inland Waters Directorate Scientific Series No. 60, 34 p.

———1978, Relations between mass-balance and meteorological variables on Peyto Glacier, Alberta, 1967/1974: Zeitschrift für Gletscherkunde und Glazialgeologie, 1977, v. 13, no. 1–2, p. 111–125.

———1980, Monitoring glacier outburst floods: Nordic Hydrology, v. 11, no. 5, p. 285–300.

———1981, The mass balance of Peyto Glacier, Alberta, Canada, 1965 to 1978: Arctic and Alpine Research, v. 13, no. 3, p. 307–318.

———1982, Hydrological relationships in a glacierized mountain basin: Symposium at Exeter 1982—Hydrological Aspects of Alpine and High Mountain Areas, International Association of Hydrological Sciences Publication No. 138, p. 51–59.

———1985, Canada case study: catastrophic floods, *in* Young, G.J., ed., Techniques for prediction of runoff from glacierized areas: International Association of Hydrological Sciences Publication No. 149, p. 137–143.

———1990, Glacier hydrology, *in* Prowse, T.D., and Ommanney, C.S.L., eds., Northern hydrology—Canadian perspectives: Saskatoon, Sask., Environment Canada, National Hydrology Research Institute Science Report No. 1, p. 135–162.

Young, G.J., and Arnold, K.C., 1978, Orthophotomaps of glaciers; an evaluation of an automated method applied to Peyto Glacier, Alberta: Zeitschrift für Gletscherkunde und Glazialgeologie, 1977, v. 13, no. 1–2, p. 99–110.

Young, G.J., and Stanley, A.D., 1976a, Canadian glaciers in the International Hydrological Decade program, 1965–1974. No. 3. Ram River Glacier, Alberta—Summary of measurements: Ottawa, Ont., Fisheries and Environment Canada, Water Resources Branch, Inland Waters Directorate Scientific Series No. 70, 54 p.

———1976b, Canadian glaciers in the International Hydrological Decade program, 1965–1974. No. 4. Peyto Glacier, Alberta—Summary of measurements: Ottawa, Ont., Fisheries and Environment Canada, Water Resources Branch, Inland Waters Directorate Scientific Series No. 71, 59 p.

Zdanowicz, C.M., Michel, F.A., and Shilts, W.W., 1996, Basal debris entrainment and transport in glaciers of southwestern Bylot Island, Canadian Arctic: Annals of Glaciology, v. 22, p. 107–113.

Zubok, O.M., 1975, Half decade study of mass balance at Sentinel Glacier, BC, Canada, *in* Snow and Ice Symposium, Moscow, August 1971, Proceedings: IAHS-AISH Publication No. 104, p. 202–207.

Glaciers of North America–

GLACIERS OF CANADA

MAPPING CANADA'S GLACIERS

By C. SIMON L. OMMANNEY

With a section on MAPPING GLACIERS IN THE *INTERIOR RANGES* AND ROCKY MOUNTAINS WITH LANDSAT DATA

By ROGER D. WHEATE, ROBERT W. SIDJAK, *and* GARNET T. WHYTE

SATELLITE IMAGE ATLAS OF GLACIERS OF THE WORLD

Edited by RICHARD S. WILLIAMS, Jr., *and* JANE G. FERRIGNO

U.S. GEOLOGICAL SURVEY PROFESSIONAL PAPER 1386–J–1

Between the mid-1940's and the mid-1990's, seven 1:1,000,000-scale, forty-eight 1:500,000-scale (Glacier Atlas of Canada), and more than 110 miscellaneous scale (1:2,500- to 1:125,000-scale) maps of selected glaciers of Canada were completed by governmental and academic institutions; the types of maps include sketch, topographic, and stereo-orthophoto maps. Satellite images of glaciers and digital elevation models can be combined to produce maps (planimetric and topographic) and three-dimensional perspectives

CONTENTS

GLACIERS OF NORTH AMERICA–

GLACIERS OF CANADA

MAPPING CANADA'S GLACIERS

By C. SIMON L. OMMANNEY[1]

With a section on MAPPING GLACIERS IN THE *INTERIOR RANGES* AND ROCKY MOUNTAINS WITH LANDSAT DATA

By ROGER D. WHEATE,[2] ROBERT W. SIDJAK,[2] *and* GARNET T. WHYTE[2]

Abstract

The extent and nature of the mapping of Canada's glaciers from the middle 1940's to the middle 1990's, covering terminus surveys and sketch maps to higher order, large-scale maps (Swiss-style publication quality) and stereo-orthophoto maps, are traced.

Introduction

In 1965, at the time of the first Symposium on Glacier Mapping, Canada was experiencing a remarkable flourishing of glacier-mapping activity. Papers at the symposium, by Blachut and Müller, and Konecny and Arnold (Gunning, 1966), reported on some of the developments at that time. The subsequent 20 years saw major developments in the large-scale mapping of Canada's glaciers, in which the Photogrammetric Research Section of the National Research Council of Canada (PRS-NRCC), the Department of Surveying Engineering of the University of New Brunswick, and the Glaciology Division of Environment Canada were the most significant contributors. A discussion of the maps produced by these agencies and others permits a general review of the growth and decline of this activity but does not necessarily reflect the overall history of glacier studies in Canada. In addition, there has been a replacement of the old system of mapping with a use of DEM and satellite images. Many of these maps appear in journal articles or reports and are in digital format.

Glacier Maps of Canada (1:1,000,000 Scale)

The decision to map Canada's glaciers at a scale of 1:1,000,000 arose from the need of the Geographical Branch, Department of Mines, to have

Manuscript approved for publication, 7 March 2002.

[1] International Glaciological Society, Lensfield Road, Cambridge CB2 1ER, England, U.K. (formerly with the National Hydrology Research Institute [now the National Hydrology Research Centre], Environment Canada, 11 Innovation Boulevard, Saskatoon, Saskatchewan S7N 3H5, Canada).

[2] Faculty of Natural Resources and Environmental Studies, 3333 University Way, University of Northern British Columbia, Prince George, British Columbia V2N 4Z9, Canada.

TABLE 1.—*Glacier maps of Canada (1:1,000,000 scale)*

[Abbreviations used: DEMR, Department of Energy, Mines and Resources; DMTS, Department of Mines and Technical Surveys; GEOG, Geographical Branch; IWB, Inland Waters Branch; NTS, National Topographic Series]

Glacier map name	Number	Contours	Survey date	Production agency	Glacier representation
Southern British Columbia and Alberta	IWB 1000	none	date of NTS base map	GEOG, DMTS	Purple glaciers on white
Northern British Columbia and southeastern Alaska	IWB 1001	none	date of NTS base map	IWB, DEMR	Purple glaciers on white
Yukon Territory and District of Mackenzie	IWB 1002	none	date of NTS base map	IWB, DEMR	Purple glaciers on white
Southern Baffin Island and northern Labrador Peninsula	IWB 1006	none	date of NTS base map	IWB, DEMR	White glaciers on brown
Northern Baffin Island[1]	IWB 1005	none	date of NTS base map	IWB, DEMR	White glaciers on brown
Southern Queen Elizabeth Islands	IWB 1004	none	date of NTS base map	IWB, DEMR	White glaciers on brown
Northern Queen Elizabeth Islands	IWB 1003	none	date of NTS base map	IWB, DEMR	White glaciers on brown

[1] Included in map supplement to Journal of Glaciology, v. 9, no. 55, 1970.

small-scale maps available that were suitable for planning glaciological research and accurately depicting the geographic distribution of glaciers. A study was made in the middle 1960's on the representation of glaciers on topographic maps published at various scales, particularly how glacier information was generalized. Glaciers were delineated with heavy black-ink lines on the best available maps in 1965 and reduced to the common scale (Falconer and others, 1966). One surprise from the study was the conclusion that small-scale maps may depict glaciers better than large-scale maps (see fig. 2 in Falconer and others, 1966). The three maps of the western cordillera show glaciers in purple on a white background (a combination that was thought to give the best visual contrast, even for small glaciers), whereas on the four Arctic maps, glaciers are white on a brown background (Henoch and Stanley, 1968a, b, 1970; table 1). The maps have been used to complement the standard topographic maps (Henoch, 1969) primarily for plotting information such as glaciation levels, equilibrium lines, ice-cored moraines, transient snowlines, and glacier mass balance (Østrem, 1973; Miller and others, 1975); as base maps for the National Atlas of Canada (see Fremlin and Mindak, 1968); and for use in schools.

Glacier Atlas of Canada (1:500,000 Scale)

Much more detailed information on all glaciers was subsequently compiled through the Canadian glacier inventory. Until 1972, identification numbers and basin designations were published in individual sheets of the Glacier Atlas of Canada. Modified 1:250,000-scale National Topographic System (NTS) maps formed the basis for the four-color plates. Glaciers appear in a blue vignette within their hydrological basins, and the maps are bordered in brown (fig. 1). Ommanney (1980) described the program, and the maps published (Ommanney, 1989) are listed in table 2. The series was used in compiling the base map (1:2,000,000 scale) for the 5th edition of the National Atlas of Canada,[3] published at a scale of 1:7,500,000 on which glaciers are shown with a light purple vignette (Gosson, 1985), and subsequently for educational maps (Royal Canadian Geographical Society, 1998).

[3] The 6th edition of the National Atlas of Canada is available online at the following URL address: [http://atlas.gc.ca/].

TABLE 2.—*Glacier Atlas of Canada (1:500,000-scale Glacier Inventory Maps[1])*

[Abbreviations used: DEMR, Department of Energy, Mines and Resources; DOE. Department of the Environment; IWB, Inland Waters Branch; IWD, Inland Waters Directorate]

Plate no.	Name	Number	Date	Producer	Printer
ELLESMERE ISLAND					
1.1.1	Glacier Strait	IWD 1147	1972	DOE	DEMR
1.1.2	Starnes Fiord	IWD 1148	1972	DOE	DEMR
1.1.3	Sydkap Ice Cap	IWD 1149	1972	DOE	DEMR
1.1.4	Bjorne Peninsula	IWD 1150	1972	DOE	DEMR
1.2.1	Raanes and Svendsen Peninsulas	IWD 1151	1972	DOE	DEMR
1.2.2	Fosheim Peninsula	IWD 1152	1972	DOE	DEMR
DEVON ISLAND					
2.0	Devon Island	IWB 1146	1972	DOE	DEMR
2.1	Grinnell Peninsula	IWB 1144	1971	DOE	DEMR
2.2	Colin Archer Peninsula	IWB 1145	1971	DOE	DEMR
2.3	South West Devon Island	IWB 1138	1971	DOE	DEMR
2.4	Maxwell Bay	IWB 1136	1970	DOE	DEMR
2.5	Bear Bay	IWB 1140	1971	DOE	DEMR
2.6	Devon Ice Cap - South West	IWB 1143	1971	DOE	DEMR
2.7	Devon Ice Cap - North	IWB 1141	1971	DOE	DEMR
2.8	Devon Ice Cap - South East	IWB 1142	1971	DOE	DEMR
SVERDRUP ISLANDS					
4.0	Axel Heiberg Island	IWB 1129	1969	DEMR	DEMR
4.1	Southern Axel Heiberg Island	IWB 1106	1969	DEMR	DEMR
4.2	Central Axel Heiberg Island	IWB 1112	1969	DEMR	DEMR
4.3	Western Axel Heiberg Island	IWB 1115	1969	DEMR	DEMR
4.4	Northern and Eastern Axel Heiberg Island	IWB 1105	1969	DEMR	DEMR
BAFFIN AND BYLOT ISLAND					
5.0	Baffin Island	IWB 1100	1969	DEMR	DEMR
5.1	Bylot Island	IWB 1102	1969	DEMR	DEMR
5.2	Brodeur Peninsula	IWB 1104	1969	DEMR	DEMR
5.3	Borden Peninsula - West	IWB 1101	1969	DEMR	DEMR
5.4	Borden Peninsula - East	IWB 1103	1969	DEMR	DEMR
5.5	Milne Inlet	IWB 1109	1969	DEMR	DEMR
5.6	Tay Sound	IWB 1111	1969	DEMR	DEMR
5.7	Pond Inlet	IWB 1107	1969	DEMR	DEMR
5.8	Cambridge Fiord	IWB 1114	1969	DEMR	DEMR
5.9	Barnes Ice Cap	IWB 1116	1969	DEMR	DEMR
5.10	Gibbs Fiord	IWB 1117	1969	DEMR	DEMR
5.11	Sam Ford Fiord	IWB 1110	1969	DEMR	DEMR
5.12	Clyde Inlet	IWB 1113	1969	DEMR	DEMR
5.13	McBeth Fiord	IWB 1108	1969	DEMR	DEMR
5.14	Home Bay	IWB 1118	1969	DEMR	DEMR
5.15	Okoa Bay	IWB 1119	1969	DEMR	DEMR
5.16	Coronation Fiord	IWB 1121	1969	DEMR	DEMR
5.17	Padle Fiord	IWB 1126	1969	DEMR	DEMR
5.18	Hoare Bay	IWB 1123	1969	DEMR	DEMR
5.19	Kingnait Fiord	IWB 1122	1969	DEMR	DEMR
5.20	Penny Ice Cap	IWB 1120	1969	DEMR	DEMR
5.21	Popham Bay	IWB 1127	1969	DEMR	DEMR
5.22	Beekman Peninsula	IWB 1128	1969	DEMR	DEMR
5.23	Blunt Peninsula	IWB 1130	1969	DEMR	DEMR
5.24	Meta Incognita Peninsula	IWB 1124	1969	DEMR	DEMR
NELSON RIVER DRAINAGE BASIN					
7.0	Nelson River Drainage Basin	IWB 1135	1970	DEMR	DEMR
7.1	Oldman River	IWB 1132	1970	DEMR	DEMR
7.2	Bow River	IWB 1134	1970	DEMR	DEMR
7.3	Red Deer River	IWB 1133	1970	DEMR	DEMR
7.4	North Saskatchewan River	IWB 1131	1970	DEMR	DEMR
PACIFIC OCEAN DRAINAGE AREA					
8.8.1	Vancouver Island - South	IWB 113719	1971	DOE	DEMR
8.8.2	Vancouver Island - North	IWB 113919	1971	DOE	DEMR

[1] The first map in each complete series (numbered X.0) is a small-scale index map showing the distribution of subsequent maps.

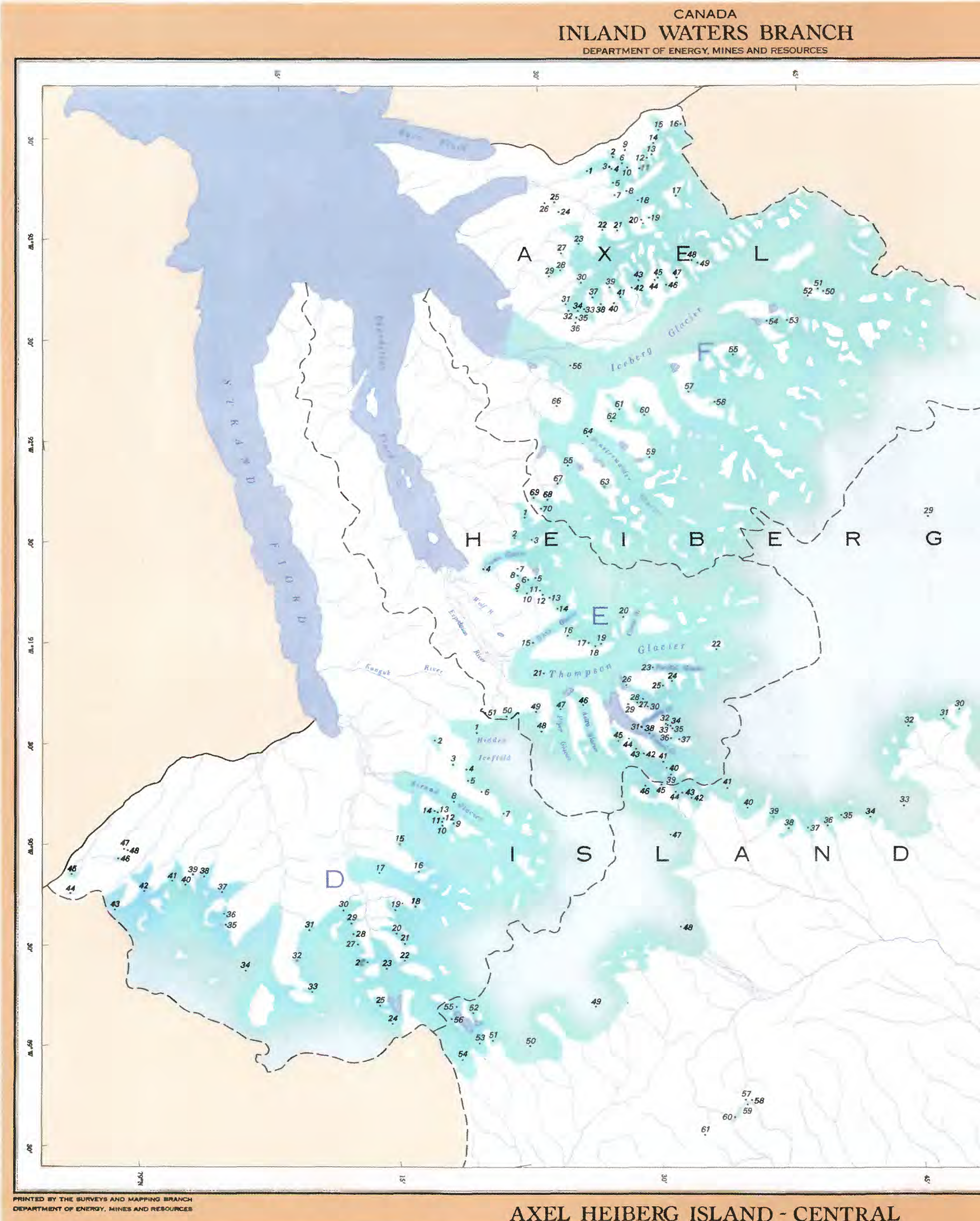

CANADA
INLAND WATERS BRANCH
DEPARTMENT OF ENERGY, MINES AND RESOURCES
A X E L
H E I B E R G
I S L A N D
STRAND FIORD
Iceberg Glacier
Thompson
Glacier
Hidden
Icefield
Kanguk
River
Expedition
River
D
E
F
PRINTED BY THE SURVEYS AND MAPPING BRANCH
DEPARTMENT OF ENERGY, MINES AND RESOURCES
AXEL HEIBERG ISLAND - CENTRAL
GLACIER INVENTORY
AREA 46444

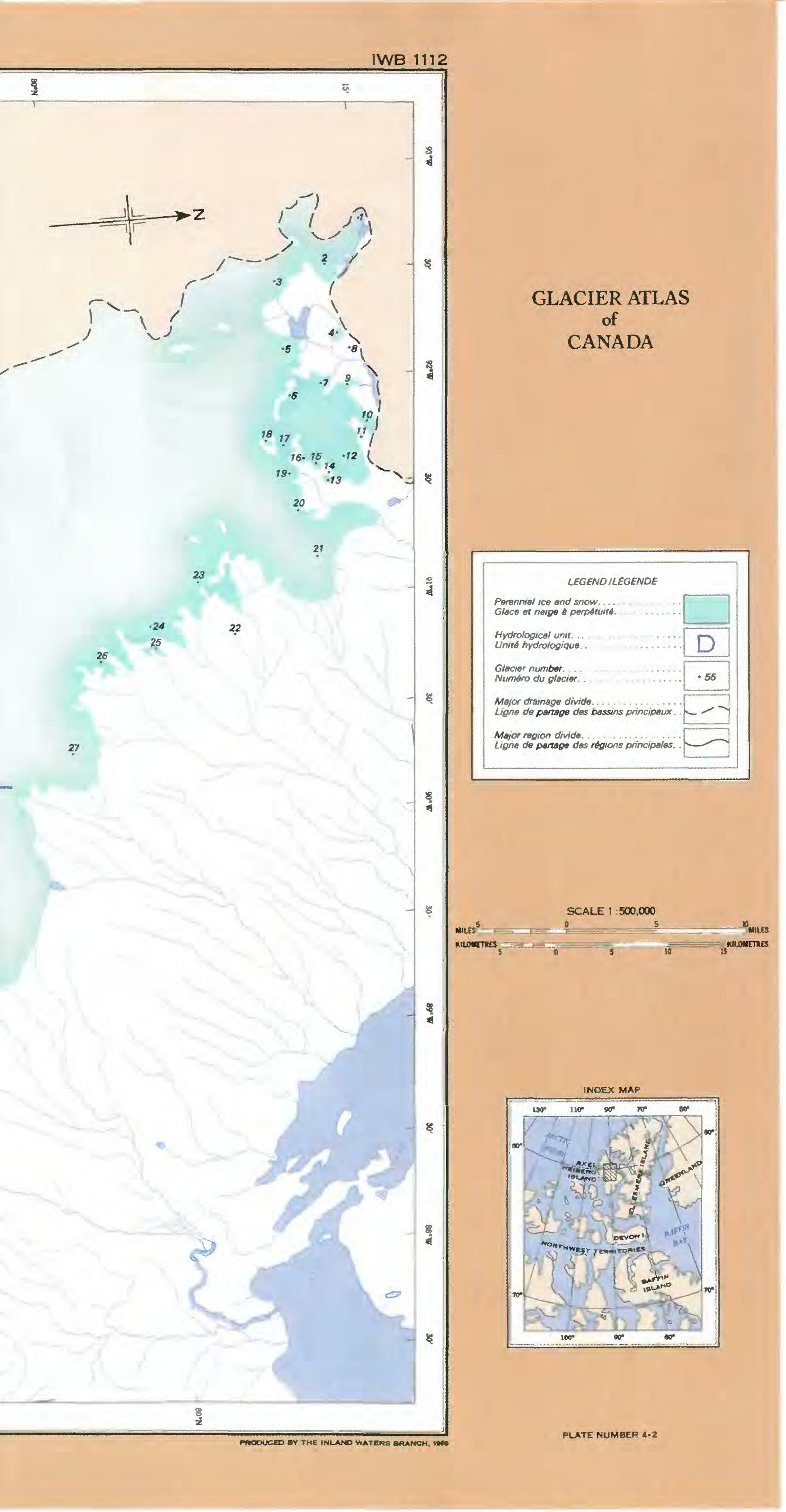

Figure 1.—Part of Glacier Atlas of Canada, Plate No. 4.2, Map No. IWB 1112, Central Axel Heiberg Island, Nunavut, that includes the White Glacier (Glacier 46444E–15) and Thompson Glacier (Glacier 46444E–21). Map published in 1969 by the Inland Waters Branch, Department of Energy, Mines and Resources; scale 1:500,000 (see table 2 for other maps in the Glacier Atlas of Canada series).

Water Survey of Canada

In 1945, the Dominion Water and Power Bureau, forerunner of the Water Survey of Canada (WSC), began annual surveys of 15 glaciers in western Canada to determine the effects of glacier variation on river runoff. The lower limits and activity of the glacier termini were measured from fixed points, and the movement and height change of the glacier surface were determined along a transverse profile of plaques in the ablation area. Glacier photographs and sketches of the relative changes were included in the annual reports of the district engineers, and some results were reported by Collier (1958). In 1950, the surveys became biennial and some surveys were terminated.

In 1959, the WSC carried out an aerial photogrammetric survey of Athabasca Glacier[4]; this was followed in 1962 by the University of New Brunswick terrestrial survey undertaken by Konecny (1964). The WSC decided that the latter technique was the most cost-effective and adopted it for future surveys of the Athabasca and Saskatchewan Glaciers in Alberta (1963 to 1979) and the Bugaboo, Kokanee, Sentinel, Sphinx, and *Nadahini*[4] Glaciers in British Columbia (1964 to 1978). Paterson (1966) assessed its accuracy and Reid (1973) discussed the procedures used. Maps were plotted at scales of 1:10,000 to 1:2,500 with topographic contours at 5 to 10 m on the ice, depending on glacier size (table 3). The biennial volumetric changes were also calculated and the maps and results published (Reid and Charbonneau, 1980, 1981). The map styles vary but generally use solid blue for ice, blue stipple for snow with blue-line contours on the glaciers; brown or gray contours are used outside the margins of the glacier. Only the exposed ice in the ablation area is mapped, however. Surveys of all these glaciers were terminated by 1980 (Reid, 1973; Reid and Charbonneau, 1980, 1981).

TABLE 3.—*Water Survey of Canada Glacier Map Series*

[DEMR, Department of Energy, Mines and Resources; DFE, Department of Fisheries and the Environment; DNANR, Department of Northern Affairs and National Resources; DOE, Department of the Environment; IWB, Inland Waters Branch; IWD, Inland Waters Directorate; UNB, University of New Brunswick; USGS, United States Geological Survey; WRB, Water Resources Branch]

Glacier map name	Number	Scale	Contours	Survey date(s)	Production agency	Glacier representation[1]
Athabasca Glacier		1:4,800		1 Aug 1959	WRB, DNANR	
Athabasca Glacier		1:4,800		1962	WRB, DNANR	
Athabasca Glacier	1–6	1:10,000	25/50/100 ft	26 Jul 1965	IWB, DEMR	C
Athabasca Glacier	2–6	1:10,000	25/50/100 ft	25 Jul 1967	IWB, DEMR	A
Athabasca Glacier	3–6	1:10,000	10/20/30 ft	25 Jul 1969	IWB, DEMR	A
Athabasca Glacier	4–6	1:10,000	5 and 10 m	12 and 16 Aug 1971	IWD, DOE	A
Athabasca Glacier[2]	5-6	1:10,000	5 and 10 m	3 Aug 1973	IWD, DOE	B, not all moraines shown
Athabasca Glacier	6–6	1:10,000	5 and 10 m	27 Aug 1975	IWD, DFE	A
Athabasca Glacier	7–6	1:10,000	5 and 10 m	13 Aug 1977	IWD, DFE	B, not all moraines shown
Athabasca Glacier	8–6	1:10,000	5 and 10 m	10 Aug 1979	IWD, DFE	A
Bugaboo Glacier	1–5	1:2,500	50 ft	9 Jul 1964	WRB, DNANR	C
Bugaboo Glacier	2–5	1:2,500	50 ft	4 Aug 1966	IWB, DEMR	C
Bugaboo Glacier	3A–5	1:2,500	50/100 ft	1 Aug 1968	IWB, DEMR	B
Bugaboo Glacier	3B–5	1:2,500	10/25 m	1 Aug 1968	IWB, DEMR	B
Bugaboo Glacier	4–5	1:2,500	10/25 m	18 Aug 1970	IWD, DOE	B
Bugaboo Glacier	5–5	1:2,500	10/25 m	29 Aug 1972	IWD, DOE	B
Bugaboo Glacier	6–5	1:2,500	10/25 m	24 Aug 1974	IWD, DOE	B
Bugaboo Glacier	7–5	1:2,500	10 m	21 Aug 1976	IWD, DFE	A
Bugaboo Glacier	8–5	1:2,500	10 m	19 Aug 1978	IWD, DOE	A

[4] The names in this section conform to the usage authorized by the Secretariat of the Canadian Permanent Committee on Geographic Names (CPCGN); URL address: [http://GeoNames.NRCan.gc.ca/]. The website is maintained by the Secretariat through Geomatics Canada, Natural Resources Canada, and combines the CPCGN server with the Canadian Geographical Names Data Base (CGNDB). Variant names and names not listed in the CPCGN/CGNDB are shown in italics.

TABLE 3.—*Water Survey of Canada Glacier Map Series*—Continued

[DEMR, Department of Energy, Mines and Resources; DFE, Department of Fisheries and the Environment; DNANR, Department of Northern Affairs and National Resources; DOE, Department of the Environment; IWB, Inland Waters Branch; IWD, Inland Waters Directorate; UNB, University of New Brunswick; USGS, United States Geological Survey; WRB, Water Resources Branch]

Glacier map name	Number	Scale	Contours	Survey date(s)	Production agency	Glacier representation[1]
Kokanee Glacier	1–4	1:2,500	20 ft	17 Aug 1964	WRB, DNANR	C
Kokanee Glacier	2–4	1:2,500	20 ft	7 and 8 Aug 1966	IWB, DEMR	C
Kokanee Glacier	3A–4	1:2,500	20/50 ft	5 and 6 Aug 1968	IWB, DEMR	B
Kokanee Glacier	3B–4	1:2,500	5 and 10 m	5 and 6 Aug 1968	IWB, DEMR	A
Kokanee Glacier	4–4	1:2,500	5 and 10 m	23 and 26 Aug 1970	IWD, DOE	A
Kokanee Glacier	5–4	1:2,500	5 and 10 m	24 and 25 Aug 1972	IWD, DOE	A
Kokanee Glacier[3]	8–4	1:2,500	5 m	17 Aug 1978	IWD, DOE	A
Nadahini Glacier	1–3	1:2,500	20 ft	26 Jul 1964	WRB, DNANR	C
Nadahini Glacier	2–3	1:5,000	20 ft	16 Aug 1966	IWB, DEMR	C
Nadahini Glacier	3A–3	1:5,000	20 and 50 ft	16 Aug 1968	IWB, DEMR	A
Nadahini Glacier	3B–3	1:5,000	5 and 10 m	16 Aug 1968	IWB, DEMR	A
Nadahini Glacier	4–3	1:5,000	5 and 10 m	3 Sep 1970	IWD, DOE	A
Nadahini Glacier	5–3	1:5,000	5 and 10 m	12 Aug 1972	IWD, DOE	A
Nadahini Glacier	6–3	1:5,000	5 and 10 m	16 and 17 Aug 1974	IWD, DOE	A
Nadahini Glacier	7–3	1:5,000	5 and 10 m	12 Aug 1976	IWD, DOE	A
Nadahini Glacier	8–3	1:5,000	5 and 10 m	10 Aug 1978	IWD, DOE	A
Saskatchewan Glacier[4]		1:24,000	50 ft	1954 and 1963	USGS, UNB, IWB	Blue/red overprint of 2 years
Saskatchewan Glacier[4]		1:20,000	10 ft	29 Jul 1963	IWB, DEMR, UNB	Black print, moraine stipple
Saskatchewan Glacier	1–7	1:10,000	20 ft	27 Jul 1965	IWB, DEMR	C
Saskatchewan Glacier	2–7	1:10,000	20 ft	26 Jul 1967	IWB, DEMR	A
Saskatchewan Glacier	3–7	1:10,000	10/50 ft	30 Jul 1969	IWB, DEMR	A
Saskatchewan Glacier	4–7	1:10,000	5 and 50 m	9 and 10 Aug 1971	IWD, DOE	B
Saskatchewan Glacier	5–7	1:10,000	5 and 50 m	1, 9, 10 Aug 1973	IWD, DOE	B
Saskatchewan Glacier	6–7	1:10,000	10/50 m	28 Aug 1975	IWD, DFE	B
Saskatchewan Glacier	7–7	1:10,000	10/50 m	14 Aug 1977	IWD, DFE	B
Saskatchewan Glacier	8–7	1:10,000	5 and 50 m	9 and 10 Aug 1979	IWD, DFE	B
Sentinel Glacier	1–1	1:2,500	20 ft	3 Sep 1964	WRB, DNANR	C
Sentinel Glacier	2–1	1:2,500	20 ft	21 Aug 1966	IWB, DEMR	C
Sentinel Glacier	3A–1	1:2,500	20 ft	24 Aug 1968	IWB, DEMR	A
Sentinel Glacier	3B–1	1:2,500	5 m	24 Aug 1968	IWB, DEMR	A
Sentinel Glacier	4–1	1:2,500	5 m	11 and 12 Sep 1970	IWD, DOE	A
Sentinel Glacier	5–1	1:2,500	5 m	20 Aug 1972	IWD, DOE	A
Sentinel Glacier[3]	8–1	1:2,500	5 m	15 Aug 1978	IWD, DOE	A
Sphinx Glacier	1–2	1:5,000	50 ft	3 Sep 1964	WRB, DNANR	C
Sphinx Glacier	2-2	1:5,000	25 ft	22 Aug 1966	IWB, DEMR	C
Sphinx Glacier	3A–2	1:5,000	25 ft	26 Aug 1968	IWB, DEMR	A
Sphinx Glacier	3B–2	1:5,000	10 m	26 Aug 1968	IWB, DEMR	A
Sphinx Glacier	4–2	1:5,000	10 m	9 and 10 Sep 1970	IWD, DOE	A
Sphinx Glacier	5–2	1:5,000	10 m	18 and 19 Aug 1972	IWD, DOE	A
Sphinx Glacier[5]	7–2	1:5,000	10 m	17 Aug 1976	IWD, DFE	A
Sphinx Glacier	8–2	1:5,000	10 m	13 Aug 1978	IWD, DOE	A

[1] A, Glaciers shown in a screened solid blue, off-ice areas in a solid buff color, contours on land and ice are gray with form lines used in the accumulation areas where adequate control is lacking. Seasonal snow cover and accumulation areas are shown in a blue stipple; old snout positions shown with a dotted line and the respective date. Symbols are used for measurement stakes and ablation mounds. B, Same as A but includes moraines depicted using a black stipple. C, Glaciers shown in a screened solid blue, off-ice areas are uncolored, contours on land are brown and on ice are blue with form lines used in the accumulation areas where adequate control is lacking. Seasonal snow cover and accumulation areas are shown in a blue stipple. Symbols are used for measurement stakes and ablation mounds. D, Glaciers shown in a screened solid blue, off-ice areas in a solid buff color, contours on land and ice are brown with form lines used in the accumulation areas where adequate control is lacking. Seasonal snow cover and accumulation areas are shown in a blue stipple, old snout positions shown with a dotted line and the respective date. Symbols are used for measurement stakes and ablation mounds. From 1976, the glacier maps were published in a bilingual format.

[2] Map included in supplement to 1970–1975 Permanent Service on the Fluctuation of Glaciers (PSFG) report (Müller, 1977).

[3] No maps made for 1974 and 1976 because of snow cover.

[4] Map included in supplement to Proceedings of Glacier Mapping Symposium (Gunning, 1966).

[5] No map made for 1974 because of snow cover.

Salmon Glacier

The PRS-NRCC has probably had a greater impact on glacier mapping in Canada than any other agency. Initially involved with the University of Toronto International Geophysical Year (IGY) Expedition, they developed and applied aerial photogrammetric techniques appropriate for mapping the lower part of Salmon Glacier (1:25,000/20 m),[5] British Columbia, and its terminus (1:12,500/20 m).[5] The color maps (five discrete colors) were published in conjunction with a detailed report on the survey by Haumann (1960). The photogrammetric base was used for assessing volumetric changes between 1949 and 1957. Details of these and subsequent maps discussed in the following paragraphs are shown in table 4.

TABLE 4.—*Miscellaneous glacier maps of Canada*

[Abbreviations: AINA, Arctic Institute of North America; ASE, Army Survey Establishment; BCIT, British Columbia Institute of Technology; DEMR , Department of Energy, Mines and Resources; DMTS, Department of Mines and Technical Surveys; DOE, Department of the Environment; DRB, Defence Research Board, Department of National Defence, Ottawa; EC, Environment Canada; ETH-Zürich, Eidgenössische Technische Hochschule, Zürich, Switzerland; FEC, Fisheries and Environment Canada; FGER, Foundation for Glacier and Environmental Research, Glaciological and Arctic Sciences Institute, Juneau, Alaska; Gestalt, Gestalt International Limited, Vancouver, B.C.; GD, Glaciology Division; IPTUK, Institut für Photogrammetrie und Topographie der Universität Karlsruhe, Germany; IWB, Inland Waters Branch; IWD, Inland Waters Directorate; McGill, McGill University, Montréal, Québec; NGS, National Geographic Society, Washington D.C., U.S.A.; NHRI, National Hydrology Research Institute; NRCC, Photogrammetric Section, Division of Physics, National Research Council of Canada; NVE, Norges Vassdrags-og Energiverk, Oslo, Norway; Parks, Parks Canada; SMB, Surveys and Mapping Branch, Department of Energy, Mines and Resources; TUH, Technical University of Hannover, German; UNB, University of New Brunswick; U of T, University of Toronto; AP, aerial photogrammetry; BP, bedrock portrayal; BW, black and white; MC, multi-colored; RS, relief shading; TP, terrestrial photogrammetry; mor., moraine; cont., contours; glac., glacier; struct., structural; crev., crevasses; unpub., unpublished; spot elev., spot elevations]

Glacier map name	Number	Scale	Contours	Survey date(s)	Production agency	Glacier representation
Athabasca Glacier						Orthophoto map
Baby Glacier		1:5,000	5 m	2 Aug 1960	McGill, NRCC, ASE	2-color, AP, mor. stipple
Berendon Glacier	IWB 1009	1:10,000	10/20 m	22 Aug 1968	IWB, DMTS	4-color, AP, blue/brown cont.
Glacier at Cathedral Peak		1:5,000	5 m	13 Aug 1975	FGER (1976), TUH	3-color, TP, RS, mor. stipple
Cathedral Massif Glacier and forefield		1:5,000	10 m	13 Aug 1975	Mauelshagen and Slupetzky (1985)	MC, AP, blue/brown cont.
Cathedral Massif, Atlin Provincial Park		1:20,000	100 ft		Cialek (1977)	
Centennial Range	M.C.R. 7	1:125,000	500 ft	from 1:250,000 maps	DEMR	4-color, AP, RS
Columbia Icefield	IWD 1011	1:50,000	20 m		NHRI, Parks, DOE	MC, RS, BP, AP + text
Crusoe Glacier Tongue[1]		1:5,000	5 m	2 Aug 1960	NRCC, McGill, DMTS	2-color, RS, blue glac., AP
Decade Glacier		1:10,000	10 m		IWB, DMTS	BW, AP, unpublished ozalid
d'Iberville Glacier		1:50,000	none		GD, EC	BW
Fox Glacier	115F/01	1:10,000	10 m		ASE, DMTS	AP, unpublished ozalid
Part of Grinnell Glacier		1:20,000	10/20 m		NVE (1991)	3-color, green glac., AP
Hare Fiord Glacier		1:20,000	20 m	1958 and 1978	Römmer and Hell (1986)	2-color, MC, blue glac., AP
Lowell Glacier		1:50,000	20 m	17 Aug 1974	IWD, DOE	3-color, RS on glac., AP
Meighen Ice Cap[1]	69H/560B	1:25,000	5 m	5 Aug 1960	DMTS	MC, AP, subglacier contours
Meighen Island N 1/2[1]	69G-H/560B	1:50,000	10 m	5 Aug 1959	DMTS	MC, AP, subglacier contours
Meighen Island S 1/2[1]	69 G-H	1:50,000	10 m	5 Aug 1959	DMTS	MC, AP, subglacier contours
Mount Logan		1:10,000	20 m	11 Aug 1972	IWD, FEC	2-color, AP, RS, BP
Mount Logan		1:10,000	20 m	1992	NHRI	BW, line map
Mount Logan		1:10,000	20 m	1993	AINA	2-color relief
The Massif of Mount Hubbard, Mount Alverstone, and Mount Kennedy		1:31,680	100 ft	1965	NGS© (1968), UNB, SMB	2-color (blue and gray), AP, RS, BP

[5] Scale of map and contour interval on the glacier.

TABLE 4.—*Miscellaneous glacier maps of Canada*—Continued

Glacier map name	Number	Scale	Contours	Survey date(s)	Production agency	Glacier representation
Oobloyah Bay, Ellesmere Island...		1:25,000	25 m	1959 and 1960	IPTUK	Orthophoto map
Otto Fiord Glacier 1959[1, 2]		1:50,000	10 m	17 Aug 1959	DRB, UNB	BW, AP
Otto Fiord Glacier 1964[1, 2]		1:50,000	10 m	16 Aug 1964	DRB, UNB	BW, AP
Per Ardua Glacier[1]		1:20,000	10 m	17 Aug 1964	DRB, UNB	BW, AP
Per Ardua Glacier toe[1]		1:5,000	5 m	Jul 1964	DRB, UNB	BW, TP
Peyto Glacier Basin[3]		1:10,000	none	20 Aug 1966	NHRI, DOE, Gestalt	Stereo-orthophoto map, AP
Peyto Glacier	IWD 1008	1:10,000	10 m	20 and 22 Aug 1966	IWB, DEMR	MC, AP, BP, RS, 1st ed.
Peyto Glacier[3]	IWD 1010	1:10,000	10 m	20 and 22 Aug 1966	NHRI, DOE, DEMR	MC, AP, RS, BP, 2nd ed.
Peyto Glacier[4]		1:10,000	10 m	1984	NHRI	BW, line map
Place Glacier	92J/07E	1:10,000	10 m	7 Sep 1965	IWB, DMTS	3-color, AP, crevasses shown
Ram River Glacier..........................	82N/16E	1:10,000	10 m	20 Aug 1966	IWB, DMTS	4-color, AP, RS, struct. shading
Rusty Glacier		1:10,000	10 m		ASE	
Salmon Glacier		1:25,000	20 m	Aug 1957	U of T, NRCC, ASE	MC, AP, mor. stipple, crev.
Salmon Glacier terminus		1:12,500	20 m	Aug 1957	U of T, NRCC, ASE	MC, AP, mor. stipple, crev.
Sentinel Glacier..............................	92G/15W	1:10,000	10 m	7 Sep 1964	IWB, DMTS	4-color, AP, crevasses shown
Steele Glacier		1:25,000	20 m	Jul 1951	IWB, DMTS	BW, AP, unpub. ozalid, 2 sheets
Steele Glacier		1:25,000	20 m	Aug 1967	IWB, DMTS	BW, AP, unpub. ozalid, 2 sheets
Steele Glacier		1:50,000	50 m	Jul 1951	IWB, DMTS	BW, AP, unpub. ozalid, 1 sheet
Thompson Glacier Region		1:50,000	25 m	28 Jul, 13 Aug 1959	McGill, NRCC, ASE	MC, AP, RS, BP
Thompson Glacier Snout		1:5,000	5 m	2 Aug 1960	McGill, NRCC	2-color, AP, mor. stipple, crev.
Thompson Glacier Snout		1:5,000	10 m		McGill, NRCC	Orthophoto map
Thompson Glacier Snout		1:5,000	5 m		McGill, NRCC	Orthophoto map
Thompson Glacier		1:5,000	10 m	Aug 1977	ETH-Zürich	Orthophoto map
Trapridge Glacier		1:10,000	10 m		Nadir Mapping Corp.	
Tweedsmuir Glacier.......................		1:50,000	20 m	1951	IWB, DOE	3-color, TP
Tweedsmuir Glacier.......................		1:50,000	20 m	31 Aug 1974	IWB, DOE	TP, unpublished ozalid
Wedgemount Glacier		1:5,000	10 m	1973	Karl Ricker, BCIT	AP, BW, fluctuations shown
White Glacier[3]		1:2,500	spot elev.	17 and 26 Jun 1969	McGill	BW, TP, comparison plotting
White Glacier..................................		1:5,000	5 m	2 Aug 1960	McGill, NRCC	MC, AP, RS, mor. stipple crev.
White Glacier[1]		1:10,000	10 m	2 Aug 1960	NRCC, McGill, DMTS	3-color, RS, blue glac., AP
Woolsey Glacier	82M/01E	1:10,000	10 m	20 Aug 1966	IWB, DMTS	MC, RS, AP

[1] Included in map supplement to Proceedings of Glacier Mapping Symposium (Gunning, 1966).
[2] Renamed Otto Glacier.
[3] Included in map supplement to the Permanent Service on the Fluctuation of Glaciers (PSFG) report 1970-1975 (Müller, 1977).
[4] Holdsworth and others (in press).

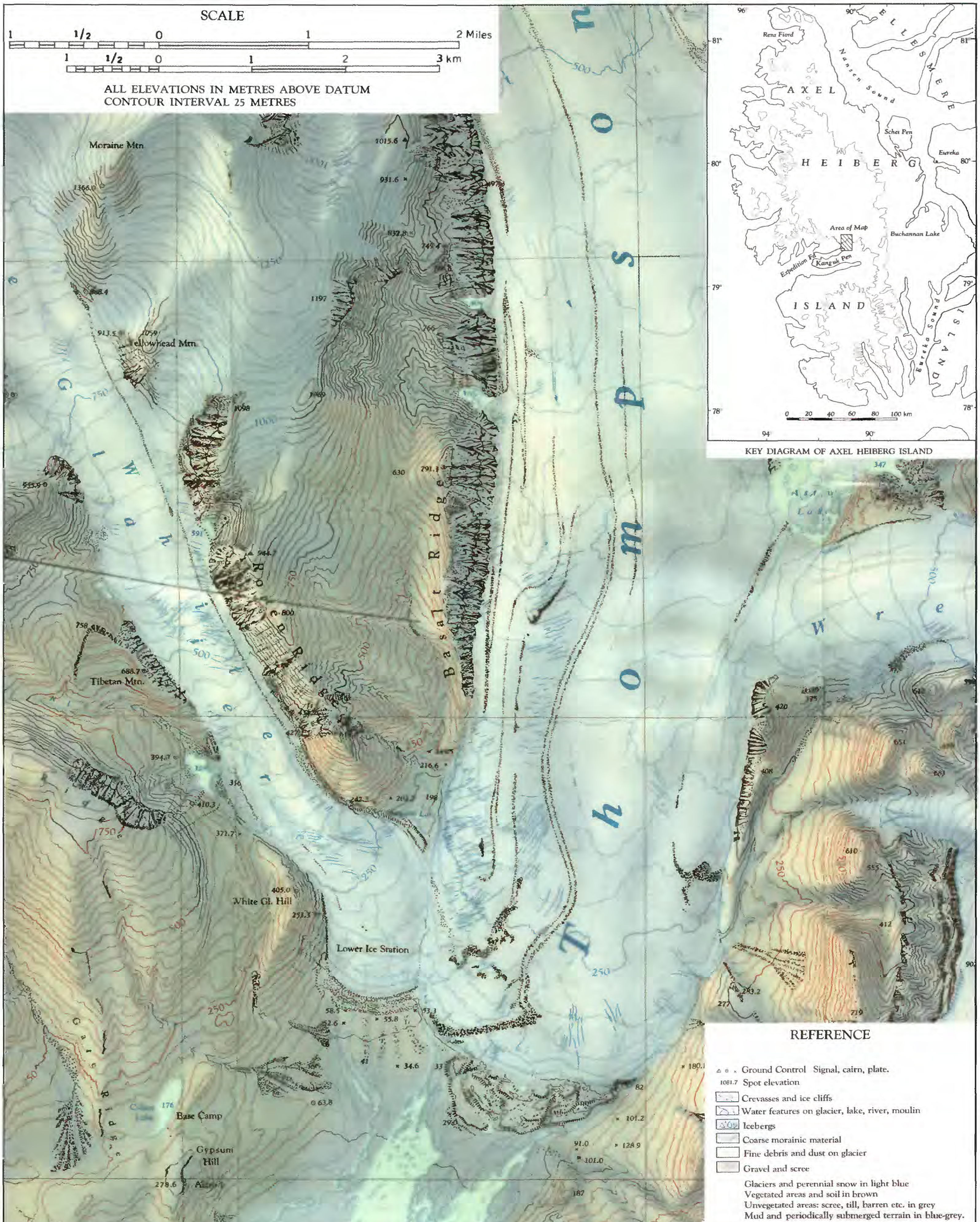
SCALE
1 1/2 0 1 2 Miles
1 1/2 0 1 2 3 km
ALL ELEVATIONS IN METRES ABOVE DATUM
CONTOUR INTERVAL 25 METRES
Moraine Mtn
Yellowhead Mtn
Tibetan Mtn.
White Gl. Hill
Lower Ice Station
Base Camp
Gypsum Hill
Basalt Ridge
Rosen Ridge
Thompson
White Glacier
Wright
KEY DIAGRAM OF AXEL HEIBERG ISLAND
AXEL HEIBERG ISLAND
Rens Fiord
Nansen Sound
ELLESMERE ISLAND
Schei Pen
Eureka
Area of Map
Buchannan Lake
Expedition Fd
Kanguk Pen
Eureka Sound
0 20 40 60 80 100 km
REFERENCE
Ground Control Signal, cairn, plate.
1081.7 Spot elevation
Crevasses and ice cliffs
Water features on glacier, lake, river, moulin
Icebergs
Coarse morainic material
Fine debris and dust on glacier
Gravel and scree
Glaciers and perennial snow in light blue
Vegetated areas and soil in brown
Unvegetated areas: scree, till, barren etc. in grey
Mud and periodically submerged terrain in blue-grey.

Figure 2.—(opposite page) Part of Thompson Glacier Region map, Axel Heiberg Island, Nunavut; scale 1:50,000; contour interval 25 m. The map was the first glacier map in Canada to use eight colors, portray bedrock outcrops, and use relief shading.

Glacier Maps of the High Arctic

After PRS-NRCC concluded the Salmon Glacier project, it became involved with the Jacobsen-McGill University Arctic Research Expedition to Axel Heiberg Island, Nunavut. This collaboration led to a remarkable set of maps, compiled using aerial photogrammetric methods; most of the maps were included in the report by Müller and others (1963). The Thompson Glacier Region map (1:50,000/25 m)[5] (fig. 2) was the first of its kind in Canada to combine eight colors, bedrock portrayal, and shading to create a strong visual impression of the landscape (McKortel, 1963). Large-scale glacier maps were made of Crusoe Glacier tongue, Baby Glacier, and the Thompson Glacier terminus (1:5,000/5 m)[5] (fig. 3). All of White Glacier, the focus of the expedition's glaciological work, was mapped and printed in two colors (1:10,000/10 m),[5] and its terminus only (1:5,000/5 m)[5] in six colors (Haumann, 1963; McKortel, 1963). The maps were used as a base for much of the scientific work of the expedition (Blachut, 1963a, b; Blachut and Müller, 1966). An overview was provided by a smaller scale map of the expedition area (1:100,000/100 m).[5] In a subsequent experiment in the use of terrestrial photogrammetry for mass-balance determination, Arnold (1977, 1981) mapped the lowest 2 km of the White Glacier (1:2,500/5 m).[5]

To the west, the Surveys and Mapping Branch, Department of Energy, Mines and Resources, and the Polar Continental Shelf Project mapped Meighen Island (1:50,000/10 m)[5] and its ice cap (1:25,000/5 m),[5] using aerial photography taken 1 year apart (see fig. 9*B* in Glaciers of the High Arctic Islands in this volume), and compared the changes. An aspect not seen on any other Canadian glacier maps is that both the surficial and subglacial topography are contoured. The maps are multicolored and have been described by Arnold (1966).

On Ellesmere Island, the surging Otto Glacier was mapped twice by the Defence Research Board (1:50,000/10 m)[5] and the results reported by Konecny (1966). The terminus of d'Iberville Glacier was mapped (1:50,000 scale), but not contoured, in a project aimed at measuring displacement values of a tidewater glacier (G. Holdsworth, 1977; unpub. data). The changes in the ice shelves along the northern coast, surveyed and mapped by Jeffries and Serson (1986), did not result in a published topographic map (see subchapter on Ellesmere Island Ice Shelves and Ice Islands in this volume). In Hare Fiord, part of the ice tongue position in 1958 has been plotted against the 1978 position (Römmer and Hell, 1986).

Figure 3.—The compound termini of the White Glacier, Axel Heiberg Island, Nunavut, High Arctic, Canada, in August 1964. The confluence of the two glaciers is marked by the medial moraine. View looking north-northeast across the outwash plain and source of the Expedition River. A low terminal moraine in front of White Glacier is visible in the center of the photograph. Photograph by C. Simon L. Ommanney, National Hydrology Research Institute. Maps of the area are shown in figures 1 and 2. A summary of historical information for White Glacier (153) and Thompson Glacier (152) is given in table 2 in the subchapter History of Glacier Investigations in Canada, by C. Simon L. Ommanney, this volume] [NTS map: 059H06].

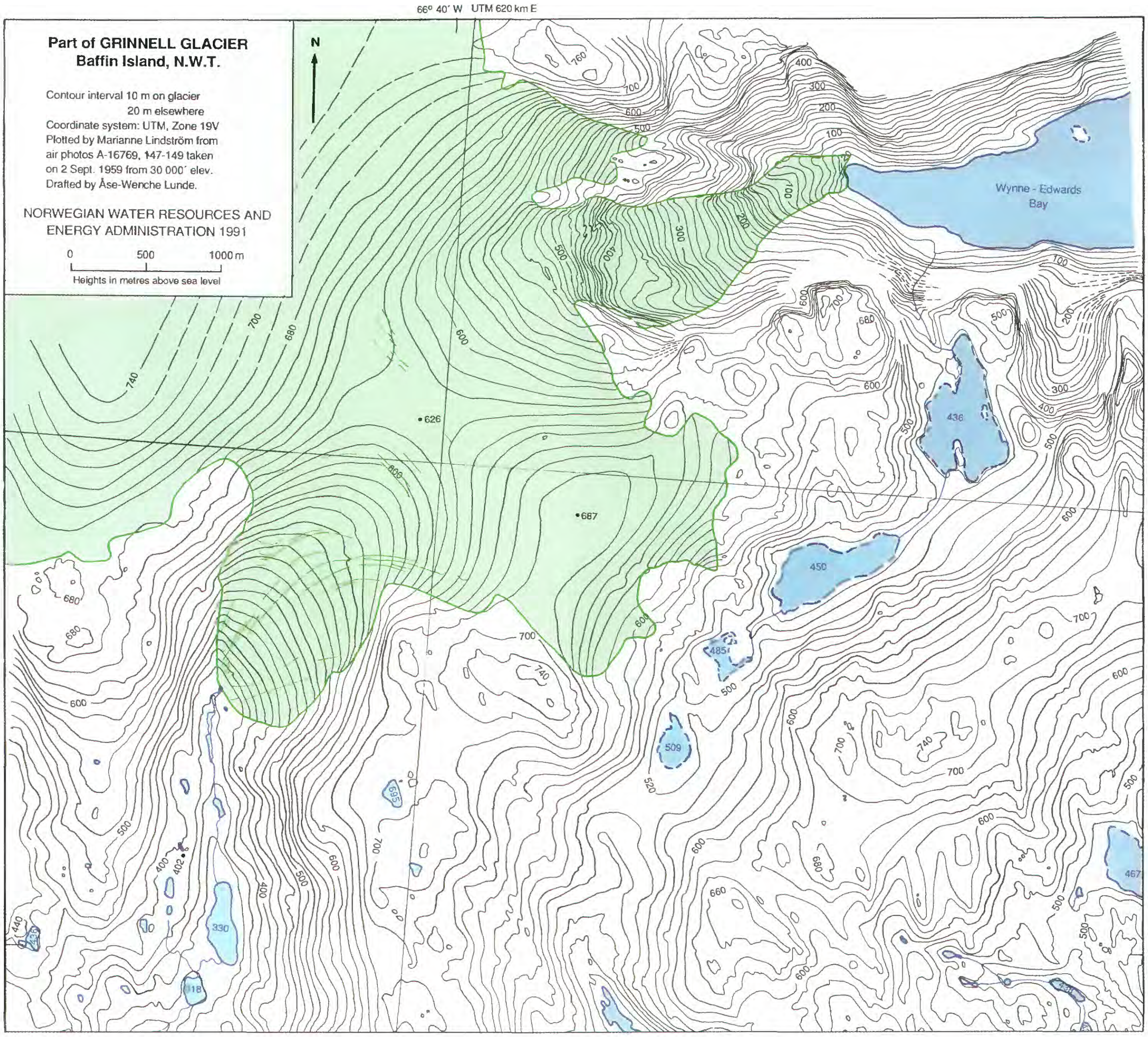

In southern Baffin Island, collaboration between Gunnar Østrem and the college in Iqaluit led to the mapping and publication of part of the Grinnell Glacier by Norges Vassdrags- og Energiverk (NVE) (1991) (fig. 4).

***Figure 4.*—A**, *Map of part of the Grinnell Glacier, Baffin Island, Nunavut; reduced from original scale of 1:20,000; contour intervals 10 and 20 m. Published by Norges Vassdrags- og Energiverk (NVE) in 1991. The map is printed in three colors (black, blue, green), with the glacier and associated glaciological features (crevasses) shown in green. NVE pioneered the use of green to depict glaciers, instead of the conventional blue, reserving blue for hydrological features.* **B**, *see opposite page.*

IHD Glacier Maps

Canadian participation in the International Hydrological Decade (IHD) included mass- balance investigations on several glaciers in western Canada and the north for which metric maps at a scale of 1:10,000 with 10-m contours were required. Those of the Berendon, Place, and Sentinel Glaciers were printed in four process colors; in addition, the maps of Ram River and Woolsey Glaciers, both in National Parks, were embellished with shaded relief. The Peyto Glacier map is discussed later. The map of Decade Glacier, Baffin Island (1:10,000/10 m)[5] was not printed. Two maps were made of Per

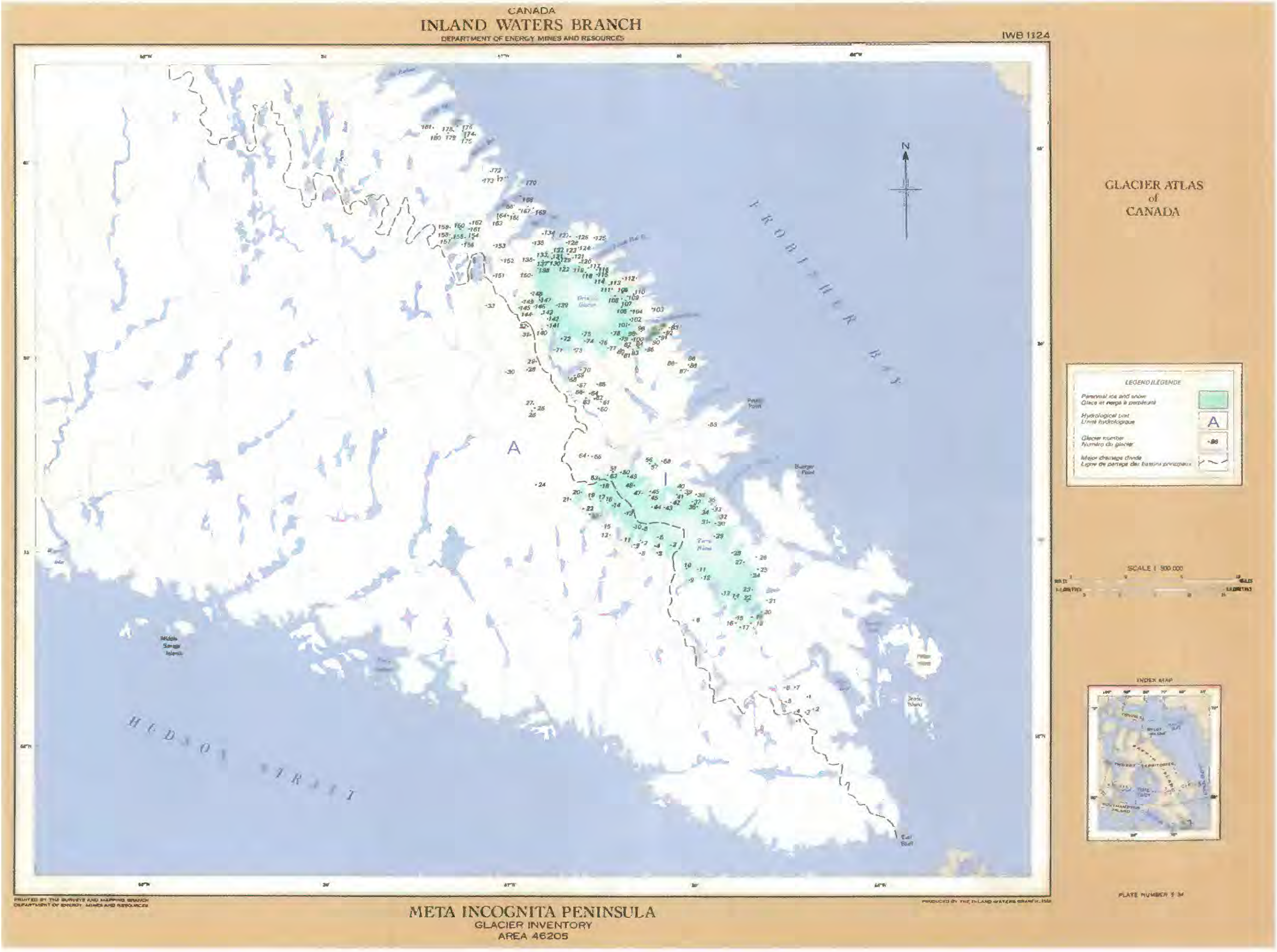

***Figure 4B**—Glacier Inventory Map (Area 46205) of the Meta Incognita Peninsula, showing the location of the Grinnell Glacier. Plate Number 5–24, Map No. IWB 1124, of the Glacier Atlas of Canada, 1969 (reduced from original scale).*

Ardua Glacier, Ellesmere Island, by Konecny (1966): the entire glacier (1:20,000/10 m)[5] and its tongue (1:5,000/5 m).[5] Maps of the Barnes Ice Cap were prepared by the Surveys and Mapping Branch as 1:50,000-scale NTS maps. Some were Arctic Provisional Maps with black contours, blue hydrography, and 25-ft contours; others were standard NTS maps with the ice shown in a blue vignette and dashed- brown 50-ft contours.

The original intent was to remap all IHD glaciers after the 10-year program was concluded to compare the accumulated mass balance with photogrammetrically determined volumetric change. This was not done, nor are there any plans to do so now. However, all glaciers in an east-west transect from Ram River Glacier to Sentinel Glacier were photographed almost simultaneously (22 to 24 August 1966). Some of the detailed glacier maps mentioned above and in tables 3 and 4 were compiled from this aerial photography. One of the objectives of the aerial photography was to map simultaneously the elevation of the transient snowline along the east-west transect (Østrem, 1973).

Miscellaneous Maps of Western Canada

Many individual glaciological projects require accurate maps for plotting results and determining changes in the glaciers. This was recognized quite early when the American Geographical Society (AGS) (1960) embarked on a project to map nine glaciers in North America, one of which was the *Little Jarvis Glacier* in the St. Elias Mountains, in a project that has been described in Brandenberger and Bull (1966). The AGS also sponsored termini mapping in Alaska by Bill Field that included the Grand Pacific Glacier, a Canadian glacier at the head of Glacier Bay (Field, 1966). Subsequent work in this region has resulted in a more general map of this glacierized area (Molenaar, 1990).

Steele Glacier, which surged during the Yukon Centennial Expedition of 1967, was mapped from 1951 aerial photography (1:50,000/25 m; 1:25,000/20 m)[5] and 1967 photography so that its velocity vectors could be plotted (Stanley, 1969). A four-color map of the Centennial Range (MCR-7, 1:125,000/500 ft),[5] that followed this expedition, had details of glaciological features normally omitted from NTS maps. Other surging glaciers in the Yukon and northern British Columbia have attracted considerable attention. The Army Survey Establishment compiled a map of Rusty Glacier (1:10,000/10 m).[5] In 1983, Nadir Mapping Corporation prepared a map of Trapridge Glacier (1:10,000/10 m)[5] for Garry K.C. Clarke, University of British Columbia.

Two maps of Tweedsmuir Glacier (1:50,000/20 m),[5] before- and after-surge, were produced under the direction of Gerald Holdsworth from 1951 aerial and 1974 terrestrial photography; the former was published in three colors. Finally, a three-color map of Lowell Glacier (1:50,000/20 m)[5] with moraine shading was prepared from 1974 photography in anticipation of a surge (see fig. 11 in Quantitative Measurements of Tweedsmuir Glacier and Lowell Glacier Imagery in the section about Glaciers of the St. Elias Mountains in this volume).

The Foundation for Glacier and Environmental Research (FGER), in collaboration with the Technical University of Hannover, Germany, has included mapping with its other studies of Cathedral Glacier near Atlin (1:5,000/5 m)[5] (Cialek, 1977; FGER, 1976; Mauelshagen, 1984; Mauelshagen and Slupetzky, 1985; Slupetzky and others, 1988).

A map of the northwest col of Mount Logan with hachured bedrock and relief shading (1:10,000/20 m)[5] was compiled in 1976 (Holdsworth and others, 1976) in connection with an ice core deep-drilling project there by Gerald Holdsworth of the Glaciology Division. It was subsequently modified in 1992 to include an area targeted for drilling in 2001 (Holdsworth and others, 1992). Two maps of the Mount Logan massif (1:75,000/40 m and 1:100,000/40 m)[5] were produced by Holdsworth and Sawyer (1993).

A joint project between the British Columbia Institute of Technology and Karl Ricker (1977) resulted in a map of Wedgemount Glacier (1:5,000/10 m).[5]

One of the finest North American examples of the cartographer's art is The Massif of Mount Hubbard, Mount Alverstone, and Mount Kennedy map (1:31,680/100 ft),[5] produced by the National Geographic Society with field surveys by the University of New Brunswick (Washburn and others, 1965; Washburn, 1971a, b). The two-color map with hachured bedrock and relief shading is a visual delight (fig. 5).

Peyto Glacier and Columbia Icefield

In 1970, a map of Peyto Glacier, Alberta, was published in nine colors using the French technique of bedrock portrayal (Sedgwick and Henoch, 1970) (1:10,000/10 m).[5] Subsequently, it was decided to experiment with the enhancement of this map to create a three-dimensional visual effect using the Swiss technique of hachured bedrock portrayal and shaded relief (Henoch and Croizet, 1976). The resultant map, published in 1975 at the same scale as the original edition, was printed in eight colors and accompanied by an explanatory booklet with the ensemble designed to cater to the scientist, teacher, and the general public.

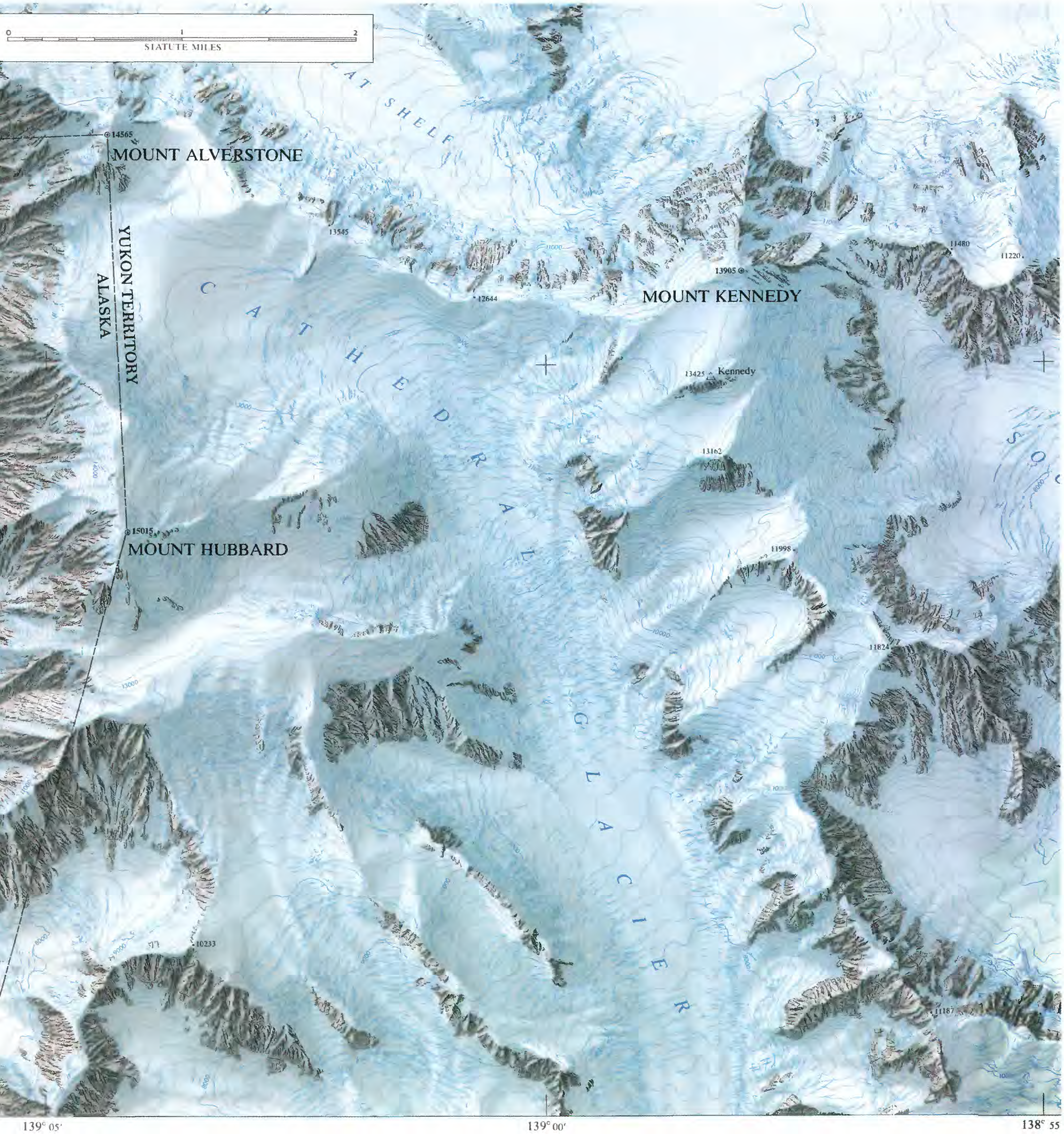

Figure 5.—Part of the Massif of Mount Hubbard, Mount Alverstone, and Mount Kennedy map, Yukon Territory, showing the highly glacierized terrain, including the source of the Hubbard and Lowell Glaciers. Map project directed by Bradford Washburn, Honorary Director, Boston Museum of Science. Published and copyrighted by the National Geographic Society (NGS), Washington, D.C., in 1968. Used with permission of Bradford Washburn and NGS. Reduced from original scale.

Following the success of the Peyto Glacier map, it was decided to experiment with a larger glaciological unit and a smaller scale, though continuing to apply the same cartographic techniques. The Columbia Icefield was selected as a joint project with Parks Canada in 1976. In 1981, a ten-color map with hachured bedrock portrayal, shaded relief, and interpretive information on the reverse side was published (1:50,000/20 m).[5]

Orthophoto Maps

Blachut and Müller concluded in 1965 that the orthophoto map would probably find extensive use in glaciological work (Blachut and Müller, 1966). Canadian experience has shown a trend toward this, although few of the resultant maps have been published or distributed widely. Once again PRS-NRCC has been a pioneer, producing stereo-orthophoto maps of Axel Heiberg Island glaciers in collaboration with Environment Canada and the Technical Universities of Vienna and Zürich: White Glacier (1:10,000/20 m),[5] Thompson Glacier and White Glacier termini (Institute of Cartography, 1998) (1:5,000/10 m)[5] (fig. 6), Crusoe Glacier terminus and Baby Glacier (1:5,000/10 m).[5] To the east, a map of Oobloyah Bay (1:25,000/25 m)[5] was prepared as a base map for the Heidelberg-Ellesmere Island Expedition 1978 (Hell, 1981).

In western Canada, the British Columbia Institute of Technology compiled a map of Wedgemount Glacier (1:10,000/20 m).[5] A stereo-orthophoto map of Peyto Glacier (1:10,000 scale) was prepared as part of a pilot study for the Forest Management Institute, Environment Canada, by Gestalt International, Ltd. Contours were not plotted on the map, but the elevation data were analyzed from the digital terrain model, which was a byproduct of the stereophotogrammetric-compilation process (Young and Arnold, 1978). The Gestalt system was further tested in the construction of three maps of the Columbia Icefield (1:25,000 scale) by the Surveys and Mapping Branch for the Glaciology Division using 1977 photography (Athabasca Glacier, Saskatchewan Glacier, Athabasca and Saskatchewan Glaciers). A larger scale map of Athabasca Glacier (1:5,000 scale), based on 1980 photography, was produced for the latter agency by Orthoshop of Calgary as part of a study of photogrammetric applications to mass-balance measurements.

Satellite Mapping

While the immediate future technology for glacier mapping in 1965 was the orthophoto map derived from aerial photographs, the current and future technology is based on satellite images and other remote-sensing devices (for example, satellite laser altimetry). Significant improvements in resolution (1-m pixel resolution of Ikonos) combined with stereo and all-weather capabilities [Synthetic Aperture Radar (SAR)] make this technology increasingly viable. The Surveys and Mapping Branch used Landsat images to revise their 1:250,000-scale NTS maps. Experiments have been carried out on the viability of using existing images to update glaciological information (Howarth and Ommanney, 1983), and some attempts were made to map with this technology (Sidjak and Wheate, 1999). The full range of potential applications has been documented in this volume and other volumes in the U.S. Geological Survey Professional Paper 1386, Satellite Image Atlas of Glaciers of the World.

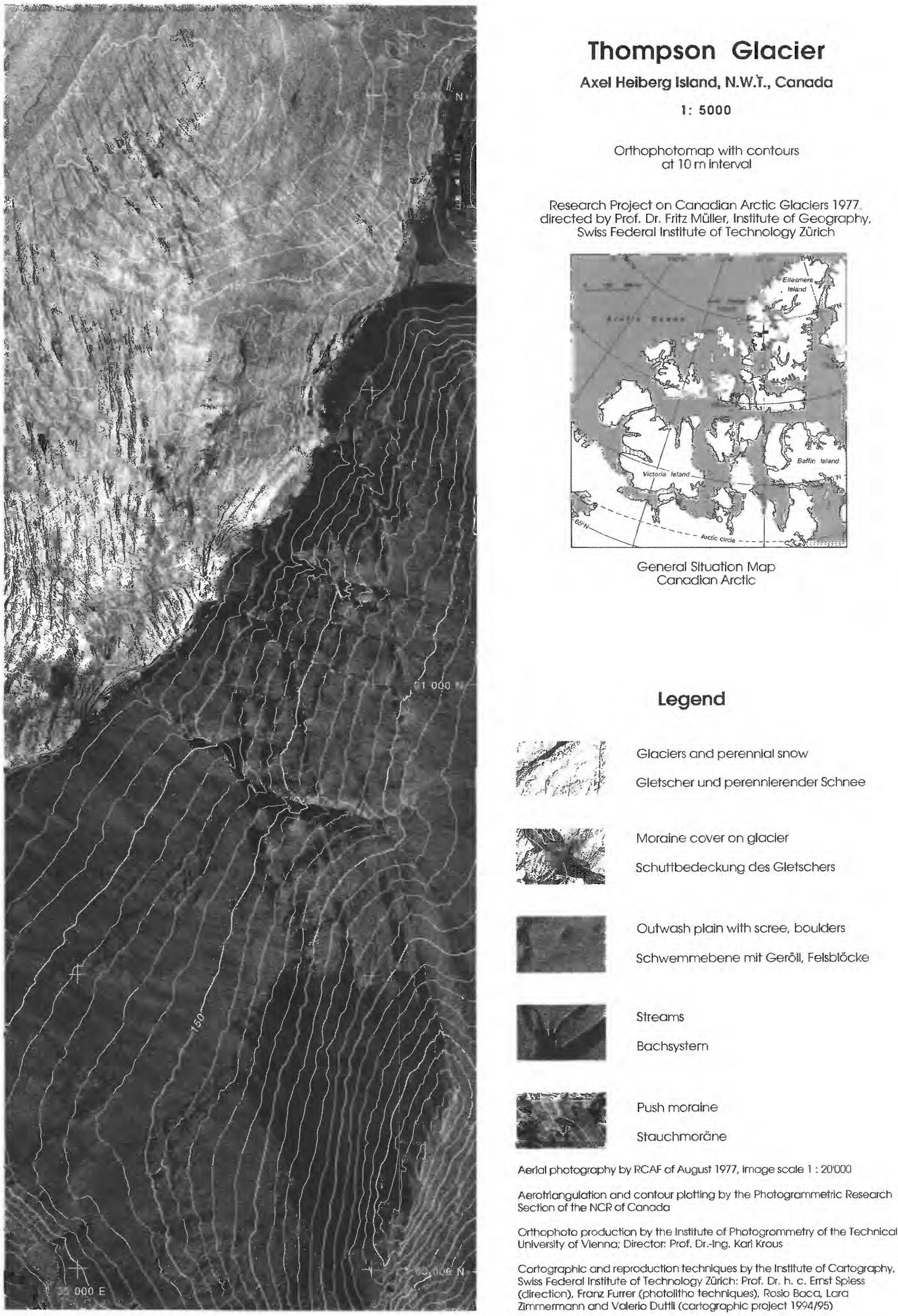

Figure 6.—*Orthophoto map of the Thompson Glacier termini, Axel Heiberg Island, Nunavut; reduced from the original scale of 1:5,000; contour interval 10 m. Map based on 1977 aerial photography by the Royal Canadian Air Force. Compiled in 1994/95 by the Institute of Cartography, Swiss Federal Institute of Technology, Zürich (Institute of Cartography, 1998).*

Mapping Glaciers in the *Interior Ranges* and Rocky Mountains with Landsat Data

By Roger D. Wheate, Robert W. Sidjak, *and* Garnet T. Whyte

Abstract

The areal extent and glacier facies of glaciers in Canada can be mapped effectively and monitored using satellite imagery especially where accessibility, size of ice mass, and large number of glaciers are limitations to conventional surveying methods. Glacier delineation, glacier facies, and surface details are enhanced by the use of specialized digital-imaging and analytical techniques, notably principal components analysis, the TM 4/5 ratio, and a normalized difference snow index (NDSI). The two examples illustrated here depict the glacier facies of the Illecillewaet Glacier, Columbia Mountains, *Interior Ranges*, British Columbia, and the retreat of the Monkman Glacier/Parsnip Glacier, Peace River, British Columbia, over a period of approximately 10 years. Retreat of glaciers in western Canada is clearly detectable using Landsat imagery with its good spatial resolution and decades of data acquisition, beginning with the launch of ERTS-1 (Landsat-1) on 23 July 1972. Three-dimensional perspectives can be produced by combining satellite images and digital elevation models.

Introduction

Glacier retreat represents a substantial change that is occurring in the Coast Mountains, *Interior Ranges*, and Rocky Mountains in western Canada. Topographic maps are revised at irregular intervals, but changes in areal extent of many Canadian glaciers and glacier facies may be significant on an annual basis. Glaciers in these mountains appear on 1:50,000- and 1:250,000-scale National Topographic System (NTS) and other map sheets. However, many of these sheets are based on glacier extent in the 1970's and 1980's and, thus, are generally outdated. Despite considerable cloud cover, it is usually possible to obtain cloud-free satellite images of western Canada during most years.

British Columbia Provincial Mapping

Glacier margins in digital format at the 1:250,000 scale for the Province of British Columbia (BC) were created in 1996 and are available to the public. The entire province has also been mapped at a scale of 1:20,000, using stereo aerial photogrammetric methods, as part of the Terrain Resource Inventory Management (TRIM) Program, which was completed between 1985 and 1996. Digital thematic datasets (layers) include glacier margins, but the accuracy of the glacier outlines may not always be reliable because of (1) masking by residual snowpack and (2) lack of experience in glacier mapping by cartographers whose primary experience is in forest-cover mapping. These two sources of error produced maps of glaciers that were initially incorrect and only become more so because of subsequent glacier changes in the more than 15 years since the mapping program began.

A second generation of mapping designed to update the changes since 1985, known as TRIM II, was begun in 1998 and is still in progress. Within the TRIM II program, orthophotographs have been produced for each 1:20,000-scale digital map quadrangle, each of which covers 12 min. longitude by 6 min. latitude (approximately 13 km x 11 km); there are 100 1:20,000-scale quadrangles in each 1:250,000-scale NTS sheet. However, an initial evaluation of some of these new data indicate that the use of early-summer aerial photography precludes the precise determination of glacier margins (concealment by snowpack). Hence, glacier-extent maps and precise location of ice-front positions for western Canada do not exist unless the glaciers were the subjects of special studies, such as Luckman and others (1987) (see also tables 1 and 4), which may now also be as dated as the first TRIM data.

The TRIM programs included the production of a digital elevation model (DEM), which contains sampled points from digital aerial stereophotogrammetry at approximately 50–70 m intervals along north-south transects, producing a 20-m contour interval. In many cases, the frequency of points decreases on glaciers because of the inability to determine elevation location under conditions of no contrast (for example, on a snow-covered glacier). Therefore, elevational inaccuracies are common in the accumulation areas of glaciers. Uncertainty in the accuracy of the DEM also complicates the calculation of the position of the equilibrium line altitude (ELA). Lodwick and Paine (1985) experimented with deriving elevation data directly from Landsat MSS data for the Barnes Ice Cap by applying principal components analysis (PCA) and utilizing the information contained in the lower components. However, their encouraging results have not been pursued with the higher resolution and spectral range of either Landsat Thematic Mapper (TM) or Enhanced Thematic Mapper (ETM+) data.

Satellite Image Data

Satellite imagery offers the dual advantages of repetitive coverage and multispectral remote sensing for updating glacier maps. The first increases the likelihood of obtaining cloud-free and snow-free scenes in mountainous areas at the latitude of western Canada and proximity to the coast, a region which typically experiences both frequent cloud cover and remnant snowpack most of the year. Ideally, satellite images are best obtained at the end-of-the-melt season, in late August to early September, to minimize snow cover, while avoiding shadows cast by the lower Sun angles in the autumn. Landsat TM data have so far offered the best combination of spatial resolution and spectral selection compared to other available sensors, such as the Système Probitoire d'Observation de la Terre (SPOT) and the Indian Remote Sensing (IRS) satellites, especially the inclusion of mid-infrared (IR) wavelength bands. The potential role of these bands [TM bands 5 (1.55µm–1.75µm) and 7 (2.08µm–2.35µm)] is based on the lower reflectance of snow and ice, in comparison to the higher reflectance and often complete saturation in the visible wavelengths. Landsat data have been shown to be effective in the mapping of the areal extent of glacier facies, including ice, wet snow, and snow (Williams, 1987; Williams and others, 1991). The 30-m picture-element (pixel) resolution has proven to be adequate here for monitoring glaciers with an area of 10 km^2 and greater, and for changes over periods of 4–5 years, as was also determined by Bayr and others (1994) in the Austrian Alps and for longer time periods in Iceland (Williams, 1986; Hall and others, 1992; Williams and others, 1997).

Digital-Image Processing for Glacier Mapping

Challenges facing the automated mapping of glacier areas include discrimination of the glacier facies, identification of debris-covered ice, topographically and cloud-shadowed areas, and water bodies marginal to the glaciers. Although glacier margins can be readily discerned visually using an optimum color composite of TM bands 3 (0.63µm–0.69µm), 4 (0.76µm–0.90µm), and 5 [or one in each part of the visible (0.4µm–0.7µm), near-IR (0.7µm–1.5µm), and mid-IR (1.5µm–8.0µm) wavelengths], the following image spectral bands and processes have been shown to greatly increase delineation of glacier facies and margins (Sidjak and Wheate, 1999).

PCA has been employed to reduce data redundancy due to correlation between TM bands and to enhance contrast in features of interest. The second principal component (PC2) is usually influenced by the mid-IR bands 5 and 7 and cleanly isolates glacier from nonglacier surfaces, unless the surface is covered with morainic material. PC4 displays more detail on the glacier surface than any of the TM bands; this has been suggested to be related to snow grain size (Brugman and others, 1996). The second component (PC2) can also be used to generate a mask to eliminate nonglacier surfaces in further analysis.

Pixel saturation is recognized as a typical problem over glacierized and snow-covered scene areas, particularly in the visible bands [Landsat TM bands 1 (0.45µm–0.52µm), 2 (0.52µm–0.60µm), and 3 (Hall and others, 1988)]. PCA reduces this problem by identifying most of the scene-brightness variance, and thus the saturation, within the first principal component (PC1). Subsequent principal components, especially the second, third, and fourth, usually depict strong, unsaturated contrast over the glacier areas, enhancing surface features and facies. Further image processing has involved the normalized difference snow index (NDSI) (Riggs and others, 1994) where NDSI = (TM2–TM5)/(TM2+TM5). The TM4/TM5 ratio has also been cited by Hall and others (1987) as effective for discriminating the ice-and-snow facies, particularly in areas of shadow.

Illecillewaet Névé and Illecillewaet Glacier

Illecillewaet Glacier (lat 51°14'N., long 117°27'W.) is the best known glacier in Glacier National Park, Columbia Mountains, east of the town of Revelstoke, B.C., and directly accessible from the Trans-Canada Highway. In the early 20th century, it formed the backdrop to a mountain lodge and was a popular climbing attraction. Champoux and Ommanney (1986) studied

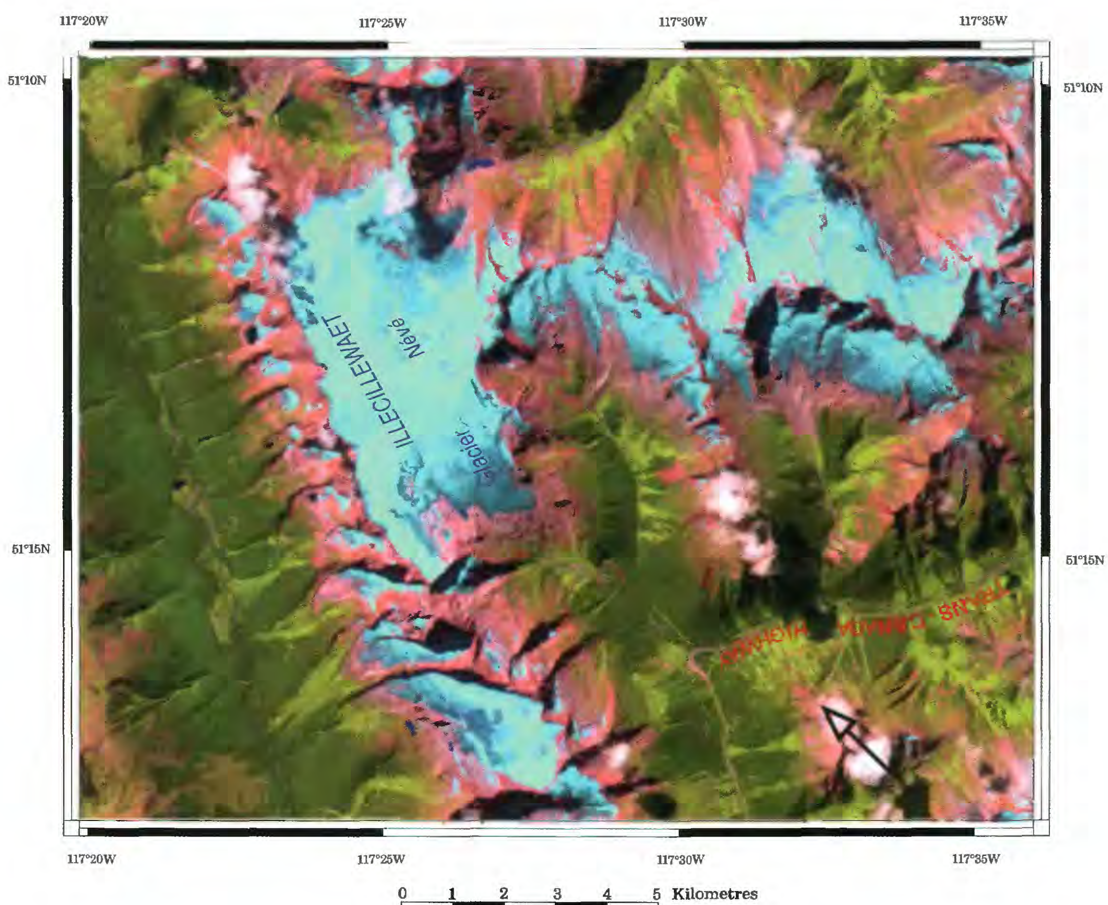

***Figure 7.**—Landsat 5 TM false-color composite image of the Illecillewaet Névé and Illecillewaet Glacier. The band combination is optimum for defining glacier extent. The image is oriented with south at the top. The Trans-Canada Highway is visible in the northwest corner of the image. The arrow indicates the perspective of the view shown in figure 8. Landsat 5 image (50440240094230T0; bands 3, 4, 5; 18 August 1994; Path 44, Row 24) from RADARSAT International, British Columbia.*

Figure 8.—**A**, *Perspective view of the Illecillewaet Glacier seen from the Trans-Canada Highway looking toward the southeast. The view is created by combining the Landsat image shown in figure 7 with the Province of British Columbia DEM. The following glacier facies are shown: accumulation area (snow): white; firn/wet snow: medium blue; bare ice (ablation area): dark blue; debris-covered ice: red; shadowed glacier: purple; meltwater lakes: green. Nonglacier surfaces are shown in gray (forested) and pink/salmon (nonforested).* **B**, *Photograph of the terminus of the Illecillewaet Glacier looking southeast from a position southeast of the Trans-Canada Highway, west of Rogers Pass, Glacier National Park, British Columbia, in August 1995. Photograph by Robert W. Sidjak, University of Northern British Columbia.*

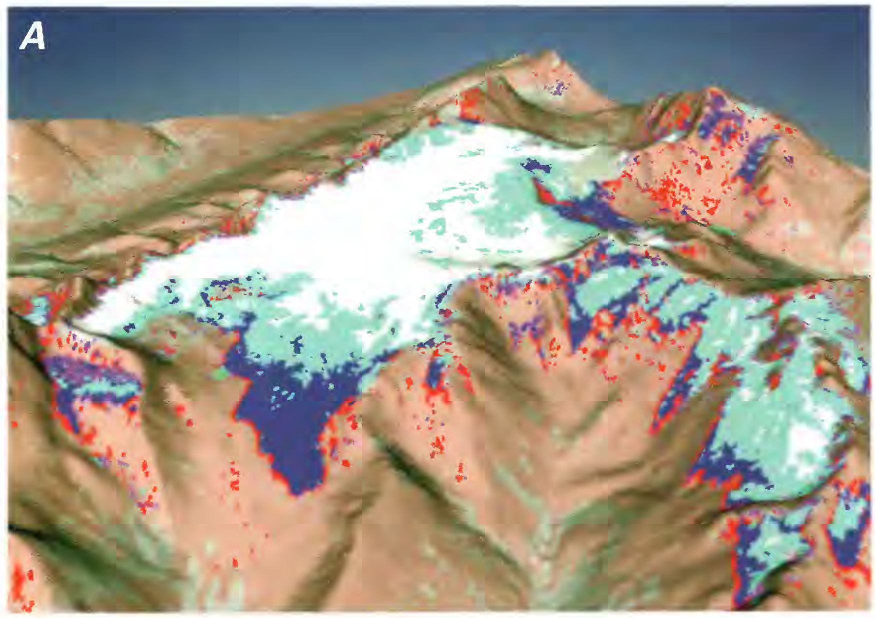

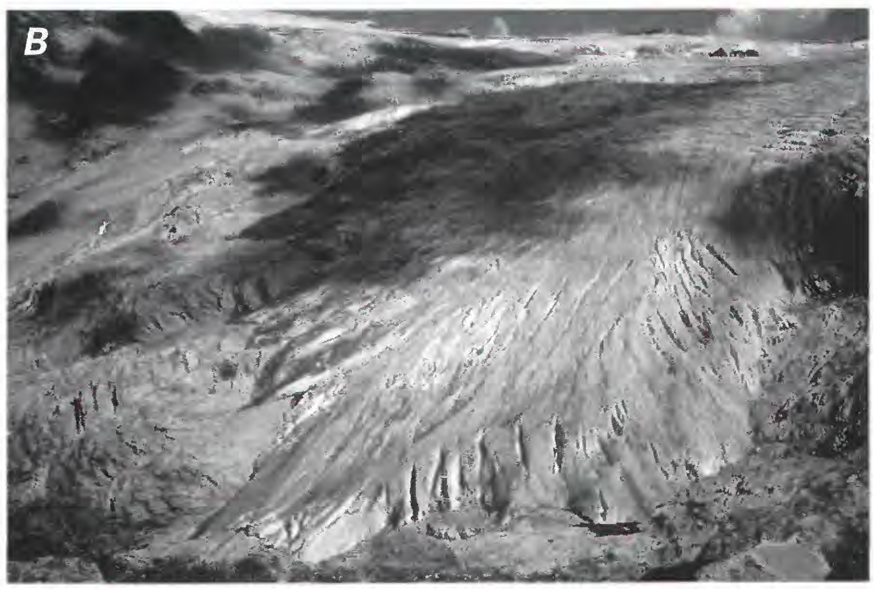

the evolution of Illecillewaet Glacier using historic data, aerial photography and satellite imagery. This study uses the above Landsat combination (TM4/TM5 ratio) of spectral bands to classify the following glacier facies and give the best estimate of transient snowline and equilibrium line location: snow (accumulation area), bare ice (ablation area), from which the accumulation-area ratio (AAR) can be calculated (see table 5); water, shadowed glacier, and debris-covered ice (recognized as a significant challenge in glacier-inventory mapping by Whalley and Martin, 1986). The Landsat 5 TM false-color composite image (50440240094230T0; bands 3, 4, 5; 18 August 1994; Path 44, Row 24) is shown in figure 7. The computer-classified image is draped on the B.C. provincial DEM in figure 8*A*, as viewed from the northwest, a similar direction from the ground photograph (fig. 8*B*). Snow (accumulation area) is shown in white, bare ice in dark blue, and firn/wet snow in medium blue. There are a few scattered clouds on the south end of the icefield (white on figure 7).

TABLE 5.—*Selected glaciological parameters of the Illecillewaet Névé and Illecillewaet Glacier*

	Illecillewaet Névé	Illecillewaet Glacier
Accumulation area	13.04 km^2	4.92 km^2
Ablation area	8.35 km^2	3.91 km^2
Total area	21.39 km^2	8.83 km^2
Accumulation-area ratio	0.61	0.56

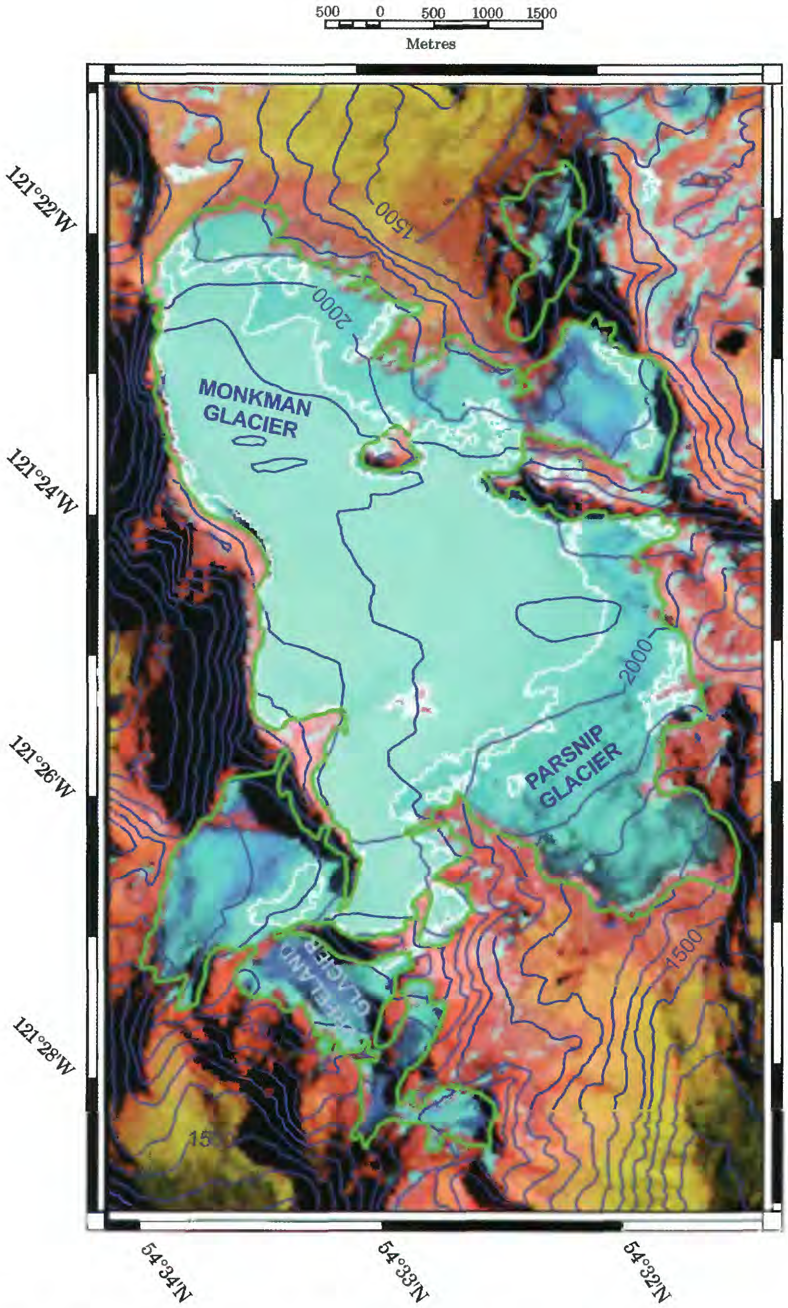

__Figure 9.__—Landsat 5 TM false-color composite image of the Monkman Glacier/Parsnip Glacier. The image is oriented with southeast at the top. The superimposed contours are taken from the Province of British Columbia DEM; the contour interval is 100 m. The ablation area/accumulation area boundary is shown in white; the 1986 margin of the glaciers, derived from the Terrain Resource Inventory Management (TRIM) Program, is shown in green. Landsat 5 image (50480220097266T0; bands 3, 4, 5; 23 September 1997; Path 48, Row 22) from RADARSAT International, Richmond, British Columbia.

Monkman Glacier/Parsnip Glacier

The Monkman Glacier/Parsnip Glacier (lat 54°30'N., long 121°30'W.) is the largest of a group of glaciers in the front ranges of the Rocky Mountains, about 100 km northwest of the city of Prince George, B.C. (see discussion of Hart Ranges in the Glaciers of the Canadian Rockies section); access to this area is very difficult except by helicopter. Comparison of image data from 23 September 1997 with the B.C. TRIM contour maps from the middle 1980's shows a decrease in glacier area from 24.8 to 23.2 km^2 and ice-front retreat ranging between about 100–200 m. Figure 9 shows a Landsat 5 TM false-color composite image (50480220097266T0; bands 3, 4, 5; 23 September 1997; Path 48, Row 22) overlain with 100-m DEM contours and includes the equilibrium line in white. The green line from the TRIM contour maps indicates the approximate areal extent of the glacier in 1986. Smaller ice patches that are not visible in dark shadow indicate some complications of using satellite images for glacier mapping and emphasize the need for derived products such as

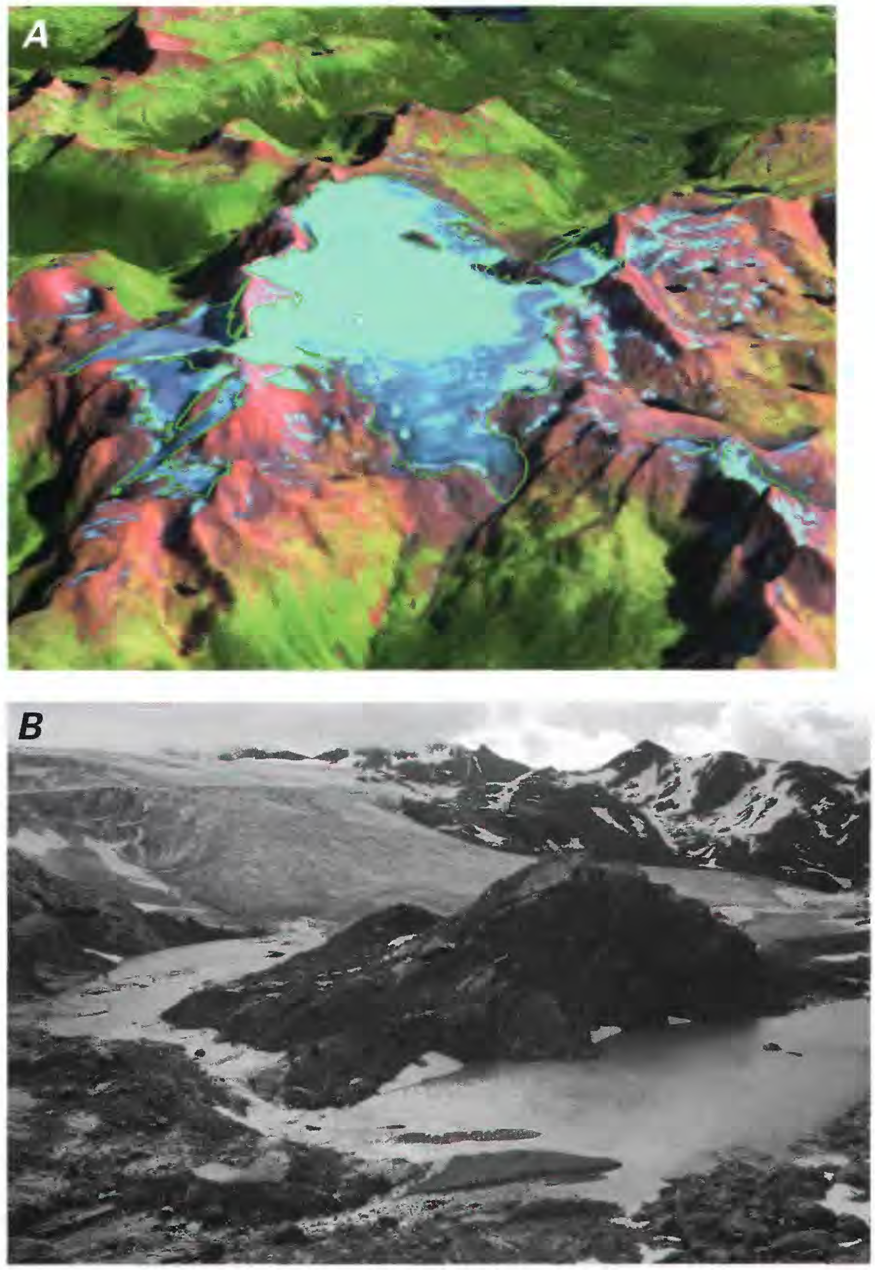

Figure 10.—**A**, *Perspective view of the Monkman Glacier/Parsnip Glacier looking toward the east. The areal extent (margins of the glaciers) in 1986, taken from the Terrain Resource Inventory Management (TRIM) Program, is shown as a green line. The view is created by draping the Landsat image shown in figure 9 with the Province of British Columbia DEM.* **B**, *Photograph of Parsnip Glacier and its proglacial lake looking toward the southeast from a terminal moraine on 26 July 2000. Photograph by Roger D. Wheate, University of Northern British Columbia.*

principal components and ratios to compensate for topographic shadows. Figure 10*A* depicts the same image (without contours), draped over the provincial DEM. Figure 10*B* is a ground photograph of the Parsnip Glacier.

Acknowledgments

The Illecillewaet Névé/Illecillewaet Glacier study was done in collaboration with Drs. Melinda M. Brugman and Alain Pietroniro of the National Water Research Institute, Saskatoon, Saskatchewan, under the cryospheric systems research initiative (CRYSYS), a Canadian contribution to the NASA Earth Observing System (EOS) program. The authors wish to acknowledge CRYSYS for providing the operating funds for the studies. The authors would also like to thank the following organizations and people for their observations, suggestions, and other support: BC Parks, Mike Demuth, and Birthe Miller. Special thanks to Nancy Alexander, Tanya Whyte, and Terry and Joyce Whyte.

National Topographic Series

While individual glaciological investigators were producing the specialized maps necessary for their work, the quality, scale, and coverage of the federal and provincial mapping was improving. There is now complete coverage of Canada at the scale of 1:250,000. Of the maps involved, 157 of them contain some depiction of glaciers, and there are possibly another 28 sheets that cover regions where one might expect to find glacier-related features such as glacierets, snow patches, and rock glaciers that may have been overlooked. The mapping of Canada at the 1:50,000 scale still remains to be completed. Unfortunately for the glaciologist, the isolated, unpopulated, ice-covered regions of the country have the lowest priority. The exception is Kluane National Park, St. Elias Mountains, Yukon Territory, which is covered with nonstandard map sheets in black and white with low-quality relief shading that are useful for glaciological applications (see section on Quantitative Measurements of Tweedsmuir Glacier and Lowell Glacier Imagery in the subchapter Glaciers of the St. Elias Mountains, by Garry K.C. Clarke and Gerald Holdsworth, this volume). It is expected that about 1,450 of these sheets might be required to provide complete coverage of all the glacierized areas in the country, but only about half have been published. However, the depiction of glaciological features has improved over the years as the mapping agencies have recognized the need for and availability of knowledge to interpret them. Glacier-inventory maps were used for reference when the 1:50,000-scale maps of Baffin Island were being compiled, leading to a vast improvement in the representation of marginal features such as moraines. Of great benefit has been the opportunity to acquire current maps in digital form so digital terrain models can be much more easily constructed. The move by some mapping agencies towards publication of new maps at scales as large as 1:20,000, also in digital form, may reduce the need for glaciologists to produce special large-scale maps of the glaciers on which they are working. Instead they may be able to concentrate their efforts on determining the changes taking place.

Conclusions

One of the most fruitful collaborations in glacier mapping was between Fritz Müller of the McGill University Axel Heiberg Island Expedition and the PRS-NRCC. This collaboration resulted in the preparation of large-scale topographic maps and stereo-orthophoto maps of several of the island's glaciers. Another productive relationship was that of Gottfried Konecny, University of New Brunswick, with the Defence Research Board, the Water Survey of Canada, and the National Geographic Society. The role of the Glaciology Division in the production of glacier maps for the IHD, specialty maps of Peyto Glacier and the Columbia Icefield, and orthophoto maps, has also been significant. Unfortunately, none of the above are still involved in any glacier mapping activity, and the Glaciology Division has since been disbanded. Glacier-mapping activity in Canada is limited to a few small projects where the product is unlikely to be published or distributed widely (Cogley, 1999), and this trend will likely continue. Scientists and lay people alike may well regret the loss of this valuable aid. However, financial resources for producing high-quality, multicolored, large-scale maps are no longer readily available. The only possible exception may be Parks Canada (the Canadian Parks Service), which has a large tourist clientele that might make such a venture viable.

With the proliferation of personal computers and growth in their storage capacity, the future may see much greater use of digital terrain models and satellite images by individual glaciologists. Optical disks permit the storing, exchange, and analysis of photographic and cartographic information so that the printed thematic map may become a collector's item.

We know that the next generation of satellites will be capable of providing greatly improved spectral and spatial resolution and more current information on glaciers. The technology for analysis of this information using personal computers is developing rapidly.

Although the heyday of the printed glacier map may be past in Canada, there are exciting prospects and challenges ahead for glaciologists in digital cartography, GIS, and analysis of remotely sensed data.

References Cited

American Geographical Society, 1960, Nine glacier maps, northwestern North America: New York, American Geographical Society, AGS Special Publication No. 34, 37 p.

Arnold, K.C., 1966, The glaciological maps of Meighen Island, N.W.T: Canadian Journal of Earth Sciences, v. 3, no. 6, p. 903–908.

———1977, White Glacier; 1:2,500, lowest 2 kilometers (terrestrial photogrammetry), *in* Fluctuations of glaciers 1970–1975, v. III: Paris, Unesco, International Association of Hydrological Sciences (IAHS), United Nations Educational, Scientific, and Cultural Organization (UNESCO), p. 255–258.

———1981, Ice ablation measured by stakes and terrestrial photogrammetry—a comparison on the lower part of the White Glacier—Axel Heiberg Island, Canadian Arctic Archipelago: Montréal, Québec, McGill University, Axel Heiberg Island Research Reports, Glaciology No. 2, 98 p., maps.

Bayr, K.J., Hall, D.K., and Kovalick, W.M., 1994, Observations on glaciers in the eastern Austrian Alps using satellite data: International Journal of Remote Sensing, v. 15, no. 9, p. 1733–1742.

Blachut, T.J., 1963a, Photogrammetric and cartographic results of the Axel Heiberg Expedition: Canadian Surveyor, v. 17, no. 2, p. 79–80.

———1963b, Photogrammetric determination of glacier movement, rate of ablation, and profiles: Canadian Surveyor, v. 17, no. 2, p. 112–122.

Blachut, T.J., and Müller, Fritz, 1966, Some fundamental considerations on glacier mapping, *in* Gunning, H.C., ed., Symposium on Glacier Mapping: Canadian Journal of Earth Sciences, v. 3, no. 6, p. 747–759.

Brandenberger, A.J., and Bull, C.[B.B.], 1966, Glacier surveying and mapping program of the Ohio State University: Canadian Journal of Earth Sciences, v. 3, no. 6, p. 849–861.

Brugman, M.M., Pietroniro, Alain, and Shi, Jiancheng, 1996, Mapping alpine snow and ice using Landsat TM and SAR imagery at Wapta Icefield: Canadian Journal of Remote Sensing, v. 22, no. 1, p. 127–136.

Champoux, André, and Ommanney, C.S.L., 1986, Evolution of the Illecillewaet Glacier, Glacier National Park, B.C., using historical data, aerial photography and satellite image analysis: Annals of Glaciology, v. 8, p. 31–33.

Cialek, C.J., 1977, The Cathedral Massif, Atlin Provincial Park, British Columbia: Department of Geography, Michigan State University, sponsored by the Foundation for Glacier and Environmental Research, Pacific Science Center, Seattle, Washington, map.

Cogley, J.G., 1999, Photogrammetric rectification of oblique trimetrogon imagery: Peterborough, Ont., Trent University, Department of Geography, Trent Technical Note No. 99–1, 9 p.

Collier, E.P., 1958, Glacier variation and trends in run-off in the Canadian Cordillera, *in* General Assembly of Toronto, v. 4, September 3–4, 1957: Association Internationale d'Hydrologie Scientifique Publication No. 46, p. 344–357.

Falconer, George, Henoch, W.E.S., and Østrem, Gunnar, 1966, A glacier map of southern British Columbia and Alberta: Geographical Bulletin, v. 8, no. 1, p. 108–112 (includes glacier map of southern British Columbia and Alberta).

Field, W.O., 1966, Mapping glacier termini in southern Alaska, 1931–1964: Canadian Journal of Earth Sciences, v. 3, no. 6, p. 819–825.

Foundation for Glacier and Environmental Research (FGER), 1976, Glacier at Cathedral Peak: compilation and printing by the Technical University of Hannover, F.R. Germany, through the Foundation for Glacier and Environmental Research, Juneau Icefield, Alaska—Atlin, B.C., Canada, Glaciological and Arctic Sciences Institute, map.

Fremlin, Gerald, and Mindak, H.E., 1968, Lakes, rivers and glaciers—a map commentary: The Canadian Cartographer, v. 5, no. 2, p. 133–137.

Gosson, C.M.C., 1985, Canada—Glaciers: Ottawa, Ontario, Energy, Mines and Resources Canada, Surveys and Mapping Branch, Geographical Services Division, map. (MCR–4080.)

Gunning, H.C., ed., 1966, Proceedings of the Symposium on Glacier Mapping: Canadian Journal of Earth Sciences, v. 3, no. 6, p. 737–915.

Hall, D.K., Ormsby, J.P., Bindschadler, R.A., and Siddalingaiah, Honnappa, 1987, Characterization of snow and ice reflectance zones on glaciers using Landsat Thematic Mapper data: Annals of Glaciology, v. 9, p. 104–108.

Hall, D.K., Chang, A.T.C., and Siddalingaiah, Honnappa, 1988, Reflectances of glaciers as calculated using Landsat-5 Thematic Mapper Data: Remote Sensing of Environment, v. 25, no. 3, p. 311–321.

Hall, D.K., Williams, R.S., Jr., and Bayr, K.J., 1992, Glacier recession in Iceland and Austria: EOS (Transactions, American Geophysical Union), v. 73. no. 12, p. 129, 135, and 141.

Haumann, Dieter, 1960, Photogrammetric and glaciological studies of Salmon Glacier: Arctic, v. 13, no. 2, p. 75–110, map.

———1963, Surveying glaciers on Axel Heiberg Island: Canadian Surveyor, v. 17, no. 2, p. 81–93.

Hell, Günther, 1981, Geodätische und photogrammetrische Arbeiten an der Oobloyah Bay, N-Ellesmere Island, N.W.T., Kanada, im Rahmen der "Heidelberg-Ellesmere Island-Expedition 1978" [Geodetical and photogrammetric studies during the Heidelberg Ellesmere Island Expedition 1978 to Oobloyah Bay, northern Ellesmere Island, N.W.T., Canada]: Heidelberger Geographische Arbeiten, v. 69, p. 35–46.

Henoch, W.E.S., 1969, Topographic maps of Canada in glaciological research: Canadian Cartographer, v. 6, no. 2, p. 118–129.

Henoch, W.E.S., and Croizet, J.L., 1976, The Peyto Glacier map—a three-dimensional depiction of mountain relief: Canadian Cartographer, v. 13, no. 1, p. 69–86.

Henoch, W.E.S., and Stanley, A.D., 1968a, Glacier map of northern Queen Elizabeth Islands (District of Franklin): produced by the Glaciology Subdivision, Inland Waters Branch, printed by the Surveys and Mapping Branch, Department of Energy, Mines and Resources, Ottawa, Ontario, map. (IWB 1003.)

Henoch, W.E.S., and Stanley, A.D., 1968b, Glacier map of southern Queen Elizabeth Islands (District of Franklin): produced by the Glaciology Subdivision, Inland Waters Branch, printed by the Surveys and Mapping Branch, Department of Energy, Mines and Resources, Ottawa, Ontario, map. (IWB 1004.)

———1970, Glacier maps of Canada: Journal of Glaciology, v. 9, no. 55, p. 149 plus map.

Holdsworth, Gerald, 1977, Ice flow and related measurements of d'Iberville Glacier, Ellesmere Island, N.W.T., Canada: Ottawa, Ontario, Environment Canada, Inland Waters Directorate, Glaciology Division, Internal report, 1977, 28 p.

Holdsworth, Gerald, Crabtree, P., and Croizet, J., 1976, Provisional map of the north-west col area of Mount Logan: Ottawa, Inland Waters Directorate, Fisheries and Environment Canada (1:10,000/20 m).

Holdsworth, Gerald, Demuth, Michael, and Beck, T.M.H., in press, Map of Peyto Glacier, in Demuth, Mich el, ed., Peyto Glacier Research: Ottawa (1:10,000/10 m).

Holdsworth, Gerald, and Sawyer, B., 1993, Mount Logan map, research and reference folio: Calgary, Alberta., Arctic Institute of North America, two map sheets.

Holdsworth, Gerald, Titus, D., and Gregory, P., 1992, Revised map of the north-west col and PR col areas of Mount Logan: Ottawa, Environment Canada (1:10,000/20 m).

Howarth, P.J., and Ommanney, C.S.L., 1983, LANDSAT digital data for updating glaciological information on topographic and glacier inventory maps, *in* Wellar, B.S., ed., Automated Cartography: International Perspectives on Achievements and Challenges v. II: p. 504–513. (Proceedings of the Sixth International Symposium on Automated Cartography, 16–21 October 1983, National Capital Region of Canada.)

Institute of Cartography, 1998, Thompson Glacier, Canada 1:5000, *in* Haeberli, Wilfried, Hoelzle, Martin, Suter, Stephan, and Frauenfelder, Regula, eds., Fluctuations of glaciers 1990–1995 with addendas from earlier years, v. VII: Wallingford, Oxfordshire, U.K., International Association of Hydrological Sciences (IAHS), Nairobi, United Nations Environment Programme (UNEP), Paris, United Nations Educational, Scientific, and Cultural Organization (UNESCO), p. 60.

Jeffries, M.O., and Serson, H.V., 1986, Survey and mapping of recent ice shelf changes and landfast sea ice growth along the north coast of Ellesmere Island, NWT, Canada: Annals of Glaciology, v. 8, p. 96–99.

Konecny, Gottfried, 1964, Glacier surveys in western Canada: Photogrammetric Engineering, v. 30, no. 1, p. 64–82.

———1966, Application of photogrammetry to surveys of glaciers in Canada and Alaska, *in* Gunning, H.C., ed., Symposium on Glacier Mapping: Canadian Journal of Earth Sciences, v. 3, no. 6, p. 783–798.

Lodwick, G.D., and Paine, S.H., 1985, A digital elevation model of the Barnes ice-cap derived from Landsat MSS data: Photogrammetric Engineering and Remote Sensing, v. 51, no. 12, p. 1937–1944.

Luckman, B.H., Harding, K.A., and Hamilton, J.P., 1987, Recent glacier advances in the Premier Range, British Columbia: Canadian Journal of Earth Sciences, v. 24, no. 6, p. 1149–1161.

Mauelshagen, L., 1984, Zur Entstehungsgeschichte und Herstellung der Karte des Cathedral Gletscher Vorfeldes in British Kolumbien (Kanada), *in* Festschrift zum 60, Geburtstag von Prof. Dr. Ing. G. Kupfer, Bonn, Germany: p. 90–99.

Mauelshagen, L., and Slupetzky, Heinz, 1985, Cathedral Massif Glacier and forefield (Atlin Provincial Wilderness Park, B.C., Canada): Salzburg, Austria, Universität Salzburg, Institut für Geographie, map. (Published in Zeitschrift für Gletscherkunde und Glazialgeologie, v. 24, no. 2, 1988.)

McKortel, T.A., 1963, The reproduction of the Thompson Glacier Map: Canadian Surveyor, v. 17, no. 2, p. 93–95.

Miller, G.H., Bradley, R.S., and Andrews, J.T., 1975, The glaciation level and lowest equilibrium line altitude in the High Canadian Arctic: maps and climatic interpretation: Arctic and Alpine Research, v. 7, no. 2, p. 155–168.

Molenaar, D., 1990, Glacier Bay, Juneau Icefield region and the glacierized ranges of Alaska-Northwestern Canada: Burley, Washington, Molenaar Maps, map.

Müller, Fritz, 1977, Fluctuations of glaciers: 1970–1975. International Hydrological Programme; Compiled for the Permanent Service on the Fluctuations of Glaciers (IUGG-FAGS/ICSU), United Nations Educational, Scientific and Cultural Organization, International Association of Hydrological Sciences, v. 3, 269 p.

Müller, Fritz, and others, 1963, Jacobsen-McGill Arctic Research Expedition 1959–1962; preliminary report 1961–1962 and map supplement: Montréal, Québec, McGill University, Axel Heiberg Island Research Reports, 241 p., 6 maps.

Norges Vassdrags- og Energiverk (NVE), 1991, Part of Grinnell Glacier, Baffin Island, N.W.T: Oslo, Norway, Norwegian Water Resources and Energy Administration, map, scale 1:20,000.

Østrem, Gunnar, 1973, The transient snowline and glacier mass balance in southern British Columbia and Alberta, Canada: Geografiska Annaler, v. 55A, no. 2, p. 93–106.

Ommanney, C.S.L., 1980, The inventory of Canadian glaciers: procedures, techniques, progress and applications, *in* World Glacier Inventory Workshop, Riederalp, Switzerland, 17–22 September, 1978: IAHS-AISH Publication No. 126, p. 35–44.

———1989, Glacier Atlas of Canada: Saskatoon, Saskatchewan, Environment Canada, National Hydrology Research Institute, Scientific Information Division, Limited edition, 2 p., 52 maps.

Paterson, W.S.B., 1966, Test of contour accuracy on a photogrammetric map of Athabasca Glacier: Canadian Journal of Earth Sciences, v. 3, no. 6, p. 909–915.

Reid, I.A., 1973, Glacier surveys by the Water Survey of Canada, *in* The Role of Snow and Ice in Hydrology, Proceedings of the Banff Symposium, September 1972: IAHS-AISH Publication No. 107, v. 2, p. 1133–1143.

Reid, I.A., and Charbonneau, J.O.G., 1980, Glacier surveys in British Columbia —1978: Ottawa, Ontario, Environment Canada. Inland Waters Directorate, Water Resources Branch, IWD Report Series No. 66, 23 p., maps.

———1981, Glacier surveys in Alberta—1979: Ottawa, Ontario, Environment Canada, Inland Waters Directorate, Water Resources Branch, IWD Report Series No. 69, 19 p., maps.

Ricker, Karl [E.], 1977, Wedgemount lake and lower Glacier basin: Map drawn by K. Ricker with additional contour information provided by K. Bracewell, W. Tupper, and the British Columbia Institute of Technology, available from Mountain Equipment Coop., 428 West 8th Avenue, Vancouver, B.C., map, scale 1:5,000.

Riggs, G.A., Hall, D.K., and Salomonson, V.V., 1994, A snow index for the Landsat Thematic Mapper and Moderate Resolution Imaging Spectoradiometer, *in* Proceedings, International Geoscience and Remote Sensing Symposium (IGARSS '94, v. 4): IEEE, Piscataway, N.J., p. 1942–1944.

Römmer, Susanne, and Hell, Günther, 1986, Veräungen der Zunge eines Gletschers am Harefjord (NWT, Kanada) zwischen 1958 und 1978: Diplomarbeit im Studiengang Kartographie, FH Karlsruhe, Germany, map, scale 1:20,000.

Royal Canadian Geographical Society, 1998, The glaciers of Canada: Canadian Geographic, v. 118, no. 7, with supplementary map.

Sedgwick, J.K., and Henoch, W.E.S., 1970, Peyto Glacier—general information. Accompanying text for Peyto Glacier map, Provisional edition: Ottawa, Ontario, Department of Energy, Mines and Resources, Inland Waters Branch, Glaciology Subdivision, text and map, scale 1:10,000. (IWD 1008.)

Sidjak, R.W., and Wheate, R.D., 1999, Glacier mapping of the Illecillewaet Icefield, British Columbia, Canada, using Landsat TM and digital elevation data: International Journal of Remote Sensing, v. 20, no. 2, p. 273–284.

Slupetzky, Heinz, Mauelshagen, L., and Gruber, W., 1988, Cathedral Massif Glacier, Canada, 1:5000 (terrestrial/aerial photogrammetric map), *in* Haeberli, W., and Müller, P., eds., Fluctuations of glaciers 1980–1985, v. V: Wallingford, Oxfordshire, U.K., International Association of Hydrological Sciences (IAHS), Nairobi, United National Environment Programme (UNEP) and United Nations Educational, Scientific, and Cultural Organization (UNESCO), p. 68–70, map.

Stanley, A.D., 1969, Observations of the surge of the Steele Glacier, Yukon Territory, Canada: Canadian Journal of Earth Sciences, v. 6, no. 4, pt. 2, p. 819–830.

Washburn, [H.]B., 1971a, The mapping of Mount Hubbard and Mount Kennedy, 1965: National Geographic Society Research Reports, v. 1965, p. 249–277.

———1971b, Oblique aerial photography of the Mount Hubbard-Mount Kennedy area on the Alaska-Yukon border: National Geographic Society Research Reports, v. 1966, p. 283–297.

Washburn, H.B., Konecny, Gottfried, Gloss, G., and Miller, M.M., 1965, Aerial photogrammetric mapping of the Mt. Hubbard-Mt. Kennedy massif, St. Elias Mountains, Alaska-Yukon, 1965, *in* Proceedings, 16th Alaskan Science Conference, 30 August–1 September 1965, Juneau, Alaska: American Association for the Advancement of Science, Alaska Division, p. 123–124.

Whalley, W.B., and Martin, H.E., 1986, The problem of "hidden" ice in glacier mapping: Annals of Glaciology, v. 8, p. 181–183.

Williams, R.S., Jr., 1986, Glacier inventories of Iceland: Evaluation and use of sources of data: Annals of Glaciology, v. 8, p. 184–191.

———1987, Satellite remote sensing of Vatnajökull, Iceland: Annals of Glaciology, v. 9, p. 127–135.

Williams, R.S., Jr., Hall, D.K., and Benson, C.S., 1991, Analysis of glacier facies using satellite techniques: Journal of Glaciology, v. 37, no. 125, p. 120–128.

Williams, R.S., Jr., Hall, D.K., Sigurðsson, Oddur, and Chien, J.Y.L., 1997, Comparison of satellite-derived with ground-based measurements of the fluctuations of the margins of Vatnajökull, Iceland, 1973–92: Annals of Glaciology, v. 24, p. 72–80.

Wood, W.A., 1963, Map of a portion of the Icefield Ranges, St. Elias Mountains, Yukon Territory, Canada: New York, American Geographical Society (1:30,000/10 m and 50 m) (see also The Geographical Review, 1963, v. 53, Plate II).

Young, G.J., and Arnold, K.C., 1978, Orthophotomaps of glaciers; an evaluation of an automated method applied to Peyto Glacier, Alberta: Zeitschrift für Gletscherkunde und Glazialgeologie, v. 13, no. 1–2, 1977, p. 99–110.

Glaciers of North America—

GLACIERS OF CANADA

GLACIERS OF THE ARCTIC ISLANDS

GLACIERS OF THE HIGH ARCTIC ISLANDS

By ROY M. KOERNER

SATELLITE IMAGE ATLAS OF GLACIERS OF THE WORLD

Edited by RICHARD S. WILLIAMS, Jr., *and* JANE G. FERRIGNO

U.S. GEOLOGICAL SURVEY PROFESSIONAL PAPER 1386-J-1

Canadian High Arctic ice caps, both dynamic and stagnant, respond only very slowly to changes in climate. Ice cores contain records of environmental change during the past 100 thousand years, temperatures ranging from −20° C to +2.5° C. The last 150 years have been the warmest in the past 1,000 years, but only slight changes in area and volume (mass-balance) of ice caps are evident

CONTENTS

GLACIERS OF NORTH AMERICA–

GLACIERS OF CANADA

GLACIERS OF THE ARCTIC ISLANDS

GLACIERS OF THE HIGH ARCTIC ISLANDS

By ROY M. KOERNER[1]

Abstract

If we exclude the massive ice sheets of Greenland and Antarctica, the Canadian High Arctic ice caps are among the oldest and largest in the world and contain long records of past environmental changes. Ice-core records indicate that these ice caps formed about 100 thousand years ago, beginning their growth as the last interglacial was coming to an end and the last glacial was beginning. However, the same ice-core records from these ice caps show that substantial climatic changes took place over their history. These changes encompass a range from a 20- degree Celsius cooling (compared to today) in the coldest parts of the last glacial to a period 10 thousand years ago that was 2.5-degrees Celsius warmer than today. Ice-core records show that the last 150 years, although still cooler than the warm period at the beginning of the present interglacial (the Holocene), are the warmest for at least the last 1,000 years. On the other hand, continuing mass-balance measurements show very few signs of warming or cooling in the eastern Canadian Arctic during the last 40 years. Satellite imagery reveals only a very slow pattern of change in the geometry of these ice caps in response to the climatic change of the last 150 years, including the very warm period from 1920 to 1960. The differences between the ablation and accumulation zones on these ice caps can be clearly seen on satellite imagery. However, because one of the modes of accumulation on these subpolar ice caps is by superimposed ice, the demarcation between the two zones cannot be clearly determined. Recent improvements in satellite sensors, however, are opening up a new approach to the mapping and study of glaciers hitherto unattainable by traditional methods.

History of Glacier Research

The Canadian High Arctic islands (Queen Elizabeth Islands, Nunavut, and Northwest Territories) (fig. 1) contain 151,057 km^2 (0.17 percent) of the world's, and 5 percent of the Northern Hemisphere's, glacierized area (Ommanney, 1970). Most of the ice masses are in the mountainous eastern part of the archipelago. The western islands are lower in elevation, and the only ice masses are on the higher parts of southwestern Melville Island.

Scientific work on the ice caps and glaciers in the Canadian High Arctic began in the 1950's with the work of the Canadian Defence Research Board (Hattersley-Smith, 1974). The Board began its work on the Ward Hunt Ice Shelf in northern Ellesmere Island in the early 1950's (Crary, 1960). In 1955, the same group established a glaciological research program on the northernmost ice caps in Canada, some of which lie north of the orbital coverage of Landsat 1–3 imagery. Toward the end of the 1950's, McGill University began work on Axel Heiberg Island (Müller, 1961, 1963a, b, 1966). The Polar Continental Shelf Project (in the Department of Energy, Mines and Resources (now Natural Resources Canada) of the Federal Government of Canada) began mapping and studying the ice cap on Meighen Island in 1959 (Arnold,

Manuscript approved for publication, 7 March 2002.

[1] Geological Survey of Canada, 601 Booth Street, Ottawa, Ontario K1A 0E8, Canada.

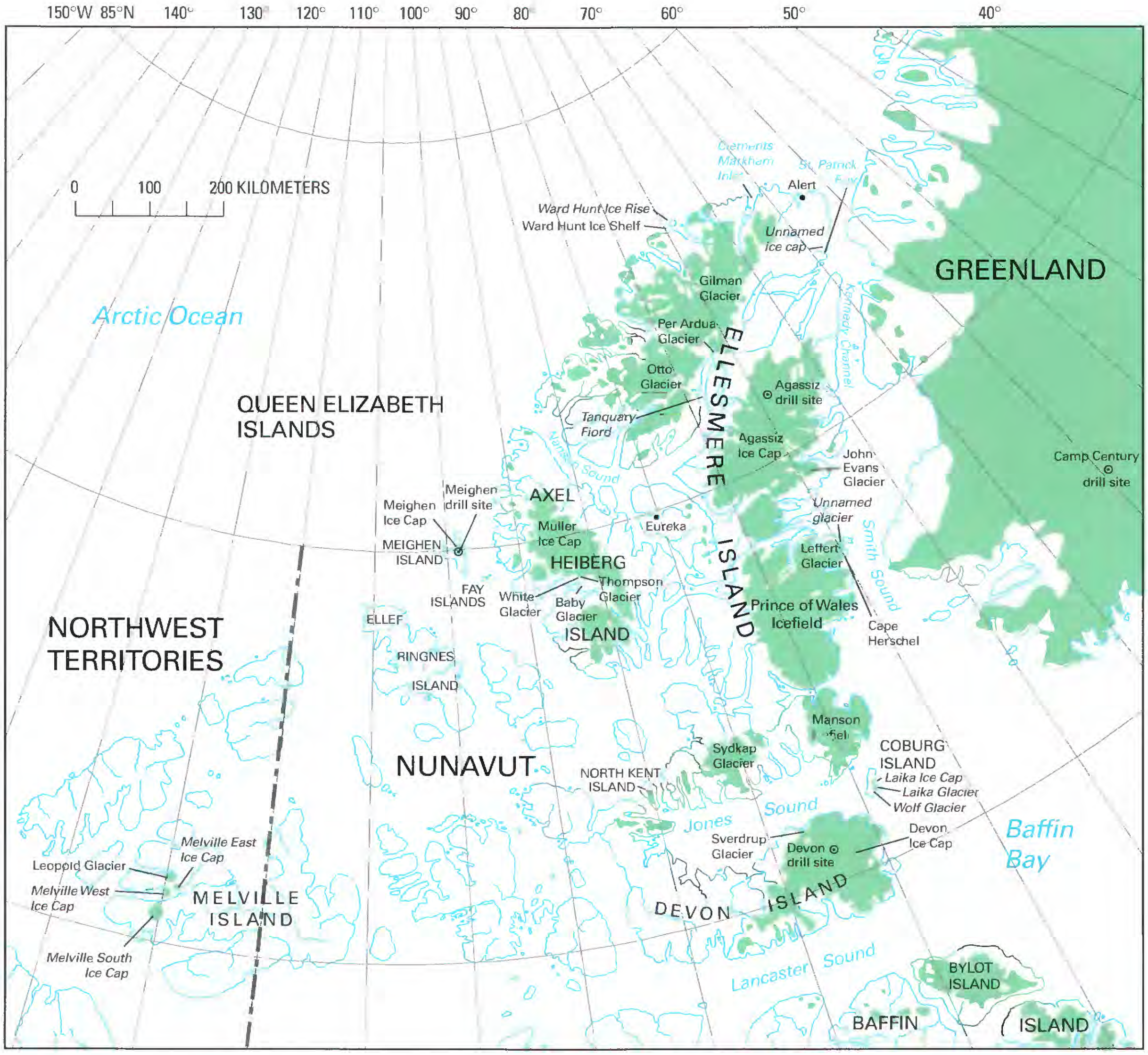

Figure 1.*—Canadian High Arctic islands. Green areas represent glacier-covered regions. The black dots within black concentric circles are ice-drilling sites.*

1965). In 1960, the Arctic Institute of North America prepared for its first year-round High Arctic expedition, and from 1961 to 1963, the Devon Island expedition included major investigations of the Devon Ice Cap and Sverdrup Glacier (Müller and Keeler, 1969; Hyndman, 1965; Koerner, 1970a, b).

In the 1960's and 1970's, various research programs were conducted on Coburg Island and in the following locations on Ellesmere Island: an ice piedmont near Cape Herschel (Müller and others, 1978), Leffert Glacier (Gerald Holdsworth, oral commun., 1984), Gilman Glacier (Arnold, 1968), an ice cap west of Tanquary Fiord (Hattersley-Smith and others, 1975), Ward Hunt Ice Shelf (Hattersley-Smith, 1963; Hattersley-Smith and Serson, 1970), and a small ice cap near St. Patrick Bay (Hattersley-Smith and Serson, 1973).

New programs were started in the 1980's on the Ward Hunt Ice Shelf (Jeffries and Serson, 1983) and the St. Patrick Bay ice cap (Serreze and Bradley, 1983). The Polar Continental Shelf Project (PCSP) conducted a climate-change and ice-physics program between 1964 and 1987, when surface-to-bedrock cores were drilled on Meighen, Devon, and Agassiz Ice Caps (Paterson, 1968, 1969; Koerner, 1968; Paterson and others, 1977). The program and staff transferred to the Geological Survey of Canada (GSC) in 1987. Since then, further cores have been drilled from the top of Agassiz and Devon Ice Caps and two from Penny Ice Cap on Baffin Island (Fisher and others, 1983; Fisher and others, 1998). The same program continues to monitor the mass balance on the Meighen, Devon, and Agassiz Ice Caps and the most southerly ice cap on Melville Island (Koerner and Lundgaard, 1995). Work on White and Baby Glaciers on Axel Heiberg Island has continued through the 1980's (Arnold, 1981) and to the present day (Cogley and others, 1995, 1996). A new, and continuing, program on John Evans Glacier in central Ellesmere Island led by the University of Alberta began in 1994 (Skidmore and Sharp, 1999).

Field reports from all these studies can be found in the annual reports of glacier research conducted in Canada and published in the following journals: Canadian Geophysical Bulletins between 1961 and 1984, Arctic from 1961 to 1965, and Ice (a publication of the International Glaciological Society) to the present day.

The Ice Caps and Glaciers

We may differentiate between the larger, dynamic glaciers and the smaller, stagnant ones. The ice shelves will be discussed in the following section on "Ellesmere Island Ice Shelves and Ice Islands" by Martin O. Jeffries.

Dynamic Ice Caps and Outlet Glaciers

It was first thought, from ice-core analysis, that the larger ice caps, such as those on Devon, Axel Heiberg, and Ellesmere Islands (fig.1), predated the last interglacial period (Koerner and others, 1987). However, further work on the same and newer data have suggested that no ice caps survived that period and that they began their growth in the very early stages of the last glacial period.

The smaller ice caps on Devon Island and southern Ellesmere Island ((D) in figs. 2, 3, 4) may be much younger. These do not reach such high elevations, have smaller accumulation areas, end well above sea level, and have very few channeled outlet glaciers. Whereas some of these ice caps may be more than 10 thousand years (kilo-annum (ka)) old, it is more likely that they began their growth during the second half of the Holocene Epoch, at less than 4.5 ka B.P. The whole question of glacial history and ice-core research will be discussed more fully later.

Topography

The surface topography of almost all the large ice caps in the Canadian High Arctic is very strongly controlled by the subglacier topography. The Prince of Wales Icefield and part of the Manson Icefield in southeastern Ellesmere Island (shown in fig. 5) are good examples. Valley glaciers on the east side descend to sea level between mountainous ridges that are often ice covered. Isachsen Glacier is a good example of this (fig. 5). Some of these glaciers are a few hundred meters thick, and the bedrock in their lower reaches is below sea level (Cadogan Glacier, figs. 5 and 6). On the west side, the ice is not as thick and often forms broad, slow-moving tongues that, in places, are almost as broad as they are long (see arrows, fig. 5). The same pattern of lobate glaciers on the one side and valley outlet glaciers on the other can be found on southern Ellesmere Island (fig. 4) and along large stretches of eastern Ellesmere Island from Baffin Bay to Kennedy Channel (fig. 1). On Axel Heiberg Island, the broad, lobate ice is on the east side, and the outlet valley-type glaciers are on the west (fig. 7). However, asymmetry is not characteristic of the most northerly of the large ice caps on Ellesmere Island (for example, Agassiz Ice Cap, fig. 8), where valley outlet glaciers emerge from all sides of the ice caps. Among all these ice caps, only that on Devon Island shows anything like the symmetry of a true ice cap, and has a nunatak-free central region. Even then, this is strictly true only of its western part (fig. 2).

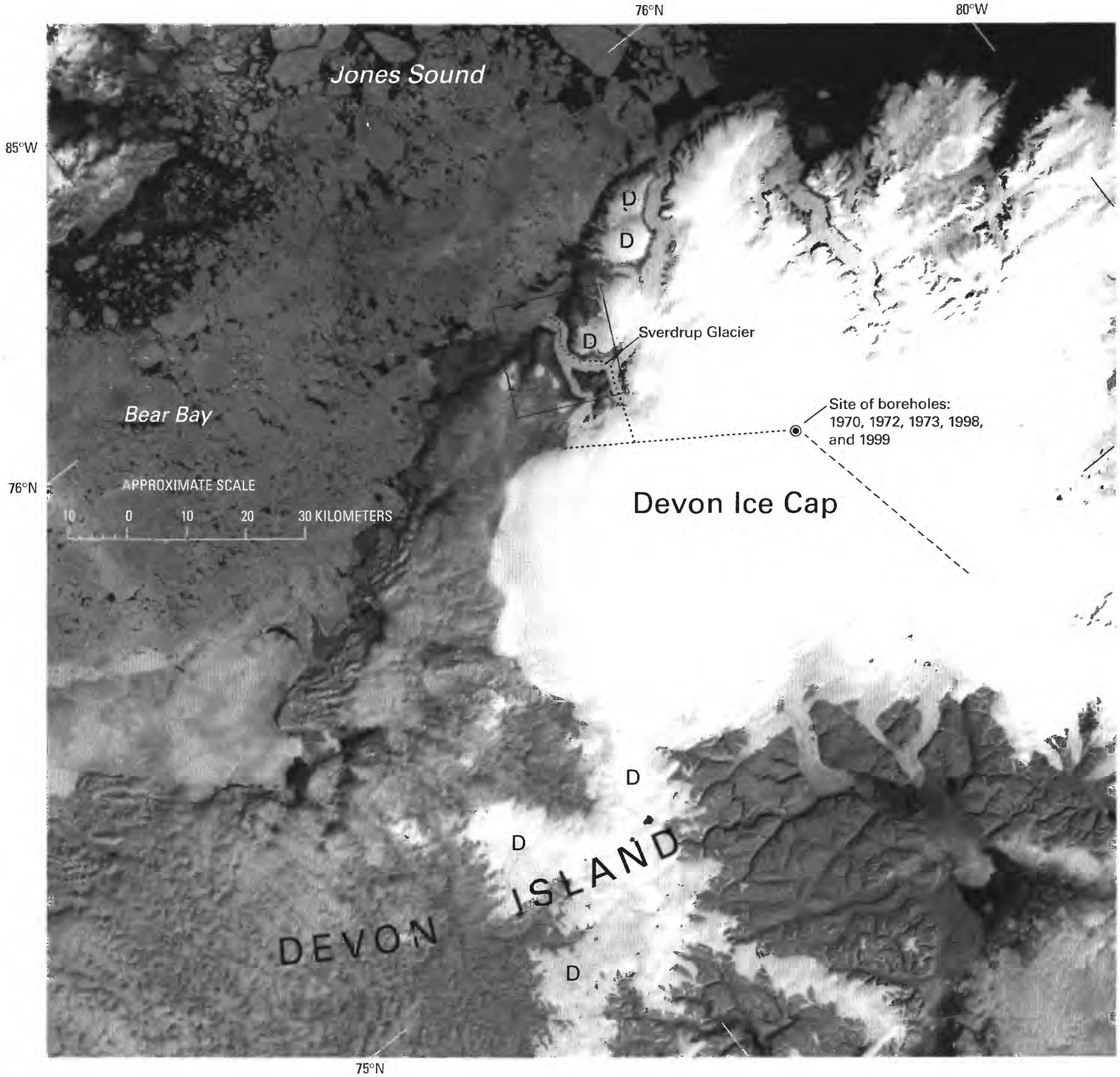

Figure 2.—*Landsat 3 MSS image showing the western part of Devon Ice Cap. The dotted lines represent the location of the stake network measured annually for mass balance; these lines (northwest side profile) and the dashed line (south side profile) are the locations of the ice-thickness profiles for Devon Ice Cap shown in figure 6. The location of the five borehole sites is shown with a concentric circle and dot symbol; the boreholes include a 230-m deep core drilled in 1970, two 299-m surface-to-bedrock cores drilled in 1972 and 1973, and nearby sites of a 305-m borehole-ice-core drilled in 1998, and one drilled in 1999. The ice caps marked with the letter (D) are dynamic and probably Holocene in origin, unlike the larger, and older, dynamic main ice cap, which has ice formed at least by 60 ka at its base. The outlined area is shown in figure 3. The Landsat image (30523–17365, band 7; 10 August 1979; Path 44, Row 6) is from the Canada Centre for Remote Sensing, Ottawa, Ontario, Canada.*

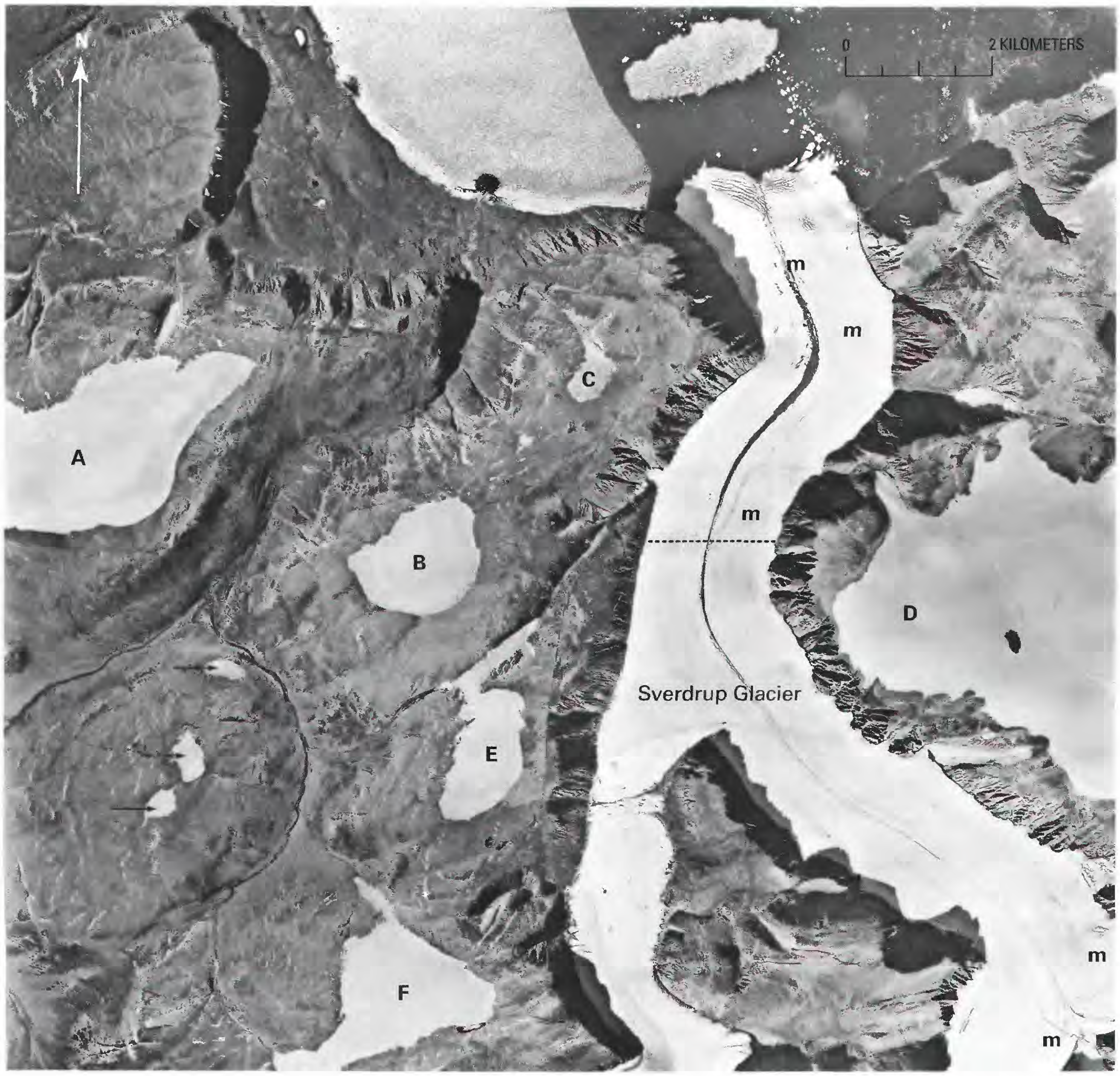

Figure 3.—Vertical aerial photograph taken in 1959 of Sverdrup Glacier on the northwest side of Devon Ice Cap (see outline in fig. 2). The letter (m) refers to supraglacier meltwater streams; the northernmost (m) is a moulin (where meltwater streams plunge into, and sometimes under, the glacier). The dotted line represents the location of the leveling profile measured for surface-height changes and is referred to in the text. Ice cap (D) is a dynamic ice cap that is much younger than the main Devon Ice Cap to its south and east. Ice caps (A), (B), (E), and (F) are all stagnant and probably less than 1 ka. Ice cap (C) is less than 200 or 300 years old, as are the three small ice caps, indicated by arrows, all of which have now melted and appear as bare ground in figure 2. All these ice caps are discussed in more detail in the text.

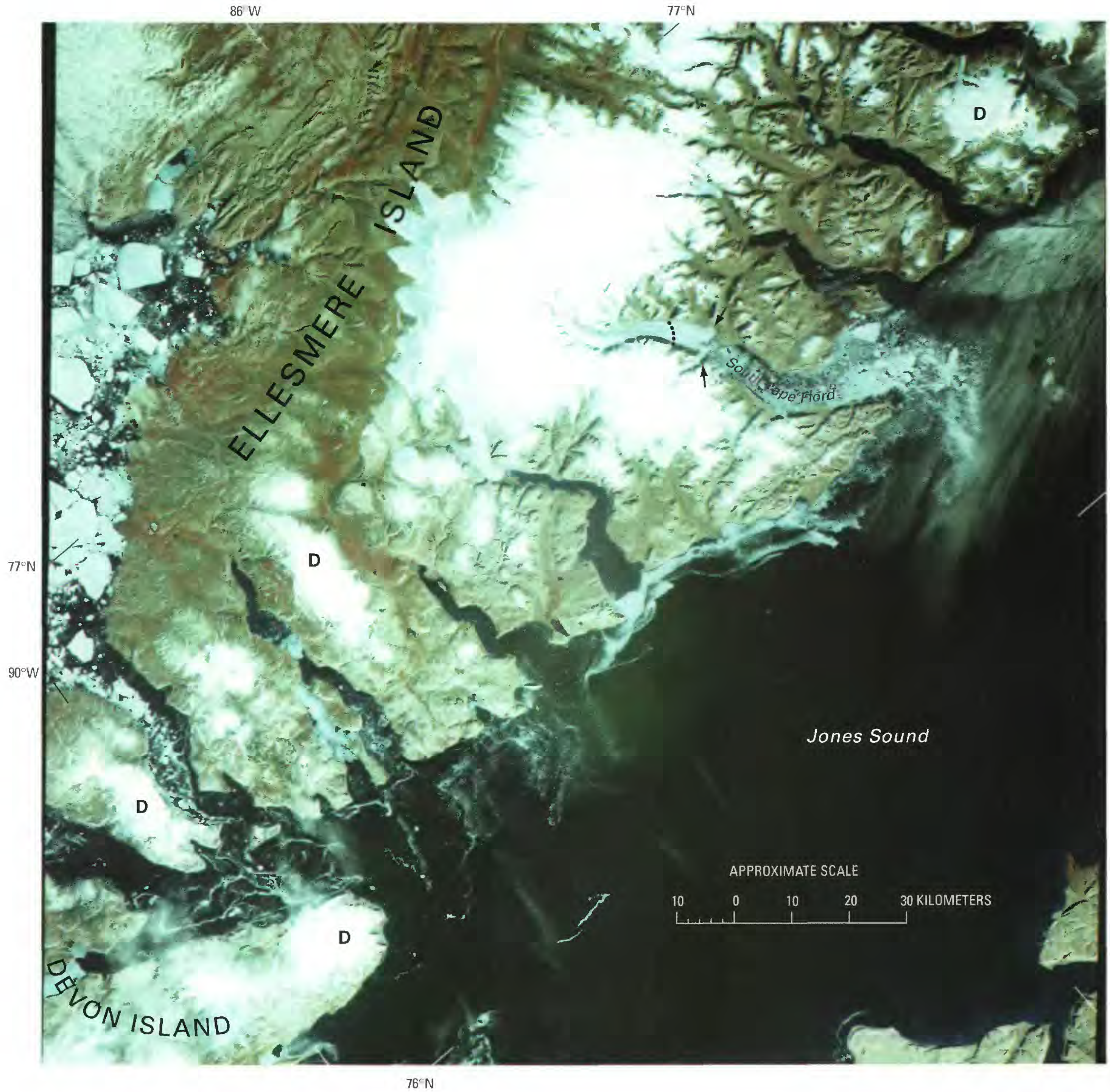

Figure 4.*—Landsat 1 MSS false-color composite image of southwestern Ellesmere Island and part of northwestern Devon Island. Ice caps marked (D) are examples of the small dynamic types discussed in the text. The arrows mark the 1957 position of a glacier in South Cape Fiord that retreated to the position marked by a dotted line sometime between 1957 and 1974. The ice between these two positions is sea ice or icebergs. The Landsat image (1760–18015, bands 4, 5, and 7; 22 August 1974; Path 48, Row 5) is from the Canada Centre for Remote Sensing, Ottawa, Ontario, Canada.*

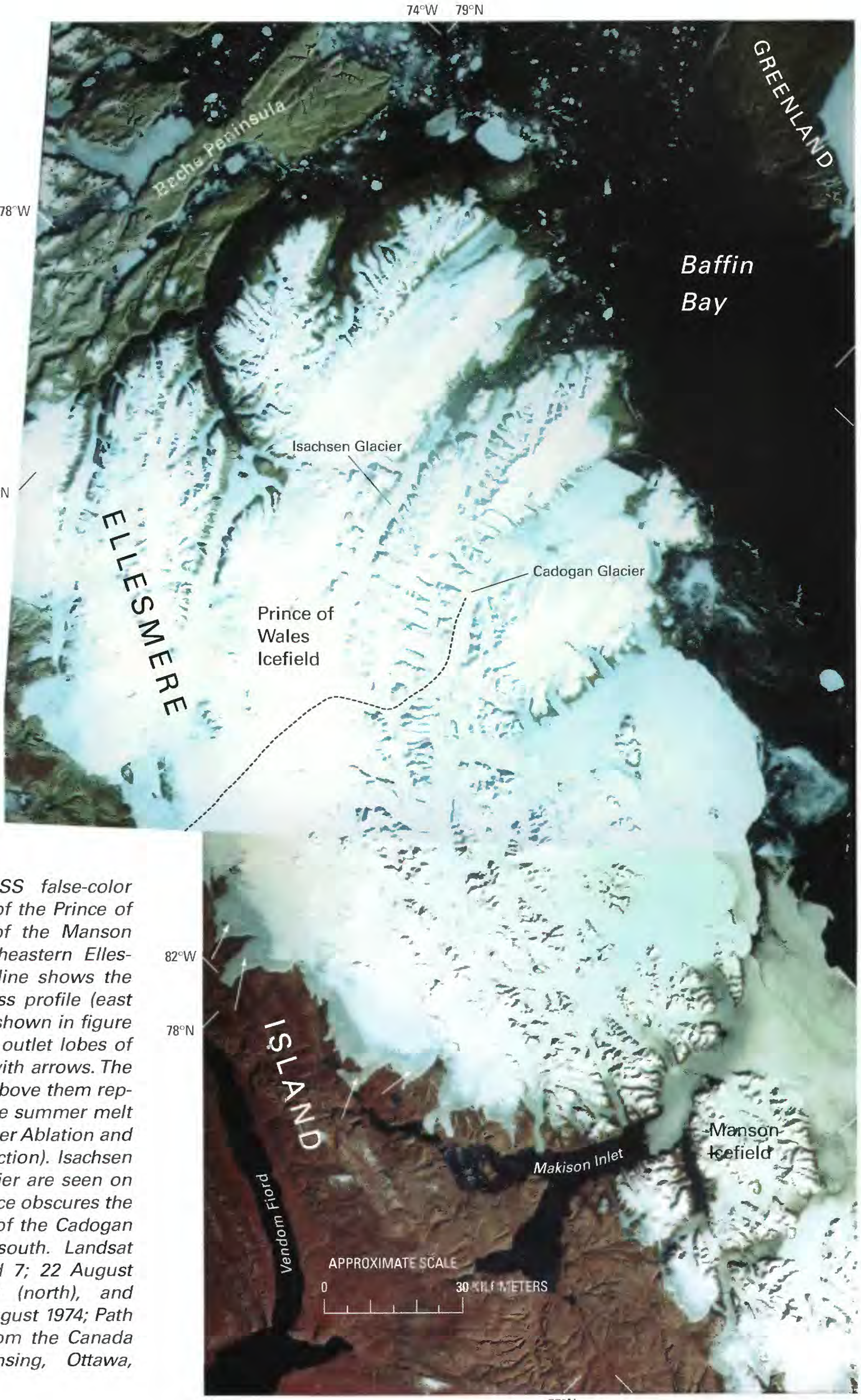

Figure 5.—*Landsat 1 MSS false-color composite image mosaic of the Prince of Wales Icefield and part of the Manson Icefield, central and southeastern Ellesmere Island. The dashed line shows the location of the ice-thickness profile (east side of central Ellesmere) shown in figure 6. The broad, slowmoving outlet lobes of the ice cap are indicated with arrows. The blue to white color tones above them represent various stages in the summer melt season (see text in "Summer Ablation and the Glacier Landscape" section). Isachsen Glacier and Cadogan Glacier are seen on the mosaic. Land-fast sea ice obscures the coastline at the terminus of the Cadogan Glacier and also to its south. Landsat images (1760–18010, band 7; 22 August 1974; Path 48, Row 3 (north), and 1758–17500, band 7; 20 August 1974; Path 46, Row 4 (south)) are from the Canada Centre for Remote Sensing, Ottawa, Ontario, Canada.*

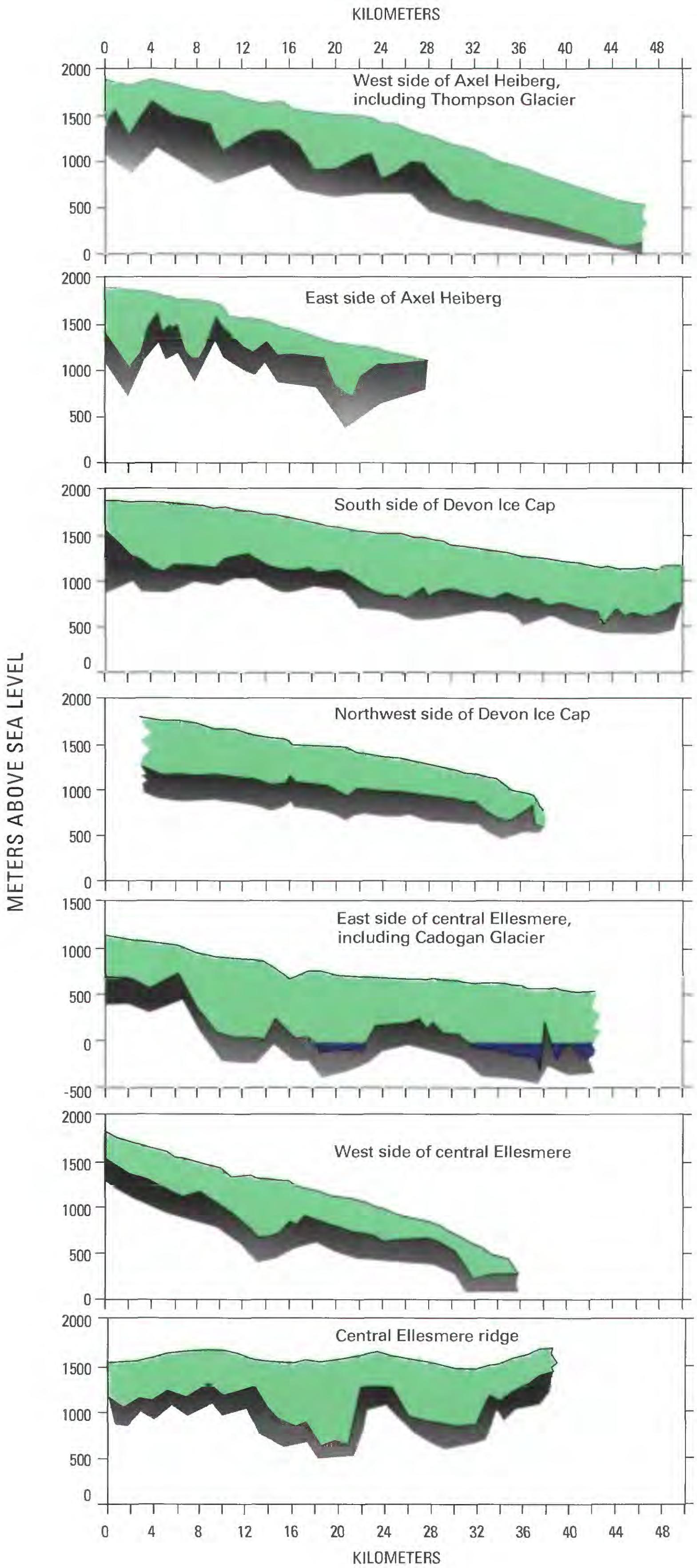

Figure 6.—*Ice-thickness profiles measured by radio-echosounding in April-May 1976 (Koerner, 1977b). The green represents ice, and the dark blue represents ice below sea level on Cadogan Glacier. See figures 2, 5, and 7 for the locations of five of the profiles. Reproduced by permission of the Canadian Journal of Earth Sciences.*

Figure 7.—*(opposite page) Mosaic of two Landsat MSS images of part of Axel Heiberg Island and Meighen Island. A concentric circle and dot symbol marks the Meighen glacier-borehole site, where a 121-m surface-to-bedrock core was drilled by the Polar Continental Shelf Project in 1965 (see also fig. 9A). The dashed lines on the Müller Ice Cap on Axel Heiberg Island represent ice-thickness profiles (east side and west side) shown in figure 6. Iceberg Glacier (see also fig. 13), White Glacier, which has been the site of glacier research since 1959, and Good Friday Bay Glacier, which advanced (surged?) sometime between 1952 and 1959, are all seen in the mosaic. The area northeast of the Fay Islands, between Meighen and Axel Heiberg Islands, is a region where sea ice persists throughout many summers. An incipient ice shelf formed here in the 1950's and 1960's and reached a few meters in thickness before it broke up in the middle 1970's. The Landsat images (1158–18455, band 7; 24 August 1977; Path 69, Row 1 (north) and 20950–18542, band 7; 29 August 1977; Path 66, Row 2 (south) are from the Canada Centre for Remote Sensing, Ottawa, Ontario, Canada.*

APPROXIMATE SCALE
0
30 KILOMETERS
MEIGHEN ISLAND
Meighen
Ice Cap
Fay Islands
Müller
Ice Cap
AXEL HEIBERG ISLAND
Iceberg Glacier
79°N
White Glacier
Thompson Glacier
Good Friday Bay
Glacier
90°W

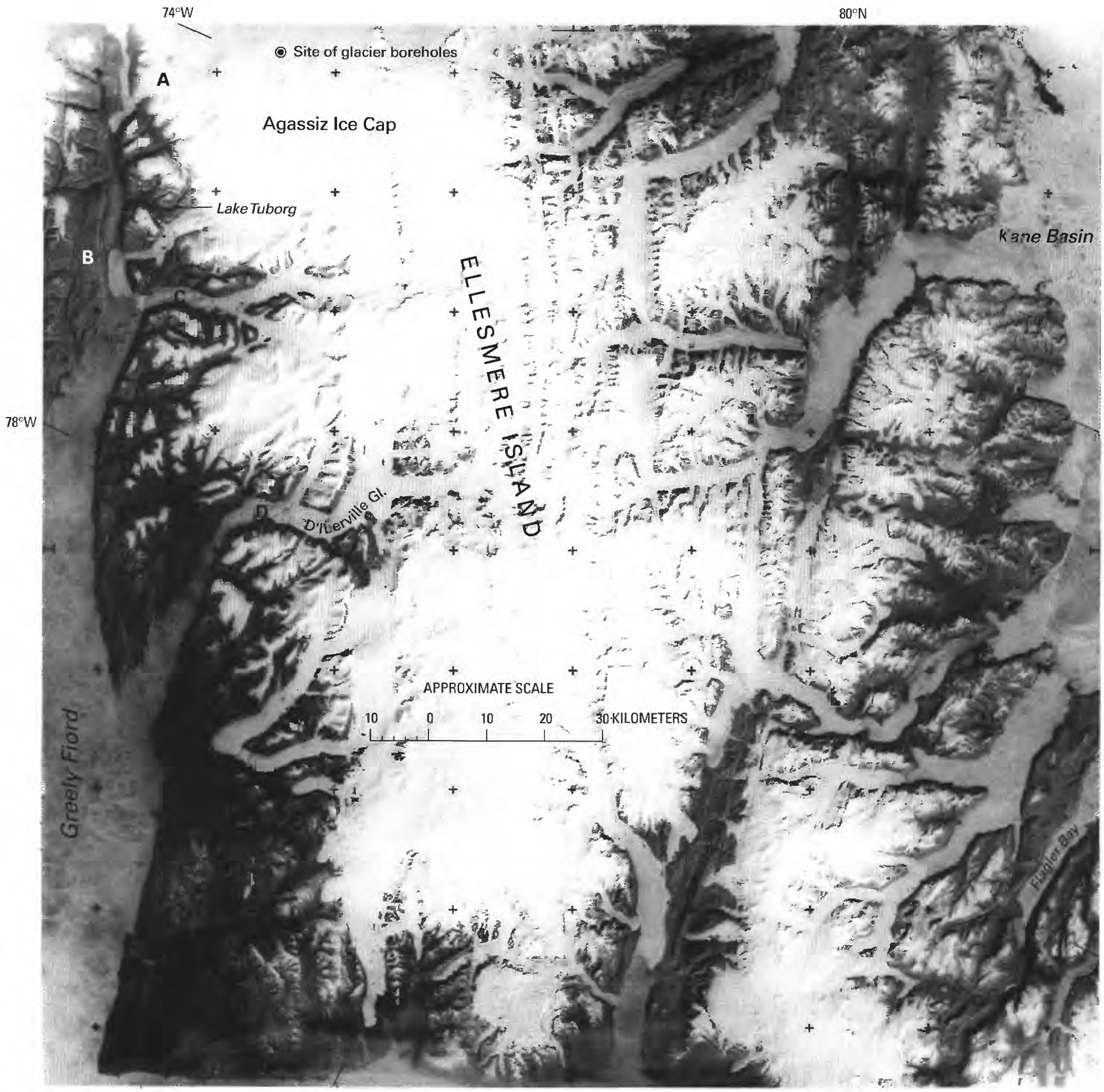

Figure 8.—*Landsat 2 return-beam vidicon (RBV) image of the Victoria and Albert Mountains, Ellesmere Island. A symbol indicates the location of six surface-to-bedrock boreholes drilled into the Agassiz Ice Cap by the Polar Continental Shelf Project: a 337-m core in 1977, a 137-m core in 1979, two 127-m cores in 1984 and 1987, and two 130-m cores in 1994. Glaciers (A), (B), (C), and (D) have either heavily crevassed or hummocky surfaces, and, therefore, very high summer ice-melt rates (see text in "Summer Ablation and the Glacier Landscape" section). Glacier (B) has advanced across the head of Greely Fiord and thereby created an ice-locked lake (Lake Tuborg). Dating of the basal waters of this lake indicate that the glacier advanced at about 3.5 ka (Hattersley-Smith and others, 1970). The Landsat image (2550–18480, band 3; 25 July 1976; Path 58, Row 1) is from the EROS Data Center, Sioux Falls, S. Dak.*

Velocity

Glacier motion has been measured by various methods. Arnold (1965, 1968, 1981) used traditional field surveying and photogrammetric techniques on Meighen Ice Cap, Gilman Glacier (Ellesmere Island), and White Glacier (Axel Heiberg Island), whereas Doake and others (1976) used radio-echosounding techniques at the top of Devon Ice Cap. The results of these and other measurements are shown in table 1. New approaches to measuring velocity, such as the Global Positioning System (GPS) of satellites and satellite radar interferometric (InSAR) techniques are quickly expanding the present slim velocity data base.

Velocities in this area are generally of the order of 10–50 m a^{-1}. However, velocity in summer can be as much as twice as high as in winter (table 1). This can be attributed to the presence of meltwater at the glacier bed in summer (Iken, 1974) and indicates that parts of some glaciers are at the melting point at their beds. Calculations of basal temperatures using known ice thicknesses and 10–15-m englacier temperatures (Müller, 1976; Paterson, 1994), as well as measured basal temperatures (Blatter, 1987), confirm the unfrozen basal condition of many High Arctic glaciers.

One consequence of relatively low glacier velocities (strictly speaking, low strain rates) is that, compared to glaciers in other areas of the world, many of these glaciers are not very crevassed. Sverdrup Glacier, although it is the major outlet for ice from the northwest side of the Devon Ice Cap, is a good example (fig. 3). Another example is the crevasse-free ice cap above, and to the east of, Sverdrup Glacier (fig. 3, (D)).

A few glaciers in the High Arctic, however, maintain high velocities, and probably comparably high strain rates, in their lower reaches and are more crevassed. Good examples are the glaciers draining the west side of Agassiz Ice Cap (fig. 8, (A), (C), and (D)). Using aerial photographs, Holdsworth (1977) calculated tongue velocities of more than 400 m a^{-1} on one of them (D'Iberville Glacier; (D), fig. 8; table 1). These glaciers act as the major outlets for Agassiz Ice Cap and drain large catchment areas.

Calving of the glaciers in the High Arctic islands has not received much attention. Although it certainly does not rule it out, very little photographic evidence exists of calving. For example, we can see very

TABLE 1.—*Velocity measurements (winter-summer) of selected Canadian High Arctic glaciers on Axel Heiberg Island, northern Ellesmere Island, central Ellesmere Island, and Devon Island*

[Note that Meighen Ice Cap and Melville ice caps are stagnant. See figure 1 for locations. Abbreviations: I., island; N., northern; C., central; do, ditto; Accum., accumulation area; Eq. line, equilibrium line; Abl., ablation area; <, less than; leaders (- -), not determined. Data archived at the Geological Survey of Canada, 601 Booth Street, Ottawa, Ontario K1A 0E8, Canada]

Location	Glacier	Velocity m a^{-1} winter	Velocity m a^{-1} summer	Location on glacier	Reference
Axel Heiberg I.	White	<13.0	- -	Accum.	Müller, 1963b
.....do...........	.....do..........	24.5	- -	Eq. line	Do.
.....do...........	.....do..........	21.4	44.0	Abl.	Do.
.....do...........	.....do..........	10.4	- -	Tongue	Do.
.....do...........	Thompson	47.0	51.0	Abl.	Do.
N. Ellesmere I.	Gilman	14.8	0	Accum.	Arnold, 1968
.....do...........	.....do..........	22.9	22.2	Eq. line	Do.
.....do...........	.....do..........	19.6	- -	Abl.	Do.
C. Ellesmere I.	D'Iberville	457.0	500.0	Tongue	Holdsworth, 1977
.....do...........	Leffert	40.0	- -	do	Gerald Holdsworth, oral commun., 1984
Devon Island	Devon Ice Cap	2.4	- -	Top of ice cap	Doake and others, 1976
.....do...........	Sverdrup	36.4	65.0	Abl.	Cress and Wyness, 1961

few icebergs adjacent to Sverdrup Glacier (fig. 3). Most of the icebergs that enter the shipping lanes south of here off the coast of Newfoundland are from the west coast of Greenland. New studies are needed to determine the importance of calving in this area.

Thickness

The ice thickness of Canadian High Arctic ice caps has been measured by radio-echosounding techniques (Hattersley-Smith and others, 1969; Paterson and Koerner, 1974; Koerner, 1977b; Oswald, 1975; Narod and Clarke, 1983). Unpublished work was done as well by the Scott Polar Research Institute at the top of Devon Ice Cap in 1974; the work is available as maps at the GSC. Some of the results (from Koerner, 1977b) are shown in figure 6, where the asymmetry in thickness of some of the ice caps can be seen. This is largely attributable to high snow-accumulation rates on the slopes facing Baffin Bay, where relatively thick ice sheets have built up. Although not shown in Koerner (1977b), areas several kilometers square were sounded at the tops of Agassiz Ice Cap and ice caps on Axel Heiberg and central Ellesmere Islands. In general, the data show that at the tops of most of the ice caps the ice is about 100–300 m thick. Downslope, the thickness may reach 1,000 m in channeled areas. However, the most common thickness is approximately 500 m, even in valley glaciers. Some of the glaciers, in their lower reaches, flow over bedrock that is below sea level (for example, Cadogan Glacier, figs. 5 and 6). In 1995, traverses were flown over many of the Canadian ice caps by a National Aeronautics and Space Administration (NASA) P–3 aircraft using ice-penetrating radar (160 MHz) and geodetic airborne laser altimetry. In Spring 2000, J.A. Dowdeswell (oral commun.) mapped glacier thicknesses by using airborne radio-echosounding surveys of the Queen Elizabeth Islands' ice caps. In May 2000, NASA, using a chartered Canadian Twin Otter aircraft, resurveyed ice caps on Ellesmere Island, Axel Heiberg Island, Devon Island, and Baffin Island, Nunavut. When published, all of these data will greatly extend our knowledge of ice-cap volumes in the Queen Elizabeth Islands. The NASA surveys also constitute a valuable baseline for monitoring the changing geometry of ice caps in an era of predicted global warming. The NASA ice-penetrating-radar data are available on the NASA website at [http://tornado.rsl.ukans.edu/1995.htm].

Stagnant Ice Caps

The smallest ice caps have no outlet glaciers. Traditional surveying and also ice-fabric analysis indicate that they are stagnant. Examples of these ice caps are shown in figure 3 ((A), (B), (E), and (F)). The first work on these ice caps was done on Meighen Ice Cap (fig. 9) by Arnold (1965), Koerner (1968), and Paterson (1969). Surveying of markers, over a 2-year period, by Arnold (1965) showed no evidence for movement. Ice-fabric analysis of an ice core from the same ice cap suggested that it has been stagnant throughout its history (Koerner, 1968). Similar ice-fabric work at the edge of a smaller ice cap on Devon Island (fig. 3, (B); R.M. Koerner, unpublished data, 1984) suggests that it too has always been stagnant. It, therefore, seems reasonable to consider that ice caps of similar and smaller size are, and always have been, stagnant. Their past and present stagnant nature puts limits on the maximum dimensions that they may have reached during their lifetime. The oxygen isotope ($\delta^{18}O$) values of the basal ice in Meighen Ice Cap are not sufficiently negative to suggest that the ice is of Pleistocene age (Koerner and Paterson, 1974). Furthermore, it is unlikely that any of these ice caps would have been large enough to survive the

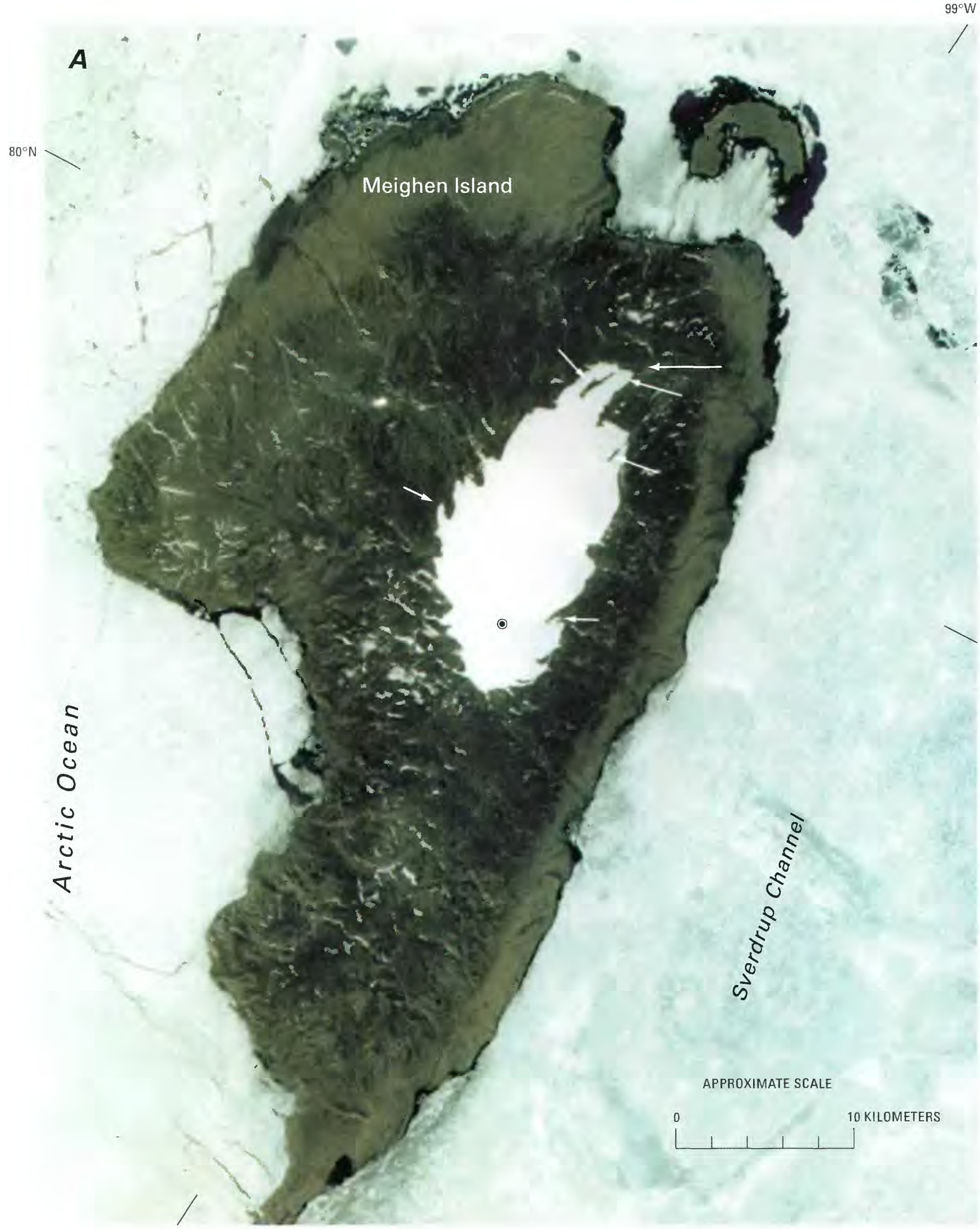

Figure 9.—*Landsat image from 1977 and an aerial photographic mosaic from 1959 showing changes in the Meighen Island Ice Cap.* **A,** *Part of an enlarged Landsat 1 MSS false-color composite image. The site of a 121-m surface-to-bedrock drill hole drilled in 1965 is shown with the concentric circle and dot symbol. Compare the margins and nunataks marked by arrows with the same locations in figure 9*B. *Landsat image (11858–18455, bands 4, 5, and 7; 24 August 1977; Path 69, Row 1) is from the Canada Centre for Remote Sensing, Ottawa, Ontario, Canada.* **B,** *see following page.*

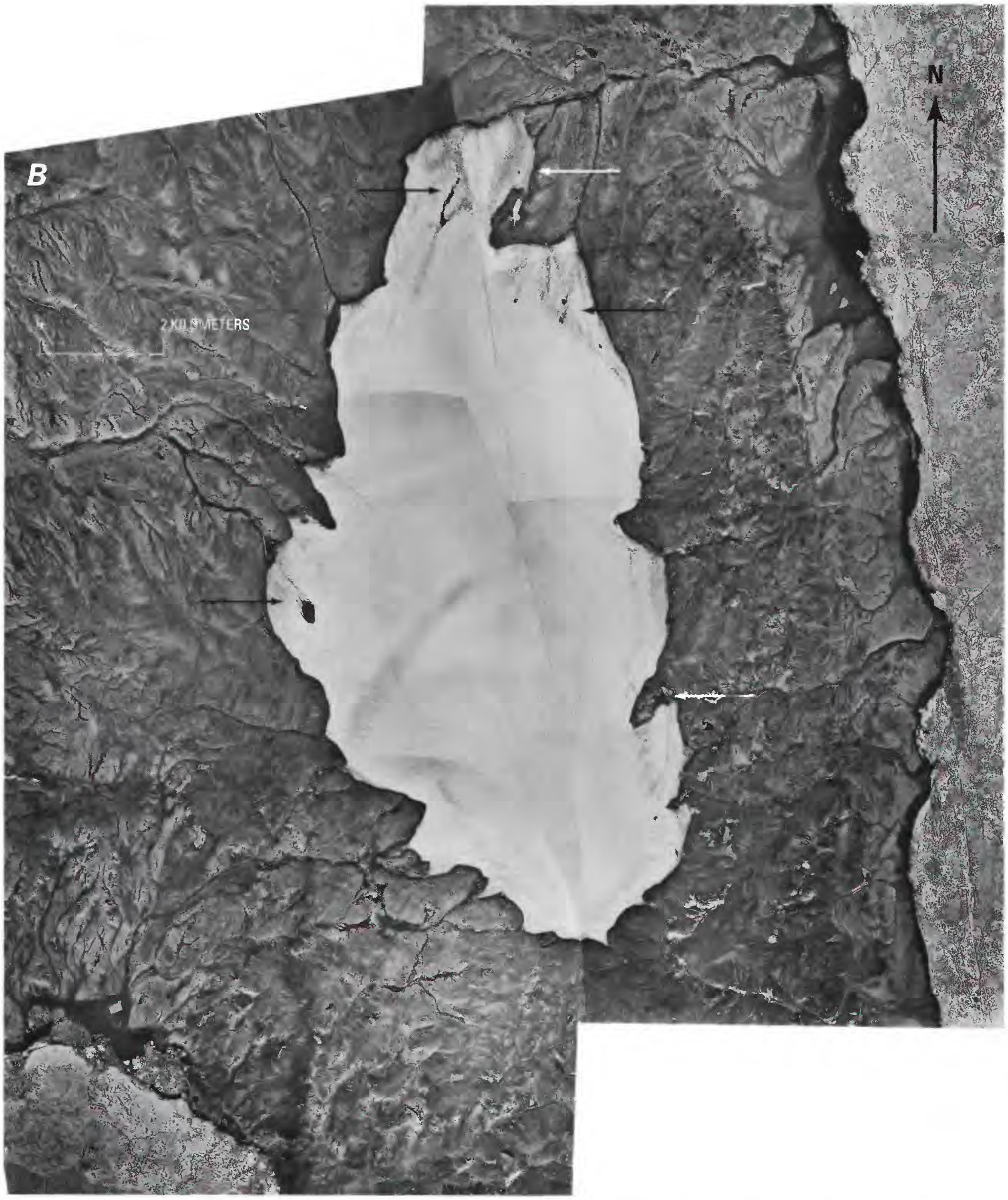

warm period between about 9 ka and 4.5 ka (Koerner and Fisher, 1990). They are, therefore, most probably less than 4.5 ka.

Ice caps smaller than Meighen Ice Cap (for example., fig. 3, ((A), (B), (E), and (F)) must be much younger than 4.5 ka, probably less than 1 ka. The smallest (e.g., fig. 3, (C) and the three ice caps indicated by arrows) may be only 200 to 300 years old; perhaps they began their growth about 300 years ago or during the "Little Ice Age" about 200 years ago. They are mostly less than 1 km in diameter and are only 10–20 m thick. The three small ice caps marked by arrows in figure 3 had melted completely by the end of 1962.

***Figure 9*B**—*Vertical aerial photographic mosaic taken on 5 August 1959. Arrows show areas of glacier recession in later years. Note the banding on the ice surface along the east margin that is caused by annual cycles of accumulation in a cold period, which have been later crosscut by ablation as the climate became warmer.*

The surface topography of stagnant ice caps depends on the geometry of the underlying bedrock topography, their age, and their mass-balance history. The surface profile of a stagnant ice cap is, in part, an integration of all the annual mass-balance gradients since its inception (where the gradient is the change in mass balance with elevation). For example, on Meighen Ice Cap (figs. 7, 9), the north-facing slopes are much less steep than those facing south. Mass-balance measurements (IAHS/UNESCO, 1985) show that the north slopes of Meighen Ice Cap are losing ice at a much greater rate than the rest of the ice cap (Koerner and Lundgaard, 1995). These slopes are unlikely to have been able to withstand long periods of warm climate (such as the one ending at about 1 ka) and are probably much younger than the southern part of the ice cap.

The annual cycle of ablation and accumulation on these ice caps exposes the sedimentary ("annual growth") layers at the surface. These bands are well depicted in figure 3 ((A), (B), and (C)), and above parts of the east margin of Meighen Ice Cap (fig. 9*A*). The light-colored bands are composed of fine-grained ice. This ice forms during cold summers, when less melting and less percolation take place than usual. An incompletely soaked, low-density, bubbly layer is then formed. Conversely, the dark bands consist of coarse-grained ice formed during warmer summers, when the surface snow layer becomes completely saturated before refreezing. An almost bubble-free layer is then formed (Koerner, 1970a). Originally, each of these surface layers may cover large areas of the ice cap. Subsequently, melting toward the outer parts of the ice cap removes part of the layers, while accumulation further in buries the rest. This type of banding should not be confused with foliation bands found on valley glaciers (Hambrey and Müller, 1978) (for example, Sverdrup Glacier, fig. 3). Foliation is a tectonic feature formed by dynamic processes in moving ice.

Mass Balance

The mass balance of a glacier is the difference between the amount of precipitation accumulating on the glacier and the amount that leaves as melt or ice calving throughout the year. The glaciers where measurements have been made between 1957 and the present (table 2) are shown in figure 1. Some of these records are more than 35 years old and are among the longest high-latitude records in the world. Mass-balance techniques are described by Østrem and Brugman (1991). However, some of these techniques do not apply to subpolar glaciers, where some of the summer snowmelt refreezes in the firn. Here, we describe the methods used by the Geological Survey of Canada on the Queen Elizabeth Islands' glaciers. The reader is referred to Geografiska Annaler (1999) for an up-to-date reference on modern methods of measurement and modeling and to Jania and Hagen (1996) for a review (with summary annual data) of Arctic mass balance covering Alaska, Canada, Greenland, Iceland, Svalbard, northern Scandinavia, and the Russian Arctic.

Winter Balance

To obtain winter balance, poles are drilled into the ice and firn in both the accumulation and ablation areas; these are used as reference points. Accumulation comes as snow throughout the winter. Each spring, snow depths are taken by using a depth probe to the easily recognized, end-of-melt-season, firn layer underneath. These depths, along with density measurements, give the winter balance. The length of the reference poles is measured at the same time each year.

TABLE 2.—*Glaciers in the High Arctic where mass-balance measurements have been carried out*

[Abbreviations: No., number; NW, northwest side; For explanation of italicized names, see text footnote 2 on p. J136]

No.	Glacier	Latitude North	Longitude West	Period observed	Years missed
	Ellesmere Island[1]				
1	Ward Hunt Ice Shelf	83°7'	73°30'	1960–85	1977, '78, '79
2	*Ward Hunt Ice Rise*	83°7'	74°10'	1958–85	1977, '78, '79
3	Gilman Glacier	82°6'	70°37'	1957–69	
4	*Unnamed ice cap*	81°57'	64°12'	1966–76	1968, '69
5	Per Ardua Glacier	81°31'	76°27'	1964–71	
6	Agassiz Ice Cap	80°	75°	1977–present	
7	Leffert Glacier	78°41'	75°01'	1979–80	
8	*Unnamed glacier*	78°39'	74°55'	1979–80	
	Coburg Island[1]				
9	*Laika Glacier*	75°53'	79°5'	1973–80	1976, '77, '78
10	*Laika Ice Cap*	75°55'	79°9'	1974–80	1976, '77, '78
11	*Wolf Glacier*	75°54'	79°12'	1979–80	
	Axel Heiberg Island[1]				
12	White Glacier	79°26'	90°40'	1959–present	1980, '81, '82, '83
13	Baby Glacier	79°26'	90°58'	1959– present	1973, 1978–88
	Meighen Island[1]				
14	Meighen Ice Cap	79°57'	99°08'	1959–present	1972, '79
	Melville Island[1]				
15	*Melville South Ice Cap*	75°25'	115°10'	1963–present	1968, '72, '75–'79
16	*Melville West Ice Cap*	75°38'	114°45'	1963–73	1968, '72
17	*Melville East Ice Cap*	75°39'	114°29'	1963–73	1968, '72
18	Leopold Glacier	75°49'	114°49'	1963–73	1968, '72
	Devon Island[1]				
19	Devon Ice Cap (NW)	75°20'	82°30'	1961–present	1968
	Baffin Island[2]				
20	Lewis Glacier[3]	70°26'	74°46'	1963–65	
21	Barnes Ice Cap	70°10'	74°46'	1963–84	
22	Decade Glacier	69°38'	69°50'	1965–73	1972
23	*Akudnirmiut Glacier*	67°35'	65°15'	1971–72	

[1] See figure 1.

[2] See figure 1 in "Glaciers of Baffin Island" section.

[3] See figures 6 and 12 in "Glaciers of Baffin Island" section.

Maps of the winter balance in the Queen Elizabeth Islands (fig. 10) show a very pronounced accumulation gradient running from the southeast to the northwest across the islands. This gradient should not be interpreted in terms of a Baffin Bay moisture source. It is rather that the major water-vapor trajectories are from the southeast (Koerner, 1979), and they probably have a source that is quite distant. Calculations, based on the stable isotope relationships of precipitation in the area, suggest that only 8 percent of the precipitation on the top of Devon Ice Cap is from Baffin Bay. The pattern of snow accumulation is associated with the growth of more dynamic glaciers in the southeast of the Queen Elizabeth Islands, that is, those facing Baffin Bay (fig. 1). This is the only area in the islands where major ice caps reach sea level. Elsewhere, they end on plateaus well above sea level and reach sea level only in the form of channeled outlet glaciers,

Figure 10.—*Winter balance in the Queen Elizabeth Islands based on pit and shallow-core analysis done in 1974. Values in Greenland are from Benson (1961) or Mock (1968). The green represents ice-covered areas, and the concentric circle and dot symbol represents ice-core sites.*

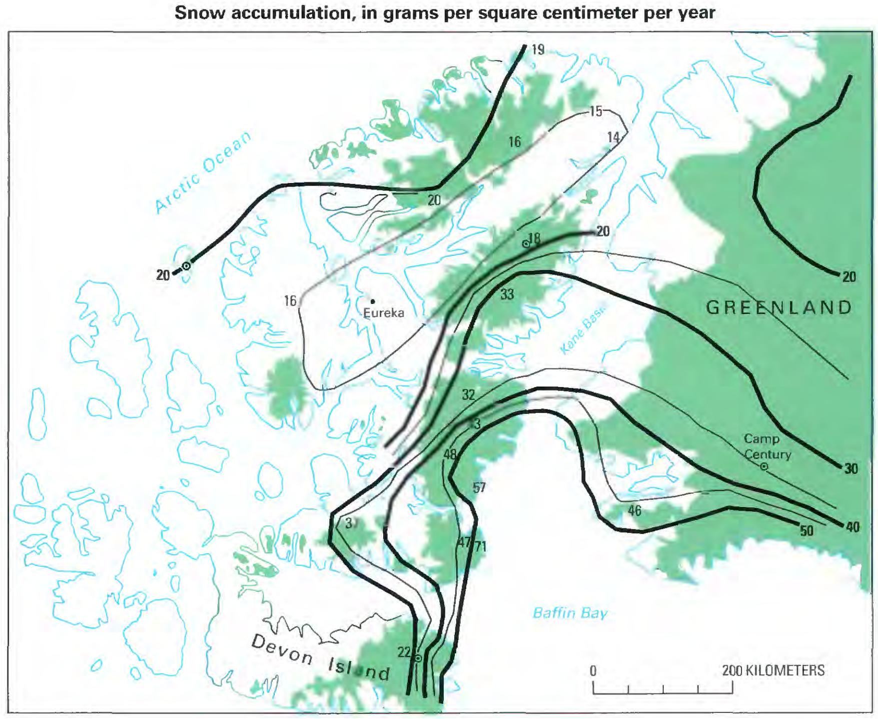

such as Sverdrup Glacier (figs. 2, 3). On the other hand, the precipitation-shadow area in north-central Ellesmere Island is very dry (fig. 10). The weather station Eureka (figs. 1, 10) sits in the middle of this area and is well known for its clear skies. Indications of slightly higher snow accumulation exist close to the Arctic Ocean, perhaps associated with northerly air-mass trajectories, rather than an Arctic Ocean moisture source.

Annual and Summer Balance

The ablation season normally covers part or all of the months of June, July, and August. The amount of melt is, in general, inversely related to elevation, and about 1–3 m of ice ablates at sea level on the glaciers each summer. However, in approximately 9 summers out of 10, melting extends right to the tops of all the ice caps, where the meltwater refreezes within the annual surface-snow layer. The effects of melting on the glacier landscape will be discussed later in the "Summer Ablation and the Glacier Landscape" section.

Measurement of the summer balance in the *ablation area,* on an annual basis, consists of measuring the length of a number of poles drilled into the ice. Their changing length gives the amount of ice melted each year. Since the introduction of automatic weather stations a few years ago, the progress of melt throughout each summer season can be recorded at a few sites (fig. 11). An ultrasonic sounder measures the distance from the sounder to the ice surface. As the ice melts, the distance increases, which thereby gives the ablation rate. Because all the winter snow melts in the *ablation area* (that is, where the **annual** balance is negative), the annual balance is the sum of winter snow and total ice melt. Very occasionally, such as in the summer of 1962, the *ablation area* may creep into the firn zone. In this case, the annual balance is the sum of snow and firn melt, although the latter is very difficult to assess, as we explain below.

The measurement of mass balance in the *accumulation area* of subpolar glaciers is not simple. In general terms, snowmelt and icemelt on *temperate glaciers* form part of the ablation process. The meltwater,

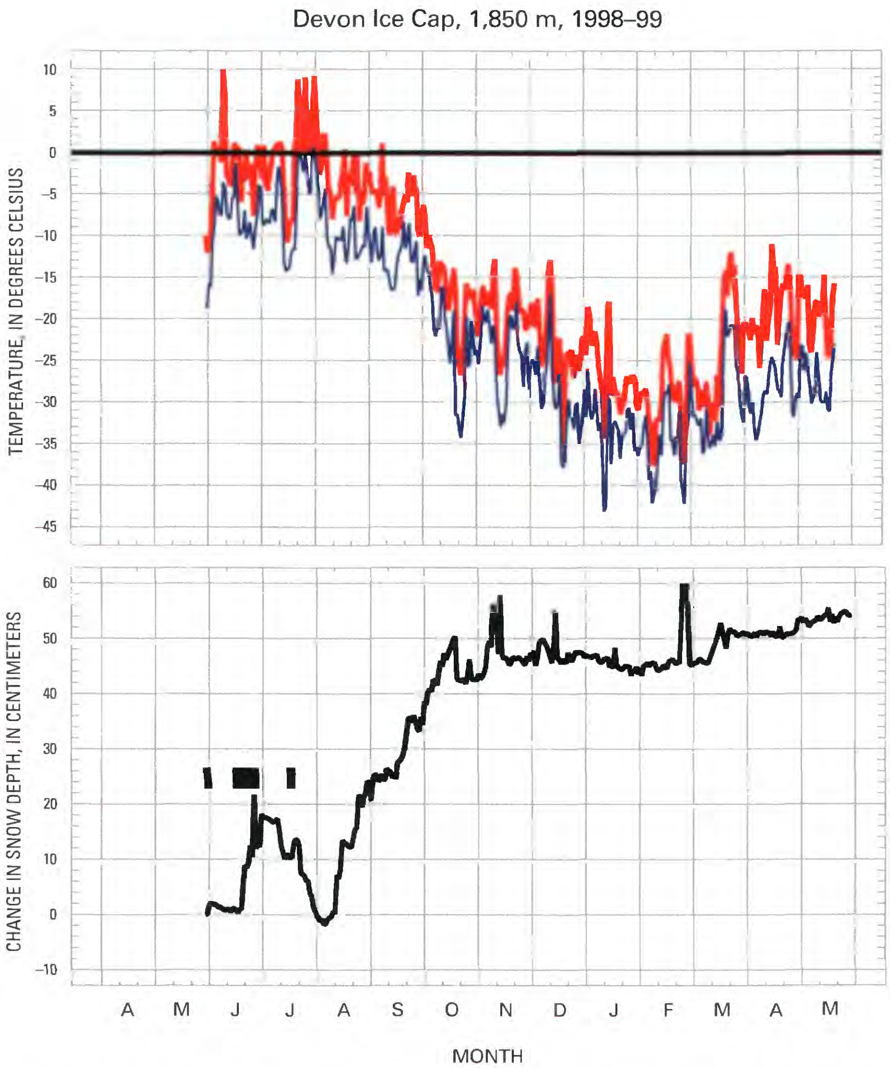

Figure 11.*—Temperatures and snow-depth changes as measured at an automatic weather station on Devon Ice Cap at 1,850 m in 1998–99. The blocks in late May, June, and July mark periods of snow accumulation during the melt season. Lowering of the snow surface in this period is due to snow melt in what was then the percolation zone. The lowering does not represent mass loss because the snowmelt refreezes at depth, in this case within the annual snow layer. The red and blue temperature traces represent maximum and minimum daily temperatures.*

whether it runs off the surface of the glacier or drains through the firn, leaves the glacier. This is not the case on subpolar glaciers where meltwater either refreezes on the ice surface under the snow or firn, or within the firn itself. Benson (1961) divided the accumulation area of polar ice caps and ice sheets into facies zones. In order, with decreasing elevation, he defined *dry-snow, percolation,* and *wet-snow facies,* as well as *superimposed ice zones.* No melting takes place at any time of year in the *dry snow zone*, which covers large parts of Greenland and Antarctica. However, High Arctic islands' ice caps lie below this zone, except in very cold summers (for example, 1965). In the *percolation facies,* melting refreezes within the current annual snow layer. The upper parts of the *accumulation areas* of the Canadian High Arctic ice caps generally fall within this zone, except in warm summers like those of 1962 and 1998 (fig. 12). In the *wet-snow facies,* melt will percolate through more than the annual layer of new snow on the surface. In warm summers, this zone may cover the entire firn *accumulation area*. In the *superimposed ice zone,* the annual snow layer melts and part of it refreezes on the ice surface beneath (Schytt, 1949, 1955; Koerner, 1970a).

On *temperate glaciers*, the equilibrium line separates an *accumulation area*, where the surface is firn, from the *ablation area*, where the surface is ice. Satellite imagery can be used to map these areas as they have very different reflective properties (Williams and others, 1991). On a subpolar glacier, the *accumulation area* includes the *superimposed ice zone*. This means that ice extends, at the surface, beyond the *ablation area* and into the *accumulation area*; hence, the equilibrium line is at the down-glacier margin of *superimposed ice zone*. Satellite imagery cannot, therefore, at present, clearly differentiate the demarcation between the *accumulation* and *ablation areas* on subpolar glaciers.

Mass-balance-measurement techniques should be unique to each of Benson's facies zones in the *accumulation area*:

(1) In the superimposed ice zone, the additional layer of ice has to be measured at the end of each melt season. This is normally done by measuring the increased height of ice on poles drilled into the ice. However, the pole may channel meltwater down to the ice under the winter snow and thereby cause a local increase in superimposed ice formation. An area around the pole has to be checked to account for this.

(2) Measuring annual accumulation in the wet-snow facies is more difficult. It is seldom possible to determine the depth to which meltwater has percolated. Consequently, no well-defined annual layer exists. Densification of the firn and snow, due to meltwater percolation and refreezing, makes pole measurement highly inaccurate. This is not always taken into account (Cogley and Adams, 1998). The practice at the GSC has been to use trays buried deeply enough in year 1 to catch meltwater percolating down in year 2. This method is adequate in most years. However, in heavy melt years (for example, 1962 and 1998 in fig. 12), the percolation tray may overflow, or, at the very least, seriously affect the melt process itself. The use of automatic weather stations (fig. 11) increases the accuracy of the mass-balance measurement, particularly in very warm summers. The automatic weather stations records the snow accumulation, on an hourly or daily basis, throughout the year. In this case, it is the part of the record between spring and the end of the melt season (that is, the summer balance) that is important. Because the automatic weather station only records the change in height of the ultrasonic snow sounder above the snow surface, the snow density

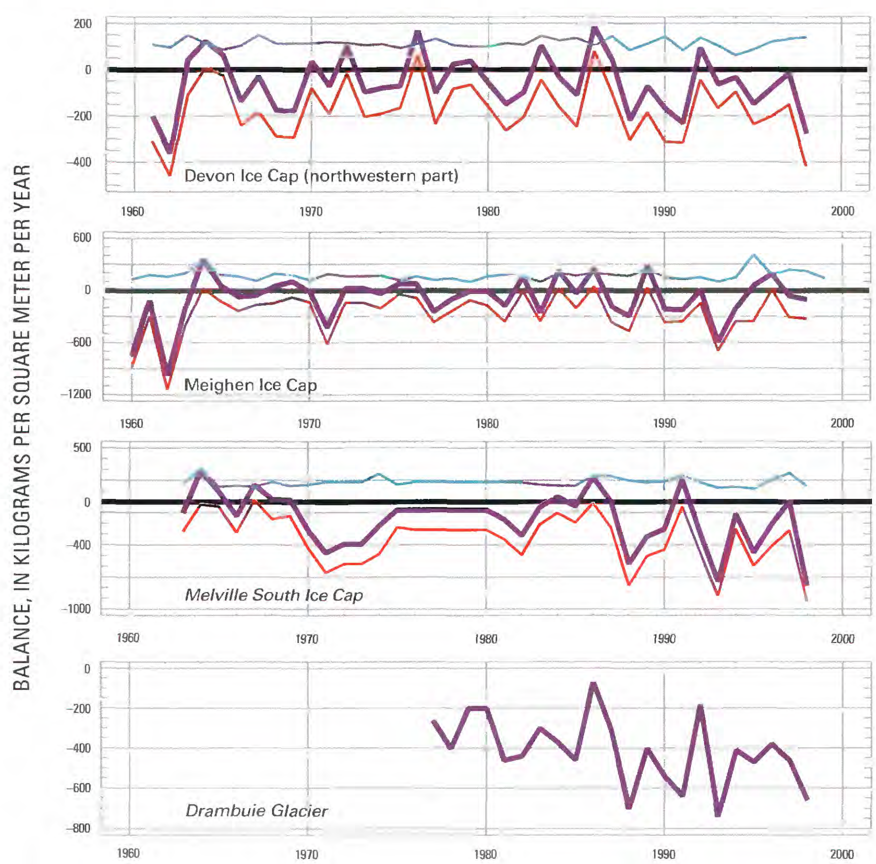

***Figure 12.**—Mass-balance records from the northwestern part of Devon Ice Cap, Meighen Ice Cap,* Melville South Ice Cap, *and* Drambuie Glacier *on the northeast side of Agassiz Ice Cap. The top (blue) line is the winter balance, the middle (purple) line is the net balance, and the lowermost (red) line is the summer balance. The figure shows that net balance is driven by summer melting rather than by winter snow accumulation, which is relatively consistent from year to year. The* Drambuie Glacier *time series is not a true mass balance because it does not include area. It is the sum of the specific balance at each of the poles, measured each year. Although the system [used for the* Drambuie Glacier*] does not represent mass balance for the ice cap and glaciers, it nonetheless serves to monitor climate change (see Koerner, 1986). The values from* Drambuie Glacier *are more negative than on the other glaciers because the measurements do not extend to the top of the ice cap. Data are from the Geological Survey of Canada.*

remains unknown. Measurements over four decades have shown that new snow, which is almost always associated with wind drift, has a density of between 0.1 and 0.2 g cm^{-2}. A density within this range is chosen according to the nature of the automatic weather station record. The method introduces a 5–10 percent error into the annual accumulation measurements between the percolation line and the upper limits of the superimposed ice zone.

(3) Mass-balance measurements in the *percolation facies* are simpler. Pole measurements are used as a guide so that the annual layer is readily recognized from its an annual sequence of refrozen melt-soaked firn overlying unsoaked firn. Depth and density measurements then give the mass balance.

Results

The mass-balance results from the GSC program are shown in figure 12. It is very clear that the net annual balance is driven by the summer melting. Each series shows that the period of record has been one of very slightly negative balance. Alt (1978, 1979) has analyzed some of these records and related them to synoptic conditions in the Arctic Islands. However, no statistically significant trend is found in the various time series (Koerner and Lundgaard, 1995; Koerner, 1996; Cogley and others, 1995, 1996). The same lack of trend extends eastward to the glaciers in Svalbard (Dowdeswell and others, 1997; Hagen and Liestøl, 1990). This contrasts with the substantial warming over the same period in the western Arctic. Regional differences in climatic change should not be unexpected, and they emphasize the need for monitoring the climate closely. As we have seen, glaciers are particularly valuable in this respect.

Summer Ablation and the Glacier Landscape

Melting produces a variety of impressive supraglacier, englacier, and subglacier features (Maaq, 1969). Melt streams can be seen in figure 3, where they are marked with a letter ‘m’. These melt streams may be up to 15-m wide and flow in channels as deep as 30 m that have vertical, or even overhanging, sides. Some even flow in tunnels just below the ice surface (for example, just downstream of the confluence of the two glaciers forming Sverdrup Glacier in fig. 3). Most of the meltwater finds its way to the margins of the glaciers, where large streams flow between the rock wall and glacier side and commonly through subglacier and englacier tunnels. Many streams disappear down moulins, especially near the terminus (for example, the northernmost ‘m’ on Sverdrup Glacier in fig. 3). Streams flow at high velocities because of the low friction between water and ice and the smooth nature of the channels. Consequently, they are able to transport boulders greater than 1 m^3 in size. Several such boulders can be found perched along the courses of abandoned streambeds.

The heavily crevassed glaciers draining the west side of Agassiz Ice Cap in northern Ellesmere Island (fig. 8, (A), (C), (D)) have much higher melting rates in their ablation areas than typical High Arctic glaciers. This is suggested by unpublished measurements by the GSC on one of these glaciers (fig. 8, (A)), as well as on highly hummocked areas of glaciers on southeastern Devon Island (Koerner, 1970b). Not only do these glaciers have relatively high specific ablation rates, which are related to their increased mesorelief and lower albedo, but they also have a greater surface area as a result of their crevassed and hummocked relief. Thus, ice loss due to melting may be up to an order of magnitude higher in their ablation zones than on glaciers elsewhere. An example of a highly hummocked glacier, Iceberg Glacier, which undergoes intense summer melting, is shown in figure 13.

A late August 1974 Landsat 1 multispectral scanner (MSS) false-color composite mosaic image (fig. 5) illustrates a High Arctic landscape at the height of the summer melt season. Various shades of blue and gray through to white (most clearly seen on the west side of the ice cap) are related to the progress of melting at different elevations. At the top of the ice cap, the snow is still highly reflective, which shows that it has melted very little, if at all. Lower down, it changes to a light gray, which indicates snow in an advanced state of melt. On the west side of the ice cap, the light-gray tone abruptly changes to either a dark gray blue or to blue. The blue tone is probably new superimposed ice, formed either during the melt season when the image was taken or during the previous melt season. The dark gray blue is older glacier ice that was formed higher up the flowline by firn compaction. The gray part of the tone becomes more pronounced closer to the glacier terminus. The light-gray tone (wet snow) extends right down to sea level on the east side of the ice cap. This is because the snow, which accumulates to much greater depths there, has not yet completely melted to expose the blue glacier ice underneath. The heads of Makinson Inlet and Vendom Fiord are already free of sea ice. The melting of the sea ice is hastened by runoff of snowmelt from ice-free terrain.

Figure 13.—*High-angle, oblique aerial photograph of Iceberg Glacier, Axel Heiberg Island (see fig. 7 for location), taken on 23 July 1964. The highly hummocked surface is associated with intense melting.*

Ice Caps and Climatic Change

Early attempts to derive climate-change records from ice caps were based on the number and thickness of ice layers and on changing stratigraphy in snow-firn pits (Hattersley-Smith 1960; Müller, 1963b; Koerner, 1970b). Hattersley-Smith (1960) detected a sharp warming of climate in the 1920's by using this method.

The Ice-Core Record

Ice cores allow climate-change studies to be carried out to much greater depth (that is, a longer length of time). As snow accumulates year by year in the accumulation area of ice caps, it traps within it atmospheric aerosols, which include cosmic and terrestrial particles (for example, dust and tephra), heavy metals, pollen, and acids. Atmospheric gases also are trapped. The oxygen-18/oxygen-16 ratio of the snow ($^{18}O/^{16}O$) and the changing percentage of ice layers in the core give a proxy record of past temperatures. At the top of the ice caps, where ice movement is mainly vertical, a continuous record of these variables exists that covers the entire history of the ice cap. This is where ice cores in the High Arctic islands have been drilled. The location of each deep drill site in the Canadian High Arctic is shown in figure 1.

One of the most important contributions of ice-core analysis to climate-change studies is a temperature proxy. This is a temperature derived from a variable measured in the core. The stable isotope-temperature relationship depends largely on the temperature of formation of precipitation; the lower the condensation temperature, the more negative the ^{18}O values of precipitation. The isotope record is either in terms of hydrogen or oxygen isotopes in water: hydrogen-deuterium-oxygen (HDO) or $H_2{}^{18}O$, both with respect to Standard Mean Ocean Water (SMOW); that is, δD or $\delta^{18}O$. This is translated into temperature on well-founded empirical relationships between surface temperatures and the δD or $\delta^{18}O$ composition of the snow (Dansgaard and others, 1973). Limitations apply to this temperature proxy. The most serious are changing sources of water vapor, variations in the length of the seasonal fractions of snowfall, and changing elevation of the drill site. However, except for the areas facing Baffin Bay, the Queen Elizabeth Islands' ice caps bear only a very weak relationship with elevation (Koerner, 1979). Ice layers that form in the snow pack in summer can be used as a *summer* temperature proxy (Koerner, 1977a). The warmer the summer, the greater the number or thickness of ice layers that form. Changing concentrations of ice layers in the ice cores can then be related to summer climate changes in the past (Koerner and Fisher, 1990).

The first task of ice-core analysis is the determination of a time scale. This may be done by counting annual cycles of some of the included "contaminants" down selected lengths of the core, by detecting acid layers from known volcanic events, by picking up well-known climatic events in the oxygen-isotope record, or, theoretically, from a knowledge of the flow law of ice. A combination of these methods has been used to develop a time scale for the Canadian High Arctic ice cores. This time scale is accurate to about 5 percent for the last 5,000 years and to about 10 percent for ice that formed at 10 ka to 5 ka. In ice older than 10 ka, the time scales have been derived from comparisons between oxygen-isotope and particulate profiles in the Canadian and the more accurately dated Greenland ice cores. This part of the record is contained in the lowermost 5–10 m of the core, where flow over uneven bedrock can produce distortions and gaps in the stratigraphy (Paterson and others, 1977).

The first deep ice core drilled from the Queen Elizabeth Islands was from the Meighen Ice Cap (figs. 1, 9*A*). Analysis of the 121-m core, which is from the highest part of the ice cap close to its southern edge (Paterson, 1968, 1969; Koerner, 1968; Koerner and others, 1973; Koerner and Paterson, 1974), originally suggested that the deepest ice is of the order of 4.5 ka. However, because of the difficulty of establishing a time scale in an ice cap formed dominantly of superimposed ice (Dowdeswell and others, 1990; Koerner, 1997), all one can say is that it began to form in the latter part of the Holocene Epoch.

Records from some of the other cores are shown in figure 14, which has three records from Canada, which show a –20 degree Celsius cooling (compared with today) in the coldest parts of the last glacial (Fisher and others, 1983, 1998), four from Greenland (Dansgaard and others, 1985; Johnsen and others, 1992), and one from Antarctica (Jouzel and others, 1993). Ice deposited during glacials is differentiated from interglacials on the basis of the presence of higher concentrations of microparticles and major ions in glacial-period ice, its more negative $\delta^{18}O$ values, and its finer grained ice texture. Despite quite different thicknesses, the main interglacial-glacial sections are common to each ice core. However, only the Vostok and Summit cores from Antarctica and central Greenland, respectively, contain ice older (fig. 14, (D)) than that deposited during the last interglacial (C) (Jouzel and others, 1993; Johnsen and others, 1992).

Basal ice in the Canadian cores (fig. 14, (C)) has high pollen concentrations and less negative oxygen-isotope $\delta^{18}O$ values, consists of much clearer (less bubbly) ice, and, on Agassiz Ice Cap, contains large amounts of dirt (Koerner and others, 1988). Such a signature, as well as its position at the base of the ice cores, suggests that it was deposited in the early growth stages of the ice cap, during the last interglacial, when the climate was entering the Wisconsinan glacial. Ice older than this must have melted during the main part of the same interglacial time, as it did at the sites of the Camp Century and Dye 3 cores in Greenland (Koerner, 1989). Because the Canadian ice-core sites are in the central and highest parts of their respective ice caps, it suggests that the Canadian High Arctic islands were ice free during some part of that same interglacial (Koerner, 1989). Similarly, it has been suggested (Koerner, 1989; Cuffey and Marshall, 2000) that the Greenland ice sheet, although it was not completely removed, must have been substantially smaller at that time.

The Holocene part of some of these records is shown in figure 15. The Penny Ice Cap and Agassiz Ice Cap $\delta^{18}O$ records show an early thermal

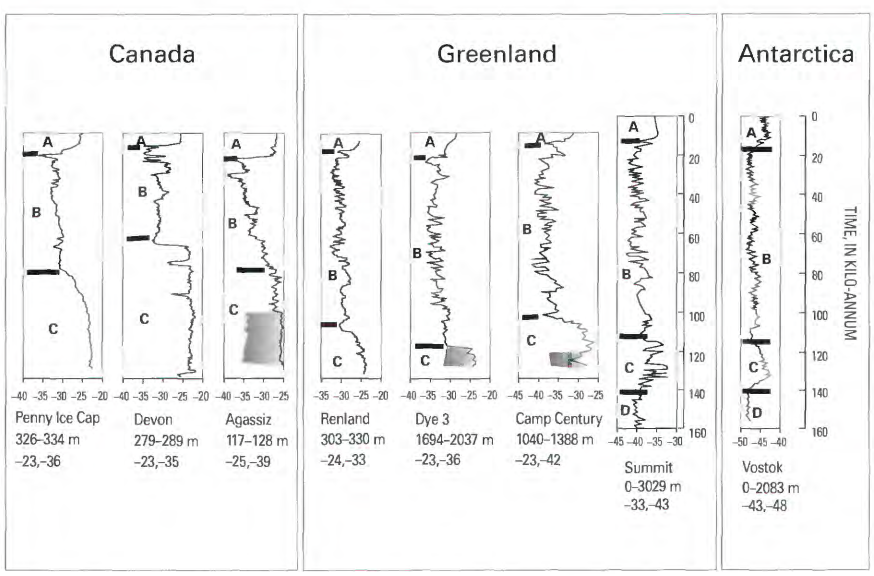

Figure 14.—*$\delta^{18}O$ profiles from Canadian ice caps (Fisher and others, 1983, 1998), the Greenland ice sheet (Dansgaard and others, 1985; Johnsen and others, 1992), and the Antarctic ice sheet (Jouzel and others, 1993). The $\delta^{18}O$ values are in parts per thousand with maximum and minimum values listed under each ice-core section. The shaded part at the base represents ice that has a high silt content. (A), Holocene; (B), Würm/Wisconsinan glacial; (C), Eemian/Sangamonian interglacial (Summit, Vostok), or early growth ice dating either from late Eemian/ Sangamonian interglacial or early Würm/Wisconsinan glacial (Penny, Devon, Agassiz, Dye 3, Camp Century); (D), earlier Pleistocene. See text for location of sections. The Summit and Vostok cores are plotted on a time scale (right-hand side of the diagram). For ice older than 110 ka, the Summit time scale is inaccurate due to dynamic disturbance of the ice at those depths. The other six cores are plotted on individual linear depth scales, where the depth interval is noted for each profile.*

maximum. However, it is not as early as that shown by the ice-layer record from Agassiz Ice Cap (percent of melt). The difference may be due to the effect of massive runoff of meltwater from the Laurentide ice sheet at this time. This water, which had very negative [oxygen-isotope] $\delta^{18}O$ values, and which may have pushed the water-vapor source farther south, is likely to have had the effect of making the [oxygen-isotope] $\delta^{18}O$ values too negative (Koerner, 1988; Fisher, 1992). The salt record from Penny Ice Cap also shows a very early Holocene maximum. Salt has been shown to have an inverse correlation with sea-ice extent in Baffin Bay (Grumet and others, 2001). The Holocene salt record, therefore, suggests that the extent of sea ice has been slowly increasing in Baffin Bay from an early Holocene minimum. Dyke and others (1996) concluded, from ^{14}C-dated fossil bones in the Arctic Islands, that Bowhead whale populations were at a maximum in the early Holocene. Together, the $\delta^{18}O$, ice-layer, and salt records suggest a varying, but overall, cooling trend has taken place throughout most of the Holocene Epoch, particularly during the last 5,000 years. The modern

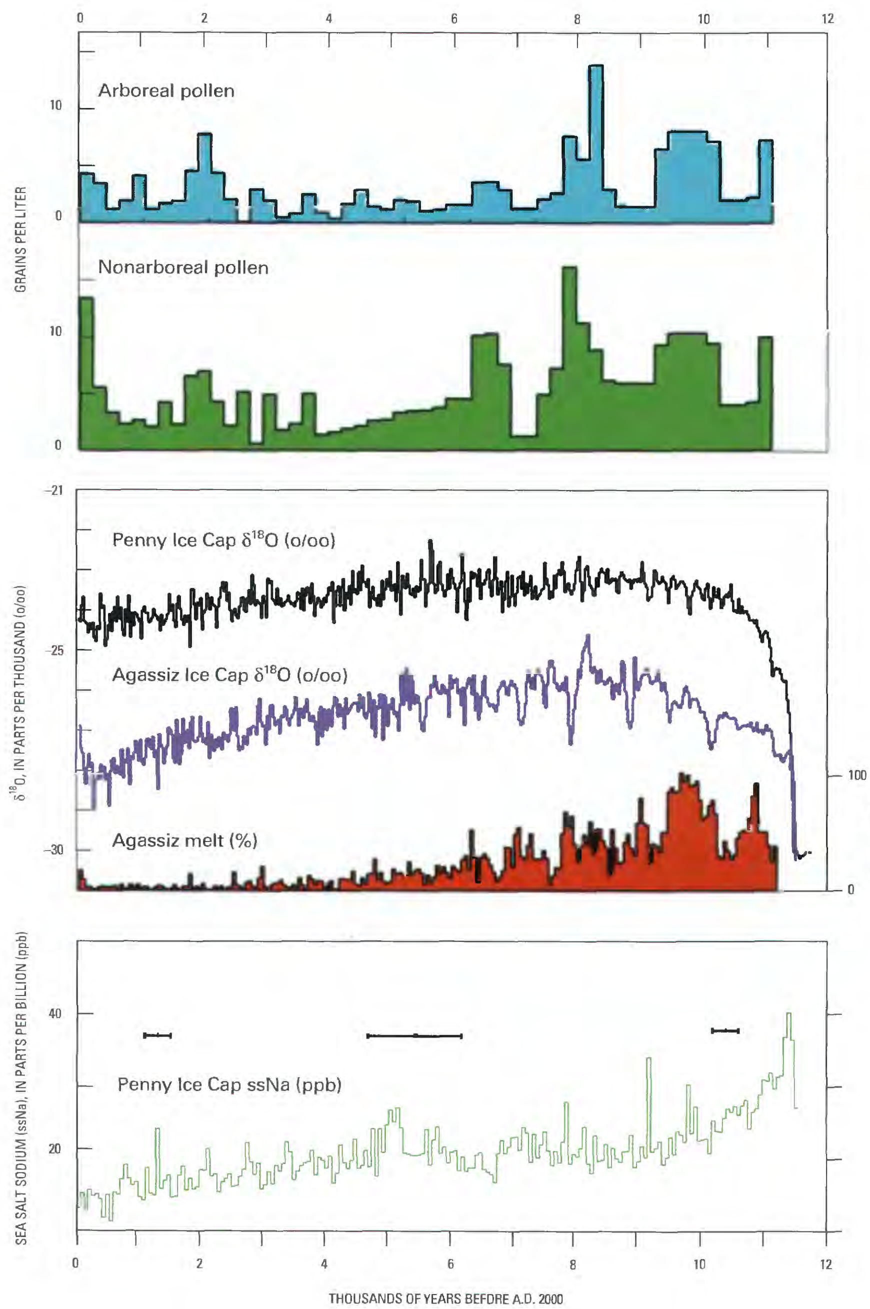

Figure 15.*—Paleoclimate records from the Holocene section of ice cores from Penny and Agassiz Ice Caps. A higher percent melt from the ice-layer record or less negative $\delta^{18}O$ values signify a warmer climate. Conditions in the early and middle Holocene were warmer than today by about 2°C and show an early Holocene thermal maximum. The sea-salt record from the Penny Ice Cap also shows a very early Holocene maximum. Salt has an inverse correlation with sea-ice extent in Baffin Bay. Therefore, the record suggests a gradually increasing sea-ice extent in Baffin Bay from an early Holocene minimum. Three horizontal error bars indicate the range of uncertainty in the sea-salt record during these intervals of time. The Holocene pollen record also suggests warmer conditions in the early Holocene and in the last 2,000 years.*

warming during the last 100–150 years appears to have produced the warmest period of at least the last 1,000 years. It follows, but highlights, a cold period ("The Little Ice Age") ending about 150 years ago. The "Little Ice Age," coming at the end of an overall cooling trend, may be nothing more than a slight cooling variation within that trend.

The Holocene pollen record, although it shows higher pollen concentrations in early Holocene ice that suggest warmer conditions, also shows increasing concentrations in the last 2,000 years. Pollen is probably not a direct temperature proxy. Whereas the other records suggest that the thermal maximum was in the early Holocene, it was a time when the Laurentide ice sheet still covered a large part of Canada. What is a pollen source today was, therefore, covered by ice at that time. An alternate early Holocene source may have been northwestern Canada, where the tree line reached farther north than today. Whether the late Holocene pollen increase represents a return to a western air-mass trajectory and pollen source has not yet been determined.

Ice-core records from Severnaya Zemlya and Svalbard to the east (Koerner, 1997) show similar Holocene $\delta^{18}O$ and ice-layer records: an early thermal maximum followed by a trend of decreasing temperatures (Koerner, 1997). It has already been shown that glacier mass balance is slightly negative today, which the ice-core records indicate is not as warm as the early Holocene (fig. 15). It suggests, therefore, that ice caps and glaciers must have had more strongly negative balances in the early Holocene than today. Only two ice cores from the Severnaya Zemlya and Svalbard group of islands show any evidence of the Pleistocene ice seen in the Canadian cores (fig. 14). The evidence for Pleistocene ice from one of these cores, Vavilov Ice Cap (Stiévenard and others, 1996), is questionable. Probably most of the Pleistocene ice caps at these sites melted during the period of negative balance in the early Holocene; only the larger ice caps in the Canadian islands and Academii Nauk Ice Cap on Severnaya Zemlya survived. Increasingly colder conditions, particularly during the last 5,000 years, have promoted regrowth of glaciers. They reached their maximum extent about 150 years ago (Müller, 1966). It was at this time that the desperate, but unsuccessful, attempts to open up the Northwest Passage were made. Success was achieved by the Norwegian explorer Roald Amundsen early this century when summer conditions promoted more open sea- ice conditions (Koerner, 1977a; Alt, 1985).

Aerial Photographic and Satellite Image Evidence of Glacier Fluctuations

Although ice cores are valuable in revealing climatic changes in the past, they do not tell much, on their own, about past changes in the dimensions of the ice caps. They show how climate changes over a broad range of wavelengths and amplitudes with respect to time and temperature. In terms of the response of glaciers to climatic changes, the waxing and waning of continental ice sheets is a response at one end of the spectrum, and the growth and disappearance of stagnant ice caps is a response at the other end of the same spectrum. Nye (1963) and Jóhannesson and others (1989) considered the problem of response times of glaciers, times that may vary from a few years to many thousands of years. In the Canadian High Arctic islands, one might expect a response time of about 2,000 years on the largest dynamic ice caps without valley outlets, such as, for example, the west side of Devon Ice Cap (fig. 2), but one might expect an immediate response on stagnant ice caps. Thus, a small glacier may be advancing in response to a recent climatic change while a larger one is retreating in response to a climatic change that ended a thousand years before. Relating these geometry changes to those of climate is further complicated because of our poor knowledge of the ice volume and bedrock topography of the Queen Elizabeth Islands' ice caps. Extensive radio-echosounding will help enormously in this respect (J.A. Dowdeswell, oral commun., 1999).

To examine changes in the areal extent of the Queen Elizabeth Islands' glaciers and ice caps, we compare vertical aerial photography taken in the 1950's with Landsat imagery taken in the 1970's. The Landsat MSS imagery, because of its 79-m pixel resolution, can only detect changes at the terminus of glaciers over a 20 year timespan, if the changes are greater than an average, cumulative change of 4 m a^{-1} (Williams and others, 1997).

Dynamic Ice Caps and Outlet Glaciers

On the basis of Landsat imagery shown in figures 2, 4, 5, and 7 and the vertical aerial photograph in figure 3, no significant marginal changes have been found on the larger ice caps. Some measurable changes are evident in glacier terminus positions that are mostly "increased-ablation" retreats in response to the warmth of the 1950's (Bradley and England, 1978). Because the time period between the aerial photography and the Landsat images includes part of the very warm period from 1920 to 1960, it may appear surprising that relatively few measurable changes are seen at the margins of the small glaciers. Similarly, why are some of the glaciers not advancing in response to the cooler climate of the "Little Ice Age" (about 1550 to 1850)? Continuing mass-balance measurements also show very few signs of warming or cooling in the eastern Canadian Arctic during the last 40 years.

The answer may be found in the low *activity index* of the High Arctic glaciers. That is, the accumulation and ablation rates are relatively small when compared with those of alpine glaciers or the maritime-nourished glaciers of Alaska. Changes are, therefore, likely to be small and not detectable by the use of 79-m pixel resolution imagery in a time period of only a few decades. The higher resolution satellite imagery, such as the Landsat Enhanced Thematic Mapper (ETM+) (15-m pixels), the Advanced Spaceborne Thermal Emission and Reflection Radiometer (ASTER) (15-m pixels), and IKONOS (1-m pixels), that is available will provide a better opportunity to detect changes.

A few documented cases do exist, however, of glaciers that have advanced dramatically in the High Arctic islands. One of them, the Otto Glacier in northern Ellesmere Island (fig. 1), has been described as a surging glacier (Hattersley-Smith, 1969). This glacier advanced 2–3 km between 1950 and 1959 and a farther 2–3 km between 1959 and 1964. The lower part of this advancing tidewater glacier was afloat. However, because the Otto Glacier is both a tidewater glacier and a surging glacier, the advance may not be related to climate (Post, 1975).

Another case of a possible surging glacier is the *Good Friday Bay Glacier*[2] (fig. 7). An advance of about 2 km began on this glacier between 1952 and 1959. Although some of the surface characteristics of this glacier suggest a surge (Müller, 1969), climatic forcing cannot be ruled out.

Figure 4 illustrates a 6.5-km retreat of a valley glacier that flows into South Cape Fiord on southwestern Ellesmere Island. The retreat took place between 1957 and July 1974. The retreat is associated with increased crevassing of the surface toward the terminus. However, no changes to surface level can be seen along the glacier. We cannot say whether the glacier is retreating *from* a more common position or *to* a more common position. None of the nearby glaciers has advanced or

---

[2] The names in this section conform to the usage authorized by the Secretariat of the Canadian Permanent Committee on Geographic Names (CPCGN); URL address: [http://GeoNames.NRCan.gc.ca/]. The Website is maintained by the Secretariat through Geomatics Canada, Natural Resources Canada, and combines the CPCGN server with the Canadian Geographical Names Data Base (CGNDB). Variant names and names not listed in the CPCGN/CGNDB are shown in italics.

retreated during the same period. On first inspection, the Landsat image in figure 4, taken only a month after a set of aerial photographs that showed the retreat, appears to show the terminus in its old, advanced position. Prior knowledge that the glacier has retreated, together with very careful examination of the image, shows that the ice in front of the terminus is either sea ice or icebergs.

Stagnant Ice Caps

Stagnant ice caps respond immediately to climatic change. A warming trend will always cause marginal retreat of these ice caps. However, retreat at its margins does not necessarily indicate that the ice cap has a negative balance. As long as the equilibrium line altitude (ELA) is low enough, the ice cap may retreat despite having a positive balance. Because the ice cap is stagnant, the margin will "advance" only if the ELA lies beyond the margin. Although Meighen Ice Cap does not have an overall positive balance, it does have a slightly positive balance at its highest elevations. Retreat of its margins, accompanied by thickening in its central parts, is steepening its slopes. Theoretically, steeper slopes could cause greater basal shear stress and change it from a stagnant to a weakly dynamic ice cap.

Figure 16*A* shows three of the ice caps on Melville Island (fig. 1). The small nunataks on one of the two more northerly of the Melville Island ice caps (arrows in fig. 16*A*) show no measurable change between a 1957 aerial photograph and the 1977 Landsat image. Some retreat is evident at (A) and (B) on the southern ice cap (compare with fig. 16*B*). Retreat elsewhere may be hidden by a late snow cover at the time the Landsat image was taken; some snow still remains on the surrounding plateau. However, even if a general retreat is present at the margins, it must be quite small.

The situation is a little different on Meighen Ice Cap (fig. 9). The nunataks marked by arrows (fig. 9*A*) are more exposed in the 1977 Landsat imagery than in earlier (1959) aerial photography (fig. 9*B*). In one case, a nunatak near the west margin that is seen on the earlier aerial photograph is part of the surrounding plateau in the later Landsat image. The ice margin has also retreated at the locations indicated by arrows. From aerial photographs, Arnold (1965) found slow wastage at the margins of Meighen Ice Cap for the period 1950–59. An oblique aerial photograph taken on 18 July 1950, and shown in Arnold (1965), shows a continuous ice cover where the Landsat image shows a long narrow nunatak at the northern end.

Clear changes can be seen on the smallest stagnant ice caps when comparing aerial photographs of the 1950's and the satellite imagery of the 1970's. Comparing figures 2 and 3 of the area close to the northwest margin of the Devon Ice Cap, we can see that three small ice caps (fig. 3, arrows) have disappeared by the 1970's, when they were replaced by bare ground (fig. 2). Another small ice cap (fig. 3, (C)) just above the terminus of Sverdrup Glacier has almost disappeared, and a slightly larger one to the southwest (fig. 3, (E)) has been separated from a section located in a nearby gully.

These are not especially dramatic changes, but they do suggest that the climate of the 20-year period between the 1950's and 1970's was warmer than the climate under which these ice caps formed. The records of negative balance from Meighen Ice Cap and Melville Island ice caps would certainly apply to these smaller stagnant ice caps. It seems most likely that they began growth during the colder parts of the last 1,000 years and are presently out of phase with modern warming. Many more may disappear within the next 50 years if the climate does not cool again.

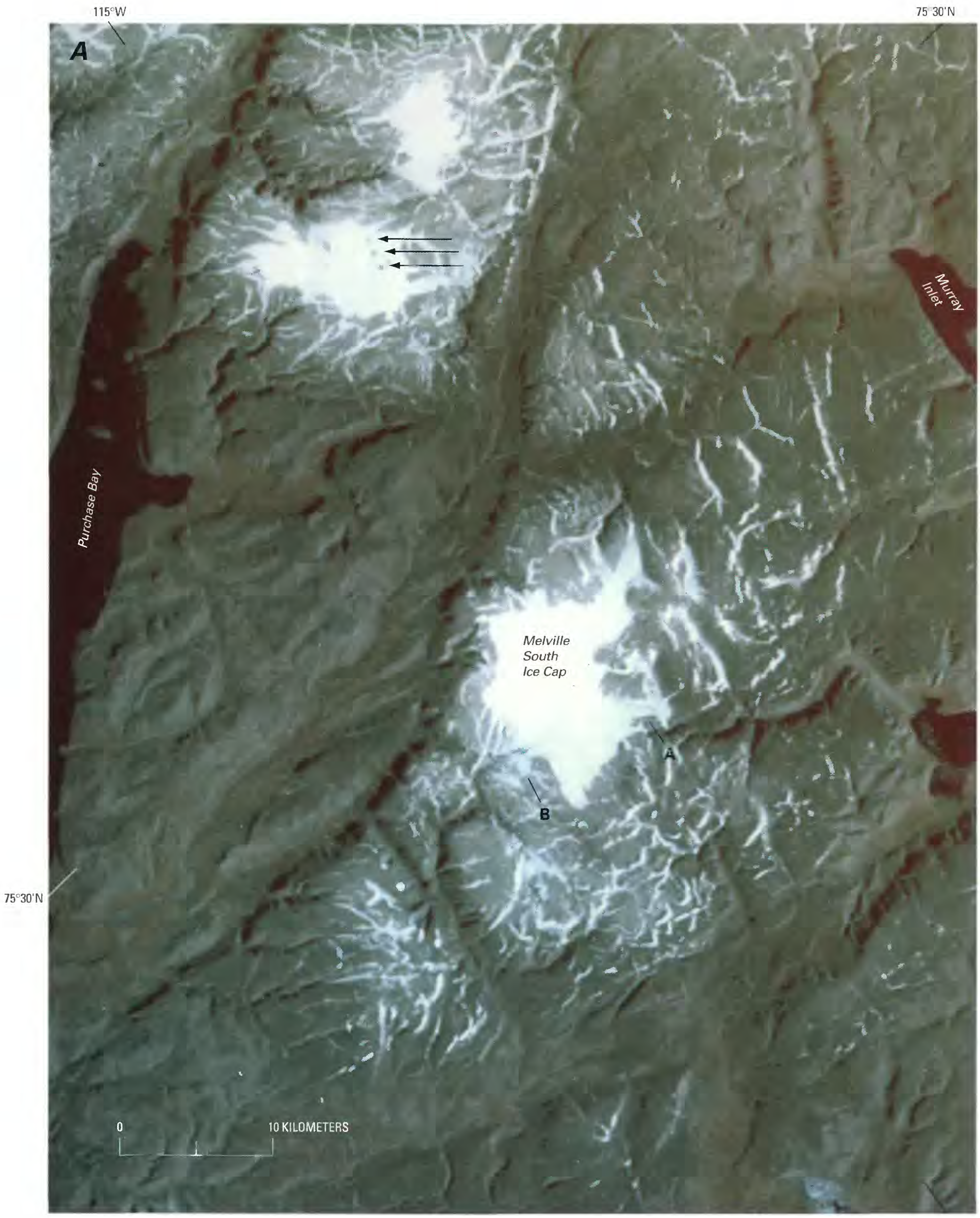
115°W
75°30'N
A
Murray Inlet
Purchase Bay
Melville South Ice Cap
A
B
75°30'N
0
10 KILOMETERS

Figure 16.—Landsat image from 1977 and an aerial photograph from 1957 showing slight changes in the Melville Island ice caps. **A**, (opposite page) Part of an enlargement of a Landsat image of three of the Melville Island ice caps. The nunataks at the top of the figure (indicated by arrows) show very little change in area compared to an aerial photograph taken 20 years earlier. A slight retreat can be seen on the southern ice cap at points (A) and (B) when compared with figure 16B. The Landsat image (11855–18310, bands 4, 5, and 7; 21 August 1977; Path 66, Row 6) is from the Canada Centre for Remote Sensing, Ottawa, Ontario, Canada. **B**, Vertical aerial photograph of Melville South Ice Cap taken in 1957. The ice margins at (A) and (B) should be compared with the same points in figure 16A. Note the "banding" on the ice surface at (C) formed by outcropping of dust layers.

Evidence of Changes in Glacier Volume

Changes of glacier thickness may be assessed by more traditional techniques. The absolute, or relative, change of glacier elevation is measured photogrammetrically, by surveying across the glacier between fixed points off the glacier, by radio-echosounding, by gravimetric methods, or by changing borehole length. These surveys measure the difference between the vertical velocity of the glacier and the ice-melt or accumulation rate for the period between the surveys. The vertical velocity in this case is a long-period, or even paleobalance, rate, representing a period of unknown length.

Arnold (1968, 1981) discussed at length the techniques used for glacier surveys. Briefly, one has to survey the surface of a glacier on at least two occasions sufficiently separated in time to detect vertical (height) changes. If markers on the glacier move, any resurveys must be made to the original coordinates. Sets of changing vertical angles, made by the use of traditional survey methods, determine height changes of the glacier surface. Modern photogrammetric techniques can give the same results; the effort involved is less, but the expense greater. Arnold (1968, 1981) has done work of both kinds on Gilman Glacier (fig. 1) and on White Glacier (figs. 1, 7).

Another method involves leveling along a straight line across a glacier between two fixed points on the valley walls. When repeated, comparison of the two surveys gives the change of elevation of the glacier surface. This method has been used on Sverdrup Glacier (fig. 3, dotted line; Cress and Wyness, 1961).

Very careful radio-echosounding, repeated after an interval of a few years, can be used to detect glacier-thickness changes (Nye and others, 1972). Precision gravimeters can also be used to achieve the same results (Bentley, 1975). The latter technique has been used at the top of Devon Ice Cap (Winter, oral commun., 1976). It is also possible to use repeated measurements of the length of surface-to-bedrock boreholes to achieve the same results (Paterson, 1976).

Arnold's (1968) measurements in the accumulation area of Gilman Glacier (fig. 1) found no significant changes during the 1957–67 period. Similarly, gravimeter measurements on Devon Ice Cap detected no change for the 1971–76 period (Peter Winter, oral commun., 1976). In contrast, Paterson's (1976) measurements of change in borehole length indicated a slight thickening of the highest part of this ice cap. Arnold (1968) measured an average surface lowering of 1.66 m (0.17 m a^{-1}) for 1957–67 in the ablation area of Gilman Glacier. He also measured an average surface lowering of 8.2 m (0.83 m a^{-1}) for the period 1960–70 on White Glacier (Arnold, 1981). The lowering of Gilman Glacier and White Glacier took place during periods that included the warmer early 1960's, including the summer of 1962 that had the most negative glacier mass balances on record (fig. 12). Farther south, on Sverdrup Glacier, leveling in 1965 and again in 1975 detected no significant height changes of the glacier 10 km from the terminus and 300 m above sea level.

The most effective method for measuring ice-thickness change, however, consists of repeated geodetic airborne laser altimetry surveys (Krabill and others, 1995). One such survey was done by NASA in 1995 and was repeated in 2000 along flightlines suggested by the GSC. The results of this survey will give broad spatial coverage of change in ice-cap thickness [relative change based on change in surface elevation] in the Canadian High Arctic islands from northern Ellesmere Island to southern Baffin Island.

Conclusions and Recommendations

The Landsat imagery (having 79-m pixel resolution) used in this chapter is barely adequate to detect changes in the margins of the larger ice caps during a 10- to 20-year period. Partly, this is due to the low *activity index* of High Arctic glaciers. Both snow-accumulation and ice-melt rates are small compared to those of alpine glaciers. Changes in both snowfall and ice melt might also be small. Unlike Greenland and Antarctica, where similarly low activity indices apply, the glaciers in the High Arctic are relatively small, so that the kinds of dramatic changes, like massive ice-shelf calving are not present. Stagnant ice caps, on the other hand, do show changes. Their response to climatic change has no lag, unlike dynamic glaciers, and marginal retreat can be directly related to summer climate even on an annual basis. A few of the smaller stagnant ice caps, detectable in the earlier aerial photography, disappeared between the 1950's and 1970's.

Satellite imagery is continually improving, however, and future coverage having improved resolution, such as coverage by the Landsat 7 (ETM+) (15-m pixel resolution), Ikonos (1-m pixel resolution), and the Global Land Ice Mapping System (GLIMS) ASTER (15-m pixel resolution), should prove to be valuable new tools for glacier monitoring in terms of changes in glacier area. The aerial photography taken in the 1940's and 1950's will, therefore, serve as an invaluable baseline for future comparative purposes. The recent application of satellite synthetic aperture interferometry techniques is enabling the mapping of velocity fields on glaciers, ice caps, and ice sheets (Mohr and others, 1998). Now, by combining interferometry and local mass-balance and ice-radar techniques, it is proving possible to calculate surface-elevation changes, as well as the velocity fields on glaciers (Reeh and others, 1999).

Recent application of airborne laser altimetry surveys (having 0.1-m vertical accuracy) to the Greenland ice sheet (Krabill and others, 1995) and smaller circumpolar ice caps (Garvin and Williams, 1993) has already shown its value. A repeat of a 1995 series of flightlines over the Canadian High Arctic islands and Baffin Island in 2000 gave, for the first time, an extensive measure of the changes in ice-cap thickness there. However, any changes on a dynamic glacier relate to climatic change that has taken place in the past, as well as in the present. It may prove difficult to relate those changes of thickness to any particular period of climatic change, although they are directly relevant to the part played by glaciers in sea-level change.

One limitation of satellite imagery over subpolar ice caps is the problem of detecting the equilibrium line. This is because superimposed ice forms part of the accumulation process. Consequently, the accumulation region includes a zone where the surface is ice. This ice has the same characteristics as the ice *below* the equilibrium line, which is superimposed ice that has flowed down the ice cap in the past from its zone of formation. With improvements in the sensors carried on satellites expected to be launched in the future, the situation of satellite monitoring of glaciers will improve. However, it will be essential to conduct field-based glacier research for accurate image interpretation.

The use of automatic weather stations is becoming more applicable and popular in the practice of glacier research and monitoring. These stations are proving especially valuable in terms of correcting for meltwater percolation and refreezing in the accumulation area. However, the effect of rime-ice and hoarfrost accumulation on automatic weather station sensors must be assessed. GSC research is showing that wind and radiation recorded during large parts of the winter (when hoarfrost develops) and summer (when rime ice forms) produce barely usable and, at worst, misleading results. Research should be directed to keeping the sensors free of these deposits.

The importance of glacier calving and basal-ice melt by the sea under floating glacier tongues in the High Arctic islands is poorly understood. Examination of aerial photography suggests that calving is not a very important factor in mass balance, and basal melt under the glacier tongues is even less so. However, this is an area deserving of future research.

Acknowledgments

I am greatly indebted to reviewers of this chapter, Drs. Martin O. Jeffries, Julian A. Dowdeswell, and W.S.B. Paterson. Dr. Paterson, in particular, suggested that I undertake a major revision of the entire chapter and made many very constructive suggestions. Although I did not agree to all the reviewers' suggestions, the chapter is the better for the time and effort that they put into their technical reviews.

References Cited

Alt, B.T., 1978, Synoptic climate controls of mass balance variations on Devon Island Ice Cap: Arctic and Alpine Research, v. 10, no. 1, p. 61–80.

———1979, Investigation of summer synoptic climate controls on the mass balance of Meighen Ice Cap: Atmosphere-Ocean, v. 3, p. 181–199.

———1985, 1550–1620—A period of summer accumulation in the Queen Elizabeth Islands *in* Harington, C.R., ed., Climatic Change in Canada 5: Ottawa, Ontario, National Museum of Natural Sciences, Syllogeus, v. 55, p. 461–479.

Arnold, K.C., 1965, Aspects of the glaciology of Meighen Island, Northwest Territories, Canada: Journal of Glaciology, v. 5, no. 40, p. 399–410.

———1968, Determination of changes of surface height 1957–1967, of the Gilman Glacier, northern Ellesmere Island, Canada: Montréal, Québec, McGill University, unpublished M.A. thesis, 74 p.

———1981, Ice ablation measured by stakes and terrestrial photogrammetry—A comparison on the lower part of the White Glacier: Montréal, Québec, McGill University, Axel Heiberg Island Research Reports, Glaciology 2, 98 p.

Benson, C.S., 1961, Stratigraphic studies in the snow and firn of the Greenland Ice Sheet: Folia Geographica Danica, v. 9, p. 13–37.

Bentley, C.R., 1975, Advances in geophysical exploration of ice sheets and glaciers: Journal of Glaciology, v. 15, no. 73, p. 113–134.

Blatter, H., 1987, On the thermal regime of an Arctic valley glacier—A study of White Glacier, Axel Heiberg Island, N.W.T., Canada: Journal of Glaciology, v. 33, no. 114, p. 200–211.

Bradley, R.S., and England, John, 1978, Recent climatic fluctuations of the Canadian High Arctic and their significance for glaciology: Arctic and Alpine Research, v. 10, no. 4, p. 715–731.

Cogley, J.G., and Adams, W.P., 1998, Mass balance of glaciers other than the ice sheets: Journal of Glaciology, v. 44, no. 147, p. 315–325.

Cogley, J.G., Adams, W.P., Ecclestone, M.A., Jung-Rothenhäusler, F., and Ommanney, C.S.L., 1995, Mass balance of Axel Heiberg glaciers, 1960–1991—A reassessment and discussion: Saskastoon, Saskatchewan, Environment Canada, National Hydrology Research Institute (NHRI) Science Report 6, 168 p.

———1996, Mass balance of White Glacier, Axel Heiberg Island, N.W.T., Canada, 1960–1991: Journal of Glaciolgy, v. 42, no. 142, p. 548–563.

Crary, A.P., 1960, Arctic ice island and ice shelf studies: Arctic, v. 13, no. 1, p. 32–50.

Cress, P., and Wyness, R., 1961, The Devon Island expedition, observations of glacial movements: Arctic, v. 14, no. 4, p. 257–259.

Cuffey, K.M., and Marshall, S.J., 2000, Substantial contribution to sea-level rise during the last interglacial from the Greenland ice sheet: Nature [London], v. 404, no. 6778, p. 591–594.

Dansgaard, W., Clausen, H.B., Gundestrup, N.S., Johnsen, S.J., and Rygner, C., 1985, Dating and climatic interpretation of two deep Greenland ice cores: Geophysical Monograph, v. 33, p. 71–76.

Dansgaard, W., Johnsen, S.J., Clausen, H.B., and Gundestrup, N., 1973, Stable isotope glaciology: Meddelelser om Grønland, v. 197, no. 2, 53 p.

Doake, C.S.M., Gorman, M., and Paterson, W.S.B., 1976, A further comparison of glacier velocities measured by radio-echo and survey methods: Journal of Glaciology, v. 17, no. 75, p. 35–38.

Dowdeswell, J.A., Drewry, D.J., and Simões, J.C., 1990, Correspondence—Comments on "6000-year climate records in an ice core from the Hoghetta ice dome in northern Spitsbergen": Journal of Glaciology, v. 36, no. 124, p. 353–356.

Dowdeswell, J.A., Hagen, J.O., Björnsson, H., Glazovsky, A.F., Harrison, W.D., Holmlund, P., Jania, J., Koerner, R.M., Lefauconnier, B., Ommanney, C.S.L., and Thomas, R.H., 1997, The mass balance of circum-Arctic glaciers and recent climate change: Quaternary Research, v. 48, p. 1–14.

Dyke, A.S., Hooper, J.E., and Savelle, J.M., 1996, A history of sea ice in the Canadian Arctic Archipelago based on postglacial remains of the Bowhead Whale (*Balaena mysticetus*): Arctic, v. 49, no. 3, p. 235–255.

Fisher, D.A., 1992, Possible ice-core evidence for a fresh melt water cap over the Atlantic Ocean in the early Holocene, *in* Bard, E., and Broecker, W.S., eds., The last deglaciation—Absolute and radiocarbon chronologies: North Atlantic Treaty Organization (NATO) Advanced Study Institute series, v. 12, p. 267–293.

Fisher, D.A., Koerner, R.M., Bourgeois, J.C., Zielinkski, Greg, Wake, Cameron, Hammer, C.U., Clausen, H.B., Gundestrup, N., Johnsen, Sigfus, Goto-Azuma, Kumiko, Hondoh, Takeo, Blake, Erik, and Gerasimoff, Mike, 1998, Penny Ice Cap cores, Baffin Island, Canada, and the Wisconsinan Foxe Dome connection—Two states of Hudson Bay ice cover: Science, v. 279, no. 5351, p. 692–695.

Fisher, D.A., Koerner, R.M., Paterson, W.S.B., Dansgaard, W., Gundestrup, N., and Reeh, N., 1983, Effect of wind scouring on climatic records from ice-core oxygen-isotope profiles: Nature [London], v. 301, no. 5897, p. 205–209.

Garvin, J.B., and Williams, R.S., Jr., 1993, Geodetic airborne laser altimetry of Breiðamerkurjökull and Skeiðarárjökull, Iceland, and Jakobshavn Isbræ, West Greenland: Annals of Glaciology, v. 17, p. 379–385.

Geografiska Annaler, 1999, Methods of mass balance measurements and modeling: Geografiska Annaler, v. 81A, no. 4, special issue, p. 461–796.

Grumet, N.S., Wake, C.P., Mayewski, P.A., Zielinski, G.A., Whitlow, S.I., Koerner, R.M., Fisher, D.A., and Woollett, J.M., 2001, Variability of sea-ice extent in Baffin Bay over the last millennium: Climatic Change, v. 49, p. 129–145.

Hagen, J.O., and Liestøl, Olav, 1990, Long-term glacier mass-balance investigations in Svalbard, 1950–88: Annals of Glaciology, v. 14, p. 102–106.

Hambrey, M.J., and Müller, F., 1978, Structures and ice deformation in the White Glacier, Axel Heiberg Island, Northwest Territories, Canada: Journal of Glaciology, v. 20, no. 82, p. 41–66.

Hattersley-Smith, G., 1960, Studies of englacial profiles in the Lake Hazen area of northern Ellesmere Island: Journal of Glaciology, v. 3, no. 27, p. 610–625.

———1963, The Ward Hunt Ice Shelf—Recent changes of the ice front: Journal of Glaciology, v. 4, no. 34, p. 415–424.

———1969, Recent observations on the surging Otto Glacier, Ellesmere Island: Canadian Journal of Earth Sciences, v. 6, no. 4, pt. 2, p. 883–889.

———1974, North of latitude 80 degrees north: Information Canada, The Defence Research Board in Ellesmere Island, DR3–1774, 121 p.

Hattersley-Smith, G., Fusezy, A., and Evans, S., 1969, Glacier depths in northern Ellesmere Island—Airborne radio-echo-sounding in 1966: Canada Department of National Defence, Defence Research Board, Defence Research Establishment Ottawa, DREO Technical Note 69–6, 23 p.

Hattersley-Smith, G., Keys, J.E., Serson, H., and Mielke, J.E., 1970, Density stratified lakes in northern Ellesmere Island: Nature [London], v. 225, no. 5227, p. 55–56.

Hattersley-Smith, G., Krouse, H.R., and West, K.E., 1975, Oxygen isotope analysis in accumulation studies on an ice cap in northern Ellesmere Island, N.W.T., in Moscow Symposium, August 1971, Proceedings: International association of Scientific Hydrology Publication 104, p. 123–128.

Hattersley-Smith, G., and Serson, H., 1970, Mass balance of the Ward Hunt Ice Rise and Ice Shelf—A 10 year record: Journal of Glaciology, v. 9, no. 56, p. 247–252.

———1973, Reconnaissance of a small ice cap near St. Patrick Bay, Robeson Channel, northern Ellesmere Island, Canada: Journal of Glaciology, v. 12, no. 66, p. 417–421.

Holdsworth, G., 1977, Ice flow and related measurements of D'Iberville Glacier, Ellesmere Island, N.W.T., Canada: Ottawa, Ontario, Canada Department of the Environment, National Hydrology Research Institute, Glaciology Division, unpublished manuscript, 28 p.

Hyndman, R.D., 1965, Gravity measurements on the Devon Island Ice Cap and an adjoining glacier: Journal of Glaciology, v. 5, no. 40, p. 489–496.

IAHS/UNESCO (International Association of Hydrological Sciences/United Nations Educational, Scientific, and Cultural Organization), 1985, Fluctuations of glaciers, 1975–1980: Zürich, Permanent Service on the Fluctuations of Glaciers, v. 4, 265 p.

Iken, A., 1974, Velocity fluctuations of an Arctic valley glacier—A study of the White Glacier, Axel Heiberg Island: Montréal, Québec, McGill University, Axel Heiberg Island Research Reports, Glaciology 5, 116 p.

Jania, J., and Hagen, J.O., eds., 1996, Mass balance of Arctic glaciers: Sosnowiec, Poland (University of Silesia, Faculty of Earth Sciences), and Oslo, Norway, International Arctic Science Committee, Working Group on Arctic Glaciology, Report No. 5, 62 p.

Jeffries, M.O., and Serson, Harold, 1983, Recent changes at the front of Ward Hunt Ice Shelf, Ellesmere Island, N.W.T.: Arctic, v. 36, no. 3, p. 289–290.

Jóhannesson, Tómas, Raymond, Charles, and Waddington, Ed, 1989, Time-scale for adjustment of glaciers to changes in mass balance: Journal of Glaciology, v. 35, no. 121, p. 355–369.

Johnsen, S.J., Clausen, H.B., Dansgaard, W., Fuhrer, K., Gundestrup, N., Hammer, C.U., Iversen, P., Jouzel, J., Stauffer, B., and Steffensen, J.P., 1992, Irregular glacial interstadials recorded in a new Greenland ice core: Nature [London], v. 359, no. 6393, p. 311–313.

Jouzel, J., Barkov, N.I., Barnola, J.M., Bender, M., Chappellaz, J., Genthon, C., Kotlyakov, V.M., Lipenkov, V., Lorius, C., Petit, J.R., Raynaud, D., Raisbeck, G., Ritz, C., Sowers, T., Stiévenard, M., Yiou, F., and Yiou, P., 1993, Extending the Vostok ice-core record of paleoclimate to the penultimate glacial period: Nature [London], v. 364, no. 6436, p. 407–412.

Koerner, R.M., 1968, Fabric analysis of a core from the Meighen Ice Cap, Northwest Territories, Canada: Journal of Glaciology, v. 7, no. 51, p. 421–430.

———1970a, Some observations on superimposition of ice on the Devon Island Ice Cap, Northwest Territories, Canada: Geografiska Annaler, v. 52A, no. 1, p. 57–67.

———1970b, The mass balance of the Devon Island Ice Cap, Northwest Territories, Canada, 1961–66: Journal of Glaciology, v. 9, no. 57, p. 325–336.

———1977a, Devon Island Ice Cap—Core stratigraphy and paleoclimate: Science, v. 196, no. 4285, p. 15–18.

———1977b, Ice thickness measurements and their implications with respect to past and present ice volumes in the Canadian High Arctic ice caps: Canadian Journal of Earth Sciences, v. 14, no. 12, p. 2697–2705.

———1979, Accumulation, ablation and oxygen isotope variations on the Queen Elizabeth Island ice caps, Canada: Journal of Glaciology, v. 22, no. 86, p. 25–41.

———1986, Novyy metod ispol'zovaniya lednikov dlya monitoringa izmeneniy klimata [A new method for using glaciers as monitors of climate]: Materialy Glyatsiologicheskikh Issledovaniy, v. 57, p. 47–52. [English text is given on p. 175–179.]

———1988, Ice core records of paleoclimate—The late glacial/early Holocene period [abs.]: American Quaternary Association, 10th meeting, Amherst, Mass., 1988, Program and abstracts: Seattle, Wash., American Quaternary Association, p. 29–32.

———1989, Ice core evidence for extensive melting of the Greenland ice sheet during the last interglacial: Science, v. 244, no. 4907, p. 964–968.

———1996, Canadian Arctic, in Jania, J., and Hagen, J.O., eds., Mass balance of Arctic glaciers: International Arctic Science Committee Report 5, p. 13–21.

———1997, Some comments on climatic reconstructions from ice cores drilled in areas of high melt: Journal of Glaciology, v. 43, no. 143, p. 90–97.

Koerner, R.M., Bourgeois, J.C., and Fisher, D.A., 1988, Pollen analysis and discussion of time-scales in Canadian ice cores: Annals of Glaciology, v. 10, p. 85–91.

Koerner, R.M., and Fisher, D.A., 1990, A record of Holocene summer climate from a Canadian High-Arctic ice core: Nature [London], v. 343, no. 6259, p. 630–631.

Koerner, R.M., Fisher, D.A., and Paterson, W.S.B., 1987, Wisconsin and pre-Wisconsin ice thicknesses on Ellesmere Island, Canada—Inferences from ice cores: Canadian Journal of Earth Sciences, v. 24, no. 2, p. 296–301.

Koerner, R.M., and Lundgaard, Leif, 1995, Glaciers and global warming: Géographie Physique et Quaternaire, v. 49, no. 3, p. 429–434.

Koerner, R.M., and Paterson, W.S.B., 1974, Analysis of a core through the Meighen Ice Cap, Arctic Canada, and its paleoclimatic implications: Quaternary Research, v. 4, no. 3, p. 253–263.

Koerner, R.M., Paterson, W.S.B., and Krouse, H.R., 1973, $\delta^{18}O$ profile in ice formed between the equilibrium and firn lines: Nature (Physical Science), v. 245, no. 148, p. 137–140.

Krabill, W.B., Thomas, R.H., Martin, C.F., Swift, R.N., and Frederick, E.B., 1995, Accuracy of airborne laser altimetry over the Greenland ice sheet: International Journal of Remote Sensing, v. 16, no. 7, p. 1211–1222.

Maaq, H., 1969, Ice dammed lakes and marginal drainage on Axel Heiberg Island, Canadian Arctic Archipelago: Montréal, Québec, McGill University, Axel Heiberg Island Research Reports, 147 p.

Mock, S.J., 1968, Snow accumulation studies on the Thule Peninsula, Greenland: Journal of Glaciology, v. 7, no. 49, p. 59–76.

Mohr, J.J., Reeh, N., and Madsen, S.N., 1998, Three-dimensional glacier flow and surface elevation measured with radar interferometry: Nature [London], v. 391, no. 6664, p. 273–276.

Müller, Fritz, 1961, Preliminary report 1959–1960, Jacobsen-McGill Arctic Research Expedition to Axel Heiberg Island: Montréal, Québec, McGill University, 219 p.

———1963a, Accumulation Studies, in Preliminary report 1961–62: Montréal, Québec, McGill University, Axel Heiberg Research Reports, p. 7–26.

———1963b, Surveying of glacier movement and mass changes, in Preliminary report 1961–62: Montréal, Québec, McGill University, Axel Heiberg Research Reports, p. 65–80.

———1966, Evidence of climatic fluctuations on Axel Heiberg Island, Canadian Arctic Archipelago, in Fletcher, J.O., ed., Symposium on the Arctic heat budget and atmospheric circulation, Santa Monica, Calif., 1966, Proceedings, Rand Corporation, p. 136–156.

———1969, Was the Good Friday Glacier on Axel Heiberg Island surging?: Canadian Journal of Earth Sciences, v. 6, no. 4, pt. 2, p. 891–894.

———1976, On the thermal regime of a High-Arctic valley glacier: Journal of Glaciology, v. 16, no. 74, p. 119–133.

Müller, F., and Keeler, C.M., 1969, Errors in short-term ablation measurements on melting ice surfaces: Journal of Glaciology, v. 8, no. 52, p. 91–105.

Müller, F., and others, 1978, Investigations of glaciers in the North Water area, in North Water Project, progress report no. 5: Zürich, Eidenössische Technische Hochschule (ETH), and Montréal, Québec, McGill University, unpublished report, p. 126–134.

Narod, B.B., and Clarke, G.K.C., 1983, UHF radar system for airborne surveys of ice thickness: Canadian Journal of Earth Sciences, v. 20, no. 7, p. 1073–1086.

Nye, J.F., 1963, The response of a glacier to changes in the rate of nourishment and wastage: Royal Society of London Proceedings, series A, v. 275, p. 87–112.

Nye, J.F., Berry, M.V., and Walford, M.E.R., 1972, Measuring the change in thickness of the Antarctic ice sheet: Nature (Physical Science), v. 240, no. 97, p. 7–9.

Ommanney, Simon, 1970, The Canadian glacier inventory, in Glaciers: Ottawa, Ontario, Secretariat Canadian National Committee for the International Hydrological Decade, p. 23–30.

Østrem, G., and Brugman, M., 1991, Glacier mass-balance measurements, a manual for field and office work: Saskatoon, Saskatchewan, Environment Canada, National Hydrology Research Institute (NHRI) Science Report 4, 224 p.

Oswald, G.K.A., 1975, Investigation of sub-ice bedrock characteristics by radio-echosounding: Journal of Glaciology, v. 15, no. 73, p. 75–87.

Paterson, W.S.B., 1968, A temperature profile through the Meighen Ice Cap, Arctic Canada: International Association of Hydrological Sciences, Publication 89, p. 440–449.

———1969, The Meighen Ice Cap, Arctic Canada—Accumulation, ablation and flow: Journal of Glaciology, v. 8, no. 54, p. 341–352.

———1976, Vertical strain-rate measurements in an Arctic ice cap and deductions from them: Journal of Glaciology, v. 17, no. 75, p. 3–12.

———1994, The physics of glaciers, (3d ed.): Oxford, Pergamon Press, 480 p.

Paterson, W.S.B., and Koerner, R.M., 1974, Radio echo sounding on four ice caps in Arctic Canada: Arctic, v. 27, no. 3, p. 225–233.

Paterson, W.S.B., Koerner, R.M., Fisher, D.A., Johnsen, S.J., Clausen, H.B., Dansgaard, W., Bucher, P., and Oeschger, H., 1977, An oxygen-isotope climatic record from the Devon Island ice cap, Arctic Canada: Nature [London], v. 266, no. 5602, p. 508–511.

Post, Austin, 1975, Preliminary hydrography and historic terminal changes of Columbia Glacier, Alaska: U.S. Geological Survey Hydrological Investigations Atlas HA-559, 3 sheets.

Reeh, Niels, Madsen, S.N., and Mohr, J.J., 1999, Combining SAR interferometry and the equation of continuity to estimate the three-dimensional glacier surface-velocity vector: Journal of Glaciology, v. 45, no. 151, p. 533–538.

Schytt, V., 1949, Re-freezing of melt water on the surface of glacier ice: Geografiska Annaler, v. 31, nos. 1–4, p. 222–227.

———1955, Glaciological investigations in the Thule Ramp area [Greenland]: Wilmette, Ill., U.S. Army Corps of Engineers, Snow, Ice, and Permafrost Research Establishment (SIPRE) Report 28, 88 p.

Serreze, M., and Bradley, R.S., 1983, Topoclimatic studies of a small plateau ice cap, northern Ellesmere Island, N.W.T., Canada [abs.], *in* Arctic Workshop, 12th, Amherst, Mass., 1983, Abstracts: Amherst, Mass., University of Massachusetts, Department of Geology and Geography, Contribution 44, p. 57–59.

Skidmore, M.L., and Sharp, M.J., 1999, Drainage system behaviour of a High-Arctic polythermal glacier: Annals of Glaciology, v. 28, p. 209–215.

Stiévenard, M., Nikolaëv, V., Bol'shiyanov, D.Y., Fléhoc, C., Jouzel, J., Klementyev. O.L., and Souchez, R., 1996, Pleistocene ice at the bottom of the Vavilov ice cap, Severnaya Zemlya, Russian Arctic: Journal of Glaciology, v. 42, no. 142, p. 403–406.

Williams, R.S., Jr., Hall, D.K., and Benson, C.S., 1991, Analysis of glacier facies using satellite techniques: Journal of Glaciology, v. 37, no. 125, p. 120–128.

Williams, R.S., Jr., Hall, D.K., Sigurðsson, O., and Chien, J.Y.L., 1997, Comparison of satellite-derived with ground-based measurements of the fluctuations of the margins of Vatnajökull, Iceland: 1973–1992: Annals of Glaciology, v. 24, p. 72–80.

Glaciers of North America–

GLACIERS OF CANADA

GLACIERS OF THE ARCTIC ISLANDS

ELLESMERE ISLAND ICE SHELVES AND ICE ISLANDS

By MARTIN O. JEFFRIES

SATELLITE IMAGE ATLAS OF GLACIERS OF THE WORLD

Edited by RICHARD S. WILLIAMS, Jr., *and* JANE G. FERRIGNO

U.S. GEOLOGICAL SURVEY PROFESSIONAL PAPER 1386-J-1

*Ellesmere Island, Nunavut, has ice shelves in several fjords along its northwest coast. They can be classified into three types: sea ice (Ward Hunt Ice Shelf), glacier (Milne Ice Shelf), and composite (*Alfred Ernest Ice Shelf*). Some ice shelves and ice plugs (multiyear landfast sea ice) calve and are the source of ice islands such as* Hobson's Choice ice island *that drift around the Arctic Ocean*

CONTENTS

GLACIERS OF NORTH AMERICA–

GLACIERS OF CANADA

GLACIERS OF THE ARCTIC ISLANDS

ELLESMERE ISLAND ICE SHELVES AND ICE ISLANDS

By MARTIN O. JEFFRIES[1]

Abstract

Within fjords along the northwest coast of Ellesmere Island, Nunavut, are several types of ice shelves. Three types have been recognized: sea ice, such as the Ward Hunt Ice Shelf; glacier, such as the Milne Ice Shelf; and composite, such as the *Alfred Ernest Ice Shelf*. Ice plugs, such as the *Nansen Ice Plug*, which are composed of multiyear landfast sea ice, and ice shelves are the source of ice islands, such as *Hobson's Choice ice island*, that drift around the Arctic Ocean. Satellite images are used to characterize the types of ice shelves, ice plugs, and ice islands. Because of winter darkness and persistent summer cloud cover, satellite synthetic aperture radar is the preferred source of image data to identify the changes in, map the areal extent of, and establish a baseline for ice shelves. Ellesmere Island ice shelves have existed since the middle Holocene Epoch and were more extensive in the past. The warming interval during the 20th century has caused a marked reduction in their areal extent. Ice islands are another element of the cryosphere that can be monitored by the use of satellite imagery and can serve as an indicator of climatic amelioration.

Introduction

Ice shelf: "A sheet of very thick ice, with a level or gently undulating surface, which is attached to the land along one side but most of which is afloat and is bounded on the seaward side by a steep cliff **ice front** rising 2–50 m or more above sea level" (Jackson, 1997, p. 317).

Ice island: "A form of large **tabular iceberg** broken away from an ice shelf and found in the Arctic Ocean, having a thickness of 15–20 m and an area between a few thousand square meters and 500 sq km or even more. The surface of an ice island is usually marked by broad, shallow, regular undulations that give it a ribbed appearance from the air" (Jackson, 1997, p. 316).

The first ice island, named *T–1*[2], was seen in 1946, when a U.S. Army Air Force (USAAF) reconnaissance mission over the Arctic Ocean reported a heart-shaped ice mass that had dimensions of 24x29 km and an area of about 500 km^2 surrounded by sea ice (Koenig and others, 1952). Subsequently, ice islands *T–2, T–3, T–4*, and *T–5* were observed from the air or identified on aerial photographs between 1946 and 1950 in the Arctic Ocean, and 59 unnamed ice islands were found in aerial photographs of the Canadian Arctic Archipelago taken in 1950 (Koenig and others, 1952).

Manuscript approved for publication 7 March 2002.

[1] Geophysical Institute, University of Alaska Fairbanks, 903 Koyukuk Drive, P.O. Box 757320, Fairbanks, Alaska 99775–7320.

[2] The names in this section conform to the usage authorized by the Secretariat of the Canadian Permanent Committee on Geographic Names (CPCGN); URL address: [http://GeoNames.NRCan.gc.ca/]. The Website is maintained by the Secretariat through Geomatics Canada, Natural Resources Canada, and combines the CPCGN server with the Canadian Geographical Names Data Base (CGNDB). Variant names and names not listed in the CPCGN/CGNDB are shown in italics.

The undulating surface topography of ice islands is accentuated in summer when meltwater lakes form in the troughs (fig. 1). An ice shelf having a similar topography of ridges and water-filled troughs (fig. 2) was observed in 1951 during U.S. Air Force (USAF) reconnaissance missions between Nansen Sound and Ward Hunt Island on the north coast of Ellesmere Island, Nunavut (fig. 3). Little doubt existed that the *Ellesmere Ice Shelf*, as it was initially called (Hattersley-Smith and others, 1955; Crary, 1958, 1960), was the source of the ice islands.

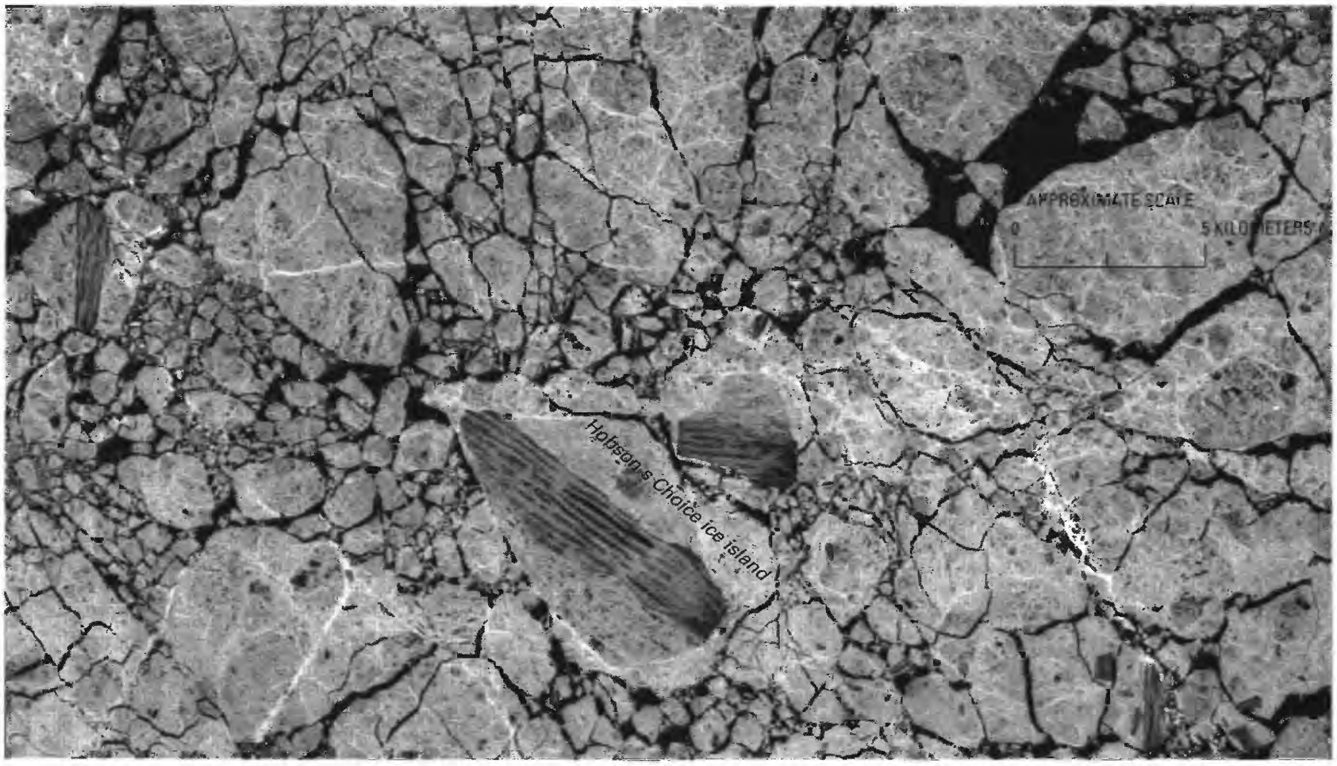

Figure 1.*—Subscene of a SPOT–1 image of* Hobson's Choice ice island *and 19 smaller ice islands on 25 July 1988.* Hobson's Choice ice island *calved from the east side of Ward Hunt Ice Shelf in 1982–83 (see fig. 4). Image number HRV2 061–108 250788 is from SPOT Image Corporation.*

Figure 2.*—Left-looking (high-angle oblique) trimetrogon aerial photograph of the Ward Hunt Ice Shelf acquired by the Royal Canadian Air Force in August 1950 from 6,096 m. The ice shelf north (to the left) of the ice rise and Ward Hunt Island ceased to exist in 1961–62, when almost 600 km^2 of ice calved. Photograph number T404L–3 from the National Air Photo Library, Ottawa, Canada.*

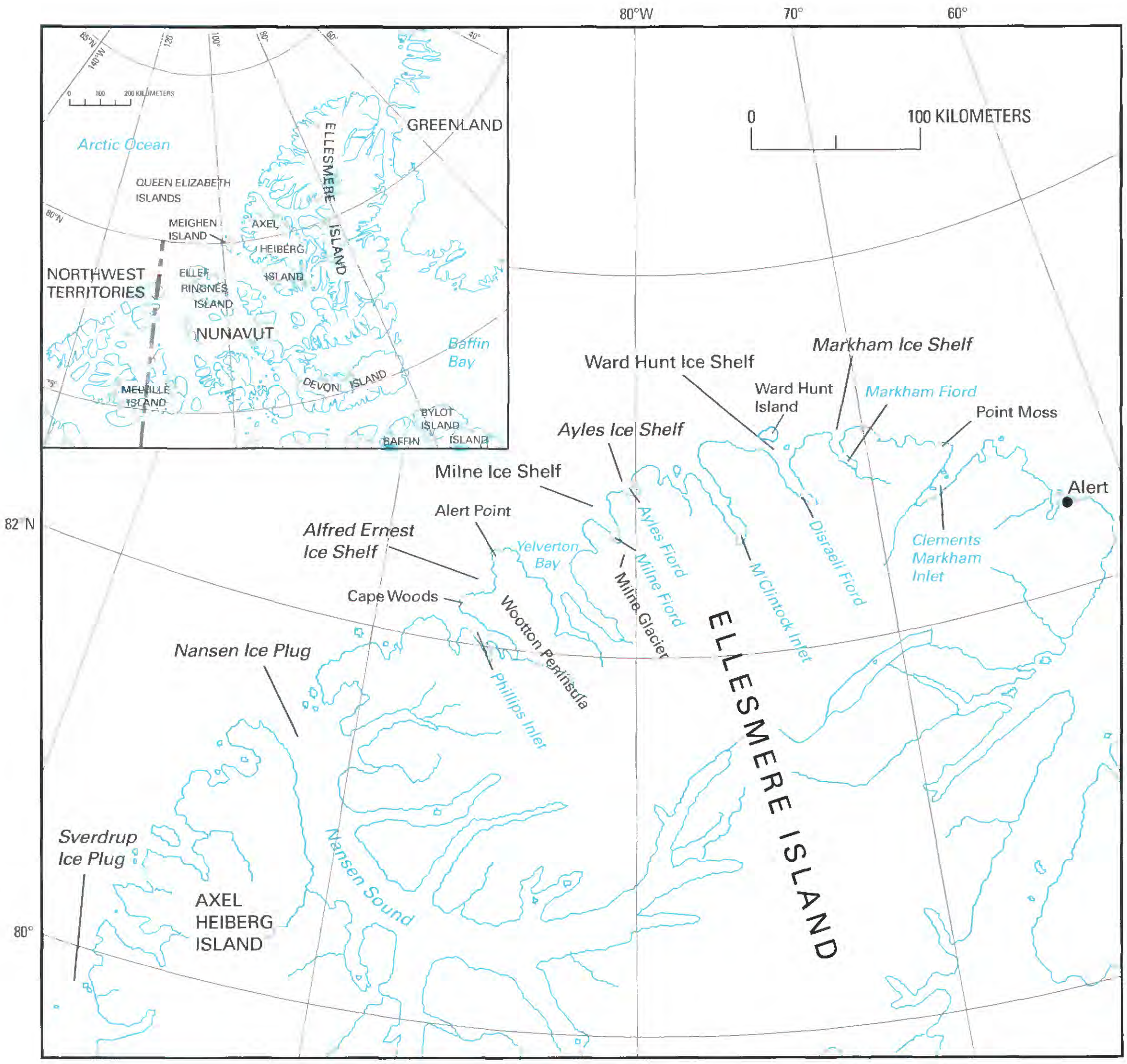

***Figure 3.**—Northern part of Ellesmere Island, Queen Elizabeth Islands, Nunavut, Canada, showing the location of the largest remaining ice shelves (*Markham Ice Shelf, *Ward Hunt Ice Shelf,* Ayles Ice Shelf, *Milne Ice Shelf, and* Alfred Ernest Ice Shelf*), as well as other locations mentioned in the text.*

The first to describe the undulating surface of the ice along the north coast of Ellesmere Island was Lt. Pelham Aldrich (Royal Navy) in 1876. Man-hauling a sledge on what is now known as the Ward Hunt Ice Shelf and looking west across the mouth of Disraeli Fiord, Aldrich wrote: "Several low ridges from 30 to 40 feet high, and varying from a few hundred yards to about a mile in length, show up in front of the cliffs. Their general direction being SE to NW, hence on the east coast of the bay to the south-westward they are nearly parallel with it. I imagine these ridges are composed of hard ice under the snow..." (Parliamentary Paper, 1877, p. 201–202). As the party passed between Ward Hunt Island and the mainland (fig. 2), he wrote: "...we crossed a ridge about 30 feet high, and a half mile in width, which runs quite a mile from about the middle of the south shore...Similar looking ridges extended to the eastward and westward of the island" (Parliamentary Paper, 1877, p. 201–202).

Thirty years later, on what is now known as the Ward Hunt Ice Shelf, Peary (1907, p. 185) noted the difficulty of dog-sled travel, which "was accentuated in the series of rolling swells which are a feature of this ice-foot? (sic) along here. These swells are on a large scale...if they are not huge drifts I do not know how to account for them. Off Ward Hunt Island and especially the western end, they are particularly marked, and here they blend into drifts formed in the lee of the island."

Elsewhere along the coast, Peary described the ice topography thus: "...what later became a constant and striking feature of the glacial fringe, the long, prairie-like swells of its surface..." (Peary, 1907, p. 181) and "...a gigantic potato field with a long blue lake or rushing stream in every furrow" (Peary, 1907, p. 220). Although Peary considered the ice surface to be a "watery hell" (Peary, 1907, p. 225), he also predicted that "the glacial fringe" "will form one of the most unique and interesting features of this region to the glacialist..." (Peary, 1907, p. 240).

The historical record suggests that the "glacial fringe" was a single ice shelf that extended from Point Moss to Nansen Sound (fig. 3), hence, the so-called *Ellesmere Ice Shelf*. At the beginning of the 20th century, it had an estimated area of 7,500 km^2 (Jeffries, 1987). A single, continuous *Ellesmere Ice Shelf* no longer exists; its disintegration, which produced the ice islands, has left a number of smaller ice shelves isolated in fjords, inlets, and bays (fig. 3). These are the Ellesmere Island ice shelves, and they are unique in North America.

Peary showed remarkable foresight with respect to the interest of "the glacialist" in the "glacial fringe." In 1953 and 1954, the Defence Research Board of Canada and the Geological Survey of Canada conducted the first glaciological, geophysical, geological, and oceanographic surveys of the *Ellesmere Ice Shelf* (Hattersley-Smith and others, 1955; Crary, 1958, 1960). Since then, numerous glaciological and related investigations have been made of the Ellesmere Island ice shelves, and a number of ice islands have been used as platforms for drifting scientific research stations in the Arctic Basin, for example, *T–3*, *ARLIS–II,* and *Hobson's Choice ice island* (fig. 1). Most scientific investigations have been on-site programs. Remote sensing has not been widely used, although imagery has been available since the first aerial photography missions of the late 1940's. Available remote sensing data now include oblique and vertical aerial photographs, Satellite pour l'Observation de la Terre (SPOT) and Landsat imagery, airborne real aperture radar (RAR), airborne and spaceborne synthetic aperture radar (SAR), and the like.

This paper describes the origin and age of the ice shelves, the different types of ice shelves (sea-ice, glacier-ice, and composite-ice shelves), the origin of the undulating surface topography, the impact of ice shelves on coastal oceanography, ice-shelf regrowth, ice islands, and ice plugs. European Remote Sensing Satellite (ERS–1) and RADARSAT SAR, Landsat, and SPOT images are used to illustrate a variety of physical characteristics and processes of the Ellesmere Island ice shelves and ice islands.

Origin and Age of the Ellesmere Ice Shelves

Most of the Earth's ice shelves are located in Antarctica, where they are almost all seaward extensions of the grounded Antarctic ice sheet. The glaciers and ice streams that flow into the large embayments of the Antarctic continent are further nourished at the surface by accumulating snow and, in places, by basal accretion of sea ice. Massive tabular icebergs calve from the Antarctic ice shelves. The largest ice shelf on Earth is the Ross Ice Shelf, West Antarctica (525,840 km^2: Swithinbank, 1988, p. B12). The calving of iceberg B–15 (37x295 km, 10,900 km^2) and a number of smaller icebergs from the Ross Ice Shelf in March 2000 reduced its area by 3 percent or less (S.S. Jacobs, oral commun., August 2000).

The Ellesmere Island ice shelves and ice islands are dwarfed by comparison with their Antarctic counterparts. *T–2* (700 km^2) was the largest reported ice island in this area (Koenig and others, 1952). The calving of almost 600 km^2 of ice from the Ward Hunt Ice Shelf in 1961–62 reduced its area by more than 50 percent (Hattersley-Smith, 1963). In 1998, Ward Hunt Ice Shelf had an area of 490 km^2 (Vincent and others, 2001). The

Ellesmere Island ice shelves have a total area of approximately 1,350 km^2 (Jeffries, 1987). Though they are much smaller, the Ellesmere Island ice shelves are no less scientifically significant than the Antarctic ice shelves.

Koenig and others (1952) recognized that some parts of the *Ellesmere Ice Shelf* were receiving inflow from grounded glaciers and other parts were not. Lemmen and others (1988a, 1988b) considered the Ellesmere Island ice shelves to be composed of genetically, dynamically, and geomorphologically distinct systems, and they proposed a simple genetic classification to differentiate among a *sea-ice ice shelf*, a *glacial- [sic, glacier-] ice shelf*, and a *composite-ice shelf*. *Sea-ice ice shelf* refers to an ice shelf that is primarily composed of multiyear landfast sea ice and has a freeboard of more than 2 m. Glacier input is either absent or negligible, although ice rises (where the ice shelf is grounded on the sea floor) may be found in and adjacent to sea-ice shelves. *Glacial- [sic, Glacier-] ice shelf* refers to an ice shelf that is, or has been, nourished directly from grounded (glacier) ice. *Composite-ice shelf* refers to an ice shelf that is composed of significant amounts of both glacier ice and sea ice. Surface accumulation and bottom freezing, as well as surface ablation and bottom melting, are known to take place or have taken place at the Ward Hunt Ice Shelf, a *sea-ice ice shelf* (see next section). It is reasonable to presume that the same processes are present at the other types of ice shelves.

Glaciological and geomorphological studies, along with radiocarbon dating of driftwood, marine mammals, and shells, indicate that the Ellesmere Island ice shelves are Holocene in age (Bradley, 1990; Evans and England, 1992). The *sea-ice ice shelves* began to form at about 4.5 kilo-annum (ka, 10^3 years) (before the present, present defined by geochronologists as A.D. 1950) during a middle Holocene climatic deterioration. Prior to that, the Pleistocene glaciers had retreated to behind their present positions, the summer sea-ice cover was much less severe with predominantly open water compared with modern conditions, and no ice shelves were present (Evans and England, 1992). The timing of glacier readvance and formation of the *glacial [sic, glacier] ice shelves* and the glacier component of the *composite ice shelves* is more difficult to ascertain. Some large glaciers are still advancing in response to the middle Holocene climatic deterioration, and some glaciers display evidence of dual advances, which may reflect both the middle Holocene and "Little Ice Age" (400–100 years before present) accumulations (Evans and England, 1992).

Ice-Shelf Types

Sea Ice: Ward Hunt Ice Shelf

The Ward Hunt Ice Shelf lies across the mouth of Disraeli Fiord (figs. 2,3, and 4) and is the most studied of the Ellesmere Island ice shelves. The undulating surface topography is manifested as a faintly ribbed texture in the SAR image (fig. 4). The undulations are commonly called "rolls" (Hattersley-Smith, 1957). On the western part of the ice shelf (the area to the west of Ward Hunt Island), the rolls have a mean (±1 standard deviation) wavelength of 267±60 m, whereas those on the eastern ice shelf (the area to the east of Ward Hunt Island) have a mean wavelength of 212±42 m (Jeffries and others, 1990). Interest in the rolls has centered primarily on their origin (see "Surface Topography" section). More recently, it has been found that the meltwater lakes on the Ward Hunt Ice Shelf harbor complex and productive microbial ecosystems that offer the opportunity to understand the Proterozoic fossil record and life on "snowball Earth" (Vincent and others, 2001).

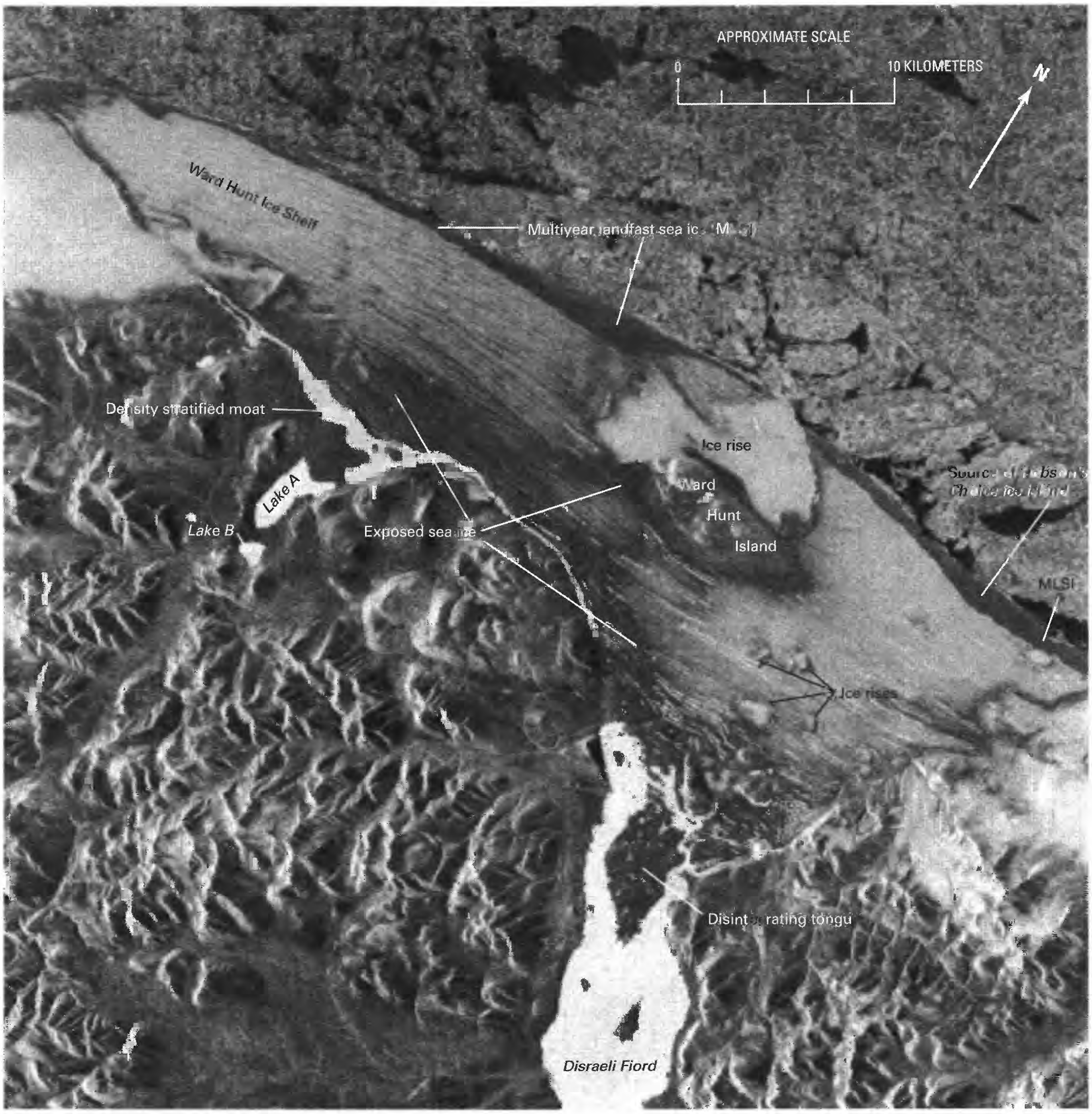

Figure 4.—Subscene of a radiometrically calibrated RADARSAT Standard Beam 5 (ST5) SAR image of the Ward Hunt Ice Shelf on 26 May 1998 that has a spatial resolution of 150 m and a pixel spacing of 100 m. Image number R113353209 from the Alaska SAR Facility. Original image is © CSA (Canadian Space Agency).

Radiocarbon dates for basally accreted marine organic compounds collected at the ice-shelf surface range between 4.5 and 3.3 ka (Lyons and Mielke, 1973). The former is the best estimate for the onset of ice-shelf formation in the middle Holocene (Evans and England, 1992). The youngest driftwood (3±0.2 ka) found along the shores of Disraeli Fiord (Crary, 1960) provides a maximum date for the complete blockage of the coast by the ice shelf (Evans and England, 1992). The only known ice rises in all the Ellesmere ice shelves are those in the Ward Hunt Ice Shelf (fig. 4). Heat-flow calculations indicate that they began to ground on the sea floor beginning at about 1.6 ka, the greatest growth taking place in the interval 1,000 to 150 years ago (Lyons and others, 1972).

Sea ice and brackish ice in ice cores reflect water salinity variability below the ice shelf (Lyons and others, 1971; Jeffries and Sackinger, 1989;

Jeffries, 1991a). This saline ice, which still has a high liquid-brine content (Jeffries, 1991a), is exposed at the surface of the ice shelf, particularly to the south and west of Ward Hunt Island (fig. 4). The dark SAR signature can be attributed to attenuation of the radar signal by the brine. The brighter SAR signatures of other parts of the ice shelf are probably due to volume scattering and strong returns from bubble-rich iced firn ("A mixture of ice and firn; firn permeated with meltwater and then refrozen," Jackson, 1997, p. 316) that overlies the sea ice.

Airborne radio-echosounding indicates that the entire area of ice shelf to the west and south of Ward Hunt Island contains sea ice and brackish ice, which has frustrated efforts to make ice-thickness measurements by electromagnetic means in these areas because of signal attenuation (Hattersley-Smith and others, 1969; Narod and others, 1988). However, seismic sounding and ice-temperature profiles in the western ice shelf indicate that it is up to 50 m thick (Crary, 1958; Lyons and others, 1972; Jeffries, 1991a).

Bottom reflections have been obtained by radio-echosounding over a large part of the eastern ice shelf. In 1966, the ice thickness was primarily in the range of 35–40 m, but some values were as high as 80 m (Hattersley-Smith and others, 1969). In 1981, the ice thickness was consistently 45–50 m (Narod and others, 1988). The acquisition of bottom reflections implied that no saline ice was present in much of the eastern ice shelf. This was confirmed by the nonsaline composition of a 42-m ice core (Jeffries and others, 1988, 1991) through *Hobson's Choice ice island* (fig. 1), which calved from the eastern ice shelf (fig. 4) in 1982–83 (Jeffries and Serson, 1983). The absence of sea ice in the eastern ice shelf has been attributed to bottom melting prior to 1952 (Jeffries and others, 1991).

The 42-m *Hobson's Choice* ice core was composed of 37 m of iced firn overlying a tritium-rich, 5-m-thick basal ice layer that had accreted since 1952 from freshwater flowing out of Disraeli Fiord (Jeffries and others, 1988, 1991). It has been estimated that the freshwater ice accreted at 1.3–1.9 times the rate of surface ablation (Jeffries, 1991b; Jeffries and others, 1991). Although the eastern ice shelf might have thickened slightly between the 1950's and the 1980's, evidence exists that significant thinning has taken place since the 1980's (Vincent and others, in 2001). This is discussed in the "Ice-Shelf Dams and Coastal Oceanography" section.

Glacier: Milne Ice Shelf

Milne Ice Shelf is the second largest of the Ellesmere ice shelves. It is 42-km long and extends from the mouth of Milne Fiord to the grounding line of Milne Glacier (figs. 5 and 6). The surface topography of the ice shelf is quite variable, as it has rolls that become shorter in wavelength as the distance from the ice-shelf front increases (fig. 5). The topographic variations are the basis for the division of the ice shelf into three units (outer, central, and inner) plus the floating part of the Milne Glacier (Jeffries, 1986).

Milne Glacier is 10–40 m thick seaward of the grounding line (Narod and others, 1988). In addition to an undulating surface, the floating ice is characterized by a number of moderately contorted medial moraines (fig. 5) that might be evidence that Milne Glacier is a surge-type glacier (Jeffries, 1984). Between 1950 and 1959, the glacier advanced at about 10 m a^{-1}; no advance took place between 1959 and 1966 (Hattersley-Smith and others, 1969). A comparison of the 1959 aerial photography and the SPOT image (fig. 5) indicates that the glacier advanced 2.5 km between 1966 and 1988. A comparison of the SPOT image and the RADARSAT image (fig. 6) indicates that the glacier advanced 2 km at 165 m a^{-1} between 1988 and 2000. These speeds are not as high as those associated with true surge-type glaciers, but they are high for a polar glacier.

__Figure 5.__— SPOT–1 haute (high) resolution visible (HRV) [high-resolution visible spectrum] image of the Milne Ice Shelf on 8 August 1988. The ice shelf is composed of the floating part of Milne Glacier north of the glacier grounding line, and the inner, central, and outer units. Abbreviation: MLSI, multiyear landfast sea ice. Image number HRV1 086–122080888 is from the SPOT Image Corporation.

No radio-echosounding bottom echoes were obtained from the inner unit (Narod and others, 1988), but ice-core drilling has shown the ice to be as little as 3 m thick (M.O. Jeffries, unpub. data, 1983). Short-wavelength (60–100 m, Jeffries, 1986), curvilinear rolls are evident in the SPOT image (fig. 5) but not in the SAR image (fig. 6). Also, the textureless SAR signature of the inner unit is brighter than that of the central and outer units (fig. 6). The bright signature might be due to surface scattering from rough ice deformed by the advance of Milne Glacier. This signature is also similar to that of Disraeli Fiord (fig. 4) where evidence exists that the cause is the same. This is discussed in the "Ice-Shelf Dams and Coastal Oceanography" section.

The central unit is 10–100 m thick (Narod and others, 1988) and is derived from tributary glaciers (figs. 5 and 6: numbers 1, 2, 3, and 6) flowing in from the east and west sides of Milne Fiord (Jeffries, 1986). The thickest ice is found in a tongue extending seaward of glacier 2 (Narod and others, 1988). The rolls (150–180 m wavelength, Jeffries, 1986) on the

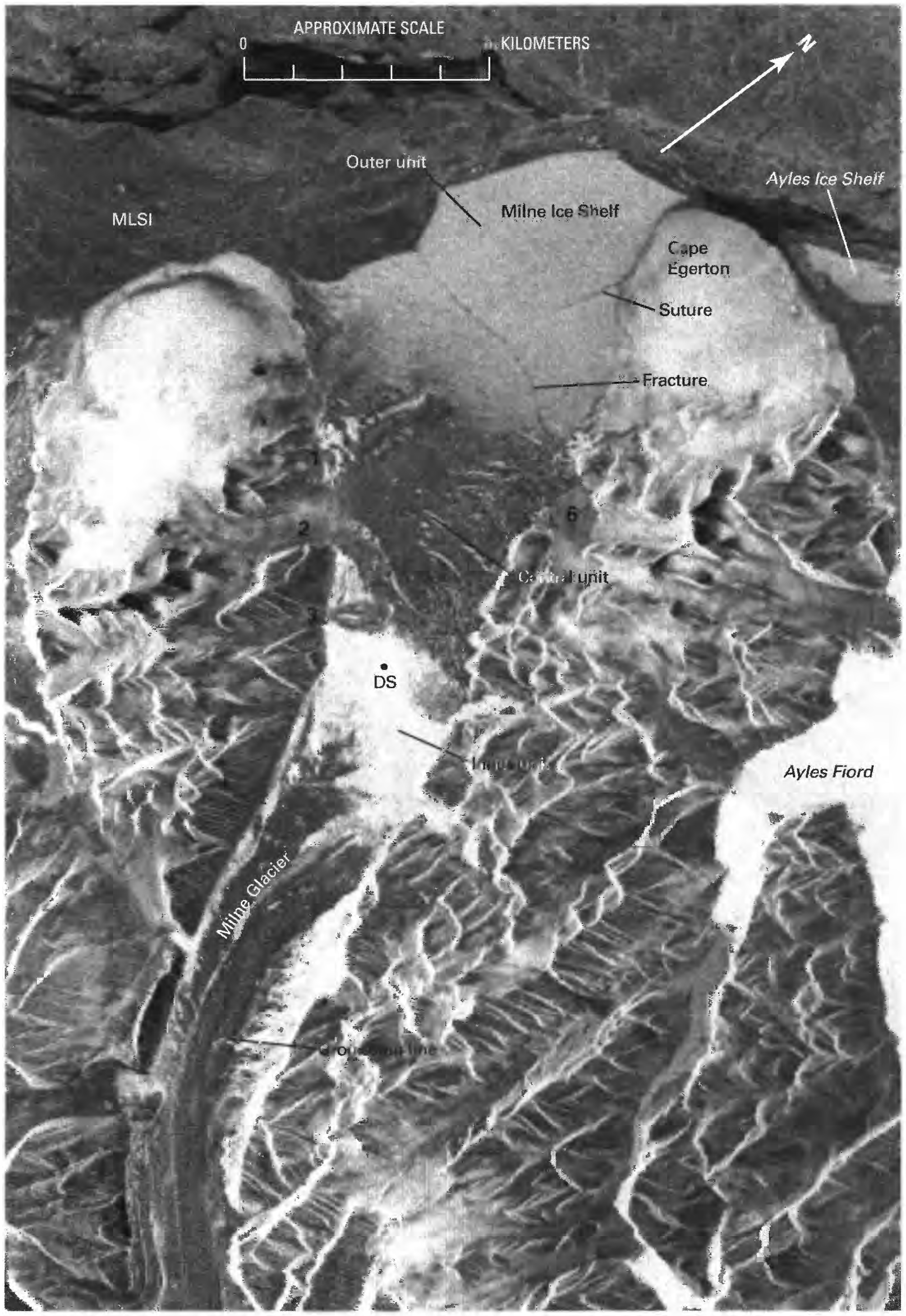

***Figure 6.**—Subscene of a radiometrically calibrated RADARSAT Standard Beam 1 (ST1) SAR image of the Milne Ice Shelf on 13 April 2000 that has a spatial resolution of 150 m and a pixel spacing of 100 m. Tributary glaciers flowing into the central unit are identified by 1, 2, 3, and 6 (after Jeffries, 1986). DS identifies the location where density stratification was observed below the ice in 1983 and 1984. Note multiyear landfast sea ice (MLSI). Image number R123185213 is from the Alaska SAR Facility. Original image is © CSA.*

central unit might be aligned with former crevasses (Hattersley-Smith, 1957), or they might reflect the flow lines of the glacier tongues derived from glaciers 1, 2, 3, and 6 (Jeffries, 1986). Extensive moraines composed of individual boulders many meters across and conical mounds of debris up to 10 m high attest to the glacial origin of the central unit (Jeffries, 1986). The debris-laden ice surface accounts for the dark tone in the SPOT image (fig. 5) and probably the dark signature of the SAR image (fig. 6).

The outer unit is 10–90 m thick, and the thickest ice is found in a tongue that extends west across the mouth of Milne Fiord from the ice field at Cape Egerton (Narod and others, 1988: fig. 6). If this thick tongue of ice is a glacier tongue, then it is likely a relict feature, as I have seen no evidence on the ground or from the air for glacier flow off the ice field today. The rolls on the outer unit have a mean wavelength of 330±62 m (Jeffries, 1986), and those adjacent to Cape Egerton are the most linear of the entire ice shelf (fig. 5). Rather than precluding a glacier origin for the outer unit, the linearity of the rolls might be due to prolonged and intense modification of the surface topography since the glacier advance from Cape Egerton.

Other features on the outer unit include a fracture and a suture (rehealed fracture) (fig. 6) that are also evident in 1959 aerial photographs (Jeffries, 1986). The precise origin of these features is unknown, although airborne radio-echosounding suggests that they might be associated with bottom crevasses where brackish or sea ice is accreting (Narod and others, 1988). Unlike the central unit, the outer unit is not debris-laden, and it has a bright SAR signature (fig. 6) probably due to volume scattering from the iced firn. Note the strong resemblance between the topography of the outer unit (fig. 5) and that of *Hobson's Choice ice island* (fig. 1).

Composite: *Alfred Ernest Ice Shelf*

The *Alfred Ernest Ice Shelf* occupies the bay between Alert Point and Cape Woods on Wootton Peninsula (figs. 3 and 7). Lemmen and others (1988b) described it as a composite-ice shelf that comprises an inner unit known to be glacial in origin, as it is derived from a valley glacier (A in fig. 7) and a trunk glacier (B), and an outer unit believed to have originated as sea ice. A radiocarbon date of 6.83±0.05 ka for a narwhal tusk at site N (fig. 7) suggests regionally abundant open water and locally no ice shelf at that time (Evans, 1989). A radiocarbon date of 4.31±0.07 ka for driftwood at site X (fig. 7) gives a maximum age for the sea-ice component (Lemmen and others, 1988b) that is consistent with the onset of formation of the Ward Hunt Ice Shelf. A radiocarbon date of 1.85±0.05 ka for marine shells from

Figure 7.—Subscene of a radiometrically calibrated RADARSAT SAR image of the Alfred Ernest Ice Shelf *on 5 April 2000 that has a spatial resolution of 150 m and a pixel spacing of 100 m. A and B identify a valley glacier and trunk glacier, respectively, and A_f and B_f are the floating tongues of those glaciers. DS is the location where density stratification was observed below the ice, and FW is the location where freshwater was found in a crack in the ice in May 1986. X and Y identify the locations of radiocarbon-dated driftwood and marine shells, respectively (Lemmen and others, 1988b). N identifies the location of a radiocarbon-dated narwhal tusk (Evans, 1989). Image number R123071212 is from the Alaska SAR Facility. Original image is © CSA.*

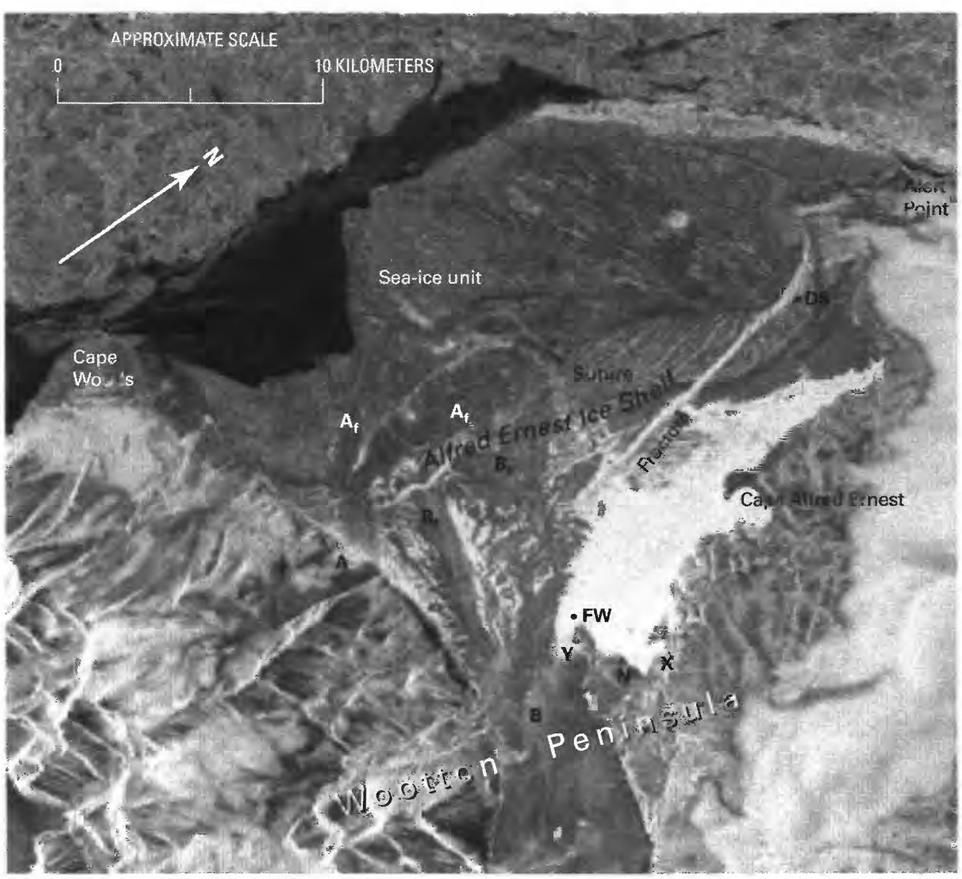

glacially thrust sediment at site Y (fig. 7) indicates that the glacier component of the ice shelf is quite young and postdates the sea-ice component.

Lemmen and others (1988b) note that the floating tongues of glaciers A and B have "surface patterns that are clearly related to transverse crevasse systems within the grounded ice." On these glacier tongues are also extensive moraines that have boulders and conical debris mounds similar to those on the Milne Ice Shelf (M.O. Jeffries, unpub. data, 1984, 1986). The sea-ice unit has some particularly dark SAR signatures that might denote sea ice exposed at the surface (fig. 7). The ribbed texture of the sea-ice unit is more pronounced than at Ward Hunt and Milne Ice Shelves (figs. 4 and 6), perhaps because of differences in the SAR incidence angle or illumination direction. The rolls on the sea-ice unit have a mean wavelength of 291±69 m (M.O. Jeffries, unpub. data, 1986).

Lemmen and others (1988b) describe a suture (fig. 7) along the east margin of the sea-ice unit and propose that it is a fracture caused by the advance of glacier B. They suggest that the suture has developed rolls since it opened. This might account for the ribbed texture of the suture (fig. 7), but given the present understanding of the processes governing the ice-surface topography (see next section), one would expect these rolls to be aligned parallel with rather than perpendicular to the rolls on the sea-ice unit.

In May 1986, I traveled on the surface of the suture and observed a number of open fractures oriented parallel with the ribbed texture. The fractures contained freshwater, and freeboard values of 0.1–0.2 m indicated relatively thin ice. The bright linear feature running through the suture and oriented parallel with the ribbed texture (fig. 7) is probably a particularly large and recent fracture. A comparison of airborne 1988 SAR data (fig. 4 in Jeffries, 1992) and 1993 ERS–1 data indicates that it opened after 1988. I suggest that the ribbed texture of the suture is due to scattering from old, rehealed fractures that record a history of glacier advances. These advances have progressively widened the suture since its initial opening at approximately 1.85 ka and have displaced the sea-ice unit seaward. The new fracture suggests the presence of some recent glacier activity.

The area adjacent to Cape Alfred Ernest and along the shore of Wootton Peninsula has a bright, textureless SAR signature (fig. 7). It is quite unlike the suture and the glacier- and sea-ice units, but it is similar to Disraeli Fiord (fig. 4) and the inner unit of the Milne Ice Shelf (fig. 6). The cause and implications of these bright signatures are discussed in the "Ice-Shelf Dams and Coastal Oceanography" section.

Surface Topography

The ice shelves and ice islands have a rolling topography of strongly aligned, bifurcating ridges and troughs, that is, the rolls (figs. 1, 2, and 5). Details of the numerous explanations for the origin of the rolls can be found elsewhere (Hattersley-Smith, 1957; Lister, 1962; Holdsworth, 1987). They are either genetic features that began to form at the time of ice-shelf formation or are superimposed features that developed after initial ice-shelf formation, or they are a combination of the two. On any given ice shelf or part of an ice shelf, the wavelength of the rolls is quite uniform and apparently increases as ice thickness increases (Hattersley-Smith, 1957). Jeffries and others (1990) found ice thickness (y) and roll wavelength (x) to be related by a polynomial expression,

$$y=0.1392x+0.0002826x^2-2.085\ m.$$

Of all the explanations for the rolls, the following meltwater-lake hypothesis has been given the most credence. In developing this hypothesis, Crary

(1960) observed that the orientation of the rolls is, in many places, parallel with the direction of prevailing winds and the shore. He suggested that winds blowing parallel to the coastline over an initially randomly distributed array of melt pools would cause them to become elongated as a result of solar heating of the water and wind-accelerated convection currents. The greater the number of summers that this happens, the more developed the rolls become.

The rolls are superimposed features according to the meltwater-lake-alignment hypothesis, but the hypothesis offers no explanation for the uniformity of their wavelength, the relationship between wavelength and ice thickness, and the bifurcations (Holdsworth, 1987). To account for these, Holdsworth hypothesized that the rolls form dynamically as an ice shelf is deformed. He showed analytically that (1) extreme pack-ice pressure against the edge of an ice shelf creates compressive strains that cause ice-shelf creep buckling at a critical stress level; (2) the undulations bifurcate because the compressive strains are nonhomogeneous as the extreme pack-ice pressure events take place over limited sections of the ice-shelf edge for limited periods of time; and (3) as the ice thickens, buckling due to further extreme events creates longer wavelength undulations. The genetic waveforms caused by the creep-buckling instabilities are perpetuated by the meltwater lakes (Holdsworth, 1987).

The creep-buckling-instability hypothesis was developed to explain the rolls on the Ward Hunt Ice Shelf but would apply to the other ice shelves, except where it can be shown that other processes are acting that are capable of compressing and buckling floating ice (Holdsworth, 1987). This would include those parts of the Milne Ice Shelf and *Alfred Ernest Ice Shelf* that are derived from the seaward advance of grounded glaciers. Although the outer unit of the Milne Ice Shelf may be glacier ice in origin, any rolls that were originally oriented parallel to ice flow lines or crevasses may have been modified due to exposure to the prevailing winds' blowing along the coast.

Ice-Shelf Dams and Coastal Oceanography

The ice cover on Disraeli Fiord, which lies to the south of the Ward Hunt Ice Shelf, has a bright, textureless SAR signature that contrasts with the darker, more textured signature of the ice shelf (fig. 4). No ice shelf is present in Disraeli Fiord, but the water there is strongly density stratified and has a layer of freshwater at the surface overlying seawater at greater depth (Keys, 1978; Jeffries, 1991b; Jeffries and Krouse, 1984; Vincent and others, 2001). It is stratified because meltwater that flows in from its catchment area is impounded behind the Ward Hunt Ice Shelf, and the perennial ice cover prevents wind-mixing.

Disraeli Fiord is covered with perennial lake ice that grows from the freshwater layer (Keys, 1978; Jeffries, 1985). The ice surface forms candles [disintegrates into ice prisms oriented perpendicular to the ice surface (Jackson, 1997, p. 94)] because of melting along grain boundaries in summer (Keys, 1978), and also many internal melt features are present (Jeffries, 1985). Consequently, the bright SAR signature is probably due to a combination of surface and volume scattering, plus any reflections from the ice-water interface. An equally bright SAR signature is observed at *Lakes A* and *B* (fig. 4), which are both density stratified and have perennial ice covers (Hattersley-Smith and others, 1970; Jeffries and others, 1984; Jeffries and Krouse, 1985). The bright signature of the moat along the south shore of the western ice shelf near *Lakes A* and *B* (fig. 4) suggests that it too is density stratified and covered with lake ice.

The freshwater ice found at the base of *Hobson's Choice ice island* was cited as evidence that some freshwater flows out of Disraeli Fiord below the ice-shelf dam, specifically below the eastern Ward Hunt Ice Shelf (Jeffries and others, 1988, 1991). In 1967, when the density stratification was discovered (Keys, 1978), the freshwater layer was 44.5 m thick; in 1983, it was 41 m thick (Jeffries, 1991b), and in 1999, it was 32 m thick (Vincent and others, 2001). It has always been assumed that the freshwater-layer thickness is equivalent to the mean draft of the ice shelf; hence, a 32-m draft was equivalent to a thickness of 35 m in 1999, which was 22 percent thinner than in 1983 and 27 percent thinner than in 1967 (Vincent and others, 2001). An increase in mean annual air temperature and melting degree days since 1967 suggests that the thinning of the freshwater layer is a genuine loss due to outflow beneath the ice shelf rather than a consequence of decreasing meltwater flow into Disraeli Fiord (Vincent and others, 2001).

Density stratification has also been observed at the Milne Ice Shelf and *Alfred Ernest Ice Shelf*. In May 1983 and 1984, a 17.5-m-thick freshwater layer was found below 3-m-thick lake ice in the inner unit of Milne Ice Shelf (M.O. Jeffries, unpub. data, 1983, 1984). With a bright SAR signature (fig. 6) similar to that on Disraeli Fiord (fig. 4), the inner unit is probably lake ice that has grown from freshwater impounded behind the central and outer units of Milne Ice Shelf. The inner unit of the Milne Ice Shelf, then, is not entirely glacier ice in origin, although it owes its unusual composition to the glacier-ice dam of the central and outer units. It is a hybrid that probably varies in composition according to the advance and retreat of Milne Glacier, as well as the hydrography of the fjord, as determined by the effectiveness of the ice-shelf dam.

In May 1986, a 7-m-thick layer of freshwater was found below 2-m-thick lake ice at the northern end of the *Alfred Ernest Ice Shelf* suture, and freshwater was observed in a seal hole in 2-m-thick ice at location FW (fig. 7) (M.O. Jeffries, unpub. data, 1986). The bright, textureless SAR signature of the ice adjacent to Cape Alfred Ernest and along the shore of Wootton Peninsula (fig. 7) suggests an extensive lake-ice cover that is growing from freshwater impounded behind the glacier- and sea-ice units of *Alfred Ernest Ice Shelf*.

Bright SAR signatures are found in other fjords and inlets of the north coast of Ellesmere Island: West Arm Yelverton Inlet, Ayles Fiord, Taconite Inlet, and M'Clintock Inlet (fig. 8). It is unlikely that the SAR signatures at these locations are due to surface and volume scattering from desalinated, near-surface layers of multiyear sea ice because the backscatter is significantly stronger than that from the multiyear ice on the nearby Arctic Ocean (fig.8). It is more likely that the bright SAR signatures denote lake ice and that these fjords and inlets are also density stratified because of ice dams that impound freshwater. Density stratification is widespread at the moment, but significant hydrographic changes at these locations might be detected by changes in the backscatter from the ice. For example, if an ice dam failed and the stratification broke down—or if the perennial ice melted, and the fjords and inlets were open each summer and subject to wind mixing—the SAR signature of the ice would become darker as the ice began to grow from seawater or brackish water.

Ice Islands, Ice-Shelf Regrowth, and Ice Plugs

Koenig and others (1952) suggested that winds, tides, and pack-ice pressure cause cracks to develop in ice shelves and hasten ice-island calving. Cracks might also develop because of thermal stress (Legen'kov, 1974). Holdsworth (1971) suggested that the massive calving from the Ward Hunt Ice Shelf

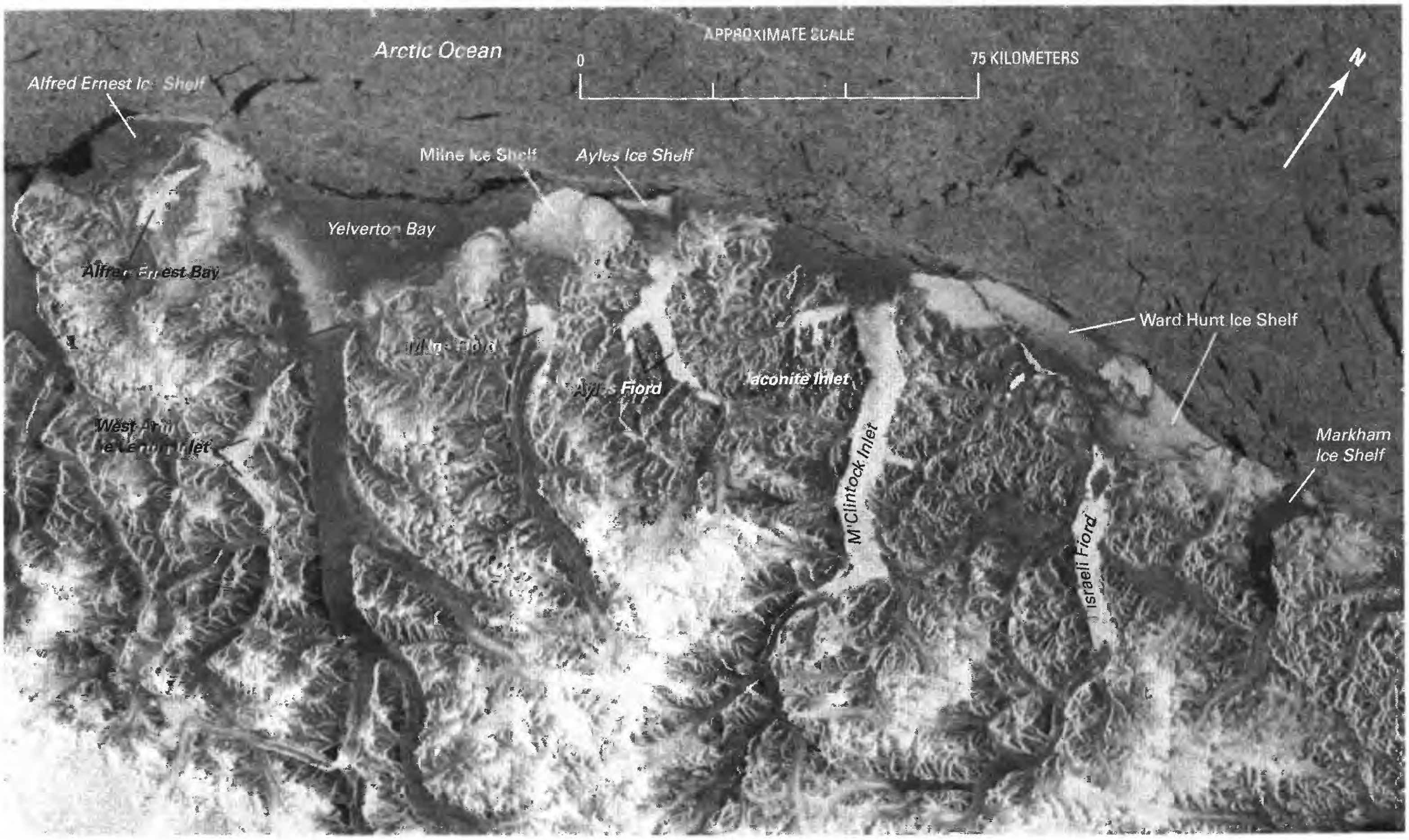

Figure 8.—Subscene of a radiometrically calibrated RADARSAT Wide Beam B ScanSAR image of northernmost Ellesmere Island on 8 April 2000 that has a spatial resolution of 150 m and a pixel spacing of 100 m. The five largest remaining ice shelves are marked; the bright SAR signature indicates an area where density stratification probably occurs from an ice dam that impounds freshwater. Image number R123114210 is from the Alaska SAR Facility. Original image is © CSA.

Shelf in 1961–62 might have been due to the coincidence of above-average tides and a seismic shock. Holdsworth and Glyn (1981) invoked a vibration mechanism, where ocean-wave energy intercepted by an ice shelf causes a resonant motion that raises stresses in the ice to the point that fracture results.

Ahlnäs and Sackinger (1988) proposed that calvings are triggered by persistent offshore winds. Frequently, after a major calving event, the lost shelf ice is replaced by multiyear landfast sea ice (MLSI). In February 1988, only 7–10 days after an episode of offshore winds, a piece of MLSI was observed by airborne SAR as it calved from the Milne Ice Shelf (Jeffries and Sackinger, 1990). The SPOT image (fig. 5) shows that that particular piece of MLSI did not move far in the 6 months after calving. ERS–1 SAR data show that the MLSI subsequently broke away completely (M.O. Jeffries, unpub. data, 1991), and the RADARSAT SAR image (fig. 6) shows that it has since been replaced by more MLSI.

Extensive areas of MLSI are observed along the north coast of Ellesmere Island, and in many cases, MLSI is found in areas that are known to have once been occupied by an ice shelf. Yelverton Bay (figs. 3, 5, and 8), the likely source of ice island *T–3* (Crary, 1960), is now covered with MLSI. Since the *M'Clintock Ice Shelf* disintegrated in the middle-1960's (Hattersley-Smith, 1967), MLSI containing ice-shelf fragments has covered the mouth of M'Clintock Inlet (fig. 8). The MLSI is a means by which the ice shelves regenerate after ice-island calvings, although the narrow strip of MLSI along the front of the Ward Hunt Ice Shelf (fig. 4), which has grown since the 1961–62 and 1982–83 calvings, is evidence that the replacement of lost ice shelf is often far from complete. The MLSI can be considered as incipient ice shelf and as analogous to the original sea-ice ice shelves.

The *Nansen Ice Plug* (fig. 9) is MLSI at the mouth of Nansen Sound (fig. 3) (Serson, 1972). The historical record (Peary, 1907, p. 203) suggests

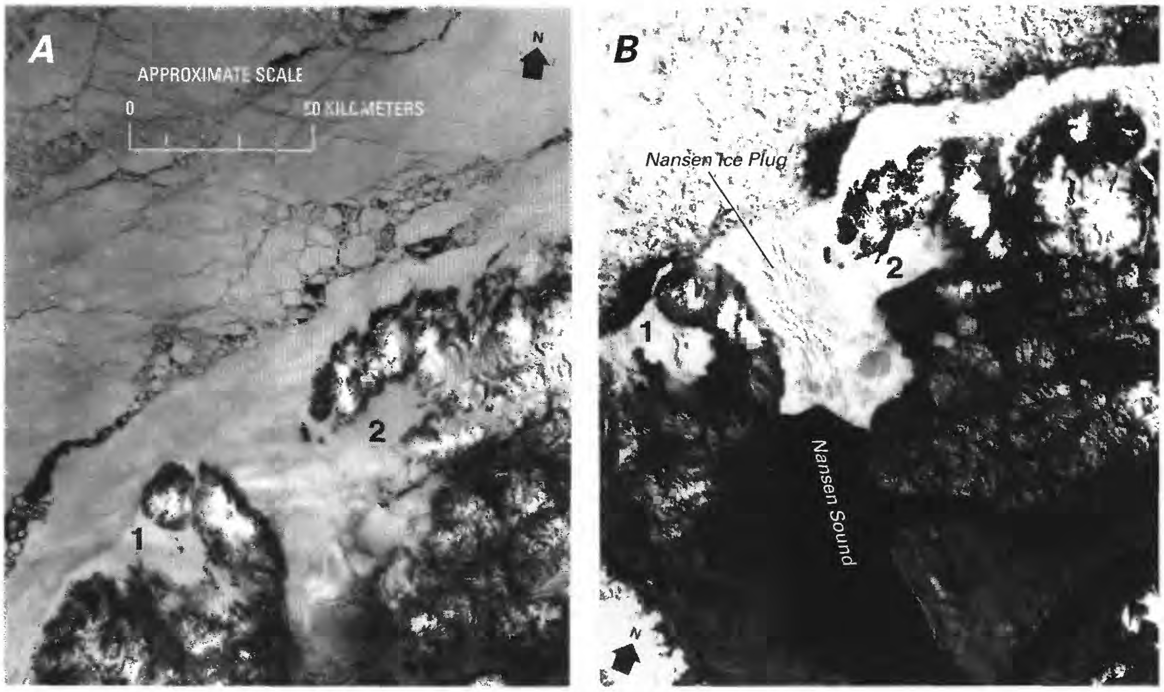

Figure 9.—Landsat multispectral scanner (MSS) images of the Nansen Ice Plug *on* **A**, *22 June 1990 and* **B**, *24 August 1990. Landsat image 52304–20574, band 4; 22 June 1990; Path 58, Row 247; and Landsat image 52367–20143, band 4; 24 August 1990; Path 51, Row 248, respectively, were acquired by the now-defunct Quick-Look Project satellite receiver at the Geophysical Institute, University of Alaska Fairbanks, Alaska. Numbers 1 and 2 are reference points that identify the same locations in each image.*

that an ice shelf was present in Nansen Sound at the beginning of the 20th century. The disintegration of that ice shelf or of a subsequent ice plug might have been the source of ice island *NP–6* (Serson, 1972). Figure 9 illustrates the effectiveness of the ice plug as a barrier to the movement of ice from the Arctic Ocean into Nansen Sound (fig. 3) and the Queen Elizabeth Islands (fig. 3 inset). A similar MLSI plug, the *Sverdrup Ice Plug*, is found in Sverdrup Channel between Axel Heiberg and Meighen Islands (fig. 3) (Serson, 1974). In Summer 1998, the warmest summer in the region since 1962, both the *Nansen* and *Sverdrup Ice Plugs* disintegrated for the first time since 1962 (Jeffers and others, 2001). The disintegration of these incipient ice shelves was not an isolated incident. Summer 1998 was a globally warm summer that saw a record reduction in the sea-ice cover of the Beaufort and Chukchi Seas (Maslanik and others, 1999) and the Queen Elizabeth Islands (Jeffers and others, 2001).

An abnormal reduction of the sea ice cover in the Queen Elizabeth Islands also took place in late summer and early autumn 1991 (Jeffries and Shaw, 1993). This allowed *Hobson's Choice ice island* (fig. 1) to drift rapidly south through the interisland channels, where it disintegrated between 13 October and 12 November 1991 (fig. 10) (Jeffries and Shaw, 1993). The demise of *Hobson's Choice ice island* was unfortunate as it forced the closure of the Canadian ice-island research station there. This station had promised to add significantly to geological, geophysical, meteorological, and oceanographic understanding of the Canadian Polar Margin (Hobson, 1989).

Conclusion

Ice shelves have existed along the north coast of Ellesmere Island since the middle Holocene when sea-ice ice shelves began to form in response to a climatic deterioration. The ice shelves were once much more extensive than they are today, and their current extent reflects a 20th century disintegration. The 20th century was a period of exceptionally high temperatures and climatic amelioration in the Canadian High Arctic (Bradley, 1990;

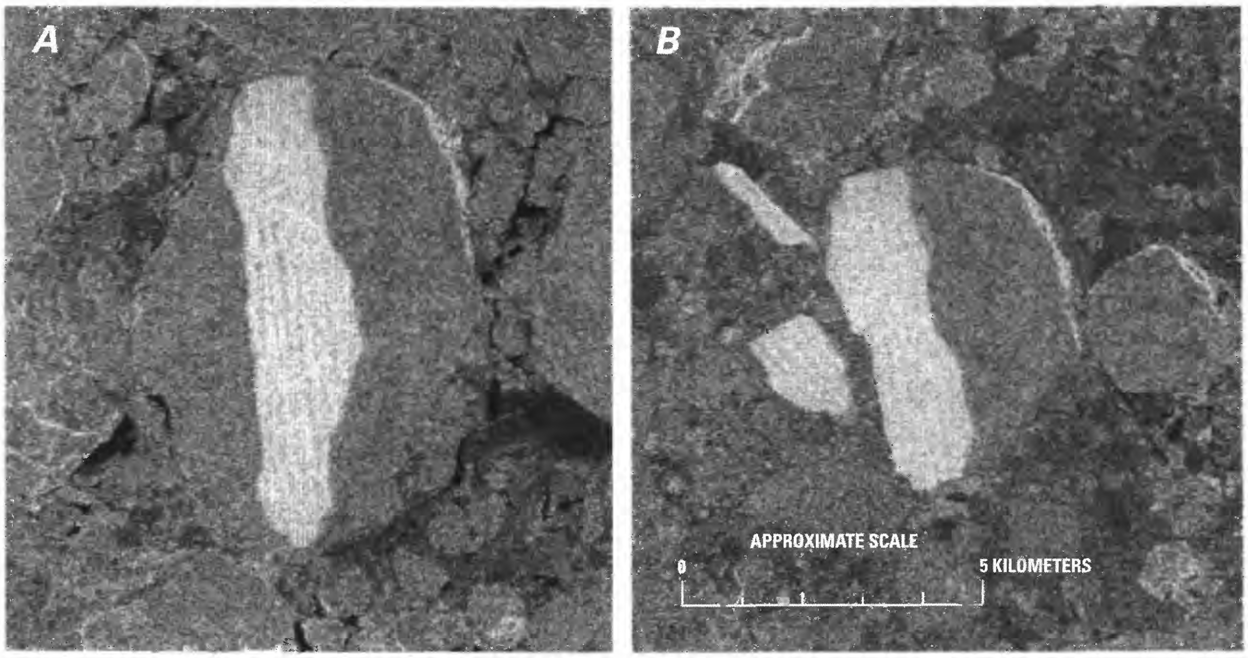

Figure 10.—Radiometrically calibrated ERS–1 SAR subscenes of Hobson's Choice ice island *on* **A**, *13 October 1991 and* **B**, *12 November 1991 as it drifted south through the channels of the Queen Elizabeth Islands and disintegrated into three large pieces and numerous smaller fragments. The spatial resolution is 30 m, and the pixel size is 12.5 m. Image numbers E101262195* (A) *and E101692193* (B) *are from the Alaska SAR Facility. Original images are © CSA.*

Evans and England, 1992), and it is reasonable to suppose that the disintegration of the *Ellesmere Ice Shelf* was a response to the pronounced warming during the last century (Jeffries, 1992). The apparent thinning of the Ward Hunt Ice Shelf in the 1980's–90's and the disintegration of the ice plugs in the late 1990's came about as significant changes were detected in the sea ice and hydrography of the Arctic Ocean (Dickson, 1999). It is difficult to ignore the connection between the state of the Ellesmere Island ice shelves, the state of the climate, and changes taking place elsewhere in the Arctic Basin. The ice shelves are bellwethers of climate change, which has the potential to cause further glaciological, hydrographic, and cryohabitat changes at these small but environmentally significant ice features (Vincent and others, 2000, 2001). Available ERS–1, ERS–2 and RADARSAT SAR data offer the opportunity to identify changes that may have taken place since 1991, as well as (1) to map the current areal extent of the ice shelves and (2) to establish a baseline for future monitoring. SAR instruments such as RADARSAT–2, ENVISAT, PALSAR, Ice, Cloud, and Land Elevation Satellite (ICESat), and current Earth Observing System (EOS) (*Terra*) instruments, such as the Moderate-Resolution Imaging Spectrometer (MODIS) and Advanced Spaceborne Thermal Emission and Reflection Radiometer (ASTER), offer unprecedented opportunities for the foreseeable future for change detection and impact assessment. These should increase the understanding of the Ellesmere Island ice shelves and ice islands and their relationship to climate variability.

References Cited

Ahlnäs, K., and Sackinger, W. M., 1988, Offshore winds and pack ice movement episodes off Ellesmere Island, *in* Sackinger, W.M., and Jeffries, M.O., eds., Port and ocean engineering under Arctic conditions: Fairbanks, Alaska, University of Alaska Fairbanks, Geophysical Institute, v. 3, p. 271–286.

Bradley, R.S., 1990, Holocene paleoclimatology of the Queen Elizabeth Islands, Canadian High Arctic: Quaternary Science Reviews, v. 9, no. 4, p. 365–384.

Crary, A.P., 1958, Arctic ice island and ice shelf studies, Part I: Arctic, v. 11, no. 1, p. 3–42.

———1960, Arctic ice island and ice shelf studies, Part II: Arctic, v. 13, no. 1, p. 32–50.

Dickson, R.R., 1999, All change in the Arctic: Nature [London], v. 397, no. 6718, p. 389–391.

Evans, D.J.A., 1989, An early Holocene narwhal tusk from the Canadian High Arctic: Boreas, v. 18, no. 1, p. 43–50.

Evans, D.J.A., and England, J., 1992, Geomorphological evidence of Holocene climatic change from northwest Ellesmere Island, Canadian High Arctic: Holocene, v. 2, no. 2, p. 148–158.

Hattersley-Smith, Geoffrey, 1957, The rolls of the Ellesmere Ice Shelf: Arctic, v. 10, no. 1, p. 32–44.

———1963, The Ward Hunt Ice Shelf—recent changes of the ice front: Journal of Glaciology, v. 4, no. 34, p. 415–424.

———1967, Note on ice shelves off the north coast of Ellesmere Island: Arctic Circular, no. 17, p. 13–14.

Hattersley-Smith, Geoffrey, Crary, A.P., and Christie, R.L., 1955, Northern Ellesmere Island, 1953 and 1954: Arctic, v. 8, no. 1, p. 3–36.

Hattersley-Smith, Geoffrey, Fusezy, A., and Evans, S., 1969, Glacier depths in northern Ellesmere Island—airborne radio echo sounding in 1966: Canada Department of National Defence, Defence Research Board, Defence Research Establishment Ottawa, Operation Tanquary, DREO Technical Note 69–6, Geophysics Hazen 36, 23 p.

Hattersley-Smith, Geoffrey, Keys, J.E., Serson, H., and Mielke, J.E., 1970, Density stratified lakes in northern Ellesmere Island: Nature [London], v. 225, no. 5227, p. 55–56.

Hobson, G., 1989, Ice island field station—New features of the Canadian Polar Margin: EOS (American Geophysical Union Transactions): v. 70, no. 37, p. 833, 835, 838–839.

Holdsworth, Gerald, 1971, Calving from the Ward Hunt Ice Shelf, 1961–62: Canadian Journal of Earth Sciences, v. 8, no. 2, p. 299–305.

———1987, The surface waveforms on the Ellesmere Island ice shelves and ice islands: National Research Council of Canada Technical Memorandum 141 (NRCC 28003), p. 385–403.

Holdsworth, Gerald, and Glyn, J., 1981, Mechanism for the formation of large icebergs: Journal of Geophysical Research, v. 86C, no. 4, p. 3210–3222.

Jackson, J.A., ed., 1997, Glossary of geology (4th ed.): Alexandria, Va., American Geophysical Institute, 769 p.

Jeffers, S., Agnew, T.A., Alt, B.T., de Abreau, R., and McCourt, S., 2001, The effects of the extreme summer of 1998 on the Canadian High Arctic ice regime: Annals of Glaciology, v. 33, p. 507–512.

Jeffries, M.O., 1984, Milne Glacier, Ellesmere Island, N.W.T., Canada—a surging glacier?: Journal of Glaciology, v. 30, no. 105, p. 251–253.

———1985, Physical, chemical and isotopic investigations of Ward Hunt Ice Shelf and Milne Ice Shelf, Ellesmere Island, N.W.T.: Calgary, Alberta, University of Calgary, unpublished Ph.D. thesis, 309 p.

———1986, Glaciers and the morphology and structure of Milne Ice Shelf, Ellesmere Island, N.W.T., Canada: Arctic and Alpine Research, v. 18, no. 4, p. 397–405.

———1987, The growth, structure and disintegration of arctic ice shelves: Polar Record, v. 23, no. 147, p, 631–649.

———1991a, Massive, ancient sea ice strata and preserved physical-structural characteristics in the Ward Hunt Ice Shelf: Annals of Glaciology, v. 15, p. 125–131.

———1991b, Perennial water stratification and the role of basal freshwater flow in the mass balance of the Ward Hunt ice Shelf, Canadian High Arctic: International Conference on the Role of the Polar Region in Global Change, 1990, Proceedings: Fairbanks, Alaska, University of Alaska Fairbanks, Geophysical Institute and Center for Global Change and Arctic System Research, v. 1, p. 332–337.

———1992, Arctic ice shelves and ice islands—Origin, growth and disintegration, physical characteristics, structural-stratigraphic variability and dynamics: Reviews of Geophysics, v. 30, no. 3, p. 245–267.

Jeffries, M.O., and Krouse, H.R., 1984, Arctic ice shelf growth, fiord oceanography and climate: Zeitschrift für Gletscherkunde und Glazialgeologie, v. 20, p. 147–153.

———1985, Isotopic and chemical investigations of two stratified lakes in the Canadian High Arctic: Zeitschrift für Gletscherkunde und Glazialgeologie, v. 21, p. 71–78.

Jeffries, M.O., and Sackinger, W.M., 1989, Some measurements and observations of very old sea ice and brackish ice, Ward Hunt Ice Shelf, N.W.T.: Atmosphere-Ocean, v. 27, no. 3, p. 553–564.

———1990, Near-real-time, synthetic aperture radar detection of a calving event at the Milne Ice Shelf, N.W.T., and the contribution of offshore winds, *in* Murthy, T.K.S., Paren, J.G., Sackinger, W.M., and Wadhams, P., eds., Ice technology for polar operations: Computational Mechanics Publications, p. 321–331.

Jeffries, M.O., and Serson, H.V., 1983, Recent changes at the front of Ward Hunt Ice Shelf: Arctic, v. 36, no. 3, p. 289–290.

Jeffries, M.O., and Shaw, M.A., 1993, The drift of ice islands from the Arctic Ocean into the channels of the Canadian Arctic Archipelago—The history of Hobson's Choice Ice Island: Polar Record, v. 29, no. 171, p. 305–312.

Jeffries, M.O., Krouse, H.R., Sackinger, W.M., and Serson, H.V., 1990, Surface topography, thickness and ice core studies of multiyear landfast sea ice and Ward Hunt Ice Shelf, northern Ellesmere Island, N.W.T., *in* Harington, C.R., ed., Canada's missing dimension—Science and history in the Canadian Arctic islands: Ottawa, Ontario, Canadian Museum of Nature, v. 1, p. 229–254.

Jeffries, M.O., Krouse, H.R., Shakur, M.A., and Harris, S.A., 1984, Isotope geochemistry of stratified Lake "A", Ellesmere Island, N.W.T.: Canadian Journal of Earth Sciences, v. 21, no. 9, p. 1008–1017.

Jeffries, M.O., Sackinger, W.M., Krouse, H.R., and Serson, H.V., 1988, Water circulation and ice accretion beneath Ward Hunt Ice Shelf (northern Ellesmere Island, Canada) deduced from salinity and isotope analysis of ice cores: Annals of Glaciology, v. 10, p. 68–72.

Jeffries, M.O., Serson, H.V., Krouse, H.R., and Sackinger, W.M., 1991, Ice physical properties, structural characteristics and stratigraphy in Hobson's Choice Ice Island and implications for the growth history of the East Ward Hunt Ice Shelf, Canadian High Arctic: Journal of Glaciology, v. 37, no. 126, p. 247–260.

Keys, J.E., 1978, Water regime of Disraeli Fiord, Ellesmere Island: Canada Department of National Defence, Research and Development Branch, Defence Research Establishment Ottawa (DREO) Report 792, 58 p.

Koenig, L.S., Greenaway, K.R., Dunbar, Moira, and Hattersley-Smith, Geoffrey, 1952, Arctic ice islands: Arctic, v. 5, no. 2, p. 67–103.

Legen'kov, A.P., 1974, Thermal stresses and deformation of the drifting ice island station North Pole 19: Oceanology, v. 13, no. 6, p. 804–808.

Lemmen, D.S., Evans, D.J.A., and England, John, 1988a, Discussion of "Glaciers and the morphology and structure of the Milne Ice Shelf, Ellesmere Island, N.W.T., Canada" by Martin O. Jeffries: Arctic and Alpine Research, v. 20, no. 3, p. 366–368.

———1988b, Ice shelves of northern Ellesmere Island, N.W.T.—Canadian landform examples, 10: Canadian Geographer, v. 32, no. 4, p. 363–367.

Lister, H., 1962, Heat and mass balance at the surface of the Ward Hunt Ice Shelf: Montréal, Québec, Arctic Institute of North America, Research Paper 19, Scientific Report 1, 54 p.

Lyons, J.B., and Mielke, J.E., 1973, Holocene history of a portion of northernmost Ellesmere Island: Arctic, v. 26, no. 4, p. 314–323.

Lyons, J.B., Ragle, R.H., and Tamburi, A.J., 1972, Growth and grounding of the Ellesmere Island ice rises: Journal of Glaciology, v. 11, no. 61, p. 43–52.

Lyons, J.B., Savin, S.M., and Tamburi, A.J., 1971, Basement ice, Ward Hunt Ice Shelf, Ellesmere Island, Canada: Journal of Glaciology, v. 10, no. 58, p. 93–100.

Maslanik, J.A., Serreze, M.C., and Agnew, T.A., 1999, On the record reduction in 1998 western Arctic sea-ice cover: Geophysical Research Letters, v. 26, no. 13, p. 1905–1908.

Narod, B.B., Clarke, G.K.C., and Prager, B.T., 1988, Airborne UHF radar sounding of glaciers and ice shelves, northern Ellesmere Island, Arctic Canada: Canadian Journal of Earth Sciences, v. 25, no. 1, p. 95–105.

Parliamentary Paper, 1877, Arctic Expedition 1875–76, journals and proceedings of the Arctic Expedition, 1875–76, under the Command of Captain Sir George S. Nares, RN, KCB, Great Britain, Admiralty (in continuation of Parliamentary Papers C1153 and C1560 of 1876): London, W.M. Harrison, printed for H.M. Stationery Office, 484 p.

Peary, R.E., 1907, Nearest the Pole—A narrative of the Polar Expedition of the Peary Arctic Club in the SS Roosevelt, 1905–1906: London, Hutchinson, 410 p.

Serson, H., 1972, Investigation of a plug of multiyear old sea ice in the mouth of Nansen Sound: Canada Department of National Defence, Defence Research Board, Defence Research Establishment Ottawa (DREO) Technical Note 72–6, 16 p.

———1974, Sverdrup Channel: Canada Department of National Defence, Defence Research Board, Defence Research Establishment Ottawa (DREO) Technical Note 74–10, 31 p.

Swithinbank, C.W.M., 1988, Antarctica, with sections on the 'Dry Valleys' of Victoria Land, by Chinn, T.J., and Landsat images of Antarctica, by Williams, R.S., Jr., and Ferrigno, J.G., *in* Williams, R.S., Jr., and Ferrigno, J.G., eds., Satellite image atlas of glaciers of the world: U.S. Geological Survey Professional Paper 1386–B, 278 p.

Vincent, W.F., Gibson, J.A.E., and Jeffries, M.O., 2001, Ice-shelf collapse, climate change and habitat loss in the Canadian High Arctic: Polar Record, v. 37, no. 201, p. 133–142.

Vincent, W.F., Gibson, J.A.E., Pienitz, R., Villeneuve, V., Broady, P.A., Hamilton, P.B., and Howard-Williams, C., 2000, Ice shelf microbial ecosystems in the High Arctic and implications for life on snowball Earth: Naturwissenschaften, v. 87, no. 3, p. 137–141.

Glaciers of North America—

GLACIERS OF CANADA

GLACIERS OF THE ARCTIC ISLANDS

GLACIERS OF BAFFIN ISLAND

By JOHN T. ANDREWS

With sections on BARNES ICE CAP: GEOMORPHOLOGY AND THERMODYNAMICS
By GERALD HOLDSWORTH

LATE 20TH CENTURY CHANGE AT THE BARNES ICE CAP MARGIN
By JOHN D. JACOBS

SATELLITE IMAGE ATLAS OF GLACIERS OF THE WORLD

Edited by RICHARD S. WILLIAMS, Jr., *and* JANE G. FERRIGNO

U.S. GEOLOGICAL SURVEY PROFESSIONAL PAPER 1386–J–1

The glaciers on Baffin Island are primarily ice caps or ice fields and associated valley outlet glaciers and include numerous small glaciers as well. The two largest ice caps, the Barnes Ice Cap (5,935 km^2) and the Penny Ice Cap (5,960 km^2) are thought to be the last remnants of the Laurentide Ice Sheet. Approximately 8 percent of Baffin Island is covered by glaciers (36,839 km^2). Nearby Bylot Island is heavily glacierized; it has 4,859 km^2 of its area covered by glaciers, about 45 percent of the island. The Barnes Ice Cap has been slowly shrinking; the recession could accelerate if significant regional warming were to take place

CONTENTS

GLACIERS OF NORTH AMERICA–

GLACIERS OF CANADA

GLACIERS OF THE ARCTIC ISLANDS

GLACIERS OF BAFFIN ISLAND

By JOHN T. ANDREWS[1]

With sections on

BARNES ICE CAP: GEOMORPHOLOGY AND THERMO-DYNAMICS

By GERALD HOLDSWORTH[2]

LATE 20TH CENTURY CHANGE AT THE BARNES ICE CAP MARGIN

By JOHN D. JACOBS[3]

Abstract

Glaciers on Baffin Island are strongly influenced by topography and climate. The major glaciers are either ice caps that occupy inland highland areas or ice fields and associated valley outlet glaciers, or they are combinations of both. Other significant glaciers are found on Cumberland Peninsula, on Hall Peninsula, and along the east fjord coast of the island. Baffin Island glaciers are covered by 1:1,000,000-scale, 1:250,000-scale, and some 1:500,000-scale and 1:50,000-scale maps, aerial photographs at 1:50,000 scale, Landsat imagery, and other satellite imagery (e.g., RADARSAT). Landsat images are used to describe individually the separate glacierized areas of the island, especially the areas of Barnes and Penny Ice Caps, which are thought to be the last remnants of the Laurentide Ice Sheet.

Introduction

Baffin Island, Nunavut, Canada[4], extends between lat 62° and 74°N. and long 62° and 90°W. (fig. 1). The island has an area of about 500,000 km^2, which makes it one of the five largest islands in the world. Most of the island is composed of Precambrian granites, granite gneisses, and other metamorphic rocks; therefore, most of the glaciers on the island overlie these hard and resistant lithologies. However, younger sedimentary rocks of Paleozoic to Cenozoic age (Kerr, 1980) crop out at the surface along the west coast of the

Manuscript approved for publication 7 March 2002.

[1] Institute of Arctic and Alpine Research, University of Colorado, Box 450, Boulder, CO 80309.

[2] Arctic Institute of North America, University of Calgary, 2500 University Drive, NW., Calgary, Alberta T2N 1N4, Canada; Institute for the Study of Earth, Oceans, and Space, Morse Hall, University of New Hampshire, Durham, NH 03824–3525; and the National Hydrology Research Centre, 11 Innovation Boulevard, Saskatoon, Saskatchewan S7N 3H5, Canada; e-mail address: [gholdswo@acs.ucalgary.ca].

[3] Department of Geography, Memorial University of Newfoundland, St. John's, Newfoundland A1B 3X1, Canada; e-mail address: [jjacobs@plato.ucs.mun.ca].

[4] The geographic place-names used in this section follow the usage approved by the Geographic Names Board of Canada. Names in common usage that are not recognized by the Board are shown in italics.

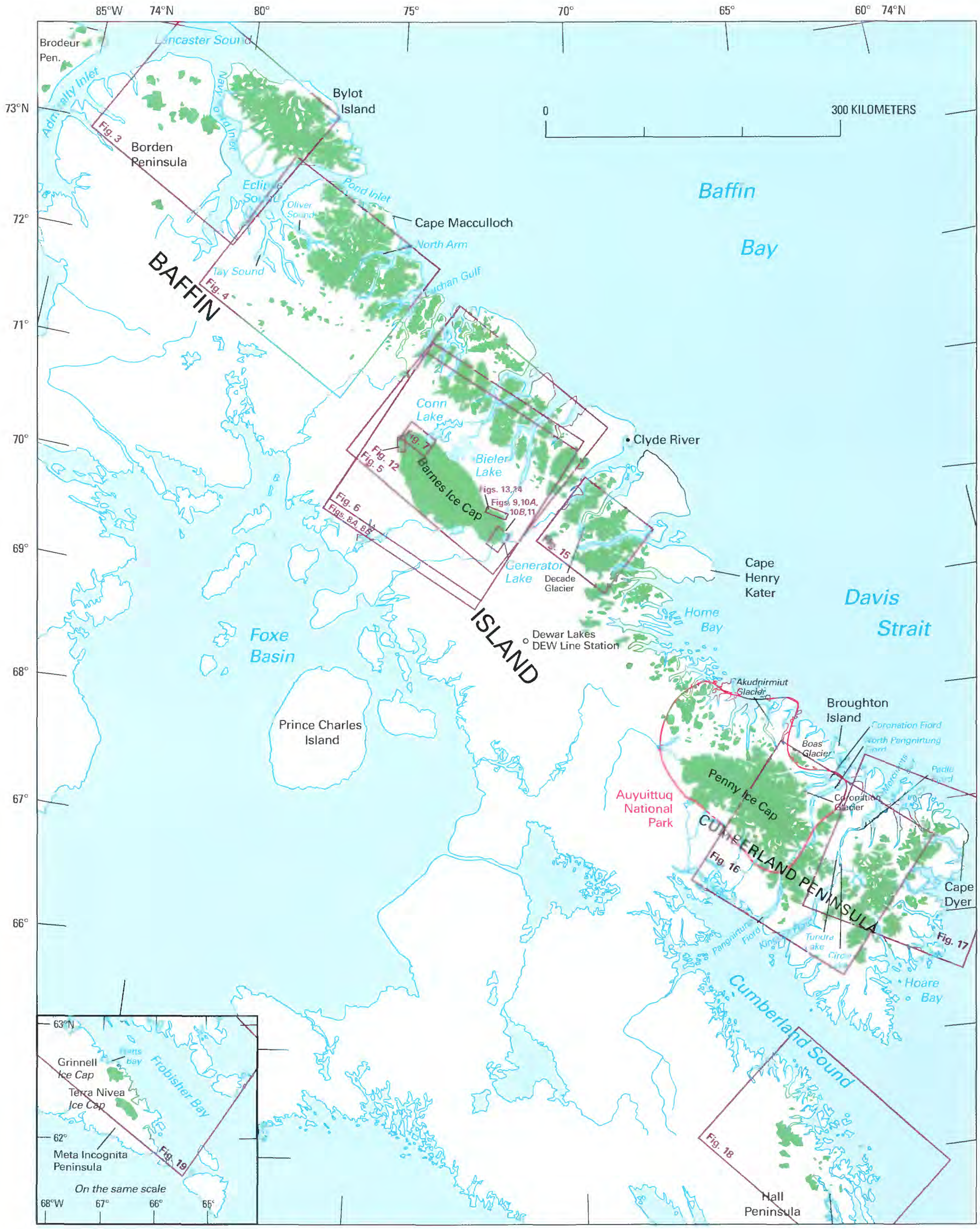

Figure 1.—*Baffin Island and adjacent regions, Nunavut, Canada, showing the location of major glaciers and other features. Also shown are the outlines for figures 3–19, including the approximate outlines of Landsat images discussed in the text and used for figures 3–6, 8, and 15–19 (see also table 3). Abbreviation: Pen., Peninsula.*

island (Paleozoic formations) and extend northward to form major uplands in the northern part of Baffin Island. Mesozoic and Cenozoic (Tertiary) rocks are found on Bylot Island, one of the most heavily glacierized tracts in the region.

The pattern of the present glacierization on Baffin Island is influenced strongly by topography and climate. Baffin Island can be represented simply in cross section (east to west) as a wedged-shaped prism that has the highest land lying within 10 to 100 km of the outer fault-bounded east coast (Ives and Andrews, 1963; Kerr, 1970). Fjords of various sizes cut through the uplifted rim (Dowdeswell and Andrews, 1985) and head toward the broad, rolling interior plateau of the island, where elevations range between 600 and 700 m and decline gradually westward toward the shores of Foxe Basin (see Bird, 1967). The maximum elevations shown on the U.S. Defense Mapping Agency's Operational Navigational Charts (ONC C–12 and B–8) are 2,057 m near the center of the Penny Ice Cap and 1,905 m on Bylot Island (fig. 1). Elevations in excess of 800 m are restricted to the areas between the heads of the fjords and the outer east coast and along the fault-bounded south side of Frobisher Bay (inset map in fig. 1).

Climatic data from Baffin Island are sparse and are biased toward meteorological data recorded at coastal stations. Selected data are shown in table 1. At the Dewar Lakes Distant Early Warning (DEW) Line Station in central Baffin Island (fig. 1), the mean annual temperature is –13°C, with a July mean temperature of 6.0°C (Maxwell, 1980, 1982). Precipitation is notoriously difficult to measure in Arctic areas and is most probably underestimated (Hare and Hay, 1971). Nevertheless, the snowfall records from the stations, combined with snowpit work on the glaciers (for example, Baird, 1951; Ward and Baird, 1954; Sagar, 1966; Weaver, 1975; Hooke and others, 1987), indicate that winter accumulation on most glaciers probably varies between 30 and 60 cm water equivalent.

Distribution of Glaciers

The interaction between topographic and climatic gradients results in a particular geographic distribution of glaciers (see Andrews and others, 1970; Andrews and Barry, 1972). A regional picture of the interaction can be obtained by mapping the glaciation level (also called glaciation limit or glaciation threshold) by the "summit method" of Østrem (1966). The glaciation level for the region of Baffin Bay is drawn from maps in Andrews and Miller (1972) and Weidick (1975) and is shown in figure 2. The glaciation level is the elevation at which, in a regional sense, the long-term net mass balance equals zero (b_n=0). Areas above this level will generally support an ice mass, whereas mountains or hills whose summits lie below this limit will be ice free under the present climate. The glaciation level on Baffin Island dips toward Baffin Bay at about 4 m km^{-1} from a maximum elevation of about 1,200 m to a minimum of 600 m (fig. 2). The proximity of the glaciation level to the broad plateau of the interior of Baffin Island and the evidence there for

TABLE 1.—*Selected climatic data showing temperature in degrees Celsius for climatic regions on Baffin Island and environs*

[Modified from Maxwell, 1982. The averages noted here are from available sources; the length of record is not uniform. For a more complete description of the climatic regions of Baffin Island, see Maxwell (1982).]

Climatic region	January	July	Total precipitation (mm)
Northern Baffin Island	–20 to –33	+3 to +5	150 to 300
Western interior	–28 to –32	+5 to +8	175 to 250
Mountains	–28 to –32	+4 to +5	300 to 600
Southeastern Baffin Island	–25	+5 to +8	400 to 500

extensive neoglacial snow cover (Ives, 1962; Andrews and others, 1976; Locke and Locke, 1977; Williams, 1978) are reasons why Baffin Island is frequently considered to be a major area for the initial growth of the Laurentide Ice Sheet (Ives and others, 1975; Andrews and others, 1972).

On Baffin Island, the major glaciers, such as the Barnes Ice Cap, either occupy inland highland areas or are ice fields and associated valley outlet glaciers (Bylot Island) (Sugden and John, 1976), or they are combinations of both (Penny Ice Cap) (fig. 1, table 2). In the southern part of the island, two significant ice caps located along the south rim of Frobisher Bay are called the Grinnell and Terra Nivea *Ice Caps* (Mercer, 1956). Other significant glaciers are found on Hall Peninsula in the south, Cumberland Peninsula to the north, and as a broad band of glacierized terrain extending along the east coast (fjord) part of the island between the northern Cumberland Peninsula and Bylot Island (fig. 1). Small, largely decaying ice caps and ice patches are present on the upland surfaces in northern Baffin Island and to some extent north and west of the Barnes Ice Cap (Falconer, 1962, 1966; Andrews and others, 1976). The major glaciers were discussed by Mercer (1975), and his work is still a basic reference on Baffin Island glaciers.

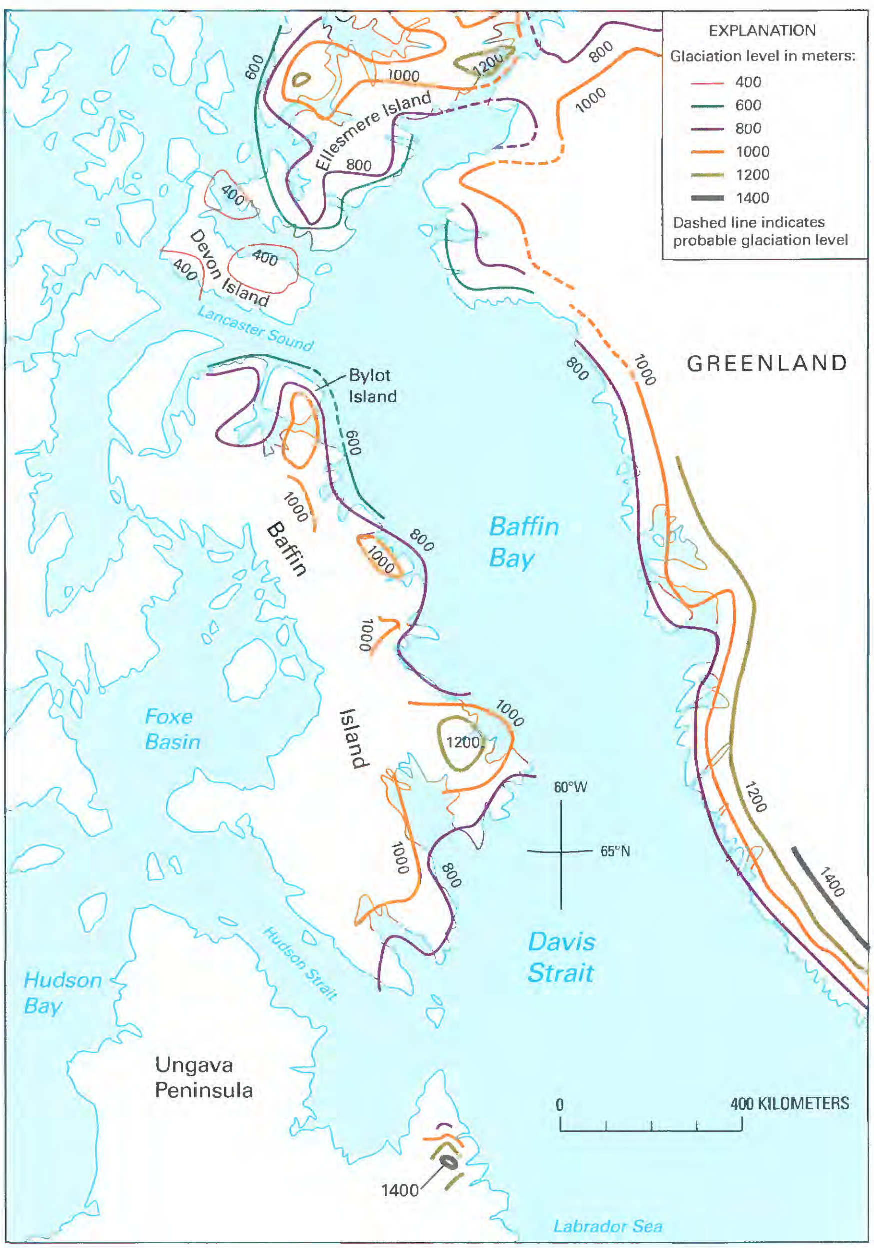

__Figure 2.__—Glaciation level (limit or threshold) on Baffin Island and West Greenland (modified from Andrews and Miller, 1972, and Weidick, 1975).

TABLE 2.—*Areas of glaciers on Baffin Island and Bylot Island*
[Modified from Mercer, 1975; Bird, 1967]

Name	Area (square kilometers)	Figure number (this section)
Baffin Island		
Penny Ice Cap	5,960	1, 16
Barnes Ice Cap	5,935	1, 5, 6, 7, 8*A*, 8*B*, 9, 10*A*, 10*B*, 11, 12, 13, and 14
"Hall" Ice Cap	490	1, 18
Terra Nivea *Ice Cap*	165	1, 19
Grinnell *Ice Cap*	139	1, 19
Other glaciers	24,150	1, 3, 4, 15, and 17
Total	36,839	
Bylot Island	4,859	1, 3

The ice caps, ice fields, outlet glaciers, and smaller glaciers of Baffin Island have been mapped and included in the Canadian National Inventory of Glaciers (Ommanney, 1980); each has a unique glacier inventory code. The area is covered by National Topographic Series (NTS) map sheets 16/26, 25, 27/37, and 48/58, all at a scale of 1:1,000,000. Specific glacier identification is available on a series of 1:500,000-scale maps (for example, the Grinnell and Terra Nivea *Ice Caps* on the Meta Incognita Peninsula, Glacier Inventory, area 46205; Glacier Atlas of Canada, plate no. 5–24; Canada Department of Energy, Mines and Resources, Inland Waters Branch, IWB 1124, 1969). The entire area is covered by 1:250,000-scale topographic maps. For Bylot Island, the glacierized parts of the northern Brodeur Peninsula, Borden Peninsula, and the nearby area southwest of Pond Inlet are covered by 1;50,000-scale topographic maps. Topographic maps at a scale of 1:50,000 cover a number of small decaying glaciers south of Eclipse Sound between lat 71° and lat 72°N.

Glaciological Studies

Falconer (1962) initiated an inventory of glaciers of Baffin and Bylot Islands from aerial photographs. Following this work, done for the former Geographical Branch of the Canadian Department of Mines and Technical Surveys (later Energy, Mines and Resources, presently Natural Resources Canada), the task of collecting historical records on glacier positions was inherited by the Glaciology Subdivision of Environment Canada. To my knowledge, a systematic survey of historical accounts has not been done. The earliest observations known are the observations of John Ross (1819) on glaciers of the Erik Harbour area, the description of glaciers of Bylot Island by P.G. Sutherland (1852), the work of Leopold M'Clintock (1860) on glaciers of the Bylot Island area, and observations of C.F. Hall, an American explorer. Hall sailed along the south coast of Frobisher Bay in 1860–62 (Hall, 1865) and noted (p. 520), "...From the information I had previously gained, and the data furnished by my Innuit companion, I estimated the Grinnell Glacier to be fully 100 miles long." This account may suggest that heavy snows mantled the high ground on Meta Incognita Peninsula, where Grinnell *Ice Cap* is located (fig. 1), to a greater extent than they do today. Another possible source of information is the logs of whalers who sailed into Baffin Bay from the 17th century onward. It would seem likely that some observations of glacier extent would appear in the ship logs.

The scientific observation of glaciers on Baffin Island was initiated in 1950, when the Arctic Institute of North America (AINA) sponsored an experienced expedition to study the Barnes Ice Cap (Baird, 1951). This was followed in 1953 by a smaller venture that focused on glaciological and glacioclimatic measurements of the Penny Ice Cap (Baird, 1953; Baird and others, 1953; Orvig, 1954; Ward and Baird, 1954). Some earlier photographic records and sketches of glaciers in Pangnirtung Pass, Cumberland Peninsula, were obtained by the naturalist Dr. J. Dewey Soper in the course of his sledge travels from 1924 to 1926 (Soper, 1981).

The next major glaciological research program on Baffin Island was promoted by the former Geographical Branch of the Canadian Department of Mines and Technical Surveys. Studies were undertaken on the Barnes Ice Cap (Sagar, 1966; Løken and Andrews, 1966; Anonymous, 1967; Church, 1972) and on the Decade Glacier to the east (Østrem and others, 1967). The Barnes Ice Cap program was continued by the Glaciology Subdivision of Environment Canada (Holdsworth, 1973b, 1977) and by R. LeB. Hooke and colleagues from the University of Minnesota (Hooke, 1973, 1976; Hooke and others, 1980, 1982, 1987; Hudleston, 1976).

In 1969, a small research program in glaciology, specifically on mass and energy balance, was started by the University of Colorado. The focus of the research was the *Boas Glacier*, a small glacier northeast of Penny Ice Cap (fig. 1) (Andrews and Barry, 1972; Jacobs and others, 1974; Weaver, 1975). This work was discontinued in 1976. Plans to extract an ice core from the Penny Ice Cap commenced in the 1980's with a survey of recent snow accumulation (Holdsworth, 1984; Short and Holdsworth, 1985). A combined Canadian, Japanese, and U.S.A. research effort extracted cores to bedrock during the middle 1990's; these cores have been examined in detail for paleoenvironmental data (Fisher and others, 1998).

Other glaciological papers dealing with Baffin Island are listed in an annotated bibliography prepared by Andrews and Andrews (1980). Given the large area covered by various glaciers (36,839 km^2), approximately 8 percent of the island, (Bird, 1967; Mercer, 1975) (table 2), glaciological research on Baffin Island is generally lacking. Virtually nothing is known of the mass balance or dynamics, for example, of the two southern ice caps situated on Meta Incognita Peninsula (Blake, 1953; Mercer, 1956), although research on neoglacial events and on glacial processes has been reported and is part of a program supported from the University of Colorado (Muller, 1980; Dowdeswell, 1982, 1984). Jacobs and others (1997) used Landsat images to evaluate the recent history of the south margin of the Barnes Ice Cap.

Maps, Aerial Photographs, and Satellite Images of Glaciers

Glacier Maps

The Canadian government flew a special series of survey flights in 1961 over north-central Baffin Island in order to provide 1:50,000-scale vertical aerial photographic coverage of Barnes Ice Cap. The photographs were subsequently used to compile, along with aerial photogrammetric methods, a special 1:50,000-scale map series of Barnes Ice Cap and environs. The area is covered by seven map sheets (37E/1W, 37E/2W, 37E/2E, 37E/3W, 37E/6W, 37E/7E, and 37E/7W). A digital elevation model of the Barnes Ice Cap, based on Landsat MSS data was prepared by Lodwick and Paine (1985). Elsewhere on the island, some good quality orthophotomaps exist of the glacierized terrain in the vicinity of Pangnirtung Pass, Cumberland Peninsula (fig.1). These maps were produced at a scale of 1:50,000 for a project associated with the establishment of a new national park (Auyuittuq National Park) that includes most of Penny Ice Cap and large areas of glacierized alpine terrain (fig. 1).

Baffin and Bylot Islands are covered by specially prepared maps produced by the former Glaciology Division, Environment Canada. These maps are at a scale of 1:1,000,000 and show the major and minor glaciers. The map identification numbers for the series are 1WB 1005 (northern Baffin Island) and 1WB 1006 (southern Baffin Island). Information about maps can be obtained by contacting Geomatics Canada, Natural Resources Canada, 130 Bentley Avenue, Ottawa, Ontario K1A 0E9, Canada (tel: 613–952–7000 [1–800–465–6277]; fax: 1–800–661–6277; World Wide Web site: [http://www.geocan.nrcan.gc.ca]).

In addition, the glaciers of the area have been inventoried by the Glaciology Division. Each ice mass has a unique identification code. The individual glaciers that have been inventoried are mapped and identified on a series of color maps at a scale of 1:500,000. Baffin Island and Bylot Island are covered by plate numbers 5–0 to 5–24. Part of Grinnell Glacier, Baffin Island, Northwest Territories [now Nunavut], was mapped by the Norwegian Water Resources and Energy Administration, and a map was published in 1991; the scale of the map is 1:20,000.

Aerial Photographic Coverage of Glacierized Areas

The National Air Photo Library (NAPL) is located in Ottawa, Ontario, and is part of the Department of Natural Resources. All government-sponsored aerial photography is kept in the library, together with index sheets showing flightlines and center points of each photograph. The index maps are normally at a scale of 1:250,000 or 1:500,000.

Much of the glacierized part of Baffin Island was flown in 1948 by using trimetrogon aerial photography. The central image (vertical aerial photograph) of the trio is at a scale of about 1:20,000. Conventional vertical aerial photographs were taken during the 1950's and into the 1970's. The flying height for these photographs appears to have been normally about 9,146 m, and a 15-cm lens was used, which gives a nominal ground scale of about 1:50,000 (assuming a terrain elevation of 1,524 m). Virtually all the glacierized terrain on Baffin and Bylot Islands is covered by this vertical aerial photography. The quality of coverage varies but is most often excellent to good. Many areas have coverage in two or more years.

Color aerial photography is rare; however, some of this coverage exists for parts of Barnes Ice Cap and the mountains between there and Clyde River on the coast (fig.1). In addition, color aerial photography at small scale was taken for part of the Auyuittuq National Park.

Information on coverage can be obtained by contacting the NAPL, Geomatics Canada, Natural Resources Canada, 615 Booth St., Ottawa, Ontario K1A 0E9, Canada (tel: 613–995–4560 [1–800–230–6275]; fax: 613–995–4568; World Wide Web site: [http://airphotos.nrcan.gc.ca]).

Landsat Coverage

Landsat images are available for Baffin Island either through the U.S. Geological Survey's EROS Data Center or through the Canada Centre for Remote Sensing[5] (see table 3 and figure 1). One particularly important product is a series of black-and-white Landsat mosaics that can be bought directly from the NAPL, Geomatics Canada (see above).

The mosaics are at a scale of 1:1,000,000, and coverage is as follows:

NTS 25	Coverage of Terra Nivea and Grinnell *Ice Caps* and parts of Hall Peninsula

[5] U.S. Geological Survey, EROS Data Center, Sioux Falls, S. Dak. 57198 (tel: 605–594–6151 [1–800–252–4547]; fax: 605–594–6589; World Wide Web: http://edc.usgs.gov/). Canada Centre for Remote Sensing, Geomatics Canada, Natural Resources Canada, 588 Booth Street, Ottawa, Ontario K1A 0Y7, Canada (tel: 613–995–4057; fax: 613–992–0285; World Wide Web: [http://www.ccrs.nrcan.gc.ca]).

NTS 16–26 Coverage of the Cumberland Peninsula (Penny Ice Cap) and northern Hall Peninsula

NTS 26–36 Koukdjuak River, includes Penny Ice Cap

NTS 27–37 Coverage of north-central Baffin Island including the Barnes Ice Cap and mountain glaciers

NTS 48–58 Coverage of most of Bylot Island, all of Devon Island, and the small ice caps on Borden Peninsula and Brodeur Peninsula (figs. 1 and 2)

The quality of the mosaics is normally excellent, and they are at the same scale and cover the same areas as the 1:1,000,000-scale topographic map series produced by the Government of Canada. The Landsat mosaics and topographic maps are an excellent combination for laboratory exercises in aspects of both glacial geology and glaciology.

Glaciological Phenomena Observed on Landsat Images

Several Landsat images have been selected for inclusion in this section. They are mostly high quality false-color composite images that reveal several important glaciological features. Their coverage area is shown in figure 1, and details of each Landsat image are tabulated in table 3. For ease of reference, they will be discussed in a north-to-south sequence.

TABLE 3.—*Landsat images used in figures 3–6, 8, and 15–19 and National Topographic Series (NTS) map sheets*

[Code symbols: ●, Excellent image (0 to ≤5 percent cloud cover), ◕, Good image (>5 to ≤10 percent cloud cover), ◐, Fair to poor image (>10 to ≤100 percent cloud cover)]

Path-Row	Scene center (lat-long)	Landsat identification number	Date	Solar elevation angle (degrees)	Code	Cloud cover (percent)	Figure	Glacier area (NTS map sheet)
017–013	66°29'N. 62°07'W.	20185–15051	26 Jul 75	42	●	0	17	(16L)
017–015	64°08'N. 64°56'W.	1747–15083	9 Aug 74	40	◐	15	18	"Hall" Ice Cap
017–016	62°46'N. 66°10'W.	1747–15090	9 Aug 74	41	◐	15	19	Terra Nivea and Grinnell *Ice Caps*
019–013	66°35'N. 64°37'W.	21663–15103	12 Aug 79	35	●	0	16	Penny Ice Cap (26I)
026–011B	69°31'N. 69°58'W.	30721–15514 subscene B	24 Feb 80	10	●	0	15	(27C)
028–010	70°25'N. 72°55'W.	10380–16182	7 Aug 73	36	●	0	5	Barnes Ice Cap (37E)
028–010	70°25'N. 72°31'W.	22050–16064	2 Sep 80	25	●	0	8*B*	Barnes Ice Cap (37E)
028–010	70°33'N. 72°23'W.	30525–16065	12 Aug 79	32	●	0	8*A*	Barnes Ice Cap (37E)
028–010	70°16'N. 73°13'W.	10740–16100	2 Aug 74	37	◕	10	6	Barnes Ice Cap (37E)
033–009	71°51'N. 77°08'W.	1403–16461	30 Aug 73	27	●	0	4	–
037–008	73°01'N. 80°47'W.	20943–16335	22 Aug 77	–	●	5	3	Bylot Island (48D)

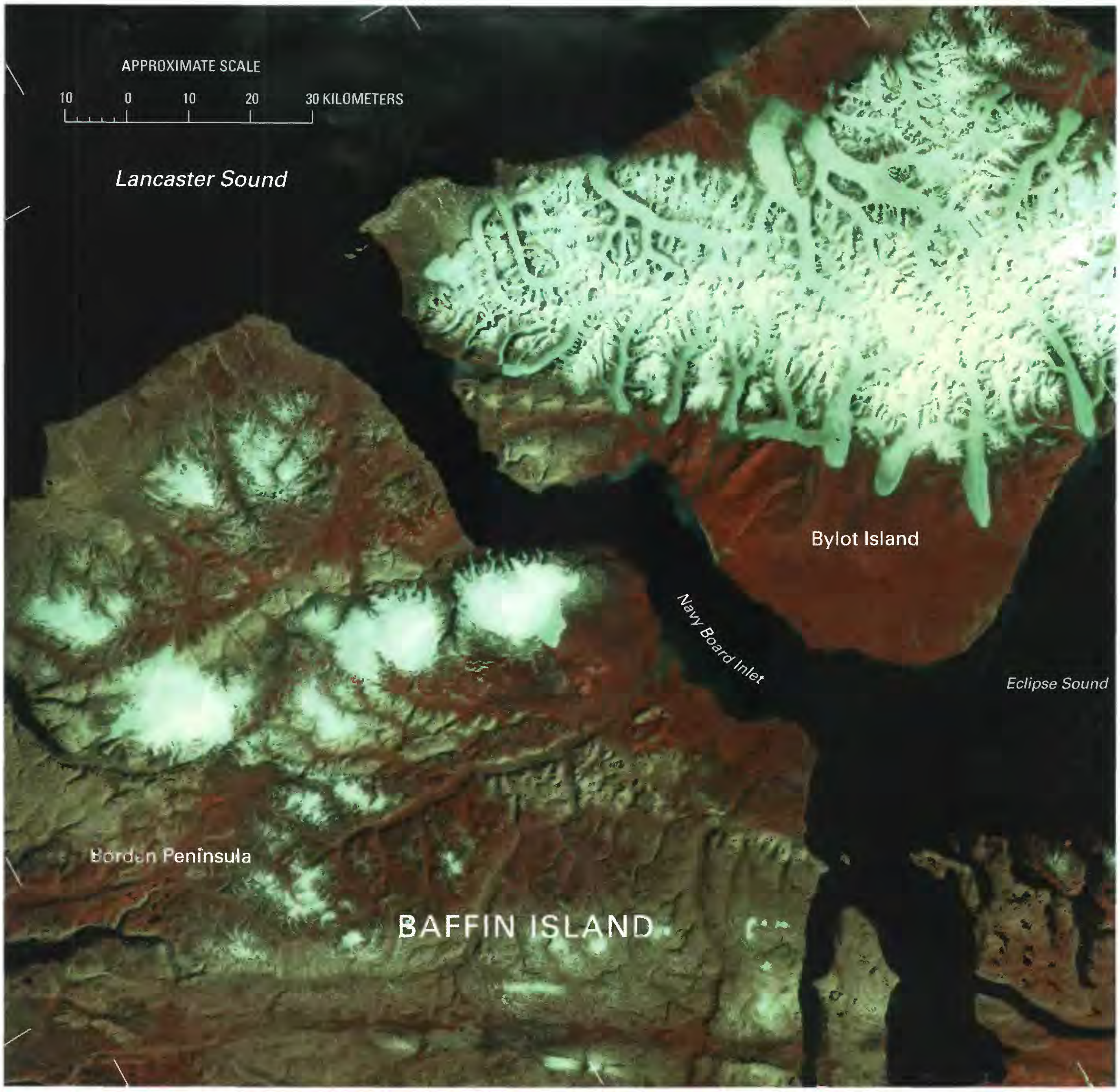

***Figure 3.**—Annotated Landsat 2 MSS false-color composite image of the Navy Board Inlet and Bylot Island glaciers. Landsat image (20943–16335, bands 4, 5, and 7; 22 August 1977; Path 37, Row 8) is from the Canada Centre for Remote Sensing, Ottawa, Ontario.*

Navy Board Inlet and Bylot Island

Figure 3 shows a false-color composite Landsat image of northern Baffin Island acquired on 22 August 1977. Variations in bedrock geology are clearly apparent. On the west side of Navy Board Inlet, several small plateau glaciers (ice caps) are visible. The general elevation of the upland surface is about 700 m, and the ice caps rise to more than 1,000 m, which suggests a possible thickness of ice of 100–200 m. The ice caps are located on high ground close to the coast, and this indicates that local orographic effects may be important in their mass balance. Although some "blue" ice can be seen, the high reflectivity of the snow strongly implies that a late summer snowstorm had come through prior to the orbital overpass. The margins of the ice caps are generally smooth on the south side, but small outlet glaciers can be seen pushing downvalley, particularly on the north margin of the ice cap that lies closest to Navy Board Inlet. The decrease in glacierization to the south, even though the topography remains relatively constant, indicates a steep gradient of the glaciation level (fig. 2; Andrews and Miller, 1972).

Bylot Island is heavily glacierized (fig. 3, cover), as it has 4,859 km^2 of its area covered by glaciers, about 45 percent of the island. The image shows that this highland ice field has a "spine" of cirque basins from which ice flows. The ice merges into a series of spectacular outlet glaciers. Sixteen major outlet glaciers can be identified on the image. The lower parts of these glaciers are clearly within the ablation zone, and the transient snowline appears to lie about 1,000 m above sea level (asl). Poorly defined medial moraines can be traced on most outlet glaciers, but no indications exist of contorted medial moraines; hence, the evidence indicates that none of these outlet glaciers exhibit surge behavior.

Small sediment plumes can be seen in the ocean waters adjacent to streams draining from these glaciers, but they are not very distinct. This may reflect the lateness of the season, because meltwater volumes dwindle rapidly after the main melting period in late June to middle July on Baffin Island (Church, 1972). The glacial geology and chronology of Bylot Island is discussed by Klassen (1981, 1982, 1985).

Pond Inlet, Oliver Sound, and North Arm

The area southeast of Bylot Island can be seen on the Landsat 1 multispectral scanner (MSS) false-color composite image taken 30 August 1973 and used for figure 4. The settlement of Pond Inlet is located in this image but is not easily visible. The bedrock geology varies from Precambrian granites and gneisses around Pond Inlet to Paleozoic limestones in the lower half of the image. Figure 4 shows an inland transition from a heavily glacierized coastal zone to scattered small ice masses on the higher ground to the southwest. The style of glacierization is different from that on Bylot Island even near the coast (compare with fig. 3). Particularly in the heavily ice-covered areas on either side of Oliver Sound and North Arm, the lack of surface relief indicates that the ice covers a broad, undissected (interfjord) upland (Ives and Andrews, 1963). Elevations are between 1,000 and 1,500 m asl. Only east of Pond Inlet is the style of glacierization reminiscent of alpine glacierization. From the upland ice caps, large outlet glaciers are channeled in major valleys and, in places, extend at right angles across major fjords—such as in Erik Harbour and toward the head of North Arm. East of Erik Harbour and west of Cape Macculloch (fig. 1), a large (20-km by 15-km) piedmont lobe covers much of a coastal foreland at only 200 m asl.

The large outlet glaciers on Bylot Island (fig. 3) are distinctive; many on this image are remarkable in that no large terminal moraines are associated with them. However, in figure 4, several outlet glaciers do have visible terminal moraines. Examples are the large outlet glaciers that flow eastward to Buchan Gulf. A large lake is dammed between one of the large neoglacial moraines and the coast. Radiocarbon dates from Pond Inlet and near outer Buchan Gulf (Hodgson and Haselton, 1974) indicate that the outer coast of this section of Baffin Island has not been glacierized for at least 30 kilo-annum (ka, 10^3 years). In a similar manner, the evidence of Klassen (1981, 1982, 1985) indicates that regional glaciation of Bylot Island took place prior to 30 ka.

Figure 4 shows good separation between "blue" ice on the lower parts of the smaller glaciers and ice caps and the "white" snow and firn of the accumulation zones. The transient snowline lies at about 700 m, and even the small ice patches on the southern part of the image show only small areas of ice. It is possible that some of the effects of the summer melt season are masked by a late summer or early fall snowstorm.

Notable features in the lower left corner of figure 4, which will be described more fully when figures 5 and 6 are discussed, are the light-toned areas that are found south of Tay Sound. A detailed examination of the margins of these areas indicates that they cannot be explained by changes in the bedrock geology; rather these are the "lichen-free" areas of eastern and northern Baffin Island that have been documented, mapped, and studied as possible analogs for the development of the Laurentide Ice Sheet (see Ives, 1962; Andrews and others, 1976; Locke and Locke, 1977). Williams (1978) used these areas to suggest changes in climate during the last several hundred years, the time of the "Little Ice Age" (Grove, 1988).

Figure 4.—*Annotated Landsat 1 MSS false-color composite image of the area around Pond Inlet, Oliver Sound, and North Arm. Landsat image (1403–16461, bands 4, 5, and 7; 30 August 1973; Path 33, Row 9) is from the Canada Centre for Remote Sensing, Ottawa, Ontario.*

Barnes Ice Cap and Environs

Barnes Ice Cap (5,935 km^2) is the most studied glacier on Baffin Island (see bibliography in Andrews and Andrews, 1980). For this reason, and because of the information content of different images on different dates,

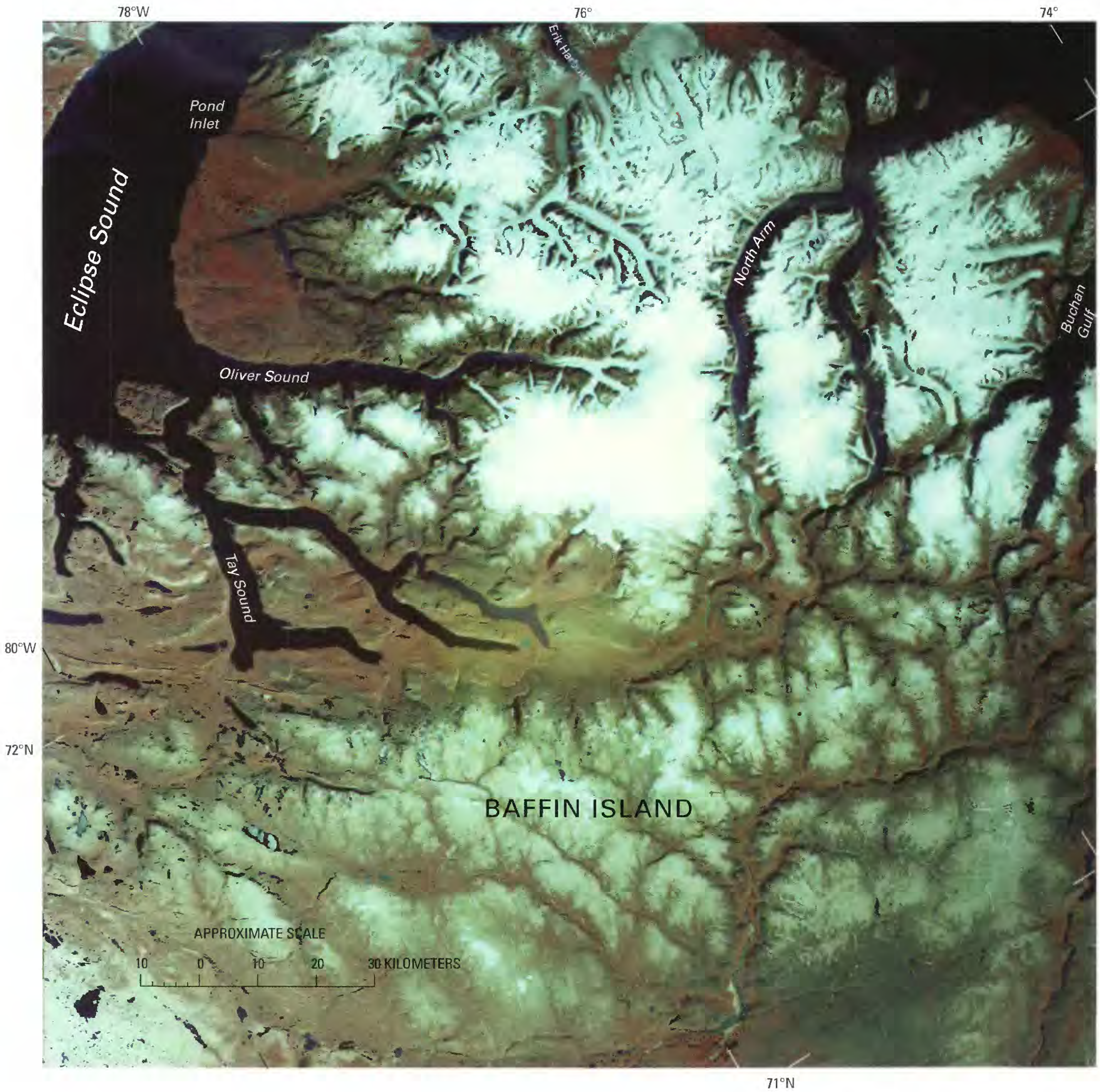

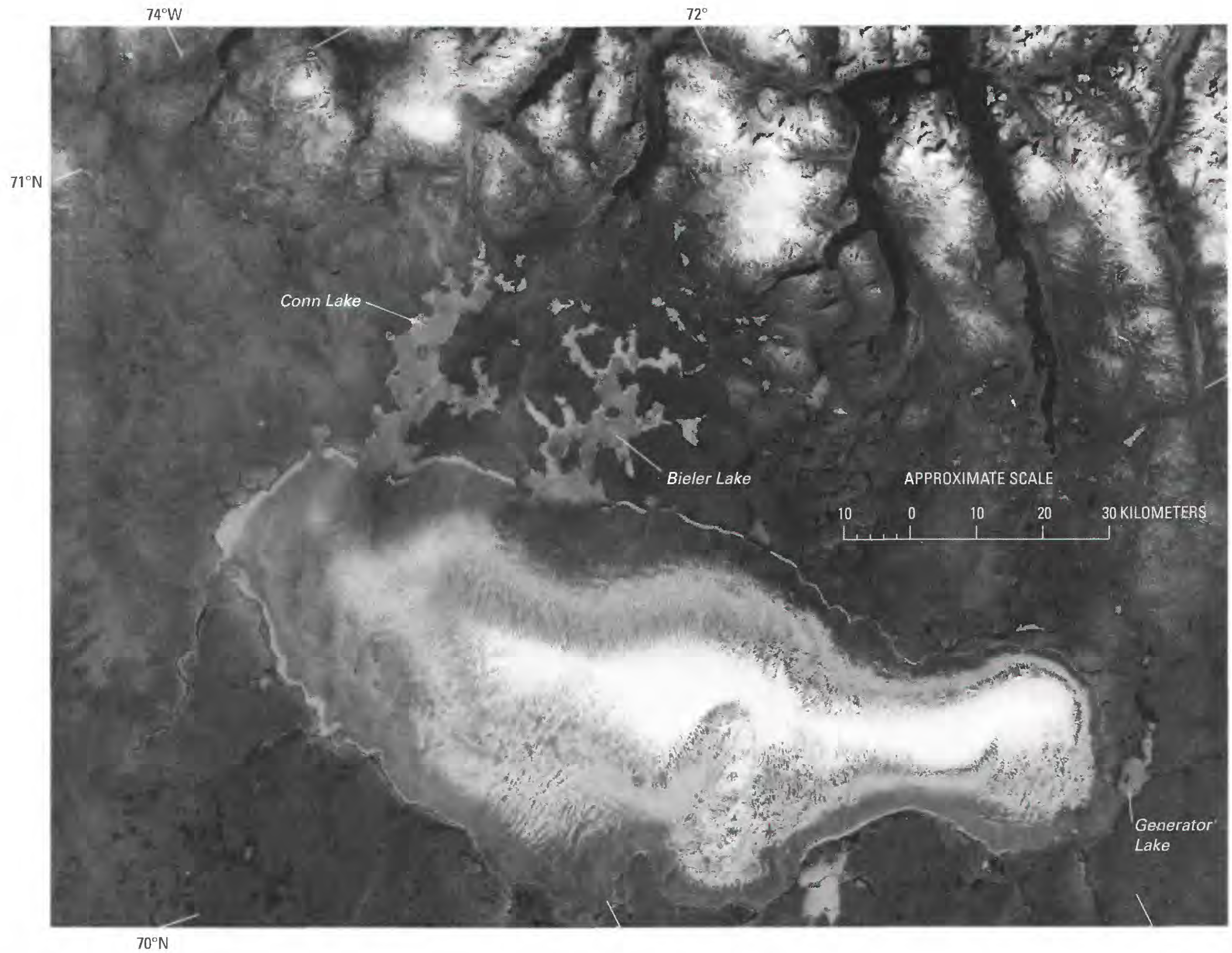

__Figure 5.__—Landsat 1 MSS black-and-white image of the Barnes Ice Cap and environs. Landsat image (10380–16182, band 7; 7 August 1973; Path 28, Row 10) is from the Canada Centre for Remote Sensing, Ottawa, Ontario.

several Landsat images and terrestrial (ground) and aerial photographs have been chosen for presentation in this section. Figure 5 is a Landsat 1 image that shows interesting glaciological and glacial geologic features on the Barnes Ice Cap and in the surrounding area. The crest of the ice cap appears as an intense white area from which surface and subsurface drainage lines diverge. The image also strikingly illustrates a series of snow-and-ice facies (see further discussion in the following section by Gerald Holdsworth on the geomorphology and thermodynamics of the Barnes Ice Cap; and in Williams and others, 1991).

Large calving bays having steep ice cliffs are present on the northeast side of the Barnes Ice Cap, where it flows into Conn and Bieler Lakes, and in the southeast, where it flows into Generator Lake (fig. 6). Icebergs are found in these lakes, but none are visible in figure 5.

North and northeast of the Barnes Ice Cap are light-toned areas that are "type-locations" for lichen-free areas (Ives, 1962; see also fig. 6). Rimrock Lake is in this area (fig. 6), and it is around that lake that Ives (1962) first studied and speculated on the significance of the lichen-free phenomenon. This area was first noted on 1:50,000-scale aerial photographs and was then studied in the field (Ives, 1962; Andrews and others, 1976).

Sugden (1978) and Andrews and others (1985) used black-and-white Landsat images to map areas of heavy, moderate, and light glacial scour. An area of heavy glacial scour is shown in the bottom left of figure 5 and is indicated by a high percentage of small lakes and obvious evidence for

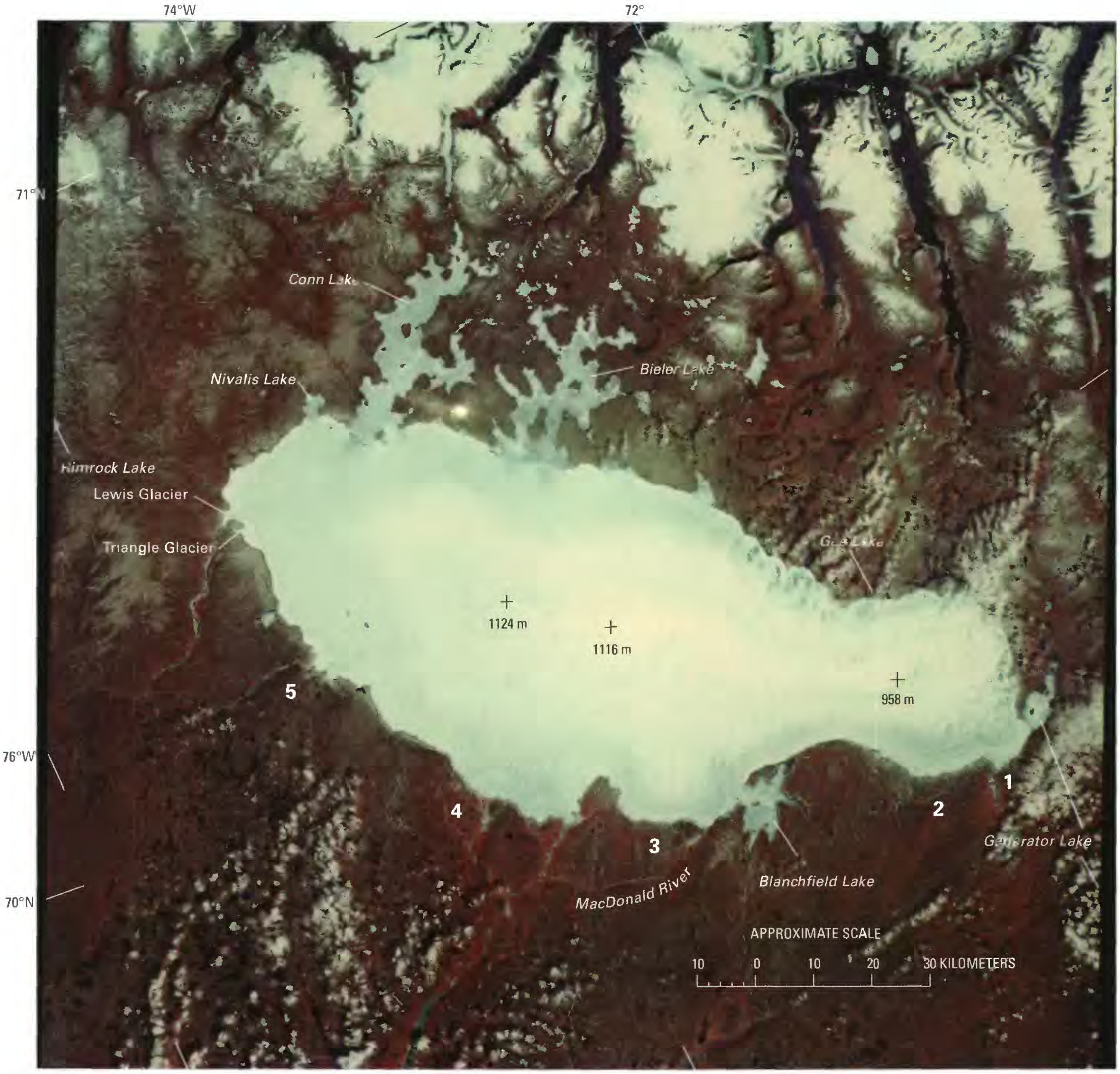

***Figure 6.**—Landsat 1 MSS false-color composite image of Barnes Ice Cap. The numbers 1 to 5 locate regions on the adjacent ice cap that have undergone anomalous advances and slumping. Landsat image (10740–16100, bands 4, 5, and 7; 2 August 1974; Path 28, Row 10) is from the Canada Centre for Remote Sensing, Ottawa, Ontario.*

structure in the Precambrian bedrock. This zone contrasts with the area northwest of the Barnes Ice Cap, where lakes are scarce and little structural detail is evident.

Not as obvious, but also present in figure 5, are moraines around the southwest margin of the Barnes Ice Cap and other major neoglacial moraines along the west margin (Davis, 1985). On the east, areas of glacial scour can be seen to occupy lowlands, whereas the major interfluves show little evidence of glacial erosion. A series of moraines can also be observed near the fjord heads that are part of the moraine system deposited during Cockburn time (Falconer and others, 1965; Andrews and Ives, 1978) between 9 and 8 ka B.P.

The southern lobe of the Barnes Ice Cap was the location of intensive research by Holdsworth (1973a, b, 1977) [see following section] and Hooke (1973, 1976). The southern lobe exhibits two major features of interest:

(1) a zone of neoglacial moraines that have been dated by lichenometry as having formed between 1.5 ka and 60 years ago (Løken and Andrews, 1966; Andrews and Webber, 1969; Andrews and Barnett, 1979); and (2) a series of moraines that are crosscut by a distinctive rectangular lobe of the Barnes Ice Cap (southwest margin), which is interpreted as being associated with a recent rapid advance (Løken and Andrews, 1966; Løken, 1969; Holdsworth, 1973b; Jacobs and others, 1997).

Barnes Ice Cap: Geomorphology and Thermodynamics

By Gerald Holdsworth

Introduction

Barnes Ice Cap (lat 70°N., long 73°W.) (fig. 1) is situated in the center of Baffin Island. Both the Barnes Ice Cap and the Penny Ice Cap (300 km to the southeast) are probably the last remnants of the Laurentide Ice Sheet, the northeastern part of which covered most of the island as recently as at 10 ka (Dyke and Prest, 1987; Prest, 1969). Prior to that time and up to about the beginning of the Holocene Epoch, mountains along the northeastern coastal strip were more heavily glacierized than now, and outlet glaciers from the ice sheet and from highland glaciers would have filled the deep fjords that run in a northeasterly direction into Baffin Bay.

Having maximum (orthogonal) dimensions of about 150 km by 60 km, the Barnes Ice Cap covers an area of about 5,935 km^2. It has three main "domes" that have a maximum elevation on the northwestern one of about 1,124 m asl (fig. 6). The thickest ice, measured in 1967 (Clough and Løken, 1968), is about 550 m near the central dome (surface elevation 1,116 m). The south dome (surface elevation 958 m) was more than 460 m thick in 1970 (Jones, 1972). The ice cap is known to be shrinking in areal extent from glacial geologic evidence seen around the margin and from direct observations made since 1950.

On the basis of its thermal regime (Holdsworth, 1977; Classen, 1977; Hooke and others, 1980), the glacier is classified as subpolar or polythermal, as parts of the base in the region of the south dome are at the pressure melting point. Except where they are in contact with large proglacial lakes (for example, Conn, Bieler, and Generator Lakes; figs. 1, 5, 6), the margins of the ice cap are frozen to the base, where the temperature is typically about –7°C. The higher interior ice is several degrees (Celsius) warmer than the marginal ice (Holdsworth, 1977; Hooke and others, 1983). Near the top of the south dome, the mean annual air temperature is estimated to be about –15°C, whereas the mean annual ice temperature is about –8°C. This is a result of the release of latent heat associated with the formation of superimposed ice under the insulating snow cover in the upper parts of the ice cap each spring. This thermal structure is indirectly responsible for certain features seen on the satellite images.

A net accumulation of iced firn and superimposed ice (refrozen meltwater) is found on the higher parts of the glacier (Hooke and others, 1987). Elsewhere, blue, white, intermediate, or debris-laden ice is exposed in the outer parts of the ice cap later in the ablation season. In many parts of the ablation zone, meltwater lakes form in depressions on the ice surface. The depressions are believed to be troughs in a series of waves or irregular undulations that formed after a section of the ice cap underwent what was described previously as a surge (Holdsworth, 1977). The sections are usually well defined by an anomalously advanced margin and by a typically "slumped" and low-gradient vertical profile extending from the divide to the margin. In at least two cases, local divides show displacement, evidently as a result of the nonsteady ice flow that involves rapid mass transfer. Such profiles are easily obtained from the special series of 1:50,000-scale topographic maps that cover the ice cap.

Although the term "surge" has been applied to specific sections of the ice cap (Løken, 1969; Holdsworth, 1973b, 1977), a more appropriate term would be "local creep slump" (Shoemaker, 1981). The latter process involves enhanced ice creep and basal sliding induced by a bottom layer of meltwater that has slowly accumulated in the warmer central parts of the ice cap.

The main features that distinguish these sections from other parts of the ice cap can be seen on satellite images. These features, which all are located on the southwest side of the ice cap, are (1) the existence of more dendritic (higher-order) meltwater stream channels compared with channels elsewhere (in particular, sections on the northeast side of the ice cap do not divide close to proglacial lakes); (2) irregular folds or offset foliation defined by light- and dark-blue colored, banded ice; (3) the existence of moraine fields that indicate that only a discrete section of the ice margin was involved in an advance or a series of advances (Løken and Andrews, 1966).

Other information that is relevant to interpreting satellite images is as follows:

(1) A marginal or nearly marginal strip of whitish, bubbly, basal ice crops out along the edge of the ice cap. This ice has a density of 0.87 Mg m^{-3}. This is much less dense than most of the ice above, which has a density approaching 0.91 Mg m^{-3} (Hooke, 1976). In addition, the whitish ice has an oxygen isotope $\delta^{18}O$) value that indicates a Wisconsinan (late Pleistocene) age (Hooke and Clausen, 1982). That such a layer can have persisted since the Pleistocene is supported by simple two-dimensional steady-state dynamic modeling of the ice mass along flow lines through the south dome (Gerald Holdsworth and G.E. Glynn, unpub. data, 1975; Hooke, 1976).

    Hooke (1976) found that the whitish Pleistocene ice layer was 13-m thick in one marginal section of the south dome region. Its surface exposure on a slope averaging about 10° to 15° is on the order of 40–70 m, so on satellite images, the exposure is at least 1–2 pixels wide. Also, it normally does not crop out exactly at the margin but is commonly underlain by younger ice that it has overridden. Elsewhere, the whitish ice could be much thicker than it is at the south dome location. Sometimes wind-drift wedges of snow may form in the depression between the ice cap proper and a marginal ice-cored moraine. When looking for the Pleistocene ice in photographs and images, these considerations have to be taken into account. Thus, not all the marginal "whitish" ice seen in the following images is necessarily Pleistocene ice.

(2) Proglacial lakes affect the flow of ice in their vicinity. Two large ice-marginal lakes are located on the north side of the ice cap, Conn and Bieler Lakes (fig. 6). Both these lakes are deep where they are dammed against the ice because the slope of the land is toward the ice cap. As a consequence, ice flow is locally focused toward the lakes, and "draw-down" of the ice has produced some of the effects also seen in the "slumped" areas. In contrast, the smaller Generator Lake on the east end of the ice cap has evidently been dammed by the local advance that resulted from "creep slump" in part of the south dome within the last century (Holdsworth, 1973b).

Analysis of Landsat Imagery

Figure 6 is a Landsat 1 MSS false-color composite image of the Barnes Ice Cap acquired 2 August 1974 and processed for standard earth-science analysis. Part of the southeast end of the glacier is obscured by clouds. However, snow, ice, and some structural detail can be seen over most of the rest of the ice cap. The sections that show evidence for local advance are the lobes numbered 1 through 5, all situated on the southwest side of the ice cap. The main observations that define the slump areas are

(1) The irregular or lobate form of the margins.

(2) The arcuate moraine loop associated with slump margin 2. Although most of the advanced lobes have enhanced moraine forms associated with them, the most obvious is this one, which is about 20 km long. These moraines can be easily seen on the NTS map sheet 37D/9 (scale 1:50,000). A detailed structural map and cross section of this moraine system is also shown in Løken and Andrews (1966). They show that, in this system of moraines, the outer one represents a major advance of a section of the ice cap about 700 years ago. Other readvances took place 400 to 500 years ago and about 300 years ago. On the other hand, slump margin 1 is probably the youngest, and its prominent ice-cored moraine ridges are still very close to the edge of the ice cap.

(3) Large supraglacial lakes can still be seen in the slump area marked 5, even in early winter images. The largest lake is about a kilometer long.

Also seen in figure 6 are the ice drawdowns associated with Conn and Bieler Lakes. Note the zone of darker blue ice entering Conn Lake. Figure 7 is part of an aerial photograph that shows this darker ice. The ice here appears darker because it is crevassed and also probably because the banded foliation seen elsewhere is destroyed by compression transverse to the extending flow direction, which is toward the lake.

Finally, notice a discontinuous strip of marginal "whitish" ice that appears much lighter than the blue ice higher on the ice cap. This is proba-

Figure 7.—*Vertical aerial photograph of the north margin of the Barnes Ice Cap showing darker ice entering Conn Lake (see fig. 6). Note crevasse traces in the ice. The Pleistocene ice is probably the 50- to 200-m-wide white band that is truncated by Conn Lake and the smaller Nivalis Lake to the northwest. See Hooke (1976) for an explanation of why this ice is often underlain by younger ice. Photograph NAPL No. A–17047–108 courtesy of the National Air Photo Library, Ottawa, Ontario, Canada. Used with permission.*

bly a combination of the Pleistocene ice and marginal wind-drift and wedges of snow, as mentioned earlier. The white strip is particularly visible in the black-and-white satellite image of figure 5. Note that it is continuous between slump margins 2 and 3, but it is absent along the slump margins where it has probably been overridden by younger (Holocene) ice. A short white strip is visible between margins 3 and 4. Also clearly seen in figure 6 are the ice-surface outlines of slump margins 1, 2, and 3. Outlines of slump margins 4 and 5 are less pronounced but are still evident. Slump margin 5 may not have experienced much advance but may be instead a mass transfer from the reservoir regions to the margin in the form of a persistent bulge, such as has been observed on the Trapridge Glacier in Yukon Territory (Clarke and others, 1984). On the other hand, drainage patterns in the moraine fields suggest that the margin may have previously advanced several kilometers more than the adjacent margin. The strip of white ice at the margin of lobe 5 is thought to be (or at least to contain) the Pleistocene ice. Even with marginal ice slopes in the northwest sector at under 3°, a 10–20 m thick Pleistocene ice layer would only cover a horizontal distance of 200–400 m.

To see more of the features mentioned above, it is necessary to examine two more satellite images. Figure 8*A* is a Landsat 3 MSS false-color composite image acquired 12 August 1979 showing a considerably greater central area of snow cover than that found in figure 5. Of particular interest are

Figure 8.*—Landsat MSS false-color composite images of Barnes Ice Cap.* ***A****, Landsat 3 image showing development of meltwater streams, lakes, and exposed underlying ice (darker blue). See text for further description. Landsat image (30525–16065, bands 4, 5, and 7; 12 August 1979; Path 28, Row 10) is from Canada Centre for Remote Sensing, Ottawa, Ontario.* ***B****, See following page.*

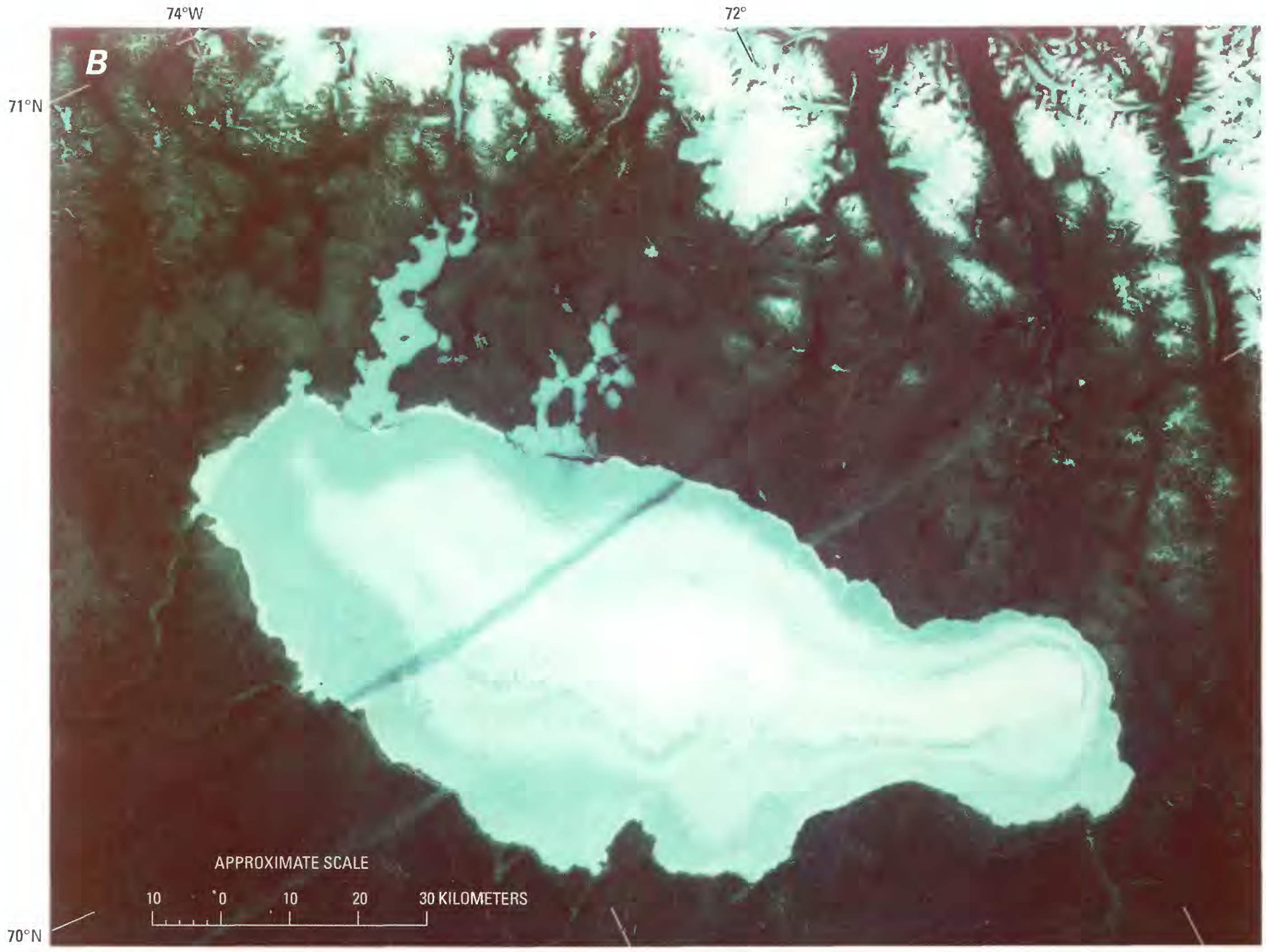

*Figure 8*B, *Landsat 2 image showing glacier-surface details near the end of the ablation season. Landsat image (22050–16064, bands 4, 5, and 7; 2 September 1980; Path 28, Row 10) is from Canada Centre for Remote Sensing, Ottawa, Ontario.*

(1) the presence of meltwater lakes appearing as dark-blue marks in the zone of sporadic, saturated snow between the central snow cover and the blue ice; (2) the development of meltwater streams appearing as linear blue streaks in areas of smooth contours (seen in the 1:50,000-scale topographic map sheets) or as dendritic networks in areas of irregular contours (typical of the slumped areas); and (3) the existence of the discontinuous narrow strip of white ice close to the edge of the ice cap.

Figure 8*B* is a Landsat 2 MSS false-color composite image taken 2 September 1980 that shows the glacier near the end of the ablation season. The prominent streak running diagonally across the image is a shadow cast by an aircraft "contrail," which is barely visible just below and to the right of it. The central divide area is still covered by residual snow; this area is the 1980–81 firn accumulation zone (Hooke and others, 1987). The shorter blue streaks at the edge of the snow mark the slush zone. Where local topography is favorable, slush avalanches are common in late summer. They drain the saturated snow facies. The prominent, arcuate indentations and converging meltwater streams help define the upper limit of the slump regions. The light-blue zone fringed by the upper and lower dark-blue (ice) probably represents areas of thin slush covering underlying blue ice. The dark-blue zone surrounding it is the outcrop of dense, bubble-poor Holocene ice. Again, the marginal strips of white ice are provisionally interpreted to be Pleistocene ice. The strip is widest in the northwestern part of the ice cap. Elsewhere, the marginal ice is commonly very complex and contains flow folds that have nearly horizontal axial planes.

Features seen in the image in figure 8*A* but not in figure 8*B* are darker areas (>1 km^2) in the blue-ice zone where a slight green hue is also apparent. The origin of these features has not been verified, but they could represent temporary or residual areas of superimposed ice associated with dirt. Such dirt, in the form of scattered small cones, is often visible to an observer traveling over lower parts of slump margin 1 (fig. 6). The dirt would have become concentrated in the bottom of supraglacier lakes. At a later time, a stream may reroute and wash the sediment away. The transient nature of these features is demonstrated by their absence from the image in figure 8*B*.

Figure 9 is a vertical aerial photograph showing slump margin 1. The banded foliation patterns are particularly striking. At Generator Lake (east edge of photograph), the margin shows finer scale foliation in a 10-m-high ice cliff, above which is a heavy moraine cover (upper right part of image). Note the supraglacial channel on the ice cap in figure 10*A*. This channel separates slump margin 1 ice on the left from essentially unslumped ice on the right. A recumbent flow fold is visible in a closer view of this exposure (fig. 10*B*). Hudleston (1976) analyzed the flow field required to produce such folds. He suggested that they can result from changes in the flow field as the shape or profile of the ice cap changes due to climatic factors. Details of the debris content in this ice may be found in Holdsworth (1973a). A 12–15-m-high ice cliff in 30-m deep water is seen in figure 11. These cliffs all show up as sharp edges on the vertical aerial photographs and satellite images.

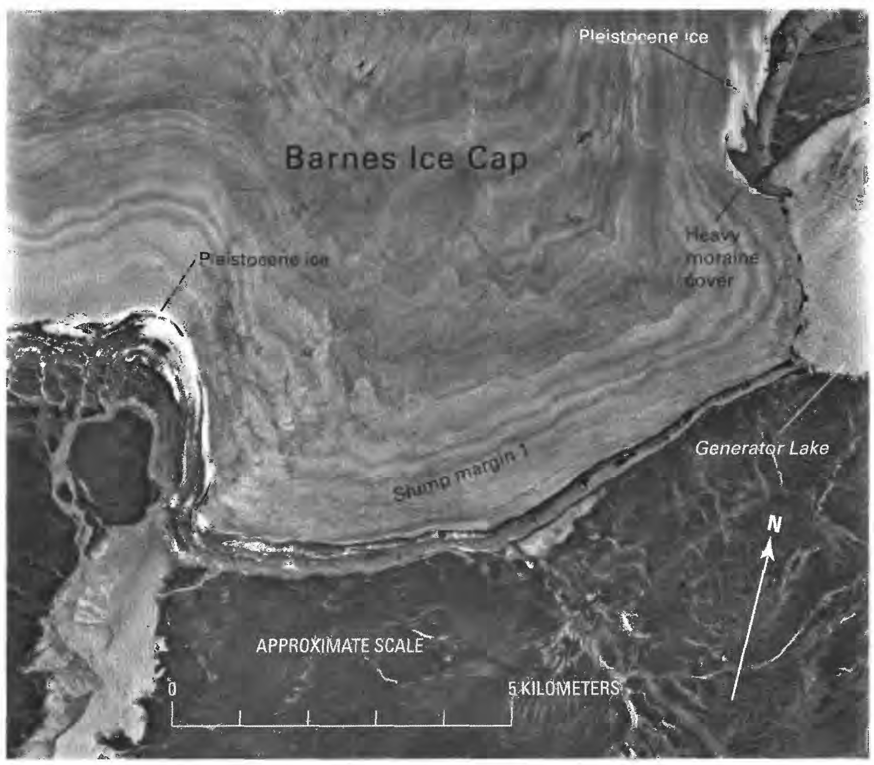

Figure 9.*—Vertical aerial photograph of Barnes Ice Cap showing part of slump margin 1 (see fig. 6 for location). Note the extremely crenulated foliation, which is typical of slumped margins. Generator Lake is on the right. At the contact between the lake and the ice cap margin is an area of heavy moraine cover (see fig. 10A). Some of the bright (white) areas seen in this location are possibly the remains of late season snow drifts. The Pleistocene ice layer is present in the bight on the northeast margin, north of the heavy moraine cover, and possibly on the southwest margin on the west edge of the photograph, according to R.L. Hooke (written commun., 22 July 1999). Elsewhere in the image, the layer would be unrecognizable because of the slump. Photograph NAPL No. A–17042–127 courtesy of the National Air Photo Library, Ottawa, Ontario, Canada. Used with permission.*

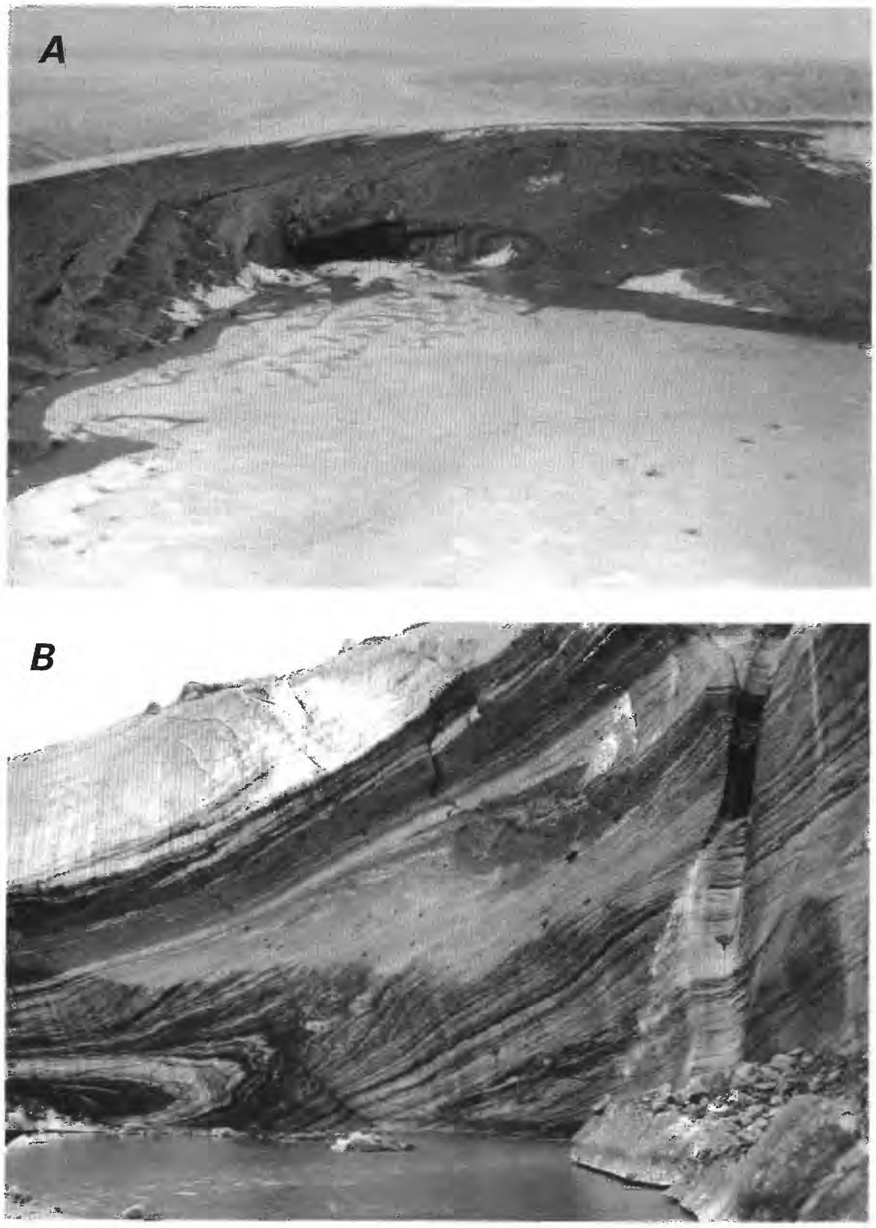

Figure 10.—Margin of Barnes Ice Cap at Generator Lake. **A**, *Oblique aerial photograph showing the heavy moraine cover on the ice seen in the previous air photograph. Also visible are remnant snow patches and an ice cliff, which has a flow fold (fig. 10B). Photograph by Gerald Holdsworth taken in July 1970.* **B**, *Ten-meter-high ice cliff in which can be seen a recumbent flow fold defined by submeter-scale layering in the ice. This is about two orders of magnitude smaller than the smallest banded foliation seen in the satellite images. Photograph by Gerald Holdsworth.*

Figure 11.—Ice cliffs 12–15-m high at the edge of the Barnes Ice Cap where it calves into Generator Lake in 30 m of water. Photograph by Gerald Holdsworth taken in August 1971.

Late 20th Century Change at the Barnes Ice Cap Margin

By John D. Jacobs

Introduction

As described in the preceding text, glaciological studies have been carried out on the Barnes Ice Cap since 1950, including several periods of intense investigation in the 1960's and 1970's. Early work recognized that recession had been taking place along the ice-cap margin for centuries, particularly in the south and west, but that the recession had not been uniform along the entire margin. Holdsworth (preceding section) interpreted forms along the west and south margins as advancing lobes associated with slump areas. In these areas and elsewhere, the ice front had receded from well-defined moraine ridges. Along the northeast and east margins, much less change was noted. Løken and Andrews (1966) concluded from lichenometric studies of moraines around the south dome of the ice cap that its northeast margin was either stationary or advancing northeastward as the ice divide migrated in that direction.

Between 1970 and 1984, repeated surveys were conducted by Holdsworth and Hooke along a 10-km-long stakeline running northeast from the summit of the south dome (Holdsworth, 1975; Hooke and others, 1987) (958-m dome in fig. 6). Although large interannual differences were found in mass balance, the net balance averaged over the transect was negative for the 14-year period. It was estimated that the ice cap in this sector had thinned by about 2 m in that time (Hooke and others, 1987). In the absence of continued surveys, subsequent changes there and over the ice cap as a whole remain unknown.

Studies of the Margin Using Landsat Imagery

From 1989 to 1991, an area of the northwest margin of the Barnes Ice Cap including the Lewis Glacier (figs. 6 and 12) was investigated by Jacobs and others (1993), with reference to surveys done in the 1960's (Andrews and Webber, 1964; Andrews and Barnett, 1979). The position of the glacier terminus was surveyed, and a section of the ice cap margin south of the Lewis Glacier was staked for monitoring. Control points were established for registration and classification of satellite imagery.

A Landsat MSS image dated 19 August 1988 was obtained that covered 40 km of the ice cap margin centered on the Lewis Glacier. The 1961 position of the glacier margin was digitized from the 1:50,000-scale map sheet for the area (NTS map sheet 37E/6W, which is based on 1961 aerial photogrammetry) and then was superimposed on the georeferenced Landsat image. The right (south) margin and central terminus of the Lewis Glacier

Figure 12.—*Lewis Glacier, an outlet glacier at the northwest margin of the Barnes Ice Cap (fig. 6). Low-angle oblique aerial photograph taken in July 1993 from the south. The width of the glacier front is approximately 500 m. Recession of the Lewis Glacier terminus averaged 25 m a^{-1} between 1961 and 1991. Photograph by J.D. Jacobs.*

were found to be well defined, but it was not possible to differentiate between debris-covered ice and the surrounding terrain in other sectors. Estimates of retreat were, therefore, most accurate in the former areas. The Lewis Glacier terminus had retreated 680 m between 1961 and 1988, or about 25 m a^{-1}, compared with an estimate of 20 m a^{-1} obtained by earlier workers from detailed surveys of the terminus in 1963 and 1965 (Anonymous, 1967). Recession along the ice cap margin south of the Lewis Glacier was 9 m a^{-1} for the same period. Recession in varying amounts was determined over the entire 40-km segment of the northwest margin contained in the 1988 Landsat MSS subscene (Jacobs and others, 1993).

Additional mapping of the Barnes Ice Cap margin in its southern sector was undertaken by using a Landsat 5 Thematic Mapper (TM) scene (3 August 1993) covering the southern one-third of the ice cap (Jacobs and others, 1997). Low-angle oblique aerial photography was obtained in August 1994 along parts of the margin as a basis for controlling the classification of the TM image. Classification of the glacier facies was based on the TM band 4 to band 5 image ratio, which is effective at identifying ice, open water, and exposed bedrock (Williams and others, 1991). The existing (1961 aerial photogrammetry) 1:50,000-scale NTS map sheet for the ice cap was digitized for digital elevation model (DEM) construction, and the georeferenced, classified image was registered to the DEM by using 47 ground-control points. The combined root-mean square (rms) error of the georeferenced image and the digitized base map was estimated to be 33 m. It was difficult to determine the position of the ice margin in the presence of debris-covered ice and where perennial snowbanks lay on the distal side of ice-cored moraines. Taking this uncertainty into account, the average recession over the 183-km length of the south and east margins between 1961 and 1993 was estimated to be at least 137 m, or about 4 m a^{-1} (Jacobs and others, 1997).

Change Detection Using RADARSAT SAR

Synthetic aperture radar (SAR) offers the advantage for glaciological investigations of coverage in any season or in any cloud conditions, although challenges arise in the interpretation (Bindschadler and Vornberger, 1992). Short (1998; Short and others, 2000) studied the feasibility of ice-margin mapping on the Barnes Ice Cap using SAR imagery from RADARSAT. The field area was the north margin of the south dome, an area of debris-covered ice, massive ice-cored moraines, and distal snowbank features (fig. 13). It was in this sector that Løken and Andrews (1966) suggested the ice cap was stationary or possibly advancing. Ambiguities in

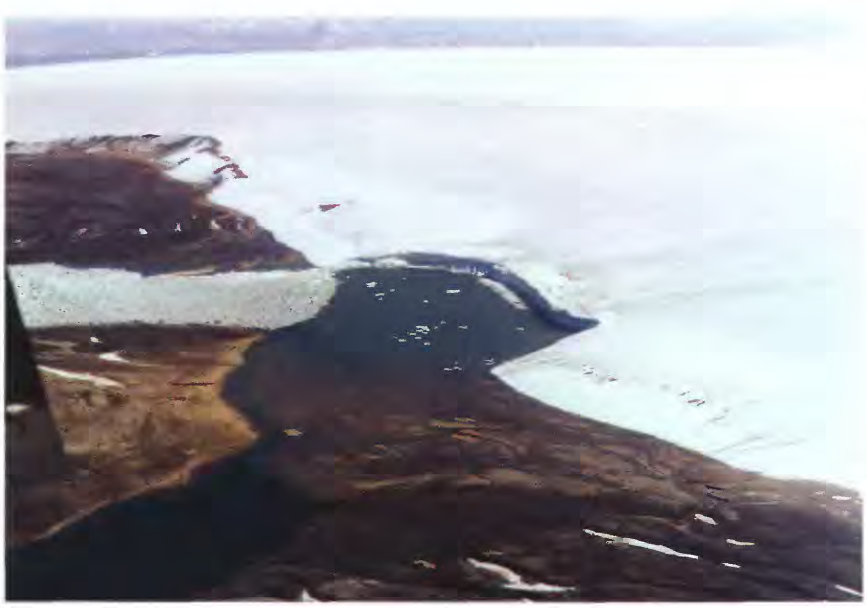

Figure 13.*—North side of the south dome of the Barnes Ice Cap at Gee Lake, view looking southward. Low-angle oblique aerial photograph by J.D. Jacobs taken in July 1997.*

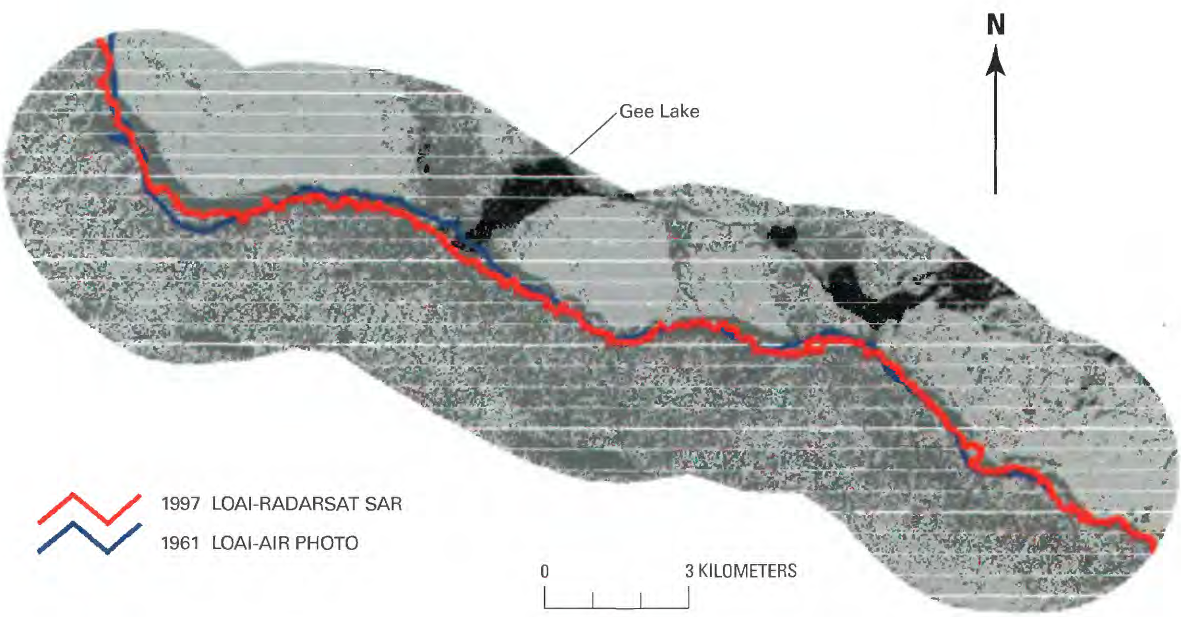

***Figure 14.**—Part of a RADARSAT SAR image centered on Gee Lake (lat 60°57'N., long 72°29'W.), Barnes Ice Cap, showing mapped 1997 limit of active ice (LOAI) and 1961 LOAI from air-photograph interpretation. RADARSAT image (S4 ASC, ID M0122606, 26 July 1997) from RADARSAT International, Richmond, British Columbia.*

what was meant by the glacier "edge" or "margin" in such a complex terrain led Short (1998) to focus on the concept *limit of active ice*, defined as the extent of ice that is still fed from the accumulation zone of the glacier.

Three RADARSAT SAR images were obtained for the summers of 1996 and 1997, including descending (view up-glacier) and ascending (view down-glacier) standard modes (picture element (pixel) resolution of 25 m) and an ascending fine-mode image (pixel resolution of 8 m). Field studies were carried out during the summer of 1997 along the 27-km stretch of the moraine selected as a test area (figs. 13 and 14). Image analysis involved image speckle filtering, texture analysis, supervised classification, image segmentation, and edge detection, in that order, and the ascending standard mode provided the best results. The approach was successful in mapping the limit of active ice with an accuracy of 49 m (Short and others, 2000). The resulting map has been used to assess the amount of change along this section of the margin (Jacobs and others, 1999). Interpretation of 1961 aerial photography and the corresponding topographic map permitted delineation of the limit of active ice in this area for 1961, which was transferred to the 1997 SAR image (fig. 14). Recession is evident in some areas, such as the ice front calving into Gee Lake, and slight advance in others; overall, however, the average change in the position of the margin during the 36 years between observations has been slight.

Conclusion

Multispectral satellite imagery has been demonstrated to provide a basis for first estimates of changes in the position of the Barnes Ice Cap margin. Sustained overall recession is evident around the margin. Recession was clearly documented at the two study sites (Lewis Glacier and Gee Lake, fig. 6). RADARSAT SAR was found to be a more sensitive tool for detecting change in the areas of complex morphology in the north part of the south dome. Results from that analysis support the conclusion that the Barnes Ice Cap is experiencing overall attrition. It should be noted that for most of the latter half of the 20th century, ablation-season temperatures in the Baffin Island region did not change significantly, in contrast to the pronounced summer warming that was recorded in the western Arctic (Chapman and Walsh, 1993). Should a regional warming take place, it is to be expected that shrinking of the Barnes Ice Cap will accelerate.

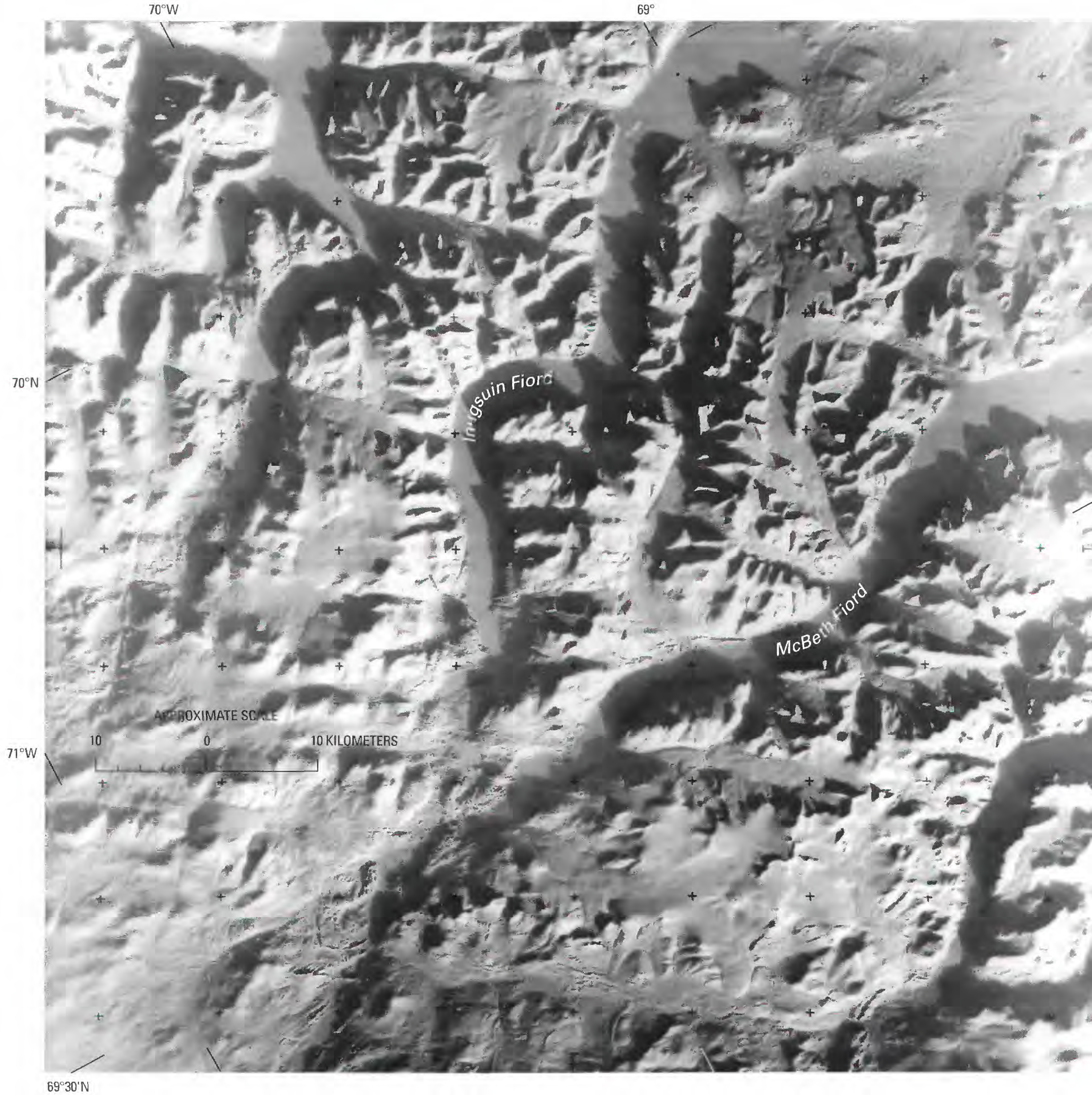

Alpine Area (Lat 69°N., Long 69°W.): Home Bay

Farther to the southeast of the Barnes Ice Cap, the transition between the alpine-sculptured area of the fjord and the more massive, rolling terrain of the interior can be seen on a Landsat 3 return beam vidicon (RBV) image taken 24 February 1980 (figs. 1 and 15). The low solar-elevation angle accentuates the position of individual cirque basins, many of which merge into mountain ice fields and are drained by large outlet glaciers. Large neoglacial moraines can be distinguished in the center bottom of the scene. To the east, the alpine terrain gives way abruptly to the low foreland of the

Figure 15.*—Landsat 3 RBV image with low Sun angle (elevation 10°) highlighting the alpine terrain northwest of Home Bay (see fig. 1 for location and text for more details). Landsat image (30721–15514 B; 24 February 1980; Path 26, Row 11) is from the Canada Centre for Remote Sensing, Ottawa, Ontario.*

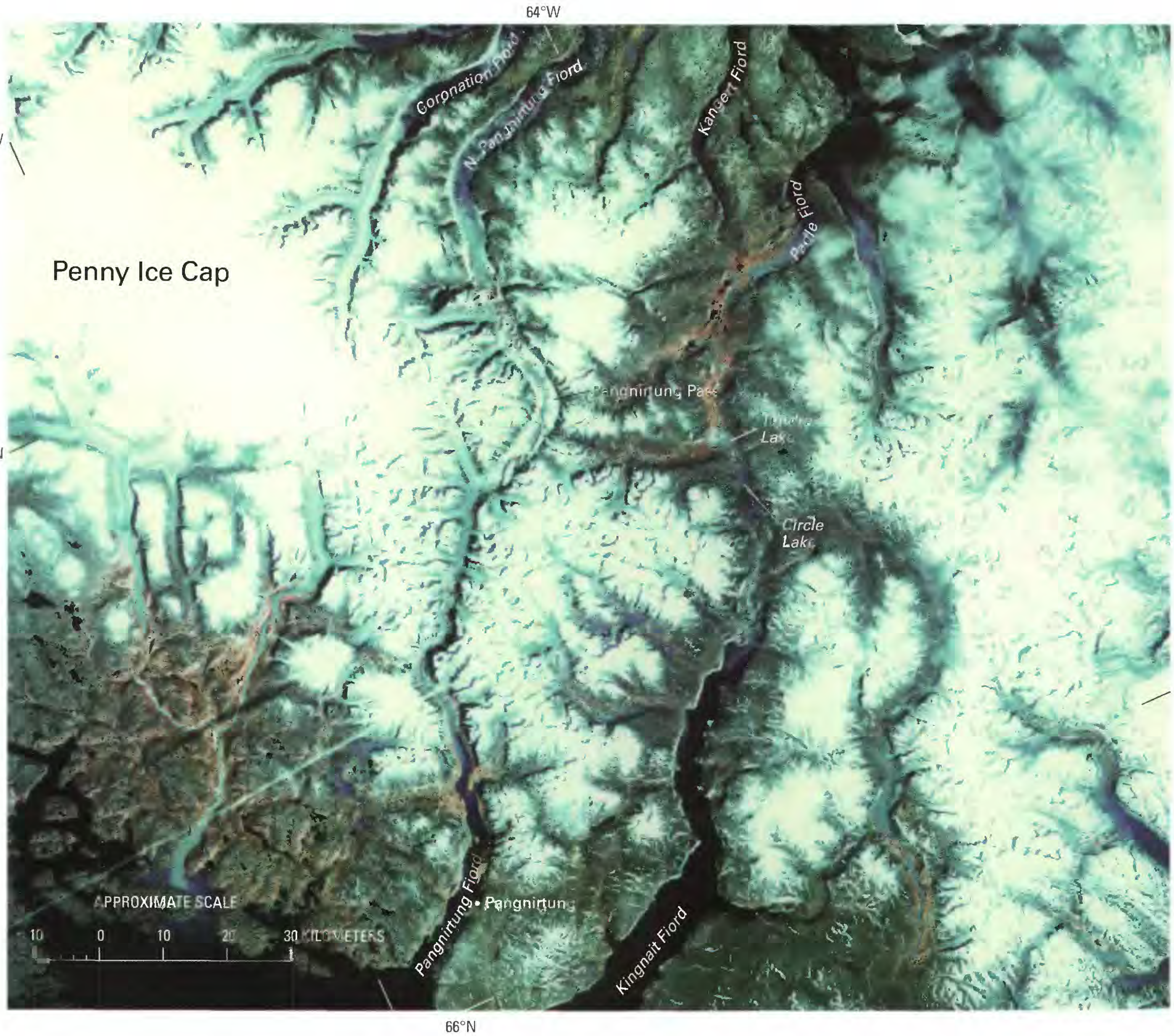

__Figure 16.__—Landsat 2 MSS false-color composite image of part of the Penny Ice Cap and the glacierized alpine terrain of the central Cumberland Peninsula (see fig. 1). Abbreviation: N., North. Landsat image (21663–15103, bands 4, 5, and 7; 12 August 1979, Path 19, Row 13) is from the Canada Centre for Remote Sensing, Ottawa, Ontario.

Cape Henry Kater area (fig. 1) (King, 1969a and b), which contains a long and complex Quaternary glacial and marine record (King, 1969b; Miller, 1985a, b). Controls on the glacierization of this area are discussed in Andrews and others (1970), and mass-balance estimates are contained in Weaver (1975).

Penny Ice Cap and the Cumberland Peninsula

One of the most spectacular regions in Baffin Island is illustrated in figure 16, a Landsat 2 MSS false-color composite image taken 12 August 1979. Most of the area in the right one-half of the image lies within the Auyuittuq National Park (fig. 1). The settlement of Pangnirtung lies within the center bottom of the image but cannot be detected.

The pattern of glacierization readily enhances major rectilinear structural details in the bedrock. Cumberland Peninsula is crossed by two major fjord-valley systems (fig. 1). To the east, Kingnait Fiord leads northward through Circle and Tundra Lakes toward Padle Fiord; farther west, Pangnirtung Fiord heads northward to Pangnirtung Pass and hence into North

Pangnirtung Fiord. Elevations along Pangnirtung Pass vary between 1,500 and 2,000 m asl. Penny Ice Cap lies northwest of Pangnirtung Pass. Near Pangnirtung Pass, the ice cap consists of interlocking cirque glaciers and outlet glaciers forming a highland ice field, but farther west, the relative relief decreases, and an ice cap covers most of the terrain. Large outlet glaciers descend from the ice cap to the north, east, and south. Coronation Glacier ends in a calving margin in Coronation Fiord (Gilbert, 1982) (figs. 1, 16). Figure 16 does not show the extent of the ablation zone, although careful examination indicates that many of the large outlet glaciers are snow-free. The snowline at this time is estimated to lie at about 750 m asl.

In the southwest corner of the image (fig. 16) is a good illustration of the character of what Sugden (1978) called "ice-scoured terrain." Little evidence exists for a thick till cover, and instead, the details of the bedrock structure are visible and are enhanced by small lakes. This area contrasts with the terrain along the north edge of Penny Ice Cap, (5,960 km^2) where outlet glaciers have been topographically steered, and complete glacial inundation, if it were present, may have happened at 1 Mega-annum (Ma, 10^6 years) to 100 ka B.P. (Boyer and Pheasant, 1974).

Cape Dyer, Cumberland Peninsula

Figure 17, a Landsat 2 MSS false-color composite image, partly overlaps figure 16, which lies to the west. However, this Landsat image was acquired on 26 July 1975 during one of the warmest summers on record. The area is heavily glacierized by individual cirque glaciers, valley glaciers, and highland ice caps. Large outlet glaciers flow from the latter and descend to 0 to 200 m asl in most localities. The glaciation level rises steeply from the outer coast (fig. 2). Because of extensive open water off Cape Dyer during a good part of the year, the snowfall around Cape Dyer is the heaviest on record for the eastern Canadian Arctic (Andrews and others, 1970). The average annual snowfall at Cape Dyer, about 5.0 m, declines rapidly to the north and west, so that at Broughton Island (just off the top left corner of figure 17 (see fig. 1)) the average recorded annual snowfall is only about 2.5 m. The transient snowline seen on the image is quite high and is estimated to lie at about 1,000 m asl.

The glacial history of the Cape Dyer area and that of Merchants Bay to the northwest (fig. 17) were studied by Locke (1980) and Hawkins (1980). They showed that neoglaciation affected both areas, but near Cape Dyer, the neoglacial moraines of the large outlet glaciers overran weathered tills that date from the earlier Sunneshine stade, dated at approximately 100 ka B.P. In contrast, Hawkins (1980) and Miller (1975), working in the fjords of Merchants Bay, were able to map extensive late Foxe (=late Wisconsinan) moraines that terminated at sea level and were associated with large deltas, the tops of which are now about 35 m below sea level. Amino-acid age estimates and uranium-series radiometric dating indicate that the outer coast in this area was deglaciated at more than 75 ka B.P. (Szabo and others, 1981). More recent research has used a combination of cosmogenic dating (=exposure age dating) of boulders and radiocarbon dating of lake sediments to provide a more detailed account of the glacial history of this region (Steig and others, 1998).

The heaviest area of sea-ice cover around Baffin Island is located between Cape Dyer and Home Bay to the northwest (fig. 1). In most years, sea ice is very close to the coast until well into late August or even early September, but in 1975, the sea ice broke up early, and most sea ice cleared the coast by the first week in August.

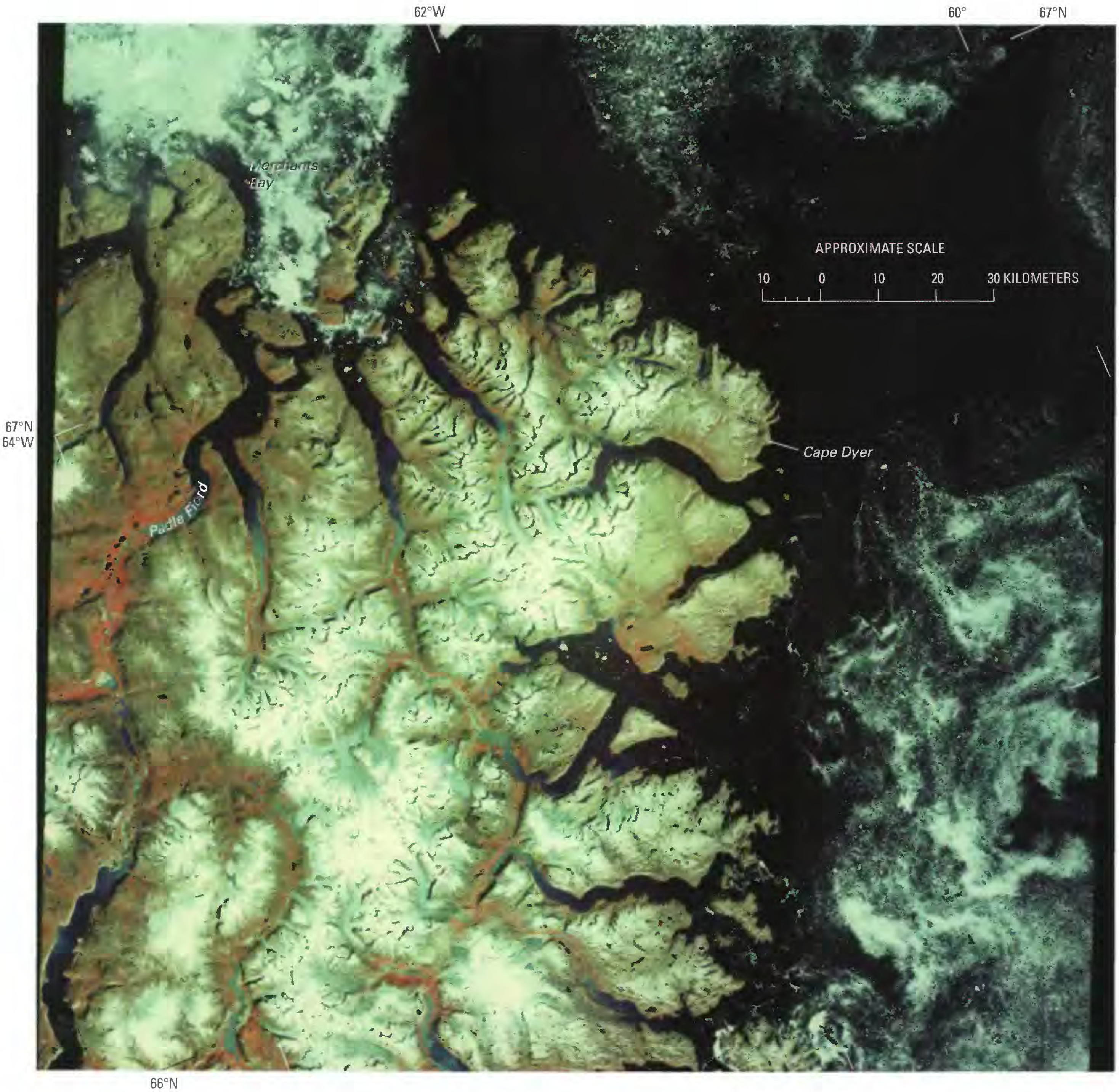

Figure 17.—*Annotated Landsat 2 MSS false-color composite image of local alpine glaciers on the eastern part of the Cumberland Peninsula (see fig. 1). Landsat image (20185–15051, bands 4, 5, and 7; 26 July 1975; Path 17, Row 13) is from the Canada Centre for Remote Sensing, Ottawa, Ontario.*

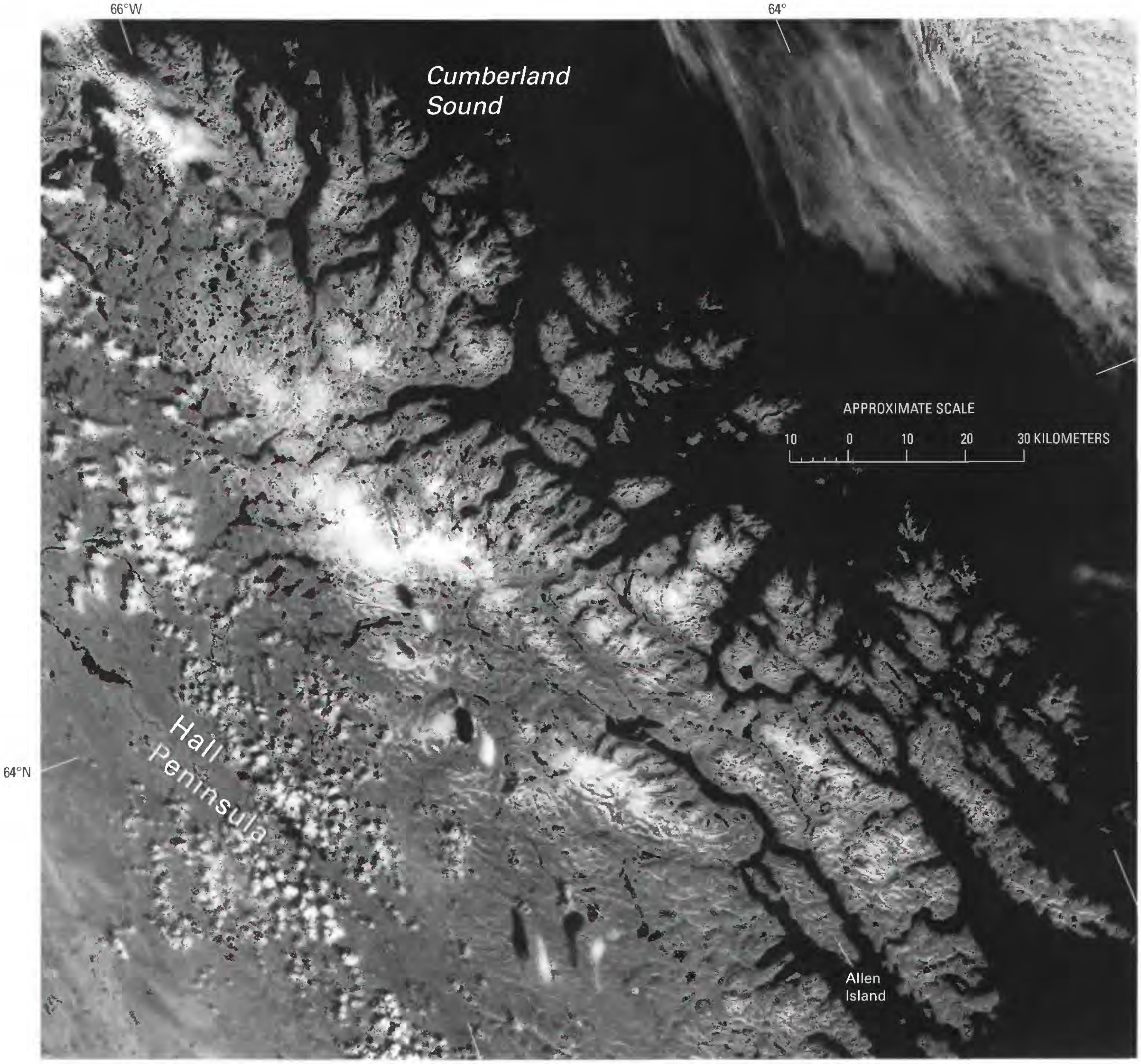

Hall Peninsula

Figure 18.—Annotated Landsat 1 MSS black-and-white image of an ice cap on the northeast coast of Hall Peninsula (fig. 1). Landsat image (1747–15083, band 7; 9 August 1974; Path 17, Row 15) is from the EROS Data Center, Sioux Falls, S. Dak.

Small ice caps and small glaciers lie in a restricted zone along the northeast and east flank of the Hall Peninsula (fig. 1). The Landsat image taken 9 August 1974 (fig. 18) illustrates the major geographic features of the glacierization. The margins of the ice caps are simple along the southwest where they terminate on uplands of Hall Peninsula, but on the seaward side, small outlet glaciers are topographically channeled, although none descend to sea level. The glaciation level for the region is shown in figure 2. No glaciological research has been undertaken on any of the glaciers on the Hall Peninsula, and few glacial geological investigations have been carried out (Miller, 1985b). Data on late Foxe deglaciation have come from marine shells in glacial marine deltas, and ages fall between 9.5 and 8.5 ka B.P. (Miller, 1979, 1980). However, amino-acid studies suggest that parts of Allen Island were deglaciated at more than 80 ka years ago. (Andrews and others, 1981).

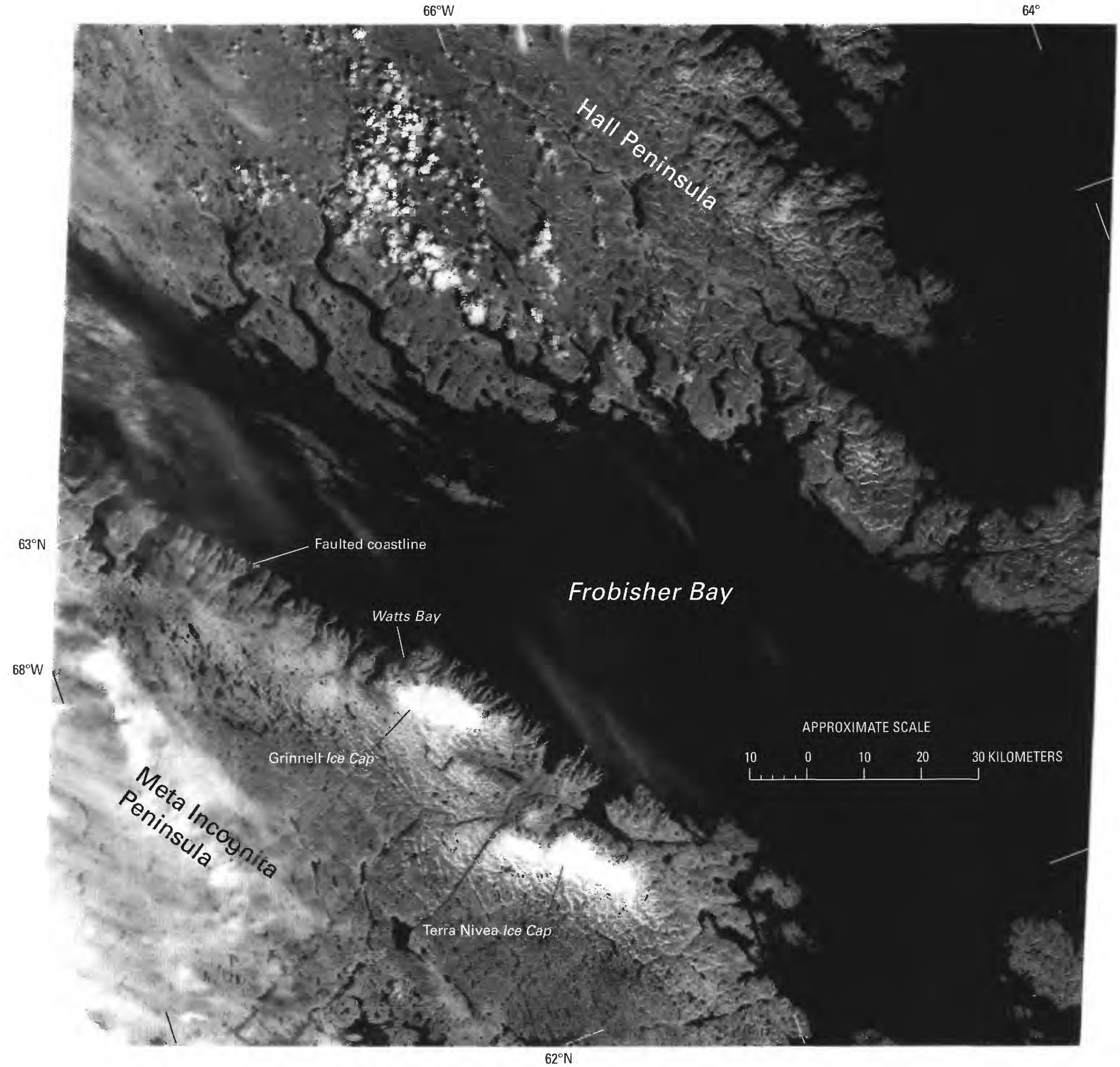

Figure 19.*—Annotated Landsat 1 MSS black-and-white image of Terra Nivea and Grinnell* Ice Caps *on the Meta Incognita Peninsula, southern Baffin Island (fig. 1). Landsat image (1747–15090, band 7; 9 August 1974; Path 17, Row 16) is from the EROS Data Center, Sioux Falls, S. Dak.*

Meta Incognita Peninsula

Figure 19 is a Landsat 1 MSS image taken 9 August 1974 that covers the small Terra Nivea and Grinnell *Ice Caps* on the uplifted rim of the Frobisher Bay half-graben. The image does not reveal much detail because of extensive snow cover on the ice caps. These two small ice caps have been studied relatively little (Dowdeswell, 1982, 1984), and no reports exist on the amount of winter accumulation, although studies have been made of the neoglacial and Holocene glacial histories (Blake, 1953; Mercer, 1956; Muller, 1980; Lind, 1983; Stravers, 1986; Duvall, 1993).

Dowdeswell (1982) studied the tidal outlet glacier from the Grinnell *Ice Cap* that ends in Watts Bay (fig. 19). This glacier is moving at about 20 m a^{-1} at its terminus, and 100 to 200 years ago, it extended much farther out into Watts Bay. The description of the two ice caps by Hall (1865) during the middle of the 19th century suggests that a significantly thicker snow (if not ice) cover may have been present, so that the appearance from Frobisher Bay was of a continuous ice body. Studies of moraines fronting glaciers around the Terra Nivea and Grinnell *Ice Caps* (Muller, 1980; Dowdeswell, 1982, 1984) indicate that the major glacier recession dates from the last 100 years. In addition to the two small ice caps, a number of small cirque glaciers face Frobisher Bay. These are not well shown on this Landsat image, although the image does indicate the presence of cirques, many of which are drowned or partly drowned, along the steep fault-bound escarpment. The escarpment is strikingly illustrated in the coastline of Frobisher Bay immediately northwest of the Grinnell *Ice Cap*.

References Cited

Andrews, J.T., and Barnett, D.M., 1979, Holocene (Neoglacial) moraine and proglacial lake chronology, Barnes Ice Cap, Canada: Boreas, v. 8, no. 3, p. 341–358.

Andrews, J.T., and Barry, R.G., 1972, Present and paleo-climatic influences on the glacierization and deglacierization of Cumberland Peninsula, Baffin Island, N.W.T., Canada: Boulder, Colo., University of Colorado, Institute of Arctic and Alpine Research, Occasional Paper 2, various paginations.

Andrews, J.T., Barry, R.G., Bradley, R.S., Miller, G.H., and Williams, L.D., 1972, Past and present glaciological responses to climate in eastern Baffin Island: Quaternary Research, v. 2, no. 3, p. 303–314.

Andrews, J.T., Barry, R.G., and Drapier, L., 1970, An inventory of present and past glacierization of Home Bay and Okoa Bay, east Baffin Island, N.W.T., Canada, and some climatic and paleoclimatic considerations: Journal of Glaciology, v. 9, no. 57, p. 337–362.

Andrews, J.T., Clark, P., and Stravers, J.A., 1985, The patterns of glacial erosion across the eastern Canadian Arctic, *in* Andrews, J.T., ed., Quaternary environments: Eastern Canadian Arctic, Baffin Bay and western Greenland: Boston, Allen and Unwin, p. 69–92.

Andrews, J.T., Davis, P.T., and Locke, C., 1976, Little Ice Age permanent snowcover in the eastern Canadian Arctic—Extent mapped from Landsat-1 satellite imagery: Geografiska Annaler, v. 58A, no. 1–2, p. 71–81.

Andrews, J.T., and Ives, J.D., 1978, “Cockburn” nomenclature and the late Quaternary history of the eastern Canadian Arctic: Arctic and Alpine Research, v. 10, no. 3, p. 617–633.

Andrews, J.T., and Miller, G.H., 1972, The Quaternary history of northern Cumberland Peninsula, Baffin Island, N.W.T., Canada; Part IV, Maps of the present glaciation limits and lowest equilibrium line altitude for north and south Baffin Island: Arctic and Alpine Research, v. 4, no.1, p. 45–59.

Andrews, J.T., Miller, G.H., Nelson, A.R., Mode, W.N., and Locke, W.W., III, 1981, Quaternary near-shore environments on eastern Baffin Island, N.W.T., *in* Mahaney, W.C., ed., Quaternary paleoclimate: Norwich, Geo Abstracts, p. 13–44.

Andrews, J.T., and Webber, P.J., 1964, A lichenometrical study of the northwestern margin of the Barnes Ice Cap; a geomorphological technique: Canada Department of Mines and Technical Surveys, Geographical Bulletin 22, p. 80–104.

Andrews, J.T., and Webber, P.J., 1969, Lichenometry to evaluate changes in glacial mass budgets, as illustrated from north-central Baffin Island, N.W.T.: Arctic and Alpine Research, v. 1, no. 3, p. 181–194.

Andrews, Martha, and Andrews, J.T., 1980, Baffin Island Quaternary environments—An annotated bibliography: Boulder, Colo., University of Colorado, Institute of Arctic and Alpine Research, Occasional Paper 33, 123 p.

Anonymous, 1967, Hydrology of the Lewis Glacier, north-central Baffin Island, N.W.T., and discussion of reliability of the measurements: Geographical Bulletin, v. 9, no. 3, p. 232–261.

Baird, P.D., 1951, Method of nourishment of an ice cap on Baffin Island, *in* Assemblée Générale de Bruxelles, 1951: Association Internationale d'Hydrologie Scientifique Publication 32, v. 1, p. 194–202.

Baird, P.D., 1953, Baffin expedition 1953: Arctic, v. 6, no. 2, p. 163–164.

Baird, P.D., and others, 1953, Baffin Island expedition, a preliminary field report: Arctic, v. 6, no. 4, p. 227–251.

Bindschadler, Robert, and Vornberger, Patricia, 1992, Interpretation of SAR imagery of the Greenland Ice Sheet using coregistered TM imagery: Remote Sensing of Environment, v. 42, no. 3, p. 167–175.

Bird, J.B., 1967, The physiography of Arctic Canada, with special reference to the area south of Parry Channel: Baltimore, Johns Hopkins Press, 336 p.

Blake, W.J., 1953, Studies of the Grinnell Glacier, Baffin Island: Arctic, v. 6, no. 2, p. 167.

Boyer, S.J., and Pheasant, D.R., 1974, Delimitation of weathering zones in the fiord area of eastern Baffin Island, Canada: Geological Society of America Bulletin, v. 85, no. 5, p. 805–810.

Chapman, W.L., and Walsh, J.E., 1993, Recent variations of sea ice and air temperatures in high latitudes: American Meteorological Society Bulletin, v. 74, no. 1, p. 33–47.

Church, M., 1972, Baffin Island sandurs: A study of arctic fluvial processes: Canada Geological Survey Bulletin 216, 208 p.

Clarke, G.K.C., Collins, S.G., and Thompson, D.E., 1984, Flow, thermal structure and subglacial conditions of a surge-type glacier: Canadian Journal of Earth Sciences, v. 21, no. 2, p. 232–240.

Classen, D.F., 1977, Temperature profiles for the Barnes Ice Cap surge zone: Journal of Glaciology, v. 18, no. 80, p. 391–405.

Clough, J.W., and Løken, O.H., 1968, Radio-echo sounding on the Barnes Ice Cap, *in* North-central Baffin Island field report 1967: Canada Department of Energy, Mines and Resources, Inland Waters Branch, Report Series 2, p. 87–102.

Davis, P.T., 1985, Neoglacial moraines on Baffin Island, *in* Andrews, J.T., ed., Quaternary environments: Eastern Canadian Arctic, Baffin Bay and western Greenland: Boston, Allen and Unwin, p. 682–718.

Dowdeswell, E.K., and Andrews, J.T., 1985, The fiords of Baffin Island—Description and classification, *in* Andrews, J.T., ed., Quaternary environments: Eastern Canadian Arctic, Baffin Bay, and western Greenland: Boston, Allen and Unwin, p. 93–123.

Dowdeswell, J.A., 1982, Debris transport paths and sediment flux through the Grinnell Ice Cap, Frobisher Bay, Baffin Island, N.W.T., Canada: Boulder, Colo., University of Colorado, unpublished Master's thesis, 176 p.

———1984, Late Quaternary chronology of the Watts Bay area, Frobisher Bay, southern Baffin Island, N.W.T., Canada: Arctic and Alpine Research, v. 16, no. 3, p. 311–320.

Duvall, M.L., 1993, Late Foxe glacial geology of the mid-bay area of Frobisher Bay, southeast Baffin Island, Northwest Territories: Boulder, Colo., University of Colorado, unpublished Master's thesis, 103 p.

Dyke, A.S., and Prest, V.K., 1987, Paleogeography of northern North America 18,000–5,000 years ago: Canada Geological Survey Map 1703A, scale 1:12,500,000.

Falconer, G., 1962, Glaciers of northern Baffin and Bylot Islands, N.W.T.: Ottawa, Canada Department of Energy, Mines and Resources, Technical Surveys, Geographical Branch, Geographical Paper 33, 31 p., 42 figs.

Falconer, G., 1966, Preservation of vegetation and patterned ground under a thin ice body in northern Baffin Island, N.W.T.: Geographical Bulletin, v. 8, no. 2, p. 194–200.

Falconer, G., Ives, J.D., Løken, O.H., and Andrews, J.T., 1965, Major end moraines in eastern and central Arctic, Canada: Geographical Bulletin, v. 7, no. 2, p. 137–153.

Fisher, D.A., Koerner, R.M., Bourgeois, J.C., and others, 1998, Penny Ice Cap cores, Baffin Island, Canada, and the Wisconsinan Foxe Dome connection: Two states of Hudson Bay ice cover: Science, v. 279, no. 5351, p. 692–695.

Gilbert, R., 1982, Contemporary sedimentary environments on Baffin Island, N.W.T., Canada—Glaciomarine processes in fiords of eastern Cumberland Peninsula: Arctic and Alpine Research, v. 14, no. 1, p. 1–12.

Grove, J.M., 1988, The Little Ice Age: London, Methuen and Co. Ltd., 498 p.

Hall, C.F., 1865, Arctic researches and life among the Esquimaux—Being the narrative of an expedition in search of Sir John Franklin, in the years 1860, 1861, and 1862: New York, Harper and Brothers, 595 p.

Hare, F.K., and Hay, J.E., 1971, Anomalies in the large-scale annual water balance over northern North America: Canadian Geographer, v. 15, no. 2, p. 79–94.

Hawkins, F.F., 1980, Glacial geology and late Quaternary paleoenvironment in the Merchants Bay area, Baffin Island, N.W.T., Canada: Boulder, Colo., University of Colorado, unpublished Master's thesis, 145 p.

Hodgson, D.A., and Haselton, G.M., 1974, Reconnaissance glacial geology, northeastern Baffin Island: Canada Geological Survey Paper 74–20, p. 1–10.

Holdsworth, Gerald, 1973a, Barnes Ice Cap and englacial debris in glaciers: Journal of Glaciology, v. 12, no. 64, p. 147–148.

———1973b, Evidence of a surge on Barnes Ice Cap: Canadian Journal of Earth Sciences, v. 10, no. 10, p. 1565–1574.

———1975, Deformation and flow of Barnes Ice Cap, Baffin Island: Ottawa, Environment Canada, Inland Waters Directorate, Scientific Series 52, 19 p.

———1977, Surge activity on the Barnes Ice Cap: Nature, v. 269, no. 5629, p. 588–590.

———1984, Glaciological reconnaissance of an ice core drilling site, Penny Ice Cap, Baffin Island: Journal of Glaciology, v. 30, no. 104, p. 3–15.

Holdsworth, Gerald, and Glynn, G.E., 1975, Two-dimensional ice flow simulation along the Barnes Ice Cap trilateration network: Ottawa, Environment Canada, unpublished internal report, 10 p.

Hooke, R.L., 1973, Structure and flow in the margin of the Barnes Ice Cap, Baffin Island, N.W.T., Canada: Journal of Glaciology, v. 12, no. 66, p. 423–438.

Hooke, R.L., 1976, Pleistocene ice at the base of the Barnes Ice Cap, Baffin Island, N.W.T., Canada: Journal of Glaciology, v. 17, no. 75, p. 49–59.

Hooke, R.L., Alexander, E.C., Jr., and Gustafson, R.J., 1980, Temperature profiles in the Barnes Ice Cap, Baffin Island, Canada, and heat flux from the subglacial terrane: Canadian Journal of Earth Sciences, v. 17, no. 9, p. 1174–1188.

Hooke, R.L., and Clausen, H.B., 1982, Wisconsin and Holocene - $\delta^{18}O$ variations, Barnes Ice Cap, Canada: Geological Society of America Bulletin, v. 93, no. 8, p. 784–789.

Hooke, R.L., Gould, J.E., and Brzozowski, J., 1983, Near-surface temperatures near and below the equilibrium line on polar and subpolar glaciers: Zeitschrift für Gletscherkunde und Glazialgeologie, v. 19, no. 1, p. 1–25.

Hooke, R.L., Johnson, G.W., Brugger, K.A., Hanson, Brian, and Holdsworth, Gerald, 1987, Changes in mass balance, velocity, and surface profile along a flow line on Barnes Ice Cap, 1970–1984: Canadian Journal of Earth Sciences, v. 24, no. 8, p. 1550–1561.

Hudleston, P.J., 1976, Recumbent folding in the base of the Barnes Ice Cap, Baffin Island, Northwest Territories, Canada: Geological Society of America Bulletin, v. 87, no. 12, p. 1684–1692.

Ives, J.D., 1962, Indications of recent extensive glacierization in north-central Baffin Island, N.W.T.: Journal of Glaciology, v. 4, no. 32, p. 197–205.

Ives, J.D., and Andrews, J.T., 1963, Studies in the physical geography of north-central Baffin Island, N.W.T.: Geographical Bulletin, v. 19, p. 5–48.

Ives, J.D., Andrews, J.T., and Barry, R.G., 1975, Growth and decay of the Laurentide Ice Sheet and comparisons with Fenno-Scandinavia: Naturwissenschaften, v. 62, no. 3, p. 118–125.

Jacobs, J.D., Barry, R.G., Bradley, R.S., and Weaver, R.L., 1974, Studies of climate and ice conditions in eastern Baffin Island, 1971–73: Boulder, Colo., University of Colorado, Institute of Arctic and Alpine Research, Occasional Paper 9, 77 p.

Jacobs, J.D., Heron, Richard, and Luther, J.E., 1993, Recent changes at the northwest margin of the Barnes Ice Cap, Baffin Island, N.W.T., Canada: Arctic and Alpine Research, v. 25, no. 4, p. 341–352.

Jacobs, J.D., Short, N.H., and Bell, T.J., 1999, Late 20th century history of Barnes Ice Cap, Baffin Island, N.W.T. [abs.]: Canadian Geophysical Union, 25th annual meeting, Banff, Alberta, Program and Abstracts, p. 123.

Jacobs, J.D., Simms, E.L., and Simms, Alvin, 1997, Recession of the southern part of Barnes Ice Cap, Baffin Island, Canada, between 1961 and 1993, determined from digital mapping of Landsat TM: Journal of Glaciology, v. 43, no. 143, p. 98–102.

Jones, S.J., 1972, Radio depth-sounding on Meighen and Barnes Ice Caps, Arctic Canada: Ottawa, Environment Canada, Inland Waters Directorate, Scientific Series 25, 13 p.

Kerr, J.W., 1970, Today's topography and tectonics in northeastern Canada: Canadian Journal of Earth Sciences, v. 7, no. 2, p. 570.

———1980, Structural framework of Lancaster aulacogen, Arctic Canada: Canada Geological Survey Bulletin 319, 24 p.

King, C.A.M., 1969a, Glacial geomorphology and chronology of Henry Kater Peninsula, east Baffin Island, N.W.T.: Arctic and Alpine Research, v. 1, no. 3, p. 195–212.

———1969b, Moraine types on Henry Kater Peninsula, east Baffin Island, N.W.T., Canada: Arctic and Alpine Research, v. 1, no. 4, p. 289–294.

Klassen, R.A., 1981, Aspects of the glacial history of Bylot Island, District of Franklin, *in* Current research, part A: Canada Geological Survey Paper 81–1A, p. 317–326.

———1982, Quaternary stratigraphy and glacial history of Bylot Island, N.W.T., Canada: Urbana, Ill., University of Illinois, unpublished Ph.D. thesis, 163 p.

———1985, An outline of the glacial history of Bylot Island, District of Franklin, N.W.T., *in* Andrews, J.T., ed., Quaternary environments: Eastern Canadian Arctic, Baffin Bay and western Greenland: Boston, Allen and Unwin, p. 428–460.

Lind, E.K., 1983, Holocene paleoecology and deglacial history of the Cape Rammelsbery area, southern Baffin Island, Canada: Boulder, Colo., University of Colorado, unpublished Master's thesis, 219 p.

Locke, C.W., and Locke, W.W., III, 1977, Little Ice Age snow-cover extent and paleoglaciation thresholds, north-central Baffin Island, N.W.T., Canada: Arctic and Alpine Research, v. 9, no. 3, p. 291–300.

Locke, W.W., III, 1980, Quaternary geology of the Cape Dyer area, southwesternmost Baffin Island, Canada: Boulder, Colo., University of Colorado, unpublished Ph.D. thesis, 348 p.

Lodwick, G.D., and Paine, S.H., 1985, A digital elevation model of the Barnes ice-cap derived from Landsat MSS data: Photogrammetric Engineering and Remote Sensing, v. 51, no. 12, p. 1937–1944.

Løken, O.H., 1969, Evidence of surges on the Barnes Ice Cap, Baffin Island: Canadian Journal of Earth Sciences, v. 6, no. 4, part 2, p. 899–901.

Løken, O.H., and Andrews, J.T., 1966, Glaciology and chronology of fluctuations of the ice margin at the south end of the Barnes Ice Cap, Baffin Island, N.W.T., Canada: Geographical Bulletin, v. 8, no. 4, p. 341–359.

Maxwell, J.B., 1980, The climate of the Canadian Arctic Islands and adjacent waters: [Ottawa] Environment Canada, Atmospheric Environment Service, Climatological Studies, v. 30, no. 1, 531 p.

———1981, The climate of the Canadian Arctic Islands and adjacent waters: [Ottawa] Environment Canada, Atmospheric Environment Service, Climatological Studies, v. 30, no. 2, 589 p.

M'Clintock, Sir Francis Leopold, 1860, The voyage of the Fox in the Arctic Seas; a narrative of the discovery of the fate of Sir John Franklin and his companions: Boston, Ticknor and Fields, 375 p.

Mercer, J.H., 1956, The Grinnell and Terra Nivea Ice Caps, Baffin Island: Journal of Glaciology, v. 2, no. 19, p. 653–656.

———1975, Glaciers of Baffin and Bylot Islands, *in* Field, W.O., ed., Mountain glaciers of the Northern Hemisphere: Hanover, N.H., U.S. Army Corps of Engineers, Cold Regions Research and Engineering Laboratory, v. 2, p. 683–721.

Miller, G.H., 1975, Glacial and climatic history of northern Cumberland Peninsula, Baffin Island, Canada, during the last 10,000 years: Boulder, Colo., University of Colorado, unpublished Ph.D. thesis, 226 p.

———1979, Radiocarbon date list IV, Baffin Island, N.W.T., Canada: Boulder, Colo., University of Colorado, Institute of Arctic and Alpine Research, Occasional Paper 29, 59 p.

———1980, Late Foxe glaciation of southern Baffin Island, N.W.T., Canada: Geological Society of America Bulletin, v. 91, no. 7, part I, p. 399–405.

Miller, G.H., 1985a, Aminostratigraphy of Baffin Island shell-bearing deposits, *in* Andrews, J.T., ed., Quaternary environments: Eastern Canadian Arctic, Baffin Bay and western Greenland: Boston, Allen and Unwin, p. 394–427.

———1985b, Moraines and proglacial lake shorelines, Hall Peninsula, Baffin Island, *in* Andrews, J.T., ed., Quaternary environments: Eastern Canadian Arctic, Baffin Bay and western Greenland: Boston, Allen and Unwin, p. 546–557.

Muller, D.S., 1980, Glacial geology and Quaternary history of southeast Meta Incognita Peninsula, Baffin Island, Canada: Boulder, Colo., University of Colorado, unpublished Master's thesis, 211 p.

Ommanney, C.S.L., 1980, The inventory of Canadian glaciers—Procedures, techniques, progress and applications, *in* World Glacier Inventory Workshop, Reideralp, Switzerland, 1978, Proceedings: International Association of Hydrological Sciences-Association Internationale des Sciences Hydrologiques Publication 126, p. 35–44.

Orvig, Svenn, 1954, Glacial-meteorological observations on ice caps in Baffin Island: Geografiska Annaler, v. 36, no. 3–4, p.197–318.

Østrem, Gunnar, 1966, The height of the Glaciation Limit in southern British Columbia and Alberta: Geografiska Annaler, v. 48A, no. 3, p. 126–138.

Østrem, Gunnar, Bridge, C.W., and Rannie, W.F., 1967, Glacio-hydrology, discharge and sediment transport in the Decade Glacier area, Baffin Island, N.W.T.: Geografiska Annaler, v. 49A, p. 268–282.

Prest, V.K., 1969, Retreat of Wisconsin and Recent ice in North America: Canada Geological Survey Map 1257A, scale 1:5,000,000.

Ross, John, 1819, A voyage of discovery, made under the orders of the Admiralty, in His Majesty's Ships *Isabella* and *Alexander*, for the purpose of exploring Baffin's Bay and inquiring into the probability of north-west passage: London, John Murray, 252 p.

Sagar, R.B., 1966, Glaciological and climatological studies on the Barnes Ice Cap, 1962–1964: Geographical Bulletin, v. 8, no. 1, p. 3–47.

Shoemaker, E.M., 1981, Creep slump in glacier reservoirs—theory and experiment: Journal of Glaciology, v. 27, no. 97, p. 393–406.

Short, Naomi, 1998, Mapping the margin of the Barnes Ice Cap using SAR imagery: St. John's, Newfoundland, Memorial University of Newfoundland, Department of Geography, unpublished Master's thesis, 163 p.

Short, N.H., Simms, É.L., and Jacobs, J.D., 2000, RADARSAT SAR applied to ice margin mapping: The Barnes Ice Cap, Nunavut, Canada: Canadian Journal of Remote Sensing, v. 26, no. 2, p. 91.

Short, S.K., and Holdsworth, Gerald, 1985, Pollen, oxygen isotope content and seasonality in an ice core from the Penny Ice Cap, Baffin Island: Arctic, v. 38, no. 3, p. 214–218.

Soper, J.D., 1981, Canadian Arctic recollections Baffin Island 1923–1931: Saskatoon, Saskatchewan, University of Saskatchewan, Institute of Northern Studies.

Steig, E.J., Wolfe, A.P., and Miller, G.H., 1998, Wisconsin refugia and the glacial history of eastern Baffin Island, Arctic Canada: Coupled evidence from cosmogenic isotopes and lake sediments: Geology, v. 26, no. 9, p. 835–838.

Stravers, J., 1986, Glacial geology of the outer Meta Incognita Peninsula, southern Baffin Island, Arctic Canada: Boulder, Colo., University of Colorado, unpublished Ph.D. thesis, 231 p.

Sugden, D.E., 1978, Glacial erosion by the Laurentide Ice Sheet: Journal of Glaciology, v. 20, no. 83, p. 367–392.

Sugden, D.E., and John, B.S., 1976, Glaciers and landscapes, a geomorphological approach: New York, John Wiley, 376 p.

Sutherland, P.C., 1852, Journal of a voyage in Baffin's Bay and Barrow Straits, in the years 1850–1851: London, Longman, Brown, Green, and Longmans, 2 v.

Szabo, B.J., Miller, G.H., Andrews, J.T., and Stuiver, M., 1981, Comparison of uranium series, radiocarbon, and amino acid data from marine molluscs, Baffin Island, Arctic Canada: Geology, v. 9, no. 10, p. 451–457.

Ward, W.H., and Baird, P.D., 1954, Studies in glacier physics on the Penny Ice Cap, Baffin Island, 1953; Part I, A description of the Penny Ice Cap, its accumulation and ablation: Journal of Glaciology, v. 2, no. 15, p. 342–355.

Weaver, R.L., 1975, Boas Glacier (Baffin Island, N.W.T., Canada)—Mass balance for five budget years, 1969–1974: Arctic and Alpine Research, v. 7, no. 3, p. 279–284.

Weidick, Anker, 1975, Estimates on the mass balance changes of the Inland Ice since Wisconsin-Weichel: Grønlands Geologiske Undersøgelse Rapport 68, 21 p.

Williams, L.D., 1978, Ice-sheet initiation and climatic influences of expanded snow cover in Arctic Canada: Quaternary Research, v. 10, no. 2, p. 141–149.

Williams, R.S., Jr., Hall, D.K., and Benson, C.S., 1991, Analysis of glacier facies using satellite techniques: Journal of Glaciology, v. 37, no. 125, p. 120–128.

Glaciers of North America–

GLACIERS OF CANADA

GLACIERS OF THE CANADIAN ROCKIES

By C. SIMON L. OMMANNEY

SATELLITE IMAGE ATLAS OF GLACIERS OF THE WORLD

Edited by RICHARD S. WILLIAMS, Jr., *and* JANE G. FERRIGNO

U.S. GEOLOGICAL SURVEY PROFESSIONAL PAPER 1386-J-1

The Rocky Mountains of Canada include four distinct ranges from the U.S. border to northern British Columbia: Border, Continental, Hart, and Muskwa Ranges. They cover about 170,000 km^2, are about 150 km wide, and have an estimated glacierized area of 38,613 km^2. Mount Robson, at 3,954 m, is the highest peak. Glaciers range in size from ice fields, with major outlet glaciers, to glacierets. Small mountain-type glaciers in cirques, niches, and ice aprons are scattered throughout the ranges. Ice-cored moraines and rock glaciers are also common

CONTENTS

Page

GLACIERS OF NORTH AMERICA–

GLACIERS OF CANADA

GLACIERS OF THE CANADIAN ROCKIES

By C. Simon L. Ommanney[1]

Abstract

The Rocky Mountains of Canada include four distinct mountain ranges (Border, Continental, Hart, and Muskwa Ranges) extending from the U.S. border to northern British Columbia, a distance of 1,350 kilometers. The Rocky Mountains encompasses about 170,000 square kilometers, are about 150 kilometers wide, and have an estimated glacierized area of 38,613 square kilometers. Mount Robson, at 3,954 meters above sea level, is the highest peak. Within the Continental Ranges are the Front, *Park*, and Kootenay Ranges; these include some of the most spectacular and heavily glacierized mountains in North America. Major glaciers, such as the Waputik, Wapta, Freshfield, Mons, Lyell, and Columbia Icefields are located in these mountains. The Columbia Icefield (325 square kilometers) is the largest ice field in the Rocky Mountains; its three largest outlet glaciers are the Columbia, Athabasca, and Saskatchewan Glaciers. Glaciers range in size from ice fields, with major outlet glaciers, to glacierets. Small mountain-type glaciers in cirques, niches, and ice aprons are scattered throughout the ranges. Ice-cored moraines and rock glaciers are also common.

Introduction

To the early explorers, the Rocky Mountains were a seemingly impenetrable barrier blocking access to the Pacific and inhibiting the coastal inhabitants in their movements to the east. The chain covers about 170,000 km^2 and stretches in a continuous series of parallel ranges 150-km wide, from the British Columbia/Alberta/United States border some 1,350 km to northern British Columbia, where the Liard River, in cutting through the chain, acts as a convenient boundary. The same mountain mass continues into the Yukon Territory, but the rocks of the mountains, named here the Mackenzie Mountains, are younger geologically. To the east, the limits of the Rocky Mountains are not sharp. From the heights of the Front Ranges, one passes through the Foothills and out into the Interior Plains. To the west, the boundary is marked by one of the world's greatest physiographic features, which can even be seen from the Moon—the Rocky Mountain Trench. The trench continues through the Yukon Territory and Alaska as the Tintina Trench. The highest elevation in the Rocky Mountains is Mount Robson, at 3,954 m above sea level (asl). The lowest elevation, 305 m, is in the north at the junction of the Liard and Toad Rivers.

Gadd (1986) gives an excellent account of the geology of the Rocky Mountains. The mountains were formed by strong compressive forces generated to the west of the Rocky Mountain Trench. During a 75-million-year period that began about 120 million years ago, a series of thrust faults forced the Precambrian, Paleozoic, and Mesozoic sedimentary rocks eastward along a fault

Manuscript approved for publication 7 March 2002.

[1] International Glaciological Society, Lensfield Road, Cambridge CB2 1ER, England, U.K. (formerly with the National Hydrology Research Institute [now part of the National Water Research Institute], Environment Canada, 11 Innovation Boulevard, Saskatoon, Saskatchewan S7N 3H5, Canada).

plane over the soft Cretaceous shales of the Great Plains. The compressive forces produced a series of folds, which give the Rocky Mountains their characteristic parallel ranges. During the last 2 million years, intense glaciation in the region has eroded the mountains into big, rugged peaks separated by deep, wide valleys, creating a striking east-facing scarp.

There are four distinct ranges within the Rocky Mountains region, known as the Border, Continental, Hart, and Muskwa Ranges (figs. 1 and 2).[2] Included in the Continental Ranges are the Front, *Park*, and Kootenay Ranges. The distinctions between the ranges are based largely on geologic structure and physiography. The entire region is characterized by limestones, quartzites, and argillites, which form massively bold peaks, best expressed in the *Park Ranges* of the Continental Ranges. The *Park Ranges* contain some of the most spectacular and heavily glacierized mountains in North America (fig. 3). Flat to gently dipping beds of quartzite or limestone have produced castellated peaks, subsequently modified by glacial oversteepening; large talus cones have developed postglacially. Summit elevations decline northward and southward from the *Park Ranges*; in particular, the Hart Ranges are considerably lower than the other three ranges. Elevations increase farther north in the Muskwa Ranges, and the castellated limestone and quartzite peaks reappear around Churchill Peak (3,200 m) and Mount Lloyd George (3,000 m) (Slaymaker, 1972).

Glaciers in the Rocky Mountains (fig. 4, table 1) are typically of the small mountain type, lying in cirques, niches, or along some of the upturned strata as ice aprons. Scattered at intervals along the range are larger ice fields,[3] with major outlet and valley glaciers. Glacierets, ice-cored moraines, and rock glaciers occur at the limits of contemporary glacierization. In some situations, the avalanching of hanging glaciers has created regenerated glaciers lower on the mountain; part of the nourishment of the well-known Victoria Glacier is of this form (fig. 5).

Unfortunately, the precise area of permanent snow and ice in the Rockies is not known. Henoch (1967) made a determination for the major Canadian drainage areas, but because the Columbia Icefield drains to the Pacific Ocean, to Great Slave Lake, and into the Nelson River system that empties into Hudson Bay, it is hard to determine what proportion of the total area should be attributed to the Rocky Mountains alone (table 2).

The nature of the ice cover within part of the Rocky Mountains is indicated in table 3 (Ommanney, 1972a), which shows the distribution of various glacier types within the Nelson River drainage basin, stretching from Waterton Lakes National Park to the southern part of the Columbia Icefield. Major ice fields,[3] such as the Waputik, Wapta, Freshfield, Mons, Lyell, and Columbia Icefields,[3] are not adequately reflected in table 3. Because of the nature of their subglacial topography and ice cover, all of the constituent glaciers can be identified individually.

Hydrometric stations in the *Park Ranges* and Muskwa Ranges typically show two prominent stream-discharge peaks that correspond to snowmelt (June) and glacier melt (July–August), in addition to a minor peak in the fall. In the Hart Ranges, the glacier-melt peak is generally absent, whereas there is neither a fall-rain peak nor a glacier-melt peak (Slaymaker, 1972) in the Border Ranges farther south.

---

[2] The names in this section conform to the usage authorized by the Secretariat of the Canadian Permanent Committee on Geographic Names (CPCGN); URL address: [http:// geonames.nrcan.gc.ca/english]. The Website is maintained by the Secretariat through Geomatics Canada, Natural Resources Canada, and combines the GPCGN server with the Canadian Geographical Names Data Base (CGNDB). Variant names and names not listed in the GPCGN/CGNDB are shown in italics. See also Canadian gazetteers for British Columbia (CPCGN, 1985) and for Alberta (CPCGN, 1988).

[3] Ice field is used in glaciological terminology to refer to "an extensive mass of land ice covering a mountain region consisting of many interconnected alpine and other types of glaciers, covering all but the highest peaks and ridges" (Jackson, 1997, p. 316). The UNESCO (1970) definition is slightly different. "Ice masses of sheet or blanket type of a thickness not sufficient to obscure the subsurface topography." In Canada, icefield is used as a synonym for glacier in many glacier place-names and in the text to refer to such place-names, but is not necessarily used in the formal glaciological sense.

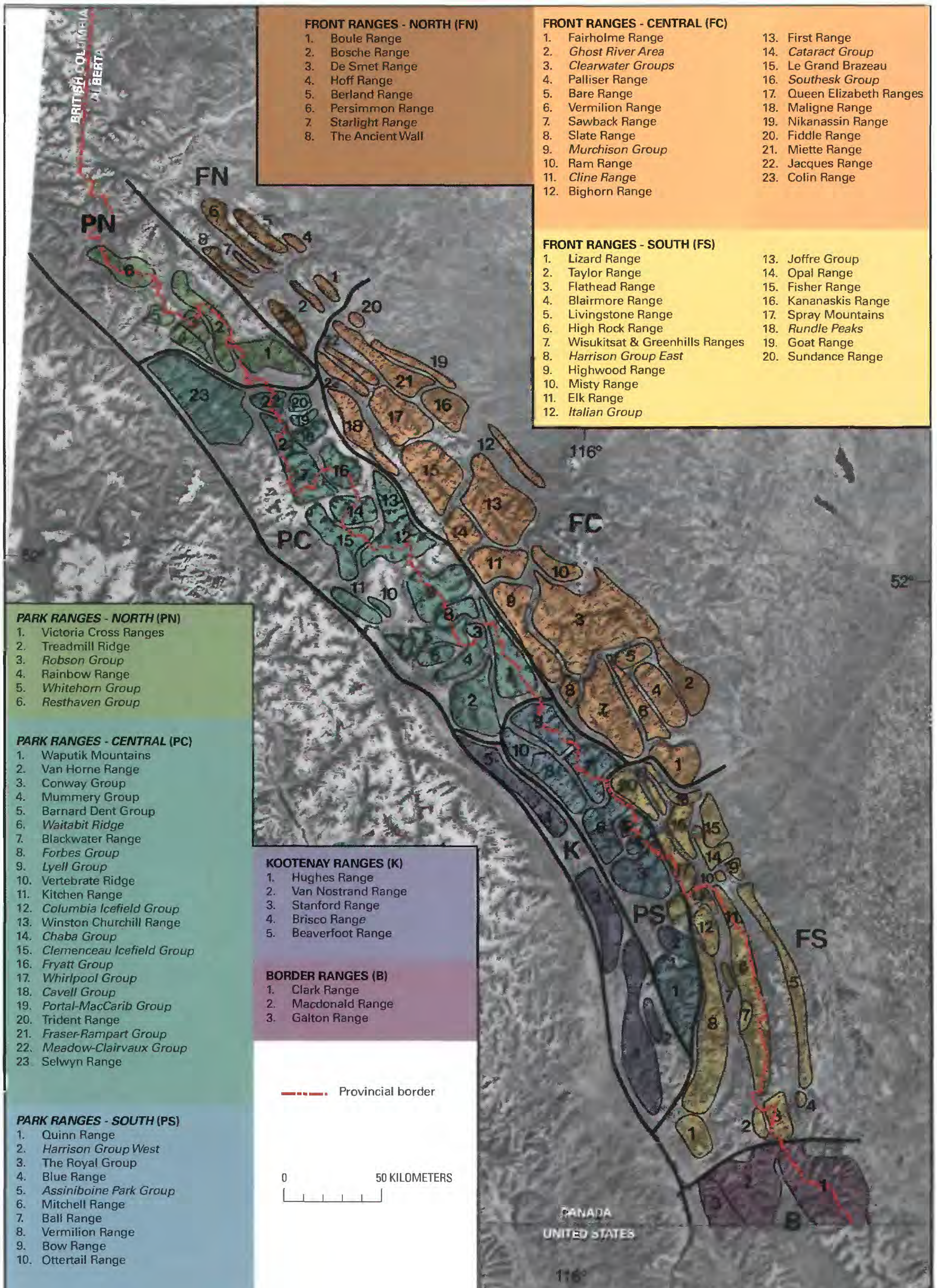

Figure 1.—*Mountain ranges of the southern Rocky Mountains. Landsat image mosaic used as map base.*

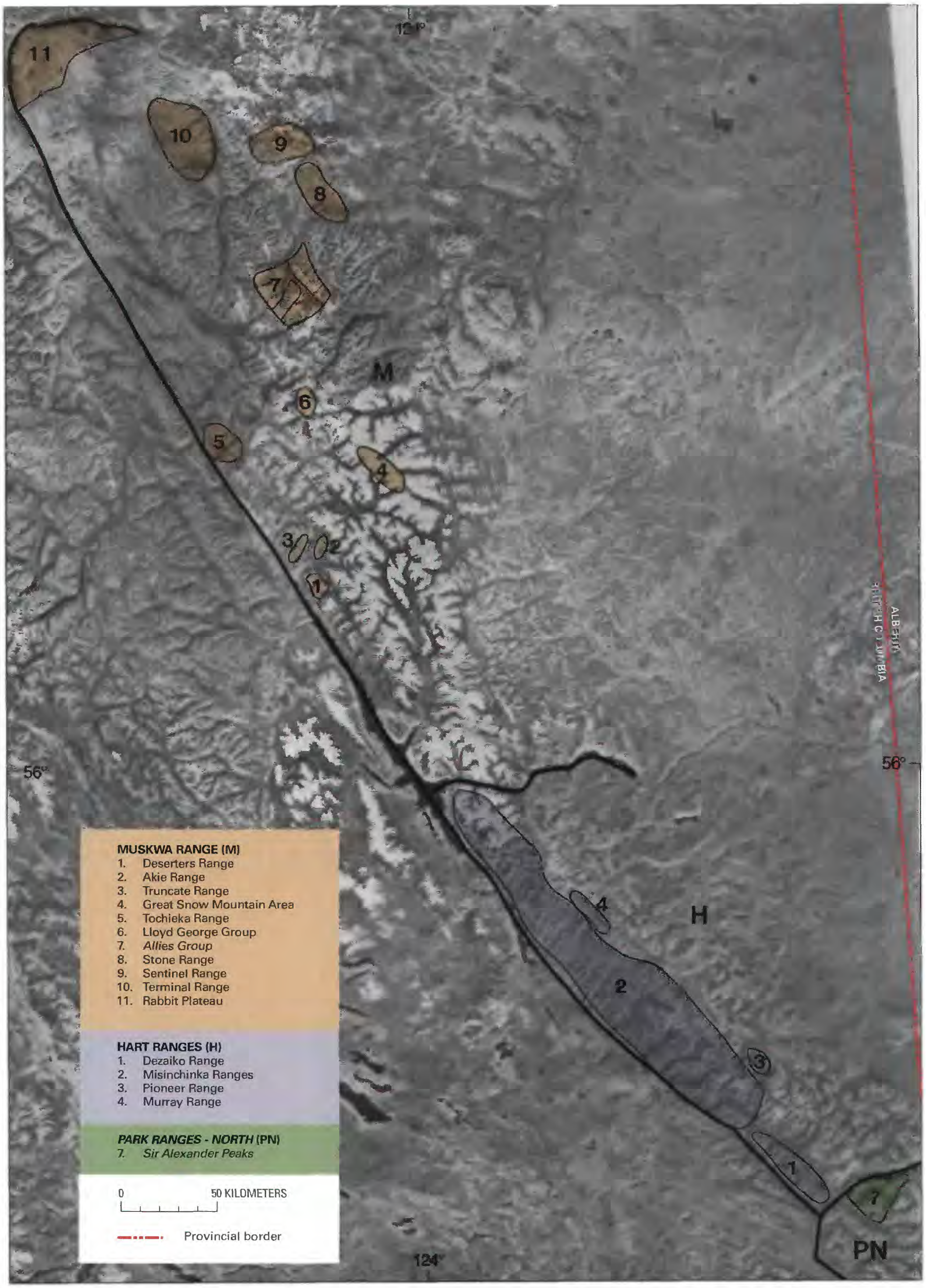

***Figure 2.**—Mountain ranges of the northern Rocky Mountains. Landsat image mosaic used as map base.*

Figure 3.*—High-angle oblique aerial photograph of Mount Assiniboine and environs, Banff National Park, Rocky Mountains, Canada, an area of spectacular relief and glacierized peaks. U.S. Geological Survey (USGS) photograph 69L2117, taken 8 September 1969 by Austin Post, is courtesy of Robert M. Krimmel, USGS.*

The glaciers and terrain of the major mountain ranges and their subsidiary mountain ranges, mountains, mountain groups, mountains peaks, and mountain ridges will be discussed here in turn, beginning with the Border Ranges at the southern end of the Rocky Mountains. All major ranges are identified by an alphanumeric code in figures 1 and 2.[4] The Continental Ranges, the largest mountain mass, are subdivided into a southern, central, and northern part because they cover such a large area. Within each subdivision, the mountains of the Front and Kootenay Ranges and *Park Ranges* are considered in turn. The terminology has been drawn from maps and alpine guides (Putnam and others, 1974; Boles and others, 1979); however, some of the names are not endorsed by the Canadian Permanent Committee on Geographical Names (CPCGN).[2] Those place-names not yet approved by the CPCGN are shown in italics.

[4] The major mountain ranges are coded with letters; subsidiary mountain ranges, mountains, mountain groups, mountain peaks, and mountain ridges are coded with numbers. It is noteworthy that many of the subsidiary mountain ranges have never been given formal names; in the subheadings in the text, they are simply referred to as "unnamed range." On figures 1 and 2 they are unnumbered. Glaciers and ice fields are described within the subsidiary mountain ranges, etc. The letters and numbers are keyed to figures 1 and 2, which delineate each major and subsidiary mountain ridge on a Landsat image mosaic base map.

Figure 4.—Sketch map showing glaciers of the Southern Canadian Rocky Mountains. Modified from the Canadian Geographic (Shilts and others, 1998). Used with permission.

TABLE 1.—*Named glaciers of the Rocky Mountains cited in the chapter*

[The geographic coordinates for glaciers whose names have not been formally approved (shown in italics) may not be accurate. N.P. = National Park; BC = British Columbia; AB = Alberta; – not shown in geonames database or glacier name is informal (italics); glacier name, map sheet, location of glacier, and province checked against the archives of the Geographical Names of Canada, Geomatics Canada, Natural Resources Canada [http://geonames.nrcan.gc.ca]]

Glacier Name	Map sheet (1:250,000-scale)	Latitude North	Longitude West	Location	Province
Abruzzi Glacier	082J06	50°25.0'	115°07.0'	Kootenay	BC
Achaean Glacier	094F08	57°22.0'	124°04.0'	Peace River	BC
Albert Glacier	082N04	51°02.5'	117°50.5'	Kootenay	BC
Alexandra Glaciers	082N14	51°59.0'	117°09.0'	Banff N.P.	AB
Alexandra Icefield	082N14	51°59.5'	117°12.0'	Banff N.P./ Kootenay	AB/BC
Angel Glacier	083D09	52°41.0'	118°04.0'	Jasper N.P.	AB
Apex Glacier	083C04	52°08.2'	117°44.0'	Kootenay	BC
Athabasca Glacier	083C03	52°11.0'	117°15.7'	Jasper N.P.	AB
Ayesha Glacier	082N10	51°38.8'	116°35.6'	Kootenay	BC
Balfour Glacier	082N09	51°34.0'	116°26.0'	Banff N.P.	AB
Barbette Glacier	082N10	51°44.0'	116°36.0'	Banff N.P.	AB
Bath Glacier	082N09	51°31.0'	116°23.0'	Banff N.P.	AB
Beatty Glacier	082J11	50°40.5'	115°17.0'	–	AB
Bennington Glacier	083D09	52°40.5'	118°19.0'	Cariboo	BC
Bennington Icefield	083D09	52°39.3'	118°17.9'	–	AB
Berg Glacier	083E03	53°07.0'	119°08.0'	Cariboo	BC
Bonnet Glacier	082O05	51°27.0'	115°55.0'	Banff N.P.	AB
Boundary Glacier[1]	083C03	52°11.5'	117°11.4'	–	AB
Bow Glacier	082N10	51°38.9'	116°30.4'	Banff N.P.	AB
Brazeau Icefield	083C11	52°32.2'	117°18.3'	--	AB
Cairnes Glacier	082N10	51°42.8'	116°46.3'	Kootenay	BC
Campbell Glacier	082N10	51°44.0'	116°59.0'	Kootenay	BC
Campbell Icefield	082N10	51°43.2'	116°58.0'	Kootenay	BC
Castelnau Glacier	082J11	50°31.5'	115°09.4'	Kootenay	BC
Castle Glacier	093H16	53°59.6'	120°23.8'	--	BC
Castleguard Glacier I[2]	083C03	52°06.7'	117°13.7'	Banff N.P.	AB
Castleguard Glacier II[2]	083C03	52°06.2'	117°14.5'	Banff N.P.	AB
Castleguard Glacier III[2]	083C03	52°05.9'	117°15.2'	Banff N.P.	AB
Castleguard Glacier IV[2]	083C03	52°04.9'	117°16.3'	Banff N.P.	AB
Cathedral Glacier[3]	082N08	51°24.3'	116°23.4'	–	BC
Cavell Glacier	083D09	52°40.9'	118°03.0'	--	AB
Center Glacier	083C13	52°50.0'	117°55.0'	--	AB
Chaba Glacier	083C04	52°14.0'	117°41.0'	Jasper N.P.	AB
Chaba Icefield	083C05	52°17.0'	117°51.0'	Kootenay	BC
Chown Glacier	083E06	53°23.0'	119°23.0'	Jasper N.P.	AB
Clairvaux Glacier	083D16	52°46.4'	118°23.8'	Jasper N.P.	AB
Clemenceau Glacier	083C04	52°14.0'	117°54.0'	Kootenay	BC
Clemenceau Icefield	083C04	52°11.0'	117°48.0'	Kootenay	BC
Coleman Glacier	083E03	53°10.0'	119°02.7'	Jasper N.P.	AB
Columbia Glacier	083C03	52°09.6'	117°22.8'	Jasper N.P.	AB
Columbia Icefield[4]	083C03	52°09.5'	117°19.0'	Kootenay	BC
Columbia Icefield[4]	083C03	52°09.5'	117°18.0'	Jasper N.P.	AB
Conway Glacier	082N15	51°46.1'	116°49.1'	Banff N.P.	AB
Cornucopia Glacier	083C11	52°33.5'	117°14.8'	–	AB
Coronet Glacier	083C11	52°31.0'	117°21.0'	Jasper N.P.	AB
Crowfoot Glacier	082N09	51°38.3'	116°25.2'	Banff N.P.	AB
Daly Glacier	082N09	51°31.0'	116°26.5'	Yoho N.P.	BC
Delta Glacier[5]	082N10	51°43.3'	116°35.0'	Banff N.P.	AB

TABLE 1.—*Named glaciers of the Rocky Mountains cited in the chapter*—Continued

Glacier Name	Map sheet (1:250,000-scale)	Latitude North	Longitude West	Location	Province
Diadem Icefield	083C06	52°19.6'	117°25.0'	–	AB
Dome Glacier[6]	083C03	52°12.1'	117°18.1'	Jasper N.P.	AB
Drummond Glacier	082N09	51°36.0'	116°03.0'	Banff N.P.	AB
Duplicate Glacier	083C04	52°12.8'	117°54.8'	Kootenay	BC
East Glacier	082N15	51°52.2'	116°55.2'	Banff N.P.	AB
East Goodsir Glacier	082N01	51°12.4'	116°21.5	Yoho N.P.	BC
East Lyell Glacier	082N14	51°57.5'	117°04.5'	Banff N.P.	AB
Elk Glacier	082J11	50°31.0'	115°09.0'	Kootenay	BC
Emerald Glacier	082N07	51°30.0'	116°32.0'	Yoho N.P.	BC
Eremite Glacier	083D09	52°38.0'	118°14.0'	Jasper N.P.	AB
Foch Glacier	082J11	50°34.5'	115°10.3'	–	AB
Fraser Glacier	083D09	52°38.2'	118°16.7'	Jasper N.P.	AB
Freshfield Glacier	082N15	51°47.0'	116°53.0'	Banff N.P.	AB
Freshfield Icefield	082N10	51°45.0'	116°54.0'	Banff N.P.	AB
Fusilier Glacier	094K07	58°22.0'	124°52.0'	Peace River	BC
Ghost Glacier	083C05	52°19.6'	117°53.6'	Kootenay	BC
Glacier des Poilus	082N10	51°34.0'	116°35.0'	Yoho N.P.	BC
Gong Glacier	083C06	52°22.0'	117°28.8'	Jasper N.P.	AB
Goodsir Glacier	082N01	51°12.2'	116°22.6'	Yoho N.P.	BC
Great Snow Icefield	094F08	57°27.0'	124°06.0'	–	BC
Haig Glacier[4]	082J11	50°43.0'	115°17.0'	–	AB
Haig Glacier[4]	082J11	50°43.0'	115°19.0'	Kootenay	BC
Hanbury Glacier	082N01	51°15.0'	116°30.0'	Yoho N.P.	BC
Hector Glacier	082N09	51°35.7'	116°15.5'	Banff N.P.	AB
Hilda Glacier	083C03	52°11.0'	117°10.0'	–	AB
Hooker Glacier	083D08	52°23.4'	118°05.0'	Kootenay	BC
Hooker Icefield[4]	083D08	52°25.0'	118°05.0'	Jasper N.P.	AB
Hooker Icefield[4]	083D08	52°25.0'	118°05.5	Kootenay	BC
Horseshoe Glacier[7]	082N08	51°20.5'	116°16.0'	Banff N.P.	AB
Huntington Glacier	083C02	52°09.8'	116°57.6'	–	AB
Ithaca Glacier	094F08	57°23.0'	124°08.0'	Peace River	BC
Kane Glacier[4]	083D08	52°24.0'	118°10.1'	Jasper N.P.	AB
Kane Glacier[4]	083D08	52°24.6'	118°09.5'	Kootenay	BC
King George Glacier	082J11	50°35.8'	115°23.6'	–	BC
Kitchi Glacier	093H16	53°54.3'	120°24.5'	–	BC
Kwadacha Glacier	094F15	57°49.0'	124°55.0'	Cassiar	BC
Lambe Glacier	082N10	51°44.5'	116°46.7'	Kootenay	BC
Lefroy Glacier	082N08	51°22.5'	116°16.1'	Banff N.P.	AB
Llanberis Glacier	094F14	57°51.0'	125°00.0'	Cassiar	BC
Lloyd George Glacier	094F15	57°55.0'	124°55.0'	Peace River	BC
Lloyd George Icefield	094F15	57°52.0'	124°58.0'	Peace River	BC
Lyautey Glacier	082J11	50°37.0'	115°13.0'	–	AB
Lyell Icefield[4]	082N14	51°55.8'	117°04.7'	Kootenay	BC
Lyell Icefield[4]	082N14	51°56.0'	117°05.0'	Banff N.P.	AB
Mangin Glacier	082J11	50°33.0'	115°13.0'	–	AB
Mary Vaux Glacier	083C11	52°34.0'	117°27.5'	–	AB
Mastodon Glacier	083D09	52°37.0'	118°16.7'	Jasper N.P.	AB
McConnell Glacier	094F14	57°57.8'	125°14.0'	Cassiar	BC
Meadow Glacier	083D16	52°45.6'	118°23.3'	Jasper N.P.	AB

TABLE 1.—*Named glaciers of the Rocky Mountains cited in the chapter*—Continued

Glacier Name	Map sheet (1:250,000-scale)	Latitude North	Longitude West	Location	Province
Menagerie Glacier	093H16	53°55.0'	120°23.5'	--	BC
Mist Glacier[8]	083E03	53°07.7'	119°10.0'	Cariboo	BC
Misty Glacier	083C05	52°17.6'	117°51.2'	Kootenay	BC
Molar Glacier	082N09	51°37.1'	116°16.0'	Banff N.P.	AB
Monkman Glacier	093I11	54°34.0'	121°22.0'	Peace River	BC
Mons Glacier	082N15	51°52.5'	116°59.3'	Banff N.P.	AB
Mons Icefield[4]	082N14	51°51.5'	117°00.7'	Banff N.P.	AB
Mons Icefield[4]	082N14	51°52.0'	117°00.0'	Kootenay	BC
Mount Brown Icefield	083D08	52°22.1'	118°136'	Cariboo; Kootenay	BC
Mount Brown Icefield	083D08	52°22.0'	118°13.0'	--	AB
Mummery Glacier	082N10	51°40.5'	116°49.0'	Kootenay	BC
Mural Glacier	083E03	53°12.0'	119°11.0'	Jasper N.P.	AB
Murchison Icefield	082N15	51°55.0'	116°38.0'	Banff N.P.	AB
Nivelle Glacier	082J11	50°31.0'	115°11.0'	Kootenay	BC
Niverville Glacier	082N15	51°47.2'	116°57.5'	Banff N.P.	AB
North Alnus Glacier	083D08	52°26.6'	118°01.6'	Kootenay	BC
North Glacier	082N15	51°52.3'	116°57.3'	Banff N.P.	AB
Odyssey Icefield	094F08	57°20.0'	124°05.0'	--	BC
Pangman Glacier	082N15	51°46.0	116°57.0'	Banff N.P.	AB
Para Glacier	083D09	52°39.7'	118°16.8'	--	AB
Paragon Glacier	083D09	52°41.0'	118°18.0'	--	BC
Parapet Glacier[4,9]	082N10	51°44.5'	116°38.3'	--	AB
Parapet Glacier[4]	082N10	51°44.5'	116°38.3'	Kootenay	BC
Parsnip Glacier	093I11	54°32.0'	121°27.0'	Peace River	BC
Peyto Glacier	082N10	51°40.6'	116°32.8'	Banff N.P.	AB
President Glacier	082N07	51°30.2'	116°34.3'	--	BC
Prince Albert Glacier	082J11	50°36.2'	115°24.7'	--	BC
Princess Mary Glacier	082J11	50°35.0'	115°24.2'	--	BC
Pétain Glacier	082J11	50°32.0'	115°10.0'	Kootenay	BC
Quentin Glacier	094F15	57°55.0'	124°58.0'	Cassiar	BC
Rae Glacier	082J10	50°37.4'	114°59.1'	--	AB
Ram River Glacier	082N16	51°51.0'	116°11.0'	--	AB
Reef Glaciers	083E03	53°07.0'	119°00.5'	Cariboo	BC
Reef Icefield[4]	083E02	53°08.5'	119°00.6'	Jasper N.P.	AB
Reef Icefield[4]	083E02	53°08.5'	119°00.6'	Cariboo	BC
Resthaven Icefield	083E06	53°26.0'	119°28.0'	Jasper N.P.	AB
Rice Glaciers	083C03	52°00.0'	117°15.0'	--	BC
Robson Glacier	083E03	53°08.0'	119°06.0'	Cariboo	BC
Saskatchewan Glacier	083C03	52°08.3'	117°12.1'	Banff N.P.	AB
Scarp Glacier	083D09	52°38.9'	118°21.4'	Cariboo	BC
Scott Glacier	083D08	52°26.0'	118°05.0'	Jasper N.P.	AB
Serenity Glacier	083C05	52°23.0'	117°59.0'	Kootenay	BC
Sharp Glacier	082N01	51°12.2'	116°20.1'	Kootenay N.P.	BC
Simon Glacier	083D09	52°38.2'	118°18.8'	Jasper N.P.	AB
Sir Alexander Icefield	093H16	53°56.0'	120°23.0'	Cariboo	BC
Sir James Glacier	082N15	51°52.1'	116°52.8'	Banff N.P.	AB
South Alnus Glacier	083D08	52°24.7'	118°00.4'	Kootenay	BC
Southeast Lyell Glacier	082N14	51°54.5'	117°01.6'	Banff N.P.	AB
Southwest Lyell Glaciers	082N14	51°54.7'	117°05.4'	Kootenay	BC

TABLE 1.—*Named glaciers of the Rocky Mountains cited in the chapter*—Continued

Glacier Name	Map sheet (1:250,000-scale)	Latitude North	Longitude West	Location	Province
Stagnant Glacier	094F14	57°52.0'	125°03.0'	Cassiar	BC
Stanley Glacier	083C04	52°08.1'	117°56.6'	Kootenay	BC
Steppe Glacier[4]	083E03	53°09.5'	119°00.6'	Cariboo	BC
Steppe Glacier[4]	083E03	53°09.0'	119°01.0'	Jasper N.P.	AB
Stutfield Glacier	083C03	52°14.0'	117°21.5'	Jasper N.P.	AB
Swiftcurrent Glacier	083E03	53°09.8'	119°17.8'	Cariboo	AB
Swiftcurrent Icefield	083E03	53°11.0'	119°15.0'	–	AB/BC
Tipperary Glacier	082J11	50°41.0'	115°24.0'	–	BC
Tumbling Glacier[10]	082N01	51°07.5'	116°14.2'	Kootenay N.P.	BC
Tusk Glacier	083C04	52°14.0'	117°56.0'	Kootenay	BC
Victoria Glacier	082N08	51°23.0'	116°16.0'	Banff N.P.	AB
Vista Glacier	083D16	52°46.3'	118°26.5'	Cariboo	BC
Vreeland Glacier	093I11	54°34.0'	121°27.0'	Peace River	BC
Vulture Glacier[4]	082N09	51°35.9'	116°27.5'	Banff N.P.	AB
Vulture Glacier[4]	082N09	51°35.9'	116°27.5'	Kootenay	BC
Waitabit Glacier	082N10	51°42.0'	116°54.7'	Kootenay	BC
Wales Glacier[4]	083C04	52°10.0'	117°37.5	Jasper N.P.	AB
Wales Glacier[4]	083C04	52°09.2'	117°39.6'	Kootenay	BC
Wapta Icefield[4]	082N09	51°38.0'	116°30.0'	Banff N.P.	AB
Wapta Icefield[4]	082N09	51°38.0'	116°30.0'	Kootenay	BC
Waputik Glacier	082N09	51°32.3'	116°22.8'	Banff N.P.	AB
Waputik Icefield[4]	082N09	51°34.5'	116°27.2'	Banff N.P.	AB
Waputik Icefield[4]	082N09	51°34.0'	116°27.0'	Yoho N.P.	BC
Washmawapta Icefield	082N01	51°10.0'	116°18.0'	Kootenay	BC
Wenkchemna Glacier	082N08	51°18.7'	116°14.2'	Banff N.P.	AB
West Alexandra Glacier	082N14	51°59.0'	117°13.0'	Kootenay	BC
West Chaba Glacier	083C04	52°15.0'	117°46.1'	–	AB
West Glacier	082N15	51°51.6'	116°59.3'	Banff N.P.	AB
West Washmawapta Glacier	082N01	51°11.0'	116°19.0'	Kootenay	BC
Wilson Icefield	083C02	52°01.1'	116°48.0'	Banff N.P.	AB
Wishaw Glacier	093H16	53°57.0'	120°12.0'	Peace River	BC
Wokkpash Glacier	094K07	58°16.0'	124°43.0'	Peace River	BC
Yoho Glacier	082N10	51°36.0'	116°33.0'	Yoho N.P.	BC

[1] Two other Boundary Glaciers, in Cassiar, BC, are listed in the geonames database.

[2] Castleguard Glacier, without roman numeral subdivisions, in Banff N.P., AB, is listed in the geonames database.

[3] Two other Cathedral Glaciers, in Cassiar, BC, and in Yukon Territory, are listed in the geonames database.

[4] Some glaciers and icefields straddle the border between the Provinces of Alberta (AB) and British Columbia; hence, they are listed twice although the ice is contiguous.

[5] There is another Delta Glacier, in Cassiar, BC, listed in the geonames database.

[6] Another Dome Glacier, in Nunavut, is listed in the geonames database.

[7] Another Horseshoe Glacier, in Kootenay, BC, is listed in the geonames database.

[8] Another Mist Glacier, in Kootenay, BC, is listed in the geonames database.

[9] In addition to the Parapet Glacier in the Rocky Mountains, there is a Parapet Glacier in Nunavut listed in the geonames database.

[10] Another Tumbling Glacier, in Nunavut, is listed in the geonames database.

*Figure 5.—Photograph of the Victoria Glacier, Rocky Mountains, Alberta, Canada, in August 1973, showing its morainic-debris-covered terminus and glacierets on the steep valley wall. Photograph by C. Simon L. Ommanney, National Hydrology Research Institute [NTS Map: 082N08]. Glacier 4*5BAA–37, Glacier Atlas of Canada, Plate 7.3, Red Deer River, Glacier Inventory, Area 4*5, Inland Waters Branch, Department of Energy, Mines and Resources, 1970, scale 1:500,000.*

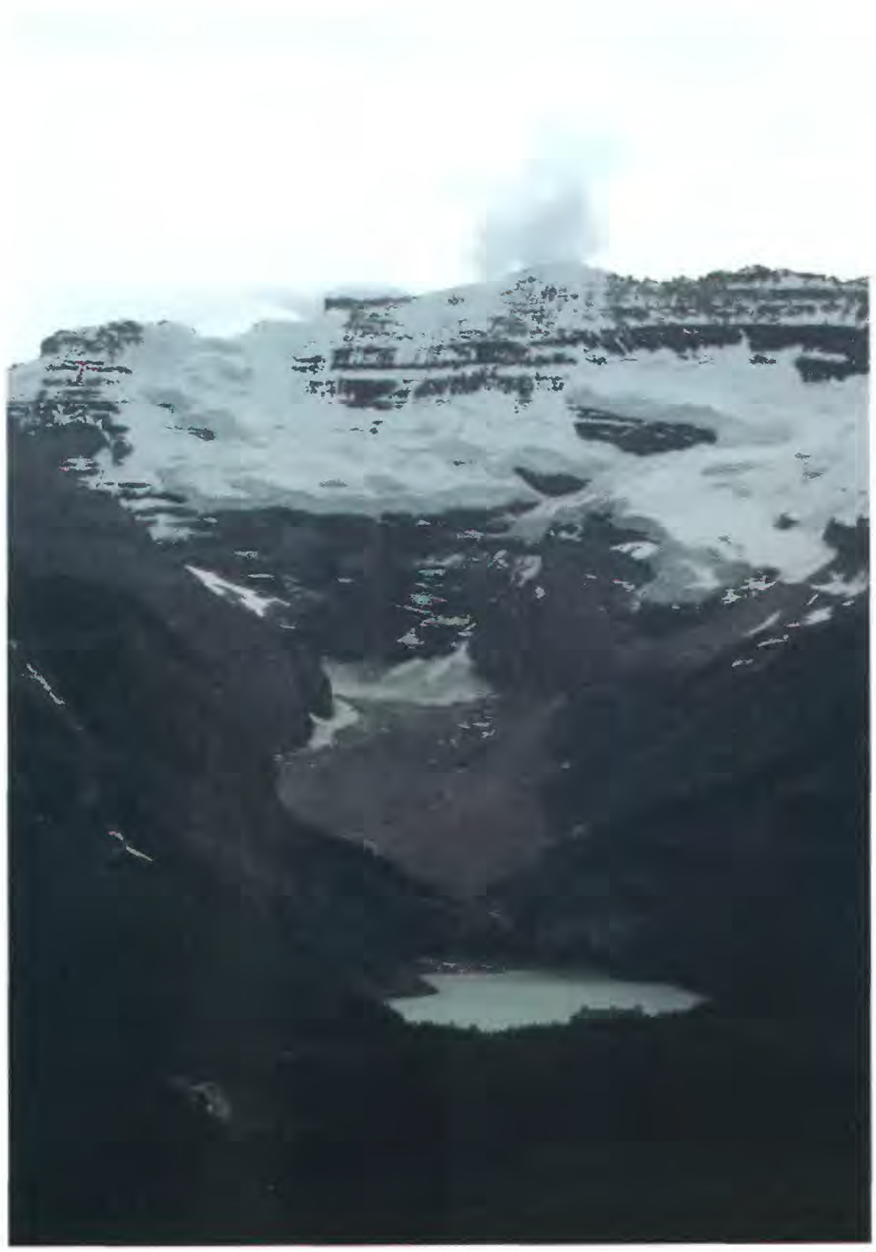

TABLE 2.—*Estimate of glacierized area of the Rocky Mountains of Canada (from Henoch, 1967)*

Drainage Areas	Area (square kilometers)
Pacific Ocean	37,659
Nelson River	328
Great Slave Lake	626
Total	38,613

TABLE 3.—*Number and types of glaciers within the Nelson River basin (from Ommanney, 1972a)*

Drainage Area	Ice Field	Outlet Glacier	Valley Glacier	Mountain Glacier	Glacieret	Rock Glacier, Ice-Cored Moraine	Total
Oldman River				2	33	18	53
Waterton River					4		4
Bow River to Lake Louise	2	1		92		8	103
Pipestone River		2		34	1	12	49
Baker Creek				12		6	18
Bow River and Brewster Creek				36		12	48
Spray River	1			75	2	13	91
Lake Minnewanka	1			23		8	32
Kananaskis Lake				69	3	7	79
Ghost River				3		3	6
Elbow River				5		4	9
Highwood River				15	1	20	36
Red Deer River				58	1	8	67
Siffleur River				97	6	16	119
Mistaya River				66	6	6	78
Howse River	1		1	79	3	7	91
Arctomys Creek				23	1	4	28
Alexander River				57	1	9	67
North Saskatchewan River		1		59	4	12	76
Cline River			1	87	5	15	108
Clearwater River		1		49	1	13	64
North Saskatchewan (middle)				29		6	35
Blackstone River				3		4	7
Opabin Creek				4			4
Job Creek				27	3	9	39
Brazeau River	3			33	2	6	44
Brazeau Lake	2			47	1	15	65
Isaac Creek				20		5	25
Southesk River				51	1	17	69
Thistle Creek				3		2	5
Cardinal River				5		1	6
Total	9	5	2	1,163	79	266	1,524

Border Ranges (B)[4]

The Border Ranges (fig. 1, B) mark the southern limit of the Rocky Mountains in Canada. They include the Galton, Macdonald, Clark, Wilson, and *Lewis Range*s. No substantial ice bodies exist here. The glacierets that are located in the Border Ranges are of little significance for water supply but may be important for some plant and animal life. Abandoned cirques, tarns, horns, and other remnants of mountain glaciation testify to the previous presence and areal extent of extensive glaciers.

Clark Range (Wilson and *Lewis Range*s) (B1)[4]

The Clark Range (fig. 1, B1) lies along the Continental Divide that forms the border between the provinces of British Columbia and Alberta in the southern Rocky Mountains. The range rises to an elevation of almost 3,000 m asl in Mount Blakiston (2,919 m) and has a mean peak elevation of about 2,500 m asl. The Wilson and *Lewis Range*s are outliers within Waterton Lakes National Park.

Although no glaciers are shown on the National Topographic System (NTS) maps for this area nor are any observable on the satellite images, interpretation of aerial photographs for the Canadian Glacier Inventory has revealed some permanent snow and ice, or glacierets, in sheltered areas of the park and farther north in the range around Mount Haig (2,611 m).

Macdonald Range (B2)

The Macdonald Range (fig. 1, B2), lies west of the Clark Range and is separated from it by the *Flathead Basin*; it also has no glaciers, according to current maps. No inventory has been completed for this area, so it is not known whether glacierets exist. Any accumulation of perennial ice is unlikely, because the mean elevation of the range is lower than that of the Clark Range and, at this latitude in the Rocky Mountains, permanent snow and ice tend to remain only on the sheltered eastern and northern slopes rather than on the more exposed western flanks.

Galton Range (B3)

At an even lower mean elevation, the Galton Range (fig. 1, B3) forms the western flank of the Border Ranges. The range abuts the Rocky Mountain Trench, which in this area includes the Kootenay River and Lake Koocanusa. Because the maximum height is 2,230 m asl and the mean height is just over 2,000 m, it is reasonably certain that not even permanent snow patches exist here.

Continental Ranges (South—Border Ranges to Kicking Horse Pass)

Because the Continental Ranges extend more than 725 km and contain thousands of glaciers, several of which have been studied and are quite well known, they have been divided into three sections—south, central, and north.

The northern boundary of the southern area is marked by the Trans-Canada Highway and the main line of the Canadian Pacific Railroad (CPR), both of which follow the Bow River from the Foothills, through Banff to the Kicking Horse Pass and its famous spiral tunnel, and then along the Yoho River to the west. This coincides with the northern limit of the Kootenay Ranges. The southern limit has been taken as the beginning of the Border Ranges, which were discussed previously. The slightly warmer climate south of Kicking Horse Pass means that generally this group of mountain ranges contains fewer and smaller ice fields and glaciers than those to the north, but there is ample evidence of previous glacierization.

The series of parallel ranges running from east to west have been grouped and are discussed according to the area within which they fall—the Front, *Park,* and Kootenay Ranges.

Front Ranges (South) (FS)

The Front Ranges (fig. 1, FS) constitute a series of parallel mountain ranges rising from the Foothills up to and beyond the Continental Divide that marks the provincial boundary. The outer, or eastern, group of ranges consists of the Blairmore, Livingstone, Highwood, Misty, Opal, and Fisher Ranges and ends in the north at the *Rundle Peaks*. The next parallel group of ranges is made up of the Flathead, Taylor, High Rock, Wisukitsat, Greenhills, Elk, and Kananaskis Ranges. The final section of the Front Ranges is made up of the Lizard Range, the *Harrison*, *Italian* and Joffre Groups, Spray Mountains, and the Sundance Range. It is this inner and higher set of ranges in which several glaciers are found, particularly in the Spray Mountains and in the *Italian* and Joffre Groups. The divide follows the central range as far as the Elk Range then swings over and passes out into the *Park Ranges*.

Lizard Range (FS1)

The Lizard Range (fig. 1, FS1) is the southernmost element of the Front Ranges and is situated on the western flank of the Rocky Mountains, south of the Kootenay Ranges. Elevations here are <2,300 m, and there are no glaciers.

Taylor Range (FS2)

Just to the west of the Continental Divide, the mountains in the Taylor Range (fig. 1, FS2) are somewhat higher in elevation, up to 2,445 m, but the orographic-precipitation regime is insufficient to sustain any permanent ice masses.

Flathead Range (FS3)

The elevation of the mountains increases within the Flathead Range (fig. 1, FS3), averaging about 2,500 m asl, but with higher peaks such as Mount Ptolemy (2,815 m) and Mount Darrah (2,745 m). Mount Ptolemy has a few rock glaciers in its vicinity (for example, Canadian glacier inventory glacier No.*4*5AA16 and 17), and there are some glacierets farther south in the headwaters of the Carbondale River. None, however, is shown on the published topographic maps.

Blairmore Range (FS4)

Moving toward the prairies and almost in the Foothills, elevations drop to close to 2,000 m in the Blairmore Range (fig. 1, FS4), and no glaciers of any size exist.

Livingstone Range (FS5)

Just to the north of the Blairmore Range, the Livingstone Range (fig. 1, FS5), a long, sinuous, limestone range, almost 100-km long, is the first of five major ranges that constitute the next group in the Continental Ranges. Some peaks, such as Centre Peak and Mount Burke, rise to about 2,500 m. Although no glaciers are visible on the Landsat images or any NTS maps, a group of four rock glaciers has been identified at the southern end of the range near the Blairmore Range.

High Rock Range (*Tornado Group*) (FS6)

Situated parallel to the Livingstone Range and to its west, the High Rock Range (fig. 1, FS6), also known as the *Tornado Group*, rises from 2,550 m in Crowsnest Mountain in the southern part of the range and extends past Tornado Mountain (3,100 m) to several 3,000-m peaks in the northern part. A small ice apron and rock glacier (*4*5BL5 and 6; Ommanney, 1989) occur at the foot of Mount Cornwell; they are remnants of the glaciers observed there during the 1916 survey (Interprovincial Boundary Commission, 1924). Small glaciers, glacierets, ice-cored moraines, and rock glaciers are mostly found at the foot of the higher peaks on the north- and east-facing slopes, though none are shown on NTS maps. This may explain Denton's (1975) conclusion that there was no glacier on Tornado Mountain.

Wisukitsat and Greenhills Ranges (FS7)

Two small ice-free ranges, the Wisukitsat and Greenhills Ranges (fig. 1, FS7), lie between the High Rock Range and the next major parallel feature of the Continental Ranges, to the west, the *Harrison Group East*. Both are fairly low, with peaks less than 2,700 m and 2,400 m in elevation, respectively, and are not known to be glacierized.

Harrison Group East (FS8)

The last major mountain block in this discussion of the Front Ranges (South) is the *Harrison Group East* (fig. 1, FS8), which is almost 100 km long and about 15 km wide. It is bounded to the east by Elk River and to the west by Bull River. Summit elevations are lowest in the southern part (<2,500 m) and rise to just over 3,000 m northward. No detailed studies have been made of the ice cover in this range, so it is not known whether glacierets and rock glaciers can be found here. It would seem likely, as well-developed glaciers are found just to the north around Mount Abruzzi in the *Italian Group*.

Highwood Range (FS9)

Moving farther north again, the next major eastern outlier of the Rockies is the Highwood Range (fig. 1, FS9). It has elevations varying from 2,782 m (Mount Head) to more than 2,800 m in the northern part of the range. Small glaciers are found at the headwaters of tributaries of Sheep River.

Misty Range (FS10)

Lying at the headwaters of Sheep River and cut off to the west by Highwood River, the Misty Range (fig. 1, FS10) rises to more than 3,000 m asl in Mist Mountain (3,138 m) and Mount Rae (3,219 m). The latter is the location of *Rae Glacier* [*4*5BJ–4] (fig. 6) (Gardner, 1983), which was studied briefly by a group from the University of Saskatchewan (Lawby and others, 1994). There are three other glaciers near *Rae Glacier*, as well as many other small ones at the head of Mist Creek. Gardner (1983) refers to several small cirque and niche glaciers above 2,900 m in elevation on shaded and leeward slopes.

Elk Range (FS 11)

The Elk Range (fig. 1, FS11) is a northerly extension of the High Rock Range. Mean maximum elevations vary from 2,600 to more than 2,800 m. Again, small glaciers are scattered along the base of the range in sheltered north- and east-facing basins.

Italian Group (FS12)

The *Italian Group* (fig. 1, FS12) is really a continuation of the *Harrison Group*. It is centered on Mount Abruzzi, a major peak rising to 3,265 m asl, with other peaks exceeding 3,000 m in its vicinity. Many small glaciers are located here in sheltered north- and east-facing cirques. Most are about 1 km long, with snouts terminating around 2,450 m. Abruzzi Glacier (4 km^2), which is the largest, is some 2 km wide, 2.5 km long, and descends to 2,500 m. This is the southernmost group of glaciers in the Canadian Rocky Mountains, if one relies solely on the existing topographic maps. However, glacier inventory studies have revealed small permanent ice

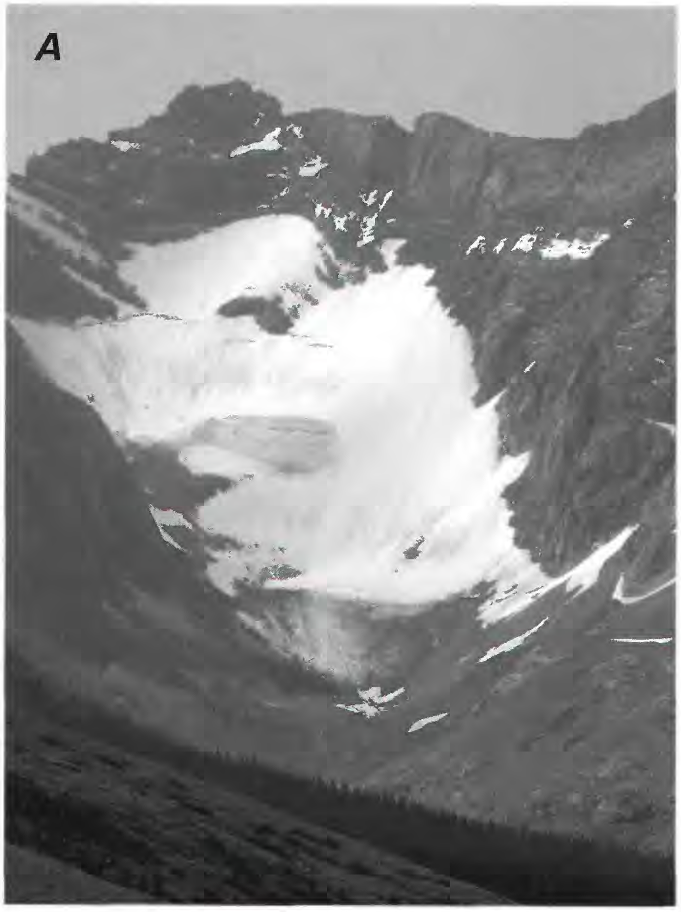

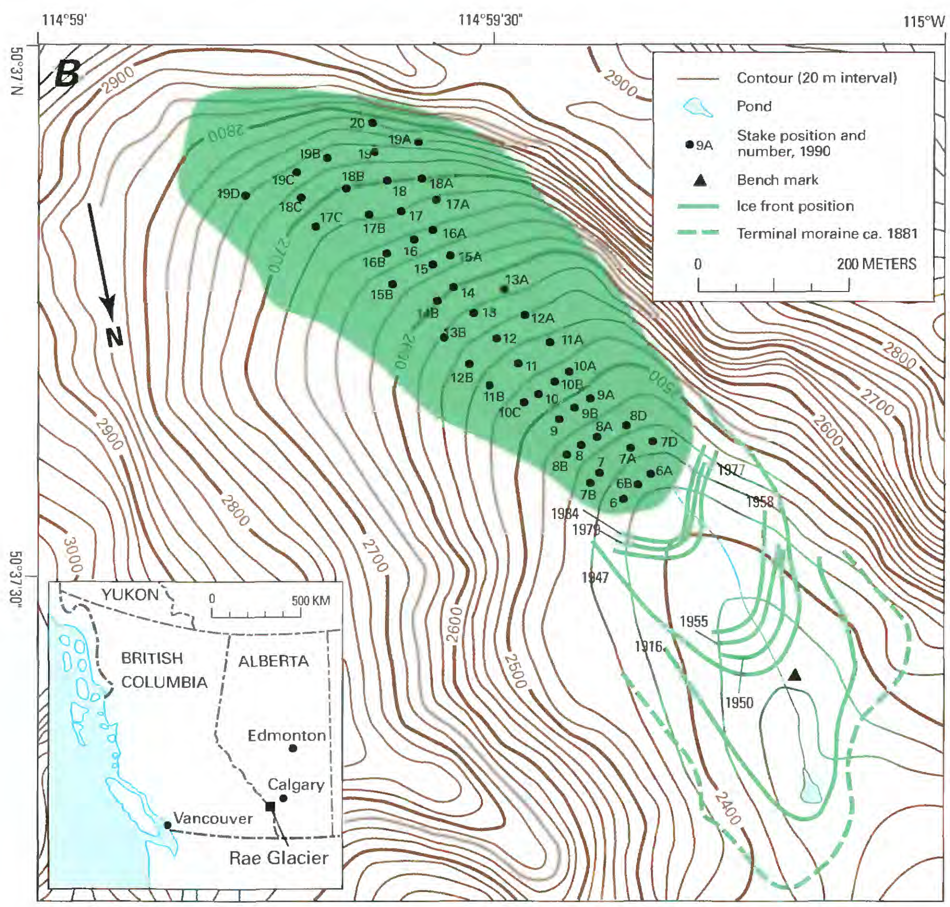

***Figure 6.**—Rae Glacier, Misty Range, Rocky Mountains, **A**, Photograph taken August 1985. Glacier 4*5BJ–4, Glacier Atlas of Canada, Plate 7.2, Bow River Glacier Inventory, Area 4*5B, Inland Waters Branch, Department of Energy, Mines and Resources, 1970, scale 1:500,000. **B**, Modification of sketch map showing historical terminus survey and stake positions for 1990 as determined by a group from the University of Saskatachewan (Lawby and others, 1994).*

masses all the way south to the U.S./Canada border. Just over the border in Glacier National Park, Montana, 37 named, small mountain glaciers have been documented within the park, and two outside. [See section "Glacier Retreat in Glacier National Park, Montana," in the Glaciers of the Western United States (J–2) part of this volume.] Glacier National Park, not to be confused with the Canadian Glacier National Park in the Selkirk Mountains of central British Columbia, near Revelstoke, is one of two contiguous national parks, north and south of the border; the other is Waterton Lakes National Park, Alberta.

Joffre Group (French Military Group) (FS13)

Bounded to the east by Elk River and to the west by the Palliser River, the Joffre, or *French Military Group* (fig. 1, FS13), is a northwesterly extension of the *Italian Group* and has peaks rising to a maximum in Mount Joffre (3,449 m) and more and larger glaciers than in the previously discussed mountain ranges. The Mangin and Pétain Glaciers are about 5 km^2 in area and 4.5 and 3.5 km in length, respectively. The *Foch Glacier*, Elk, Castelnau, Lyautey and Nivelle Glaciers are 1.5 to 2 km in length, and there are several other unnamed glaciers nearby of comparable size. Only the Nivelle Glacier is located on the western side of the main range. The average lowest elevation of the ice varies from 2,400–2,600 m. The equilibrium line altitude (ELA) likely lies between 2,600 and 2,700 m.

Opal Range (FS14)

The toe of an L-shaped range, the Opal Range (fig. 1, FS14), provides part of the initial buttress of the Rocky Mountains, which face the Foothills to the east, and has the upper part of the "L" tucked in behind the more northerly Fisher Range. Along with the following two ranges, it forms part of what has been called the *Kananaskis Range*. The western limits are marked by the broad valley of the Kananaskis River. There is a slight east-to-west gradient in maximum peak elevations from 2,900 m to slightly more than 3,000 m. The peaks to the west resemble the Sawback Range. The sharp and jagged peaks were created by erosion of the nearly vertical, steeply dipping beds of the Rundle Limestone. No glaciers are shown on the published maps, but the glacier inventory identified some small ice aprons, glacierets, and rock glaciers in parts of the range.

Fisher Range (FS15)

Fisher Range (fig. 1, FS15) marks the northern limit of the easternmost ranges of the Rocky Mountains considered in this part of the Continental Ranges. Elevations are similar to those in the Opal Range, rising to a maximum of just over 3,000 m asl at Mount Fisher, where the glacier inventory identified two small cirque glaciers, the only permanent ice here.

Kananaskis Range (FS16)

Although there are no glaciers large enough for skiing, this is the area of Mount Allan in the Kananaskis Range (fig. 1, FS16), which includes the area chosen for Canada's winter Olympic downhill skiing events in 1988. The range lies across the Kananaskis River valley and is bounded on the west by Smith-Dorrien Creek with mountains rising slightly to just over 3,100 m asl. Numerous small ice aprons and cirque glaciers have been identified here, as well as several small rock glaciers.

Spray Mountains (British Military Group) (FS17)

Otherwise known as the British Military Group, after the association of peak and glacier names, the Spray Mountains (fig. 1, FS17) contain several glaciers along the divide—a continuation of those found farther south in the Joffre Group. The largest, about 4 km^2, 3 km long, and descending to 2,225 m, is the Haig Glacier. *Beatty Glacier*, just to the south of the Haig Glacier, is only about 1.5 km long and terminates a little higher at 2,380 m. Other glaciers vary in length from 0.5 to 3 km and have average snout elevations of about 2,500 m asl. The ELA in this range is estimated to be about 2,650 m on the east side and 2,670 m on the west side.

Rundle Peaks (FS18)

Paralleling the Trans-Canada Highway on its southern margin, as the highway enters the Rocky Mountains and curves northward toward Banff and Banff National Park, are the *Rundle Peaks* (fig. 1, FS18). Peak elevations are less than 3,000 m and include the Three Sisters above the town of Canmore, Alberta, and Mount Rundle, all of which afford the scenic backdrop to the Banff townsite from Mount Norquay. There are no glaciers in this range.

Goat Range (FS19)

West of the *Rundle Peaks* is the small Goat Range (fig. 1, FS19), stretching from the Spray Lakes Reservoir, which can be seen clearly on Landsat images, to the southern end of Sulphur Mountain in Banff. The lower part of the range has elevations comparable to those of the *Rundle Peaks*, approximately 2,900 m, but, unlike the latter, it does have several small cirque glaciers and ice aprons around Mount Nestor (2,960 m).

Sundance Range (FS20)

As viewed from space, the Sundance Range (fig. 1, FS20) looks like a giant tuning fork; it extends south-southeast from the Banff area before splitting into the two tines that reach to the head of the Spray Lakes Reservoir. Mean peak elevations vary from 2,800–2,950 m asl. Although not shown on NTS maps, the southern part, from Cone Mountain to Fatigue Mountain (2,959 m), contains numerous small glaciers (*4*5BC61–78, 84–91; Ommanney, 1989) that lie along benches and terraces eroded in the tilted strata. Some climbers include this range with the *Assiniboine Park Group* [and the Blue and Mitchell Ranges, as part of the *Assiniboine Park Group*] in the *Park Ranges*. Such trans-range mountain groups make the delineation of meaningful groups of mountain ranges extremely difficult, because differentiation may be based on physiographic, geologic, or other considerations.

Park Ranges (South) (PS)

The *Park Ranges* (fig. 1, PS) lie between the Kootenay and Front Ranges. They are generally higher and more heavily glacierized than the Front Ranges (South). The northern limit of this area is composed of the Ball, Vermilion, Bow, and Ottertail Ranges; the latter includes the Washmawapta Icefield. In the vicinity of Mount Assiniboine—the "Matterhorn" of the Rocky Mountains—are found the *Assiniboine Park Group* and Royal Group, as well as the Blue and Mitchell Ranges. In the southern part, the ranges narrow into the western part of the *Harrison Group* and terminate in the Quinn Range. Glaciers are concentrated in the northern part of the *Park Ranges* (South) and also around Mount Assiniboine.

Quinn Range (PS1)

The Quinn Range (fig. 1, PS1) is about 50 km long; it is nestled between the *Harrison Group East* of the Front Ranges and the Van Nostrand

Range of the Kootenay Ranges. The range rises to a maximum height of 3,300 m asl at Mount Mike, and maximum elevations are generally close to 3,000 m, yet no glaciers are shown on the maps.

Harrison Group West (PS2)

The Bull and White Rivers separate the western and eastern sections of the *Harrison Group*, the *Harrison Group East* (fig. 1, FS8), and the *Harrison Group West* (fig. 1, PS2). The western part of the *Harrison Group West* is somewhat higher than the eastern part, having several peaks >3,000 m asl; Mount Harrison rises to 3,359 m. Despite the fact that Mount Harrison is higher than Mount Abruzzi and about 40 km farther north, there are apparently no glaciers in the vicinity.

The Royal Group (PS3)

The centerpiece of the Royal Group (fig. 1, PS3) is Mount King George (3,422 m), an impressive landform of towers and massive walls, but there are several other peaks that also rise above 3,000 m. The *Princess Mary*, *King George*, and *Prince Albert Glaciers* are located on the flanks of Mount King George. They vary in area from 0.5 to 1.5 km^2 and have termini at about 2,450 m asl. More than 2 km long, the *Tipperary Glacier* is located on Mount Cradock; another small glacier (Albert Glacier) fills a cirque north of Mounts Queen Elizabeth and King Albert. Part of The Royal Group, with elevations ranging up to 2,950 m asl, lies to the west, separated from the rest of the group by the Albert and Cross Rivers.

Blue Range (PS4)

The small mountain block of the Blue Range (fig. 1, PS4) straddles the Continental Divide south of Mount Assiniboine, from which it is separated by Aurora and Owl Creeks. Elevations do not reach 2,900 m even along the border, and no glaciers are shown on current maps, even though glacier inventory work on the eastern end of the range revealed numerous cirques having small ice bodies and large moraines.

Assiniboine Park Group (PS5)

The dominant peak in the southern Rockies and the highest in the southern Continental Ranges, Mount Assiniboine (3,618 m) (fig. 3) rises as a majestic horn above its surrounding glaciers, which lie on shelves around the main mountain core, the *Assiniboine Park Group* (fig. 1, PS5). The Indian name means "stone-boiler," after the practice of using hot stones for cooking. Of the dozen glaciers on Mount Assiniboine, the largest is about 2.5 km^2 in area. The average elevation of the glacier tongues ranges from 2,450 to 2,550 m. On the east side of the group, the equilibrium line probably lies at about 2,650 m. Rock-glacier forms in the area have been studied by Yarnal (1979). Although a popular stop for tourists and climbers, no scientific studies have been done on the glaciers in this area. The *Assinboine Park Group* is well-defined on all sides, limited by the Mitchell River and the Aurora, Bryant, and Owl Creeks.

Mitchell Range (PS6)

The main part of the Mitchell Range (fig. 1, PS6) lies along the east side of the Kootenay River south of the Simpson River. This part has peaks rising to >2,900 m. The western slopes of the Mitchell Range are deeply incised with well-developed cirque basins that probably show evidence of recent glaciation, if not some permanent ice. The range spreads out eastward in a series of four connected blocks ending at Simpson Ridge, where a small glacier (0.5 km^2) is located beneath Nestor Peak; its snout is at 2,485 m.

Ball Range (PS7)

As one drives from Banff northward to the Kicking Horse Pass, the Ball Range (fig. 1, PS7) can be seen where it forms part of the eastern section of the *Park Ranges*. Limited on three sides by the broad valleys of the Vermilion and Bow Rivers, the Ball Range has peaks varying from 2,800 to 3,100 m that reach a maximum elevation at Mount Ball (3,312 m). The six glaciers plotted on the NTS maps are all located on this mountain. They are less than 1 km long and have lower elevations differing by as much as 1,000 m (2,057–3,050 m). The largest has an area of about 0.75 km^2. Stanley Glacier (0.6 km^2 in area) is the only one lying on the western side of the range.

Vermilion Range (PS8)

Not to be confused with the Vermilion Range of the Front Ranges, 45 km to the northeast, this Vermilion Range (fig. 1, PS8) forms a major ridge to the west of the Continental Divide between the Vermilion and Beaverfoot Rivers, rising to maximum elevations of >3,000 m. Although maps include the Washmawapta Icefield in the Ottertail Range, the Vermilion Range should probably be considered as ending at Wolverine Pass. Six glaciers lie in cirques along the eastern slope of the range, the largest being Tumbling Glacier about 1 km^2 in area. Average snout elevations are at about 2,100 m asl and lengths vary from 0.2 to 1.5 km.

Bow Range (PS9)

The Bow Range (fig. 1, PS9) is the focal point of the visit of most tourists to Banff National Park. The range marks the northern limit of the area considered as the southern Continental Ranges. It is some 21 km long, 19 km wide, and has peaks that are amongst the highest of the mountain ranges discussed so far—Mounts Allen (3,301 m), Lefroy (3,423 m) and Victoria (3,646 m), and Deltaform (3,424 m) and Hungabee Mountains (3,492 m). Glaciers occur on both sides of the main range and include several debris-covered and rock-glacier forms. Many glaciers exceed 1 km in length. On the western side, the lowest elevation of glaciers is about 2,600 m asl, but several termini end at lower elevations; on the east, the glaciers tend to be at even lower elevations. The popular Lake Louise is dammed by an early Holocene moraine formed by the Victoria Glacier; it probably formed during the Eisenhower Junction glaciation, some 10,000 years before present (B.P.) (Kucera, 1976). Ironically, Moraine Lake is dammed by a rock slide from the Tower of Babel (Kucera, 1976) rather than by a moraine. Kucera (1976) and Gardner (1978b) provide popular accounts of the glaciers and landforms in this area. Several glaciers that have been the subject of specific studies and comments are discussed below.

Horseshoe Glacier

Horseshoe Glacier, with an area of 4.3 km^2, is about the same size as Victoria Glacier (3.5 km^2 in area) but has not been studied in detail. It is fed by snow avalanches from Ringrose Peak, Mount Lefroy, Hungabee Mountain, and The Mitre at the head of Paradise Valley. It extends some 1.3 km from 2,800 m to 2,220 m asl, through a heavily debris-covered ablation zone that makes up over half its area and retards its rate of retreat. The glacier was described by the Vauxes and Sherzer in the early part of the century (Sherzer, 1907, 1908; G. and W.S. Vaux, 1907b). The snout, which is an ice cliff, calves directly into a proglacial lake dammed by deposits left by the retreating glacier. The lake is fed by glacier meltwater from a terminus that has receded 945 m from its "Little Ice Age" maximum (Gardner, 1978b).

Wenkchemna Glacier

Wenkchemna Glacier, located in the Valley of the Ten Peaks at the head of Moraine Lake, is 3.7 km^2 in surface area, of which two-thirds is covered in moraine. Wenkchemna Glacier extends more than 4 km, from a number of independent ice streams that flow from the mountain wall below the Wenkchemna Peaks at about 2,700 m to a tongue at 1,900 m asl. These streams turn down valley to create the 1-km-wide ice-and-debris tongue that is estimated to be from 30 to 100 m thick. The glacier surface is irregular and hummocky, and thaw pits have formed where surface lakes have penetrated the underlying ice and drained. The comparative inactivity of the glacier, and the effectiveness of the debris as a sediment trap, means that the meltwater stream is clear, and a delta is not forming at the head of Moraine Lake. Around the margin and terminus are arcuate ridges up to 3 m high that are characteristic of rock glaciers. The early observations made here by Sherzer (1907, 1908), by the Vaux family (G. and W.S. Vaux, 1907b; by G. Vaux, 1910; M.M. and G. Vaux, 1911), by Field and Heusser (1954), along with more recent observations by Gardner (1977, 1978a), all show very little change in the glacier limits since 1903. Gardner reported the glacier had thinned by up to 50 m. Although several people have observed the debris-covered ice terminus encroaching on the surrounding forest, Kucera (1976) is of the opinion that Wenkchemna Glacier is shrinking.

Victoria Glacier

Victoria Glacier (fig. 5), lying at the head of Lake Louise, is probably one of the most frequently photographed glaciers in the Rocky Mountains, although some visitors may not recognize the debris-covered tongue for what it is. The glacier is visible and easily accessible from Chateau Lake Louise by a good trail that passes beside the lake.

The continuous ice stream flows northward from Abbot Pass (2,923 m) for about 2 km before turning sharply to the northeast, where it degenerates into an indistinct debris-covered ice tongue after another 2 km. The Abbot Pass basin contains less than 20 percent of the accumulation area. The rest, some 1.8 km^2 in area, lies in a broad apron that stretches from Popes Peak past Mount Victoria toward Abbot Pass and avalanches 300 m or more to form a reconstituted ice mass where the Abbot Pass ice stream changes direction. It is mainly an interrupted valley glacier; of its 3.5 km^2 area, 24 percent is debris-covered. Lefroy Glacier (1.3 km^2) flows from the basin between Mount Lefroy and The Mitre and is separated from Victoria Glacier by a band of moraine.

The earliest known record is a 1897 photo by William Hittel Sherzer (Collie, 1899). The following year, long-term studies were initiated by the Vaux family of Philadelphia—George Jr., William, and Mary—who carried out observations in 1898, 1899, 1900, 1903, 1907, 1909, 1910, and 1912 (G. and W.S. Vaux, 1901, 1907a, b, 1908; G. Vaux, 1910; M.M. and G. Vaux, 1911; M.M. Vaux, 1911, 1913; Cavell, 1983). These observations were interspersed with those of Sherzer, who returned to the area in 1904 and 1905 on behalf of the Smithsonian Institution (Sherzer, 1905, 1907, 1908). Studies in the inter-war years were sparse, apparently limited to surveys in 1931 and 1933 by the Alpine Club of Canada (Wheeler, 1932, 1934). The reasonably good historical record led to the selection of this glacier by the Calgary office of the Dominion Water and Power Bureau (DWPB) in 1945 for its network of glaciers being assessed for their contribution to runoff. The position of the terminus and changes in its areal extent were measured, and a set of plaques were placed on the ice surface to measure velocity (McFarlane, 1945, 1946a, 1947; McFarlane and May, 1948; Meek, 1948a, b; McFarlane and others, 1949, 1950; May and others, 1950; Carter, 1954). The surveys continued every year until 1950, then biennially until 1954, when the snout was so covered in debris that it was almost impossible to identify the toe

(Ommanney, 1971). Recession from various surveys is shown in figure 9; the average value is about 13.5 m a^{-1}. Average velocities, measured upstream of the junction with the Lefroy Glacier, are given in table 4.

Osborn (1975) reported on the penetration of the "Little Ice Age" moraines by advancing rock glaciers. Luckman and others (1984) extended their studies of the Holocene to this area, and some investigations have been initiated on sedimentation in Lake Louise (Hamper and Smith, 1983).

TABLE 4.—*Average annual surface movement of Victoria Glacier (m a^{-1})*

1899–1900	44.8	1947–1948	23.8
1899–1905	34.4	1948–1949	32.0
1906–1918	31.7	1949–1950	25.6
1945–1946	20.7	1950–1952	25.3
1946–1947	39.6	1952–1954	31.4

Cathedral Glacier

The *Cathedral Glacier* (0.84 km^2 in area) is poised like a Sword of Damocles above one of Canada's main transportation routes through the Rocky Mountains. Situated on Cathedral Mountain on the south side of *Kicking Horse Valley*, between approximately 2,410 m and almost 3,000 m elevation, *Cathedral Glacier* has, at least five times in 1925, 1946, 1962, 1978, and 1982, generated mudflows that blocked the Canadian Pacific Railroad (CPR) line and even buried the Trans-Canada Highway. Both Jackson (1979a, b, 1980) and Holdsworth (1984) speculated on the possible cause of these jökulhlaups. It is thought that the surface topography of the glacier, particularly a giant snowdrift ridge, permits development of a surface lake at 2,960 m asl, which is recharged by normal snowmelt and rain. A pulse discharge through the glacier and down a narrow ravine picks up speed and unconsolidated till to create a mudflow that heads towards the CPR tracks in the spiral tunnel section and the Trans-Canada Highway. The regional firn line at 2,890 m asl is situated below the lake level. This is one of two major glacier hazards identified in the Rockies, the other being associated with Hector Glacier and Peyto Glacier.

Ottertail Range (PS10)

The Ottertail Range is a northwesterly extension of the Vermilion Range and is similar to it in many respects. The highest peak is Mount Goodsir at 3,562 m. Glaciers in the northern part of the range, including the Hanbury Glacier, Goodsir Glacier, *East Goodsir Glacier*, and Sharp Glacier, also lie in east- and north-facing basins, except for the West Washmawapta Glacier and Washmawapta Icefield, which fills a large basin below Limestone Peak. The Washmawapta Icefield is only about 4 km^2 in area and hardly warrants its name. Glaciers terminate at about 2,500 m asl on this side of the range but are generally lower (some 2,300 m) on the eastern side. Hanbury Glacier is about the same size as the Washmawapta Icefield.

Kootenay Ranges (K)

South of Kicking Horse Pass, the Kootenay Ranges (fig. 1) form the western limit of the Rocky Mountains. The physiographic transition farther westward is very sharp, because the mountains drop down steeply into the Rocky Mountain Trench and the Kootenay and Columbia River systems. The range is narrow in the north, where it consists of the Beaverfoot (fig. 1, K5), Brisco (fig. 1, K4), and Stanford Ranges (fig. 1, K3), having peak heights varying from 2,500–2,700 m. Farther south it broadens into the 90-km-long Hughes Range (fig. 1, K1), which joins Lizard Range to form the southwestern limit of the Continental Ranges. The mountains here are slightly higher, up to 2,800 m, and are higher still in the eastern, parallel Van Nostrand Range (2,905 m) (fig. 1, K2). However, none of the topographic maps show any evidence of perennial ice features in the Kootenay Ranges.

Continental Ranges (Central—Kicking Horse Pass to Yellowhead Pass)

This central region, extending 300 km between Lake Louise and Mount Robson, is the most heavily glacierized part of the Continental Ranges. The mountains in this region trend northwest to southeast and are divided into the Front Ranges and the *Park* (or *Main*) *Ranges* (fig. 1). The former consist of Devonian and younger limestones, dolomites, and shales, all of which dip steeply to the west, whereas the latter are made up of nearly horizontal beds of Cambrian and older quartzitic sandstones, limestones, dolomites, and shales (Gardner, 1972). At the northern end is Mount Robson (3,954 m), the highest mountain in the Rockies. Most peaks in the Front Ranges have elevations between 2,800 m and 3,280 m asl, whereas those in the *Park Ranges* vary in elevation between 3,125 m and 3,600 m. Local relief is generally on the order of 1,400 m to 1,900 m.

The ranges become progressively drier from west to east toward the prairies. Hence the eastern ranges do not contain many glaciers or ice fields. Westward, the first large glacier is the Bonnet Glacier, on the east side of Castle Mountain and hidden from the view of the average tourist by the 18-km-long bulk of that impressive mountain. The glaciers take a variety of forms, including ice fields such as the Columbia Icefield, outlet glaciers such as the Athabasca and Saskatchewan Glaciers, valley glaciers such as Robson Glacier, and mountain glaciers of the cirque, niche, and ice-apron type such as the Angel Glacier. Located north of Kicking Horse Pass, the Waputik Icefield is the first of a long series of ice fields that straddle the Continental Divide (figs. 7, 8). The second is the Wapta Icefield, source of the Yoho and Peyto Glaciers, followed by the Campbell and Freshfield Icefields, which send a magnificent valley glacier to feed the Howse River. Next come the Mons and Lyell Icefields, southeast of the largest ice field in the Rocky Mountains, the Columbia Icefield (fig. 4). This last ice field culminates in the Snow Dome, which is the hydrographic apex of the continent and drains into three oceans. Located immediately northwest of the Columbia Icefield, the Continental Divide is capped by the Clemenceau, Chaba, and Hooker Icefields (fig. 4). The only ice fields off the main divide are the Wilson Icefield and *Brazeau Icefield*, which lie just east of the valleys of the North Saskatchewan and Athabasca Rivers.

The glaciation level is lowest in the western parts of the *Park Ranges* and through the Yellowhead Pass (about 2,600 m asl) but rises in the vicinity of Mount Robson to more than 2,900 m and climbs eastward toward the Front Ranges to more than 3,100 m (Østrem, 1973b).

In this part of the Continental Ranges, moraines of the "Little Ice Age" are evidence of the most significant regional Holocene glacial event in the Rocky Mountains. The best developed moraines are those from the early 1700's, when about one-third of the glaciers showed maximum advance, and from the mid- to late-nineteenth century, when major readvances built moraines close to or beyond that earlier extent (Luckman, 1986).

Rock glaciers are distributed throughout the area. Luckman and Crockett (1978) reported on those in the southern half of Jasper National Park. The 119 rock glaciers identified range in area from 0.035 km^2 to 1.57 km^2 and lie between 1,710 and 2,670 m asl; that is 400 to 600 m below the glaciation level. Their distribution seems to be controlled strongly by lithology, and they are predominantly oriented to the north. In Banff National Park, Papertzian (1973) found no evidence for lithological control of the 80 rock glaciers there. They range in area from 0.011 km^2 to 1.26 km^2 and lie between 1,737 and 2,743 m asl. Østrem and Arnold (1970) mapped both rock glaciers and ice-cored moraines in southern British Columbia and

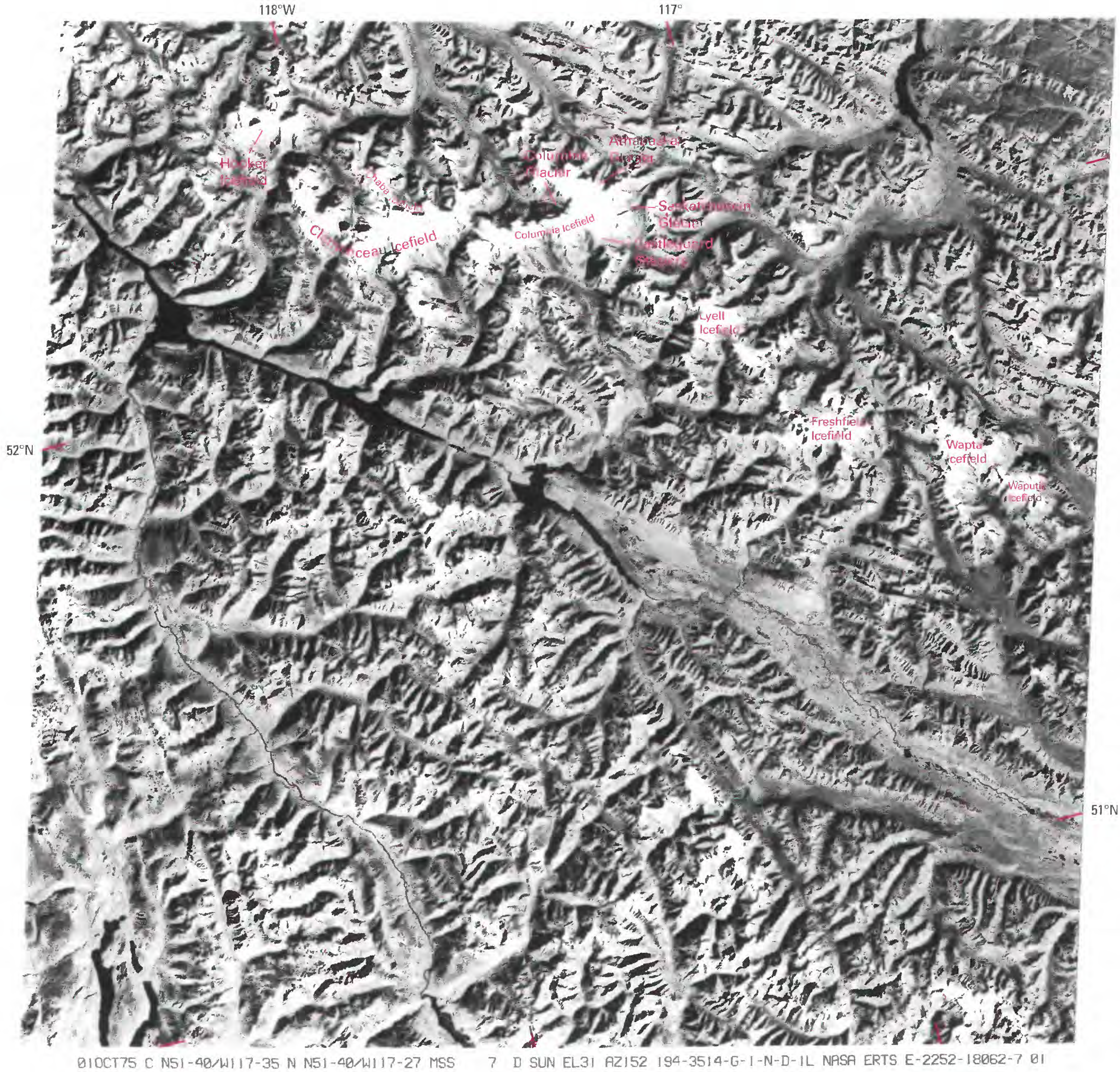

Alberta without distinguishing between them. An intermediate form that is quite common is the debris-covered glacier, such as Dome Glacier.

Descriptions of Rocky Mountain glaciers date from the time when Athabasca Pass was a major fur-trade thoroughfare, and they became more common once the Canadian Pacific Railroad line was completed. Despite the fairly long history of formal and informal glacier study, data for the whole range are sporadic. This is especially true for glaciers of the Front Ranges and for ice masses away from the main transportation routes such as the Clemenceau Icefield. However, virtually all of the detailed information on glaciers in the Rockies comes from the central Continental Ranges, primarily through investigations at the Peyto, Saskatchewan, and Athabasca Glaciers.

***Figure 7.**—Landsat 2 MSS image of several ice fields and outlet glaciers in the Rocky Mountains, including the Columbia, Wapta and Waputik Icefields. Landsat image (2252- 18062, band 7; 1 October 1975; Path 48, Row 24) from the EROS Data Center, Sioux Falls, S. Dak.*

Figure 8.—*Slightly reduced segment of the 1:250,000-scale topographic map of the Golden quadrangle (82N) showing the major ice fields along the crest of the Rocky Mountains from Waputik Icefield in the south to Lyell Icefield in the north. ©1997. Produced under licence from Her Majesty the Queen in Right of Canada, with permission of Natural Resources Canada.*

Front Ranges (Central) (FC)

The Front Ranges (Central) (fig. 1, FC) are a continuation of the series of parallel ridges described from the region to the south, although the parallelism may be less pronounced. Mountain outliers are found to the east in the Bighorn (fig. 1, FC12), Nikanassin (fig. 1, FC19), and Fiddle Ranges (fig. 1, FC20). The southern section, starting with the Fairholme Range (fig. 1, FC1) just north of the Bow River, continues northwest of Lake Minnewanka, with the Ghost River area bordering the Foothills, and extends westward through the Palliser (fig, 1, FC4), Bare (fig. 1, FC5), Vermilion (fig. 1, FC6), Sawback (fig. 1, FC7), and Slate Ranges (fig. 1, FC8). Between the Red Deer River and the North Saskatchewan River, the Front Ranges are more blocky in outline, with only two large groups, *Clearwater* (fig. 1, FC3) and *Murchison Groups* (fig. 1, FC9), and the Ram Range (fig. 1, FC10) as a northeasterly outlier. Between the Ram Range and the Athabasca River are a series of mountain blocks and groups whose boundaries are not very distinct. From south to north these are *Cline Range* (fig. 1, FC11), First Range (fig. 1, FC13), the *Cataract Group* (fig. 1, FC14), Le Grand Brazeau (fig.1, FC15), the *Southesk Group* (fig. 1, FC16), Queen Elizabeth Ranges (fig. 1, FC17), and Maligne Range (fig. 1, FC18), with the parallel Colin (fig. 1, FC23), Jacques (fig. 1, FC22), and Miette Ranges (fig. 1, FC21) rounding out this section in the north. The characteristics of the ranges and their glaciers will be discussed in turn.

Figure 9.—*(opposite page) Variations of glaciers in the Rocky Mountains, compiled by C.S.L. Ommanney; based on the published work of many glaciologists.*

Fairholme Range (FC1)

The Fairholme Range (fig. 1, FC1) is a large S-shaped feature that is clearly visible in satellite images. It extends some 25 km from where the Trans-Canada Highway passes through the towns of Exshaw and Canmore to Lake Minnewanka. Several peaks lie between 2,800 and 3,000 m asl, but the range is essentially free of ice.

Ghost River Area (FC2)

The Ghost River area (fig. 1, FC2), including the irregular mountain mass lying north of Lake Minnewanka and east of the Ghost River, has a few tiny cirque glaciers around Mount Oliver. These are the easternmost glaciers in the central Front Ranges. Elevations range to a maximum of slightly more than 2,900 m.

Clearwater Groups (FC3)

Probably the largest mountain block in this section of the Continental Ranges is the *Clearwater Groups* (fig. 1, FC3). They adjoin the northern part of the *Ghost River Area* and extend northwestward, encompassing the headwaters of the Clearwater River to end where the North Saskatchewan River cuts through the Front Range. The *Clearwater Groups* are bounded to the west by the Pipestone and Siffleur Rivers, and most of the glaciers are concentrated in the part of the group just to the east of these two river valleys. In the southwestern sector is found Drummond Glacier. There are about a dozen glaciers in the headwaters of the Clearwater River, which range in area from 0.5 km^2 to 3 km^2 and which generally terminate at elevations between 2,450 and 2,550 m. The equilibrium line altitude (ELA) probably lies between 2,600 and 2,650 m asl. Average peak elevations rise to well over 3,000 m, with a maximum at 3,373 m. To the north, the glaciers flow into the Escarpment and Ram Rivers, the latter having as its source the glacier of the same name.

Drummond Glacier

About 8.5 km^2 in area and 3.5 km in length, Drummond Glacier flows from just over 3,000 m to 2,375 m; it is the largest glacier in the *Clearwater Groups*. It is part of a small ice field about 13 km^2 in area just west of Mount Drummond at the headwaters of the Red Deer River. Historical photographs taken in 1884, 1906, 1917–20, 1930, and 1939 and 1963, were used by Brunger and others (Brunger, 1966; Nelson and others, 1966; Brunger and others, 1967) to reconstruct its recession (fig. 9). The University of Calgary group also made measurements of ablation and surface movement from 1962 to 1965.

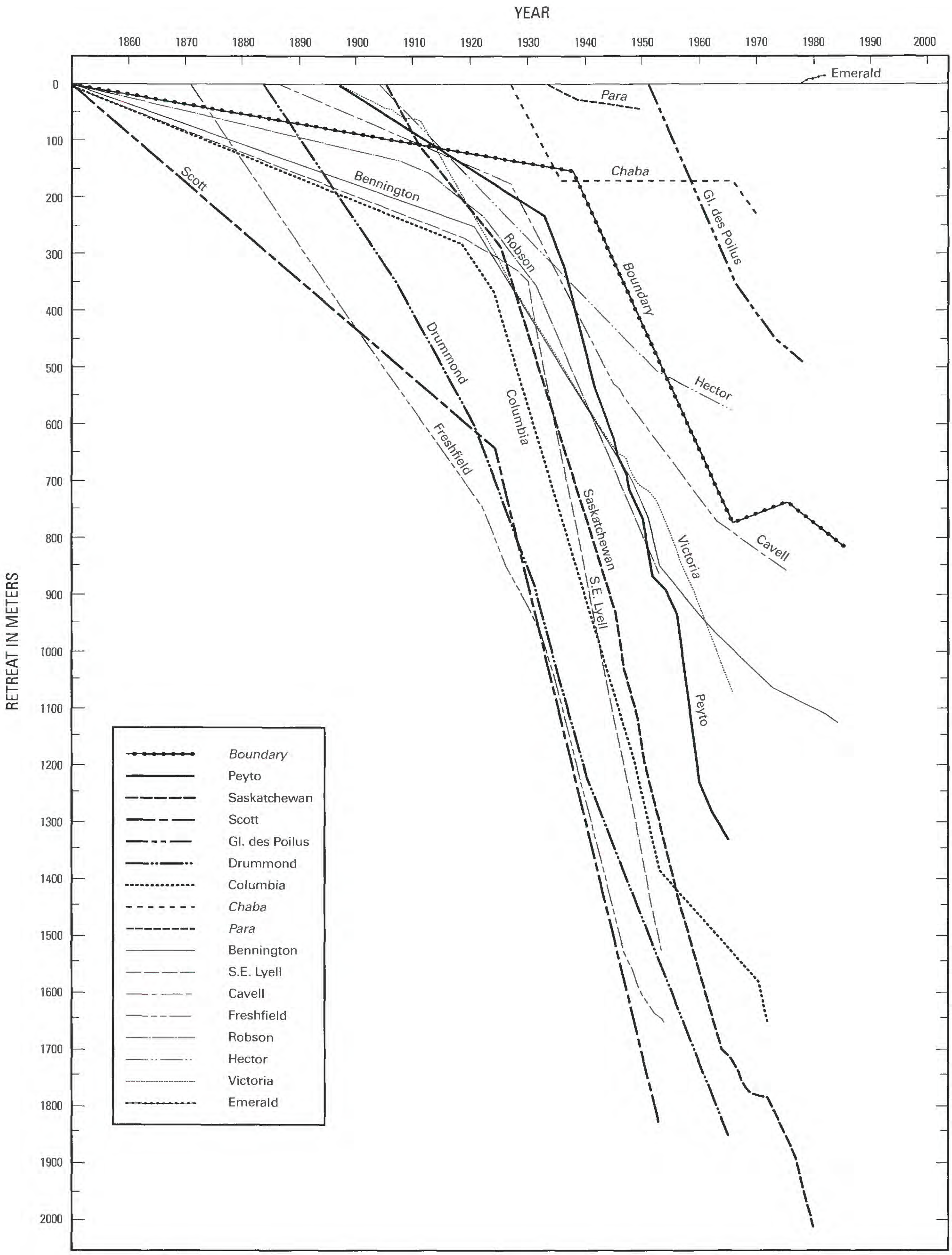

YEAR
1860
1870
1880
1890
1900
1910
1920
1930
1940
1950
1960
1970
1980
1990
2000
RETREAT IN METERS
0
100
200
300
400
500
600
700
800
900
1000
1100
1200
1300
1400
1500
1600
1700
1800
1900
2000
Emerald
Para
Chaba
Gl. des Poilus
Scott
Bennington
Robson
Boundary
Hector
Drummond
Columbia
Freshfield
Saskatchewan
S.E. Lyell
Victoria
Cavell
Peyto
Boundary
Peyto
Saskatchewan
Scott
Gl. des Poilus
Drummond
Columbia
Chaba
Para
Bennington
S.E. Lyell
Cavell
Freshfield
Robson
Hector
Victoria
Emerald

Ram River Glacier

The Ram River Glacier (fig. 10) was the most easterly, and hence most continental, of the five selected by the Canadian Government as representative glacier basins for the International Hydrological Decade (IHD) in an east-west transect of the cordillera. It was the smoothest, the smallest (1.89 km^2), the most compact, and, because of a mean elevation of 2,750 m, at the highest elevation of those studied. Possibly because of this, it is also the least dynamic. It lies in a cirque dominated by high, steep cliffs. A standard mass-balance measurement program was carried out here from 1965 to 1975, and the results (fig. 11) have been published (Young and Stanley, 1976a). A base map at a scale of 1:10,000 was published in 1967. The mean specific winter balance for the decade was 0.88 m water equivalent (w.e.), the annual balance was –0.43 m, and the mean equilibrium line was 2,838 m asl.

Palliser Range (FC4)

Surrounded by Lake Minnewanka and Cascade and Ghost Rivers, and south of Red Deer River, Palliser Range (fig. 1, FC4) is a westerly extension of the *Ghost River Area*. The maximum elevation in the range is 3,162 m at Mount Aylmer, with other peaks ranging from 2,900 to 3,100 m, which is

Figure 10.—*Photograph of the Ram River Glacier, Rocky Mountains, Alberta, Canada, in August 1973. Glacier 4*5DC–2, Glacier Atlas of Canada, Plate 7.4, North Saskatchewan River Glacier Inventory, Area 4*5D, Inland Waters Branch, Department of Energy, Mines and Resources, 1970, scale 1:500,000. Photograph by A.D. Stanley, National Hydrology Research Institute [NTS Map: 082N16].*

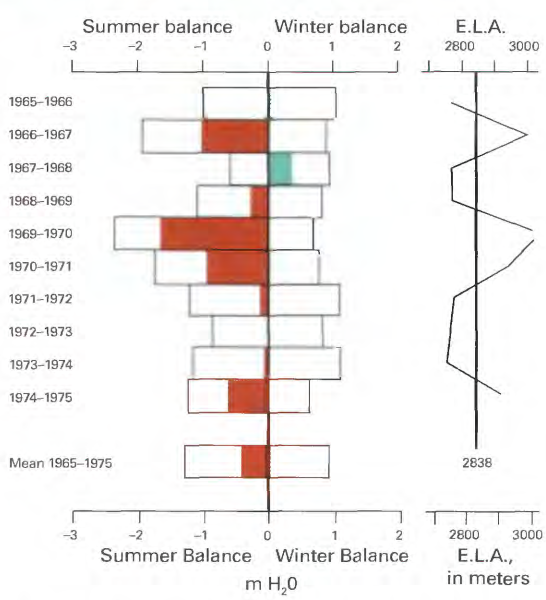

Figure 11.—*Mass-balance measurements of the Ram River Glacier, Rocky Mountains, Alberta, from 1965 to 1975 (from Young and Stanley, 1976a).*

roughly the elevation of the glaciation level. Three small glaciers have been identified in the central part of the range.

Bare Range (FC5)

Slightly lower in height, 2,750–2,950 m, the Bare Range (fig. 1, FC5) is a 20-km extension of the Palliser Range through which flows the Panther River. Because it is below the regional glaciation level, no glaciers have been observed here.

Vermilion Range (FC6)

The Vermilion Range (fig. 1, FC6) lies west of Cascade River; it is bounded to the south by Banff and to the north by the Red Deer River. Elevations through its 60-km extent are on the order of 2,850–2,950 m. Just south of Prow Mountain is a cluster of small glaciers along the headwaters of a tributary of Red Deer River.

Sawback Range (FC7)

Farther westward, the last major mountain block in this transect before reaching the *Park* or *Main Ranges*, is the Sawback Range (fig. 1, FC7). It adjoins the Vermilion Range on the east and has a sharp boundary on the west created by the Bow River valley, through which runs the Trans-Canada Highway. To the north it is limited by the Red Deer River valley. Elevations increase here above the regional glaciation level to more than 3,200 m in Mounts Douglas and St. Bride and in Bonnet Peak. Ice cover lies predominantly along the east side of the range in a series of almost continuous masses north of Bonnet Peak. The largest of these is Bonnet Glacier, 3.3 km long and about 6 km^2 in area with a snout at 2,560 m asl. Other glaciers from 0.5 to 1.2 km in length also terminate below 2,600 m asl.

Slate Range (FC8)

Bounded by Pipestone River and Baker Creek, the Slate Range (fig. 1, FC8) lies at the northwest corner of the Sawback Range. Peaks rise to slightly more than 3,000 m in elevation. The ice cover is concentrated in a small ice field around Mount Richardson. Glaciers range from 0.5 to 1.0 km in length, and their lower limits are from 2,410 to 2,570 m asl.

Murchison Group (FC9)

The *Murchison Group* (fig. 1, FC9) is more than 50 km long and generally 10 km wide, although becoming broader northward. It is bounded on the west by the broad valley of the Mistaya and Bow Rivers, on the east by the Siffleur and Pipestone Rivers, and in the north by the North Saskatchewan River trench. Many peaks rise to more than 3,000 m asl, and the range tends to climb northward to a maximum of 3,210 m in Mount Loudon, well above the regional glaciation level. About 20 glaciers are found here. They average just over 1 km in length, with termini at 2,500 m asl. The largest are the Hector and Molar Glaciers, 3.0 km and 2.0 km long, respectively. The ELA probably lies at about 2,750 m asl. This range includes the smallest named ice field in the Rocky Mountains, the *Murchison Icefield*, which is about 0.3 km^2 in area.

Hector Glacier

Hector Glacier lies in the southern part of the *Murchison Group*. It flows from Mount Hector, at about 3,350 m, northward for 3 km to 2,430 m asl. In the 1960's, this glacier was heavily crevassed and split into several tongues. Brunger (1966) and Brunger and others (1967) used historical photographs to reconstruct the recession of the western snout (fig. 9). In the late summer of 1938, a large ice mass separated from the glacier and fell into the Molar Creek valley, uprooting trees and destroying everything in its path. The glacier traveled more than 3 km and spread a broad carpet of ice over the valley up to 60-m-deep. Old-timers in the district reported no similar occurrence during the previous 40 years (B.C. Mountaineer, 1939). This represents the second major known glacier hazard in the Rocky Mountains, in addition to the repeated mudflows from the *Cathedral Glacier*, previously discussed.

Ram Range (FC10)

Guarding the southern side of the pass through the Front Ranges created by the valley of the North Saskatchewan River, Ram Range (fig. 1, FC10) is a small, L-shaped block on the northern end of the Clearwater Group. Elevations average about 2,500 m with a maximum of 2,844 m. A few tiny ice masses are found in sheltered north-facing valleys.

Cline Range (FC11)

Bounded by the North Saskatchewan River to the south and the Cline River to the north, *Cline Range* (fig. 1, FC11) contains numerous small cirque glaciers, generally less than 1 km^2 in area and terminating on average at about 2,400 m asl. The Wilson Icefield, 12 km^2 in area, which rises to 3,261 m on Mount Wilson, lies above the regional glaciation level at 3,000 to 3,100 m in elevation. It is located in the southwestern corner of the range and contains about a dozen outlet glaciers, which range in length from 2 to 4 km and have termini that flow down to 2,000 m. The highest peak is Mount Cline (3,361 m), with small glaciers on its north and south slopes. One of these was, for a short time, subject to some commercial exploitation as the Ice Age Company mined it for "pure" freshwater and "gourmet" ice for sale in Alberta (Brugman, 1989; Rains, 1990). An application to expand the operation led to an environmental impact assessment (Ice Age Co., 1989) and non-renewal of the mining licence. Although there are several other peaks with elevations of more than 3,000 m, average peak elevations are about 2,800 m.

Bighorn Range (FC12)

The Bighorn Range (fig. 1, FC12) is about 5 km broad at its widest part and 44 km long. It lies well outside the main body of the Rockies and could be considered part of the transition to the Rocky Mountain Foothills. It has no glaciers, and its peaks average less than 2,500 m in elevation.

First Range (FC13)

The next major mountain block in the Front Ranges is the First Range (fig. 1, FC13). The Brazeau River marks its northern boundary and the Cline River its southern one. The 40x25 km block is cut by Job and Coral Creeks, with the section to the west being known as the *Job Creek Peaks*. Peak elevations average between 2,750 and 2,900 m asl, rising to a maximum of 3,150 m. Detailed aerial photographic analysis in this area revealed more than 40 small glaciers in the western section, with a particularly heavy concentration at the head of Job Creek. About the same number have been plotted in the main First Range. Most lie in the headwaters of the Bighorn River and Littlehorn Creek and in the eastern basin of Job Creek. The glaciers are too small to see on Landsat images and are not shown on current topographic maps.

Cataract Group (FC14)

Nestled in behind *Job Creek Peaks*, and divided from the *Park Ranges* by the valley of the North Saskatchewan River, is the *Cataract Group* (fig. 1, FC14). Peak elevations here average more than 3,000 m and have a maximum in Mount Stewart (3,312 m). Increased elevation and proximity to the source of moisture mean that the area covered by glaciers is now a little denser. Almost 70 small glaciers can be found in this group, of which the Huntington (1.5 km^2) and Coleman Glaciers (2 km^2) are amongst the largest. The regional equilibrium line altitude is thought to lie at about 2,550 m asl. Large proglacial moraine areas and rock glaciers are common.

Le Grand Brazeau (FC15)

Stretching some 50 km from the Rocky Mountain Foothills to the *Park Ranges* is the mountain block referred to as Le Grand Brazeau (fig. 1, FC15), not be to be confused with the Brazeau Range, which is a small feature 75 km to the east in the Foothills. Officially the name is applied only to that part of the mountain block centered on Poboktan Mountain (3,323 m), but climbers have used the wider application. Peaks rise to more than 3,000 m asl with several reaching about 3,200 m. The regional glaciation level is at about 2,900 m. As in the mountain group to the south, glacier density increases westward, and there is a predominance of rock glaciers, debris-covered glaciers, and large expanses of proglacial moraine. West of Poboktan Mountain, the glaciers drain to the Arctic Ocean, and to the east they contribute to the Nelson River system that flows into Hudson Bay. Most of the 25 larger ice bodies terminate between 2,350 and 2,500 m asl. Their lengths range from 1 to 2.5 km, but some extend to 3.5 km, and one is 4.2 km long. *Cornucopia Glacier* is probably typical of those in the area; it is 2.5 km long and has a snout at 2,550 m asl. It forms part of *Brazeau Icefield*, which lies at the junction with the Queen Elizabeth Ranges and is the largest ice field in the Front Ranges, having an area of 40 km^2.

***Southesk Group* (FC16)**

North of Southesk River and south of Rocky River lies the 25- by 30-km-wide *Southesk Group* (fig. 1, FC16). There are a few tiny glaciers in the headwaters of Ruby and Thistle Creeks and the Cairn River. To the west, glaciers become larger, and three are more than 1 km in length, terminating at about 2,400 m asl. Peak elevations tend to lie below 3,000 m, although Mount Balinhard rises to 3,130 m and is the site of North Glacier.

Queen Elizabeth Ranges (FC17)

Extending northwestward from *Brazeau Icefield* for more than 50 km are the Queen Elizabeth Ranges (fig. 1, FC17). Whereas the largest ice-covered area is that around Mount Brazeau (3,470 m), others are found around Maligne Mountain (3,193 m) and Mount Unwin (3,268 m). Coleman (1903) visited the area in 1902 and described the ice field as rising into two white mounds to the south and sinking away to dirty surfaces of ice in the valleys to the east. All glacier tongues show signs of recession. Kearney (1981) dated the moraines here and in the vicinity of *Mary Vaux* and *Center Glaciers.* Peak elevations decline northward from more than 3,200 m to about 2,500 m. As a result, most of the glaciers are found around the upper part of Maligne Lake. Almost 20 glaciers average 1 to 2.54 km in length and have lower snout elevations of about 2,300 m asl. Coronet Glacier (3.5 km long), an outlier of *Brazeau Icefield*, is one of the largest, exceeded only by the 5-km-long glacier flowing north from Mount Brazeau.

Maligne Range (FC18)

Somewhat lower and lying between the Maligne and Athabasca Rivers, the Maligne Range (fig. 1, FC18) extends for more than 60 km in a northwestward orientation and marks the western limit of this section of the Front Ranges. Average peak elevations are about 2,600 m. About two dozen small cirque glaciers and ice aprons are located in sheltered north- and east-facing basins, the largest being those on the slopes of Mount Kerkeslin (2,956 m).

Nikanassin Range (FC19)

The ranges in the northern section of the central Front Ranges (FC) begin to decline in height and break up into a series of more isolated, parallel ridges in the region of the Nikanassin Range. Elevations in the Nikanassin Range (fig. 1, FC19) are less than 2,500 m and there are no glaciers.

Fiddle Range (FC20)

An extension northward of the Nikanassin Range, Fiddle Range (fig. 1, FC20) has an even lower elevation and likewise no glaciers.

Miette Range (FC21)

West of and parallel to the Fiddle and Nikanassin Ranges lies the Miette Range (fig. 1, FC21). It is slightly higher than these two ranges, rising to a maximum of 2,795 m asl. Some tiny permanent ice masses may exist in north-facing cirques, but all would be too small to be visible from space or to be shown on topographic maps.

Jacques Range (FC22)

To the west of the Miette Range lies the Jacques Range (fig. 1, FC22), which has an unnamed extension of the range to the southeast. Mountain elevations in the Jacques Range are comparable to those in Miette Range; it is unlikely that there are any glaciers here.

Colin Range (FC23)

The northwesternmost parallel range in this transect of the Front Ranges is the Colin Range (fig. 1, FC23). Mountain elevations here rise to 2,600 m asl. No glaciers are plotted on any of the topographic maps, and because the highest peaks lie below the regional glaciation level, it is not expected that any glaciers will be found here.

Park Ranges (Central) (PC)

The central section of the *Park*, or *Main*, *Ranges* (fig. 1, PC) consists of three more-or- less parallel sets of mountains between the valley of the Athabasca River on the east and the Rocky Mountain Trench on the west. The southern part of the central section (PC) is separated from the southern section (PS) by Kicking Horse Pass with the Canadian Pacific Railroad (CPR) and the Trans-Canada Highway. The northern limit of the central section is marked by Yellowhead Pass, which is the route of the Canadian National Railroad (CNR) from Edmonton to the west. This part of the *Park Ranges* contains the greatest concentration of glaciers in the Rocky Mountains, including all of the main ice fields (figs. 7, 8). Moving northward through the inner chain, one passes the Waputik Mountains, with the Wapta and Waputik Icefields; the Conway, Barnard Dent, and *Forbes Groups*, with the Freshfield Icefield, Campbell Icefield, and Lyell Icefield; the Columbia Icefield and the Winston Churchill Range, and thence through the *Fryatt*, *Cavell*, and *Portal-MacCarib Groups* to the Trident Range. The central chain includes the Van Horne Range, the *Chaba* and *Clemenceau Icefield Groups* with their extensive ice covers, and the *Whirlpool*, *Fraser-Rampart*, and *Meadow-Clairvaux Groups*. The westernmost chain is largely unnamed, apart from the large block of the Selwyn Range at the northern end. All are discussed below, with particular emphasis being given to the areal coverage of glacier ice and those glaciers that have been studied in the most detail.

Waputik Mountains (PC1)

Extending northward from Kicking Horse Pass is a triangular, elevated area of peaks and ridges bounded on the east by the Bow and Mistaya Rivers and the mass of the Front Ranges, and on the west by the valleys of the Amiskwi and Blaeberry Rivers. The Waputik Mountains (fig. 1, PC 1) contain the subsidiary President and Waputik Ranges as well as the two southernmost major ice fields of the Rockies, the Waputik and Wapta Icefields (figs. 7, 8). An inventory of the glaciers in this region was completed by Stanley (1970) as a pilot study for the world inventory of perennial snow and ice masses. He found more than 100 glaciers that covered an area of 146 km^2. They ranged in elevation from 2,100 to 3,200 m and had an average snowline in the vicinity of 2,400 m. The Waputik Range lies east of the Waputik Icefield (fig. 8) between Bow River and Bath Creek. It rises to about 2,750 m and contains one major ice mass from which drains the Waputik Glacier (3 km^2). Just west of the Yoho River is the President Range. Peaks here are on the order of 3,000 m asl, and a number of small glaciers are nestled around them, including the Emerald Glacier and the *President Glacier*. The Emerald Glacier is a small ice apron whose northern section is almost detached; it covers an area of only 0.6 km^2. Part of the tongue has a continuous supraglacier debris cover and part is relatively debris free. Batterson (1980), Rogerson and Batterson (1982), and Rogerson (1985) determined rates of advance for the push moraine of Emerald Glacier (fig. 9).

President Glacier flows from the north slope of The President toward Little Yoho River. Its present snout is at 2,353 m asl, but it formerly extended downslope an additional 2 km. The *President Glacier* had one advance about 1714 and a second about 1832 (Bray, 1964). In 1937, McCoubrey (1938) noted a marked shrinkage of ice (32–36 m) on the left side of the glacier as compared to the earlier survey by Roger Neave in 1933 (Wheeler, 1934). Later, Bray (1965) discussed the relationship between solar activity and glacier variation here.

Waputik Icefield

The main feature in the southern section of these mountains is the Waputik Icefield (figs. 7, 8, and 12). It is some 53 km^2 in area, straddles the Continental Divide between Mount Bosworth and Balfour Pass, and is the source of a number of quite large glaciers. The Waputik Icefield can easily be identified on Landsat images (fig. 7). Bath Glacier (4.3 km^2) has a large ice apron that extends 7 km southward from the slopes of Mount Daly and can be seen from the Trans-Canada Highway. Most of the ice field drains westward through Daly Glacier (13.7 km^2 in area) with much of the remainder flowing northward in Balfour Glacier (5.9 km^2 in area). Glaciers terminate at about 2,100 m, and the equilibrium line altitude lies close to 2,450 m asl.

Balfour Glacier

At the time of the initial photographs by Wilcox (1900), Balfour Glacier (fig. 13) was a compound valley glacier draining about 14 km^2 of the northeast sector of the Waputik Icefield (figs. 7, 8). The glacier is now about half that size (8.8 km^2). Its main stream is a northwesterly flowing mass that no longer coalesces with the glaciers draining the ice aprons north and east of Mount Balfour. McFarlane (1945) did not include this glacier in the Dominion Water and Power Bureau (DWPB) network because of the high cost of visiting it.

Studies of proglacial Hector Lake established a chronology of proglacial-lake sedimentation back to 1700 (Smith, 1978; Leonard, 1981, 1985; Smith and others, 1982). Most sediment in the lake is provided by nival and glacial meltwater from Balfour Creek. Sediment input varies with inflow discharge and is controlled mainly by melting rates (Smith, 1978).

Leonard (1986a, b) documented the changing glacial outwash sedimentation and glacial activity over a period of about 1,000 years. He concluded that the very regular rhythmic laminations were indeed true varves and could be correlated with the climate record from Lake Louise. Multiple cores were used to assess lake-wide sedimentation characteristics likely related to changes in total sediment input. The maximum ice stand occurred about 1847. Recession rates averaged about 10 m a^{-1} from the late 1840's to 1900 and then increased fourfold from 1900 to 1948. Since 1948, recession has been almost negligible. The major moraine-building episodes of 1700–1720 and 1840–1860 were periods of persistent high sedimentation

Figure 12.—*High-angle oblique aerial photograph of the 53 km^2 Waputik Icefield looking northwest. The ice field straddles the Continental Divide and is the source of a number of large outlet glaciers. University of Washington photograph F2116, taken 7 August 1961 by Austin Post, U.S. Geological Survey, is courtesy of Robert M. Krimmel, USGS.*

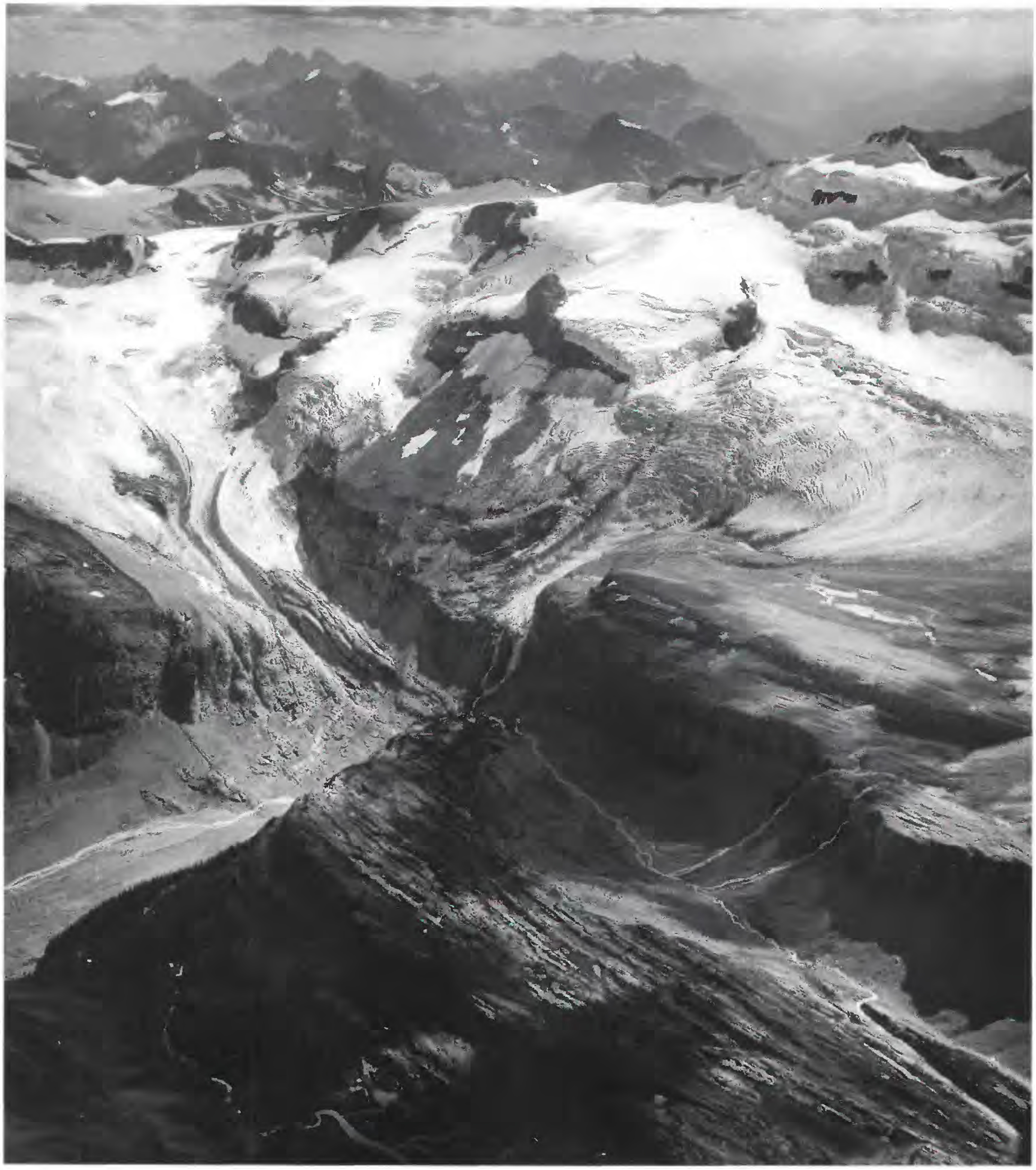

Figure 13.—*High-angle oblique aerial photograph of the Balfour Glacier, a major northward flowing outlet glacier on the Alberta side of the Waputik Icefield. The glacier drains east into Hector Lake and the Bow River to the left of the photograph. Glacier *4*5BAA–63, 64, 65, Glacier Atlas of Canada, Plate 7.3, Red Deer River, Inland Waters Branch, Department of Energy, Mines and Resources, 1970, scale 1:500,000. University of Washington photograph F2113, taken 7 August 1961 by Austin Post, U.S. Geological Survey, is courtesy of Robert M. Krimmel, USGS.*

rates as was that of the very rapid ice recession period, 1910–1945. The two earlier periods were probably because of high glacial erosion rates and the later period almost certainly due to high sediment availability.

Wapta Icefield

Wapta Icefield (fig.8) lies northwest of the Waputik Icefield; it is about 80 km^2 in area and has been one of the focal points of glaciological research in the Rocky Mountains. It is drained on the Alberta side by the Vulture (4.9 km^2 in area), Bow (5.1 km^2 in area) and Peyto (12.6 km^2 in area) Glaciers and, on the British Columbia side, by the Yoho (20.9 km^2 in area) and Ayesha (3.2 km^2 in area) Glaciers, as well as by the Glacier des Poilus (12.8 km^2 in area). The Glacier des Poilus is the southwestern extension of the Wapta Icefield and occupies two large basins. It flows from almost 3,000 m down to 2,240 m and has an equilibrium line altitude at about 2,450 m asl. Bigras (1978) reported on the sediment transport, discharge, volumetric change, and geomorphology of this glacier. He concluded that it had lost 4.5×10^6 m^3 of ice during the last century. Average recession since 1951 is shown in figure 9.

Crowfoot Glacier (1.5 km^2 in area), part of a separate outlier glacier (5 km^2 in area) which lies east of the Wapta Icefield (figs. 7, 8), is frequently photographed by motorists traveling on what Parks Canada now refers to as the Icefields Parkway. Leonard (1981) investigated lichen growth curves here and found them to be 35 percent lower than those reported by Luckman (1977), thus casting doubt on some regional growth curves. Elevations of mountain peaks rise to more than 3,100 m, and the regional ELA lies at about 2,440 m. Northward, the range narrows. There are significant ice accumulations around Mistaya Mountain, namely, the Delta (2.2 km^2 in area), Barbette (4.5 km^2 in area) and Parapet (1.1 km^2 in area) Glaciers, and also around Mount Sarbach (1.5 km^2 in area). Howse Peak (3,289 m), the highest in these mountains, is located in this part of the *Park Ranges* (Central).

Bow Glacier

Bow Glacier (fig. 14) flows northeast for 3 km from the Wapta Icefield (figs. 7, 8) and begins to descend steeply from about 2,600 m asl. Its terminus rests at just over 2,300 m asl, about 200 m above the recent maximum position. The lower part of the glacier is quite heavily crevassed where the ice flows out of the ice field over a series of ridges. The popular Num-Ti-Jah Lodge, just off the Icefields Parkway, affords an excellent view of the glacier across Bow Lake.

The glacier was first visited in 1897 (Stutfield and Collie, 1903) when the ice extended below the base of the main cliff. The terminus remained there until 1922 before retreating above the base of the cliff by 1933 (Wheeler, 1934). Further retreat from the 1933 position appears to have been comparatively minor. The glacier was photographed in 1945 by the DWPB but not investigated further, as it was then hanging over the cliff (McFarlane, 1945). Heusser (1956) concluded that the glacier retreated 1,100 m from 1850 to 1953. Aerial photographs taken in 1952 show a narrow lake developing between the glacier and cliff edge. By 1966, only a quarter of the

Figure 14.—*Photograph of the terminus of the Bow Glacier, Rocky Mountains, Alberta, Canada, in September 1973, showing its snowline. Photograph by C. Simon L. Ommanney, National Hydrology Research Institute [NTS Map: 082N10]. (Glacier 4*5BAA–78, Glacier Atlas of Canada, Plate 7.3, Red Deer River, Glacier Inventory, Area 4*5, Inland Waters Branch, Department of Energy, Mines and Resources, 1970, scale 1:500,000).*

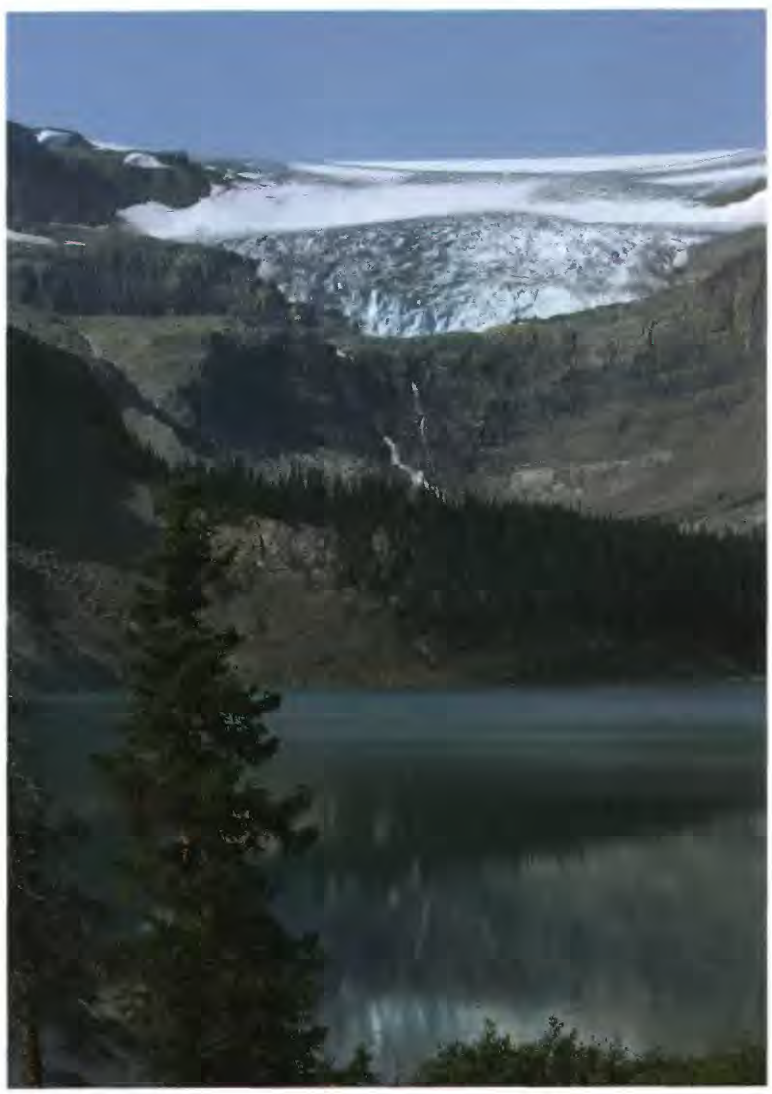

present-day lake was visible, and by the 1980's, the entire lake could be seen and the glacier tongue was a few meters above it (Smith, 1981).

A number of studies have been carried out on sedimentation in Bow Lake and the reduction in sediment input caused by the development of the proglacial pond (Kennedy, 1975; Leonard, 1981, 1985; Smith, 1981; Smith and Syvitski, 1982; Smith and others, 1982). Leonard (1981, 1985) was able to explain up to 70 percent of the sedimentation rate variance when he compared the Bow Lake varve record to the ablation-season temperature record from Lake Louise. The sediment load carried by the stream flowing from the glacier was substantial enough to create a large delta at the western end of Bow Lake. Church and Gilbert (1975) have looked at the long profile and mean clast size of the outwash fan. In 1997 a group from the University of Alberta installed an automatic weather station at Bow Glacier and commenced a continuing study of sedimentation and runoff chemistry (M.J. Sharp, oral commun., 2000).

Peyto Glacier

The first records of Peyto Glacier (fig. 15) were photographs taken by Wilcox in 1896 and by Thorington in 1923. Recession since 1923 was recorded by Thorington, Kingman, Dickson, and Vanderburg in 1933 (Wheeler, 1934) and again by Kingman in 1936 (McCoubrey, 1938). In 1945, it was selected as a representative glacier by the DWPB, and for the next 17 years the position of the snout, changes in the areal extent of Peyto Glacier, and ice velocities were measured (fig. 9). The glacier gradually retreated into a narrow gorge, which made it less representative. After 1962, the survey was terminated. Detailed reports, prepared by the DWPB as internal documents, were summarized by Ommanney (1972b), and some results have been published (McFarlane, 1946a; Meek, 1948b; McFarlane and others, 1950; Collier, 1958).

Heusser (1954, 1956) used photographic and botanical techniques to reconstruct the recent history of Peyto Glacier. The recessional moraine was dated to 1863 and four other moraines were identified. Retreat from 1865 to 1953 was determined to be about 1,009 m. Brunger and others (1967) concluded that an ecesis interval (colonization of flora and fauna in deglacierized terrain) of 25 years was more appropriate than the 12-year interval used by Heusser. They found glacier response lagged climate by about 15 years, close to the 20-year lag estimated by Collier (1958).

In 1965, Peyto Glacier was selected as one of the representative International Hydrological Decade (IHD) glacier basins in the Rocky Mountains by

Figure 15.—*Photograph of the Peyto Glacier, Rocky Mountains, Alberta, Canada, in July 1967. A prominent, sharp-crested lateral moraine can be seen on the right valley wall grading into a less prominent terminal moraine, evidence of significant thinning and retreat of the Peyto Glacier. Photograph by C. Simon L. Ommanney, National Hydrology Research Institute [NTS Map: 082N10]. (Glacier 4*5DB–32, Glacier Atlas of Canada, Plate 7.4, North Saskatchewan River. Glacier Inventory, Area 4*5D, Inland Waters Branch, Department of Energy, Mines and Resources, 1970, scale 1:500,000.)*

the Canadian Government. The 13.4 km^2 glacier originates at an elevation of 3,185 m asl; its tongue is at about 2,100 m asl, and the mean elevation is 2,635 m. The measurement program was described by Østrem and Stanley (1969). Young (1976) modified this methodology and proposed a grid square technique to produce accumulation, ablation, and mass-balance maps using associations between snow depth and terrain geometry (for example, surface slope, azimuth, and local relief). The technique could be used to assess the recurrence patterns of accumulation, bias in sampling networks, effects of different sized sampling networks, progress of melt throughout an ablation season, as well as being able to extrapolate to unvisited parts of the glacier (Young, 1974a). The assumption of a linear function for snow accumulation produced results that seemed realistic but were substantially different from those derived from the normal stake network (Young, 1974b).

A report on the glaciological, hydrological, and meteorological data collected for the IHD program (1965 to 1974) has been published (Young and Stanley, 1976b). A plot of the mass balance, including more recent data (Mokievsky-Zubok and others, 1985; IAHS/UNEP/UNESCO, 1988, 1993, 1999; IAHS/UNESCO, 1998) is given in figure 16. Young (1977a, 1981) found that the same annual balance was produced by different combinations of winter accumulation and summer ablation; the patterns did not necessarily repeat themselves. Fluctuations in meltwater discharge over a few days closely parallel the air-temperature curve, that from Lake Louise being a better predictor than the Peyto Glacier station. The elevation of the transient snowline was a good indicator of the health of the glacier. Letréguilly (1988) found mass balance to be almost entirely related to summer temperature. The correlation was best with data from the meteorological station in Jasper, some 200 km away, rather than with the closest station at Lake Louise. This is in line with Tangborn's conclusion (1980) that mass balance here was likely most dependent on summer ablation. Letréguilly also found that the correlation coefficients of meteorological data with the ELA were as good or better than with the mass balance. Yarnal (1984) demonstrated that the mass balance of Peyto Glacier is also related to the 500-mbar patterns. Synoptic atmospheric pressure patterns having cyclonic circulation favor glacier accumulation, whereas anticyclonic types inhibit the buildup of the regional snowpack. Ablation is suppressed by synoptic patterns associated with cloudy days and (or) low temperatures and is enhanced by patterns associated with warm sunny days. Peyto Glacier accumulation appears to be associated with the large-scale patterns. According to Xie and Zhang (1986), the glacier has a reasonably stable regime with a coefficient of glacial stability of 0.33. Others, in analyzing global mass-balance data, which include those from Peyto Glacier, have concluded that representative mass-balance values might be obtained from observations at the ELA (Ohmura and others, 1986), at the weighted mean altitude (Valdeyev, 1986), or another single point (Konovalov, 1987). Attempts to develop appropriate indices for these and other glacier characteristics, using data from Peyto Glacier, are continuing (Bahr and Dyurgerov, 1999; Dyurgerov and Bahr, 1999).

The glacier's accessibility, only a 2- to 3-hour walk from Peyto Lookout off the Trans-Canada Highway, and the availability of semipermanent facilities soon led to the development of many other complementary studies, often in collaboration with Canadian and other universities.

A map of the glacier, at a scale of 1:10,000 with 10-m contours, was prepared as a base for glaciological research. A nine-color edition using a French bedrock-portrayal technique was published in 1970 (Sedgwick and Henoch, 1975), followed in 1975 by a Swiss-style eight-color map; bedrock portrayal and shaded relief added a three-dimensional effect (Henoch and Croizet, 1976).

A subsequent experiment produced an orthophotograph, stereomate, digital-terrain model, and contour map of part of the glacier (Young and Arnold, 1977). There was good agreement in the ablation area with elevations of the existing map (<1 m) but large discrepancies in the freshly snow-covered accumulation area. The accumulation area had thinned by about 20 m since 1966–76.

Holdsworth and others (1983) and Goodman (1970), using a radio-echo-sounder, measured depths of 40–192 m in the ablation area and 120–150 m in the accumulation area, indicating that the 1967 seismic survey by Hobson and Jobin (1975) was seriously in error, and the volume of 532×10^6 m^3 of water equivalent was wrong by at least a factor of 2–3.

Power and Young (1979a, b), using a modified University of British Columbia (UBC) model, compared simulated discharge for 1967–74 to that

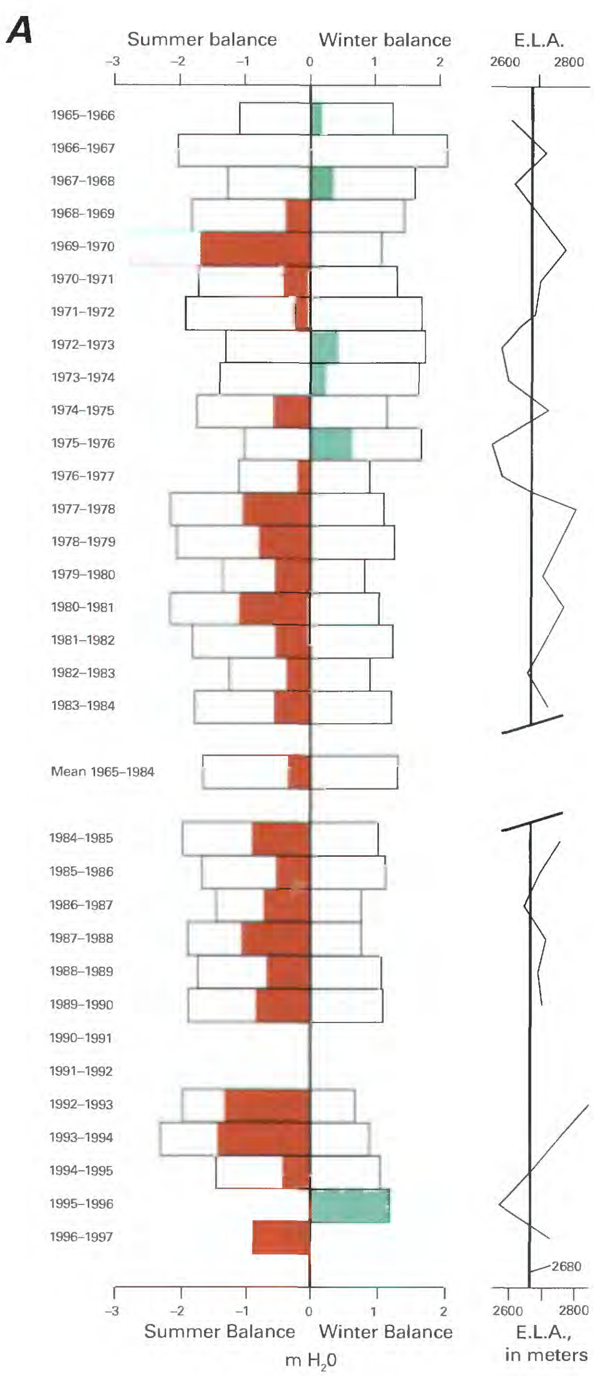

***Figure 16.*—A**, *Mass-balance measurements of the Peyto Glacier, Rocky Mountains, Alberta from 1965 to 1997 (from Mokievsky-Zubok and others, 1985; IAHS/UNEP/UNESCO, 1988, 1993, 1999; IAHS/UNESCO, 1998, and Demuth (written commun., 2001);* **B**, *Cumulative specific net balance of Peyto Glacier from 1965 to 1997 (IASH/UNEP/UNESCO, 1999). Asterisk indicates absence of measurements in mass-balance series.*

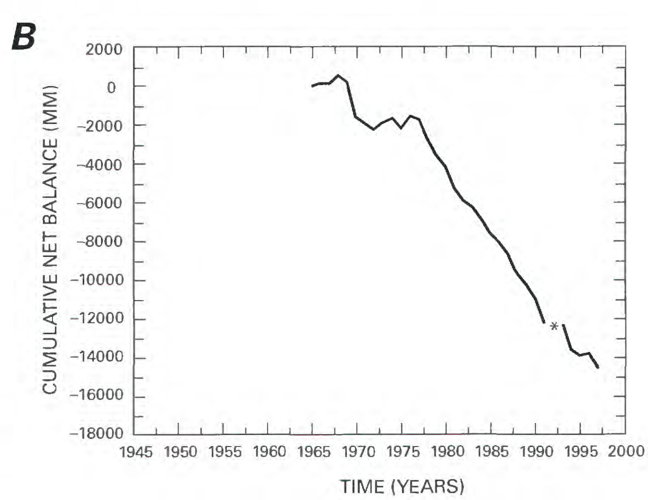

predicted using algorithms derived from mean daily temperature and then extended the results using a lapse rate of $0.65°C^{-100m}$ with an arbitrary reduction of 15 percent melt applied to the accumulation area (Young, 1980). The model simulates snowmelt and icemelt processes reasonably well. The results confirm that the Peyto Glacier tends to compensate for changes in snowmelt runoff; for example, lower winter snowpacks produce high glacier-melt runoff. The response time of the basin and its various flow components is closely linked to the progression of the snowline upglacier, although summer hydrographs can vary markedly over the seasons. The difference between the calculated and measured discharge over an 8-year period averaged 5×10^6 m^3, which could be accounted for by an average evaporation over the basin of 200 mm a^{-1} (Young, 1982). Gottlieb (1980) obtained reasonably good overall agreement using a degree-day approach and simplified water routing procedures, but his model did not seem to be able to predict peak flows.

Derikx (1973) considered a glacier analogous to a ground-water system and developed a black-box model to predict meltwater runoff in response to meteorological data. Although a linearized equation with simple boundary conditions is a very crude approximation of reality, the results showed a fair correspondence between the calculated and measured meltwater discharge. Derikx and Loijens (1971) refined the model by adding inputs distributed by different elevation bands and by separating the four hydrological components (exposed ice, snow-covered ice, firn, and rock). Daily discharge calculated by the model was 21 percent higher or lower than the measured value. In the warm, dry period of 2–27 August 1967, when the snowcover had been removed, Peyto Glacier contributed 40 percent of the Mistaya River streamflow. Applied to the other glaciers in the basin, this means glacier-melt contribution in August can reach 80 percent. Loijens (1974) observed that 46 percent of the annual flow in the river in 1967 occurred in a 7-week period and that 70 percent of this was supplied by glacier runoff and 31 percent by glacier icemelt. Average ice ablation contributed 15 percent to annual streamflow. Young (1977b) reported that 4 years of negative balance contributed some 37×10^6 m^3 of water from storage, or 20 percent of total streamflow, and 4 positive years retained 13.8×10^6 m^3. Hence he proposed a revision in the contribution to annual flow in the North Saskatchewan River at Saskatchewan River Crossing caused by the 1948–66 reduction in glacier volume. He suggested 8–10 percent compared to Henoch's (1971) original estimate of 4 percent.

Prantl and Loijens (1977) and Collins and Young (1979, 1981) used hydrochemical characteristics to separate the various flow components and to study their temporal variation. Conductivity falls rapidly as dilute meltwater arrives at the gauge and rises steadily as chemically enriched meltwater routed more slowly through basal tunnels, cavities, and subglacier moraines reaches the portal.

Johnson and Power (1985, 1986) reported on a high-magnitude catastrophic event that substantially modified the proglacial area of Peyto Glacier. A major storm led to the overtopping of a drainage tunnel and the collapse of a large section of ice-cored moraine. The downstream area was subjected to alternate damming, flooding, and draining. Flood waves up to 26 m^3 s^{-1} deposited an estimated 6,000 m^3 of gravel in the valley, destroying the gauging facility. Other major flooding episodes occurred in 1984, again in association with extreme rainfall events.

Goodison (1972a) derived a snowmelt-rainfall recession curve and found that any particular day's rainfall takes about 5 days to pass through a completely snow-covered basin. The response time shortens as the season progresses. Regression models developed using 1968 data accounted for 82.4 percent of the discharge variation in the 1969 hydrograph and provided a particulary good fit to the June–July runoff. Another study found no statistically meaningful relationship between global radiation and ablation (Goodison, 1972b). Østrem (1973a) came to a similar conclusion in the course of developing an operational model based on temperature, wind, and precipitation. Daily computed runoff values were within about 21 percent of the observed values. The negative correlation between glacier discharge and radiation has been observed for other glaciers where liquid precipitation, usually associated with low incoming short-wave radiation, is a dominating influence on glacier runoff. However, Munro (1975) found that short-term variations in the meltwater hydrograph were closely controlled by the net radiative flux; the sensible heat flux was also an important energy source. Munro and Young (1982) concluded that net shortwave radiation was the prime determinant of meltwater discharge. Estimates were a fair approximation of energy equivalents of ablation derived from stake measurements. An unexpectedly thin boundary layer, about 1 m deep, was attributed to katabatic control of flow (Munro and Davies, 1976). Such a finding has implications for the long-term effectiveness of the turbulent-transfer approach (Munro and Davies, 1977). Another factor in the long-term suitability of turbulent transfer theory for glacier-melt prediction is the finding by Stenning and others (1981) that katabatic layer development and characteristics are also subject to synoptic-scale influences.

Föhn (1973) found fair agreement between energy- and mass-balance results. About 20 percent of daily snowmelt takes place internally as a result of the penetration of solar radiation. At the base of the snowpack, the water table fluctuated 10–50 mm throughout the first 9 days under conditions of continuous snowcover. At some times, lateral inflow of water made up for actual mass loss at the upper end of the snowpack.

By studying the weathering surface in a 5,320-m^2 ablation-area site, Derikx (1975) concluded that the hydrological response time was extremely short and closely followed melt calculated from the hourly energy balance. Any delay seemed to be mainly the result of the channel network. Dye-tracer tests by Collins (1982) gave average flow-through velocities of 0.13–0.35 m s^{-1}, with delays of up to 5 h at low flows and under 2 h during times of peak surface ablation, thus showing a strong dependence on discharge.

The glacier has fairly extensive ice-cored moraines. A simple model suggested that their ablation could be estimated from meteorological variables, if the surface temperature of the debris layer were available (Nakawo and Young, 1982).

Krouse (1974) demonstrated that the isotopic record retains characteristics of the winter precipitation record, but he and West (1972) have both attributed some of the large isotope fluctuations to wind drainage on the glacier and to the topographic shape of the ice surface (Krouse and others, 1977). This conclusion was supported by Foessel (1974), who found "cool-air pooling" in the ablation area in response to dish-shaped terrain, and who developed an equation that proved very reliable in predicting daily mean temperatures at any elevation in the basin. He also found that seasonal temperature trends behaved in a cyclic manner in response to migration of synoptic weather systems over western Canada (in line with the findings of Yarnal (1984) in relation to mass balance).

The suspended sediment regime is very irregular seasonally and diurnally; pulses of sediment occur independently of discharge variations. Sediment concentrations averaged about 660 mg l^{-1} and ranged from 19 to 3,379 mg l^{-1}, with one extreme event at 14,000 mg l^{-1}. The total suspended sediment output in 1981 was in excess of 68,000 tonnes. Subglacier reorganization of outflow streams that change sediment availability seemed to be the main factor influencing sediment output (Binda and others, 1985). Downstream in the drainage basin of the Peyto Glacier, Smith and others (1982) estimated that over a 75-day measurement period in 1976 some

40×10^3 tonnes of material was transported to and deposited in Peyto Lake. In 1996, a special session of the annual Canadian Geophysical Union scientific meeting in Banff, Alberta, was devoted to past and present work on Peyto Glacier. Papers from this session will be published by the National Water Research Institute in its science report series (M.N. Demuth, oral commun., 2000).

Yoho Glacier

Yoho Glacier is the largest southern outflow from the Wapta Icefield (figs. 7, 8). It flows 7 km from the center of the ice field at 3,125 m asl to a terminus at 2,150 m asl. The ELA on the glacier surface lies at about 2,450 m. The first description of Yoho Glacier was published by Habel (1898) when the ice was close to its maximum (Bray and Struik, 1963). At that time the Yoho Glacier had a magnificent ice fall that attracted visitors for many years. Subsequently, studies were conducted by W.H. Sherzer of the Smithsonian Institution (Sherzer, 1907, 1908), and the Yoho Glacier was included in a set of observations undertaken by the Vaux family (Vaux, G., Jr., and Vaux, W.S., 1907a, b, 1908; Vaux, G., 1910; Vaux, M.M. and Vaux, G., Jr., 1911; Vaux, M.M., 1911, 1913). These studies were extended by A.O. Wheeler and members of the Alpine Club of Canada (ACC), which held a number of field camps in that valley (Wheeler, 1907, 1908, 1909, 1910, 1911, 1913, 1915a, 1917, 1920a, b, 1932, 1934). The Yoho Glacier was inspected in 1945 by the DWPB, but by then had retreated up the valley and was a hanging glacier unsuitable for recording purposes (McFarlane, 1945, Meek, 1948a, b). Heusser (1956) concluded that a series of recessional moraines had formed in about 1865, 1880, and 1884. Parks Canada became interested in the hydrology of Yoho National Park, and an attempt was made to extend the record of glacier recession (Kodybka, 1982). For a short time, the National Hydrology Research Institute extended their Peyto Glacier program to include observations on the glaciers and streams around the Yoho Glacier. No report of that work has been published.

Van Horne Range (PC2)

Between the Amiskwi River and the Rocky Mountain Trench and south of Blaeberry River lies the Van Horne Range (fig. 1, PC2). Maximum elevations here are less than 2,900 m asl, which is the height of the regional glaciation level. Some of the deep, north- and east-facing cirques may contain small glaciers, but none is shown on the topographic maps. The range consists of a number of northwest- and southeast-trending ridges.

Conway Group (PC3)

The Conway, Mummery, and Barnard Dent Groups all form part of the same range that lies west of the Blaeberry River and is centered on the Freshfield Icefield (figs. 7, 8). The Conway Group (fig. 1, PC3) is the easternmost of the three groups. Many peaks rise above 3,000 m, reaching a maximum elevation of 3,260 m asl at Solitaire Mountain. The ice-covered area of more than 20 km^2 contains several glaciers, of which the most notable are the Cairnes, Lambe, and Conway Glaciers, which range in length from 4 to 5 km with ELA's at about 2,400 m.

Mummery Group (PC4)

Southwest of the Conway Group, running parallel to and north of the Blaeberry River, is the Mummery Group (fig. 1, PC4). Elevations trend southwesterly from above 3,000 m at the apex of the Freshfield Icefield (fig. 8) downward to the 2,500-m range near the Rocky Mountain Trench. The main glaciological feature is Mummery Glacier, a southward-flowing extension of Freshfield Icefield. This 7-km-long glacier is joined near its tongue by a large glacier flowing eastward from Mount Mummery (3,320 m). Its ELA is about 2,450 m asl.

Barnard Dent Group (PC5)

The Barnard Dent Group (fig. 1, PC5) contains three major ice masses, including the bulk of the 78-km^2 Freshfield Icefield (fig. 8). This ice field is situated in a northeasterly basin that flows into Howse River through a magnificent valley glacier. The Campbell Icefield (13 km^2) lies to the west of the Continental Divide. A significant ice accumulation is also on Mount Alan Campbell. Summit elevations generally exceed 3,000 m, with the highest being that of Mount Freshfield (3,325 m). Apart from the Freshfield (11 km), Campbell (5.5 km), Pangman (4.2 km), and Niverville (2.5 km) Glaciers, most are 1 to 2 km long and terminate between 2,200 and 2,400 m. Waitabit Glacier, just to the south of the Freshfield Icefield, has been reduced to three small, disconnected ice masses that total slightly more than 1 km^2.

Freshfield Glacier

Field (1979) provided a comprehensive and illustrated report on Freshfield Glacier (figs. 7, 8, and 17) following the American Geographical Society (AGS) expedition there in 1953, and Ommanney (1984) has compiled a list of publications about work on Freshfield Glacier. The Freshfield Glacier was determined to be slightly over 14 km long when mapped by the Interprovincial Boundary Survey in 1917 (Interprovincial Boundary Commission, 1924). According to Heusser (1956), the glacier began to retreat in 1871. Short readvances took place in 1881 and 1905 (Heusser, 1956); in

*__Figure 17.__—High-angle oblique aerial photograph of Freshfield Glacier, a major northeastward flowing outlet glacier of the 78 km^2 Freshfield Icefield. According to Heusser (1956), the glacier began to retreat in 1871. It was more than 14 km long in 1917 when mapped by the Interprovincial Boundary Survey. Most recently it has been mapped as 11 km long. A series of ogives can be seen on the tongue of the glacier that has been created as the slope of the glacier increases down glacier. Glacier 4*5DAC–22, Glacier Atlas of Canada, Plate 7.4, North Saskatchewan Glacier Inventory, Area 4*5D, Inland Waters Branch, Department of Energy, Mines and Resources, 1970, scale 1:500,000. Photograph F642–89, taken 21 August 1964 by Austin Post, U.S. Geological Survey, is courtesy of Robert M. Krimmel, USGS.*

1897, Collie (1899) reported on a small push moraine formed in that year. For most of the 20th century, retreat has been continuous and rapid, with a total recession of 1,640 m (fig. 9). The Freshfield Glacier was discovered by Hector (1861) in 1859, a time when the snout was within 100 m of the ancient terminal moraine. The Freshfield Glacier had a row of angular blocks running down the center of the ice stream. One of the largest boulders was used by all the early observers as a common reference point, thus minimizing errors (McFarlane, 1947). The glacier was observed by Stutfield and Collie (1903) in 1897 and 1902, by Hickson (1915) in 1913, by Palmer (1924a, b) in 1922, and by Thorington (1927, 1932, 1938, 1945) in 1926, 1930, 1934, 1937 and 1944.

The long historical record was one reason why the DWPB selected Freshfield Glacier for their studies of the water resources of mountainous rivers in 1945. The position of the snout and changes in its areal extent were measured, and a set of plaques was placed on the ice surface to measure velocity. The survey was abandoned after 1954 due to the expense, including logistics of accessing the glacier. Detailed reports were prepared by the DWPB as internal documents, but some results were published (McFarlane, 1947; McFarlane and May, 1948; Meek, 1948a, b; McFarlane and others, 1949, 1950; May and others, 1950; Carter, 1954). The AGS expedition used photographic and botanical techniques (Field and Heusser, 1954; Heusser, 1954; 1956) to identify glacier limits and variations. Some subsequent visits were made by the ACC (Gray, 1962) but little new scientific information was added. In 1922, Palmer (1924a) estimated the firn line at 2,400 m; today it is closer to 2,600 m. Because the ice field has a low gradient, any change of the firn limit will have far-reaching effects on the glacier's mass balance.

Waitabit Ridge (PC6)

Nestled in between the Mummery and Barnard Dent Groups is *Waitabit Ridge* (fig. 1, PC6). The maximum elevation is in the center of the Ridge in Robinson Peaks (2,925 m), but the average tends to be on the order of 2,600 m. Only one glacier is visible, a 1.5-km-long ice body flowing to the northwest in the section adjoining the Campbell Icefield.

Blackwater Range (PC7)

In the Blackwater Range (fig. 1, PC7), the elevations are lower than those of *Waitabit Ridge*, but there is a small glacier (<1 km^2) in a south-facing cirque between Felucca and Blackwater (2,732 m) Mountains. The range runs parallel to the Rocky Mountain Trench, with one spur pointing eastward along Bluewater Creek. Northward is a small, unnamed range, running from Frigate Mount to the large artificial water body of Bush Arm. It rises to 2,800 m and has two small glaciers.

Forbes Group (PC8)

North and west of Forbes Creek and Howse River lies the *Forbes Group* (fig. 1, PC8), centered on the 3,612-m peak of that name. Elevations in the *Forbes Group* exceed 3,000 m, and several are greater than 3,200 m. The area is heavily glacierized and forms part of the Mons Icefield (<30 km^2), which spreads out along the range between Mount Outram and Mons Peak. Much of the ice drains through Mons Glacier, which was joined with neighboring Southeast Lyell Glacier in 1902 (Outram,1905). In 1918, the two glaciers were 300 m apart. Between 1918 and 1953, Mons Glacier receded 1,100 m horizontally and 350 m vertically (Field, 1979). Part of the ice field drains westward from the Continental Divide. Several glaciers, including the East, West, and Sir James Glaciers, are on the order of 3 km long. Termini generally lie between 2,300 and 2,500 m asl, though the ice field ELA is thought to be about 2,450 m.

Lyell Group (PC9)

The *Lyell Group* (fig. 1, PC9) consists of two ranges separated by the valleys of Lyell and Arctomys Creeks. In the southern part of the *Lyell Group* glaciers are scattered in cirques along the ridge that runs from Mount Erasmus (3,265 m) up to the main body of Lyell Icefield (fig. 8). To the west, this ridge trends to the southwest and Rostrum Peak (3,322 m), along which there are numerous glaciers, 1- to 2-km long, in southeast-facing cirques. The focal point here is Lyell Icefield itself, with its outlet glaciers—East, Southwest, and Southeast Lyell Glaciers, that cover an area of about 50 km^2. The bulk of the ice field spreads southward from Mount Lyell (3,500 m) before flowing east and west from the Continental Divide and pushing tongues of ice well below 2,000 m. The ELA is probably about 2,500 m asl.

Southeast Lyell Glacier

The Southeast Lyell Glacier (fig. 18) flows eastward from Lyell Icefield (figs. 7, 8). The accumulation area of the Southeast Lyell Glacier extends along the provincial boundary some 9 km between Mount Lyell and Division Mountain at elevations ranging from 2,440 to 3,050 m. As recently as 1902, the Southeast Lyell Glacier was connected with Mons Glacier (Outram, 1905), but, subsequently, the Mons Glacier receded so far up valley as to be scarcely visible (Field and Heusser, 1954). The glacier is strongly broken and crevassed where it travels steeply downward, and a prominent, broad, lateral moraine exists along the northern edge. In 1858, the Southeast Lyell Glacier so intrigued James Hector (1861) of the Palliser Expedition, the first European to investigate this area, that he left a detailed description of it that Thorington used to establish a datum from which to

Figure 18.—*Terrestrial photograph of Southeast Lyell Glacier, an outlet glacier from the approximately 50-km^2 Lyell Icefield. The glacier has a steep, crevassed surface. The first recorded observation was in 1858. The glacier receded gradually from 1858 until about 1930, and then more rapidly since then, probably because the terminus was resting in a lake from about 1930 to 1953 (Field and Heusser, 1954) (fig. 9). Glacier 4*5DAC–89, Glacier Atlas of Canada, Plate 7.4, North Saskatchewan Glacier Inventory, Area 4*5D, Inland Waters Branch, Department of Energy, Mines and Resources, 1970, scale 1:500,000. Photograph taken in August 1953 by William O. Field, American Geographical Society, is courtesy of Calvin J. Heusser, Professor Emeritus, New York University.*

measure frontal recession (Gardner, 1972). Following Hector's visit, the positions of the terminus were recorded in 1902 by Outram (1905), in 1918 by the Interprovincial Boundary Survey (Interprovincial Boundary Commission, 1924), and in 1926, 1930, and 1944 by Thorington (1927, 1932, 1945). Heusser (1956) dated the moraines to 1841, 1855, 1885, 1894, 1902, and 1906. In 1947, the DWPB visited the glacier to see whether it might be suitable for inclusion in their network. It was found to have receded so much that what was left of the forefoot was too steep for their purpose (McFarlane, 1947), although it was photographed and a reference baseline established (Meek, 1948a, b). Glacier limits and variations for the Southeast Lyell Glacier were documented by an AGS expedition in 1953 using photographic and botanical techniques (Field and Heusser, 1954; Heusser, 1954, 1956). The AGS expedition concluded, on the basis of field observations, that the reason for the rapid recession since 1930 was a proglacial lake in which the terminus was situated for much of the 1930 to 1953 period. By 1953, the terminus was 60 m beyond the lakeshore and some 4 m above its surface. Available information of the retreat of the Southeast Lyell Glacier is plotted in figure 9.

North of Lyell Icefield is another mountain block running east from Mount Amery (3,329 m) across the ice-covered divide to Cockscomb Mountain (3,140 m). Ice flows east and west from the Continental Divide, pushing down to below 2,400 m in fairly large glaciers such as the *Rice Glaciers* group (2–3 km long) and to below 2,200 m in the Alexandra Glaciers (5.5 and 4 km long) (fig. 19), which were joined in 1918. This ice mass, which might more properly be called the *Alexandra Icefield*, covers an area of about 25 km^2. Average peak elevations are usually well above 3,000 m asl. The western part of the *Lyell Group* consists of up to two dozen small cirque and niche glaciers, averaging 1 km in length and about 0.5 km^2 in area, on either side of the ridges in that part of the range.

Unnamed Range (—)

Between Bush River and Prattle Creek, south of the western extension of the Columbia Icefield, is an umbrella-shaped range with no name. Its axis is almost 40 km long and 5 km wide at its narrowest, whereas the arc of the umbrella frame is 25 km long. Peak elevations range between 2,500 and 2,800 m in the south, and as much as 3,100 m in the north. Some glaciers, as much as 1.5 km^2 in area, are scattered along the ridge of the shaft, but the majority are concentrated in the northerly part of the range. On the eastern side, facing the headwaters of Bush River, is an elongated ice apron spread along 8 km of the range. Other glaciers in this sector take the form of cirque glaciers or small ice fields with outlet glaciers ranging from 2 to 4 km in length and about 4 km^2 in area. Whereas some glaciers push their snouts below 2,000 m asl, some as low as 1,710 m, most terminate at about 2,300 m.

Vertebrate Ridge (PC10)

Vertebrate Ridge (fig. 1, PC10) extends to the northwest about 20 km; its main feature is a 7-km^2 ice field centered on Stovepipe Mountain (2,804 m). A 4-km-long outlet glacier drains from the ice field northward to an elevation of 2,000 m. The southern part of the ice field is drained to the east by a glacier reaching to 1,800 m. Heights along the ridge are generally about 2,550 to 2,650 m in elevation.

Kitchen Range (PC11)

Parallel to Vertebrate Ridge, and marking the western edge of the *Park Ranges* in this section, is the 30-km-long Kitchen Range (fig. 1, PC11).

Summit elevations range between 2,800 and 2,950 m. About eight glaciers are situated on either side of the main ridge, the largest being a 4-km^2 ice mass east of Poker Mountain. Lower ice limits vary between 2,025 and 2,530 m, and glacier lengths are generally less than 1.5 km.

Columbia Icefield Group (PC12)

Seen from space, the Columbia Icefield (fig. 1, PC12) (figs. 7, 20), about midway between Lake Louise and Jasper, appears as an extensive snow-covered upland with comparatively little relief. Shaped like a stylistic "T," it runs almost 40 km from east to west, and 28 km from northwest to southeast. Its area depends on how many of the peripheral ice masses are included, but an acceptable figure would be 325 km^2. It is situated on a plateau 3,000–3,325 m in elevation that dips slightly to the south and culminates in the Snow Dome (fig. 21), a gently-sloping 3,520-m peak, completely covered with ice and snow, which is the hydrographic apex of the continent, draining into three oceans (Freeman, 1925; Lang, 1943). Harmon and Robinson (1981) provided a poetic and pictorial commentary on the beauties of the area. Numerous peaks more than 3,500 m asl fringe

Figure 19.—*High-angle oblique aerial photograph of West Alexandra Glacier and* South Alexandra Glacier. *The glaciers were joined before 1918. Glacier 4*5DAE–32, 33, 34, 35, Glacier Atlas of Canada, Plate 7.4, North Saskatchewan Glacier Inventory, Area 4*5D, Inland Waters Branch, Department of Energy, Mines and Resources, 1970, scale 1:500,000. The University of Washington photograph F2–131, taken 7 August 1961 by Austin Post, U.S. Geological Survey, is courtesy of Robert M. Krimmel, USGS.*

the Columbia Icefield, so that ice flowing to the margin of the ice field forms huge cliffs above high rock walls and avalanches to the base of the rock walls to form reconstituted glaciers (Boles, 1974). The ice discharges radially through outlet glaciers; the three largest (Columbia, Athabasca, and Saskatchewan Glaciers) flow in deeply incised valleys. There are many other small ones such as Stutfield, Dome, and the *Castleguard Glaciers* [*I, II, III, IV*; see footnote 2 in table 1] (Baranowski and Henoch, 1978). Several have been studied in some detail and will be discussed further. Not only is the Columbia Icefield (fig. 7) the largest ice field in the Rocky Mountains, but together with the Clemenceau and Chaba Icefields, it drapes the peaks, mainly along the Continental Divide, in a continuous glacier cover for more than 60 km.

A comprehensive inventory of the glaciers (some of which are listed in table 5) and of the landforms in the Columbia Icefield area, particularly near the Athabasca (figs. 7, 20) and Dome Glaciers, was undertaken by Baranowski and Henoch (1978) and Kucera and Henoch (1978). Detailed geomorphological maps were prepared at scales of 1:25,000 and 1:2,500. Unfortunately, little is known about the bulk of the ice field that lies in British Columbia.

Several federal government agencies and university departments undertook a joint project in 1977 to map the surface of the ice field and to calculate the amount of water held in its snow and ice (Canada, Energy, Mines and Resources, 1978). Preliminary findings showed that the part feeding the Athabasca and Saskatchewan Glaciers (figs. 7, 20) was thinner than previously thought (100–365 m). Surveyors used stereoscopic, vertical aerial photography and an Inertial Survey System (ISS) to fix additional

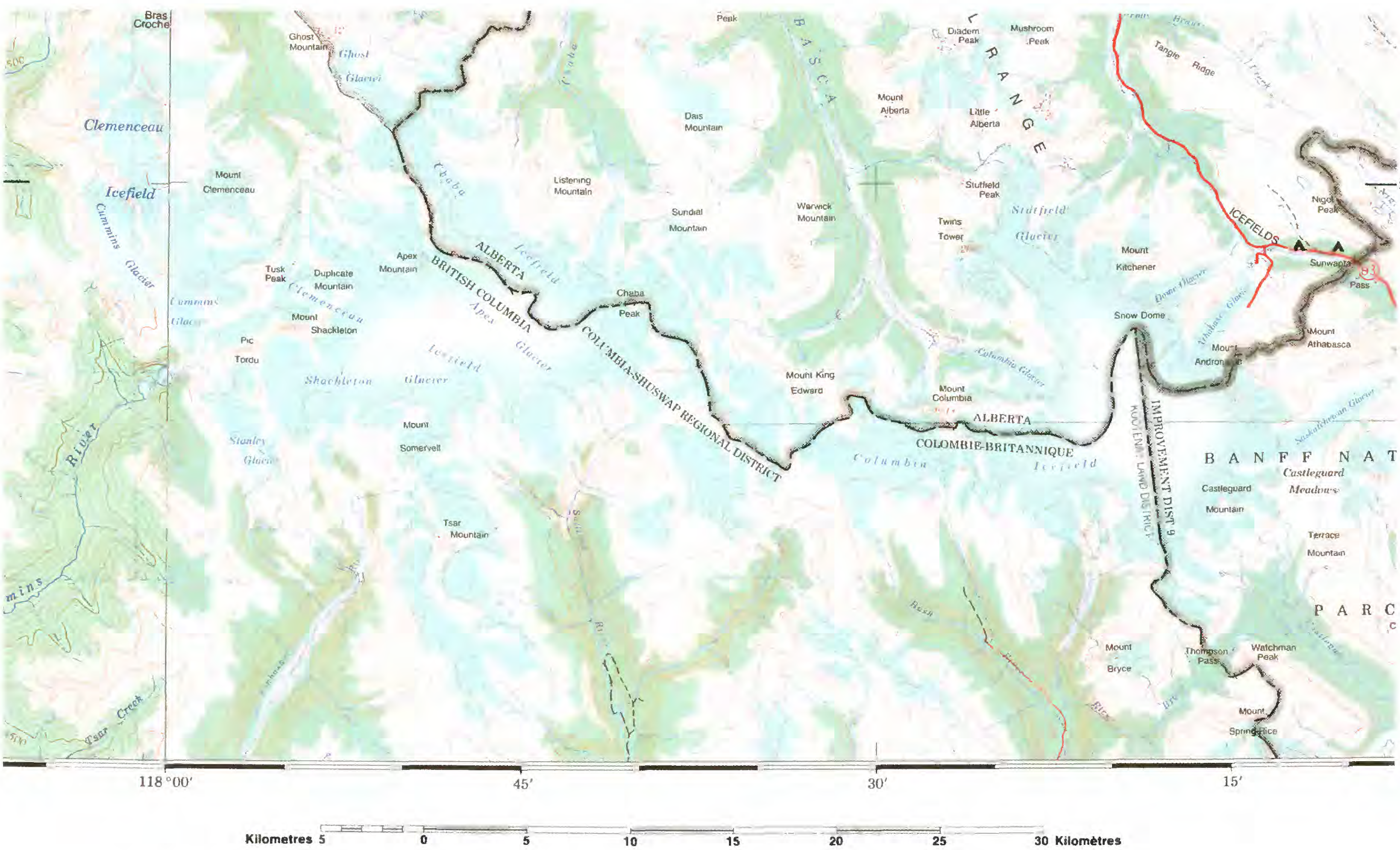

Figure 20.—*Mosaic of reduced segments of the 1:250,000-scale topographic maps of the Brazeau Lake and Canoe River quadrangles (83C and 83D) showing the area around Columbia and Clemenceau Icefields. ©1995 and 1986. Produced under licence from Her Majesty the Queen in Right of Canada, with permission of Natural Resources Canada.*

ground control points on the ice. The aerial survey aircraft also carried a thermal infrared (IR) line-scanner from which radiometric temperature isolines at 1°C were to be plotted. One of the thermal IR images generated was used for the cover of a new map of the Columbia Icefield (Canada, Environment Canada, 1980).

The accessibility of the Columbia Icefield, particularly the Athabasca and Saskatchewan Glaciers, and the availability of a fairly good historical sequence of observations, probably favored its selection as the site for a wide variety of glaciological studies. These have included investigations of glacier chemistry, glacier flow, depth measurement, photogrammetry, resistivity, sediment transport, and temperature, among others. Each will

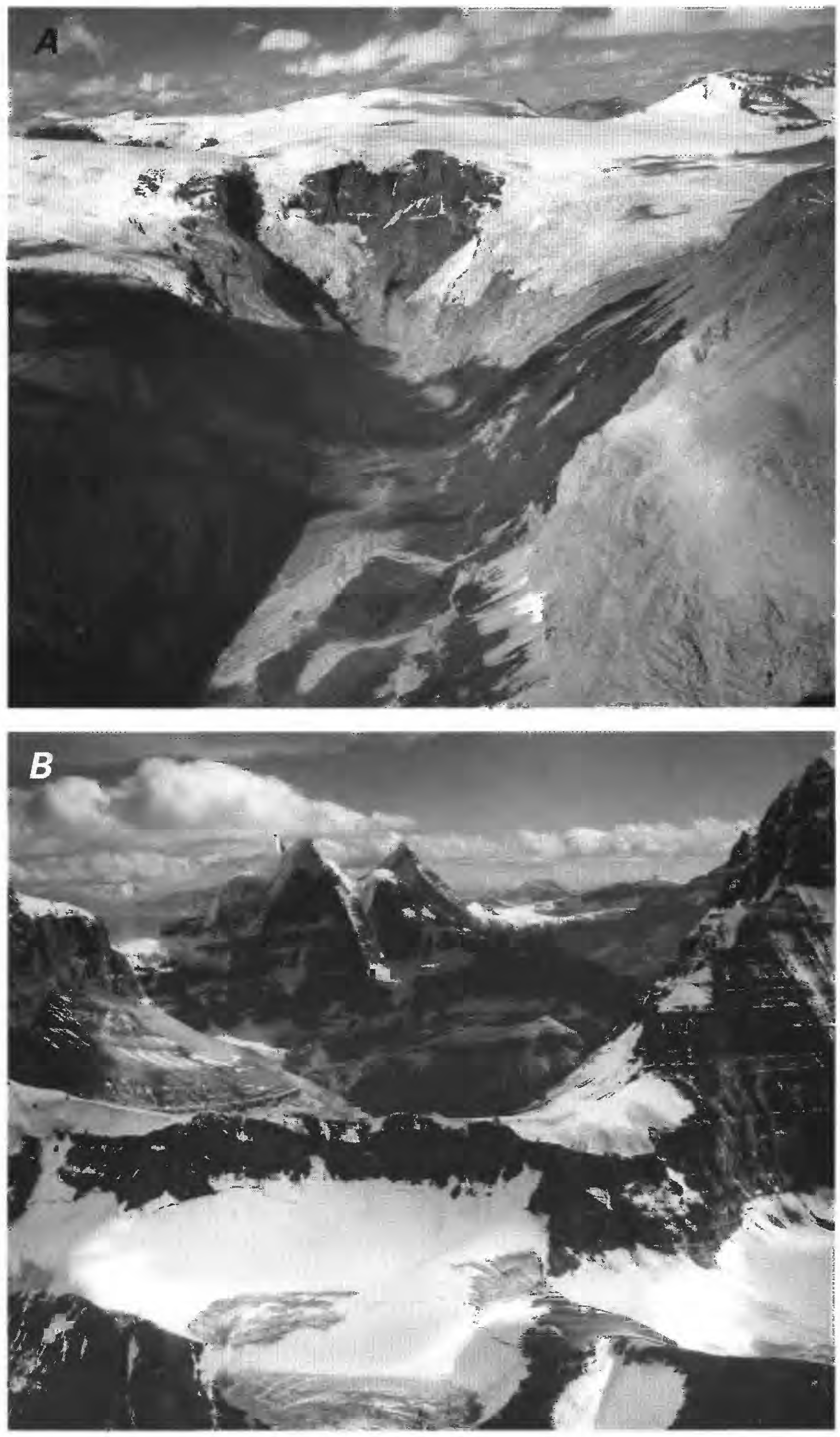

***Figure 21.**—High-angle oblique aerial photographs of the Columbia Icefield, the largest ice field in the Rocky Mountains, having an area of more than 300 km^2. Together with Clemenceau and Chaba Icefields, it provides continuous glacier-ice cover along the Continental Divide for more than 60 km.* **A**, *Columbia Icefield from the south looking up Bryce Creek to Snow Dome. U.S. Geological Survey photograph F642–115.* **B**, *The northern part of Columbia Icefield. Twins Tower is in the center. U.S. Geological Survey photograph K641–44. Both photographs taken 21 August 1964 by Austin Post, U.S. Geological Survey, are courtesy of Robert M. Krimmel, USGS.*

TABLE 5.—*Characteristics of glaciers in the vicinity of Athabasca Glacier*

Glaciers	Area (square kilometers)	Length (kilometers)	Elevations (meters) Top	Elevations (meters) Bottom	Debris-cover (square kilometers)
Dome	5.92	5.7	3200	1980	2.16
Stutfield	5.68	5.2	2740	1770	3.41
Kitchener	2.17	2.8	3020	2070	1.35
Little Athabasca	2.03	2.4	3290	2290	
Sunwapta	0.97	2.3	3140	2300	
Athabasca trib. (E)	0.75	1.7	2940	2350	
Athabasca trib. (W)	0.50	1.3	3050	2380	
Stutfield trib.	0.43	1.0	2320	2090	
Kitchener trib.	0.39	1.2	2860	2510	
Little Dome	0.16	0.6	2590	2440	
Nigel Peak	0.15	0.8	2700	2470	

be discussed in the context of those parts of the Columbia Icefield on which the work was carried out.

Castleguard Glaciers

The southern limit of the Columbia Icefield is marked by a group of glaciers (collectively known as the *Castleguard Glaciers* [*I, II, III, IV*; see footnote 2 in table 1] (fig. 7)) at the head of Castleguard River. Livingston and Field visited them in 1949 and numbered them I to IV from northeast to southwest. *Castleguard Glacier IV* (fig. 22), the principal southern outlet glacier of the Columbia Icefield was called *South Glacier* by Ford (1983) and his colleagues from McMaster University working on the *Castleguard Cave* system. *Castleguard Glacier I*, situated at 2,300–2,700 m asl, was first photographed by the Interprovincial Boundary Survey in 1918 and subsequently by others in 1919, 1923, 1924, and 1949. Until 1924, it abutted a massive moraine which probably formed near the turn of the century (Denton, 1975). *Castleguard Glaciers II* and *III* have shrunk enormously since the 1920's, as has *Castleguard Glacier IV.* Ice fronts have receded an average of 500 m since the end of the "Little Ice Age." Sporadic observations by the McMaster group indicate a reduced average recession of the *Castleguard Glaciers* of about 20 m from 1967 to 1981. This is a key alpine karst locality, because the cave and glacier systems are still in contact. Recent work has focused on the karst cave system (Ford, 1975, 1983), subglacial chemical deposits (Hallet, 1976a, b, 1977; Hallet and Anderson, 1980), and the interaction between glaciers and the limestone bedrock (Smart, 1983, 1984, 1986).

Saskatchewan Glacier

The next major outlet glacier from the Columbia Icefield, the Saskatchewan Glacier (figs. 7, 20, 23) is about 13 km long and some 30 km^2 in area. It declines gradually from east to northeast, without ice falls, to its terminus at 1,800 m. Several tributary glaciers were formerly active in providing nourishment, although by the late 1980's only one of these supplied the Saskatchewan Glacier. The ELA lies almost at the junction of the ice field and outlet tongue and ranges from 2,440 to slightly more than 2,530 m. Based on ice discharge, Meier (1960) computed the annual accumulation to be 1 m water equivalent (w.e.) and its gradient 13 mm m^{-1} below the firn limit, indicating a high degree of activity. Average ablation ranged from 1 m a^{-1} near the ice field through 2.6 m a^{-1} to 4 m a^{-1} at the snout. The ice was 442 m thick 8 km upglacier and, because of the valley's marked U-shape and very steep walls, was as much as 305 m thick, even quite close to the margin (Meier, 1960).

***Figure 22.**—High-angle oblique aerial photograph of* Castleguard Glacier IV, *the principal southern outlet glacier of the Columbia Icefield. This glacier and the other Castleguard Glaciers have receded considerably since the 1920's. Glacier 4*5DAE–47, Glacier Atlas of Canada, Plate 7.4, North Saskatchewan Glacier Inventory, Area 4*5D, Inland Waters Branch, Department of Energy, Mines and Resources, 1970, scale 1:500,000. Photograph K642–108, taken 21 August 1964 by Austin Post, U.S. Geological Survey, is courtesy of Robert M. Krimmel, USGS.*

In 1953, the American Geographical Society expedition used photographic and botanical techniques to determine the history of the Saskatchewan Glacier (Field and Heusser, 1954; Heusser, 1954, 1956). It withdrew from its terminal moraine in 1893 and by the time of their visit had retreated 1,364 m. The rate of recession from 1948 to 1953 was quite fast at 55 m a^{-1}.

In 1945, the Saskatchewan Glacier was investigated by the DWPB Calgary office. At this time the toe was very irregular and the surface of the glacier very rough. The position of the snout and changes in its areal extent were measured every year, and a set of plaques was placed on the ice surface to measure velocity; in 1950, the measurement interval became biennial. Detailed reports were prepared by the DWPB as internal documents, but some results were published (Lang, 1943; McFarlane, 1946b; Meek, 1948a, b; McFarlane and others, 1950; Collier, 1958). In the mid-1960's, following recommendations made at the Glacier Mapping

Symposium, the Water Survey of Canada began to use terrestrial photogrammetry to determine volumetric change, with results as shown in table 6 (Campbell and others, 1969; Reid, 1972; Reid and Charbonneau, 1972, 1975, 1979, 1981; Reid and others, 1978). Snout and plaque surveys were continued in the intervening years by the Calgary office of the Water Survey of Canada (WSC) (Warner and others, 1972; Canada, Environment Canada, 1976, 1982), but all were terminated by 1980 (fig. 9).

Meier (1960) measured the velocities on the surface and at depth, the surface and bedrock topography, and the ablation and flow structures in a project designed to test theories of glacier flow. Summer velocities were generally greater than annual ones, though there were significant velocity fluctuations in the short-term and there was even intermittent backward movement. Maximum surface velocities of 117 m a^{-1} at the firn limit decreased unevenly downglacier to 3.5 m a^{-1} at the snout. The flow law of ice was determined by analysis of a 140-m-deep vertical-velocity profile and a surface transverse-velocity profile. Three main classes of structural ice features were distinguished: (1) primary sedimentary layering,

Figure 23.*—High-angle oblique aerial photograph of Saskatchewan Glacier, a major eastward-flowing outlet glacier from the Columbia Icefield. The glacier is about 13 km long, has an area of 30 km^2, and has been studied since 1945 (see text). Glacier 4*5DAF–18, Glacier Atlas of Canada, Plate 7.4, North Saskatchewan Glacier Inventory, Area 4*5D, Inland Waters Branch, Department of Energy, Mines and Resources, 1970, scale 1:500,000. Photograph K642–102, taken 21 August 1964 by Austin Post, U.S. Geological Survey, is courtesy of Robert M. Krimmel, USGS.*

TABLE 6.—*Changes in the area and volume of the snout of Saskatchewan Glacier, 1965–1979*

Changes	1965–67	1967–69	1969–71	1971–73	1973–75	1975–77	1977–79
Volume (m^3x10^6)	–43.96	+12.45	–44.11	–30.85	–10.75	–3.09	–23.88
Surface height (m)	–6.51	+1.89	–6.84	–4.51	–1.76	–0.53	–3.73
Terminus (m)	–33.80	–28.00	–9.60	–23.00	–45.40	–53.60	–91.20
Snout elevation(m asl)	1,786	1,789	1,789	1,790	1,790	1,790	1,790
Area (km^2)	6.75	6.58	6.45	6.84	6.10	5.84	6.40

(2) secondary flow foliation, and (3) secondary cracks and crevasses. Meier (1958) also studied crevasse patterns as part of this general study of flow. Preliminary results showed that crevasse formation was preceded by a buildup in extension rate. Crevasses then formed so as to relieve the extension rate on intercrevasse blocks. Intense deformation resulting in pure shear preceded an extending crevasse. No crevasses deeper than 30 m were observed.

Rigsby's (1958, 1960) fabric diagrams did not show preferred orientations as strong as those for other temperate glaciers. Any strong patterns observed were thought to be in the more extensively metamorphosed, presumably older, ice flowing from depth. Melt recrystallization probably changed the strong orientation of crystals from a single maximum with optic axes normal to the foliation plane to 3–4 maxima, none of which necessarily coincided with the pole of the foliation plane.

Sharp and Epstein (1958) and Epstein and Sharp (1959) analyzed the oxygen-isotope ratios in different firn strata and found differences that reflected the elevation of accumulation, seasonal influences, differences among individual storms, and subsequent diagenetic changes. Ice along the centerline showed an irregular trend to lower ratios downglacier, which was thought to reflect ice transport along flow lines from different parts of the accumulation area.

McPherson and Gardner (1969) observed large cross-valley topographic highs, composed of till, in front of the Saskatchewan Glacier, which were old landforms emerging from beneath the ice. They might have been interpreted as end moraines. If so, they were not disturbed when overridden during the neoglacial advance.

Columbia Glacier

The Columbia Glacier (figs. 7, 20, 24), 8.5 km in length and about 16 km^2 in area, is the major outlet glacier flowing from the northwest section of the ice field, draining ice as well from the western slopes of Snow Dome and the eastern slopes of Mount Columbia (3,747 m). Columbia Glacier drops rapidly from the plateau area over a major ice fall, which creates a series of very well-defined ogives, to flow in a 0.6- to 0.7-km-wide glacier to an elevation of about 1,500 m. Its ELA lies at about 2,140 m. Habel (1902), Schaffer (1908), Palmer (1924–1926, 1925), Field (1949), and Field and Heusser (1954) recorded the location of the terminus in 1901, 1907, 1920, 1924, 1948, and 1953. The Interprovincial Boundary Survey photographed the glacier in 1919 (Interprovincial Boundary Commission, 1924). Heusser (1954) established a chronology of recessional moraines and dated the outer one at 1724 and others at 1842, 1854, 1864, 1871, 1907, 1909, and 1919; he concluded that the glacier had retreated 394 m between 1724 and 1924. A plot of the recession data is given in figure 9; it assumes no change from 1725 to 1850. Baranowski and Henoch (1978) observed that the Columbia Glacier had advanced as much as 1 km from 1966 to 1977. Since the Columbia Icefield map was published, the glacier has advanced farther to completely fill the large proglacial lake, a distance of some 800 m (Parks

Canada, oral commun., 1986). The glacier is not being surveyed regularly, so it is not known whether this advance is continuing.

Athabasca Glacier

The most-visited glacier in Canada is without a doubt the Athabasca Glacier (figs. 20, 25). Situated only 1 km from the Icefields Parkway, which passes through Banff and Jasper National Parks, it is one of the primary destinations for tourists and tours. It has also become the focus of Parks Canada interpretive program and provides, through the Brewster snowmobiles, one of the few easy opportunities for the general public to get up on the ice. However, most would probably identify it as the Columbia Icefield. Its accessibility and the need for information about it have led to numerous scientific studies, which are summarized below.

The 6.5-km-long glacier leaves the ice field at 2,800 m, descends in a series of three ice falls as it passes over successive rock thresholds and continues as a gentle 1-km-wide tongue with a slope of 3–7° to its terminus at 1,925 m asl. It cuts through the axis of a gentle anticline and is flanked by walls of limestone, dolostone, and shale. Crevasses are well developed in the lower two ice falls and extend almost across the entire width of the glacier. Kucera (1987) measured 15 of the largest crevasses and found them to be no deeper than 36 m. Part of the glacier front is formed by moraine-covered ice that continues up valley, forming about two-fifths of

*__Figure 24.__—High-angle oblique aerial photograph of Columbia Glacier, a major outlet glacier draining the northwest section of the Columbia Icefield, including the western slopes of Snow Dome (off left side of photograph) and the eastern slopes of Mount Columbia (off right side of photograph). The glacier drops over a major ice fall (center of photograph) creating ogives. The glacier receded rapidly from the 1920's to the 1960's (fig. 9), but has advanced about 2 km between 1966 and 1986. Glacier 4*7AAG–71, Glacier Atlas of Canada, Inland Waters Branch, Department of Energy, Mines and Resources, scale 1:500,000. Photograph K641–42, taken 21 August 1964 by Austin Post, U.S. Geological Survey, is courtesy of Robert M. Krimmel, USGS.*

the glacier along the northwest side. Benoît and others (1984) published a key to the photointerpretation of features on and around the Athabasca and Dome Glaciers. Elements that are important for the analysis of remote-sensing imagery, such as the characteristics of various features, their texture, and reflectivity are all discussed. This study complements an earlier glaciological and geomorphological investigation by Kucera and Henoch (1978). Howarth (1983) and Howarth and Ommanney (1983) reported some difficulty in interpreting Landsat scenes for this area.

It is surprising that no systematic annual mass-balance studies have been carried out on the Athabasca Glacier. However, geochemical studies within the 2,600–2,700-m elevation band were used by Butler and others (1980) to estimate a net annual mass balance here of 1.5 and 2.4–2.7 m w.e., respectively, for 1976–77 and 1977–78. Average snowfall on the ice field is estimated to be more than 7 m, and the ELA is at about 2,600 m asl. Holdsworth and others (1985) obtained an 11.5-m core from the top of Snow Dome to evaluate the site for a deep core drilling. Preliminary analysis indicated a lack of evidence of regular seasonal variations in the stable-isotope data but evidence of percolation and homogenization of the isotopic and chemical constituents. It is clear that the overall mass-balance trend during the 20th century has been strongly negative. In 1870, the glacier was about 1.5 times its present total volume ($1{,}013 \times 10^6$ m^3) and 2.5 times its area (6×10^6 m^2 vs. 2.6×10^6 m^2). The average rates of decrease in volume

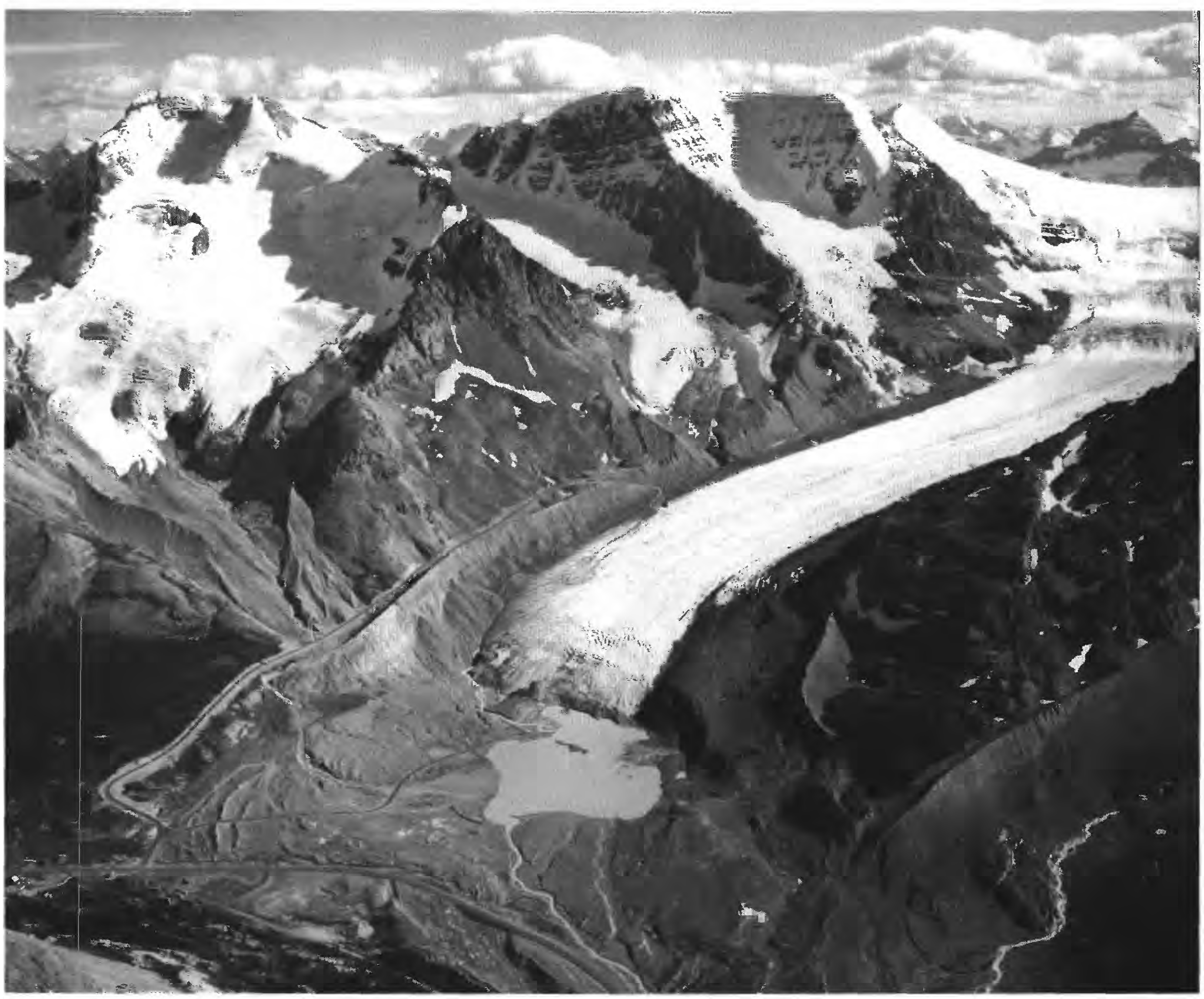

Figure 25.—*High-angle oblique aerial photograph of Athabasca Glacier, the most visited glacier in Canada. The 6.5 km glacier drains the Columbia Icefield to the northeast and has been studied extensively (see text). Glacier 4*7AAF–4, Glacier Atlas of Canada, Inland Waters Branch, Department of Energy, Mines and Resources, scale 1:500,000. Photograph K64L–133, taken 21 August 1964 by Austin Post, U.S. Geological Survey, is courtesy of Robert M. Krimmel, USGS.*

have declined: $3.2x10^6$ m^3 a^{-1} for 1870–1971 to $2.5x10^6$ m^3 a^{-1} for 1959–1971 (Kite and Reid, 1977). Ice volume has also been reconstructed by Mayewski and others (1979) as shown in table 7.

Observations of the retreat of the terminus of the Athabasca Glacier have been carried out for many years and are shown in table 8. Figure 26 shows the position of the terminus of Athabasca Glacier in 1952 and 1977. Hermann Woolley and J. Norman Collie visited and named Athabasca Glacier in 1898, at which time it coalesced with the Dome Glacier. Athabasca Glacier was photographed in 1908 (Schaffer, 1908) and again in 1919 (Interprovincial Boundary Commission, 1924). Field photographed it in 1919. In 1945, the DWPB commenced a series of annual surveys from their Calgary office. The position of the snout and the changes in the areal extent of Athabasca Glacier were measured every year, and a set of plaques was placed on the ice surface to measure velocity. Detailed reports were prepared as internal documents (McFarlane, 1945, 1946b, 1947; McFarlane and May, 1948; MacFarlane and others, 1949; May and others, 1950; Carter, 1954; Carter and others, 1956; Fowler and others, 1958; Chapman and

***Figure 26.**—Two photographs of the receding terminus of the Athabaska Glacier, Jasper National Park, Alberta.* ***A**, View in 1952 by A. MacS. Stalker, Geological Survey of Canada, Photograph GSC 147803.* ***B**, View in 1977 from Applied Hydrology Division, Environment Canada, Photograph GSC 203797–M. Modified from figure 9 in Prest, V.K., 1983, p. 20. ©Produced under licence from Her Majesty the Queen in Right of Canada, with permission of Natural Resources Canada.*

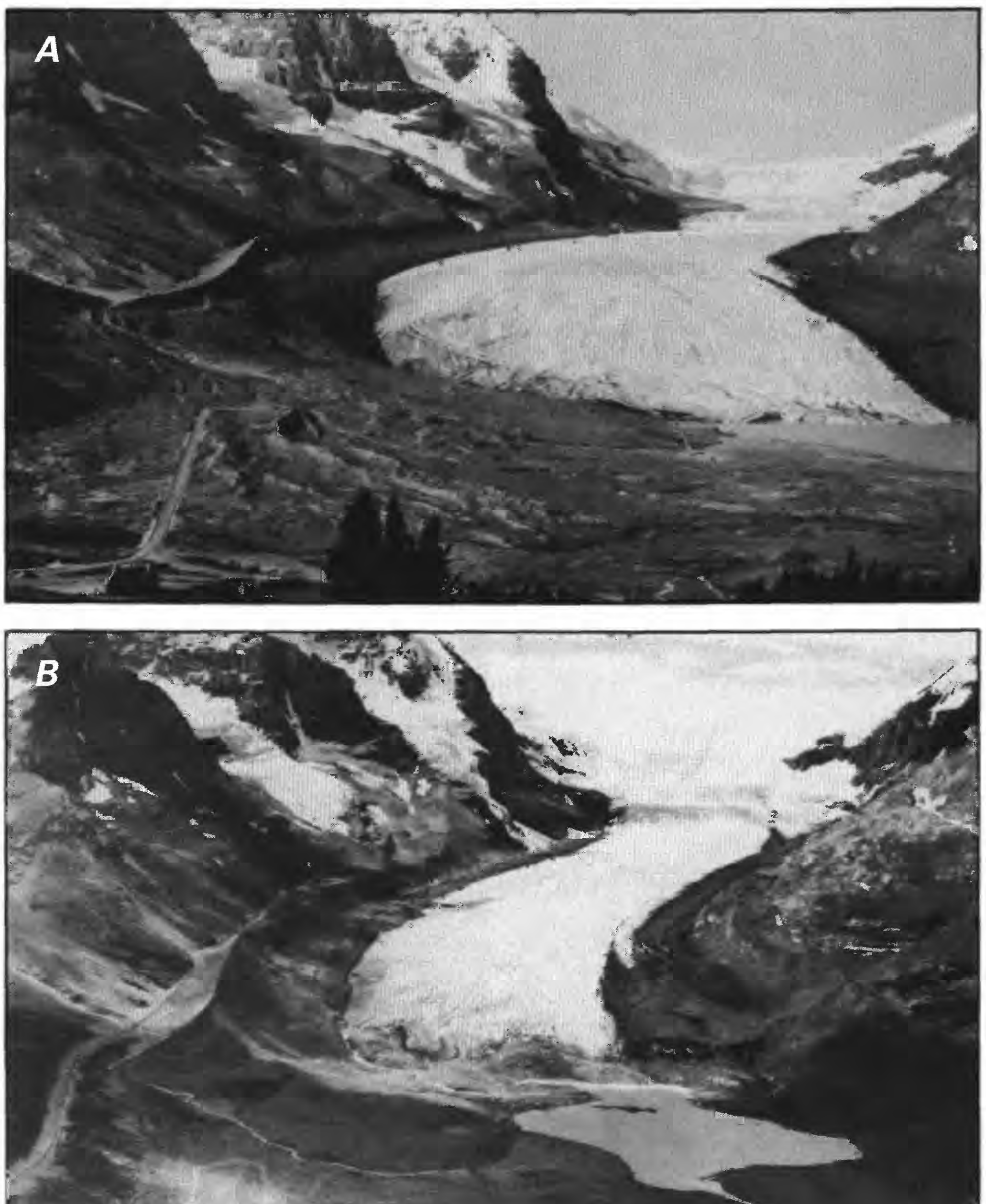

Figure 27.—*Terrestrial photograph of Angel Glacier on the north slope of Mount Edith Cavell, Cavell Group, Alberta, in August 1953, taken by William O. Field, American Geographical Society. Photograph and caption courtesy of Calvin J. Heusser, Professor Emeritus, New York University.*

representative (McFarlane, 1945, 1946a, b, 1947; Meek, 1948b). Field and Heusser (1954) reckoned that the glacier started to retreat in 1733 and that the separation of the lower glacier took place in the 1920's; they also noted a substantial reduction in volume. Heusser (1956) established moraine positions for 1723, 1783, 1871, and 1901. Early measurements were made by E.M. Kindle in 1927 and E.L. Perry in 1929.

Luckman (1976, 1977) attempted to establish the Neoglacial history of this and neighboring areas. Based on ground measurements and aerial photographs, a tentative reconstruction of the recent recessional history of *Cavell Glacier* has been determined (fig. 9).

Portal-MacCarib Group (PC19)

North of Astoria River is the small *Portal-MacCarib Group* (fig. 1, PC19). It is 13.5 km long, trends southwest from the Athabasca River, has summit elevations near 2,750 m, and has a few small glaciers and rock glaciers.

Trident Range (PC20)

The northernmost mountain block in the interior part of the central *Park Ranges* is Trident Range (fig. 1, PC20). It is bounded on the north by the Miette River and on the east by the Athabasca River. At the junction of the Miette and Athabasca Rivers is Jasper, one of the famous resort towns of the Rockies. Numerous small glaciers and rock glaciers can be found here, ranging in length up to 1.5 km, but none is much bigger than 0.5 km^2 in area. Apart from one rock glacier that pushes below 2,000 m, the lower limits of the glaciers is in the range of 2,300–2,400 m. Østrem's (1966) map shows a lowering of the glaciation level here to below 2,600 m, possibly caused by storm tracks being channeled through Yellowhead Pass. Whereas average peak elevations are 2,600–2,800 m, a few rise to about 3,000 m.

Fraser-Rampart Group (PC21)

Between the Tonquin Valley and the Fraser River lies a heavily glacierized mountain range, the *Fraser-Rampart Group* (fig. 1, PC21), centered on what might be called the *Bennington Icefield*. The *Fraser-Rampart Group* extends 13 km north from Mastodon Mountain to join The Ramparts, a bastion that extends about 10 km from east to west. At the base of The Ramparts are very extensive rock-glacier formations. Furthermore, there are substantial debris-covered ice features associated with many of the glacier tongues. Bennington Peak and Mount Geikie rise to more than 3,200 m, and the other peaks range from 2,900–3,100 m asl. Some of the larger glaciers that form part of *Bennington Icefield* are the Fraser (3.5 km), Mastodon (4.4 km), Simon (4.8 km), Eremite (2.7 km), and Scarp (2.8 km) Glaciers that end at 1,800–2,000 m. These are 2 to 4 km^2 in size, but the majority are 1 km^2 or less and have higher termini, at 2,200–2,400 m. Several studies have been carried out on glaciers in this group, including the Bennington Glacier, *Para Glacier,* and *Paragon Glacier*. The latter is a tongue-shaped glacier about 300 m wide and 1 km long with an area of roughly 0.3 km^2. Although its terminus is now at 2,000 m asl, it formerly coalesced with the *Bennington Icefield*. In 1982, its ELA was 2,250 m, about the same as on the Bennington Glacier (McCarthy, 1985).

Bennington Glacier

The Bennington Glacier is a fairly large alpine glacier, about 5 km in length, with a spectacular series of "Little Ice Age" moraines from which it has retreated some 1,300 m. The Bennington Glacier descends 1,600 m in elevation from the west face of Mount Fraser. In the early 1980's, the firn line was at about 2,130 m. Retreat can be determined from available photographs. The earliest photograph, taken in 1921 by the Interprovincial Boundary Commission, gave a post-"Little Ice Age" recession of 250 m. McCarthy (1985) reconstructed the history and the development of the forefield of Bennington Glacier through a comprehensive lichenometric study that paid particular attention to eight moraine complexes and an ice-front esker. The recessional history of the Bennington Glacier is plotted in figure 9.

Para Glacier

The *Para Glacier* is a small cirque glacier about 2 km in length on the east side of Parapet Peak. It flows into Chrome Lake. The main stream of ice flows east and is fed by a steep and much-broken ice fall from the eastern arête of Bennington Peak. There is very little debris on the glacier. Initial observations made by C.G. Wates in 1933 (Wheeler, 1934) and McCoubrey (1938) plotted in figure 9 were apparently filed with the American Geographical Society (Denton, 1975).

Meadow-Clairvaux Group (PC22)

The mountains that form the southern slopes of Yellowhead Pass are part of the small *Meadow-Clairvaux Group* (fig. 1, PC22). The *Meadow-Clairvaux Group* is situated west of the Trident Range and Meadow Creek and is separated from Selwyn Range by the valley of the Fraser River. Peaks here do not rise above 3,000 m in elevation but generally lie close to 2,600–2,900 m asl. The 10 glaciers here, such as the Vista, Clairvaux, and Meadow Glaciers, are small (<1.5 km^2) in area, terminate below 2,300 m, and include a number of rock- and debris-covered features.

Selwyn Range (PC23)

The last major feature in this central part of the *Park Ranges* is the Selwyn Range (fig. 1, PC23), which lies between the Fraser and Canoe Rivers and extends as a series of transverse ridges, about 25 km wide,

TABLE 7.—*Recession and volume changes of Athabasca Glacier, 1870–1970 (from Mayewski and others, 1979)*

Date	Retreat (meters a^{-1})	Area Loss (square kilometers a^{-1})	Volume Loss (cubic kilometers a^{-1})
1870–1877	6	0.025	0.0024
1877–1882	11	0.011	0.0030
1882–1886	11	0.011	0.0014
1886–1900	6	0.022	0.0020
1990–1908	5	0.023	0.0015
1908–1922	4	0.018	0.0033
1922–1938	13	0.035	0.0035
1938–1945	27	0.043	0.0069
1945–1950	27	0.033	0.0068
1950–1956	21	0.028	0.0062
1956–1960	38	0.040	0.0043
1960–1965	8	0.019	0.0040
1965–1970	4	0.013	0.0026

others, 1960; Davis and others, 1962; Davies and others, 1964, 1966, 1970; Glossop and others, 1968), but some results were published (McFarlane, 1946a; Meek, 1948a, b; McFarlane and others, 1950; Collier, 1958).

Following experimental aerial photogrammetric surveys of the Athabasca Glacier in 1959 and 1962 (Reid, 1961), the University of New Brunswick examined the use of terrestrial photogrammetry for measuring the melt of the Athabasca Glacier (Konecny, 1963, 1966; Reid and Paterson, 1973). From 1959 to 1962 the surface was reduced an average of 1.7 m, and the glacier lost $3.936 x 10^5$ m^3, representing a 35 percent contribution to average annual streamflow (Reid and Paterson, 1973). The Water Survey of Canada then switched to a program of terrestrial surveys every 2 years (Campbell and others, 1969; Reid, 1972; Reid and Charbonneau, 1972, 1975, 1979, 1981; Reid and others, 1978) for the measurement of volumetric change (table 8); snout and plaque surveys were continued in the intermediate years by the Calgary office (Warner and others, 1972; Canada, Environment Canada, 1976, 1982). Paterson (1966) showed that the difference between individually surveyed markers and map heights was less than three times the theoretical error, or about 15 percent of the contour interval. Additional surveys were made of the Athabasca Glacier in August 1977 as part of a program to remap the Columbia Icefield and surrounding areas and to test the relatively new orthophoto-mapping process. Young and others (1978) reported that there was little to choose amongst the various techniques, although the orthophoto mapping might be faster and cheaper and produced a digital-terrain model in computer-compatible form of use for further computations. Errors in the three methods ranged from about 1–2 m on the lower glacier to about 10–20 m on the upper.

Some other records are also available from Field, who revisited the glacier in 1948, 1949, 1953 and 1963 (Denton, 1975). He and Heusser, using photographic and botanical techniques (Field and Heusser, 1954; Heusser, 1954, 1956), were able to develop the history further. Athabasca Glacier reached its maximum about 1714 and began to withdraw from different parts of its end moraine in 1721 and 1744. It readvanced in the first half of the 19th century, reaching almost to its maximum extent. Recession began between 1841 and 1866 and has continued with minor fluctuations marked by moraines formed about 1841, 1900, 1908, 1925, and 1935.

The glacier has been used as a test area for a variety of depth-measurement techniques, some of which have been designed to provide information for physical studies of glacier flow.

Kanasewich (1963) used gravity techniques to obtain ice-thickness values along eight transverse profiles, whereas Paterson and Savage (1963a) used seismic waves to determine depths for 2- km downglacier from the lowest ice fall. During the summer of 1959, five holes were drilled into the glacier with a prototype hotpoint drill (Stacey, 1960). Rossiter (1977) tested a 1–32 MHz radio interferometry depth-sounding technique on Athabasca Glacier. High scattering levels above 8 MHz were attributed to water-filled cavities within the glacier on the order of 3–6 m in width, having typical separations of 10–30 m. Strangway and others (1974) found that at 1, 2, and 4 MHz the ice had a dielectric constant of about 3.3,

TABLE 8.—*Changes in the area and volume of the snout of Athabasca Glacier, 1959–1979*

Changes	1959–62	1962–65	1965–67	1967–69	1969–71	1971–73	1973–75	1975–77	1977–79
Volume ($m^3 x 10^6$)	–1.76	–3.07	+3.10	+0.66	–16.76	+6.19	–6.13	–6.50	–2.79
Surface height (m)	–0.68	–1.35	+1.36	+0.29	–7.71	+2.49	–2.45	–2.61	–1.09
Terminus	–38.1	–36.3	–10.6	–20.4	–14.9	–6.0	–19.0	+7.8	–7.0
Snout elevation (m asl)			1930	1930	1935	1930	1953	1941	1944
Area (km^2)	2.57	2.28	2.28	2.28	2.17	2.48	2.50	2.49	2.56

corresponding to that for ice near 0°C. Measured depths were not always consistent with previous seismic, gravity, and borehole results. Radio-echo-sounding has featured prominently in depth investigations. A sophisticated mobile system linked to fixed transponders (Goodman, 1970, 1975) provided results that agreed within 14 m with the seismic and borehole measurements of Savage and Paterson (1963). Repetitive soundings at individual locations revealed the presence of intraglacier structures that appeared to be related to changing hydrological or glaciological conditions within the glacier (Goodman, 1973). Waddington and Jones (1977), using a 1–5 MHz radio-echosounder, sampled the accumulation area of the Athabasca Glacier from below Castleguard Mountain northward to the ice falls and westward to the divide. They found depths ranging from 100 to 365 m. Contour maps of ice thickness and basal elevations have been produced by Trombley (1986), based on 300 depth measurements of the lower 3.6 km of the glacier with a portable radio-echosounder. A summary of some of the results, based on Paterson (n.d.) and Trombley (1986) is given in table 9.

Measurements show that in the ablation area, below the lowermost ice fall, the longitudinal and transverse profiles of ice thickness are geometrically regular and simple. A bedrock depression and two bedrock rises influence the flow. The ice is thickest (>320 m) in the deepest part of the depression, which appears to be a relic valley carved by what is now a small hanging glacier. Removal of the glacier would create a chain of paternoster lakes (Kanasewich, 1963).

In an interesting variant on their seismic study, Neave and Savage (1970) used natural seismic activity to monitor icequakes. These appeared as single events in the zone of marginal crevasses resulting from extensional faulting near the glacier surface. Swarms of icequakes were occasionally recorded that were distinguished from the crevasse-forming icequakes by their intense activity (20 events s^{-1}), by their distribution along a line several hundred meters long, and by their location, crossing the crevasse-free center strip of the glacier. Propagation velocities on the order of 30 m s^{-1} were observed. Not only did the individual events in a swarm migrate across glacier, but they also appeared to migrate downglacier at a velocity of about 30 m h^{-1}.

TABLE 9.—*Depths of Athabasca Glacier [based on Paterson (n.d.) and Trombley (1986)]*

Elevation (m asl)	Depth (meters)	Year of measurement	Elevation (meters asl)	Depth (meters)	Year of measurement
2036	60	1979	2231	250	1960
2048	73	1960	2232	322	1959–61
2115	176	1979	2234	316	1966–67
2122	194	1959–61	2234	298	1966–67
2130	195	1979	2235	314	1959–61
2135	209	1959–61	2237	265	1966–67
2141	209	1966–67	2237	251	1979
2195	248	1959–61	2238	297	1966–67
2202	210	1979	2238	300	1979
2206	235	1960	2239	306	1979
2228	310	1979	2240	306	1979
2229	319	1979	2240	308	1966–67
2229	318	1979	2240	311	1966–67
2229	315	1979	2250	311	1966–67
2230	291	1979	2250	312	1979
2230	313	1966–67	2250–55	309	1966–67

It is possible to tell from velocity measurements that ice now at the tongue of the Athabasca Glacier fell as snow on the ice field 150–200 years ago. Observations in 1959 and 1960, along the center line of the glacier, showed that ice velocity varied from 74 m a^{-1} below the ice fall to 15 m a^{-1} at the terminus and that the longitudinal strain rate varied from –0.1 to 0.0 a^{-1} (Savage and Paterson, 1963, 1965). Paterson (1962) found that the longitudinal strain rate was not constant with depth and at 100 m was slightly greater than at the surface. He concluded that the quasi-viscous Glen flow law provided the best fit to the available data (Paterson and Savage, 1963b). Ice takes about 2 years to travel down the lowest ice fall, corresponding to a velocity there of about 130 m a^{-1}. Seasonally unexpected velocity variations 2.5 km upglacier were explained by variations in the amount of water available at the bed for lubrication, being positively correlated with streamflow from the lake, with a lag of 3–4 days (Paterson, 1964). However, Meier (1965) pointed out that measurements on meltwater discharge from Athabasca Glacier by Mathews (1964a, 1964b) showed that maximum runoff occurs within a few hours of maximum melt. Paterson (1965) replied that some runoff may be delayed. Short-term velocity variations have been studied by Kucera (1971, 1987), using time-lapse photography. Ice within 60 m of the terminus is moving at an average rate of 57 mm d^{-1} (20.8 m a^{-1}) and, during the summer, as much as 5 mm h^{-1}. During a two-and-a-half month period, ice descended the lowest ice fall at a velocity of about 0.35 m d^{-1}, or 125 m a^{-1}. The glacier moves faster in summer than in winter and seems to move faster during the day than at night.

The velocity of ice deep within Athabasca Glacier has been measured in a number of boreholes. Savage and Paterson (1963), Paterson (1970), and Raymond (1971b) demonstrated that the upper part of the glacier is moving faster than the base. Velocity varies little with depth in the upper half of the borehole (209 m deep), but in the lower half, velocity decreases but at an increasing rate as the bottom is approached. Savage and Paterson (1963, 1965) estimated basal slip in two boreholes to be 30 m a^{-1} and 3 m a^{-1}. These boreholes lie along the same streamline and are separated by only six times the average depth. Raymond (1971a) applied a new method for determining the three-dimensional velocity field of the Athabasca Glacier. His measurements of ice deformation at depth revealed the pattern of flow in a nearly complete cross section of a valley glacier (Raymond, 1971b). He found that the relative strength of marginal and basal shear strain-rate was opposite to that expected. He further developed methods for determining the distributions of stress and effective viscosity in a glacier (Raymond, 1973) that did not support the results obtained by Paterson and Savage (1963a, b).

Using two different techniques, Reid and Paterson (1973) determined that the average annual loss of ice is 14.7x10^6 m^3, equivalent to 13.4x10^6 m^3 a^{-1}, or about 35 percent of the average annual streamflow measured at the gauging station. This compares to Collier's figure of 10–20 percent (Collier, 1958). The figure for glacier-melt contribution is much higher. Reid (1972) determined the 20-year average for mid-May to the end of October to be 35.1x10^6 m^3. Collier (1958) pointed out how effective glacier melt is in sustaining streamflow in August and September. The addition of 106 percent to the drainage area in Edmonton only increased the September 1955 flow by 1 percent (Collier, 1958).

Mathews (1964a) developed a moderately successful regression equation relating discharge of the Sunwapta River to temperature in Jasper. Correlations commonly better than +0.8 and reaching +0.96 were obtained for individual periods of from 1 to 2 months. He concluded that the daily streamflow was related, first, to the temperatures of the current day and, second, to the temperatures of the previous few days. There were pronounced diurnal fluctuations in meltwater flow from Athabasca Glacier (Mathews, 1964a)

An interesting feature of the streamflow record noted by Mathews (1964a) was the occurrence of jökulhlaups. These interrupted the normal diurnal cycle and were apparently unrelated to weather conditions. Records covering 13 summers showed at least 10 glacier-outburst floods having a discharge volume of 250,000 m^3 or more and one flood that released 1,400,000 m^3 of water. Because there are no ice-dammed lakes near the Athabasca Glacier, the water must have been stored within the glacier itself. Drainage of the floodwaters from a single chamber within the ice would certainly have caused some surface subsidence of the ice, but this was not observed. Mathews (1964a) concluded that the water must have been contained in a number of smaller cavities. Such cavities were noticed by Savage and Paterson (1963) during their drilling program in 1962. In 1968, they punctured a cavity at a depth of 9.2 m (Paterson and Savage, 1970). Water gushed from the borehole for about 55 s, indicating an excess pressure of at least 25 kPa. This pressure was thought to have been generated by the reduction in volume of the cavity caused by freezing of some of the water within it. Other evidence of unusual flows is provided by Kucera (1987), who reported that a meltwater stream near the snowmobile access road tripled in discharge from 0800 to 1600 h during one day in August 1980. Conditions were clear and air temperatures increased from 1 to 8°C during the same period.

During periods of high discharge, the meltwater streams carry a heavy sediment load, shifting position and migrating across the "Sunwapta" delta throughout the summer (Kucera, 1971, 1987). The sequence of WSC glacier maps shows that the delta has advanced 40 m into Sunwapta Lake, an effective sediment trap, during a 14-yr period. During one 24-h period in 1957, an estimated 380 tonnes of sediment and 190 tonnes of sand were brought into the lake by two glacier streams. Of this amount, only 4–7 tonnes of the sediment and none of the sand left by way of the Sunwapta River (Mathews, 1964b).

Particle-size distribution, roundness, striations, fabric, and lithologic composition have been used to distinguish between basal till, lateral- and recessional-moraine tills, ablation till, and outwash (Mills, 1977a, 1977b, 1977c). Glacial debris in a 120-m-wide zone in front of the Athabasca Glacier is not spread haphazardly across the forefield but, rather, occurs as low discontinuous ridges 0.7–2 m high that lie 2–20 m apart and trend roughly parallel to the glacier front. These are annual moraines produced by an advance of ice during the winter months. Measurements by Kucera since 1967 indicate that although the glacier advances 6–10 m during the winter months, the rate of retreat during the ablation season has slowed from 18–30 m to 10–16 m in recent years. This explains why the annual moraines are now spaced more closely together than in the past; for example, the position of the 1977 moraine lies only 2 m from the 1976 annual moraine (Kucera, 1987).

On the west side of Sunwapta Lake, the toe of the Athabasca Glacier consists of a dirty ice cliff. Rock debris, 1–2 m thick, extends upglacier along the western margin. Supraglacial debris cover, such as that also found on the neighboring Dome Glacier, creates significant problems in the interpretation of remote sensing imagery for these areas. The cliff is marked by rills that collect ice-and-rock fragments that cascade down the steep ice front: the slope of 40° has been maintained for several years (Kucera, 1987).

Some other aspects of the Athabasca Glacier have also been studied. Paterson (1971, 1972) determined that the temperature in the ablation area of Athabasca Glacier is about –0.5°C at a depth of 10 m. Below 17 m, it is slightly below the calculated pressure-melting point. The observed temperature regime is accounted for partly by heat produced by ice deformation and partly by freezing of water within the ice. The required water content is between 0.5 and 1 percent and is thought to be water trapped between grains when the ice formed from firn. Clee and others (1969) investigated the mechanism of internal friction of ice near its melting point by observing the attenuation of elastic waves. They decided that attenuation appears to be best explained by grain-boundary slip. Watt and Maxwell (1960) measured the electrical properties of snow and glacier ice and concluded that their properties were appreciably different from pure ice. Keller and Frischknecht (1960, 1961) used electrical resistivity. Stanley (1965) found that most of the lower part of the glacier, below the ice falls, is composed of either fine or coarse bubbly ice in alternating layers. Cryoconite holes have been described by Wharton and Vineyard (1983). They observed seven species of pennate diatoms and several species of green algae in the holes, probably transported onto the glacier from nearby aquatic and terrestrial sources.

Dome Glacier

Dome Glacier is poorly nourished in comparison to Athabasca Glacier. Dome Glacier's bifurcated terminus is fed largely by avalanching from Snow Dome. Most of the surface of Dome Glacier is covered by ablation, lateral, and medial moraines, which make it difficult to determine its true areal extent. The basic characteristics of Dome Glacier are given in table 5. The ablation moraine is commonly less than 1 m thick and the ice beneath is clean. Stream courses usually follow the margin of rubble-covered ice, but Kucera (1987) observed one on the glacier in a channel 4 m wide and 3 m deep which dropped to a depth of about 10–15 m to become an englacier stream leaving a route marked by abandoned moulins up to 3 m in diameter. Probably because of the insulating moraine cover, Dome Glacier has receded comparatively less than the Athabasca Glacier, with which it coalesced at one time. Starting about 1875, it receded 530 m from 1875 to 1919 and 318 m from 1919 to 1953. At least four recessional moraines appear between the terminal moraine remnants and the present ice front: 1900, 1908, 1913, and 1918 (Heusser, 1954).

Boundary Glacier

The *Boundary Glacier* is a 2-km-long cirque glacier, 1.18 km^2 in area. It is located on the divide between the Saskatchewan and Athabasca watersheds and on the boundary between Banff and Jasper National Parks. It flows from the slopes of Mount Athabasca at 3,320 m asl to a low-gradient accumulation basin at 2,750 m and thence to two ice tongues at 2,365 m asl. The ELA lies at about 2,730 m. Gardner and Jones (1985) and Gardner (1987) have studied the sediment budget and bergschrund/randkluft erosion here. Sloan (1987) reported that debris deposition along the 350-m tongue is at a rate of 4,400 kg d^{-1}. A retreat of 810 m from the "Little Ice Age" maximum has been determined. Intermediate snout positions have been mapped (fig. 9). This is one of the few glaciers in the Rockies for which there is recent evidence of a significant advance.

Hilda Glacier

Hilda Glacier is a small cirque glacier fed largely by avalanching from the eastern slopes of Mount Athabasca (3,491 m). It is about 2.5 km long, 1.35 km^2 in area. It has a large debris-rich proglacial area 1 km long that starts at the prominent Neoglacial moraine (2,055 m), rises to the snout at 2,170 m, and thence to the upper accumulation area at 2,900 m. The glacier surface is covered by a thin mantle of supraglacier debris supplied by rockfalls and avalanches. According to Heusser (1954), retreat began around 1790, but he made no measurements because the lower end of the glacier was hidden by debris (Field and Heusser, 1954). During 1977 and 1978, while the glacier was still receding, a study of sediment supply and transport was initiated (Hammer and Smith, 1983). When seen by Heusser (1956), the lower part was a boulder mass with humps and pockets that gave the appearance of concentric "waves" in several places. This morainal complex characterizes the mass as an incipient rock glacier. In the continuum from glacier (mostly ice) to rock glacier (mostly rock fragments), the morainal complex falls into the rock glacier classification. Folds of soil that have been pushed up along the down-valley periphery suggest that the mass continues to exhibit motion.

Winston Churchill Range (PC13)

Stretching north-northeast from the Columbia Icefield some 30 km to the fork in the Athabasca and Sunwapta Rivers is the Winston Churchill Range (fig. 1, PC13). Summit elevations in the main part of the range exceed 3,100 m and reach a maximum at Mount Alberta (3,619 m). The *Diadem Icefield* includes a number of individual glaciers around Mounts Alberta and Woolley, extends northward in a continuous 10-km mass from Diadem Peak to Mount McGuire, and encompasses Gong Glacier (3.5 km) to the west. Lying outside this ice field are additional small glaciers, usually located in deep cirques on north- to northeast-facing slopes. Glaciers average 2 to 3 km in length, up to 1 km^2 in area, and have snouts close to 2,000 m. A characteristic of this region is the large amount of morainal debris lying on and around many of the glacier termini, in a number of cases grading into classic rock glaciers. Stutfield and Collie (1903) concluded that the rock glaciers were formed from massive rockfalls from the limestone cliffs at some time in the past.

Chaba Group (PC14)

Northwest of the Columbia Icefield, and contiguous with it and the Clemenceau Icefield, lies the Chaba Icefield (fig. 20). This 97-km^2 irregular, elongated ice mass runs along and beyond the Continental Divide for some 27 km. Its northeast side drains into the Athabasca River through a number of outlet glaciers, chief of which are Chaba Glacier (9-km long), *West Chaba Glacier* (7 km long) and Misty Glacier (3.5 km long). The ice field and its environs include some 30 glaciers that range from 1 to 3 km in length, with snouts reaching to elevations of 2,000–2,300 m asl. The ELA probably lies at about 2,300 m, some 500 m below the regional glaciation level established by Østrem (1966). J.M. Thorington, in one of the few reports from this area, reported a recession of 170 m from the 1927 position established by the Harvard University group in 1936 (McCoubrey, 1938). Summit elevations in the central portion of the ice field exceed 3,100 m. Northward, toward Fortress Lake and Wood River, summit elevations decline to below 2,800 m.

Clemenceau Icefield Group (PC15)

Previous writers have stated confidently that the Columbia Icefield is the largest in the Rocky Mountains, yet the Clemenceau Icefield (figs. 7, 20), including its outliers south of Tsar Mountain (*Clemenceau Icefield Group*; fig. 1, PC15), is only slightly smaller (313 km^2). It is linked to both the Chaba and Columbia Icefields (figs. 7, 20) by Wales Glacier, which has one major accumulation basin in each ice field. Most of the drainage is through two outlet glaciers: (1) a major compound glacier on the northern part of the ice field that reaches a maximum length of 13 km and consists of the Tusk, Clemenceau, and Duplicate Glaciers, whose cumulative moraines have created an extensive debris-covered tongue that feeds Clemenceau Creek and (2) Apex Glacier, a triangular-shaped outlet glacier that flows 13.5 km south from the mountain of the same name. The larger outlet glaciers push down to below 1,500 m asl, with one debris-covered tongue reaching to 1,035 m. The ELA is about 2,200 m and the glaciation level at

2,700 m. The highest point of this ice field is appropriately Mount Clemenceau (3,630 m); most of the other major peaks in the group exceed 3,000 m. The isolation and inaccessibility of the region have inhibited glaciological research, visits being limited to a few climbing parties.

Fryatt Group (PC16)

West of the Athabasca River and north of Fortress Lake and Alnus Creek is the *Fryatt Group* (fig. 1, PC16), a series of mountain ridges stretching to the northeast some 15 km from a 30–km ridge that follows the provincial boundary. Apart from Catacombs Mountain (3,292 m), elevations in the southern part are generally below 3,000 m but rise northward to about 3,100 m, attaining a maximum at Mount Fryatt (3,361 m). Most of the glaciers lie in northeast-facing cirques below the boundary ridge; they are <2 km long and terminate between 2,000 and 2,100 m. A 5–km-long glacier flows north and northwestward from Catacombs Mountain. Around Mount Fryatt the glaciers are shorter and at higher elevations.

Whirlpool Group (PC17)

The ranges surrounding Whirlpool River, west of the *Fryatt Group* and north of Clemenceau Icefield, have been referred to as the *Whirlpool Group* (fig. 1, PC17). The *Whirlpool Group* consists of two separate blocks, or ranges, divided by the valley of the Whirlpool River and Athabasca Pass, which for many years was a major fur-trade thoroughfare that effectively split the Hooker and Mount Brown Icefields (fig. 4). The former ice field is an irregular mass of contiguous glaciers covering about 90 km^2 and includes the Kane, Hooker, North Alnus, South Alnus, and Serenity Glaciers, each about 4 to 5 km long, as well as the main body of the ice field itself. Other glaciers in this part of the group tend to be 1 to 2 km long. Several snouts push down to 1,800 m or lower. Apart from contributions to Whirlpool River, the glaciers drain west through Fortress Lake and Wood River. Mount Brown Icefield is a more regular ice mass <5 km^2 in area. Glaciers in the northern extension of the range, south of Simon Creek, tend to be slightly smaller than those to the south and include several debris-covered tongues and rock glaciers. Some descriptions of the glaciers around Athabasca Pass date from the time of the fur traders. Scott Glacier was first observed by David Douglas in 1827 (Douglas, 1914). Schafer (1954) reported that its retreat began in 1780 and that by 1924 the glacier had contracted 650 m. In 1952, the Alpine Club of Canada (1953) reported that the lower part of Scott Glacier, which in 1924 covered a large part of the outwash plain, had almost disappeared after a recession of some 1.2 km in 28 years (fig. 9). Despite early miscalculations of the elevation of Mount Brown that led to suggestions that it might be the highest peak in the Rocky Mountains, its highest point is only 2,799 m asl. Summit elevations are generally lower here than in the *Park Ranges* to the east. Although some peaks in and around the Hooker Icefield exceed 3,200 m asl, most are below 3,000 m, and northward they tend to even lower elevations.

Unnamed Ranges (—)

West of the Clemenceau Icefield, the Whirlpool, and the *Fraser-Rampart Groups*, and south of the Selwyn Range, is a group of unnamed ranges that mark the western limits of the *Park Ranges* in this section. Individual ranges within the group generally trend to the southwest; runoff from the ranges drains into what used to be the Canoe River in the Rocky Mountain Trench but what is now Canoe Reach of the artificial McNaughton Lake. West of Clemenceau Icefield, there are numerous small glaciers, usually <1 km in length, that terminate between 2,200 and 2000 m, along with some evidence of debris-covered tongues and rock glaciers. The largest glaciers in the southern section are no larger than 1 km^2 in area. Average peak heights are usually below 2,700 m, considerably lower than in the ranges to the east. Østrem's (1966) investigations put the regional glaciation level at 2,500–2,600 m.

The central section of the unnamed ranges, west of the Hooker and Mount Brown Icefields, contains one range with much larger ice bodies than those found in the southern part of the unnamed ranges, including a contiguous mass of glacier ice that is about 17 km^2 in area and lies south of the Mount Brown Icefield. However, as in the area in the southern part of the unnamed ranges, the other ranges have a profusion of small glaciers; usually in well-developed cirques, <1.5 km long and about 0.5 km^2 in area. Most end below 2,200 m, with several reaching as low as 1,700 m. Large moraines are much in evidence. Peaks here are slightly higher, some exceeding 3,000 m asl, but most are in the 2,600- to 2,800-m range.

The final, northern section of these unnamed ranges consists of mountains within and west of Mount Robson Provincial Park (fig. 4) bounded by Fraser River and Ptarmigan Creek. Peaks here are lower than to the south, with the highest rising to just over 2,800 m asl. Most of the ice is concentrated in a small ice field about 6 km^2 in area. Lengths of the some 15 glaciers here range from 0.5 to 1.5 km, with two at 2.5 km. Snouts are between 2,100 and 2,300 m asl.

Cavell Group (PC18)

Just west of the Banff-Jasper Highway rises the impressive Mount Edith Cavell (3,363 m), named after a First World War nurse who was shot for helping Allied troops trapped behind enemy lines to escape. It is the focal point of the *Cavell Group* (fig. 1, PC18), a small range with summit elevations ranging from 2,800 m to more than 3,000 m and with a number of small glaciers and rock glaciers that terminate as low as 2,100 m and that are from 0.5 to 2 km in length. A trail leads from the highway to the foot of Angel Glacier.

Angel Glacier

On the north side of Mount Edith Cavell lies a group of ice masses that at one time formed part of the same glacier. The lower part, a reconstituted, debris-covered ice mass, is known as *Cavell Glacier*. The long, thin ice stream, which once joined to the upper Angel Glacier, was known as Ghost Glacier; appropriately this glacier has now vanished. Angel Glacier, named for the two "wings" of ice adhering to the slopes of Mount Edith Cavell (Lang, 1943), occupies a cirque with a collection area of 0.89 km^2. The bulk of the ice mass lies between 2,250 and 2,600 m (fig. 27). According to Østrem (1966, 1973b), the glaciation level is at about 2,600 m asl, with the equilibrium line altitude some 300 m below. This implies that Angel Glacier has a generally positive balance; something that seems to be confirmed by the small hanging glacier (150–190 m long) that flows from it; frequent ice falls confirm its active nature.

Cavell Glacier

The lower *Cavell Glacier* is a gently sloping, heavily debris-laden mass of ice barely reaching 2,000 m asl; its snout is at 1,750 m. The glacier thus lies entirely below the equilibrium line altitude and survives thanks to its heavy, insulating debris cover and the shelter from the Sun provided by the neighboring mountains. Curiously, this was one of the glaciers selected by the DWPB in 1945 for routine surveys, which was abandoned in 1947 when it was realized that the tongue was completely separated from the accumulation area and hence that the debris-covered tongue was not toward the northwest for more than 60 km. Peaks here tend to be lower than in many other parts of the *Park Ranges* discussed so far. Average elevations are close to 2,600 m; the highest peak reaches to just over 2,800 m. About 40 small glaciers and ice fields are scattered throughout the range, though most are found in the three southernmost transverse ridges. The largest of the ice fields is some 3 km^2 in area. The glaciers average about 1 km in length with snouts between 2,100 and 2,300 m. The regional glaciation level lies between 2,600 and 2,700 m.

Continental Ranges [North—Yellowhead Pass to Muskwa Ranges (M)]

The final section of the Continental Ranges lies north of Yellowhead Pass. The indistinct zone of the Foothills marks the eastern boundary, while the western boundary continues as the Rocky Mountain Trench, which contains the Fraser River. Except for the area around Mount Robson, elevations of the mountain ranges generally decrease farther to the north. The mountains themselves becoming less distinct and less glacierized than those to the south that have just been described. In addition, the isolation and inaccessibility of this part of the Continental Ranges has meant that far fewer geographical names are available to aid in their description. The glaciers are usually of the small, mountain variety. They are larger and more numerous in the mountains along and west of the divide around Mount Robson, in the *Swiftcurrent Icefield*, and northward in the vicinity of the Resthaven Icefield (figs. 28, 29).

Front Ranges (North) (FN)

The Front Ranges here (fig.1, FN) are narrow and long; they include the Boule, Bosche, De Smet, Hoff, Berland, Persimmon, and Starlight Ranges and one called The Ancient Wall. North of these ranges are additional unnamed ranges before the northern limit at Mount May and the valley of the Kakwa River.

Boule Range (FN1)

Lying between Moosehorn Creek and the Rocky Mountain Foothills, Boule Range (fig. 1, FN1) is the easternmost section of this part of the Front Ranges. It is just over 20 km in length and is 3 to 5 km wide. Because summit elevations generally lie below 2,300 m and only reach a maximum of 2,429 m in Mount Kephala, it is not surprising there is no permanent ice cover here.

Bosche Range (FN2)

Slightly longer (25 km) than the Boule Range to the east, the Bosche Range (fig. 1, FN2) is bounded on the west by the Snake Indian River. Peak heights average around 2,400 m, and therefore glaciers are not in evidence.

De Smet Range (FN3)

The innermost of the three parallel ranges that form the southern section of the northern Front Ranges, the De Smet Range (fig. 1, FN3) consists of a series of mountains and ridges strung out over 30 km as a northwesterly extension of the Jacques Range. Elevations here also average about 2,300 to 2,400 m, so there is no evidence of glacierization.

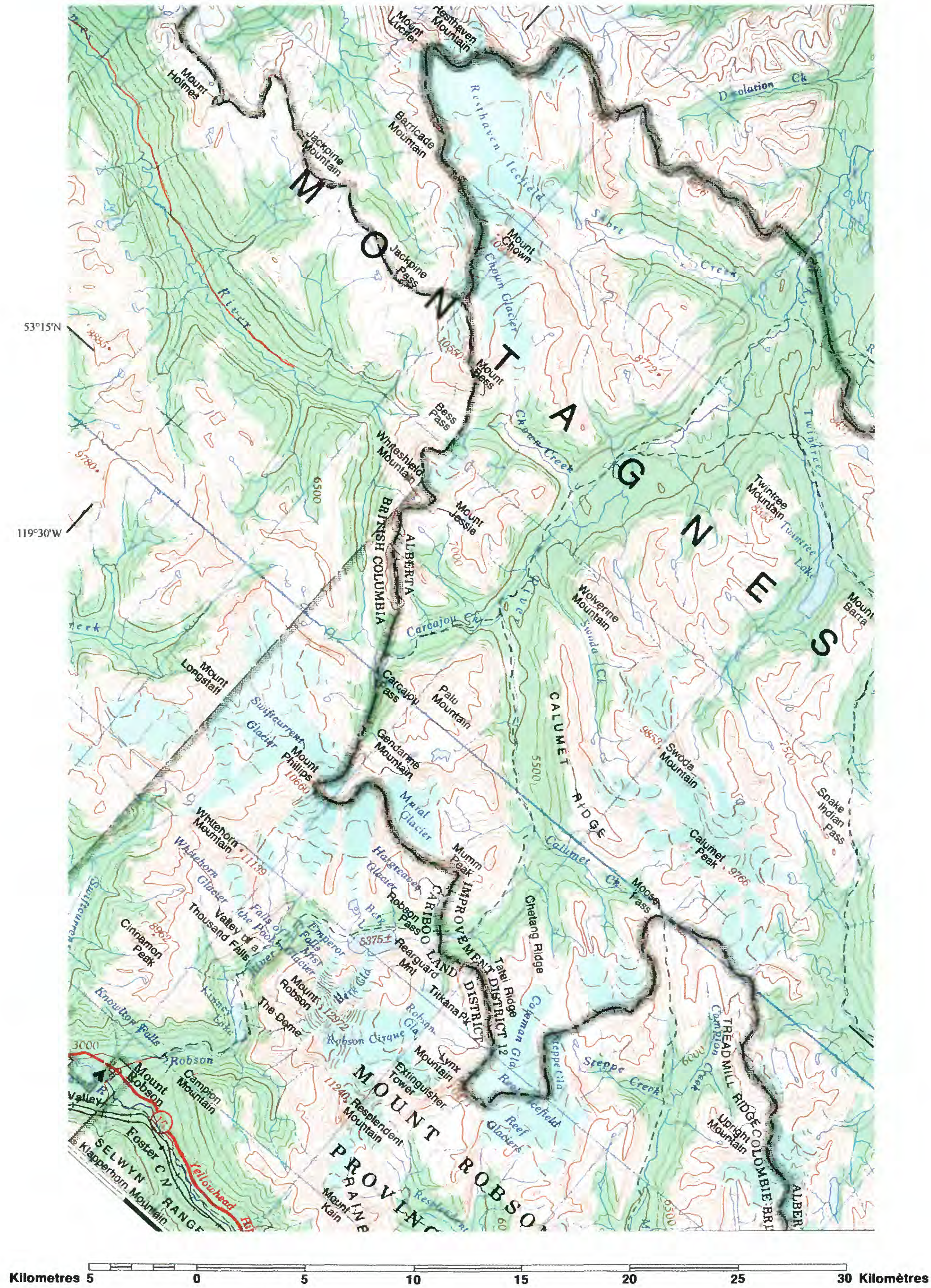

Mount Lucifer
Resthaven Mountain
Mount Holmes
Desolation Ck
Barricade Mountain
Jackpine Mountain
Resthaven Icefield
MONTAGNES
Mount Chown
Jackpine Pass
Chown Glacier
River
53°15'N
10650
Mount Bess
9772
Bess Pass
Chown Creek
Whiteshield Mountain
9780
6500
Mount Jessie
Twintree Mountain
Twintree Lake
119°30'W
BRITISH COLUMBIA
ALBERTA
7000
Wolverine Mountain
Mount Barra
Carcajou Ck
Smoky River
Swoda Ck
Mount Longstaff
Carcajou Pass
Palu Mountain
CALUMET RIDGE
Swiftcurrent Glacier
Gendarme Mountain
Mount Phillips
10660
9853
Swoda Mountain
5500
7500
Snake Indian Pass
Whitehorn Mountain
11130
Mural Glacier
Calumet Ck
Calumet Peak
9766
Whitehorn Glacier
Mumm Peak
Hargreaves Glacier
Moose Pass
Cinnamon Peak
8962
Valley of a Thousand Falls
Falls of the Pool
Emperor Falls
Robson Pass
CARIBOO LAND
IMPROVEMENT DISTRICT 12
Chetang Ridge
5375±
Berg Lake
Rearguard Mtn
Mount Robson
12972
Berg Gla
Tatei Ridge
Tilkana Pk
Robson Gla
Coleman Gla
The Dome
Knowlton Falls
Kinney Lake
Robson Cirque
Lynx Mountain
Steppe Creek
Campion Creek
TREADMILL RIDGE
3000
Robson
Mount Robson
Campion Mountain
Extinguisher Tower
Resplendent Mountain
11240
MOUNT ROBSON PROVINCIAL
Reef Icefield
Reef Glacier
Upright Mountain
COLOMBIE-BRITANNIQUE
ALBERTA
Valley
Foster
CN
SELWYN RANGE
Yellowhead
Klapperhorn Mountain
Mount Kain
RAINBOW
6000
6500
Kilometres 5
0
5
10
15
20
25
30 Kilomètres

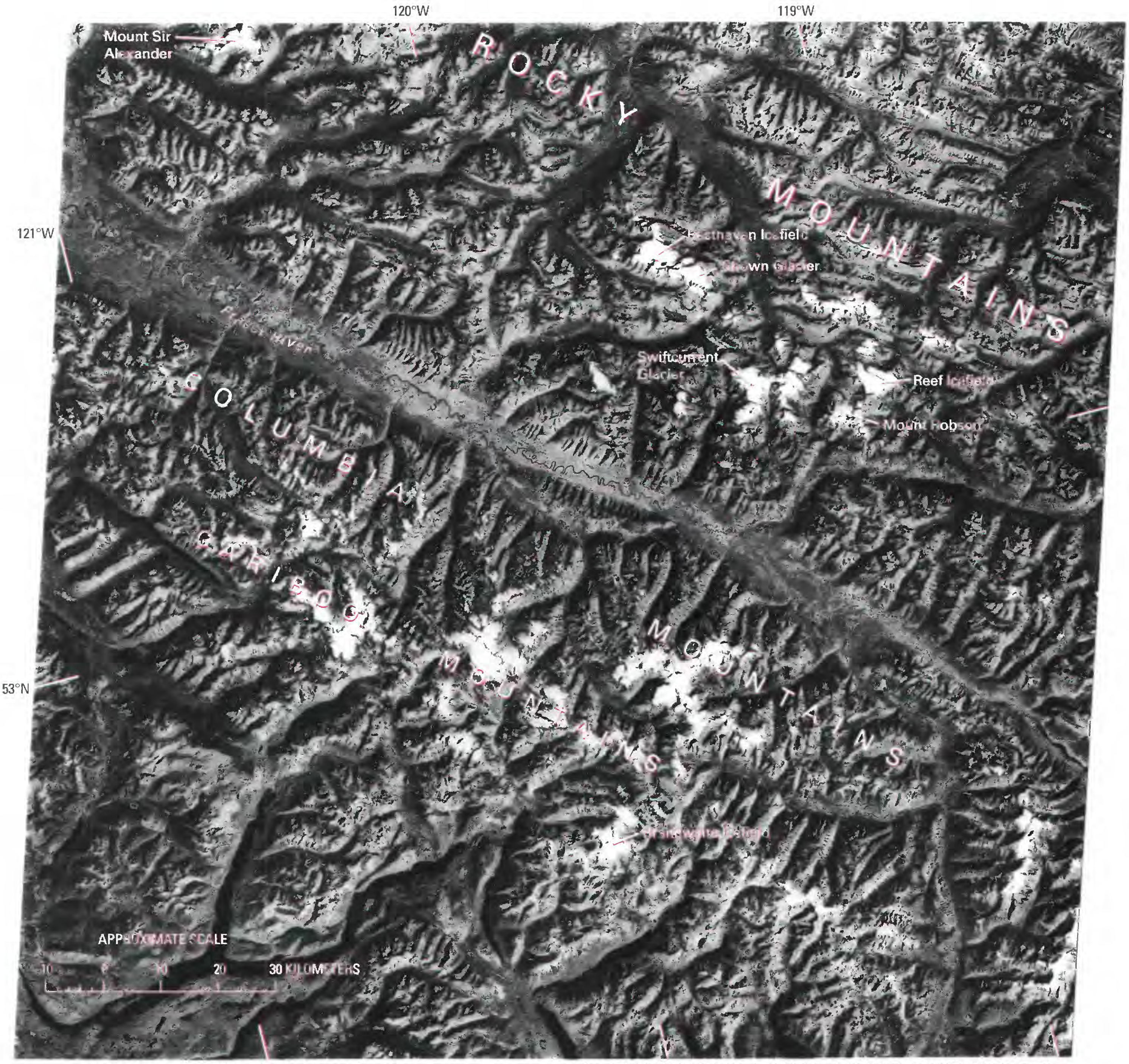

Figure 28.—*(opposite page) Segment of the 1:250,000-scale topographic map (Mount Robson, 83E) of Mount Robson and environs, Jasper National Park, Alberta, and Mount Robson Provincial Park, British Columbia, showing ice fields along the divide from Reef Icefield to Resthaven Icefield. ©1988. Produced under licence from Her Majesty the Queen in Right of Canada, with permission of Natural Resources Canada.*

Figure 29.—*Annotated Landsat 1 MSS image of part of the glacierized northern Rocky Mountains from Mount Robson (3,954 m), the highest mountain in the Canadian Rockies, to Mount Sir Alexander (3,291 m), and the northern Columbia Mountains (Cariboo Mountains), British Columbia, east and west of the Fraser River, respectively. Landsat image (1420–18291, band 7; 16 September 1973; path 50, Row 23) from the EROS Data Center, Sioux Falls, S. Dak.*

Hoff Range (FN4)

North of Wildhay River lies the Hoff Range (fig. 1, FN4), another in a series of many parallel, northwest-trending ranges that comprise the Front Ranges. The maximum elevation is 2,440 m on Mount Campion, but most of the higher peaks are 100 m or more lower. No glaciers are found in this range.

Berland Range (FN5)

The Berland Range (fig. 1, FN5), which lies between the Hoff and Persimmon Ranges, has two peaks more than 2,600 m asl but no evidence of a present-day ice cover. As with the Hoff Range, there are mountains north of Berland River that seem to be a natural extension of the Hoff Range, although that name is not now applied to them.

Persimmon Range (FN6)

The next parallel range to the west is the 50-km-long Persimmon Range (fig. 1, FN6) having peak elevations on the order of 2,500 to 2,800 m. As currently applied, the northern limit of this range appears to be the valley of Sulphur River, though that of the Smoky River, 15 km to the north, represents a more significant physiographic break.

Starlight Range (FN7)

West of Rock Creek is the Starlight Range (fig. 1, FN7), which forms part of a mountain block whose northern boundary is marked by the valley of the South Sulphur River. Peaks lie below 2,500 m asl, so this area is also unglacierized. Although unnamed, an extension of the Starlight Range extends northwestward to the valley of the Smoky River, paralleling the Persimmon Range, with similar heights and no glaciers.

The Ancient Wall (FN8)

The final range in this transect is known as The Ancient Wall (fig.1, FN8). It forms a massive rampart overlooking Blue Creek and has heights comparable to those in the eastern ranges. The extension of the mountain block of which this forms a part is northwestward to the deeply incised Rockslide Creek and northward to Hardscrabble Creek. Summit elevations are below 2,800 m and no glaciers are visible.

Unnamed Ranges (—)

The remaining groups in the northern Front Ranges are unnamed. North and east of the Smoky and Muddywater Rivers and south of Sheep Creek is what might be called the *Llama Group*. The summit elevations are below 2,500 m, and there are no glaciers. North of the *Llama Group* and south of Kakwa River is the last of the mountain blocks in the Front Ranges. Mount May at 2,450 m asl is representative of the average height of the peaks in this area. Lack of adequate precipitation and low elevation account for the fact that there are no glaciers here.

Park Ranges (North) (PN)

The northern section of the *Park Ranges* (fig. 1, PN), the last group of mountains of the Continental Ranges, includes the Victoria Cross and Rainbow Ranges, the *Robson*, the *Whitehorn*, and *Resthaven Groups*, and Treadmill Ridge. As in the Front Ranges in this northern section of the Continental Ranges, there are several other significant unnamed ranges and groups. They extend as far as the *Sir Alexander Peaks* and Jarvis Creek, a headwater tributary of McGregor River and include the Reef Icefield, the

Swiftcurrent Icefield, the Resthaven Icefield, and significant ice accumulations around Mount Robson and Mount Sir Alexander (fig. 29).

Victoria Cross Ranges (PN1)

The Victoria Cross Ranges (fig. 1, PN1), 30 by 20 km in size, lie northwest of Jasper and south of Snaring River. Summit elevations generally rise westward from 2,500–2,600 m near the Athabasca River to more than 2,900 m in the section facing Treadmill Ridge. These elevations influence the distribution of the few existing glaciers. In the southern part of the ranges are well-developed cirques with tarns. In the west, overlooking Miette River, are several glaciers 0.5 km^2 in area, and one as large as 1 km^2. These glaciers terminate at around 2,000 m asl.

Unnamed Ranges (—)

Between the De Smet Range and The Ancient Wall in the east and the Victoria Cross Ranges and Treadmill Ridge in the west is an 80-km-long mass of mountains and ranges without a collective name that straddles the boundary between the *Park Ranges* and Front Ranges. Peaks heights average between 2,700 and 2,900 m, with a slight trend to lower elevations toward the northwest. Only one peak exceeds 3,000 m asl. More than 25 glaciers are scattered through a section just north of the Victoria Cross Ranges. Seven of these are more than 1 km in length, but most are 0.5 km or less in length, and only one glacier exceeds 1 km^2 in area. Between Snake Indian and Monte Cristo Mountains, at the northern end of these ranges, is a small ice field about 5 km^2 in area. Five of the associated glaciers are >1 km long and have termini 2,300 m asl.

Treadmill Ridge (PN2)

The provincial boundary, which in this section of the Rocky Mountains still lies on the Continental Divide, follows Treadmill Ridge (fig. 1, PN2) from Yellowhead Mountain in the south to Twintree Mountain in the north; streams from Treadmill Ridge drain eastward into Snaring River and westward into the Fraser River. Summit elevations increase northward from the 2,400 to 2,500-m range, through 2,600 to 2,800 m in the middle section, to a maximum of 3,003 m at Swoda Mountain. Increased glacierization of Treadmill Ridge follows this trend. A few small ice masses, <0.5 km^2 in area, can be seen in the southern section. The middle section contains almost 50 glaciers. They average between 0.5 and 1.5 km in length, terminate between 2,100 and 2,300 m, and the larger ones tend to lie on the eastern side of the divide. About 10 km^2 of the ice is concentrated around Upright Mountain. The densest glacier cover is in the north, between Calumet Peak and Swoda Mountain. Here, numerous glaciers cover almost 20 km^2 in area and include ones more than 3.5 km in length. The termini of the glaciers are located between 2,300 and 1,950 m asl. According to Østrem (1966), the glaciation level here is more than 2,700 m asl.

Robson Group (PN3)

The *Robson Group* (fig. 1, PN3) lies between Moose River on the east and the Smoky and Robson Rivers on the west. Mount Robson will be discussed below, as it lies within the subsidiary Rainbow Range. Peaks here are not unusually high, averaging less than 2,800 m, although Lynx Mountain does rise to 3,140 m asl. Glaciers are concentrated in Reef Icefield and its associated outlet glaciers, the Steppe, Coleman, and Reef Glaciers and cover about 24 km^2. The largest of these is Coleman Glacier with a length of 7.1 km. A northern outlier, about 6 km^2 in area, lies south of Moose Pass. Some of the larger glaciers extend below 2,000 m asl but most end between 2,100 and 2,200 m.

Rainbow Range (PN4)

The southern part of the *Robson Group*, a block of mountains extending some 30 km in a northwest direction, is known as the Rainbow Range (fig. 1, PN4). This part contains Mount Robson (fig. 30), at 3,954 m the highest mountain in the Rocky Mountains and thus one of the best known to Canadians. Although Resplendent Mountain exceeds 3,400 m asl, the other peaks in the range are less than 2,900 m. The western and southern sides of Mount Robson are so precipitous that little snow adheres to them. However, on the northeastern side, avalanching ice and snow contribute to a number of glaciers, of which the largest is Robson Glacier. Mist (2.5 km) and Berg (3.3 km) Glaciers discharge northward from the mountain; Berg Glacier produces small icebergs in the lake at its foot (1,638 m), which gives rise to both its name and that of the lake. A number of small glaciers lie along the ridge southeast of Resplendent Mountain and north toward the Reef Icefield. They average less than 2.5 km long and most end below 2,000 m.

Robson Glacier

Robson Glacier (fig. 30) heads in a magnificent snow-filled cirque (Robson Cirque) and flows for 7 km northeast and north to terminate in a small proglacial lake at about 1,700 m asl. Subsidiary ice streams join from Resplendent Mountain and Extinguisher Tower. Robson Glacier was visited by an American Geographical Society expedition in 1953. Glacier limits and variations were documented using photographic and botanical techniques (Field and Heusser, 1954; Heusser, 1954, 1956). Although Heusser (1956) dated moraines to 1801, 1864, 1891, 1907, 1912, 1922, 1931, Watson (1983) and Luckman (1986) resampled some of his sites and concluded, based on lichenometric evidence, that some of the trees had been likely overridden by ice advances in the late 12th or 13th centuries. Some recession values, including those reported by Wheeler (1915b, 1923), are given in figure 9. Coleman (1910) observed that the uplift of some warm air masses from the west by the 3,000 vertical meters of Mount Robson led to almost daily falls of snow on the summit and that this heavy precipitation must compensate for the small accumulation area of Robson Glacier.

Whitehorn Group (PN5)

The last large group of glaciers in this area is found northwest of Mount Robson in the 20 by 15 km *Whitehorn Group* (fig. 1, PN5). Peaks here range from 2,800 m asl to well over 3,000 m and include Whitehorn Mountain (3,395 m) and Mount Phillips (3,249 m). The glacier cover stretches in an almost continuous mass from Mural Glacier in the east past the two large mountains to the western edge of the group. This ice cover has been referred to as the *Swiftcurrent Icefield* after the largest of the outlet glaciers, the 7.5-km long Swiftcurrent Glacier, which pushes down to 1,814 m asl close to the tree line. Other outlet glaciers range in length from 3 to 5 km and most end below 2,000 m.

Unnamed Ranges (—)

The western part of the northern *Park Ranges*, between the valley of the Fraser River, which flows in the Rocky Mountain Trench, and the *Whitehorn* and *Resthaven Groups* consists of a number of unnamed ranges and groups. Generally the peaks are lower in this western part, on the order of 2,500 to 2,800 m asl. One higher area at the head of Horsey Creek contains a small ice field and some small local glaciers just less than 10 km^2 in size. Two small glaciers also lie in cirques below Whiteshield Mountain between the *Swiftcurrent Icefield* and Resthaven Icefields.

Figure 30.—*High-angle oblique aerial photograph of Mount Robson (3,954 m) and Mount Robson Glacier looking toward the southwest into Robson Cirque on 22 August 1964. The upper part of Berg Glacier can be seen on the right, partly hidden by Rearguard Mountain. U.S. Geological Survey photograph F642 taken by Austin Post is courtesy of Robert M. Krimmel, USGS.*

Resthaven Group (PN6)

One of the most significant major ice accumulations in the northern *Park Ranges* in the *Resthaven Group* (fig. 1, PN6) is the Resthaven Icefield and associated glaciers (fig. 31), including the Chown Glacier, which covers nearly 50 km^2. It lies on the provincial boundary between the Smoky and Jackpine Rivers. Many peaks rise above 3,000 m asl, the two tallest being Mounts Bess (3,215 m) and Chown (3,331 m). The glaciers lie predominantly east of the divide. The two major units are the ice field itself, more than 10 km in length, and Chown Glacier, 7.2-km long. These two glaciers penetrate to quite low elevations, terminating below 1,600 m asl. The ELA is likely to be about 2,400 m.

Unnamed Ranges (—)

Although the northern boundary of the *Resthaven Group* runs westward from Short Creek, the natural physiographic boundaries of the group lie farther north, extending to the junction of the Smoky and Jackpine Rivers. Despite one peak of 3,019 m, average elevations are below 2,600 m. The glacier-ice cover consists of a few small outliers of the Resthaven Icefield. Two outliers are about 2 km long and the other <0.5 km long.

Figure 31.—High-angle oblique aerial photograph of an outlet glacier from Resthaven Icefield, taken on 8 August 1961 looking toward the west-northwest. The cloud-shrouded summit of Resthaven Mountain is in the background. Prominent ogives downglacier from the ice fall are visible. U.S. Geological Survey photograph F313 taken by Austin Post is courtesy of Robert M. Krimmel, USGS.

Other Unnamed Ranges (—)

The largest area of unnamed mountains in the Continental Ranges can be found in the northwestern corner of the northern *Park Ranges*. This area is bounded on the south by the broad valley of the Jackpine River, on the west by the Rocky Mountain Trench, and on the north by a broad valley containing the McGregor River. Peak elevations average between 2,300 and 2,450 m and the highest peak here is only 2,650 m. Physiographically, the mountains could be divided into a number of individual ranges. Most of the glaciers in these unnamed ranges are very small and are scattered through the northeastern part of the mountains close to the large ice field around the *Sir Alexander Peaks*. Three exceed 1 km in length and, of these, the largest is the Wishaw Glacier at 3 km^2. There are also a handful of glaciers about 0.5 km long in the central part.

Sir Alexander Peaks (PN7)

The northern limit of the Continental Ranges (fig. 2, PN), *Sir Alexander Peaks* (fig. 2, PN7), is marked by one major ice field centered on Mount Sir Alexander (3,291 m) and two smaller ones farther north. Although one other mountain exceeds 3,000 m, summit elevations generally lie between 2,550 and 2,900 m, increasing slightly toward the northwest. The *Sir Alexander Icefield* fills the range lying between the valley of the McGregor River, to the south, and Jarvis Creek, which forms the boundary between the *Park Ranges* and Hart Ranges. Glacier ice covers some 65 km^2 and includes the *Kitchi*, *Menagerie*, and *Castle Glaciers*. Several glaciers more than 4 km in length can be found here with snouts pushing to below 1,600 m asl. The ELA lies below 2,000 m, the lowest ELA documented in the Rocky Mountains. Immediately north, above Kitchi Creek, lies a small ice field (<10 km^2) with several outliers, and to the northeast, south of Edgegrain Creek, is a 5-km^2 glacier flowing north from Mount St. George. Again, there are several other small glaciers in the vicinity, most of which are 0.5 to 0.7 km long. Terminus elevations are usually between 1,750 and 1,950 m. The other significant ice body lies in the northwest sector of the *Sir Alexander Peaks*, radiating from an unnamed peak (2,858) between Mount Dimsdale (2,805) and Cheguin Mountain (2,470 m). It covers an area of about 25 km^2 and consists of a number of glaciers longer than 3 km. One of these, flowing due north, has a snout at 1,250 m asl, although the norm is between 1,600 and 2,000 m.

Hart Ranges (H)

Up to the Hart Ranges (fig. 2, H), we have discussed only about half of the total areal extent of the Canadian Rocky Mountains. However, we have now reached a geographic location where there are far fewer glaciers and very little information in the literature on which to base a comprehensive discussion of the glacierization of the other half of the Rocky Mountains in Canada. The climber's guide dismisses this northern portion in a scant three pages, and Denton (1975) states that there are no glaciers marked on the maps from here to the Peace River, the northern boundary of the Hart Ranges.

The Hart Ranges extend northwestward from the *Park Ranges* (North) for some 275 km and are bounded laterally by the Rocky Mountain Foothills and the Rocky Mountain Trench. There is a steady decline in average peak elevations northward from about 2,800 m asl just north of the *Sir Alexander Peaks* to a low of about 2,000 m around Mount Reynolds in the center of the ranges before the elevations begin to increase as the Hart Ranges near the Peace River. The decline in glacierization of the southern part of the Hart Ranges is reflected in the elevation of the glaciation level determined by Østrem (1972); the elevation of the glaciation level declines from 2,400 m asl at the boundary with the Continental Ranges to 2,100 m in the center of the Hart Ranges.

Despite Denton's (1975) conclusion, there are, in fact, a number of glaciers in the Hart Ranges. In the area immediately east of the Dezaiko Range, between Narraway River and Hanington Creek on the east and Herrick Creek on the west, are dozens of small glaciers. The highest peaks here range from 2,500 to 2,900 m with glacier snouts terminating between 1,700 and 1,900 m asl. The glacier ice lies on both sides of the main Rocky Mountain spine with somewhat larger glaciers, on the order of 5 to 7 km^2 in area, on the western slopes. Average glacier lengths are from 1.5 to 2.5 km. North of Framstead Creek, several small glaciers can be found southeast of *Mount Pulley* (2,470 m). Most are less than 2 km in length and range up to 2.5 km^2 in area. To the east, between Framstead Creek and *Red River Creek*, is a glacierized outlier with several small ice masses, all having areas less than 0.5 km^2.

Just to the northeast of the Dezaiko Range lies the aptly named Ice Mountain, which has two fairly large ice fields about 4 km^2 and 8 km^2 in area, respectively. The largest glacier has an ice stream more than 6 km long that flows from 2,350 m to 1,400 m asl. The mountain is isolated from the main range.

Dezaiko Range (H1)

The Dezaiko Range (fig. 2, H1) has three small glaciers, each about 1 km^2 in area, situated around Mount Hedrick in the central part of the range. Maximum elevations here are more than 2,000 m, and the lower limit of permanent ice lies between 1,650 and 1,850 m asl.

Misinchinka Ranges (H2)

Herrick Creek cuts through the Rocky Mountains, forming the boundary between the Dezaiko and Misinchinka Ranges (fig. 2, H2). Both ranges have a northwest trend and parallel the Rocky Mountain Trench for some 250 km, terminating at the northern limit of the Hart Ranges, where the Peace River separates them from the Muskwa Ranges. Thanks to a major hydroelectric development, this limit can be clearly seen on Landsat images where the Peace Reach of Williston Lake follows the Peace River valley. The eastern limits are not well-defined, being marked by a number of river valleys such as those of Imperial Creek and the Anzac, Misinchinka, and Pine Rivers. These ranges have no glaciers according to modern topographical maps.

Pioneer Range (H3)

In the Pioneer Range (fig. 2, H3), the Monkman (5 km^2 in area), Parsnip (14 km^2 in area) (fig. 32), and Vreeland (2 km^2 in area) Glaciers can all be found, together with other small glaciers, on the southwestern part of the range, where the maximum elevation is found at Mounts Barton (2,400 m) and Vreeland (2,440 m). [See section "Mapping Glaciers in the *Interior Ranges* and Rocky Mountains with Landsat Data" for a further discussion of Monkman and Parsnip Glaciers.] These glaciers represent the most significant ice fields in the Hart Ranges.

Murray Range (H4)

By following the divide northward to the Murray Range (fig. 2, H4), one can find two small glaciers (<1 km^2) east of Sentinel Peak (2,500 m) and one (<0.5 km^2) in a sheltered spot northeast of Mount Dudzic (2,150). About 18 km to the northeast of the Murray Range, there are a few more small scattered ice bodies around Alexis Peak (2,123 m). Here the average maximum elevation of the peaks hovers around 2,000 m asl. This sector marks the northern limit of glaciers within the Hart Ranges.

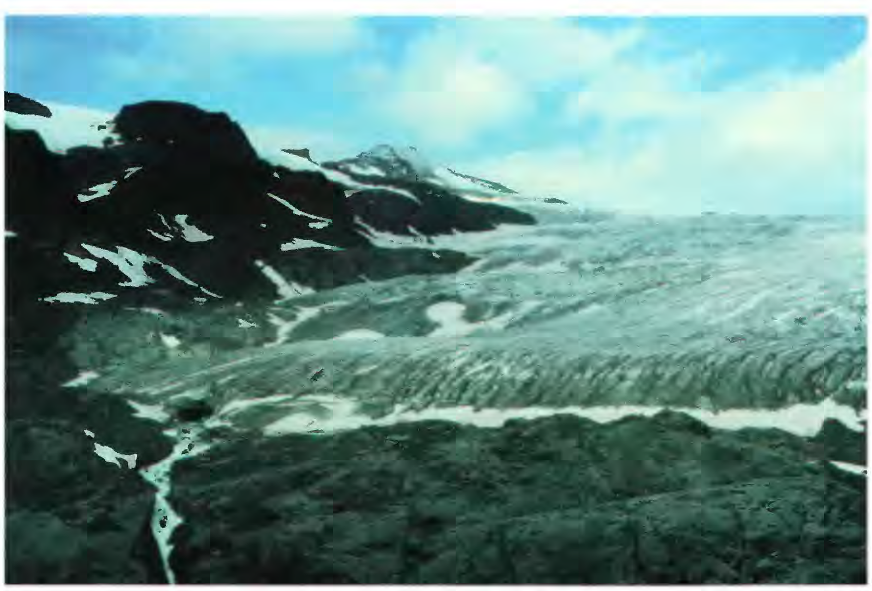

Figure 32.—*Photograph of Parsnip Glacier, Hart Ranges, northern Rocky Mountains, British Columbia. © 2000. Produced under licence from Her Majesty the Queen in Right of Canada, with permission of Natural Resouces Canada. Photograph No. A89S1, taken August 1989 by David Seeman, Canadian Forest Service, formerly with the Geological Survey of Canada.*

Muskwa Ranges (M)

The northernmost part of the Rocky Mountains is known as the Muskwa Ranges (fig. 2, M, and fig. 33), which contain many unnamed glaciers (fig. 34). From the Finlay and Peace Reaches of Williston Lake, the ranges extend in a northwesterly direction for some 500 km to their northern boundary, where the Liard River flows eastward to join the Mackenzie River. The ranges are bounded on the east by the Foothills, which at this latitude are a less-easily defined transition zone, and on the west by the northern Rocky Mountain Trench, here occupied by the Kechika and Finlay Rivers and Williston Lake.

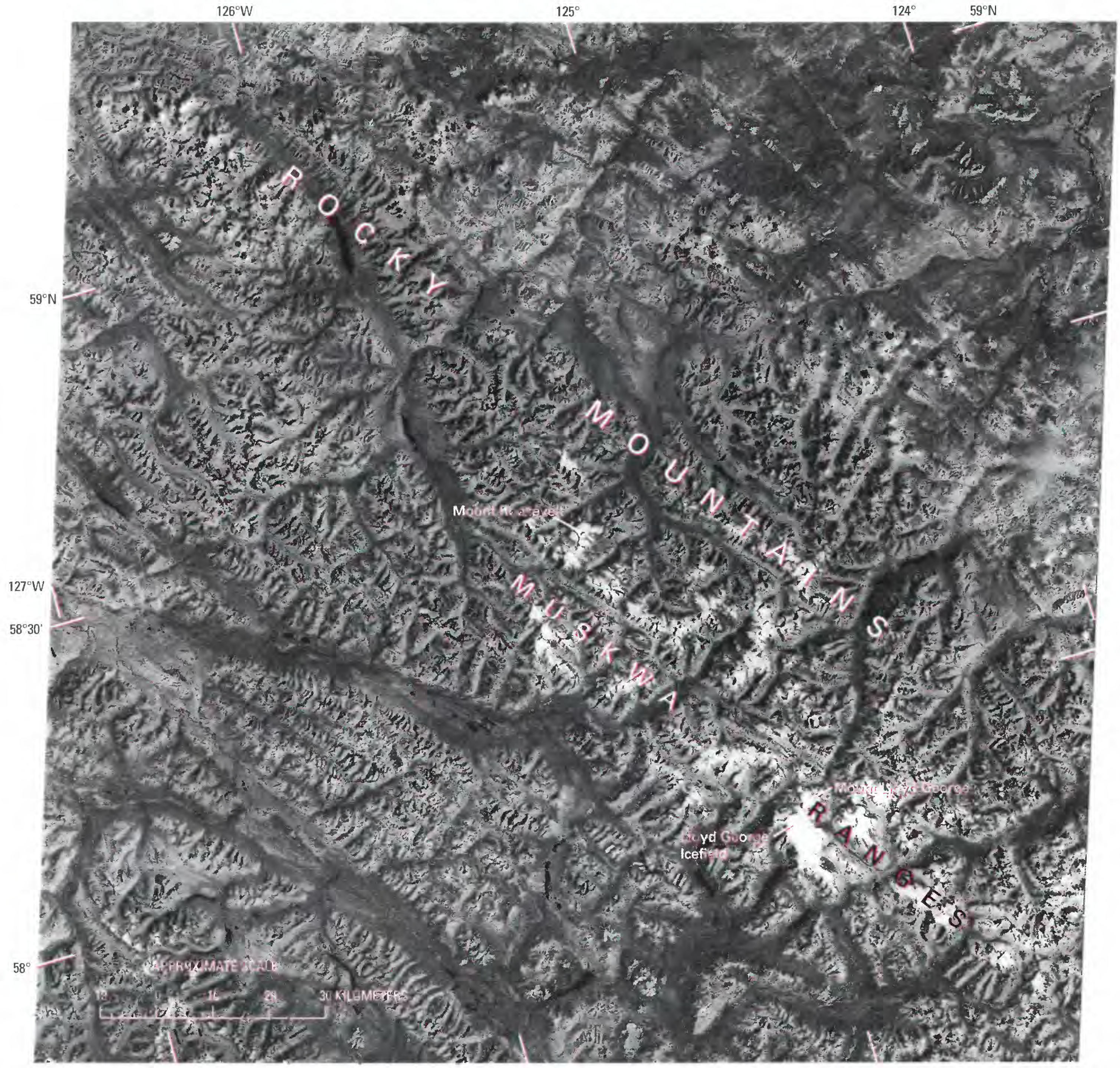

Figure 33.*—Annotated Landsat 1 MSS image mosaic showing the Muskwa Ranges, the northernmost part of the Canadian Rocky Mountains, including Mount Roosevelt (2,815 m), Mount Lloyd George (about 2,990 m), and the Lloyd George Icefield. There is substantial glacier cover in the area and the Lloyd George Icefield is more than 70 km^2. The Landsat images (1750–18535 and 1750–18542, band 7; 12 August 1974; Path 56, Rows 19 and 20) are from the EROS Data Center, Sioux Falls, S. Dak.*

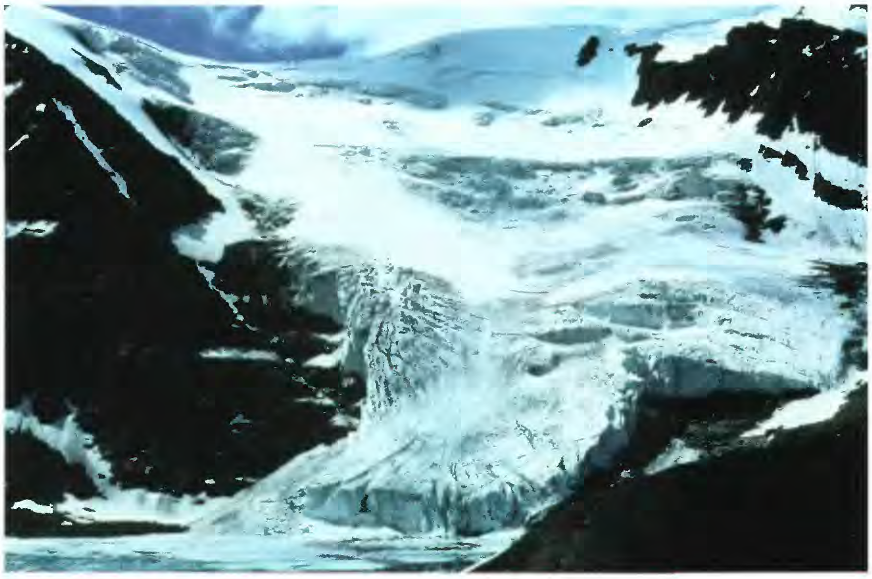

Figure 34.—Terrestrial photograph of an unnamed glacier in the Muskwa Ranges, northern Rocky Mountains. ©2000. Produced under licence from Her Majesty the Queen in Right of Canada, used with permission of Natural Resources Canada. Photograph A 89S2, taken August 1989 by David Seeman, Canadian Forest Service, formerly with the Geological Survey of Canada.

The first significant concentration of glaciers in the Muskwa Range is in the vicinity of the Great Snow Mountain area (fig. 2, M4). Several groups of glaciers are found northward from the Great Snow Mountain area along the main divide extending to the next concentration of glaciers in the Lloyd George Icefield—the final agglomeration in what the Climber's Guide (Putnam and others, 1974) calls the *Roosevelt-Churchill-Stalin Group*. With the name change of *Mount Stalin* to Mount Peck, this area will be referred to here as the *Allies Group* to reflect the remaining names of the Allied commanders and the numerous peak names that record the conferences they and other leaders attended.

The southern section of the Muskwa Ranges is a fairly broad, dissected mountain region with peaks trending from more than 2,200 m asl on the eastern side to an average of less than 2,000 m in the west, where many river valleys cut into the ranges. The block containing the Deserters (fig. 2, M1) and Akie Ranges (fig. 2, M2) is separated from the rest of the Muskwa Ranges by the broad valleys of the Ospika and Akie Rivers. The western section of the Muskwa Ranges, from the Truncate Range (fig. 2, M3) north of Akie River valley to the Tochieka Range (fig. 2, M5) and thence to Rabbit Plateau, is all free of glacier ice. East of Deserters Range, there are a few small glaciers on the eastern side of the main ranges below Mount Robb (2,500 m) and Mount Kenny (2,677 m). The largest is about 1.5 km^2 in area.

As the Great Snow Mountain area (fig. 2, M4) is approached, summit elevations increase and the glaciation level rises from 2,500 to 2,600 m asl. Around Mount McCusker (2,592 m) there are some small glaciers, all less than 0.5 km^2 in area, lying in entrenched, east-facing valleys. Immediately south of Great Snow Mountain area there are several small glaciers (<0.5 km^2) and ice fields. About 2 km^2 of ice is spread out along the eastern slope of Mount Helen, and another small ice field (1.5 km^2) lies southwest of Redfern Lake. However, most of the glacier ice in this section of the Muskwa Ranges is found just to the north.

Great Snow Mountain Area (M4)

The glacier cover in the Great Snow Mountain area (fig. 2, M4) can be divided conveniently into a northern component around Great Snow Mountain and a southern one centered on Mount Ulysses, separated by the valley of the Besa River and a tributary of Akie River. The former will here be called the *Great Snow Icefield* and the latter the *Odyssey Icefield*, reflecting the Homeric theme established in the local names. The fact that ice covers an area of more than 58 km^2 here is not properly reflected in Denton's (1975) observation that there are small glaciers in the vicinity. Østrem's (1972) map places the glaciation level here at close to 2,600 m.

Odyssey Icefield

Glaciers 3 to 4 km in length flow from Mount Ulysses (3,024 m) and the adjoining ridge to Cyclops Peak and Mount Penelope. The total area of ice here is about 38 km^2, of which outliers contribute about 4 km^2. The ice field includes Achaean Glacier (3.5 km^2), a 4-km-long glacier dropping to 1,600 m in elevation from the summit of Mount Penelope, and Ithaca Glacier, a broad ice mass on the northern side of *Odyssey Icefield*, covering over 7 km^2 and terminating at about 1,840 m asl.

Great Snow Icefield

East from Great Rock Peak (2,931 m), a number of small cirque glaciers and ice streams are found on either side of the ridges stretching to Redfern Mountain and Mount Stringer (2,795 m). Outliers here and to the west cover about 7 km^2 in area. The main ice field lies north and west of Great Snow Mountain and has an area in excess of 20 km^2, including two glaciers about 4 km^2 in area. Termini generally lie between 1,800 and 2,000 m asl.

Lloyd George Group (M6)

A major concentration of glaciers is found around Mount Lloyd George (approximately 2,990 m in elevation on the U.S. aeronautical chart ONC D–12), about 50 km to the northwest. In between are several small glaciers and ice fields, ranging in size up to 5 km^2, lying on either side of the divide between the Prophet and Muskwa Rivers on the east and the North Kwadacha River on the west.

Lloyd George Icefield

The Lloyd George Icefield (fig. 35) is bounded by the Warneford and Tuchodi Rivers. It extends about 19 km north to south and 13 km east to west. Peaks in this area range from 2,700 to over 2,900 m asl. The ice field covers about 70 km^2, much less than the area of 116 km^2 estimated by Odell (1949). Even with the attendant glaciers to the north and west, including McConnell Glacier (1.85 km^2), the total ice cover only approaches 180 km^2 in area.

An account of a visit to the *Lloyd George Group* (fig. 2, M6) has been given by Odell (1948, 1949), who reported on Llanberis Glacier, described as the main outlet glacier from the Lloyd George Icefield. This small glacier (2.7 km^2) flows westward towards Haworth Lake. He concluded that there had been no advance of the glacier since the end of the last "Ice Age" and that recession to its present snout position, 800 m from the moraine, had been slow. Much more ice is in fact drained from the ice field by the Kwadacha (15.5 km^2) and Lloyd George (10 km^2) Glaciers to the east. The latter lies on the divide between Mount Smythe and Mount Lloyd George; two-thirds of the ice drains to the south and one-third northward where it lies parallel to, but some 2 km to the east of, Quentin Glacier (2 km^2).

At the base of Mount Glendower, Odell's party discovered a large dying glacier, Stagnant Glacier (1 km^2), which filled the floor of the canyon and which was covered with a thick blanket of moraine, on the surface of which were growing plants up to 4.5-m high. The glacier is 3.5 km in length, 400 m wide, and has an upper limit at 1,800 m asl and a snout at about 1,350 m. Dead ice could be seen in thermokarst depressions and along the glacier margins. Odell observed that meltwater issuing from the glacier was of moderate amount and scarcely turbid.

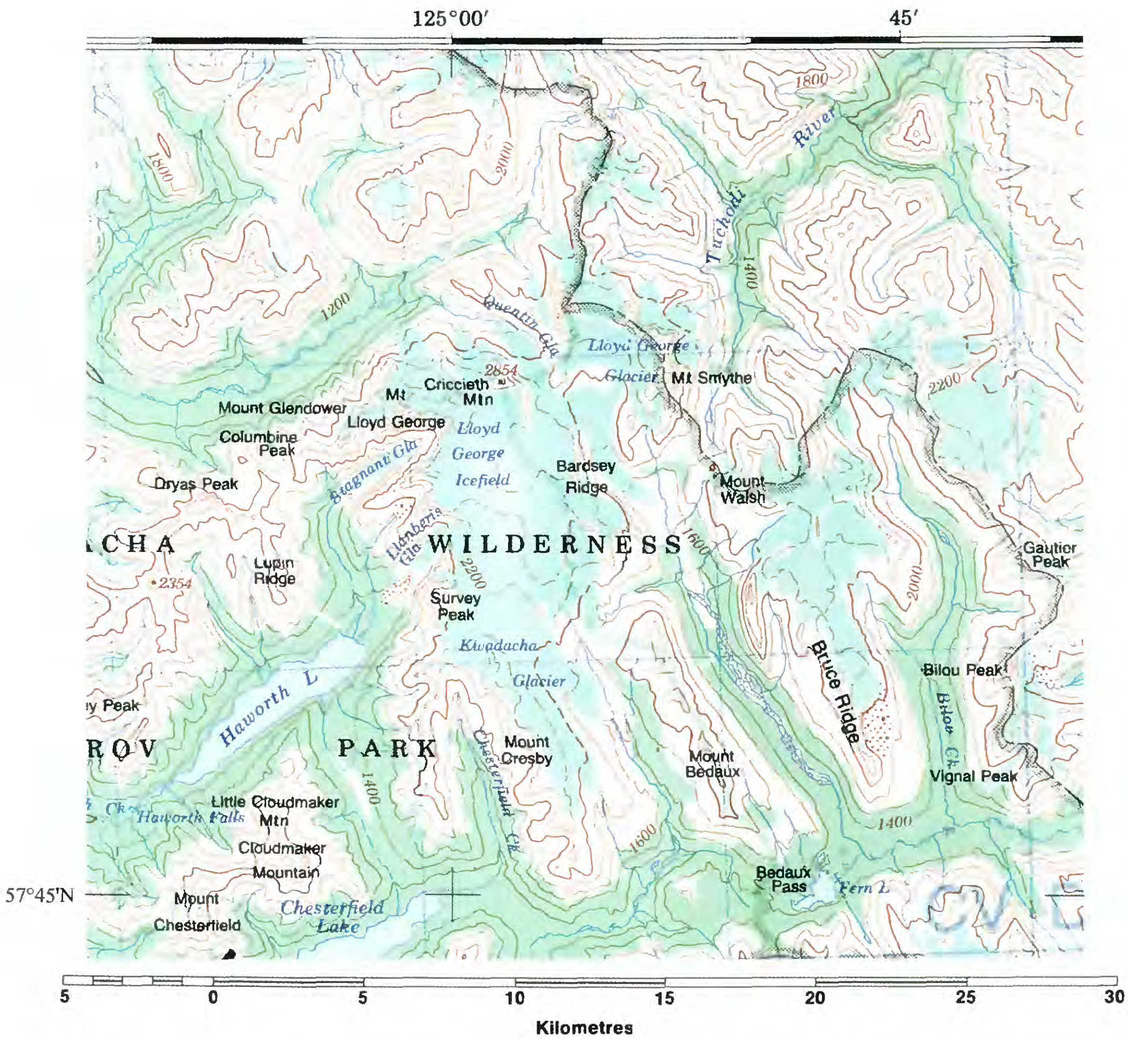

Figure 35.—Segment of the 1:250,000-scale topographic map of the Ware quadrangle (94F) showing the glacierized area around Mount Lloyd George, Muskwa Ranges, northern Rocky Mountains. ©1990. Produced under licence from Her Majesty the Queen in Right of Canada, with permission of Natural Resources Canada.

The final glacierized area within the Muskwa Ranges is situated just north of Lloyd George Icefield, in and around the *Allies Group*.

Allies Group (M7)

The *Allies Group* (fig. 2, M7) consists of four main mountain masses about equally covered in glaciers. Running the full length of the group on the eastern side is the Tower of London Range, bounded by Wokkpash Creek and separated from the rest of the group by the Racing River valley. To the west, and in the center, is the Battle of Britain Range. South of this, across the valley of a tributary of Gataga River, is an unnamed mountain mass with glaciers extending from Savio Mountain to Sicily Mountain. Because there are several Italian names here, this range will be referred to as the *Italy Range*. North of the Battle of Britain Range, separated by Churchill Creek, is the last mountain block of this group; glaciers extend from Tehran Peak northward to Mount Roosevelt and Delano Creek. For convenience this will be referred to as the *Allied Leaders Range* because of the association of Churchill and Roosevelt. No mention has previously been made of glaciers in this area by either Denton (1975) or Gadd (1986), which is surprising considering that the glacierized area here amounts to almost 200 km^2. However, Østrem (1972) did plot a glaciation level for this region rising toward the east from 2,600 to 2,700 m asl and shows many glaciers at the head of Racing River.

Battle of Britain Range

About 37 km^2 of this range is covered by glaciers. The glaciers lie within the hydrological basins of Churchill Creek and of rivers draining northeastward to Racing River and southwestward to Gataga River. Summit elevations along this divide, from Churchill Peak to the Exploration and Lindisfarne Peaks, range from 2,200 m to more than 2,600 m asl. Most of the glaciers are between 1 km^2 and 3 km^2 in area, but the largest is almost 5 km in length and 4.5 km^2 in area. Glaciers tend to be situated on the northern slopes of the northeast- to southwest-trending Battle of Britain Range.

Tower of London Range

The area of ice in the Tower of London Range is about 30 km^2; glaciers are situated on either side of the main range line running from Mount Aida northward to Fusilier Peak. Mountain heights rise to a maximum of 2,815 m at Mount Peck. Glaciers range in size from 0.5 to 2 km^2 to two glaciers at about 4 km^2, including Fusilier Glacier, to the largest, Wokkpash Glacier, at 9 km^2, a compound glacier consisting of four "ice streams" and well-developed medial moraines. Some 5 km^2 of glacier ice is found outside the range to the east.

Italy Range

Summit elevations in this range are comparable to those in the Tower of London Range, rising to a maximum of 2,853 m at King Peak. The glaciers, many of which exceed 2 km^2 in area, lie on either side of the main divide, which trends to the southwest. They cover a total area of almost 55 km^2. The largest glacier (8 km^2) is more than 10 km long and flows northward from Sicily Mountain.

Allied Leaders Range

This range can be divided into three sections. The southern section, centered on Tehran Peak (2,734 m) lies south of Grizzly Pass; the largest glacier in this section is about 5 km^2 in area. In the central section, extending eastward from Mount Caen (2,762 m) through Normandy Mountain (2,856 m) to Falaise Mountain (2,743 m), glaciers covering an area of 15 km^2 are spread out on both sides of the divide; the largest glacier is 3.7 km^2 in area. The final section, south of Delano Creek, extends from Scheldt Mountain (2,759 m) through Mount Roosevelt (2,815 m) to the east. Glaciers cover more than 20 km^2 with two exceeding 4 km^2.

Total glacier-ice cover in the *Allied Leaders Range* is about 45 km^2. The largest glaciers extend to about 1,700 m, but most terminate between 1,800 and 1,900 m asl.

North and West of *Allies Group*

Outside the *Allies Group*, glaciers are found up to 10 km to the west. Glaciers cover some 23.5 km^2 with one glacier 5.5 km^2 in size.

Finally, there are still a few glaciers in the Muskwa Ranges up to 30 km to the northwest of the *Allies Group*. The main concentration is a few kilometers north in the vicinity of Yedhe Mountain (2,685 m), where 8 km^2 of ice lies on the east slope, flowing down to elevations below 2,000 m and scattered in patches toward Toad River.

West of Toad River, and north of Gataga River, are several moraine and rock-glacier systems amongst which can be found a few small glaciers amounting in total to less than 1 km^2 of exposed ice. The northern limit of glaciers in the Muskwa Ranges lies at 58°25'N. The remaining mountain blocks (fig. 2), Stone Range (fig. 2, M8), Sentinel Range (fig. 2, M9), Terminal Range (fig. 2, M10), and Rabbit Plateau (fig. 2, M11), are unglacierized.

References Cited

Alpine Club of Canada, 1953, Changes in Scott Glacier—1924–1952: Canadian Alpine Journal, v. 36, p. 168.

Bahr, D.B., and Dyurgerov, M.[B.], 1999, Characteristic mass-balance scaling with valley glacier size: Journal of Glaciology, v. 45, no. 149, p. 17–21.

Baranowski, Stanislav, and Henoch, W.E.S., 1978, Glacier and landform features in the Columbia Icefield area, Banff and Jasper National Parks, Alberta, Canada: Ottawa, Environment Canada, Inland Waters Directorate, Glaciology Division, (Supplementary report on a study carried out for Parks Canada), 175 p. (with maps)

Batterson, M.J., 1980, Contemporary frontal moraine formation in the Yoho Valley, British Columbia: St. John's, Newfoundland, Department of Geography, Memorial University of Newfoundland, M.Sc. thesis, 150 p.

Benoît, Isabelle, Champoux, A., Ommanney, S., and Dubois, J.-M.M., 1984, Clef pour la photo-interprétation des glaciers tempérés (le glacier Athabasca, Canada): Photo Interprétation, no. 84–4, p. 29–32.

Bigras, S.C., 1978, Glacier des Poilus: Ottawa, Carleton University, Department of Geography, B.A. thesis, 86 p.

Binda, G.G., Johnson, P.G., and Power, J.M., 1985, Glacier control of suspended-sediment and solute loads in a Rocky Mountain basin, *in* Water Quality Evolution within the Hydrological Cycle of Watersheds, Canadian Hydrology Symposium No. 15, 1984, Québec, 10–12 June 1984, Proceedings: National Research Council of Canada, Associate Committee on Hydrology, NRCC No. 24633, v. 1, p. 309–327.

Boles, Glen, 1974, The Columbia Ice Field: Canadian Alpine Journal, v. 57, p. 33–34.

Boles, G.W., Kruszyna, R., and Putnam, W.L., 1979, The Rocky Mountains of Canada—American Alpine Club, Alpine Club of Canada Climber's Guide, 7th ed.: New York, American Alpine Club, and Banff, Alberta, Alpine Club of Canada, 473 p.

Bray, J.R., 1964, Chronology of a small glacier in eastern British Columbia: Science, v. 144, no. 3616, p. 287–288.

———1965, Forest growth and glacier chronology in north-west North America in relation to solar activity: Nature, v. 205, no. 4870, p. 440–443.

Bray, J.R., and Struick, G.J., 1963, Forest growth and glacial chronology in eastern British Columbia and their relation to recent climatic trends: Canadian Journal of Botany, v. 41, no. 8, p. 1245–1271.

B.C. Mountaineer, 1939, Glacier crashes in Banff National Park: The B.C. Mountaineer, v. 17, no. 2, p. 2–3.

Brugman, M.M., 1989, Mining glaciers on Mount Cline, Alberta; an assessment: Saskatoon, Sask., Environment Canada, National Hydrology Research Institute, Hydrology Division, NHRI Contribution No. 89054, 25 p.

Brunger, A.G., 1966, The Drummond, Hector and Peyto Glaciers—Their wastage and deposits: Edmonton, Alberta, University of Alberta, Department of Geography, M.Sc. thesis, 100 p.

Brunger, A.G., Nelson, J.G., and Ashwell, I.Y., 1967, Recession of the Hector and Peyto Glaciers—Further studies in the Drummond Glacier, Red Deer Valley area, Alberta: Canadian Geographer, v. 11, no. 1, p. 35–38.

Butler, Dana, Lyons, W.B., Hassinger, J.[M.], and Mayewski, P.A., 1980, Shallow core snow chemistry of Athabasca Glacier, Alberta: Canadian Journal of Earth Sciences, v. 17, no. 2, p. 278–281.

Campbell, P.I., Reid, I.A., and Shastal, John, 1969, Glacier surveys in Alberta: Ottawa, Department of Energy, Mines and Resources, Water Survey of Canada, Inland Waters Branch Report Series No. 4, 16 p.

Canada, Energy, Mines and Resources, 1978, Surveying Columbia Icefield. How big is the Columbia Icefield? Is it shrinking or growing? Swelling or reducing river systems? New techniques help find out: GEOS, Winter, p. 9–12.

Canada, Environment Canada, 1976, 1974–1976 survey of the Athabasca and Saskatchewan Glaciers: Calgary, Alberta, Environment Canada, Inland Waters Directorate, Western Region, Calgary District Office, Water Survey of Canada, Internal report, 36 p.

———1980, Columbia Icefield: Ottawa, Department of Energy, Mines and Resources, Surveys and Mapping Branch, map, scale 1:50,000, produced by National Hydrology Research Institute, Inland Waters Directorate and Parks Canada, Western Region, Department of the Environment.

———1982, 1978–1980 survey of the Athabasca and Saskatchewan Glaciers: Calgary, Alberta, Environment Canada, Inland Waters Directorate, Calgary District Office, Water Survey of Canada, Internal Report, 36 p.

Canadian Permanent Committee on Geographical Names, 1985, Gazeteer of Canada—British Columbia, 3rd ed.: Ottawa, Canada Department of Energy, Mines, and Resources, 281 p.

———1988, Gazeteer of Canada—Alberta, 3rd ed.: Ottawa, Canada Department of Energy, Mines, and Resources, 64 p.

Carter. R.L., 1954, Study of glaciers in Banff and Jasper National Parks, 1952 and 1954: Calgary, Alberta, Department of Mines and Resources, Forests and Scientific Services Branch, Dominion Water and Power Bureau, Report No. 2160–(52 and 54), surveys under the direction of R.D. May, mimeo, 32 p.

Carter, R.L., Blair, R.V., Fowler, E.D., and Thorson, K.M., 1956, Study of glaciers in Banff and Jasper National Parks, 1956: Calgary, Alberta, Department of Northern Affairs and National Resources, Water Resources Branch, Report No. 2160–(56), mimeo, 27 p.

Cavell, Edward, 1983, Legacy in ice—The Vaux family and the Canadian Alps: Banff, Alberta, Altitude Publishing, 98 p.

Chapman, E.F., Morton, G.H., Thorson, K.M., McGeachy, D.A., Elder, V.S., and Loeppky, K.D., 1960, Survey of glaciers in Banff and Jasper National Parks, 1960: Calgary, Alberta, Department of Northern Affairs and National Resources, Water Resources Branch, Report No. 2160–(60), mimeo, 31 p.

Church, Michael, and Gilbert, Robert, 1975, Proglacial fluvial and lacustrine environments, *in* Jopling, A.V., and MacDonald, B.C., eds., Glaciofluvial and glaciolacustrine sedimentation: Society of Economic Paleontologists and Mineralogists Special Publication No. 23, p. 22–100.

Clee, T.E., Savage, J.C., and Neave, K.[G.], 1969, Internal friction in ice near its melting point: Journal of Geophysical Research, v. 74, no. 4, p. 973–980.

Coleman, A.P., 1903, The Brazeau Ice-field: Geographical Journal, v. 21, no. 5, p. 502–510.

———1910, Geology and glacial features of Mt. Robson: Canadian Alpine Journal, v. 2, no. 2, p. 108–113.

Collie, J.N., 1899, Climbing in the Canadian Rockies: Alpine Journal, v. 19, no. 144, p. 441–446.

Collier, E.P., 1958, Glacier variation and trends in run-off in the Canadian Cordillera, *in* General Assembly of Toronto, v. 4, September 3–14, 1957: Association Internationale d'Hydrologie Scientifique Publication No. 46, p. 344–357.

Collins, D.N., 1982, Flow-routing of meltwater in an alpine glacier as indicated by dye tracer tests: Bern, Beitrage zur Geologie der Schweiz—Hydrologie, v. 28, no. 2, p. 523–534.

Collins, D.N., and Young, G.J., 1979, Separation of runoff components in glacierized alpine watersheds by hydrochemical analysis, *in* Canadian Hydrology Symposium 79, Cold Climate Hydrology, Vancouver, B.C., 10–11 May 1979, Proceedings: Ottawa, National Research Council of Canada (NRCC 17834), Associate Committee on Hydrology, p. 570–581.

———1981, Meltwater hydrology and hydrochemistry in snow- and ice-covered mountain catchments: Nordic Hydrology, v. 12, no. 4–5, p. 319–334.

Davies, K.F., Froelich, C.R., Heinze, L., and Kerber, R., 1966, Surveys of glaciers on the eastern slope of the Rocky Mountains in Banff and Jasper National Parks, 1966: Calgary, Alberta, Department of Northern Affairs and National Resources, Water Resources Branch, Report No. 2160–(66), mimeo, 30 p.

Davies, K.F., Loeppky, K.D., Sapp, E., and Wagner, H.M., 1964, Survey of glaciers on eastern slope of Rocky Mountains in Banff and Jasper National Parks, 1964: Calgary, Alberta, Department of Northern Affairs and National Resources, Water Resources Branch, Report No. 2160–(64), mimeo, 21 p.

Davies, K.F., Warner, L.A., Anderson, J.E., and Dahl, B.M., 1970, Survey of glaciers on the eastern slopes of the Rocky Mountains in Banff and Jasper National Parks—1970 report: Calgary, Alberta, Department of Energy, Mines and Resources, Inland Waters Branch, Water Survey of Canada Division, Internal Report, 29 p.

Davis, D.A., Loeppky, K.D., Sapp, E., and Adams, R.E., 1962, Study of glaciers on eastern slope of Rocky Mountains in Banff and Jasper National Parks, 1962: Calgary, Alberta, Department of Northern Affairs and National Resources, Water Resources Branch, Report No. 2160–(62), mimeo, 32 p.

Denton, G.H., 1975, Glaciers of the Canadian Rocky Mountains, *in* Field, W.O., ed., Mountain Glaciers of the Northern Hemisphere, v. 1: United States Army Cold Regions Research and Engineering Laboratory, p. 603–653.

Derikx, Leo, 1973, Glacier discharge simulation by ground-water analogue, *in* Symposium on the Hydrology of Glaciers, Cambridge, 7–13 September 1969, Association Internationale d'Hydrologie Scientifique Publication No. 95, p. 29–40.

———1975, The heat balance and associated runoff from an experimental site on a glacier tongue, *in* Snow and Ice Symposium, Moscow, August 1971, Proceedings: IAHS-AISH Publication No. 104, p. 59–69.

Derikx, L., and Loijens, H.[S,], 1971, Model of runoff from glaciers, *in* Hydrology Symposium No. 8, v. 1: Canada National Research Council, Associate Committee on Geodesy and Geophysics, Subcommittee on Hydrology, p.153–199.

Douglas, David, 1914, Journal kept by David Douglas during his travels in North America, 1823–1827: London, Wesley, 364 p.

Dyurgerov, M.B., and Bahr, D.B., 1999, Correlations between glacier properties—Finding appropriate parameters for global glacier monitoring: Journal of Glaciology, v. 45, no. 149, p. 9–16.

Epstein, Samuel, and Sharp, R.P., 1959, Oxygen-isotope variations in the Malaspina and Saskatchewan Glaciers: Journal of Geology, v. 67, no. 1, p. 88–102.

Field, W.O., 1949, Glacier observations in the Canadian Rockies, 1948: Canadian Alpine Journal, v. 32, p. 99–114.

———1979, Freshfield Glacier, 1953: Ottawa, Environment Canada, National Hydrology Research Institute, Snow and Ice Division, Unpublished report, 45 p.

Field, W.O., Jr., and Heusser, C.J., 1954, Glacier and botanical studies in the Canadian Rockies, 1953: Canadian Alpine Journal, v. 37, p. 128–140.

Foessel, D.G., 1974, An analysis of the temperature distribution over the Peyto Glacier, Alberta: Guelph, Ontario, Guelph University, Department of Geography, M.Sc. thesis, 137 p.

Föhn, P.M.B., 1973, Short-term snow melt and ablation derived from heat- and mass-balance measurements: Journal of Glaciology, v. 12, no. 65, p. 275–289.

Ford, D.C., 1975, Caving six miles under an Alberta glacier: Canadian Geographical Journal, v. 91, no. 4, p. 20–24.

———ed., 1983, Castleguard Cave and Karst, Columbia Icefields area, Rocky Mountains of Canada—A symposium: Arctic and Alpine Research, v. 15, no. 4, p. 425–560.

Fowler, E.D., Chapman, E.F., Thorson, K.M., and Rainsberry, K.C., 1958, Study of glaciers in Banff and Jasper National Parks, 1958: Calgary, Alberta, Department of Northern Affairs and National Resources, Water Resources Branch, Report No. 2160–(58), unpublished, 29 p.

Freeman, L.R., 1925, On the roof of the Rockies: Toronto, Ontario, McClelland and Stewart, 270 p.

Gadd, B., 1986, Handbook of the Canadian Rockies; geology, plants, animals, history and recreation from Waterton Glacier to the Yukon: Jasper, Alberta, Corx Press, 876 p.

Gardner, J.[S.], 1972, Recent glacial activity and some associated landforms in the Canadian Rocky Mountains, *in* Slaymaker, H.O., and McPherson, H.J., eds., Mountain Geomorphology—Geomorphological Processes in the Canadian Cordillera: Vancouver, Tantalus Research Limited, B.C. Geographical Series no. 14, p. 55–62.

———1977, The Wenkchemna Glacier: Canadian Alpine Journal, v. 60, p. 58–59.

———1978a, Wenkchemna Glacier—Ablation complex and rock glacier in the Canadian Rocky Mountains: Canadian Journal of Earth Sciences, v. 15, no. 7, p. 1200–1204.

———1978b, What glaciers do for western Canada: Canadian Geographical Journal, v. 96, no. 1, p. 28–33.

———1983, Accretion rates on some debris slopes in the Mt. Rae area, Canadian Rocky Mountains: Earth Surface Processes and Landforms, v. 8, no. 4, p. 347–355.

———1987, Evidence for headwall weathering zones, Boundary Glacier, Canadian Rocky Mountains: Journal of Glaciology, v. 33, no. 113, p. 60–67.

Gardner, J.S., and Jones, N.K., 1985, Evidence for a Neoglacial advance of the Boundary Glacier, Banff National Park, Alberta: Canadian Journal of Earth Sciences, v. 22, no. 11, p. 1753–1755.

Glossop, J., Morton, G.H., Anderson, J.E., Slobosz, F., and Clayton, V., 1968, Survey of glaciers on the eastern slope of the Rocky Mountains in Banff and Jasper National Parks, 1968: Calgary, Alberta, Department of Energy, Mines and Resources, Inland Waters Branch, Water Survey of Canada, Report No. 2160–(68), mimeo, 29 p.

Goodison, B.[E.], 1972a, An analysis of climate and runoff events for Peyto Glacier, Alberta: Ottawa, Environment Canada, Water Resources Branch, Inland Waters Directorate Scientific Series No. 21, 29 p.

———1972b, The distribution of global radiation over Peyto Glacier, Alberta: Ottawa, Environment Canada, Water Resources Branch, Inland Waters Directorate Scientific Series No. 22, 22 p.

Goodman, R.H., 1970, Radio-echo sounding on temperate glaciers—A Canadian view, *in* Gudmandsen, P.[E.], ed., Proceedings of the International Meeting on Radio Glaciology, May 1970: Lyngby, Technical University of Denmark, Laboratory of Electromagnetic Theory, p. 135–146.

———1973, Time-dependent intraglacier structures: Journal of Glaciology, v. 12, no. 66, p. 512–513.

———1975, Radio echo sounding on temperate glaciers: Journal of Glaciology, v. 14, no. 70, p. 57–69.

Gottlieb, Lars, 1980, Development and applications of a runoff model for snowcovered and glacierized basins: Nordic Hydrology, v. 11, no. 5, p. 255–272.

Gray, J.K., 1962, The Mummery and Freshfield Glaciers: Canadian Alpine Journal, v. 45, p. 27–33.

Habel, Jean, 1898, The north fork of the Wapta: Appalachia, v. 8, no. 4, p. 327–336.

——1902, At the western source of the Athabaska River: Appalachia, v. 10, no. 1, p. 28–43.

Hallet, Bernard, 1976a, Deposits formed by subglacial precipitation of $CaCO_3$: Geological Society of America Bulletin, v. 87, no. 7, p. 1003–1015.

———1976b, The effect of subglacial chemical processes on glacier sliding: Journal of Glaciology, v. 17, no. 76, p. 209–221.

———1977, Subglacial chemical deposits and the composition of basal ice, *in* Isotopes and Impurities in Snow and Ice Symposium, proceedings of the Grenoble Symposium, August/September 1975: IAHS-AISH, Publication No. 118, p. 289–292.

Hallet, Bernard, and Anderson, R.S., 1980, Detailed glacial geomorphology of a proglacial bedrock area at Castleguard Glacier, Alberta, Canada: Zeitschrift für Gletscherkunde und Glazialgeologie, v. 16, no. 2, p. 171–184.

Hammer, K.M., and Smith, N.D., 1983, Sediment production and transport in a proglacial stream—Hilda, Alberta, Canada: Boreas, v. 12, no. 2, p. 91–106.

Hamper, M.J., and Smith, N.D., 1983, Suspended sediment transport in glacier-fed Lake Louise, Alberta, Canada [abs.]: Geological Society of America 17th Annual Meeting, North-Central Section, Madison, Wisconsin, 28–29 April 1983, Abstracts with Programs, v. 15, no. 4, March, p. 227.

Harmon, Don, and Robinson, Bart, 1981, Columbia Icefield—A solitude of ice: Banff, Alberta, Altitude Publishing Ltd., 103 p.

Hector, James, 1861, On the geology of the country between Lake Superior and the Pacific Ocean and between the 48th and 54th parallels of latitude: Quarterly Journal of the Geological Society of London, v. 17, p. 388–445.

Henoch, W.E.S., 1967, Surface measurements of glacierized area in Canada: Ottawa, Department of Energy, Mines and Resources, Water Research Branch, Glaciology Section, Unpublished report, 4 p.

———1971, Estimate of glaciers' secular (1948–1966) volumetric change and its contribution to the discharge in the upper North Saskatchewan River basin: Journal of Hydrology, v. 12, no. 2, p. 145–160.

Henoch, W.E.S., and Croizet, J.L., 1976, The Peyto Glacier map—A three-dimensional depiction of mountain relief: The Canadian Cartographer, v. 13, no. 1, p. 69–86.

Heusser, C.J., 1954, Glacier fluctuations in the Canadian Rockies: General Assembly of Rome, International Association of Hydrological Sciences, International Union of Geodesy and Geophysics, IASH Publication No. 39, p. 493–497.

———1956, Postglacial environments in the Canadian Rocky Mountains: Ecological Monographs, v. 26, no. 4, p. 263–302.

Hickson, J.W.A., 1915, Notes of trip to the Saskatchewan River and Freshfield Glacier (1913): Canadian Alpine Journal, v. 6, p. 93–98.

Hobson, G.D., and Jobin, Claude, 1975, A seismic investigation—Peyto Glacier, Banff National Park and Woolsey Glacier, Mount Revelstoke National Park: Geo-exploration, v. 13, no. 2, p. 117–127.

Holdsworth, Gerald, 1984, Preliminary report on the dynamics and hydrology of Cathedral Glacier, Yoho National Park, B.C.: Calgary, Alberta, Environment Canada, National Hydrology Research Institute, Internal Report, 19 p.

Holdsworth, Gerald, Krouse, H.R., Shakur, A., and Peake, E., 1985, Reconnaissance of an ice core site, Columbia Ice Fields, Alberta: Calgary, Alberta, Environment Canada, Inland Waters Directorate, National Hydrology Research Institute, Internal report, 22 p.

Holdsworth Gerald, Power, J.[M.], and Christie, R.[O.], 1983, Radar ice thickness measurements on Peyto Glacier: Ottawa, Environment Canada, National Hydrology Research Institute, Snow and Ice Division, Internal report, 18 p.

Howarth, P.J., 1983, Evaluation of Landsat digital data for providing glaciological data: Ottawa, Environment Canada, National Hydrology Research Institute, Snow and Ice Division, Perennial Snow and Ice Section, Final report, Contract No. KN107–1–4656, March, 43 p.

Howarth, P.J., and Ommanney, C.S.L., 1983, Landsat digital data for updating glaciological information on topographic and glacier inventory maps, *in* Wellar, B.S., ed., Auto-Carto 6—Automated Cartography—International Perspectives on Achievements and Challenges, v. 2: p. 504–513.

IAHS/UNEP/UNESCO, 1988, Fluctuations of glaciers, 1980–1985, v. 5: Zürich, World Glacier Monitoring Service.

———1993, Fluctuations of glaciers, 1985–1990, v. 6: Zürich, World Glacier Monitoring Service.

———1999, Glacier mass balance bulletin, no. 5: Zürich, World Glacier Monitoring Service.

IAHS/UNESCO, 1998, Fluctuations of glaciers, 1990–95, v. 7: Zürich, World Glacier Monitoring Service.

Ice Age Co., The 1989 Cline Glacier ice mining project—Environmental impact assessment: Edmonton, Alberta, August, The Ice Age Co., Inc., 62 p.

Interprovincial Boundary Commission, 1924, Report of the Commission appointed to delimit the boundary between the Provinces of Alberta and British Columbia, Part II: Ottawa, Office of the Surveyor General, 155 p. (with maps)

Jackson, J.A., ed., 1997, Glossary of geology; 4th ed.: Alexandria, VA, American Geological Institute, 769 p.

Jackson, L.E., Jr., 1979a, A catastrophic glacial outburst flood (jökulhlaup) mechanism for debris flow generation at the Spiral Tunnels, Kicking Horse River basin, British Columbia: Canadian Geotechnical Journal, v. 16, no. 4, November, p. 806–813.

———1979b, Mystery flood solved—CPR records revealed the 1978 catastrophe was not unique...were other debris flows also triggered by jökulhlaups?: Ottawa, GEOS, Summer, Department of Energy, Mines and Resources, p. 2–4.

———1980, New evidence on the origin of the September 6, 1978 jökulhlaup from Cathedral Glacier, British Columbia: Geological Survey of Canada Paper No. 80–1B, p. 292–294.

Johnson, P.G., and Power, J.M., 1985, Flood and landslide events, Peyto Glacier terminus, Alberta, Canada, 11–14 July 1983: Journal of Glaciology, v. 31, no. 108, p. 86–91.

———1986, The role of high magnitude run-off events in glacierized basins: International Symposium “Glacier Mass-balance, Fluctuations and Run-off,” Alma-Ata, 30 September–5 October 1986, Proceedings: Moscow, Soviet Geophysical Committee, Academy of Sciences of the U.S.S.R., Data of Glaciological Studies No. 58, p. 82–87, 195–200.

Kanasewich, E.R., 1963, Gravity measurements on the Athabasca Glacier, Alberta, Canada: Journal of Glaciology, v. 4, no. 35, p. 617–631.

Kearney, M.C., 1981, Late Quaternary vegetation and environments of Jasper National Park, Alberta: London, Ontario, University of Western Ontario, Department of Geography, Ph.D. thesis, 318 p.

Keller, G.V., and Frischknecht, F.C., 1960, Electrical resistivity studies on the Athabasca Glacier, Alberta, Canada: Journal of Research, National Bureau of Standards, v. 64D, no. 5, p. 439–448.

———1961, Induction and galvanic resistivity studies on the Athabasca Glacier, Alberta, Canada, *in* Raasch, G.O., ed., Geology of the Arctic, v. 2: Toronto, Ontario, University of Toronto Press, p. 809–832.

Kennedy, S.K., 1975, Sedimentation in a glacier-fed lake: Chicago, University of Illinois at Chicago Circle, Department of Geological Sciences, M.Sc. thesis, 55 p.

Kite, G.W., and Reid, I.A., 1977, Volumetric change of the Athabasca Glacier over the last 100 years: Journal of Hydrology, v. 32, no. 3–4, February, p. 279–294.

Kodybka, R.J., 1982, History of the Yoho Glacier, British Columbia: Canadian Alpine Journal, v. 65, p. 56–57.

Konecny, Gottfried, 1963, Glacier surveys in western Canada: Photogrammetric Engineering, v. 30, no. 1, p. 64–82.

———1966, Applications of photogrammetry to surveys of glaciers in Canada and Alaska: Canadian Journal of Earth Sciences, v. 3, no. 6, p. 783–798.

Konovalov, V.G., 1987, Methods of calculation and remote-sensing measurements for the spatial distribution of glacier annual mass balance: Journal of Glaciology, v. 33, no. 114, p. 212–217.

Krouse, H.R., 1974, Stable isotopes in the study of snow and ice resources, *in* Advanced Concepts and Techniques in the Study of Snow and Ice Resources—An interdisciplinary symposium, Monterey, California, 2–6 December 1973: Washington, D.C., National Academy of Sciences, p. 651–660.

Krouse, H.R., Hislop, R.[W.P.], Brown, H.M., West, K.[E.], and Smith, J.L., 1977, Climatic and spatial dependence of the retention of D/H and O^{18}/O^{16} abundances in snow and ice of North America, *in* Isotopes and impurities in snow and ice, Proceedings of the Grenoble Symposium, August/September 1975: IAHS-AISH Publication No. 118, p. 242–247.

Kucera, R.E., 1971, What happens in front of a glacier: Ottawa, National Science Film Library, Research film, 16 mm, 15 minutes, listed in Cinematography in Research.

———1976, Exploring glaciers and mountains—Guide to Lake Louise and Moraine Lake: Canmore, Alberta, High Country, Box 5000, 61 p.

———1987, Exploring the Columbia Icefield, Rev. ed.: Canmore, Alberta, High Country, Box 5000, 64 p.

Kucera, R.E., and Henoch, W.E.S., 1978, Glacier and landform features in the Columbia Icefield area, Banff and Jasper National Parks, Alberta, Canada: Ottawa, Environment Canada, Inland Waters Directorate, Glaciology Division, Unpublished study carried out for Parks Canada, 131 p. (with maps)

Lang, A.H., 1943, Glaciers of the Rockies and Selkirks: Canadian Geographical Journal, v. 26, no. 2, p. 56–67.

Lawby, C.P., Smith, D.J., Laroque, C.P., and Brugman, M.M., 1994, Glaciological studies at Rae Glacier, Canadian Rocky Mountains: Physical Geography, v. 15, no. 5, p. 425–441.

Leonard, E.M., 1981, Glaciolacustrine sedimentation and Holocene glacial history, northern Banff National Park, Alberta: Boulder, Colorado, University of Colorado, Ph.D. thesis, 271 p.

———1985, Glaciological and climatic controls on lake sedimentation, Canadian Rocky Mountains: Zeitschrift für Gletscherkunde und Glazialgeologie, v. 21, no. 1–2, p. 35–42.

———1986a, Use of lacustrine sedimentary sequences as indicators of Holocene glacial history, Banff National Park, Alberta, Canada: Quaternary Research, v. 26, no. 2, p. 218–231.

———1986b, Varve studies at Hector Lake, Alberta, Canada, and the relationship between glacial activity and sedimentation: Quaternary Research, v. 25, no. 2, p. 199–214.

Letréguilly, Anne, 1988, Relation between the mass balance of western Canadian mountain glaciers and meteorological data: Journal of Glaciology, v. 34, no. 116, p. 11–18.

Loijens, H.S., 1974, Streamflow formation in the Mistaya River basin, Rocky Mountains, Canada: Proceedings of the Western Snow Conference, 42nd Annual Meeting, Anchorage, Alaska, p. 86–95.

Luckman, B.H., 1976, Glacial geomorphology at Mount Edith Cavell: London, Ontario, University of Western Ontario, Department of Geography, submitted to Parks Canada, Department of Indian Affairs and Northern Development, Unpublished report, 70 p.

———1977, Lichenometric dating of Holocene moraines at Mount Edith Cavell, Jasper, Alberta: Canadian Journal of Earth Sciences, v. 14, no. 8, p. 1809–1822.

———1986, Reconstruction of Little Ice Age events in the Canadian Rocky Mountains: Géographie Physique et Quaternaire, v. 40, no. 1, p. 17–28.

Luckman, B.H., and Crockett, K.J., 1978, Distribution and characteristics of rock glaciers in the southern part of Jasper National Park: Canadian Journal of Earth Sciences, v. 15, no. 4, p. 540–550.

Luckman, B.H., Frazer, G.W., Hamilton, J.P., and Harry, D.G., 1984, Field activities in the Canadian Rockies in 1983: London, Ontario, University of Western Ontario, Department of Geography, Report to Parks Canada and Mount Robson Provincial Park, 26 p.

Mathews, W.H., 1964a, Discharge of a glacial stream, *in* General Assembly of Berkeley, Symposium on Surface Waters, 19–31 August 1963: Association Internationale d'Hydrologie Scientifique Publication No. 63, p. 290–300.

———1964b, Sediment transport from Athabasca Glacier, Alberta, *in* General Assembly of Berkeley, Continental Erosion, Precipitation, Hydrometry, Humidity and Soil, August 19–31, 1963: Association International d'Hydrologie Scientifique Publication No. 65, p. 155–165.

May, R.D., Blair, R.V., and Harry, R.M., 1950, Study of glaciers in Banff and Jasper National Parks, 1950: Calgary, Alberta, Department of Mines and Resources, Surveys and Engineering Branch, Dominion Water and Power Bureau, Report No. 2160–(50), Unpublished, 34 p.

Mayewski, P.A., Pregent, G., Armstrong, T., Brown, P., Butler, D., Hassinger, J., Deschke, P., Palais, J., and Trombley, T., 1979, Results of the 1978 Athabasca Glacier Expedition: Durham, New Hampshire, University of New Hampshire, Department of Earth Science, Glaciology Report Series, 56 p.

McCarthy, D.P., 1985, Dating Holocene geomorphic activity of selected landforms in the Geikie Creek Valley, Mount Robson Provincial Park, British Columbia: London, Ontario, University of Western Ontario, Department of Geography, M.Sc. thesis, 303 p.

McCoubrey, A.A., 1938, Glacier observations, 1936 and 1937: Canadian Alpine Journal, v. 25, p. 113–116.

McFarlane, W.T., 1945, Study of glaciers in Banff, Yoho and Jasper National Parks, 1945: Vancouver, B.C., Department of Mines and Resources, Surveys and Engineering Branch, Dominion Water and Power Bureau, Report No. 2160–(45), Unpublished, 23 p.

———1946a, Glacier investigation in Banff, Yoho and Jasper National Parks: Canadian Alpine Journal, v. 29, no. 2, p. 265–273.

———1946b, Study of glaciers in Banff and Jasper National Parks, 1946: Vancouver, B.C., Department of Mines and Resources, Surveys and Engineering Branch, Dominion Water and Power Bureau, Report No. 2160–(46), Unpublished, 34 p.

———1947, Study of glaciers in Banff and Jasper National Parks 1947: Vancouver, B.C., Department of Mines and Resources, Surveys and Engineering Branch, Dominion Water and Power Bureau, Report No. 2160–(47), Unpublished, 40 p.

McFarlane, W.T., Blair, R.V., and Ozga, W.J., 1949, Study of glaciers in Banff and Jasper National Parks, 1949: Calgary, Alberta, Department of Mines and Resources, Surveys and Engineering Branch, Dominion Water and Power Bureau, Report No. 2160–(49), Unpublished, 34 p.

———1950, Glacier survey in Banff and Jasper National Parks, 1949: Canadian Alpine Journal, v. 33, p. 120–126.

McFarlane, W.T., and May, R.D., 1948, Study of glaciers in Banff and Jasper National Parks, 1948: Calgary, Alberta, Department of Mines and Resources, Surveys and Engineering Branch, Dominion Water and Power Bureau, Report No. 2160–(48), Unpublished, 32 p.

McPherson, H.J., and Gardner, J.S., 1969, The development of glacial landforms in the vicinity of the Saskatchewan Glacier: Canadian Alpine Journal, v. 52, p. 90–96.

Meek, Victor, 1948a, Glacier observations in the Canadian Cordillera: Canadian Geographical Journal, v. 37, no. 5, p. 190–209.

———1948b, Glacier observations in the Canadian Cordillera, *in* General Assembly of Oslo: IASH Publication No. 30, v. 2, p. 264–275.

Meier, M.F., 1958, The mechanics of crevasse formation, *in* General Assembly of Toronto, v. 4, September 3–14, 1957: Association Internationale d'Hydrologie Scientifique Publication No. 46, p. 500–508.

———1960, Mode of flow of Saskatchewan Glacier, Alberta, Canada: U.S. Geological Survey Professional Paper 351, 70 p.

———1965, Correspondence—Comments on Paterson's paper "Variations in velocity of Athabasca Glacier with time": Journal of Glaciology, v. 5, no. 41, p. 761–762.

Mills, H.H., 1977a, Basal till fabrics of modern alpine glaciers: Geological Society of America Bulletin, v. 88, no. 6, p. 824–828.

———1977b, Differentiation of glacier environments by sediment characteristics; Athabasca Glacier, Alberta, Canada: Journal of Sedimentary Petrology, v. 47, no. 2, p. 728–737.

———1977c, Textural characteristics of drift from some representative cordilleran glaciers: Geological Society of America Bulletin, v. 88, no. 8, p. 1135–1143.

Mokievsky-Zubok, Oleg, Ommanney, C.S.L., and Power, J.[M.], 1985, NHRI glacier mass balance, 1964–1984 (Cordillera and Arctic): Ottawa, Environment Canada, National Hydrology Research Institute, Surface Water Division, Glacier Section, NHRI internal report, 59 p.

Munro, D.S., 1975, Energy exchange on a melting glacier: Hamilton, Ontario, McMaster University, Department of Geography, Ph.D. thesis, 182 p.

Munro, D.S., and Davies, J.A., 1976, Diurnal energy flux variations and glacier surface hydrology, *in* Lvovitch, M.I., Kotlyakov, V.M., and Rauner, Yu.L., eds., International Geography '76, Section 2: Climatology, Hydrology, Glaciology: International Geographical Congress 23rd, 22–26 July 1976, Proceedings, p. 75–77.

———1977, An experimental study of the glacier boundary layer over melting ice: Journal of Glaciology, v. 18, no. 80, p. 425–436.

Munro, D.S., and Young, G.J., 1982, An operational net shortwave radiation model for glacier basins: Water Resources Research, v. 18, no. 2, p. 220–230.

Nakawo, Masayoshi, and Young, G.J., 1982, Estimate of glacier ablation under a debris layer from surface temperature and meteorological variables: Journal of Glaciology, v. 28, no. 98, p. 29–34.

Neave, K.G., and Savage, J.C., 1970, Icequakes on the Athabasca Glacier: Journal of Geophysical Research v. 75, no. 8, p. 1351–1362.

Nelson, J.G., Ashwell, I.Y., and Brunger, A.G., 1966, Recession of the Drummond Glacier, Alberta: Canadian Geographer, v. 10, no. 2, p. 71–81.

Odell, N.E., 1948, Stagnant glacier in British Columbia: Journal of Glaciology, v. 1, no. 4, p. 191.

———1949, Exploration of the Lloyd George Mountains in British Columbia: Canadian Geographical Journal, v. 38, no. 1, p. 48–63.

Ohmura, Atsumu, Kasser, Peter, and Funk, Martin, 1986, Parameterization of glacierization for a climate model: ISLSCP Conference, Rome, Italy, 2–6 December 1985, Proceedings; European Space Agency, Report ESA SP-248, p. 113–123.

Ommanney, C.S.L., 1971, Glacier surveys by District personnel of the Water Survey of Canada. 1. The Victoria Glacier: Ottawa, Department of the Environment, Inland Waters Branch, Glaciology Division, Glacier Inventory Note No. 6, 18 p.

———1972a, Glacier inventory, *in* Guidebook to the international symposia on the role of ice and snow in hydrology, Banff, Alberta, 6–20 September 1972: Canadian National Committee for the International Hydrological Decade, p. 84–87.

———1972b, Glacier surveys by District personnel of the Water Survey of Canada. 2. Peyto Glacier: Ottawa, Department of the Environment, Inland Waters Directorate, Water Resources Branch, Glaciology Division, Glacier Inventory Note No. 7, 20 p.

———1984, Bibliographic information on the Freshfield, Lyell and Mons Glaciers, Alberta: Ottawa, Environment Canada, National Hydrology Research Institute, Surface Water Division, Glacier Inventory Project, Internal report, 9 p.

———1989, Glacier atlas of Canada, limited ed.: Saskatoon, Saskatchewan, Environment Canada, National Hydrology Research Institute, Scientific Information Division, 2 p. (with 52 maps)

Osborn, G.D., 1975, Advancing rock glaciers in the Lake Louise area, Banff National Park, Alberta: Canadian Journal of Earth Sciences, v. 12, no. 6, p. 1060–1062.

Østrem, Gunnar, 1966, The height of the glaciation limit in southern British Columbia and Alberta: Geografiska Annaler, v. 48A, no. 3, p. 126–138.

———1972, Height of the glaciation level in northern British Columbia and southeastern Alaska: Geografiska Annaler, v. 54A, no. 2, p. 76–84.

———1973a, Runoff forecasts for highly glacierized basins, *in* The role of snow and ice in hydrology, Proceedings of the Banff Symposia, September 1972: IAHS-AISH Publication No. 107, v. 2, p. 1111–1132.

———1973b, The transient snowline and glacier mass balance in southern British Columbia and Alberta, Canada: Geografiska Annaler, v. 55A, no. 2, p. 93–106.

Østrem, Gunnar, and Arnold, K.C., 1970, Ice-cored moraines in southern British Columbia and Alberta, Canada: Geografiska Annaler, v. 52A, no. 2, p. 120–128.

Østrem, Gunnar, and Stanley, A.D., 1969, Glacier mass balance measurements, a manual for field and office work: A guide for personnel with limited backgrounds in glaciology, prepared jointly by the Canadian Department of Energy, Mines and Resources, and the Norwegian Water Resources and Electricity Board, Norwegian edition 129 p.

Outram, J., 1905, In the heart of the Canadian Rockies: New York, Macmillan, 466 p.

Palmer, Howard, 1924a, Observations on the Freshfield Glacier, Canadian Rockies: Journal of Geology, v. 32, no. 5, p. 432–441.

———1924b, The Freshfield Glacier, Canadian Rockies: Smithsonian Miscellaneous Collection, Publication No. 2757, v. 76, no. 11, p. 1–16.

———1924–26, Travels and ascents among the highest Canadian Rockies: Appalachia, v. 16, no. 3, p. 257–277.

———1925, The first ascent of Mt. King Edward, Canadian Rockies, with a note on Mt. Alberta: The Alpine Journal, v. 37, no. 231, p. 306–315.

Papertzian, V.C., 1973, A study of rock glaciers in Banff National Park, Canada: Kingston, Ontario, Queen's University, Department of Geology, B.Sc. thesis, 107 p.

Paterson, W.S.B., 1962, Observations on the Athabasca Glacier and their relation to the theory of glacier flow: Vancouver, British Columbia, University of British Columbia, Department of Physics, Ph.D. thesis, 158 p.

———1964, Variations in the velocity of Athabasca Glacier with time: Journal of Glaciology, v. 5, no. 39, p. 277–285.

———1965, Correspondence—Reply to Meier's letter on "Variations in velocity of Athabasca Glacier with time": Journal of Glaciology, v. 5, no. 42, p. 875–876.

———1966, Test of contour accuracy on a photogrammetric map of Athabasca Glacier: Canadian Journal of Earth Sciences, v. 3, no. 6, p. 909–915.

———n.d. [ca. 1968], Canadian drilling program—Summary of deep drilling in glaciers in Canada: Department of Energy, Mines and Resources, Unpublished report, 14 p.

———1970, The sliding velocity of Athabasca Glacier, Canada: Journal of Glaciology, v. 9, no. 55, February, p. 55–63.

Paterson, W.S.B., 1971, Temperature measurements in Athabasca Glacier, Canada: Journal of Glaciology, v. 10, no. 60, p. 339–349.

———1972, Temperature distribution in the upper layers of the ablation area of Athabasca Glacier, Alberta, Canada: Journal of Glaciology, v. 11, no. 61, p. 31–41.

Paterson, W.S.B., and Savage, J.C., 1963a, Geometry and movement of the Athabasca Glacier: Journal of Geophysical Research, v. 68, no. 15, p. 4513–4520.

———1963b, Measurement on Athabasca Glacier relating to the flow law of ice: Journal of Geophysical Research, v. 68, no. 15, p. 4537–4543.

———1970, Excess pressure observed in a water-filled cavity in Athabasca Glacier, Canada: Journal of Glaciology, v. 9, no. 55, p. 103-107.

Power, J.M., and Young, G.J., 1979a, Application of an operational hydrologic forecasting model to a glacierized research basin: Proceedings, Third Northern Research Basin Symposium Workshop, The State of the Art in Transposable Watershed Models, convened by the IHP Regional Working Group on Northern Research Basins, 10–15 June 1979, Québec City, Québec, Abstract No. 11. Also - Ottawa, Environment Canada, Snow and Ice Division, Preprint, 20 p.

———1979b, Application of the UBC watershed model to Peyto Glacier basin, *in* Canadian Hydrology Symposium 79, Cold Climate Hydrology, Vancouver, B.C., 10–11 May 1979, Proceedings: Ottawa, Ontario, National Research Council of Canada (NRCC 17834), Associate Committee on Hydrology, p. 217–228.

Prantl, F.A., and Loijens, H.S., 1977, Nuclear techniques for glaciological studies in Canada, *in* Isotopes and Impurities in Snow and Ice Symposium, proceedings of the Grenoble Symposium, August/September 1975: IAHS-AISH Publication No. 118, p. 237–241.

Prest, V.K., 1983, Canada's heritage of glacial features: Ottawa, Geological Survey of Canada, Miscellaneous Report 28, 119 p.

Putnam, W.L., Kruszyna, R., and Jones, C., 1974, Climber's guide to the Rocky Mountains of Canada—North, 6th ed.: New York, American Alpine Club, and Banff, Alberta, Alpine Club of Canada, 289 p.

Rains, R.B., 1990, Cline Glacier and Shoe Leather Creek, Alberta—Morphology and hydrology: Edmonton, Alberta, University of Alberta, Department of Geography, 20 p.

Raymond, C.F., 1971a, Determination of the three-dimensional velocity field in a glacier: Journal of Glaciology, v. 10, no. 58, p. 39–53.

———1971b, Flow in a transverse section of Athabasca Glacier, Alberta, Canada: Journal of Glaciology, v. 10, no. 58, p. 55–84.

———1973, Inversion of flow measurements for stress and rheological parameters in a valley glacier: Journal of Glaciology, v. 12, no. 64, p. 19–44.

Reid, I.A., 1961, Triangulation survey of the Athabasca Glacier, July 1959: Ottawa, Department of Northern Affairs and National Resources, Water Resources Branch, 20 p. and 2 maps. [Internal report]

———1972, Glacier surveys by the Water Survey of Canada, *in* The role of snow and ice in hydrology, Proceedings of the Banff Symposia, September 1972: IAHS-AISH Publication No. 107, v. 2, p. 1133–1143.

Reid, I.A., and Charbonneau, J.O.G., 1972, Glacier surveys in Alberta: Ottawa, Department of the Environment, Inland Waters Directorate Report Series No. 22, 17 p. and maps.

———1975, Glacier surveys in Alberta—1971: Ottawa, Department of the Environment, Water Resources Branch, Inland Waters Directorate Report Series no. 43, 18 p. and maps.

———1979, Glaciers surveys in Alberta—1977: Ottawa, Environment Canada, Water Resources Branch, Inland Waters Directorate Report Series No. 65, 17 p. and 2 maps.

———1981, Glaciers surveys in Alberta—1979: Ottawa, Environment Canada, Water Resources Branch, Inland Waters Directorate Report Series No. 69, 19 p. (with maps)

Reid, I.A., Charbonneau, J.O.G., and Warner, L.A., 1978, Glacier surveys in Alberta—1975: Ottawa, Fisheries and Environment Canada, Water Resources Branch, Inland Waters Directorate Report Series No. 60, 17 p. and 4 maps.

Reid, I.A., and Paterson, W.S.B., 1973, Simple method of measuring the average amount of water produced annually by melting of ice on a glacier, *in* Symposium on the Hydrology of Glaciers, Cambridge, 7–13 September 1969, Association Internationale d'Hydrologie Scientifique Publication No. 95, p. 215–218.

Rigsby, G.P., 1958, Fabrics of glacier and laboratory deformed ice, *in* Symposium of Chamonix, September 16–24, 1958: Association Internationale d'Hydrologie Scientifique Publication No. 47, p. 351–358.

———1960, Crystal orientation in glacier and in experimentally deformed ice: Journal of Glaciology, v. 3, no. 27, p. 589–606.

Rogerson, R.J., 1985, Measured re-advance of a debris-covered glacier terminus in the President Range, Yoho National Park, British Columbia, Canada: Journal of Glaciology, v. 31, no. 107, p. 13–17.

Rogerson, R.J., and Batterson, M.J., 1982, Contemporary push moraine formation in the Yoho Valley, B.C., *in* Davidson-Arnott, Robin, Nickling, William, and Fahey, B.D., eds., Research in glacial, glacio-fluvial and glacio-lacustrine systems, Symposium on geomorphology, 6th, Guelph, 9–10 May 1980, Proceedings: University of Guelph, Department of Geography, Guelph, Ontario, p. 71–90.

Rossiter, J.R., 1977, Interpretation of radio interferometry depth sounding, with emphasis on random scattering from temperate glaciers and the lunar surface: Toronto, Ontario, University of Toronto, Department of Physics, Ph.D. thesis, 223 p.

Savage, J.C., and Paterson, W.S.B., 1963, Borehole measurements in the Athabasca Glacier: Journal of Geophysical Research, v. 68, no. 15, p. 4521–4536.

———1965, Additional borehold measurements in the Athabasca Glacier: Journal of Geophysical Research, v. 70, no. 14, p. 3511–3513.

Schafer, J.P., 1954, Scott Glacier notes, 1953: Canadian Alpine Journal, v. 37, p. 124–126.

Schaffer, M.T.S., 1908, Untrodden ways: Canadian Alpine Journal, v. 1, no. 2, p. 288–294.

Sedgwick, J.K., and Henoch, W.E.S., 1975, Peyto Glacier: Ottawa, Environment Canada, Inland Waters Directorate, Water Resources Branch, Glaciology Division, map and booklet, 30 p.

Sharp, R.P., and Epstein, Samuel, 1958, Oxygen-isotope ratios and glacier movement, *in* Symposium of Chamonix, September 16–24, 1958: Association Internationale d'Hydrologie Scientifique Publication No. 47, p. 359–369.

Sherzer, W.H., 1905, Glacial studies in the Canadian Rockies and Selkirks (Smithsonian Expedition of 1904) preliminary report: Smithsonian Miscellaneous Collections (Quarterly Issue), v. 47, no. 1567, Part 4, Smithsonian Institution, Washington, D.C., p. 453–496.

———1907, Glaciers of the Canadian Rockies and Selkirks (Smithsonian Expedition of 1904): Washington D.C., Smithsonian Institution, Smithsonian Contributions to Knowledge, v. 34, art. 4, no.1692, 135 p.

———1908, The nature and activity of Canadian glaciers: Canadian Alpine Journal, v. 1, no. 2, p. 249–263.

Shilts, Elizabeth, Fick, Steven, Murray, Andrew, and McLean, Janice, 1998, The glaciers of Canada: Canadian Geographic, v. 118, no. 7, p. 51–52 (8-page foldout, color map).

Slaymaker, H.O., 1972, Physiography and hydrology of six river basins, *in* Robinson, J.L., ed., Studies in Canadian geography—British Columbia: Toronto, Ontario, University of Toronto Press, p. 32–68.

Sloan, V.F., 1987, Relationships between glacier terminus melt processes and climatic conditions, Boundary Glacier, Alberta: 43rd Annual Meeting, Eastern Snow Conference, Hanover, New Hampshire, 5–6 June 1986, Proceedings, p. 222–227.

Smart, C.C., 1983, Hydrology of a glacierized alpine karst - Castleguard Mountain, Alberta: Hamilton, Ontario, McMaster University, Department of Geography, Ph.D. thesis, 343 p.

———1984, Glacier hydrology and the potential for subglacial karstification: Norsk Geografisk Tidsskrift, v. 38, no. 3–4, p. 157–161.

———1986, Some observations on subglacial ground-water flow: Journal of Glaciology, v. 32, no. 111, p. 232–234.

Smith, N.D., 1978, Sedimentation processes and patterns in a glacier-fed lake with low sediment input: Canadian Journal of Earth Sciences, v. 15, no. 5, p. 741–756.

———1981, The effect of changing sediment supply on sedimentation in a glacier-fed lake: Arctic and Alpine Research, v. 13, no. 1, p. 75–82.

Smith, N.D., and Syvitski, J.P.M., 1982, Sedimentation in a glacier-fed lake: The role of pelletization on deposition of fine-grained suspensates: Journal of Sedimentary Petrology, v. 52, no. 2, p. 503–514.

Smith, N.D., Vendl, M.A., and Kennedy, S.K., 1982, Comparison of sedimentation regimes in four glacier-fed lakes of western Alberta, *in* Davidson-Arnott, Robin, Nickling, William, and Fahey, B.D., eds., Research in glacial, glacio-fluvial and glacio-lacustrine systems, Symposium on geomorphology, 6th, Guelph, 9–10 May 1980, Proceedings: University of Guelph, Department of Geography, Guelph, Ontario, p. 203–238.

Stacey, J.S., 1960, A prototype hotpoint for thermal boring on the Athabasca Glacier: Journal of Glaciology, v. 3, no. 28, p. 783–786.

Stanley, A.D., 1965, Relation between secondary structures in Athabasca Glacier and laboratory deformed ice: Vancouver, B.C., University of British Columbia, Department of Geology, Ph.D. thesis, 214 p.

———1970, A pilot study for the inventory of the glaciers in the Rocky Mountains. Inventory of glaciers in the Waputik Mountains, *in* Perennial Ice and Snow Masses: UNESCO/IASH Technical Papers in Hydrology No. 1, International Association of Scientific Hydrology, UNESCO A. 2486, p. 36–46.

Stenning, A.J., Banfield, C.E., and Young, G.J., 1981, Synoptic controls over katabatic layer characteristics above a melting glacier: Journal of Climatology, v. 1, no. 4, p. 309–324.

Strangway, D.W., Simmons, Gene, LaTorraca, G., Watts, R., Bannister, L., Baker, R., Redman, J.D., and Rossiter, J.R., 1974, Radio-frequency interferometry—A new technique for studying glaciers: Journal of Glaciology, v. 13, no. 67, p. 123–132.

Stutfield, H.E.M., and Collie, J.N., 1903, Climbs in the Canadian Rockies: New York, Longmans Green & Co., 343 p.

Tangborn, W.V., 1980, Dolia lednikovogo stoka v formirovanii gidroenergetiches-kikh resursov reki Kolumbii [Contribution of glacier runoff to hydroelectric power generation on the Columbia River]: Materially Gliatsiologicheskikh Issledovanii, Khronika, Obsuzhdeniia, Mezhduvedomstvennyi Geofizicheskii Komitet, Sektsiia Gliatsiologii, Institute Geografii, Academy Nauk SSSR [Data of Glaciological Studies, Chronicle, Discussion, Section of Glaciology of the Soviet Geophysical Committee and Institute of Geography, Academy of Sciences of the U.S.S.R.], No. 39, Moskva [Moscow], Iiuni [July], in Russian, p. 62–67, in English, p. 140–143.

Thorington, J.M., 1927, The Lyell and Freshfield Glaciers, Canadian Rocky Mountains, 1926: Smithsonian Miscellaneous Collection, v. 78, no. 6, Publication No. 2911, p. 1–8.

———1932, Lyell and Freshfield Glaciers: Canadian Alpine Journal, v. 20, p. 138–140.

———1938, Notes on Saskatchewan and Freshfield Glaciers: American Alpine Journal, v. 3, no. 2, p. 219–220.

———1945, Notes on Freshfield and Lyell Glaciers: American Alpine Journal, v. 5, no. 3, p. 435–436.

Trombley, T.J., 1986, A radio-echosounding survey of Athabasca Glacier, Alberta, Canada: Durham, New Hampshire, University of New Hampshire, Department of Earth Science, M.Sc. thesis, 64 p.

UNESCO, 1970, Perennial ice and snow masses: A guide for compilation and assemblage of data for a world inventory: United Nations Educational, Scientific, and Cultural Organization and International Association of Scientific Hydrology (IASH), 19 p.

Valdeyev, A.E., 1986, Glacier mass balance estimations from the measurements made at the mean weighted altitude: International Symposium "Glacier Mass-balance, Fluctuations and Runoff," Alma-Ata, 30 September–5 October 1986, Proceedings: Moscow, Soviet Geophysical Committee, Academy of Sciences of the U.S.S.R., Data of Glaciological Studies No. 57, p. 110–111 and p. 228–229.

Vaux George, Jr., 1910, Observations on glaciers in 1909: Canadian Alpine Journal, v. 2, no. 2, p. 126–130.

Vaux, George, [Jr.,] and Vaux, W.S.[Jr.,] 1901, Observations made in 1900 on glaciers in British Columbia: Proceedings of the Academy of Natural Sciences of Philadelphia, v. 53, p. 213–215.

———1907a, Glacier observations: Canadian Alpine Journal, v. 1, no. 1, p. 138–148.

———1907b, Observations made in 1906 on glaciers in Alberta and British Columbia: Proceedings of the Academy of Natural Sciences of Philadelphia, v. 58, p. 568–579.

———1908, Observations made in 1907 on glaciers in Alberta and British Columbia: Proceedings of the Academy of Natural Sciences of Philadelphia, v. 59, p. 560–563.

Vaux, M.M., 1911, Observations on glaciers in 1910: Canadian Alpine Journal, v. 3, p. 127–130.

———1913, Observations on glaciers: Canadian Alpine Journal, v. 5, p. 59–61.

Vaux, M.M., and Vaux, George, Jr., 1911, The glaciers of the Canadian Rockies and Selkirks (2d ed.): Bryn Mawr, Pennsylvania, privately printed, 20 p.

Waddington, E.D., and Jones, D.P., 1977, A radio-echo ice thickness survey of the Columbia Icefield: Vancouver, B.C., University of British Columbia, Department of Geophysics and Astronomy, Unpublished report, 8 p.

Warner, L.A., Anderson, J.E., Kerber, R.E., and Robinson, C.P., 1972, 1972 survey of the Athabasca and Saskatchewan Glaciers: Calgary, Dept. of Environment, Water Survey of Canada, 34 p. [Internal report]

Watson, H.M., 1983, A dendrochronological study of two sites in Mount Robson Provincial Park: London, Ontario, University of Western Ontario, Department of Geography, B.A. thesis, 147 p.

Watt, A.O., and Maxwell, E.L., 1960, Measured electrical properties of snow and glacial ice: Washington, D.C., Journal of Research of the National Bureau of Standards, v. 64D, no. 4, p. 357–363.

West, K.E., 1972, H_20^{18}/H_20^{16} variations in ice and snow of mountainous regions of Canada: Edmonton, Alberta, University of Alberta, Department of Physics, Ph.D. thesis, 123 p.

Wharton, R.A., Jr., and Vinyard, W.C., 1983, Distribution of snow and ice algae in western North America: Madroño, v. 30, no. 4, p. 201–209.

Wheeler, A.O., 1907, Observations of the Yoho Glacier: Canadian Alpine Journal, v. 1, no. 1, p. 149–156.

———1908, Motion of the Yoho Glacier: Canadian Alpine Journal, v. 1, no. 2, p. 271–275.

———1909, Motion of the Yoho Glacier: Canadian Alpine Journal, v. 2, no. 1, p. 97–99.

———1910, Motion of the Yoho Glacier: Canadian Alpine Journal, v. 2, no. 2, p. 121–125.

———1911, Motion of the Yoho Glacier: Canadian Alpine Journal, v. 3, p. 123–126.

———1913, Motion of the Yoho Glacier: Canadian Alpine Journal, v. 5, p. 53–58.

———1915a, Motion of the Yoho Glacier: 1912–1914: Canadian Alpine Journal, v. 6, p. 133–138.

———1915b, Robson Glacier: Canadian Alpine Journal, v. 6, p. 139–142.

———1917, Motion of the Yoho Glacier: 1914–1916: Canadian Alpine Journal, v. 8, p. 118–120.

———1920a, Motion of the Yoho Glacier: 1917, 1918 and 1919: Canadian Alpine Journal, v. 11, p. 182–185.

———1920b, Notes on the glaciers of the Main and Selkirk Ranges of the Canadian Rocky Mountains: Canadian Alpine Journal, v. 11, p. 121–146.

———1923, Motion of the Robson Glacier: Canadian Alpine Journal, v. 13, p. 158–159.

———1932, Glacial change in the Canadian Cordillera, the 1931 Expedition: Canadian Alpine Journal, v. 20, p. 120–137.

———1934, Records of glacial observations in the Canadian Cordillera, 1933 and 1934: Canadian Alpine Journal, v. 22, p. 172–187.

Wilcox, W.D., 1900, The Rockies of Canada: New York, G.P. Putnam's Sons, and London, The Knickerbocker Press, 309 p.

Xie, Zichu, and Zang, Jinhua, 1986, A study in the mass balance of the glaciers in China: International Symposium "Glacier Mass-balance, Fluctuations and Runoff," Alma-Ata, 30 September–5 October 1986, Proceedings: Moscow, Soviet Geophysical Committee, Academy of Sciences of the U.S.S.R., Data of Glaciological Studies No. 57, p. 105–110 and 223–227.

Yarnal, B.M., 1979, The sequential development of a rock glacier-like landform, Mount Assiniboine Provincial Park, British Columbia: Calgary, Alberta, University of Calgary, Department of Geography, M.Sc. thesis, 146 p.

Yarnal, Brent, 1984, Relationships between synoptic-scale atmospheric circulation and glacier mass balance in south-western Canada during the International Hydrological Decade, 1965–74: Journal of Glaciology, v. 30, no. 105, p. 188–198.

Young, G.J., 1974a, Glacier mass-balance and terrain shape—a methodological study: Montréal, Québec, McGill University, Department of Geography, Ph.D. thesis, 320 p.

———1974b, A stratified sampling design for snow surveys based on terrain shape: the Western Snow Conference, 42nd Annual Meeting, Anchorage, Alaska, Proceedings, p. 14–22.

———1976, An approach to glacier mass-balance analysis utilizing terrain characterization: Ottawa, Environment Canada, Water Resources Branch, Inland Waters Directorate Scientific Series No. 60, 34 p.

———1977a, Relations between mass-balance and meteorological variables on Peyto Glacier, Alberta, 1967–1974: Zeitschrift für Gletscherkunde und Glazialgeologie, 13, no. 1-2, p. 111–125.

———1977b, The seasonal and diurnal regime of a glacier-fed stream, *in* Swanson, R.H., and Logan, P.A., compilers, Alberta Watershed Research Program Symposium Proceedings, 31 August–2 September 1977: Edmonton, Alberta, Fisheries and Environment Canada, Forestry Service, Northern Forest Research Center, Information Report NOR–X–176, p. 111–126.

Young, G.J., 1980, Formirovanie pechnogo stoka v lednikovom basseine v Skalistykh gorakh Kanady [Streamflow formation in a glacierized watershed in the Rocky Mountains Canada]. Materialy Gliatsiologicheskikh Issledovanii, Khronika, Obsuzhdeniia, Mezhduvedomstvennyi Geofizicheskii Komitet, Sektsiia Gliatsiologii, Institut Geografii, Academy Nauk SSSR, Moskva [Moscow], Academy of Sciences of the U.S.S.R., Section of Glaciology of the Soviet Geophysical Committee and Institute of Geography, Discussion, Chronicle, Data of Glaciological Studies No. 39, in Russian, p. 55–62; in English, p. 134–139.

———1981, The mass balance of Peyto Glacier, Alberta, Canada, 1965 to 1978: Arctic and Alpine Research, v. 13, no. 3, August, p. 307–318.

———1982, Hydrological relationships in a glacierized mountain basin, *in* Glen, J.W., ed., Hydrological Aspects of Alpine and High Mountain Areas: Proceedings of the Exeter Symposium, 19–30 July 1982: IAHS-AISH Publication No. 138, p. 51–59.

Young, G.J., and Arnold, K.C., 1977, Orthophotomaps of glaciers—An evaluation of an automated method applied to Peyto Glacier, Alberta: Zeitschrift für Gletscherkunde und Glazialgeologie, v. 13, no. 1-2, p. 99–110.

Young, G.J., Glynn, J.E., Reid, I.A., and Sherstone, D.A., 1978, Mapping the Athabasca Glacier, Alberta, Canada, by orthophotography and by conventional methods: International Symposium on New Technology for Mapping, International Society for Photogrammetry, Commission 4, Ottawa, Ontario, 2–6 October 1978, Proceedings, p. 643–659.

Young, G.J., and Stanley, A.D., 1976a, Canadian glaciers in the International Hydrological Decade program, 1965–1974. No. 3: Ram River Glacier, Alberta—Summary of measurements: Ottawa, Fisheries and Environment Canada, Water Resources Branch, Inland Waters Directorate Scientific Series No. 70, 54 p.

———1976b, Canadian glaciers in the International Hydrological Decade program, 1965–1974. No. 4: Peyto Glacier, Alberta - summary of measurements: Ottawa, Fisheries and Environment Canada, Water Resources Branch, Inland Waters Directorate Scientific Series No. 71, 59 p.

Glaciers of North America–

GLACIERS OF CANADA

GLACIERS OF THE COAST MOUNTAINS

By GARRY K.C. CLARKE *and* GERALD HOLDSWORTH

SATELLITE IMAGE ATLAS OF GLACIERS OF THE WORLD

Edited by RICHARD S. WILLIAMS, Jr., *and* JANE G. FERRIGNO

U.S. GEOLOGICAL SURVEY PROFESSIONAL PAPER 1386–J–1

The Coast Mountains of Canada extend from southwestern British Columbia to southwestern Yukon Territory. Highland ice fields and associated outlet glaciers are present along the erosionally dissected mountain blocks. Mining is difficult in this area because of the glaciers, and prehistoric and historic jökulhlaups have resulted from glacier-dammed lakes

CONTENTS

GLACIERS OF NORTH AMERICA–

GLACIERS OF CANADA

GLACIERS OF THE COAST MOUNTAINS

By GARRY K.C. CLARKE[1] *and* GERALD HOLDSWORTH[2]

Abstract

The Coast Mountains follow the Pacific coast of Canada and extend from southwestern British Columbia to southwestern Yukon Territory. The predominantly granitic bedrock forms elevated blocks that have been deeply dissected by erosion, yielding a distinctive pattern of disjointed highland ice fields that are drained by radiating outlet glaciers. Popular interest in the glaciers of the Coast Mountains centers on the hazards and problems that they engender and on their attractions as a recreational resource. Scientific interest has largely focused on their status as climate indicators. We touch on these various themes by discussing the glacier-associated problems of the Granduc mining operation near Leduc Glacier in northwestern British Columbia, the outburst floods of glacier-dammed Flood Lake, and the recreational and scientific roles of small glaciers in Garibaldi Provincial Park near Vancouver, British Columbia.

Introduction

The Coast Mountains of Canada lie almost entirely within British Columbia and extend from near the Fraser River slightly north of the lat 49° N. boundary between Canada and the United States to just across the lat 60° N. boundary between British Columbia and Yukon Territory, a distance of some 1,500 km (fig.1). The section north of the Skeena River that follows the irregular border between the Alaskan "panhandle" and British Columbia is sometimes called the Boundary Ranges, and the section south of the Skeena River, the Pacific Ranges. Physiographically, the Coast Mountains resemble deeply dissected elevated blocks (Bostock, 1948). This gives the present-day glacierization a characteristic pattern: highland ice fields, drained by radiating outlet glaciers, are separated from one another by deep valleys. In late Wisconsinan time, when the region was covered by the Cordilleran ice sheet, these valleys were ice-filled, and the tops of the highest peaks protruded as nunataks; drainage to the Pacific Ocean was mainly by calving from tidewater glaciers. The end of this last glaciation left a spectacular fjord coastline and a network of U-shaped valleys that, in places, cut completely across the Coast Mountains. These valleys are now occupied by the major westward-flowing rivers of Canada. The pattern of highland ice fields broken by deep valleys is repeated over the entire length of the Coast Mountains. Some typical examples are the Frank Mackie highland glacier complex and

Manuscript approved for publication 7 March 2002.

[1] Department of Earth and Ocean Sciences, University of British Columbia, 6339 Stores Road, Vancouver, British Columbia V6T 1Z4, Canada.

[2] Arctic Institute of North America, University of Calgary, 2500 University Drive, NW., Calgary, Alberta T2N 1N4, Canada; Institute for the Study of Earth, Oceans, and Space, Morse Hall, University of New Hampshire, Durham, NH 03824–3525; and the National Hydrology Research Centre, 11 Innovation Boulevard, Saskatoon, Saskatchewan S7N 3H5, Canada; e-mail address: [gholdswo@acs.ucalgary.ca].

Figure 1.*—Coast Mountains, British Columbia, and surrounding area in Canada and the United States.*

Cambria Snowfield at the head of Portland Canal (fig. 2) and the highland ice fields of the Stikine River basin (fig. 3).

Although the scientific literature on the glaciers of the Coast Mountains is surprisingly sparse, no region in Canada has such close interaction between glaciers and humans as in this area. We shall take this interaction as our theme.

Hazards and Problems Created by Glaciers

Glaciers and Mining

Rich mineral deposits lie within the Coast Mountains, and the difficulty of exploring and mining these deposits has stimulated valuable glaciological work. The experience of the Granduc Operating Company in exploiting a copper deposit near Leduc Glacier illustrates these problems and is a fertile source of cautionary tales. Figure 2 shows the Coast Mountains at the head of Portland Canal, a remarkable fjord less than 5 km across, that extends

Figure 2.—Annotated Landsat MSS image of part of the Coast Mountains near Stewart, British Columbia, and the Granduc mining development. Copper ore is transported through an 18-km tunnel from a mine (shown by a small box) near Leduc Glacier east to a concentrator at the terminus of Berendon Glacier, then by truck to an ocean dock near Stewart. Annotations: 1, the Frank Mackie highland glacier complex; 2, Cambria Snowfield. Landsat image (21288–18435, band 7; 2 August 1978; Path 58, Row 21) is from the EROS Data Center, Sioux Falls, S. Dak. Map references: Leduc Glacier sheet 104B/1 and 104B/2, 1:50,000; Iskut River sheet 104B, 1:250,000.

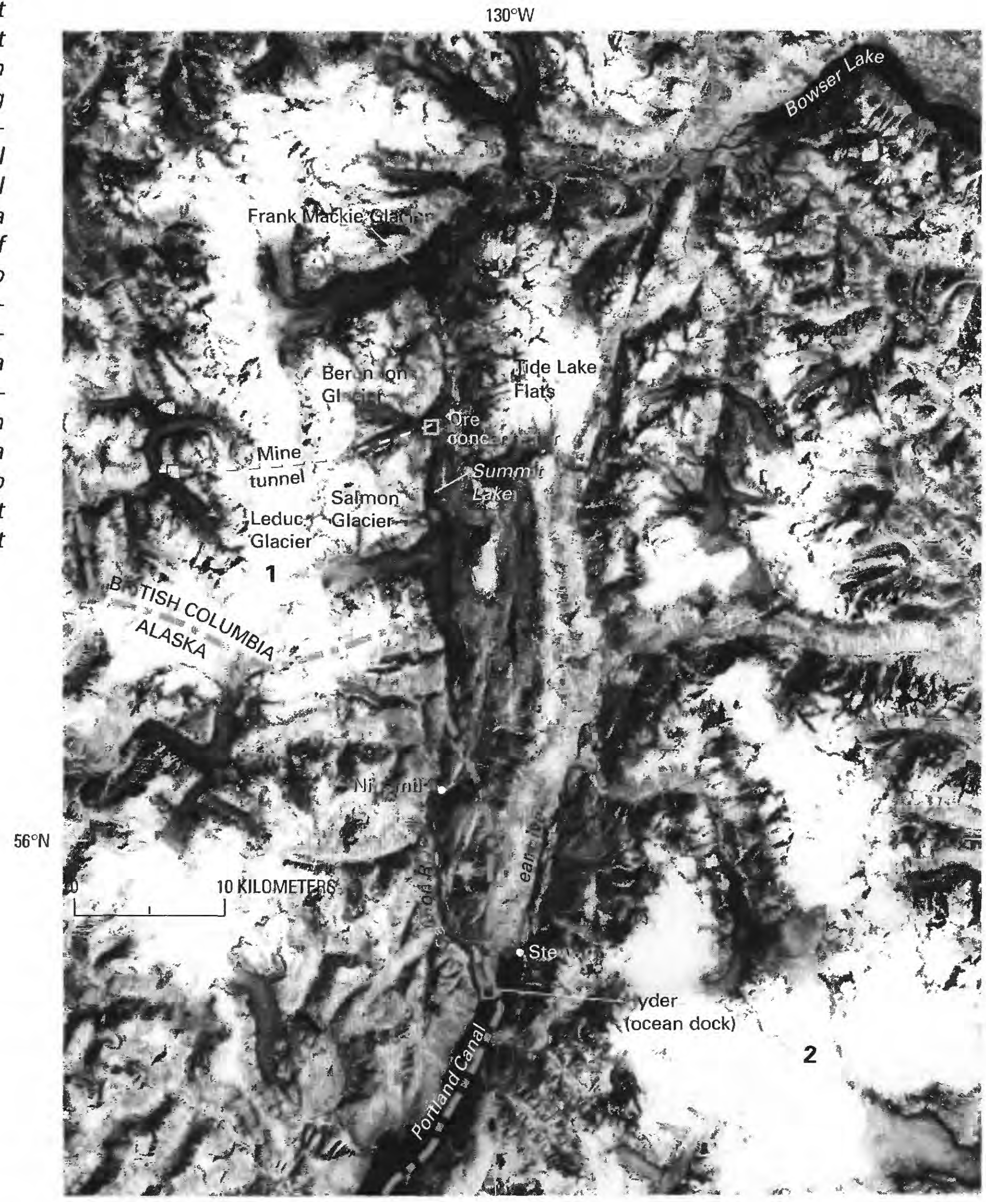

105 km from near Stewart, British Columbia, southwest to Portland Inlet. Annotations on this figure show the Granduc mine and associated developments for transporting and concentrating the ore. The main practical problem is to transport ore through rough glacier-covered terrain to a dock near Stewart. This is done in two steps: an 18-km-long access tunnel passing beneath Berendon, Frank Mackie, and Leduc Glaciers allows unconcentrated ore to be moved from the mine to a mill at Tide Lake Camp near the terminus of Berendon Glacier. Tide Lake Camp is situated between glacier-dammed Summit Lake and Tide Lake Flats, the bed of a former proglacial lake dammed by Frank Mackie Glacier (Hanson, 1932; Haumann, 1960; Field, 1975). From Tide Lake Camp, the concentrated ore is transported by truck along an access road that follows the margin of Salmon Glacier, then crosses the international boundary and follows the Salmon River from Nine-mile, Alaska, to a dock at Hyder, Alaska, near Stewart.

Initial supply of Tide Lake Camp and the mine site was by tractor-hauled sled along routes that passed over Salmon, Berendon, Frank Mackie, and Leduc Glaciers. Crevasses restricted use of these ice roads to the winter months when snow cover made safe crossings possible. In 1955, a fixed-wing landing strip was established on the surface of Leduc Glacier near the

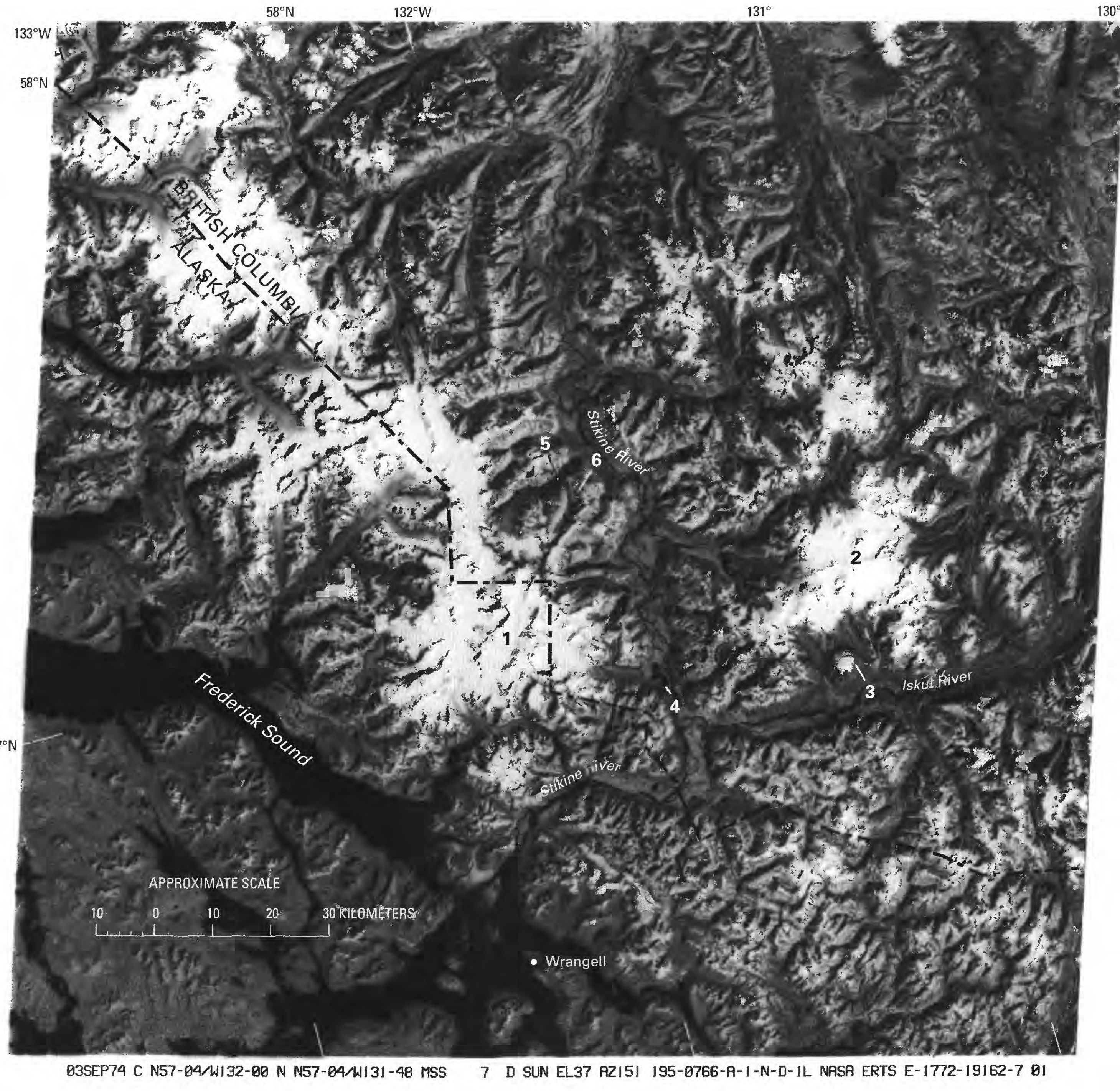

Figure 3.—*Annotated Landsat MSS image of part of the Boundary Ranges of the Coast Mountains near the confluence of the Stikine and Iskut Rivers, British Columbia and Alaska. Hydroelectric development plans for the Stikine-Iskut basin make it necessary to consider glacier hazards. Annotations: 1, 2, highland ice fields; 3, Hoodoo Mountain (a volcano); 4, Great Glacier (according to Native American oral tradition, this glacier once bridged the Stikine River); 5, Flood Glacier; 6, site of glacier-dammed Flood Lake (the 1979 outburst flood released 200 × 10^6 m^3 of water and gave a peak discharge of roughly 3,000 m^3 s^{-1}). Landsat image (1772–19162, band 7; 3 September 1974; Path 60, Row 20) is from the EROS Data Center, Sioux Falls, S. Dak. Map references: Stikine River sheet 104 SE. and part of 104 SW., 1:506,880; Iskut River sheet 104B, 1:250,000.*

mine site. As ice roads and air transport are not practical for transporting ore from the mine to an ocean port, much of the early glaciological work was directed at selecting possible routes for a tunnel connecting the mine to a concentrator. One of these routes passed beneath Salmon Glacier, so deep drilling, gravity surveys, and seismic soundings were undertaken to ensure that the planned tunnel did not intersect glacier ice (Jacobs, 1958; Mathews, 1959; Russell and others, 1960; Doell, 1963); excellent mapping and glaciological studies were carried out by Haumann (1960). Four of five deep holes drilled through Salmon Glacier in 1956 were believed to have reached bedrock at depths ranging from 495 m to 756 m.

An exploratory cross-cut tunnel at the mine site was driven beneath Leduc Glacier in 1957, and holes were drilled upward from the tunnel into the base of the glacier. These holes eventually became connected to the subglacier drainage network, which caused the lower level of the mine to fill with water (Mathews, 1964). The inflow of water was sufficiently high in volume so that the tunnel could not be reclaimed by pumping; therefore, a complicated engineering operation involving holes that were drilled through Leduc Glacier and that intersected the tunnel had to be employed in an effort to stem the water flow (Walsh, 1963). The problem eventually solved itself when, in midsummer, water level dropped below the tunnel elevation.

Annual snowfall at Stewart is high, averaging 5.5 m a^{-1}, and at Tide Lake Camp, a record annual snow fall of 25 m has been recorded. Such high snowfall in an alpine area obviously creates a grave avalanche hazard. In February 1965, an avalanche destroyed the Granduc Mine Camp near Leduc Glacier and claimed more than 20 lives. Defensive measures were subsequently taken to control avalanches and protect the camp and access road.

Because the tunnel portal and ore concentrator were sufficiently close to the terminus of Berendon Glacier, they could have been destroyed by a glacier advance. Glaciologists contributed to the discussion of a possible advance by measuring mass balance and by predicting glacier variations from a kinematic wave model (Untersteiner and Nye, 1968; Fisher and Jones, 1971). They also suggested methods of prevention or mitigation that used albedo modification (Eyles, 1977; Eyles and Rogerson, 1977b) or that involved pumping 30°C waste water from the copper mill onto the glacier (Eyles and Rogerson, 1977a).

Tide Lake Camp originally drew its water from Summit Lake, but in December 1961, the lake drained unexpectedly through a 12-km melt tunnel beneath Salmon Glacier. The resulting jökulhlaup (glacier outburst flood) released 251×10^6 m^3 of water into the Salmon River drainage. Maximum discharge exceeded 3,000 m^3 s^{-1}, and the flood badly damaged the access road and a bridge at Ninemile. Until 1961, Summit Lake had drained stably to the north through Bowser River, but since 1900, Salmon Glacier has thinned considerably. The resulting reduction of ice pressure favors the formation of a drainage tunnel. The lake now fills and drains annually, but floods are less severe than the 1961 flood. Jökulhlaups from Summit Lake are among the best studied of any in the world (Mathews, 1965, 1973; Gilbert, 1971, 1972; Fisher, 1973; Clarke and Mathews, 1981).

In a fascinating account of the problems facing the mine developers, Mamen (1966) wrote: "When production is finally achieved.... It will mark man's triumph over some of the severest obstacles Nature has ever placed in the path of mineral discovery and mine development." This was hardly an overstatement. By 1970, when production began, practically every conceivable glacier-related problem had been faced.

Glaciers and Outburst Floods

Figure 3 shows an annotated Landsat image of the Stikine-Iskut River system in the Boundary Ranges of the Coast Mountains. These rivers join near the British Columbia-Alaska boundary and flow to the Pacific Ocean near Wrangell, Alaska. Two unnamed highland glacier systems are shown in figure 3: one (labeled 1 in figure) lies along the international boundary and is truncated to the south by the Stikine River valley, and the other (labeled 2) lies between the Stikine and Iskut Rivers. Hydroelectric and other development plans for the Stikine-Iskut basin make it necessary to consider glacier-related hazards to downstream structures. As an example, the 1979 jökulhlaup from Flood Lake (labeled 6) released 200×10^6 m^3 of water into the Stikine River, and peak flood discharge was roughly 3,000 m^3 s^{-1} (Mokievsky-Zubok, 1980; Clarke and Waldron, 1984). Similar floods have taken place for at least the past century and were well known to local inhabitants when John Muir visited in 1879 (Muir, 1915). Other large glacier-dammed lakes existed in the past. According to Native American oral tradition, Great Glacier once bridged the Stikine River (Kerr, 1936; Field, 1975). Perchanok (1980) reports that 78 active or potential glacier-dammed lake sites lie within the Stikine-Iskut basin and that jökulhlaups from 10 of these could have significant downstream effects. Apart from explorers' reports and geological reconnaissance work (for example, Kerr, 1948), scientific studies of the glaciers in this part of the Coast Mountains are practically nonexistent.

Recreational and Scientific Roles of Glaciers

Besides creating problems for mining and hydroelectric developments, glaciers give pleasure to hikers and skiers. Figure 4 shows the Coast Mountains in the region of Garibaldi Provincial Park, a popular alpine recreation area near the Whistler-Blackcomb ski resort and the city of Vancouver, British Columbia. Perennial snow patches make individual glaciers difficult to distinguish and give a misleading impression of the amount of ice cover. All the glaciers are small and tend to be associated with major peaks. Garibaldi Névé and its outlet glaciers are the largest glacier feature and lie on the slopes of Mount Garibaldi (2,678 m, labeled 8). Other examples are Cheakumus, Wedge, and Weart Glaciers associated, respectively, with Castle Towers Mountain (2,676 m, labeled 4), Mount Wedge (2,890 m, labeled 3), and Mount Weart (2,834 m, labeled 2). According to Mathews (1951), these peaks projected as nunataks above the Cordilleran ice sheet. Mount Garibaldi and several lesser features are volcanic, and Mathews' suggestion that "volcanism ceased about the time of disappearance of the last ice sheet" makes for interesting speculation. The climatic deterioration of the "Little Ice Age" led to a period of glacier growth that culminated around 1750–1850. At this climax, many of the glaciers were at their greatest extent since the Cordilleran ice sheet had disappeared. The climax has been followed by a period of rapid recession that has lasted to the present time.

Although the glaciers are small, they are relatively well studied owing to their accessibility from the Squamish-Pemberton road. Sentinel and Sphinx Glaciers (labeled 7 and 5), near Garibaldi Lake (labeled 6), have received intermittent scientific attention since 1945 and are well mapped. Their contribution to annual runoff is important; mass-balance variations have been measured, but ice-thickness and flow-velocity measurements are lacking (for example, Reid and Shastal, 1970; Mokievsky-Zubok, 1973; Mokievsky-Zubok and Stanley, 1976a). Wedge Glacier has been mapped, its retreat monitored, and ice-thickness measurements taken. Its maximum measured thickness was only 150 m, and this is likely to be typical for other glaciers in the region (Tupper and others, 1978). Place Glacier, north of Garibaldi Park, has also been mapped, and mass-balance measurements have been

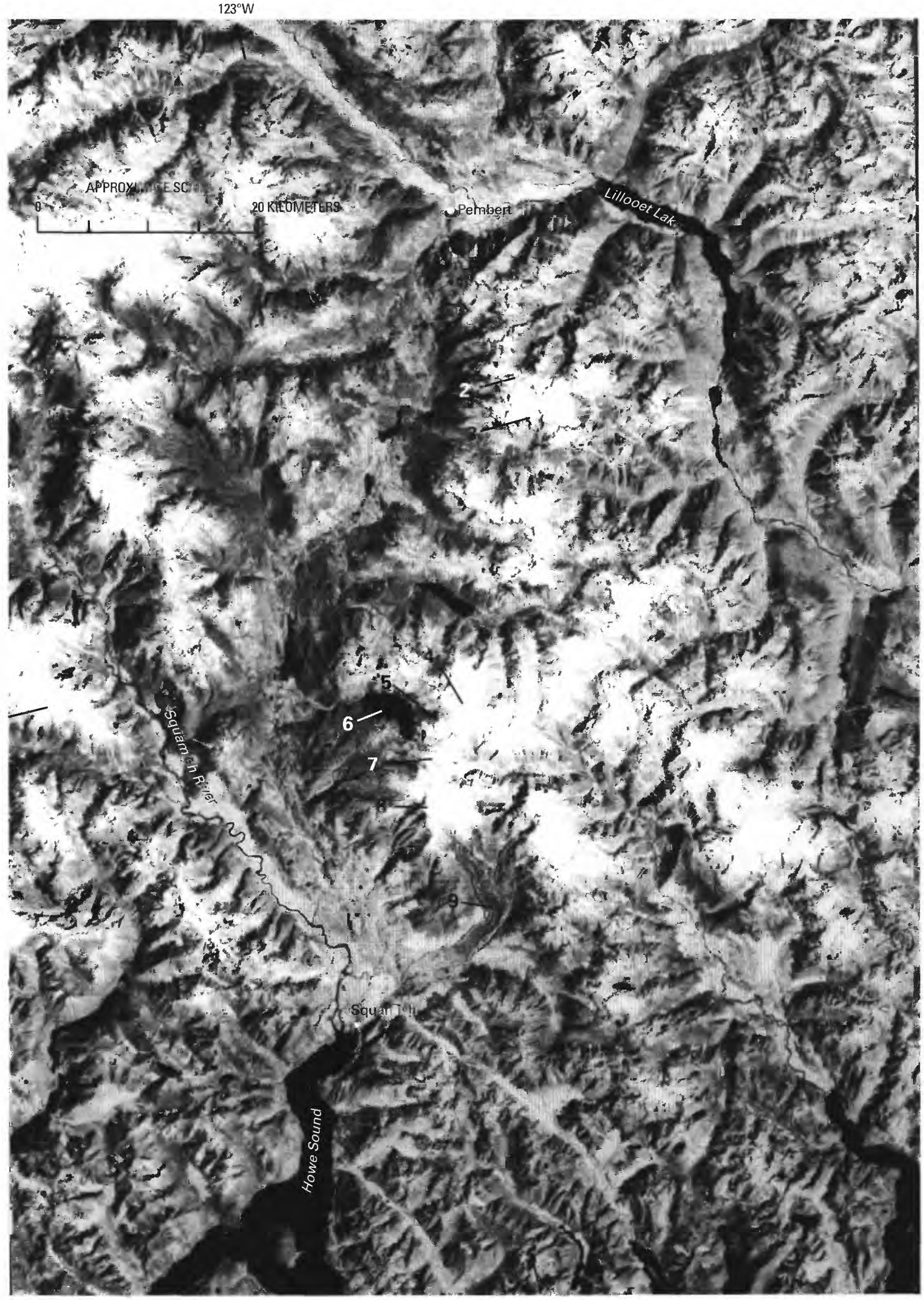

Figure 4.—*Annotated Landsat MSS image showing the region of Garibaldi Provincial Park, an alpine recreation area in the Coast Mountains to the north of Vancouver, British Columbia. Annotations: 1, Place Glacier; 2, Mount Weart; 3, Mount Wedge; 4, Castle Towers Mountain; 5, Sphinx Glacier; 6, Garibaldi Lake; 7, Sentinel Glacier; 8, Mount Garibaldi (elevation 2,678 m); 9, Ring Creek lava flow (note its similarity to a glacier). Landsat image (1385–18362, band 7; 12 August 1973; Path 51, Row 25) is from the EROS Data Center, Sioux Falls, S. Dak. Map references: Pemberton sheet 92J, 1:250,000; Vancouver sheet 92G, 1:250,000.*

taken since 1964 (Mokievsky-Zubok and Stanley, 1976b). Place and Sentinel Glaciers (labeled 1 and 7) are among the three glaciers of the Canadian Cordillera that have been the object of long-term mass-balance measurements, and their role as climate indicators has been examined by Letréguilly (1988) and Letréguilly and Reynaud (1989). A decline in field activity in the 1990's has been somewhat compensated by increasing use of satellite observations (Adam, Pietroniro, and Brugman, 1997; Adam, Toutin, and others, 1997).

References Cited

Adam, Steve, Pietroniro, Alain, and Brugman, M.M., 1997, Glacier snow line mapping using ERS–1 SAR imagery: Remote Sensing of Environment, v. 61, no. 1, p. 46–54.

Adam, Steve, Toutin, Th., Pietroniro, Alain, and Brugman, M.M., 1997, Using ortho-rectified SAR imagery acquired over rugged terrain for thematic applications in glacier hydrology: Canadian Journal of Remote Sensing, v. 23, no. 1, p. 76–80.

Bostock, H.S., 1948, Physiography of the Canadian Cordillera, with special reference to the area north of the fifty-fifth parallel: Canada Geological Survey Memoir 247, 106 p.

Clarke, G.K.C., and Mathews, W.H., 1981, Estimates of the magnitude of glacier outburst floods from Lake Donjek, Yukon Territory, Canada: Canadian Journal of Earth Sciences, v. 18, no. 9, p. 1452–1463.

Clarke, G.K.C., and Waldron, D.A., 1984, Simulation of the August 1979 sudden discharge of glacier-dammed Flood Lake, British Columbia: Canadian Journal of Earth Sciences, v. 21, no. 4, p. 502–504.

Doell, R., 1963, Seismic depth study of the Salmon Glacier, British Columbia: Journal of Glaciology, v. 4, no. 34, p. 425–437.

Eyles, Nicholas, 1977, Stop the glacier!: Canadian Alpine Journal, v. 60, p. 54–57.

Eyles, Nicholas, and Rogerson, R.G., 1977a, Artificially induced thermokarst in active glacier ice: An example from northwest British Columbia, Canada: Journal of Glaciology, v. 18, no. 80, p. 437–444.

———1977b, How to save your mine from a glacier: Canadian Mining Journal, v. 98, no. 7, p. 32.

Field, W.O., 1975, Mountain glaciers of the Northern Hemisphere: Hanover, N.H., U.S. Army Corps of Engineers, Cold Regions Research and Engineering Laboratory, v. 2, 932 p.

Fisher, D.A., 1973, Subglacial leakage of Summit Lake, British Columbia, by dye determinations, *in* Symposium on the hydrology of glaciers, Cambridge, England, 1969: Association Internationale d'Hydrologie Scientifique Publication No. 95, p. 111–116.

Fisher, D.A., and Jones, S.J., 1971, The possible future behavior of Berendon Glacier, Canada: A further study: Journal of Glaciology, v. 10, no. 58, p. 85–92.

Gilbert, R., 1971, Observations on ice-dammed Summit Lake, British Columbia, Canada: Journal of Glaciology, v. 10, no. 60, p. 351–356.

———1972, Drainings of ice-dammed Summit Lake, British Columbia: Canada, Inland Waters Directorate, Scientific Series 20, 17 p.

Hanson, George, 1932, Varved clays of Tide Lake, British Columbia: Royal Society of Canada Transactions, ser. 3, v. 26, sec. 4, p. 335–339.

Haumann, Dieter, 1960, Photogrammetric and glaciological studies of Salmon Glacier: Arctic, v. 13, no. 2, p. 74–100.

Jacobs, J.A., 1958, Geophysical investigations on the Salmon Glacier, British Columbia, *in* Symposium of Chamonix, 1958: Association Internationale d'Hydrologie Scientifique Publication No. 47, p. 43–44.

Kerr, F.A., 1936, Quaternary glaciation in the Coast Range, northern British Columbia and Alaska: Journal of Geology, v. 44, no. 6, p. 681–700.

———1948, Lower Stikine and western Iskut River areas, British Columbia: Canada Geological Survey Memoir 246, 94 p.

Letréguilly, Anne, 1988, Relation between the mass balance of western Canadian mountain glaciers and meteorological data: Journal of Glaciology, v. 34, no. 116, p. 11–18.

Letréguilly, Anne, and Reynaud, Louis, 1989, Spatial patterns of mass-balance fluctuations of North American glaciers: Journal of Glaciology, v. 35, no. 120, p. 163–168.

Mamen, Chris, 1966, Granduc drives tunnel under glacier: Canada Mining Journal, v. 87, no. 1, p. 45–49.

Mathews, W.H., 1951, Historic and prehistoric fluctuations of alpine glaciers in the Mount Garibaldi map area, southwestern British Columbia: Journal of Geology, v. 59, no. 4, p. 357–380.

———1959, Vertical distribution of velocity in Salmon Glacier, British Columbia: Journal of Glaciology, v. 3, no. 26, p. 448–454.

———1964, Water pressure under a glacier: Journal of Glaciology, v. 5, no. 38, p. 235–240.

———1965, Two self-dumping ice-dammed lakes in British Columbia: Geographical Review, v. 55, no. 1, p. 46–52.

———1973, Record of two jökulhlaups, *in* Symposium on the hydrology of glaciers: Cambridge, England, 1969: Association Internationale d'Hydrologie Scientifique Publication No. 95, p. 99–110.

Mokievsky-Zubok, O., 1973, Determination of the mass balance on Sentinel Glacier, British Columbia, Canada: Canada, Inland Waters Directorate, Scientific Series 30, 39 p.

———1980, Sudden discharge of glacier-dammed Flood Lake, August 1979: Ottawa, Fisheries and Environment Canada, National Hydrology Research Institute, Summary Report, 17 p.

Mokievsky-Zubok, O., and Stanley, A.D., 1976a, Canadian glaciers in the International Hydrological Decade Program, 1965–1974: No. 1, Sentinel Glacier, British Columbia—Summary of measurements: Ottawa, Fisheries and Environment Canada, Inland Waters Directorate, Scientific Series No. 68, 75 p.

———1976b, Canadian glaciers in the International Hydrological Decade Program, 1965–1974: No. 2, Place Glacier, British Columbia—Summary of measurements: Ottawa, Fisheries and Environment Canada, Inland Waters Directorate, Scientific Series No. 69, 77 p.

Muir, John, 1915, Travels in Alaska: Boston, Houghton Mifflin Co., 327 p.

Perchanok, M.S., 1980, Reconnaissance of glacier-dammed lakes in the Stikine and Iskut River basins, British Columbia: Ottawa, Fisheries and Environment Canada, National Hydrology Research Institute, unpublished internal report, 45 p.

Reid, I.A., and Shastal, J., 1970, Glacier surveys in British Columbia—1968: Ottawa, Canada Department of Energy, Mines and Resources, Inland Waters Branch, Report Series No. 10, 26 p.

Russell, R.D., Jacobs, J.A., and Grant, F.S., 1960, Gravity measurements on the Salmon Glacier and adjoining snow field, British Columbia, Canada: Geological Society of America Bulletin, v. 71, no. 8, p. 1223–1230.

Tupper, W.A., Waddington, E.D., and Ricker, K.E., 1978, Wedgemount Lake and glacier studies, northern Garibaldi Park, 1977: Canadian Alpine Journal, v. 61, p. 69–70 and map.

Untersteiner, N., and Nye, J.F., 1968, Computation of the possible future behavior of Berendon Glacier, Canada: Journal of Glaciology, v. 7, no. 50, p. 205–213.

Walsh, D.C., 1963, Reclaiming the shaft of Granduc Mines: Western Miner and Oil Review, v. 36, no. 3, p. 86–93.

Glaciers of North America—

GLACIERS OF CANADA

GLACIERS OF THE ST. ELIAS MOUNTAINS

By GARRY K.C. CLARKE *and* GERALD HOLDSWORTH

With a section on QUANTITATIVE MEASUREMENTS OF TWEEDSMUIR AND LOWELL GLACIER IMAGERY

By GERALD HOLDSWORTH, PHILIP J. HOWARTH, *and* C. SIMON L. OMMANNEY

SATELLITE IMAGE ATLAS OF GLACIERS OF THE WORLD

Edited by RICHARD S. WILLIAMS, Jr., *and* JANE G. FERRIGNO

U.S. GEOLOGICAL SURVEY PROFESSIONAL PAPER 1386–J–1

The St. Elias Mountains, which straddle the Canadian and U.S. border, are highly glacierized; ice fields and associated outlet glaciers, plateau glaciers, valley glaciers, and piedmont glaciers are common. The mix of sub-polar and cold glaciers range in area from a few km^2 to more than 1200 km^2 (Seward Glacier). At least 136 of the sub-polar glaciers are surge-type glaciers; the looped medial moraines of surging glaciers are distinctive features on Landsat images. The dynamics of two surging glaciers, Tweedsmuir and Lowell Glaciers, are analyzed on sequential Landsat images

CONTENTS

GLACIERS OF NORTH AMERICA–

GLACIERS OF CANADA

GLACIERS OF THE ST. ELIAS MOUNTAINS

By GARRY K.C. CLARKE[1] *and* GERALD HOLDSWORTH[2]

With a section on QUANTITATIVE MEASUREMENTS OF TWEEDSMUIR GLACIER AND LOWELL GLACIER IMAGERY

By GERALD HOLDSWORTH,[2] PHILIP J. HOWARTH,[3] *and* C. SIMON L. OMMANNEY[4]

Abstract

The St. Elias Mountains region of Canada is made up of a series of mountain ranges that contain a particularly wide variety of glacier types, defined both morphologically and thermally. This variety is a result of the extreme topography, which has a maximum relief of 4,200 meters within a few kilometers, coupled with the large gradients recorded in precipitation and temperature throughout the ranges. Glacier types seen here are valley glaciers, high-elevation plateau glaciers, ice fields and associated outlet glaciers,[5] and piedmont glaciers of different shapes and sizes. Glacier lengths range from about a kilometer to more than 70 kilometers (Hubbard Glacier, which ends in Alaska, has a length of 72 kilometers in Canada and a total length of 112 kilometers); their areas range from a few square kilometers to more than 1,200 square kilometers for Seward Glacier. Temperate glaciers are common at low elevations, particularly on the Pacific Ocean side of the axis (drainage divide). Subpolar glaciers are present on the north (continental) side of the axis even at low elevations. Cold glaciers, at "polar" temperatures, exist on high-elevation plateaus such as on Mount Logan (5,956 meters). The presence of a large concentration of generally subpolar surging glaciers in the region is particularly noteworthy. This topic receives the most attention here because features diagnostic of surges are easily detected on satellite images, from which time-series measurements, related to the dynamics of the glacier, may be made, as shown for Tweedsmuir Glacier and Lowell Glacier.

Introduction

The St. Elias Mountains, straddling the international border between Alaska and Canada (fig. 1), are among the world's most rugged and spectacular glacierized landscapes. This is a region of great scientific interest, particularly to the glaciologist, because few other areas combine such a

Manuscript approved for publication 7 March 2002.

[1] Department of Earth and Ocean Sciences, University of British Columbia, 6339 Stores Road, Vancouver, British Columbia V6T 1Z4, Canada.

[2] Arctic Institute of North America, University of Calgary, 2500 University Drive, NW., Calgary, Alberta T2N 1N4, Canada; Institute for the Study of Earth, Oceans, and Space, Morse Hall, University of New Hampshire, Durham, NH 03824–3525; and the National Hydrology Research Centre, 11 Innovation Boulevard, Saskatoon, Saskatchewan S7N 3H5, Canada; e-mail address: [gholdswo@acs.ucalgary.ca].

[3] Department of Geography, University of Waterloo, Waterloo, Ontario N2L 3G1, Canada.

[4] International Glaciological Society, Lensfield Road, Cambridge CB2 1ER, England, U.K. (formerly with the National Hydrology Research Institute [now the National Hydrology Research Centre], 11 Innovation Boulevard, Saskatoon, Saskatchewan S7N 3H5, Canada).

[5] In Canada, icefield is commonly used in place-names instead of ice field. In the volumes of the Satellite Image Atlas of Glaciers of the World, ice field is used (compare Jackson, 1997, p. 316) in the glaciological sense of the term.

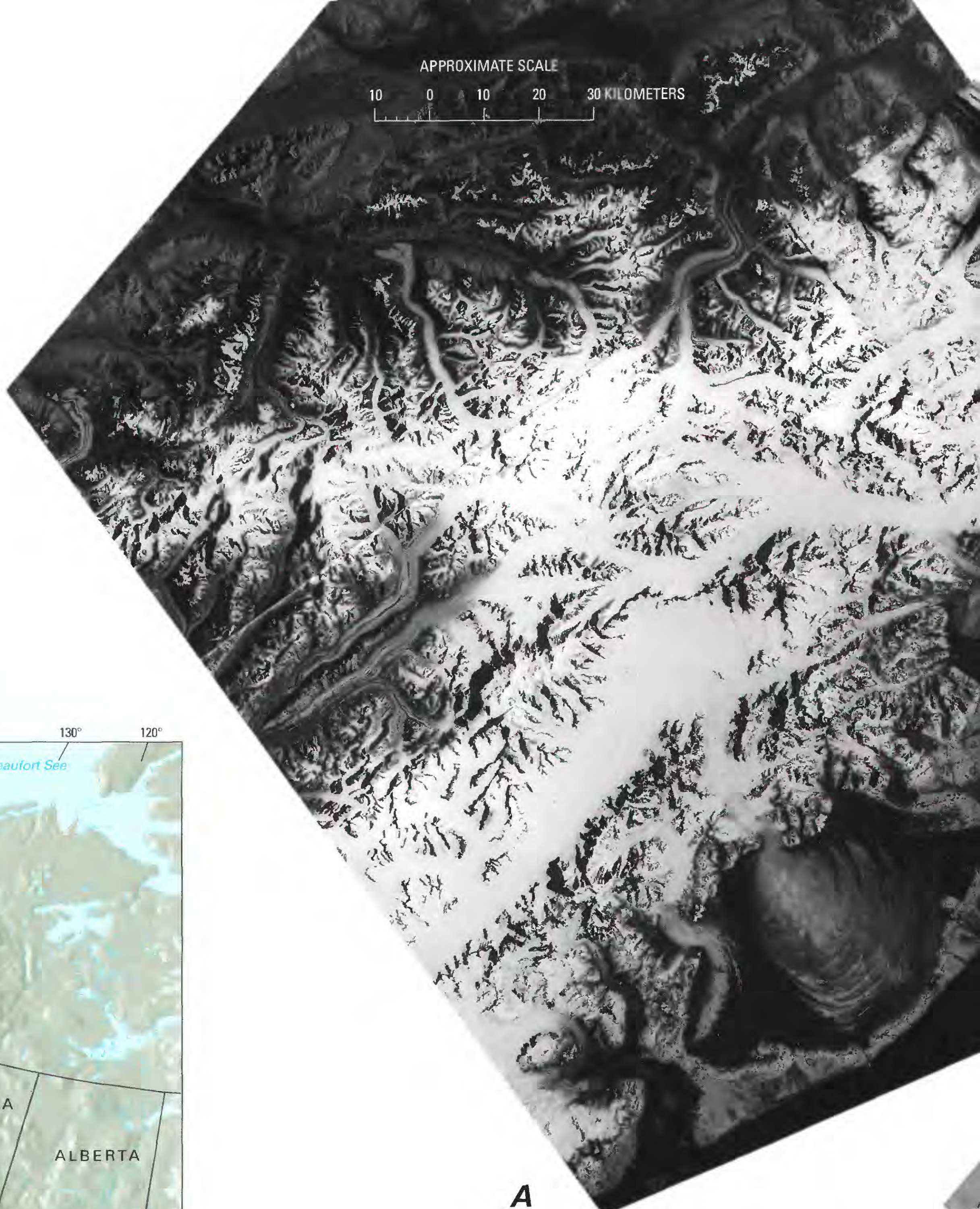

Figure 1.—*Location of the St. Elias Mountains, Yukon Territory-Alaska, and Landsat image mosaics of the mountains.* **A**, *Landsat 2 and 3 multispectral scanner (MSS) image mosaic of the St. Elias Mountains. Landsat images (21314–19295, band 7; 28 August 1978; Path 66, Row 18; 2952–19124, band 7; 31 August 1977; Path 64, Row 19; 2955–19285 and 2955–19292, band 7; 3 September 1977; Path 67, Rows 17 and 18; 3157–19514, band 7; 23 June 1982; Path 66, Row 18) are from the EROS Data Center, Sioux Falls, S. Dak.* **B**, *Annotated Landsat 2 and 3 MSS image mosaic of the St. Elias Mountains using the same Landsat images as for* A. *Abbreviations: Gl., Glacier; Mt., Mount; Mtn., Mountain; N., North; S., South.*

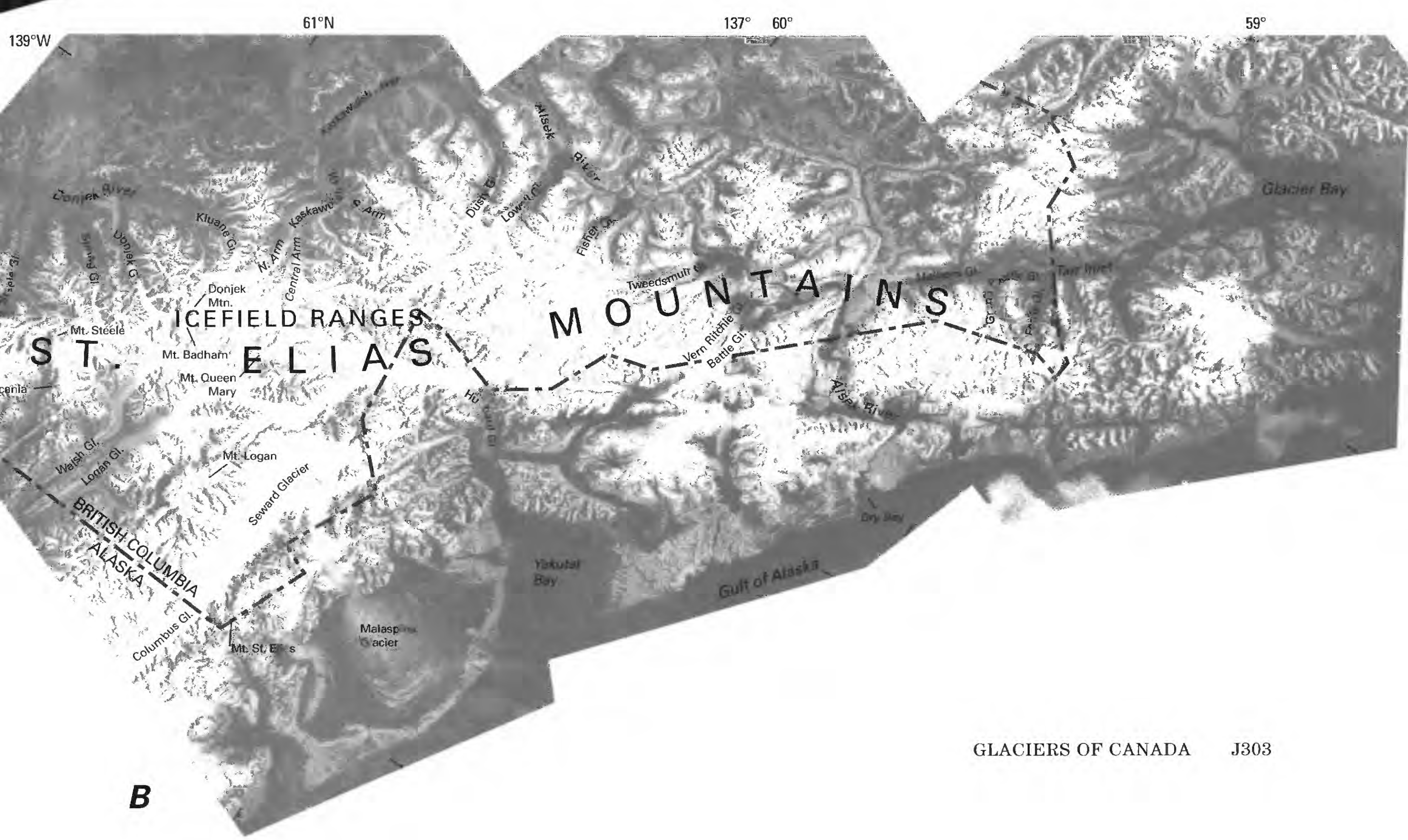
139°W
61°N
137°
60°
59°
Donjek River
Donjek Gl.
Kluane Gl.
Kaskawulsh
N. Arm
Central Arm
S. Arm
Alsek River
Dusty Gl.
Lowell Gl.
Fisher Gl.
Donjek
Mtn.
ICEFIELD RANGES
Mt. Steele
Mt. Badham
Mt. Queen
Mary
ST. ELIAS MOUNTAINS
Tweedsmuir Gl.
Melbern Gl.
Tarr Inlet
Glacier Bay
Vern Ritchie Gl.
Battle Gl.
Alsek River
Walsh Gl.
Logan Gl.
Mt. Logan
Seward Glacier
BRITISH COLUMBIA
ALASKA
Yakutat
Bay
Dry Bay
Gulf of Alaska
Columbus Gl.
Mt. St. Elias
Malaspina
Glacier

B

concentration of glaciers with such a wide variety of glacier types. The explanation for both the concentration and the variety lies in the region's proximity to the Gulf of Alaska and in the large elevation change found between the Alaskan coast and the central axis of the mountain ranges that make up the St. Elias Mountains. In fact, the elevation rises within a few kilometers of the coast to a maximum relief of 4,200 m. Some of the highest precipitation rates in Canada are present in this region, and snow may fall at any time of the year.

The Icefield Ranges (fig. 2) form the central axis or crest of the St. Elias Mountains and act as both a hydrologic and climatic divide. This is the region of the most intense glacier activity and the location of the highest peaks: Mount Logan (5,956 m, labeled 1 in fig. 2), Canada's highest mountain; Mount St. Elias (5,489 m, labeled 2 in fig. 2); Mount Lucania (5,227 m, labeled 21 in fig. 2), and Mount Steele (5,067 m, labeled 22 in fig. 2). The topographic barrier formed by the Icefield Ranges imposes a strong gradient in precipitation and mean annual temperature from the Alaskan coast to the edge of the Yukon interior. Glaciers, representing every geophysical class from temperate to cold (high polar), are found here. In general, temperate glaciers are common at low elevations, particularly on the Pacific Ocean side of the axis (drainage divide). Subpolar glaciers are present on the north (continental) side of the axis even at low elevations. Temperatures, as measured at 10 m depth in the firn, range from 0°C on the Seward Glacier (labeled 17 in fig. 2) at 1,800 m (Sharp, 1951b) to about –29°C on Mount Logan at 5,340 m (Holdsworth and others, 1992). Some glaciers are subpolar in their ablation areas and temperate elsewhere; others are apparently temperate in their ablation areas and slightly cold on their névés. An example of this is the transect glacier system of Kaskawulsh and Hubbard Glaciers (labeled 12 and 18 in fig. 2) which share a common divide at 2,674 m.

A remarkable feature of the valley glaciers of the St. Elias Mountains is that so many of them surge (Meier and Post, 1969). Of the 204 surging glaciers identified by Post (1969) in western North America, 136 are in the St. Elias Mountains, and most of these are in Canada. The most important, generally subpolar, surging glaciers located entirely or partly in the Canadian part of the St. Elias Mountains are the Anderson (labeled 6 in fig. 2), Chitina (5), Walsh (4), Klutlan (7), Steele (8), Donjek (10), Kluane (11), Dusty (13), Lowell (14), and Tweedsmuir Glaciers (fig. 1). The surging character of most of these glaciers can easily be identified by the characteristically looped medial moraines that can be seen so well on Landsat imagery. Whereas it is striking that so many of the very large glaciers surge, size alone is not the key to understanding surges because many medium-sized and even very small glaciers surge (Clarke, 1991). Also, no one obvious explanation exists for the remarkable geographical concentration of surging glaciers in the St. Elias Mountains. [For a discussion of surging glaciers, the reader is referred to Chapter K, Glaciers of Alaska; see also Chapter E, Glaciers of Svalbard, Norway, another glacierized region that has a variety of glacier types and a large number (86) of surging glaciers documented from the end of the 19th century to 1993.]

The following commentary discusses the major glaciers in the region and, following Field (1975), is organized according to recognized hydrologic-drainage systems. Glacier lengths have been measured from current (usually 1:250,000-scale) topographic maps and are given in square brackets, although some discrepancies are present between the values given here and those given by Field (1975). Glacier lengths range from about a kilometer to more than 70 kilometers (Hubbard Glacier, which ends in Alaska, has a length of 72 kilometers in Canada and a total length of 112 kilometers); their areas range from a few square kilometers to more than 1,200 square kilometers for Seward Glacier.

***Figure 2.**—(opposite page) Annotated mosaic of Landsat 2 MSS images of the Icefield Ranges, St. Elias Mountains, Yukon Territory-Alaska. Annotations: 1, Mount Logan (elevation 5,956 m), highest mountain in Canada; 2, Mount St. Elias (elevation 5,489 m), second highest mountain in Canada; 3, Logan Glacier; 4, Walsh Glacier; 5, Chitina Glacier; 6, Anderson Glacier; 7, Klutlan Glacier; 8, Steele Glacier; 9, Spring Glacier; 10, Donjek Glacier; 11, Kluane Glacier; 12, Kaskawulsh Glacier; 13, Dusty Glacier; 14, Lowell Glacier; 15, Fisher Glacier; 16, Malaspina Glacier; 17, Seward Glacier; 18, Hubbard Glacier; 19, Russell Fiord; 20, Columbus Glacier; 21, Mount Lucania; 22, Mount Steele. The Landsat images (2955–19285 and 2955–19292, band 7; 3 September 1977; Path 67, Rows 17 and 18) are from the EROS Data Center, Sioux Falls, S. Dak. Map reference: Mount St. Elias map sheet 115B and 115C, 1:250,000 scale.*

140°W
139°
138°
141°W
61°N
60°
Kluane Lake
ICEFIELD RANGES
1
2
3
4
5
6
7
8
9
10
11
12
13
14
15
16
17
18
19
20
21
22
APPROXIMATE SCALE
0
50 KILOMETERS

Most of the glaciers discussed are of the valley type. However, another important class of glaciers is mentioned here because of its relevance to ice coring. These are the high-elevation plateau glacier systems such as on Mount Logan (fig. 1). They are in the permanent accumulation area and thus appear white on satellite images throughout the year. In addition, ice fields and piedmont glaciers are found here as well.

Chitina River Valley System

The major glaciers of the Chitina River valley system are the Anderson [40 km], Chitina [70 km], Walsh [70 km], and Logan [70 km] Glaciers (fig. 3). All have their accumulation zones in the Icefield Ranges of Canada and flow across the 141st meridian, which defines the border between the Yukon Territory and Alaska. In the recent past, these glaciers were tributaries of a large trunk glacier that occupied the upper Chitina River valley. On the 1975 National Topographic Series (NTS) map sheet 115SW and 115SE (1:500,000 scale), these four glaciers are seen to merge. Now, the

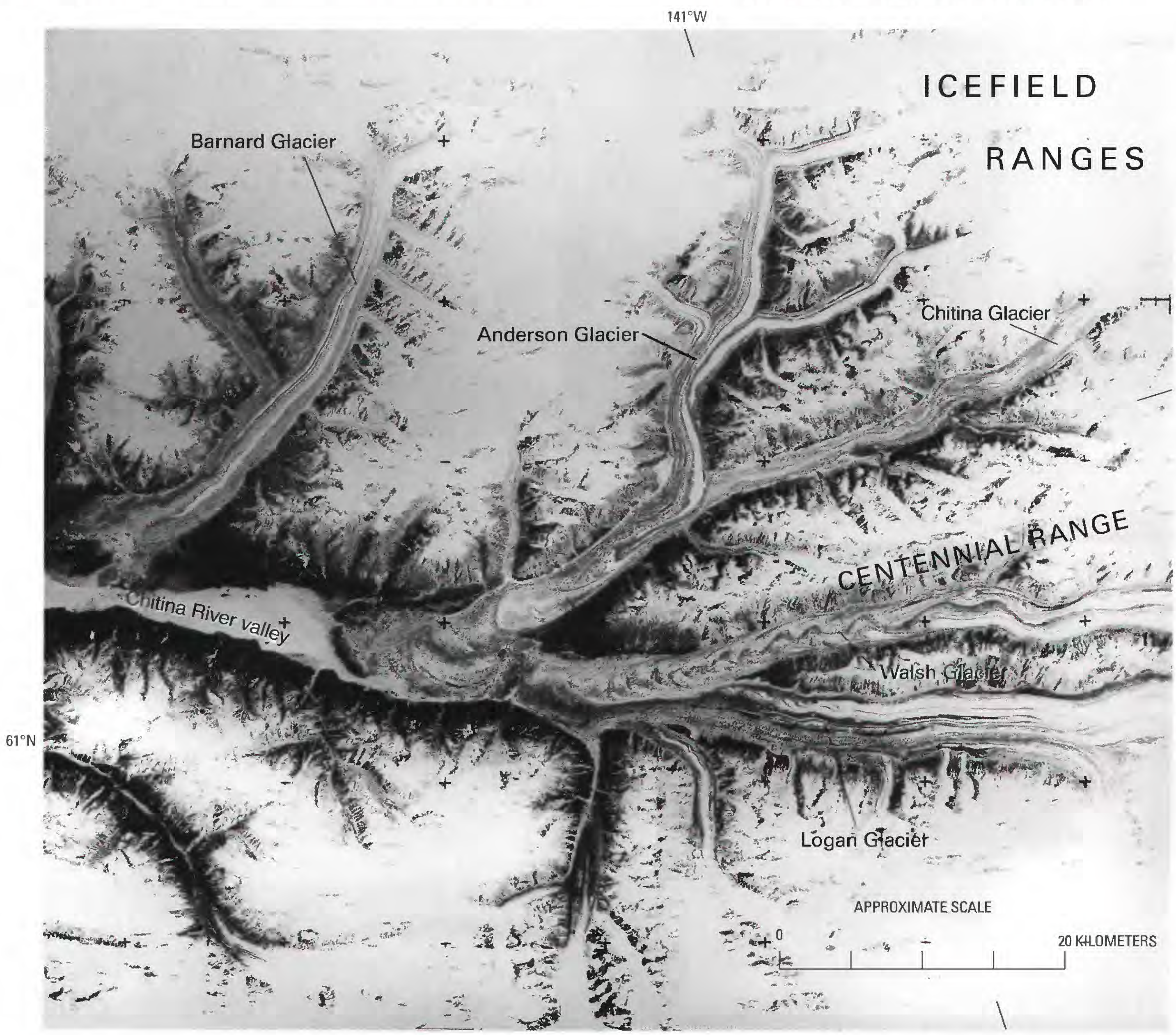

***Figure 3.**—Annotated enlargement of part of a Landsat 3 return beam vidicon (RBV) image showing the glaciers of the upper Chitina River valley basin, St. Elias Mountains, Yukon Territory-Alaska. Walsh Glacier shows well-defined moraine loops that identify the glacier as surging. Its 1960–64 surge displaced ice as much as 11.5 km—a record for North America. The approximate 1968 surge of Anderson Glacier truncated the terminus of Chitina Glacier, another surging glacier. Logan Glacier is not included in Post's (1969) catalog of surging glaciers; the moraine loops near its confluence with Walsh Glacier indicate variations in flow velocity, but these may be in response to surges of Walsh Glacier. The Landsat 3 RBV image (30853–19510; 5 July 1980; Path 68, Row 17, Subscene C) is archived by the U.S. Geological Survey Glacier Studies Project. Map references: Kluane Lake map sheet 115G and 115F (E 1/2); Mount St. Elias map sheet 115B and 115C; Bering Glacier map sheet N6000–W14100/60x180; McCarthy map sheet N6100–W14100/60x180; all 1:250,000 scale.*

Logan-Walsh merger and the Anderson-Chitina merger do not appear to connect with each other. The glacier system also does not appear to merge on two satellite images taken 3 years apart (Landsat 1, 7 August 1974; Path 69, Row 17; and 4 September 1977; Path 68, Row 17). However, inspection of a later image (Landsat image, 1 Nov 1978; Path 68, Row 17, the same scene illuminated by a low (13°) Sun angle on thin snow cover) shows that a (1- to 1.5-km) section of ice-cored moraine probably still bridges the two glacier pairs. The same pitted surface topography that is characteristic of the terminus of all the glaciers is also seen in that section. The glaciers look essentially the same on the three images, which indicates that they were in a quiescent phase.

A surge of Walsh Glacier, thought to have started in late 1960 or early 1961, lasted 4 years and displaced ice as much as 11.5 km—a record for North America (Post, 1966, 1967). Conspicuous medial moraine loops can be traced on the glacier surface, and their spacing can be used to infer a fairly regular surge-cycle periodicity for Walsh Glacier. Note that the Walsh Glacier apparently overrides the end of Logan Glacier (fig. 3). In 1966, the Anderson Glacier showed signs of entering a surge phase (Post, 1967) and was observed to be surging in 1968. It was reported (Field, 1975) that the surge was slowing down in early 1971. Landsat images of 1974, 1977, and 1980 (see fig. 3) show the Chitina Glacier totally overridden by the Anderson Glacier surge.

White River Valley System

Klutlan Glacier (fig. 1) [approximately 72 km measured from the base of Mount Bona, Alaska] is a large surging glacier that has numerous tributaries feeding ice into it. Only the last 25 km of the glacier is in Canada where it has two important tributaries entering it on the south side. These are the Nesham and Mount Wood Glaciers—both of which surge. On the Landsat images, evidence of surging of the Klutlan is seen only below the Nesham Glacier, despite Field's claim that "the entire Klutlan system is subjected to repeated surges" (Field, 1975). The same Landsat images of 7 August 1974 (Path 69, Row 17) and 4 September 1977 (Path 68, Row 17) mentioned above show virtually no change in configuration of the lower glacier or of the tributaries, so the system was in the quiescent phase then. Field (1975) states that "a small left-hand tributary of the Nesham surged independently in 1966." The end of the glacier is quite indistinct, and ice-cored moraine may stretch more than 12 km beyond the last visible white ice. Recent surges have not disturbed this terminal area, and a spruce forest has grown up on the moraine cover. Past major surges blocked regional drainage and formed glacier-dammed lakes; two of these lakes had estimated volumes exceeding 10^8 m^3. The catastrophic emptying of these lakes might have produced substantial jökulhlaups (glacier-outburst floods) in the White River valley. The glacial geology and paleolimnology of this lower deglaciated region have received considerable attention (Rampton, 1970; Bradbury and Whiteside, 1980; Driscoll, 1980; Whiteside and others, 1980; Wright, 1980).

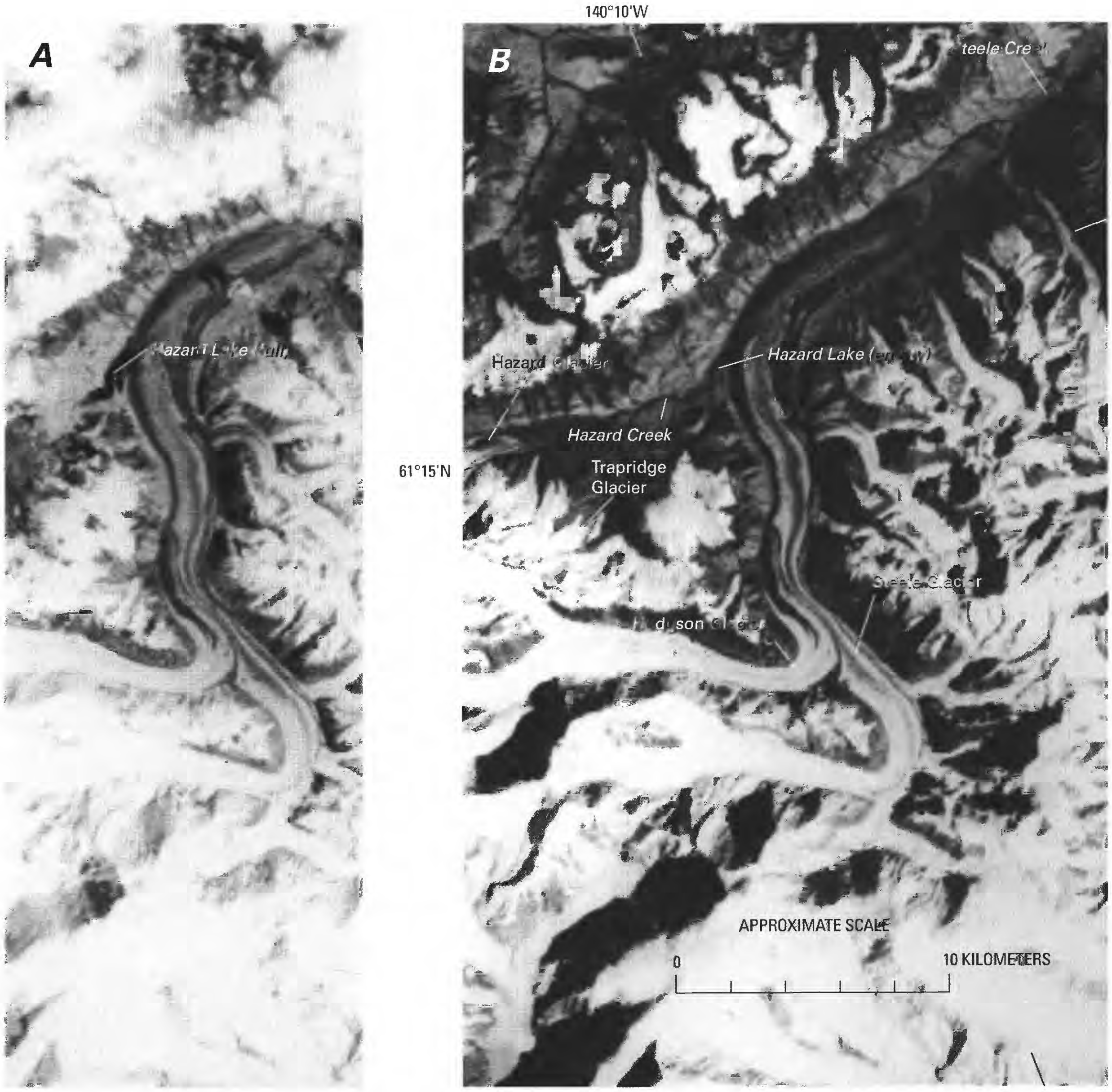

Donjek River Valley System

Figure 4.—*Annotated enlargements of parts of two Landsat 2 MSS images showing glaciers of Steele Creek drainage basin, Yukon Territory. Steele Glacier surged in 1965-66, and displaced ice as much as 9.5 km, which dammed Hazard Creek in the process. The resulting proglacial lake, known as Hazard Lake, now fills and drains annually. A surge of Hodgson Glacier, a tributary of the Steele, followed the Steele surge by several years and may have been triggered by it.* **A**, *A part of Landsat image 2901–19315, band 7; 11 July 1977; Path 67, Row 17, showing glacier-dammed Hazard Lake full and partial cloud cover.* **B**, *A part of Landsat image 2955–19285, band 7; 3 September 1977; Path 67, Row 17, showing the empty basin of Hazard Lake after an outburst flood that took place between 2 and 5 August 1977. The lake drains through a subglacial tunnel that runs from the ice dam to the Steele Glacier terminus at the head of Steele Creek. The Landsat images are from the EROS Data Center, Sioux Falls, S. Dak. Map reference: Kluane Lake map sheet 115G and 115F (E 1/2), 1:250,000 scale.*

Steele Glacier [approximately 40 km long] is best known for its 1965–66 surge. Figure 4 shows the glacier in its quiescent phase. Note that the large western tributary apparently overrides the southeast, or main, trunk of the glacier. This feature is a relict of the surge a decade earlier. The ice-cored moraine of the overextended lower glacier, now shrunken, can also be clearly seen. Steele Glacier was one of the few glaciers in the region to receive early scientific attention (Sharp, 1943, 1951a; Wood, 1936, 1942, 1972). A minor surge in the early 1940's did not affect the lower glacier. The last surge, in contrast, was quite spectacular. It started in late 1965, and by summer 1966, a large wavelike bulge was seen moving down the glacier. By summer 1967, the total ice displacement was as much as 9.5 km (Stanley, 1969). The peak speed during the approximately 3-year duration of the surge phase was 24 m d^{-1}, reached in early 1966. By the beginning of 1968, the speed was down to 1 m d^{-1} and dwindling. Between surges, the lower (ablation) zone is virtually stagnant, and the ice is covered by rock debris. The Steele Glacier and several of the smaller glaciers (such as Trapridge Glacier) in the Steele Creek drainage basin are known to be subpolar;

hence, it is postulated that their surge mechanism is thermally controlled (Jarvis and Clarke, 1974, 1975, and Clarke and Jarvis, 1976).

The 1965 surge dammed Hazard Creek and created Hazard Lake on the left margin of Steele Glacier near the sharp bend in the glacier. This lake is a transient feature that disappears entirely when the ice level ablates sufficiently. During the 1970's and 1980's, the annual cycle of filling and self-draining of the lake was studied in detail (Collins and Clarke, 1977; Clarke, 1982). The draining of the lake generated small (600 $m^3 s^{-1}$) jökulhlaups in Steele Creek. Figure 4*A* shows the lake full on 11 July 1977; figure 4*B* shows it empty on 3 September 1977 following the draining of 2–5 August 1977.

Southeast of Steele Glacier are the following glaciers: Spring [approximately 26 km long], Donjek [55 km], and Kluane [35 km] Glaciers (fig. 5). All are known to surge, but only the Donjek has received much attention. The Donjek Glacier terminus spreads out as it flows into a river valley to form a small piedmont lobe. Former (major) surges have caused this lobe to expand and to butt against the Donjek Ranges to the east, which blocked the flow in the river that is fed by Kluane Glacier and numerous other smaller glaciers to the east.

Just prior to July 1974, the last tributary on the southeast margin of Donjek Glacier surged. A Landsat image of 15 September 1973 (Path 67, Row 17) shows the presurge condition, and an image of 4 September 1977 (Path 68, Row 17) shows the relict effect of the surge on the main glacier 3 years after the event (also see fig. 5, 10 August 1980). Donjek Glacier did not respond to the surge. In 1978, a minor surge of Donjek Glacier failed to dam the river. Several centuries ago, the glacier formed an ice dam that created Lake Donjek, estimated to have had a volume of 230 $x10^6$ m^3 (see lake site in fig. 5). This transient lake was thought to have drained catastrophically on at least one occasion (Clarke and Mathews, 1981). The terminal moraines of this glacier have been studied by Johnson (1972a, b).

In one of the major accumulation basins of the Donjek Glacier, between Donjek Mountain and Mount Badham, is an ice-core drill site, referred to in the literature (for example, Holdsworth and Peake, 1985) as *Eclipse*. The site is at lat 60°50'N., long 139°50'W. at an elevation of 3,017 m (maps 115B and 115C, Mount St. Elias map sheet, 1:250,000 scale) and has been core drilled on several occasions. Here, the 10-m firn temperature is –6°C, which makes this part of the glacier subpolar. The mean annual air temperature here is –13°C, as determined from an automatic weather station (Holdsworth, 1992). The annual accumulation rate is determined from pit and core studies to be 1,500 kg m^{-2} a^{-1} (1,500 mm water equivalent). The depth of ice as determined by radar is about 550 m. The site awaits deep drilling in order to acquire a long ice core.

Slims River Valley System

Kaskawulsh Glacier [75 km long] (fig. 6) flows from a divide that it shares with the Hubbard Glacier (fig. 1) and ends at the head of two river valleys: the Slims and the Kaskawulsh. Thus, the glacier contributes water to two rivers simultaneously; the relative contributions, which vary from year to year, depend on snout position and varying hydrologic-sedimentation conditions. Although Slims River now flows into Kluane Lake (fig. 2), in earlier times, Kluane Lake drained through the (reversed) Slims River down the Kaskawulsh River and into the Alsek River (fig. 1) (and thence to the Pacific Ocean) (Bostock, 1969). Kaskawulsh Glacier is not known to surge, and this is confirmed by the regular pattern of medial moraines seen in satellite images (fig. 6). However, the last tributary flowing into the *central arm* contains wavy moraines and a "beaded" suture, indicating that this tributary has surged at least once in

__Figure 5.__—Annotated enlargement of part of a Landsat 3 MSS image showing the Donjek Glacier region, St. Elias Mountains, Yukon Territory. Spring, Donjek, and Kluane Glaciers are surge-type glaciers. Surges of Donjek Glacier have historically closed the Donjek River channel near Mount Hoge to form a large lake. An outburst flood from the lake could release roughly 230 x 10^6 m^3 of water across the Alaska Highway and the route of a proposed natural gas pipeline. A weak surge of Donjek Glacier, noted in 1978, almost dammed Donjek River. The Landsat image (30889–19492, band 7; 10 August 1980; Path 68, Row 17) is from the EROS Data Center, Sioux Falls, S. Dak. Map reference: Kluane Lake map sheet 115G and 115F (E 1/2), 1:250,000 scale.

Figure 6.*—Annotated enlargement of part of a Landsat 3 RBV image of Kaskawulsh Glacier, Yukon Territory. Kaskawulsh Glacier is one of the few large glaciers of the St. Elias Mountains that does not surge. It is a classic example of a trunk glacier that has many tributary branches. The uncontorted medial moraines indicate steady, rather than irregular, flow. The glacier terminus is at a major hydrologic divide, as Slims River flows to the Arctic Ocean and Kaskawulsh River flows to the Pacific Ocean. The Landsat 3 RBV image (30167–19491; 19 August 1978; Path 66, Row 18, Subscene A) is archived by the U.S. Geological Survey Glacier Studies Project. Map reference: Mount St. Elias map sheet 115B and 115C, 1;250,000 scale.*

the past. Low-altitude aerial photographs acquired in the 1970's and 1980's also suggest a similar conclusion. This is an example where surging tributaries do not necessarily trigger surges in the main glacier.

Measured ice thicknesses vary from 780 m near the divide (Clarke, 1967) to 650 m at the entrance to the *north arm* (Holdsworth, 1965) to 1,040 m in the ablation zone below the confluence of the *north* and *central arms* (Dewart, 1970). Surface-flow rates reach 150 m a^{-1} at the entrance to the *north arm* (Brecher, 1966) and have an ice discharge of more than 10^8 m^3 a^{-1} (Holdsworth, 1965). Ice-flow rates increase through an ice fall and then decrease to 179 m a^{-1} below the confluence (Dewart, 1970). Although some suggest that the divide region contains some "cold" firn [see Field (1975)], the general consensus is that the glacier is temperate. Holdsworth (1965) found that deep temperatures in partial water-filled crevasses at the entrance to the *north arm* are 0°C during the summer.

The intensity of research on the Kaskawulsh Glacier, and in the Icefield Ranges in general, was due to the Icefield Ranges Research Project, which was initiated jointly in 1961 by the Arctic Institute of North America and the American Geographical Society (Bushnell and Ragle, 1969, 1970, 1972, and Bushnell and Marcus, 1974).

Alsek River Valley System

The major glaciers of the Alsek hydrologic system in Canada are the Dusty [38 km long], Lowell [70 km], Fisher [48 km], Tweedsmuir [70 km], Vern Ritchie [46 km], Battle [27 km], and Melbern [20 km] Glaciers (fig. 1). The Alsek River cuts through the eastern part of the St. Elias Mountains and discharges into Dry Bay, Alaska. The surging glaciers in this group are the Dusty, Lowell, Fisher, and Tweedsmuir Glaciers (in sequence from the north), and all flow directly into the Alsek River valley.

Dusty Glacier surged about 1966; Lowell Glacier surged in 1948–50, in 1968–70, and in early 1983 (the last known surge). Dusty Glacier has a particularly simple, but distinctive, pattern of medial moraine loops, accentuated by a dark debris cover on the north side, which suggests that the north tributary is the surging one. An interesting through-flow of ice from the Dusty Glacier into the Lowell Glacier is also present, and this may be seen in figure 2, where it is evident from the transient snowline on both glaciers that Dusty Glacier is the higher of the two at that location. Also, it is possible to deduce from the ice structure and deformed or truncated medial moraines on Lowell Glacier that the flow is coming in from Dusty Glacier. On the 1:250,000-scale map sheet, this cannot be ascertained, but the newer (1987) 1:50,000-scale map (115B/8) shows the situation correctly. The deformed medial moraines on the lower part of Lowell Glacier are not easily interpreted. Post and others (1976) used easily identifiable points in the deformed moraine field, on successive images, to compute ice displacements between 1954 and 1973.

The next glacier south, Fisher Glacier, surged around 1970, but little information about this event is available. In 1973, Tweedsmuir Glacier began a surge (Holdsworth, 1973) that lasted only into early 1974. A quantitative analysis of glacier-surge dynamics using Landsat images of Tweedsmuir and Lowell Glaciers can be found in the separate section that follows. Tweedsmuir Glacier has a large piedmontlike lobe that expanded to dam the Alsek River temporarily in the winter of 1973–74. Because no flow was observed below the dam, the glacier ice must have been cold (that is, below 0°C). By the summer of 1974, the Alsek River was flowing past the glacier and caused massive ice calving into the river.

Glaciers in this group all have the potential for impeding the flow of the Alsek River, which has a peak summer discharge generally in the range 1,000–1,400 $m^3 s^{-1}$. Past surges of Lowell Glacier have been the most significant. Clague and Rampton (1982) documented the history of historic Lake Alsek, which formed several times during the past 1,000 years as a result of major damming of the Alsek River by Lowell Glacier. The last such event was thought to have been around 1900.

When these large historic lakes drained, they did so catastrophically and caused jökulhlaups downstream, as well as discharged meltwater and sediment into Dry Bay, Alaska. Evidence of these past floods is visible on the forested sides of the gorge between Fisher and Tweedsmuir Glaciers.

Quantitative Measurements of Tweedsmuir Glacier and Lowell Glacier Imagery

By Gerald Holdsworth, Philip J. Howarth, *and* C. Simon L. Ommanney

Introduction

Tweedsmuir and Lowell Glaciers (lat 59°52'N., long 138°19.3'W., and lat 60°17.8'N., long 138°17.2'W., respectively) are located in the St. Elias Mountains in the watershed of the Alsek River, a river that they both have dammed in the recent past. The terminal regions of both glaciers exhibit prominent surface features typical of surging glaciers (Meier and Post, 1969). It is likely that their surges are, at least in part, thermally controlled (Clarke, 1976). Both glaciers are about 70 km long and average 1 km wide, although they are considerably wider in their terminal regions. One of the most distinctive aspects of their surface features is the folded structure seen in the exposed ice in the lower part of each glacier. The folds are defined by medial moraines and by different ice types, which may appear white, blue, or gray depending on the content of air bubbles and fine-grained sediment. The folds can clearly be identified on both terrestrial and aerial photographs (figs. 7 and 8) at most scales and very easily on Landsat images given favorable conditions. For the features to be seen on visible-band satellite images,

***Figure 7.**—High-angle oblique aerial photograph of Tweedsmuir Glacier showing folded medial moraine loops and ice margin contact with the Alsek River. View is toward the south. Photograph no. 73R2–197 taken on 11 September 1973 by Austin Post, U.S. Geological Survey.*

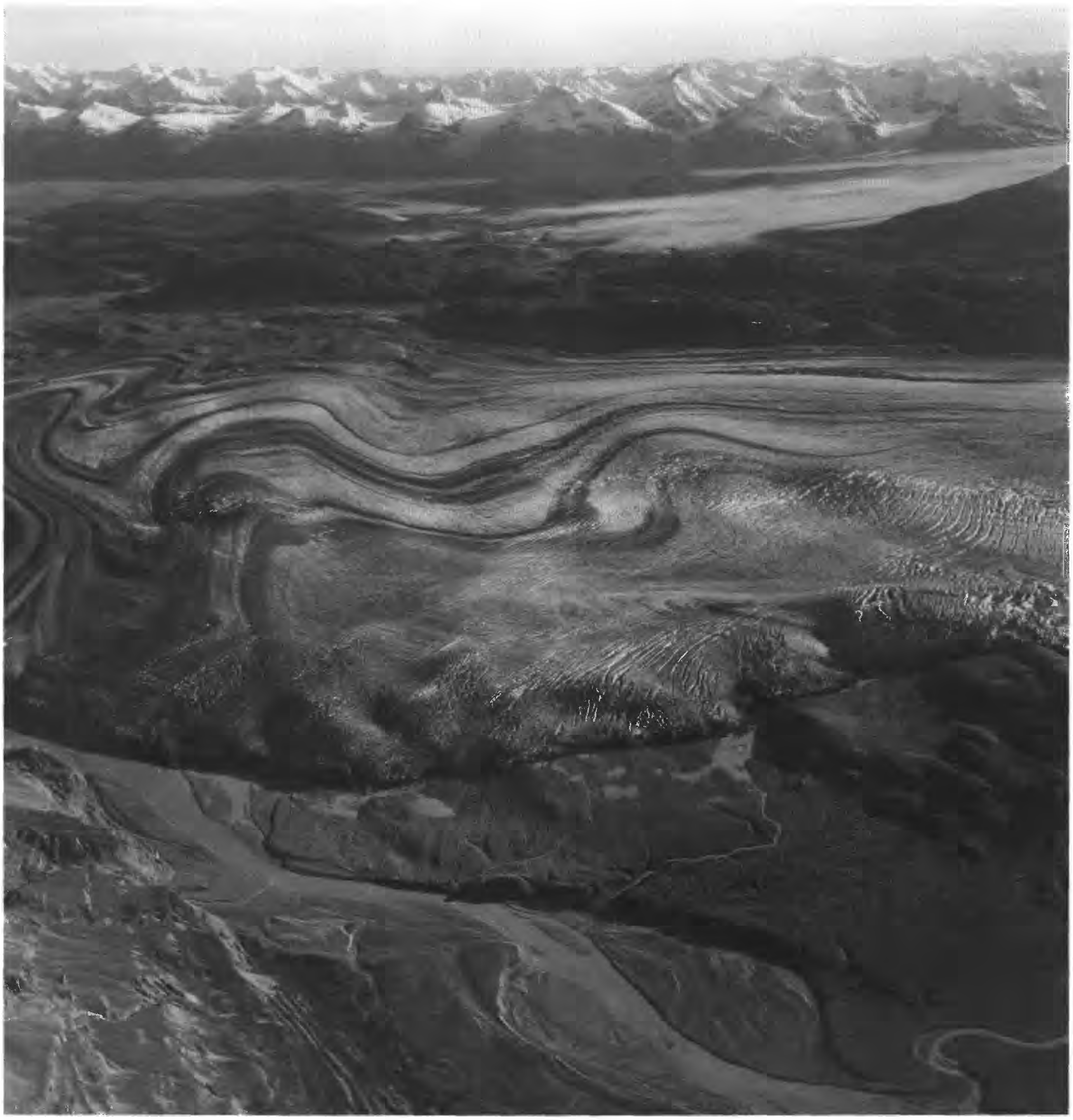

the lower (ablation) region of the glacier, where the fold fields are found, needs to be totally free of seasonal snow cover. Because of this, and because of a high incidence of cloud cover in the region, the best period to obtain imagery to study moraine movement is normally in August or September, when, also, the low Sun angle provides optimum scene contrast and relief detail.

The two glaciers studied surge at slightly irregular intervals, typically, on average, at 20–30-year intervals, but not concurrently. During a surge, any preexisting curvilinear feature on the glacier will become folded because of nonhomogeneous strains in the ice. If surface folds are already present from a previous surge, they will be amplified during a subsequent surge. In addition to large longitudinal displacements, significant transverse displacements also result, which enable flow vectors (in two dimensions) to be obtained quite accurately. Employing conventional analyses of Landsat

Figure 8.—*High-angle oblique aerial photograph of Lowell Glacier showing complex structure in the medial moraines near the terminus. Icebergs can be seen in the proglacial lake. Alsek River flows south out of the lake toward the bottom of the picture. Photograph no. 69R1–287 taken on 25 August 1969 by Austin Post, U.S. Geological Survey.*

images, we used the spatial changes that took place in these surface fold fields over time to generate displacement, velocity, and strain-rate data. From these data, it is also possible to deduce something about the movement of the ice in the vertical direction.

By using Landsat images and aerial photographs, we studied Tweedsmuir Glacier during the late-surge (1973) and postsurge (1974) phases of a recent surge cycle. Lowell Glacier was studied in the presurge (1973–82) to the surge (1983) phase of the last surge cycle. From point-displacement measurements made on Landsat images taken about 5 years apart for Tweedsmuir Glacier and spanning about 10 years for Lowell Glacier, useful information relating to glacier-surge dynamics was obtained. In particular, the application of this information could be used to predict whether the Alsek River will be dammed again by a future surge of either glacier.

Observations on the Tweedsmuir Glacier Imagery

Tweedsmuir Glacier ends in an expanded lobe that is in contact with the Alsek River in several places during a surge. Its thickness has not been measured, but ice cliffs at the river valley contact were estimated to be about 25–30 m high in 1973. On the northern land-based sublobe, the cliff thickness was about 15 m. Thicknesses in the center of the lobe are probably about 50 to 100 m, based on marginal thicknesses, surface slopes, and the surrounding topographical detail seen on the 1:50,000-scale map sheets.

The glacier began to advance at its terminus in early 1973 (Holdsworth, 1973), possibly during April. Because surging evidently involves a series of linked processes, some delay may have been present before the ice edge actually began to move forward. The marginal ice was known to have been below the melting point, and hence, it was effectively frozen to the bedrock before the surge. During the surge, basal sliding and enhanced flow in any basal till would have been the most important mechanisms for ice transport. By direct observation, the peak activity would seem to have been in June or July 1973, and by the end of that year, the movement of the transient margin had decreased to very low levels. The speed of the ice flow in at least the lower 7 km of the glacier increased by about an order of magnitude during the surge (Post and others, 1976). This demonstrates the importance of basal sliding during a surge, a hypothesis further substantiated by Kamb and others (1985) in their study of the 1982–83 surge of Variegated Glacier, southeastern Alaska.

Krimmel and Meier (1975) show velocity vectors that indicate speeds in excess of 10 m d^{-1} between 22 July 1973 and 13 September 1973 in the same lower part of the glacier. These data were obtained from the Earth Resources Technology Satellite (ERTS-1, later renamed Landsat 1) satellite images that were enlarged to a scale of 1:50,000 and then analyzed by L.R. Mayo. Additional analyses were later done by Miller (1974).

In this paper, we are making types of measurements similar to these earlier ones, except that we used 1:25,000-scale plots obtained by processing digital Landsat data on a Canadian Image Analysis System (CIAS) at the Canada Centre for Remote Sensing in Ottawa. Enhanced and mutually registered electrostatic printer plots were produced for the excellent Landsat images of 13 September 1973 and 28 August 1978 (fig. 9), which cover the end of the surge and the postsurge period. The registration points used were all sufficiently far from the glacier to be safely assumed to be fixed. The same digital images at 1:50,000 scale registered acceptably with a 1:50,000-scale map compiled from 17 August 1974 vertical aerial photographs. Even if registration with a digital terrain map or a conventional map is not exact, registration between two satellite images of the same area is sufficient to provide acceptable displacement and, hence, velocity values for transient features in the scenes. Registration of the images was achieved by a least squares optical procedure that has a

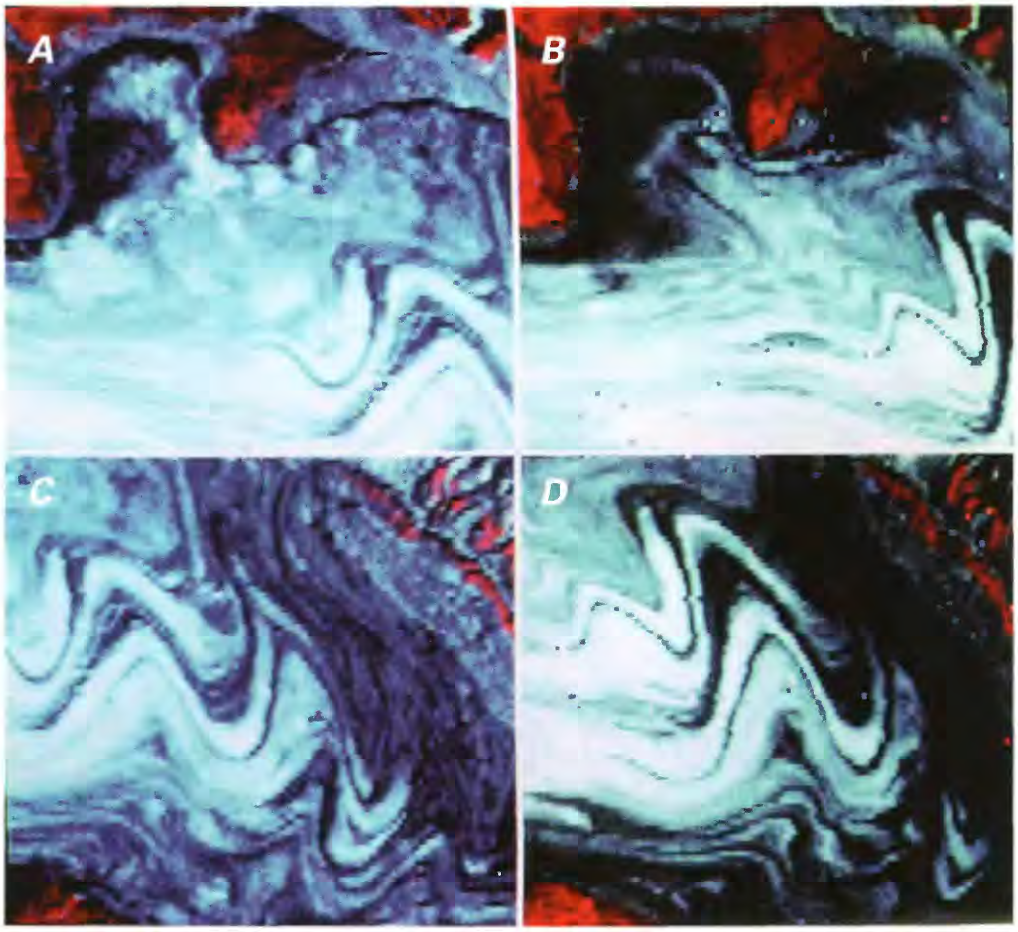

precision dictated by the picture element (pixel) dimension, approximately 57 m x 79 m. Displacements of the best defined points on the glacier were scaled directly from the registered transparencies and had an estimated error of between ±40 m and ±45 m.

Figure 9*A* shows very well the dark margin in 1973 on the north edge of the glacier caused by the 15-m high (and probably still advancing) ice cliff at that location. By 1978 (fig. 9*B*), this margin is poorly defined because of subsequent postsurge downwasting of the ice edge. Of great significance here is the observed displacement of the fold fields by 1978 (figs. 9*C*, *D*). The best measurement points in this area were mainly apices of folds. A total of 36 such points and 11 other miscellaneous points (of lesser reliability) were used to obtain a displacement field.

The resulting postsurge flow rates (fig. 10*A*) (~1 m d^{-1}) are seen to be about an order of magnitude less than the corresponding flow rates derived from L.R. Mayo's surge-phase data referred to earlier (Post and others, 1976, fig. 132). These findings are consistent with current knowledge of surge and intersurge behavior. Figure 10*B* is derived from figure 10*A* by generating 14 flow lines, starting at the left, that have equal (250-m) spacings. It was necessary to apply trial-and-error procedures in order to achieve a solution. The flow-line geometry illustrates the strongly divergent nature of the ice flow line in the terminal region. A similar conclusion was reached by L.R. Mayo from his earlier observations of the surge (see Krimmel and Meier, 1975).

Where sufficient velocity information is available along a particular flow line, or sufficiently close to it, as is the case for flow lines 5, 10, and 12 (fig. 10*B*), we computed longitudinal strain rates in a curvilinear coordinate system according to the equation:

$$\dot{\varepsilon}_{xx} = \Delta V_x / \Delta x \qquad (1)$$

where $\dot{\varepsilon}_{xx}$ is the time- and area-averaged longitudinal strain-rate compo-

Figure 9.*—Landsat 1 and 2 MSS false-color composite images of the north margin (***A*** and ***B****) and the main fold field (***C*** and ***D****) of Tweedsmuir Glacier showing changes that took place during the postsurge period.* A *and* C *are sections of a Landsat image (1417–19532; Path 65, Row 18) acquired on 13 September 1973, and* B *and* D *are sections of an image (21314–19295; Path 66, Row 18) acquired on 28 August 1978. The picture elements (pixels) measure approximately 57 m x 79 m. See figures 10*A*, 10*B*, 13*A*, and 13*B *for correct geographic orientation. Image was processed by Canada Centre for Remote Sensing, Ottawa, Ontario.*

nent of the total strain-rate tensor, and ΔV_x is the incremental change in the velocity component (V_x) over the distance Δx along the flow line. Lower order terms due to curvature are neglected.

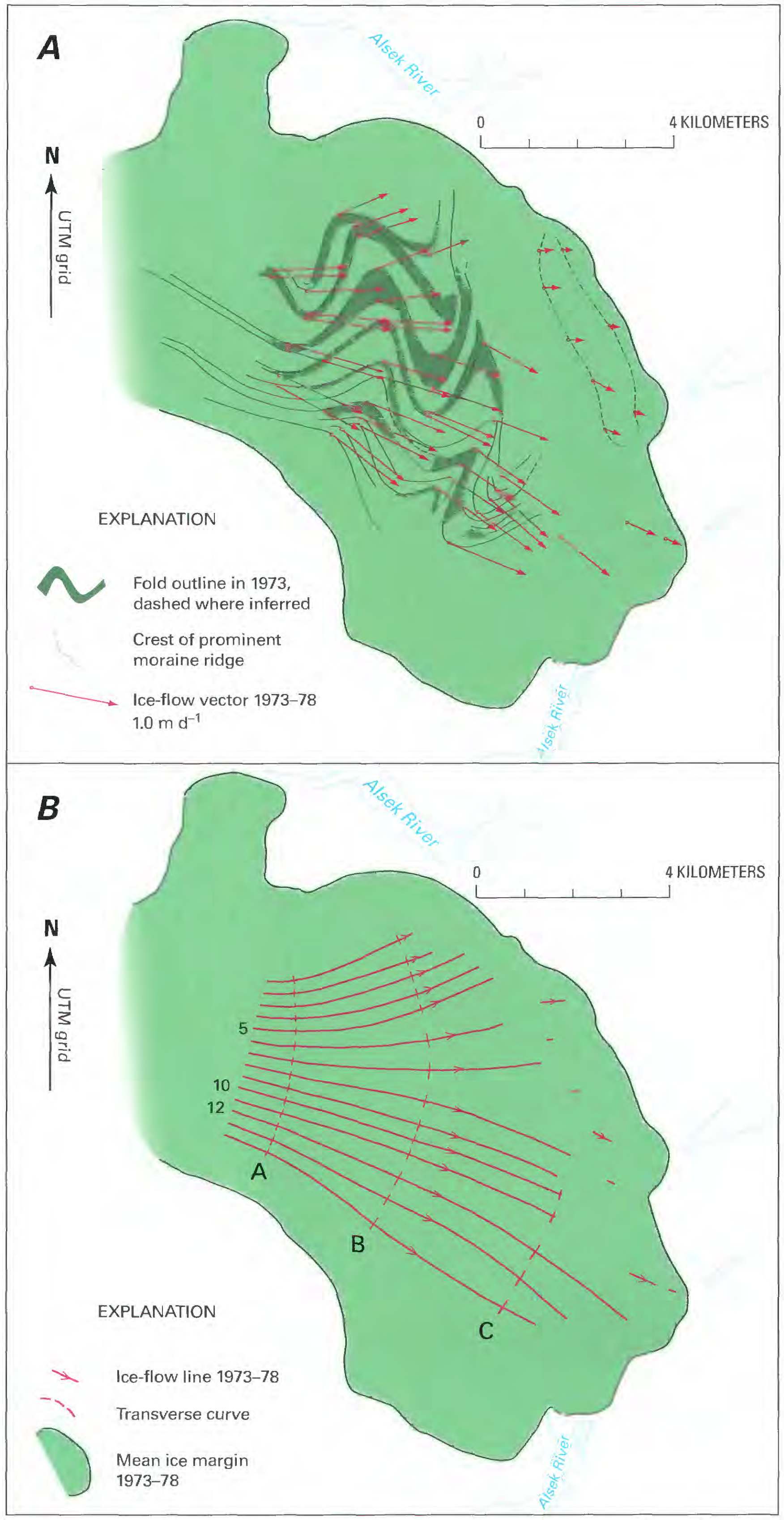

Figure 10.—*Tweedsmuir Glacier terminus showing ice-flow vectors and ice-flow lines for 1973–78.* **A**, *1973 fold geometry and ice-flow vectors based on analysis of the Landsat images shown in figure 9.* **B**, *Ice-flow lines based on the ice-flow vector field in* A. *Flow lines 5, 10, and 12 are discussed in the text, as are transverse curves A, B, and C.*

The time- and area-averaged transverse component of the strain-rate tensor $\dot{\varepsilon}_{yy}$ is obtained from the expression:

$$\dot{\varepsilon}_{yy} = W^{-1} V_x \Delta W / \Delta x \qquad (2)$$

where, if we refer to a curvilinear cell defined by adjacent flow lines and the transverse curves labeled A, B, or C in figure 4*B*, W is the initial width of a cell, and $\Delta W / \Delta x$ is its gradient along the flow lines. V_x is the mean ice-flow rate along a flow line passing through the center of the cell. These flow rates are averaged over 2-km distances on much larger, smoothed curves of velocity versus distance.

So far, our analysis scheme has applied to two dimensions in the plane of the glacier surface, and as the reference frame moves with the surface (even vertically as ablation takes place), it is "Lagrangian" in character. It is possible to take advantage of a key property of glacier ice that allows us to infer what is happening in the direction perpendicular to the glacier surface. Because of the typically flat slopes of these glaciers in the ablation area (Clarke, 1991), this direction is approximately vertical.

The key property is the "incompressibility" of the ice, which allows us to write:

$$\Sigma \dot{\varepsilon}_{ii} = 0 \qquad (3)$$

where $i = x, y, z$. This equation holds for any (orthogonal) reference-axis orientation and for ice of density near the maximum value of about 0.91 Mg m^{-3}.

Equation 3 expresses the conservation of volume and is used extensively in theoretical glaciology (Lliboutry, 1965; Paterson, 1994). From this equation, the vertical strain rate, $\dot{\varepsilon}_{zz}$, at a point can easily be calculated:

$$\dot{\varepsilon}_{zz} = -(\dot{\varepsilon}_{xx} + \dot{\varepsilon}_{yy}) \qquad (4)$$

We will show later that our directions (x, y, z) correspond approximately to the principal axes of strain in the ice, so that we do not have to take the shear strains formally into account.

Results

Table 1 shows the values of $\dot{\varepsilon}_{xx}$, $\dot{\varepsilon}_{yy}$, and $\dot{\varepsilon}_{zz}$ computed from equations 1, 2, and 4 for selected points along flow lines 5, 10, and 12 (fig. 4*B*). Positive values indicate extension; negative values, contraction.

It may be seen that longitudinal compressive flow [down-glacier flow] is taking place consistently in this region of overall divergent flow [spreading flow, see Lliboutry, 1965, tome 2, p. 460–461]. Because of the large lateral creep, the vertical strain rate is consistently negative and indicates creep thinning (vertical compression), which is to be expected during the post-surge phase of a cycle. If we assume an ice thickness of 50 m, then for a mean vertical strain rate of -6×10^{-2} a^{-1}, the surface would be dropping by 3 m a^{-1}. This result is independent of any decrease in ice thickness that is caused by surface ablation, which could be of the same order.

We are not able to identify crevasse fields positively from the satellite imagery, but they may be seen on the excellent aerial photographs of Austin Post (fig. 7). These photographs show many splaying crevasses; that is, crevasses parallel to flow direction in the center but curving toward the

TABLE 1.—*Values of longitudinal, transverse, and vertical strain rates derived from analysis of Landsat images*[1]

Flow line	Longitudinal strain rate $\dot{\varepsilon}_{xx}(\pm 0.5 \times 10^{-2} a^{-1})$	Transverse strain rate $\dot{\varepsilon}_{yy}(\pm 0.5 \times 10^{-2} a^{-1})$	Vertical strain rate $\dot{\varepsilon}_{zz}(\pm 0.5 \times 10^{-2} a^{-1})$
5	–4.7	+18.3	–13.6
10	–6.1	+7.7	–1.6
12A	–2.6	+10.0	–7.4
12B	–1.8	+3.5	–1.7

[1] Errors given for values in the first two columns are not standard errors of a mean. They are derived through equation 1 and are the maximum for any flow line. The larger error in column two reflects the larger relative error in the transverse direction.

margin down the glacier. Splaying crevasses tend to be oriented along flow lines in the ablation area of spreading snouts (see, for example, Lliboutry, 1965). This result is consistent with the earlier assumption that the strain-rate components given in table 1 are probably close to the principal strain rates, which influence the direction of ice flow.

The strain-rate data in table 1 contrast with what would be expected during the surge phase. The longitudinal strain rates midway in 1973 may be estimated from some of the displacement data of L.R. Mayo (Krimmel and Meier, 1975). Between 22 July and 13 September 1973, along a section of the glacier corresponding to our flow line 7 (fig.10*B*), the vertical strain rates were between (+) 10^{-2} and 10^{-1} a^{-1}. This deduced thickening of the ice is consistent with our knowledge of peak surge behavior in the terminal region.

Observations on the Lowell Glacier Imagery

Lowell Glacier surged in 1983 after a quiescent phase of about 15 years. Conditions during the quiescent phase are documented in figures 11 and 12. From observations made by Parks Canada personnel and others, it is thought to have begun surging on or before middle April 1983. Figure 12 shows a synopsis of changes in the lower 30 km of the glacier between September 1973 and August 1983. The changes in the ice front (table 2), the changes in

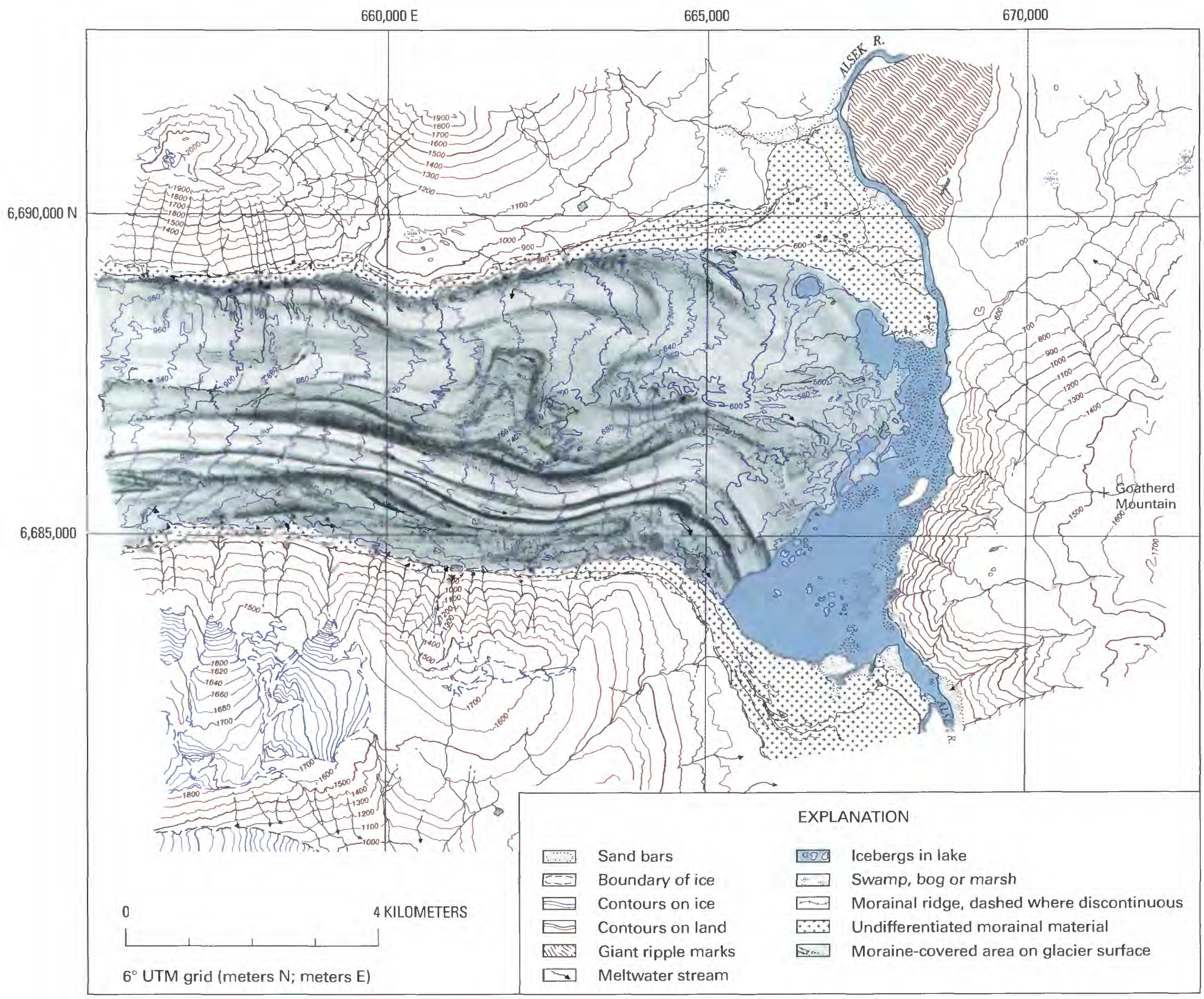

Figure 11.—*Modified, digitally scanned reproduction of topographic map of Lowell Glacier, Yukon Territory. Map prepared by Gerald Holdsworth and D. Sherstone of the former Glaciology Subdivision, Inland Waters Directorate, Department of the Environment, from 17 August 1974 vertical aerial photographs. Contour interval on land, 100 m; contour interval on ice, 20 m. Original map scale, 1:50,000. Aerial photographs archived by the National Air Photo Library, Natural Resources Canada, Ottawa, Ontario. Goatherd Mountain, indicated by plus (+) symbol, is the ground-photograph station for figure 14. Abbreviations: UTM, Universal Transverse Mercator; N., north; E., east.*

the lake area, and the development of dense clusters of icebergs can all be seen on the satellite imagery at the 1:1,000,000 scale; the images in figure 12 are annotated with these features. In interpreting the satellite images, we made extensive use of aerial and terrestrial photography. The 1983 images were interpreted with the help of terrestrial photographs taken by Lloyd Freese of Kluane National Park.

Figure 13 shows two Landsat 3 and 4 MSS (multispectral scanner) images taken on 23 June 1982 and 19 August 1983. In figure 13*A*, presurge

TABLE 2.—*Measurements of changes in the position of the terminus of the Lowell Glacier using Landsat imagery (see fig. 12)*

[Distances given are relative to the 13 September 1973 snout positions. —, not applicable. Abbreviations: ID no., identification number; N, North; S, South]

Date	Imagery	ID no.	Snout position change (meters)			Note
			N	Central	S	
13 Sep 1973	Landsat 1	1417–19532	—	—	—	Reference
17 Aug 1974	Aerial photographs	A23819/#50–60	—	—	—	Minor change
28 Aug 1978	Landsat 2	21314–19295	–2250	–500	–750	Retreat
17 Sep 1982	Landsat 4	Unknown	–2250	–2500	–2250	Retreat
9 Jun 1983	Landsat 4	40328–19482	–2050	–2000	–1450	Advance
19 Aug 1983	Landsat 4	40399–19540	–2050	–1250	–1050	Advance
28 Aug 1983	Landsat 4	40408–19475	–1250	–1000	–950	Advance

Figure 12.*—Lowell Glacier showing the changes in the geometry of the ice structure and margin from 1973 to 1983. The first three maps show presurge conditions. The second three show evidence of the surge. The maps were prepared from 1:500,000-scale photographic prints of Landsat images transferred to a 1:250,000-scale base map by the use of a Bausch and Lomb Zoom Transfer Scope. Fiducial marks are at 10-km spacing on the 6° UTM grid, zone 7 (see fig. 11). Symbols: L, lake water; B, icebergs; R, Alsek River. The Goatherd Mountain bluffs are shown shaded to the right in each map. Landsat images used for constructing each map are as follows:* **A**, *Landsat 1 (formerly ERTS-1) MSS image 1417–19532; 13 September 1973; Path 65, Row 18.* **B**, *Landsat 2 MSS image 21314–19295; 28 August 1978; Path 66, Row 18.* **C**, *Landsat 4 MSS image identification number unknown; 17 September 1982; Path 61, Row 18.* **D**, *Landsat 4 MSS image 40328–19482; 9 June 1983; Path 60, Row 18.* **E**, *Landsat 4 MSS image 40399–19540; 19 August 1983; Path 61, Row 18.* **F**, *Landsat 4 MSS image 40408–19475; 28 August 1983; Path 60, Row 18. The Landsat images are from the EROS Data Center, Sioux Falls, S. Dak.*

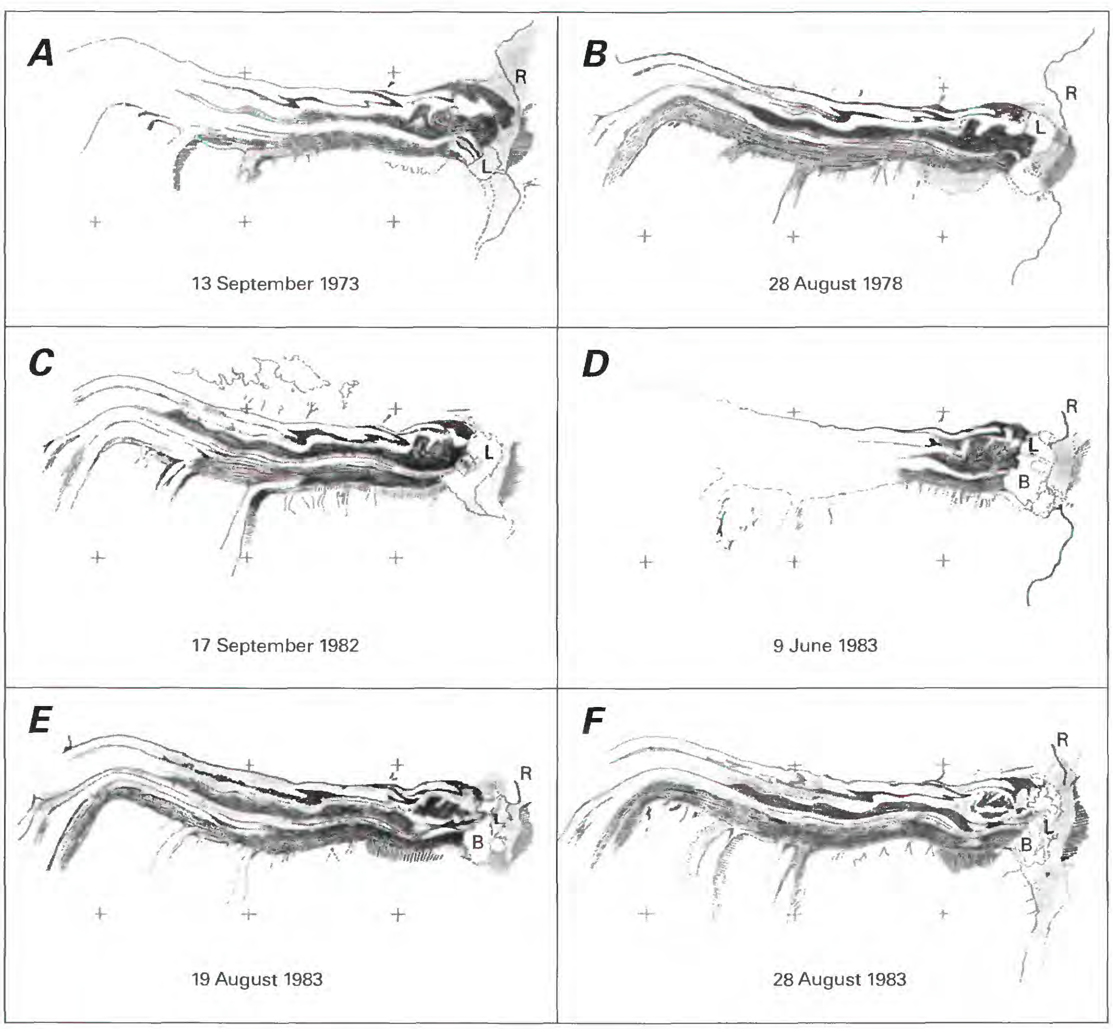

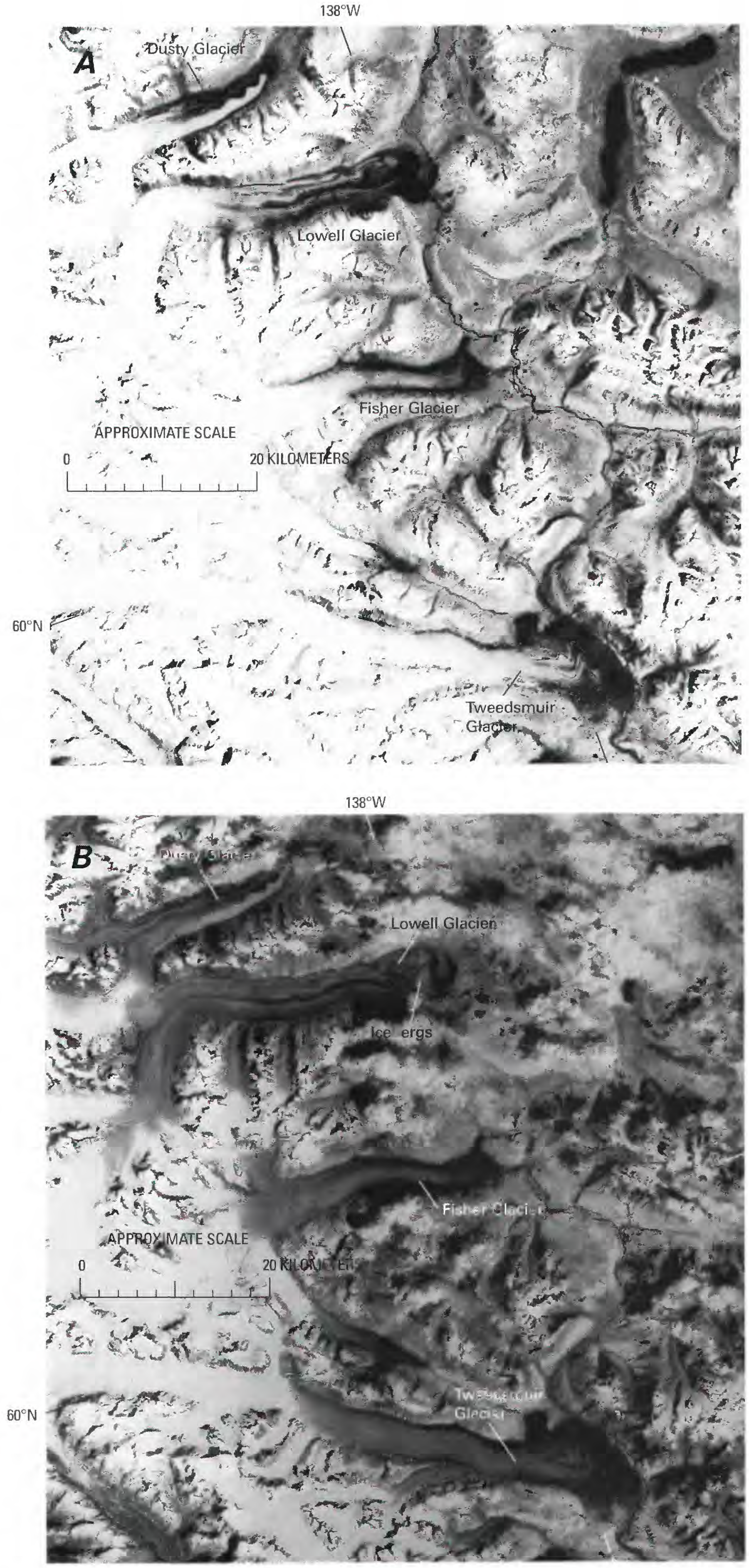

Figure 13.—*Landsat 3 and 4 MSS images of the Lowell Glacier showing conditions* **A** *just before and* **B** *during the 1983 surge. Dusty, Fisher, and Tweedsmuir Glaciers are also visible. The advance of the terminus is noticeable, and many icebergs are present in* B. *The Landsat images (*A, *31571–19514; 23 June 1982; Path 66, Row 18; and* B, *40399–19540; 19 August 1983; Path 61, Row 18) are from the EROS Data Center, Sioux Falls, S. Dak.*

conditions apply, and in 13*B*, evidence of the surge can be seen, including a noticeable advance of the terminus. The existence of the proglacial lake and the river modify the terminal region to a great extent. The icebergs that cover the surface of the lake have an appearance similar to clouds. Observations of later satellite images (into 1984) and a visit to the glacier in summer 1984 (fig. 14) made it possible to predict that the ice front would not flow against Goatherd Mountain and dam the Alsek River, as had happened in earlier surges, perhaps as recently as near the beginning of the 20th century (Clague and Rampton, 1982).

In order to observe glacier behavior during a significant part of the quiescent phase (the previous, known surge was between 1968 and 1970), we have again selected excellent Landsat images of 13 September 1973 and 28 August 1978, enhanced the imagery, and prepared digital (Versatec) terrain plots of the glacier and adjacent areas. The plots were not mutually registered images, so in order to get acceptable registration for off-glacier reference points, we had to register the images by a visual iterative procedure for 10-km-square blocks per step. This, and the smaller relative displacements of Lowell Glacier for this period compared with Tweedsmuir Glacier, mean that less reliability can be placed on any velocity results from Lowell Glacier.

Figure 15*A* shows an array of easily identifiable reference points on the glacier surface. These were selected for the ice-displacement measurements. If we refer to figure 12, these points may be identified with prominent distortions of moraine bands or different (colored) ice types. Measurement of the displacement of these points was made between 1973 and 1978 by using the first two processed images in figure 12. For the following years, we used 1:500,000-scale photographic images transferred directly to the 1:250,000-scale NTS base map by the use of a Bausch and Lomb Zoom Transfer Scope. The results are shown in figure 15*B*, where the start of the (early) 1983 surge can be identified. [Note that some points were superior to others for making measurements, and in order to avoid interference of lines, not all the point displacements have been plotted. These points coincide with the center of each of the short vertical lines or error bars. These errors (~ ±45 m) are similar to the measurements made on Tweedsmuir Glacier and reflect pixel size, as well as errors due to "point" definition in different scenes.]

The average speed of each point (which is changing with position and time) is given by the slope of each curve at a given time. For the quiescent phase, 1973–82, the speeds decrease down the glacier from about 0.34 ± 0.03 m d^{-1} (point 1) to 0.04 ± 0.03 m d^{-1} (point 13). This indicates a general longitudinal compressive strain rate on the order of 10^{-2} a^{-1}, which is typical of many valley glaciers (Lliboutry, 1965). From a review of terrestrial photographs, a low rock knoll seen in figure 8 in August 1969 was apparently covered soon after and then uncovered again after 1973 in the

Figure 14.*—Two composite terrestrial photographs of the terminus of Lowell Glacier on 20 September 1984 showing the ice cliffs, Alsek River, flowing in from the right, and the transient lake containing some icebergs. Photograph by Gerald Holdsworth from Goatherd Mountain. See figure 11 for location of photograph station.*

region immediately down the glacier from the prominent "square" fold seen in the images. This knoll or *nunatak* was again overridden in the 1983 surge. The ice in this region is evidently quite thin.

During the surge, ice-flow rates increased to values of 12 m d^{-1} (curve 8, fig. 15*B*; point 8, fig. 15*A*) and 45 m d^{-1} (curve 1; point 1), representing an increase of more than two orders of magnitude above quiescent phase flow rates. Although some uncertainty exists in the magnitude of the errors in the last results (possibly up to 30 percent), they do seem to indicate a much greater relative increase in activity of the Lowell Glacier compared with the surge of Tweedsmuir Glacier a decade earlier.

Figure 15.—Terminal ice margin positions of the Lowell Glacier, relative point displacements, and ice speeds from 1973 to 1983. **A**, *The location of terminal ice margin positions at different dates and the location of selected reference points on the glacier.* **B**, *The displacement versus time plots for six of the reference points shown in* A. *Errors in the displacement measurements are indicated by the length of the short vertical bars (estimated to be 90 m). Slopes of the curves give the ice speeds. Curve numbers in* B *correspond to point numbers in* A.

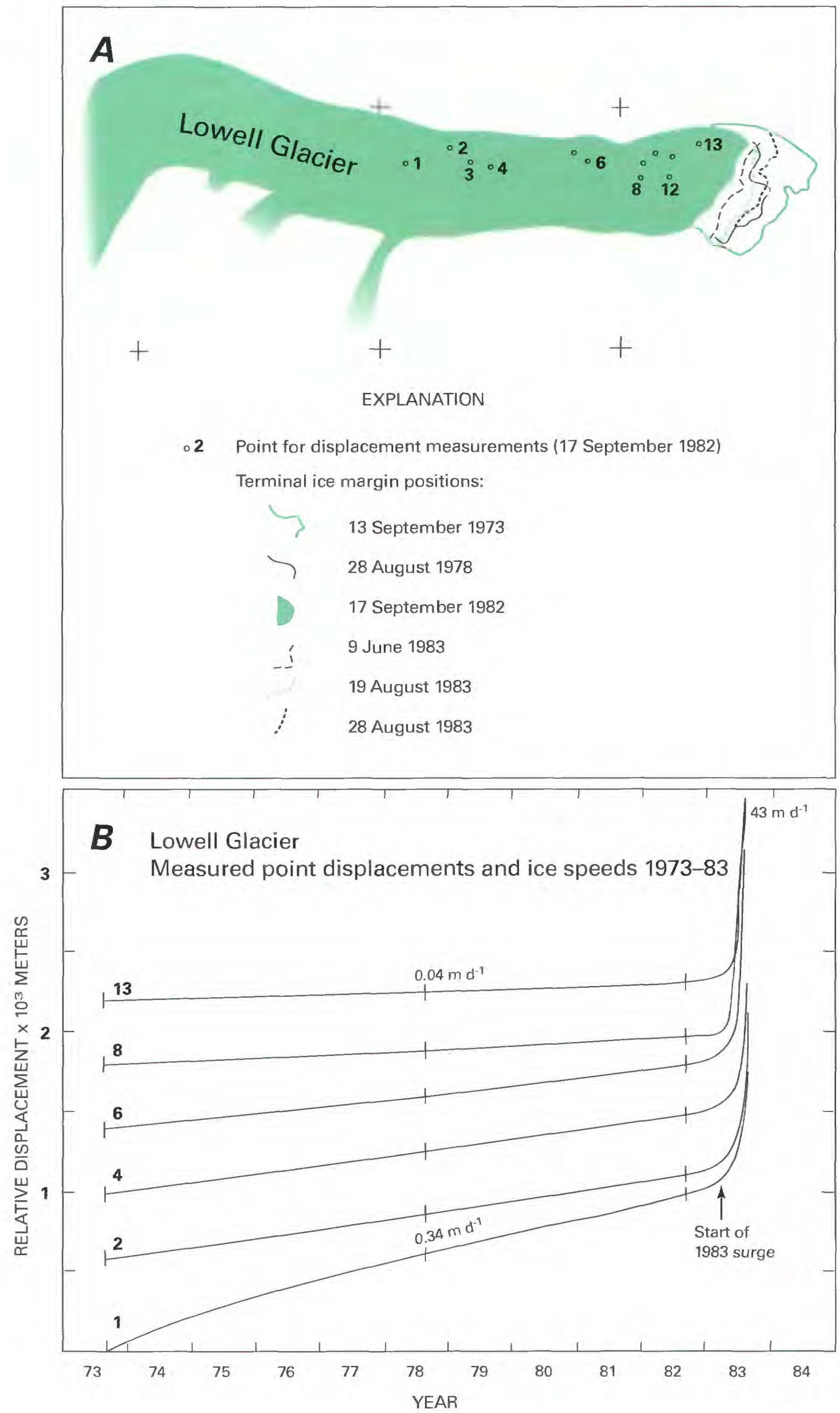

The unfavorable distribution of reference points, biased toward the north margin of the glacier (fig. 15*A*), and the lower accuracy of the registration for the Lowell Glacier have discouraged us from computing the components of the strain-rate tensor, as was done for Tweedsmuir Glacier. This deficiency is partially compensated by the excellent opportunity to determine longitudinal flow rates, which are biased toward the northern one-half of the glacier.

Value of Satellite Imagery

Significant information has been obtained about the dynamics of two large surging glaciers that occupy segments of a major Yukon-British Columbia-Alaska river system (the Alsek). This information has come from analysis of suitably selected Landsat imagery, supplemented by minimal ground-based observations. It is impractical to obtain such information in any other way (except by the much more expensive and time-consuming methods of aerial or terrestrial photogrammetry) because of the broken and dangerous nature of the glacier surface during a surge. (Even airborne radar does not work for determining ice thicknesses during a surge.) Satellite surveillance is also a practical way upon which to base predictions about potential hydrological hazards, such as jökulhlaups, that might result from the breaching of temporary ice dams of the Alsek River, as has happened several times in the past few centuries.

Seward Glacier Drainage System

Seward Glacier (labeled 17 in fig. 2) is actually an immense ice field of more than 1,200 km^2, the surface of which lies entirely in the accumulation area. This is the result of the extremely high snow-precipitation rate there. The glacier is temperate, and large crevasses are partially water filled in summer (Sharp, 1951a). Two major outlets come from the ice field: the narrow ice stream that feeds south into the vast Malaspina (Piedmont) Glacier (labeled 16 in fig. 2), which lies wholly in Alaska, and the Columbus Glacier (figs. 1 and 2), which feeds into the Bering Glacier, Alaska.

The spectacular medial moraine loops seen on the Malaspina Glacier are indicative of surging that can be traced to the outlet ice stream coming from Seward Glacier, and it is deduced that part of this system surges (Post, 1969).

In this glacier system, we will mention the ice-core sites on Mount Logan (labeled 1 in fig. 2), although hydrologically they properly should be placed in the Chitina River system, as most of the ice flowing from the upper plateau is to the north through Logan Glacier (labeled 3 in fig. 2). However, climatically, the sites are more aligned with the Pacific Ocean-Seward side of the mountain. The two sites are on the Northwest Col (5,340 m) and on the Prospectors-Russell Col (5,343 m), where 10-m firn temperatures are close to –29°C and –30°C, respectively. Ice thicknesses are generally between 100 and 200 m in the vicinity of the cols (saddles), although they increase out on the ice plateau, which has an area of about 15 km^2. Glaciological activities for the Northwest Col site are summarized in Holdsworth and others (1992). Information on the 2001-2 drilling project can be found at http://sts.gsc.nrcan.gc.ca/ice 2001/home.asp

Hubbard Glacier System

Hubbard Glacier [112 km] (labeled 18 in fig. 2) originates from a number of névés and divides that it shares with other valley glaciers (for example, Kaskawulsh and Logan Glaciers, labeled 12 and 3 in fig. 2, respectively). It flows across the Yukon-Alaska border [length to that point is 72 km] and ultimately calves into Yakutat Bay (fig. 1). The Alaskan section is discussed further in Chapter K, Glaciers of Alaska. Within Canada, the glacier appears to be wholly in the accumulation area. Geophysical studies on the Canadian part are restricted to the Hubbard-Kaskawulsh divide area, where the maximum firn-ice transition depth was found to be about 40 m. Ice depths are more than 500 m, and an ice-flow rate of 132 m a^{-1} was found about 10 km from the divide (Clarke, 1967). Glaciers on Mount Queen Mary (lat 60°37'N.; long 139°43'W.; 3,890 m; fig. 1) on the east side of the glacier are a source of lateral ice supply. In 1981, a surge was observed in one of the glaciers on the side of Mount Queen Mary, and a surge bulge moved out onto Hubbard Glacier. Areas of transient crevasse formation were often observed on the upper parts of Hubbard Glacier during the 1980's and early 1990's. Thus, even though the glacier is not formally identified as a surging glacier, it is dynamically very active, especially in its terminal region.

Grand Pacific-Melbern Glacier System

In the far southeastern part of the St. Elias Mountains, we find two interesting low-elevation transect glaciers that share a common divide at about 500 m above sea level. The south one of the pair is the Grand Pacific Glacier, well known for its numerous and apparently erratic

***Figure 16**—Annotated Landsat 5 MSS mosaic of two images (Path 59, Row 19) showing the Grand Pacific, Ferris, and Melbern Glaciers, as well as other glaciers. Landsat images are from the EROS Data Center, Sioux Falls, S. Dak.*

oscillations across the British Columbia-Alaska boundary (figs.1, 16). Following a catastrophic retreat up Tarr Inlet in the early part of the 20th century (see Chapter K, Glaciers of Alaska), its terminus retreated behind the border, where it stayed for several decades. In 1925, the (probably grounded) ice-front position was the farthest back on record, but by 1948, it had begun to approach the border, and by 1966, the ice front eventually extended at least 1 km into Alaskan waters before starting a steady retreat. By 1986, the ice front had retreated 0.8 km (Hall and others, 1995) but was still, barely, across the border in Alaska. Maps [for example, U.S. Operational Navigation Chart (ONC) D–12, scale 1:1,000,000] [all editions up to edition 6] typically show the ice front essentially coinciding with the border. Field (1958) [map 1.11] also shows the ice front coinciding with the border. The current status of the front has not been checked. Recent fluctuations have been connected with activity of the Ferris Glacier (fig. 16), one of the major tributaries of the Grand Pacific Glacier and probably a surging glacier.

On the other side of the divide, the situation is completely different. Melbern Glacier has generally thinned 300–600 m, and the terminus has retreated 15 km since the "Little Ice Age" maximum. About 7 km of this retreat took place between the middle 1970's and 1987 and caused the formation of one of the largest existing ice-dammed lakes. In 1987, the lake was full of tabular icebergs up to 200 m in diameter (Clague and Evans, 1994). Satellite imagery is particularly suitable for monitoring these types of major changes in Melbern Glacier, as well as in Grand Pacific Glacier.

References Cited

Bostock, H.S., 1969, Kluane Lake, Yukon Territory, its drainage and allied problems (155G and 115SE): Canada Geological Survey Paper 69–28, 19 p.

Bradbury, J.P., and Whiteside, M.C., 1980, Paleolimnology of two lakes in the Klutlan Glacier region, Yukon Territory, Canada: Quaternary Research, v. 14, no. 1, p. 149–168.

Brecher, H.H., 1966, Surface velocity measurements on the Kaskawulsh Glacier, Yukon Territory, Canada: Ohio State University Institute of Polar Studies Report 21, 73 p.

Bushnell, V.C., and Marcus, M.G., eds., 1974, Icefield Ranges Research Project scientific results: New York, American Geographical Society, and Montréal, Arctic Institute of North America, v. 4, 385 p.

Bushnell, V.C., and Ragle, R.H., eds., 1969, Icefield Ranges Research Project scientific results: New York, American Geographical Society, and Montréal, Arctic Institute of North America, v. 1, 224 p.

———1970, Icefield Ranges Research Project scientific results: New York, American Geographical Society, and Montréal, Arctic Institute of North America, v. 2, 139 p.

———1972, Icefield Ranges Research Project scientific results: New York, American Geographical Society, and Montréal, Arctic Institute of North America, v. 3, 263 p.

Clague, J.J., and Evans, S.G., 1994, Historic retreat of Grand Pacific and Melbern Glaciers, Saint Elias Mountains, Canada—An analogue for decay of the Cordilleran ice sheet at the end of the Pleistocene?: Journal of Glaciology, v. 40, no. 134, p. 205–210.

Clague, J.J., and Rampton, V.N., 1982, Neoglacial Lake Alsek: Canadian Journal of Earth Sciences, v. 19, no. 1, p. 94–117.

Clarke, G.K.C., 1967, Geophysical measurements on the Kaskawulsh and Hubbard Glaciers, Yukon Territory: Arctic Institute of North America Technical Paper 20, 36 p.

———1976, Thermal regulation of glacier surging: Journal of Glaciology, v. 16, no. 74, p. 231–250.

———1982, Glacier outburst floods from "Hazard Lake," Yukon Territory, and the problem of flood magnitude prediction: Journal of Glaciology, v. 28, no. 98, p. 3–21.

———1991, Length, width, and slope influence on glacier surging: Journal of Glaciology, v. 37, no. 126, p. 236–246.

Clarke, G.K.C., and Jarvis, G.T., 1976, Post-surge temperatures in Steele Glacier, Yukon Territory, Canada: Journal of Glaciology, v. 16, no. 74, p. 261–268.

Clarke, G.K.C., and Mathews, W.H., 1981, Estimates of the magnitude of glacier outburst floods from Lake Donjek, Yukon Territory, Canada: Canadian Journal of Earth Sciences, v. 18, no. 9, p. 1452–1463.

Collins, S.G., and Clarke, G.K.C., 1977, History and bathymetry of a surge-dammed lake: Arctic, v. 30, no. 4, p. 217–224.

Dewart, Gilbert, 1970, Seismic investigation of the ice properties and bedrock topography at the confluence of the north and central arms of the Kaskawulsh Glacier, *in* Bushnell, V.C., and Ragle, R.H., eds., Icefield Ranges Research Project scientific results: New York, American Geographical Society, and Montréal, Arctic Institute of North America, v. 2, p. 77–102.

Driscoll, F.G., Jr., 1980, Formation of the neoglacial surge moraines of the Klutlan Glacier, Yukon Territory, Canada: Quaternary Research, v. 14, no. 1, p. 19–30.

Field, W.O., 1958, Atlas of mountain glaciers in the Northern Hemisphere: Natick, Mass., Quartermaster Research and Engineering Command, Headquarters, U.S. Army Technical Report EP 92, unpaginated.

———ed., 1975, Mountain glaciers of the Northern Hemisphere: Hanover, N.H., U.S. Army Corps of Engineers, Cold Regions Research and Engineering Laboratory, v. 2, 932 p.

Hall, D.K., Benson, C.S., and Field, W.O., 1995, Changes of glaciers in Glacier Bay, Alaska, using ground and satellite measurements: Physical Geography, v. 16, no. 1, p. 27–41.

Holdsworth, Gerald, 1965, An examination and analysis of the formation of transverse crevasses, Kaskawulsh Glacier, Yukon Territory, Canada: Ohio State University Institute of Polar Studies Report 16, 90 p.

———1973, Surge of Tweedsmuir Glacier, British Columbia, Canada: Ice, no. 43 (3d issue), p. 23.

———1992, Ice cores as a source of long-term net precipitation data—A North American perspective, *in* Kite, G.W., and Harvey, K.D., eds., Using hydrometric data to detect and monitor climatic change: National Hydrology Research Institute Symposium 8, Saskatoon, Saskatchewan, 1992, p.107–120.

Holdsworth, Gerald, Krouse, H.R., and Nosal, M., 1992, Ice core climate signals from Mount Logan, Yukon, A.D. 1700–1987, *in* Bradley, R.S., and Jones, P.D., eds., Climate since A.D. 1500: New York, Routledge, p. 483–504.

Holdsworth, Gerald, and Peake, E., 1985, Acid content of snow from a mid-troposphere sampling site on Mt. Logan, Yukon Territory, Canada: Annals of Glaciology, v. 7, p. 153–160.

Jackson, J.A., ed., 1997, Glossary of geology (4th ed.): Alexandria, Va., American Geological Institute, 769 p.

Jarvis, G.T., and Clarke, G.K.C., 1974, Thermal effects of crevassing on Steele Glacier, Yukon Territory, Canada: Journal of Glaciology, v. 13, no. 68, p. 243–254.

———1975, The thermal regime of Trapridge Glacier and its relevance to glacier surging: Journal of Glaciology, v. 14, no. 71, p. 235–250.

Johnson, P.G., 1972a, A possible advanced hypsithermal position of the Donjek Glacier: Arctic, v. 25, no. 4, p. 302–305.

———1972b, The morphological effects of surges of the Donjek Glacier, St. Elias Mountains, Yukon Territory, Canada: Journal of Glaciology, v. 11, no. 62, p. 227–234.

Kamb, B., Raymond, C.F., Harrison, W.D., Engelhardt, Hermann, Echelmeyer, K.A., Humphrey, N., Brugman, M.M., and Pfeffer, T., 1985, Glacier surge mechanism, 1982–83 surge of Variegated Glacier, Alaska: Science, v. 227, no. 4686, p. 469–479.

Krimmel, R.M., and Meier, M.F., 1975, Glacier applications of ERTS images: Journal of Glaciology, v. 15, no. 73, p. 391–402.

Lliboutry, Louis, 1965, Traité de glaciologie, tome 2: Glaciers, variations du climat, sols gelés [Treatise of glaciology, v. 2: Glaciers, climatic variations, and frozen ground]: Paris, Masson et Cie, 612 p.

Meier, M.F., and Post, Austin, 1969, What are glacier surges?: Canadian Journal of Earth Sciences, v. 6, no. 4, pt. 2, p. 807–817.

Miller, J.M., 1974, Environmental surveys in Alaska based upon ERTS data, *in* Freden, S.C., Mercanti, E.P., and Friedman, D.B., eds., Third Earth Resources Technology Satellite Symposium, II: U.S. National Aeronautics and Space Administration Special Publication 356, p. 12–40.

Paterson, W.S.B., 1994, The physics of glaciers (3d ed.): Oxford, U.K., Elsevier Science, 480 p.

Post, Austin, 1966, The recent surge of Walsh Glacier, Yukon and Alaska: Journal of Glaciology, v. 6, no. 45, p. 375–381.

———1967, Walsh Glacier surge, 1966 observations: Journal of Glaciology, v. 6, no. 47, p. 763–765.

———1969, Distribution of surging glaciers in western North America: Journal of Glaciology, v. 8, no. 53, p. 229–240.

Post, Austin, Meier, M.F., and Mayo, L.R., 1976, Measuring the motion of the Lowell and Tweedsmuir surging glaciers of British Columbia, Canada, *in* Williams, R.S., Jr., and Carter, W.D., eds., ERTS–1, a new window on our planet: U.S. Geological Survey Professional Paper 929, p. 180–184.

Rampton, V.N., 1970, Neoglacial fluctuations of the Natazhat and Klutlan Glaciers, Yukon Territory, Canada: Canadian Journal of Earth Sciences, v. 7, no. 5, p. 1236–1263.

Sharp, R.P., 1943, Geology of the Wolf Creek area, St. Elias Range, Yukon Territory, Canada: Geological Society America Bulletin, v. 54, no. 5, p. 625–650.

Sharp, R.P., 1951a, Glacial history of Wolf Creek, St. Elias Range, Canada: Journal of Geology, v. 59, no. 2, p. 97–117.

———1951b, Thermal regimen of firn on upper Seward Glacier, Yukon Territory, Canada: Journal of Glaciology, v. 1, no. 9, p. 476–487.

Stanley, A.D., 1969, Observations on the surge of Steele Glacier, Yukon Territory, Canada: Canadian Journal of Earth Sciences, v. 6, no. 4, pt. 2, p. 819–830.

Whiteside, M.C., Bradbury, J.P., and Tarapchak, S.J., 1980, Limnology of the Klutlan moraines, Yukon Territory, Canada: Quaternary Research, v. 14, no. 1, p. 130–148.

Wood, W.A., 1936, The Wood Yukon expedition of 1935—An experiment in photographic mapping: Geographical Review, v. 26, no. 2, p. 228–246.

———1942, The parachuting of expedition supplies—An experiment by the Wood Yukon expedition of 1941: Geographical Review, v. 32, no. 1, p. 36–55.

———1972, Steele Glacier, 1935–1968, *in* Bushnell, V.C., and Ragle, R.H., eds., Icefield Ranges Research Project scientific results: New York, American Geographical Society, and Montréal, Arctic Institute of North America, v. 3, p. 1–8.

Wright, H.E., Jr., 1980, Surge moraines of the Klutlan Glacier, Yukon Territory, Canada—Origin, wastage, vegetation succession, lake development, and application to the late-glacial of Minnesota: Quaternary Research, v. 14, no. 1, p. 2–18.

Glaciers of North America–

GLACIERS OF THE CONTERMINOUS UNITED STATES

GLACIERS OF THE WESTERN UNITED STATES

By ROBERT M. KRIMMEL

With a section on GLACIER RETREAT IN GLACIER NATIONAL PARK, MONTANA

By CARL H. KEY, DANIEL B. FAGRE, *and* RICHARD K. MENICKE

SATELLITE IMAGE ATLAS OF GLACIERS OF THE WORLD

Edited by RICHARD S. WILLIAMS, Jr., *and* JANE G. FERRIGNO

U.S. GEOLOGICAL SURVEY PROFESSIONAL PAPER 1386–J–2

Glaciers, having a total area of about 580 km^2, are found in nine western states of the United States: Washington, Oregon, California, Montana, Wyoming, Colorado, Idaho, Utah, and Nevada. Only the first five states have glaciers large enough to be discerned at the spatial resolution of Landsat MSS images. Since 1850, the area of glaciers in Glacier National Park has decreased by one-third

CONTENTS

SATELLITE IMAGE ATLAS OF GLACIERS OF THE WORLD

GLACIERS OF NORTH AMERICA–

GLACIERS OF THE CONTERMINOUS UNITED STATES

GLACIERS OF THE WESTERN UNITED STATES

By ROBERT M. KRIMMEL[1]

With a section on GLACIER RETREAT IN GLACIER NATIONAL PARK, MONTANA

By CARL H. KEY,[2] DANIEL B. FAGRE,[2] *and* RICHARD K. MENICKE[3]

Abstract

Glaciers are found in the following States of the Western United States: Washington, Oregon, California, Montana, Wyoming, Colorado, Idaho, Utah, and Nevada. According to the most recent sources, these glaciers have a total area of about 580 km^2. The earliest recorded glacier observations were made in 1857, and all the major glacier areas were known by the early part of the 20th century. Glacier inventories have been completed or are in progress for several major glacierized areas. The major source materials for modern glacier inventories of the Western United States are the various U.S. Geological Survey topographic map series at scales of 1:24,000, 1:62,500, 1:100,000, and 1:125,000 and the vertical aerial photographs used to compile these maps. Where these sources are not available, oblique aerial photographs have been used to delineate the extent of glaciers and to update glacier margins where significant change has taken place. Landsat images and digital data have been used in glacier studies in the conterminous United States. However, the spatial resolution of Landsat is such that only glaciers in the States of Washington, Oregon, California, Montana, and Wyoming can be effectively observed from Landsat 1, 2, and 3 data. In the remaining States, the Landsat data can often offer regional views of moraines from past glaciation and can also be useful in the study of glacial geology and the variations in seasonal snow cover.

Introduction

Glaciers are found in the following States of the Western United States: Washington, Oregon, California, Montana, Wyoming, Colorado, Idaho, Utah, and Nevada. The single most comprehensive work on the glaciers in these States is volume 1 of "Mountain Glaciers of the Northern Hemisphere," edited by William O. Field (Field, 1975), and he relied on the expertise of numerous people as coauthors. The work attempted to list all glaciological literature and other reference material (including maps, aerial photographs, and terrestrial photographs available for each area), in addition to creating a comprehensive glacier inventory. Numerous references are cited at the end of each chapter.

Manuscript approved for publication 7 March 2002.

[1] U.S. Geological Survey, 1201 Pacific Avenue - Suite 600, Tacoma, WA 98402.

[2] U.S. Geological Survey, Glacier National Park, West Glacier, MT 59936.

[3] U.S. National Park Service, Glacier National Park, West Glacier, MT 59936.

Perhaps the single most referenced source on the distribution of glaciers in the conterminous United States is a paper by Meier (1961a), who reported on a survey of United States glaciers carried out from 1957 to 1959. Brown (1989) summarized the status of work on compiling a glacier inventory of the United States. Snyder (1996) compiled a bibliography of glacier studies by the U.S. Geological Survey (USGS) that includes numerous citations to studies of glaciers in the Western United States. This section in "Satellite Image Atlas of Glaciers of the World" must, by the nature of the subject, parallel the work of Meier (1961a) and Field (1975), but it will also stress those data available from the Landsat 1, 2, and 3 series of satellites.

The distribution of glaciers in the Western United States can be most logically categorized by using the physiographic provinces that encompass various mountain ranges. These mountain ranges can be divided arbitrarily by States, which are used as the primary geographic categorization in this section for glaciers in the Western United States.

Historical Observations

All of the major glacier areas in the Western United States were known by the early 20th century. The earliest recorded glacier observations were made by Kautz in 1857 (Kautz, 1875). Other pre-1900 glacier observations include those of Clarence King (1871), John Muir (1894), and I.C. Russell, who published two comprehensive works: "Existing Glaciers of the United States" (Russell, 1885) and "Glaciers of Mount Rainier" (Russell, 1898). These reports contained maps of glacier cover for a small area of the Sierra Nevada (fig. 1), Mount Shasta, the Lyell Glacier[4] (Yosemite National Park), and Mount Rainier (fig. 2), as well as numerous sketches of glaciers. A series of reports by F.E. Matthes from 1931 to 1945, published in the Transactions of the American Geophysical Union (Matthes, 1931, 1932, 1933, 1934, 1935, 1936, 1937, 1938, 1939, 1940, 1941, 1942, 1944, and 1945), attempted to summarize contemporary glacier research for that period. With the advent of regionally comprehensive vertical aerial photographs and topographic maps compiled from these photographs, some detailed glacier inventories have subsequently been compiled (Post and others, 1971; Graf, 1977; Raub and others, 1980; and Spicer, 1986). Another comprehensive source of glacier data that includes information on United States glaciers is the Permanent Service on the Fluctuations of Glaciers (now part of the World Glacier Monitoring Service), which has published seven volumes since 1967 summarizing glacier changes during seven successive 5-year periods (Kasser, 1967 and 1973; Müller, 1977; Haeberli, 1985; Haeberli and Müller, 1988; Haeberli and Hoelzle, 1993; Haeberli and others, 1998).

The long-term measurement of changes in termini position and mass balance of glaciers (Fountain and others, 1991; Østrem and Brugman, 1991) is important to understanding both the relationship of glacier fluctuation to climate change and to the contribution of glacier meltwater to the total annual discharge of a hydrologic basin (Fountain and Tangborn, 1985a,b). The latter application is especially important where the drainage basin is used for irrigation or for the generation of hydroelectric power.

[4] The geographic place-names given in the text have been approved for each State by the U.S. Board on Geographic Names. Unapproved names for glaciers are shown in italics.

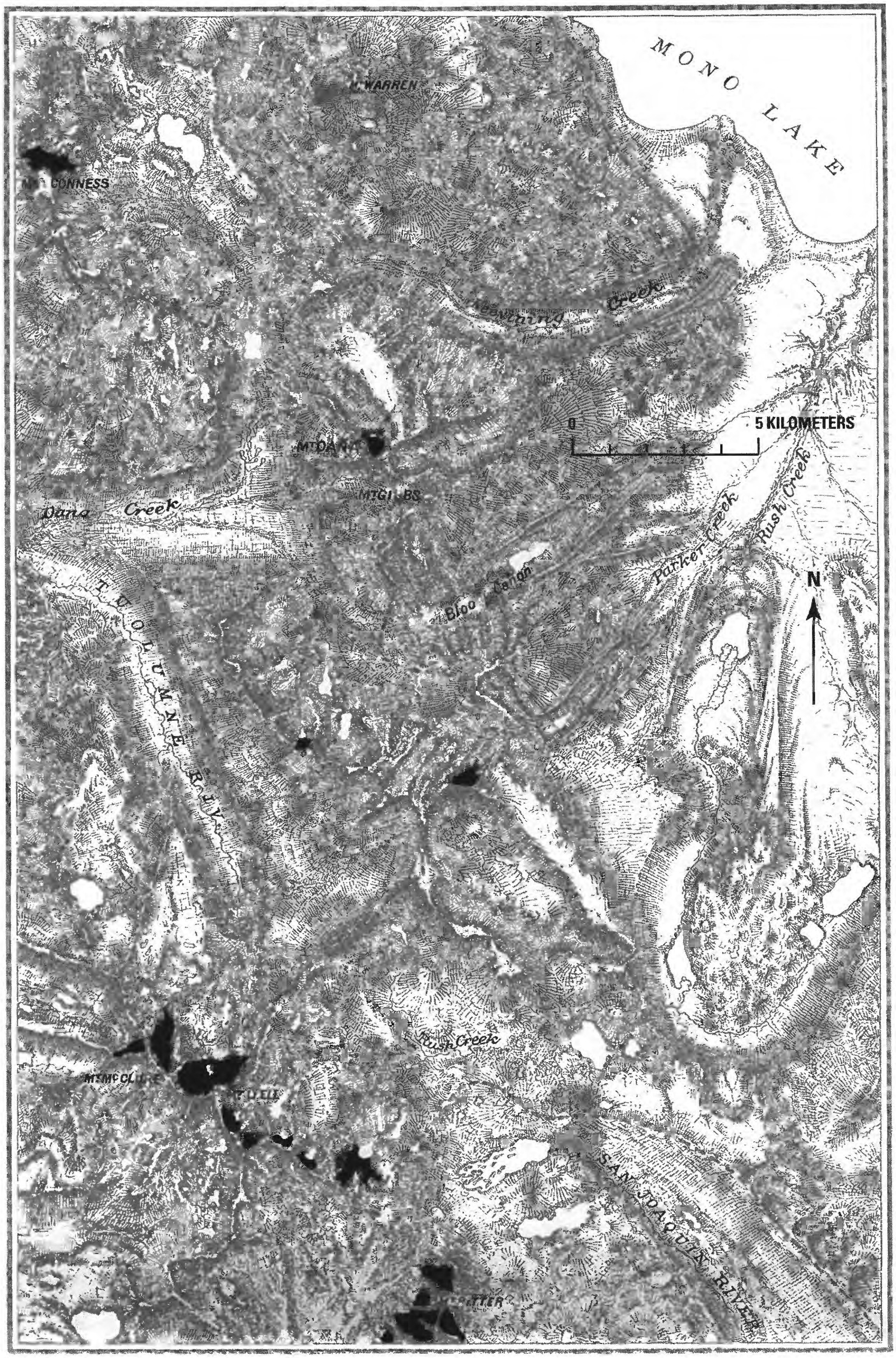

__Figure 1__.—Historical map of a part of the Sierra Nevada, Calif., taken from "Existing Glaciers of the United States" (Russell, 1885). The coverage of this early map is shown in figure 14. Glaciers are indicated by solid black.

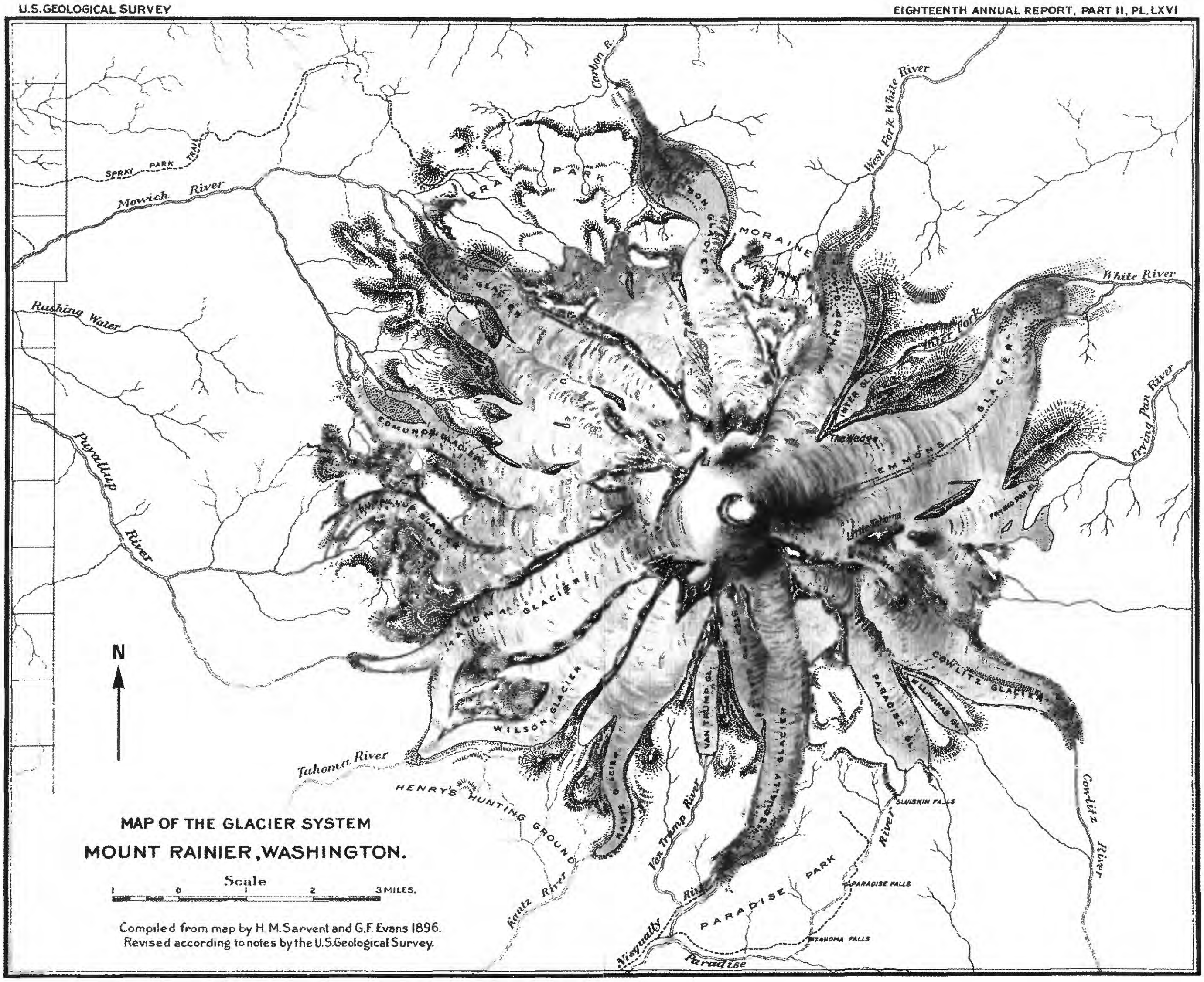

Glacier Inventories

Figure 2.—Early map of the glaciers of Mount Rainier, Wash., taken from Russell (1898). Compare with figure 10, a Landsat 3 return beam vidicon (RBV) image of Mount Rainier. All the glaciers retreated between 1900 and 1980; retreat was minor at the Carbon Glacier but was greater than 1 km at the Cowlitz Glacier.

Any work that attempts to list pertinent glaciological data on all the glaciers in a given area can be considered to be a glacier inventory, and international guidelines are available for the preparation of glacier inventories (UNESCO, 1970; Müller and others, 1977). Glacier inventories have been completed or are in progress for several major glacierized areas in the Western United States and Alaska (Brown, 1989), and these will be discussed as appropriate under each area. The definition of the term glacier is critical to any glacier inventory, as well as to an evaluation of the utility of Landsat images for the observation of glaciers. Broad definitions of glacier normally require that the snow or ice is perennial and that the mass moves under its own weight (UNESCO, 1970). Qualifications of this definition must be made for specific purposes. For example, the hydrologist may be interested in all perennial snow or ice, but the person who studies glacier mass transport is interested only in ice movement.

For glacier inventories, the most important factor is that the snow and ice be perennial. Discrepancies in measurements of area may result when a relatively wet winter is followed by a cool summer. Under these circumstances, many snow patches that could be called glaciers may remain at the end of the ablation season. The end result would be widely fluctuating glacierized areas in short time periods, which is generally unacceptable for inventory work. Therefore, most inventories are made during a year, or multiple years, of abnormally light winter snow and (or) a hot, dry summer, which reduce snow-patch areas to a minimum.

Another practical problem in most glacier inventories is that it is normally impossible to record every small mass of snow and ice that might fit the glacier definition. For this reason, a minimum size limit, in addition to the more common definition of glacier, is often stipulated in glacier inventories. The minimum size is determined by the quality of data, the hydrologic importance of the snow and ice, and the interest spurred by tourists and recreationalists. For an inventory in the north Cascades (northern Cascade Range) of Washington State, a minimum area of 0.1 km^2 was used (Post and others, 1971). For an inventory in the Sierra Nevada of California, a minimum area of 0.01 km^2 was used (Raub and others, 1980; unpub. data). It is not the intent of this Landsat image atlas to inventory glaciers, and no arbitrary minimum size for glaciers has been assigned; however, the effective spatial resolution of Landsat's sensors imposes a minimum on the order of 1 km^2 where used for glaciological studies.[5] However, 1 km^2 as the minimum glacier size would be absurd in California because only one glacier, Palisade Glacier, is more than 1 km^2 in area (Raub and others, 1980; unpub. data).

Mapping of Glaciers

In the Western States, numerous small glaciers exist over a very large area. Glacier distribution and area are listed in table 1. Because of the scattered distribution, no comprehensive study of glacier extent was done previous to the compilation of modern topographic maps. A few studies were made of isolated areas before 1960, however. Most of these consisted of general observations and, in some cases, photographic records; they are, for the most part, referenced in Field (1975). In some areas, a few outstanding photographs of glaciers, taken primarily for artistic purposes or the promotion of tourism, exist from as early as 1900. Some of these have found their way into modern reports and are used to compare glaciers qualitatively.

The major source materials for modern glacier inventories are the various USGS topographic map series at scales of 1:24,000, 1:62,500, 1:100,000, and 1:125,000 and the vertical aerial photographs that were used to compile these maps. In some instances, modern maps are not available for important glacierized areas, in which case modern oblique aerial photographs have been used to delineate the extent of each glacier. This oblique aerial photography also has been used to update glacier margins in areas where significant change has taken place.

The tool most useful in describing the geometry of a glacier is a topographic map. Commonly, the USGS topographic map series do not show sufficient detail to satisfy a specific glaciological need, and a special map must be produced for a specific glacier. Such special maps, mostly unpublished, have been made for the South Cascade, Nisqually, and Klawatti Glaciers (Meier, 1966), Blue Glacier (Tangborn and others, 1990), and Shoestring Glacier in Washington; the Eliot and Collier Glaciers in Oregon; the McClure and Palisade Glaciers in California; the Grinnell and Sperry Glaciers in Montana; the Dinwoody Glacier in Wyoming; and several glaciers in Colorado. Normally the vertical aerial photographic surveys used for these maps were done in the early fall, a time particularly advantageous to the mapping of

[5] Theoretically, for the 79-m pixel size of the Landsat multispectral scanner image, a glacier 0.2 km^2 in area could be resolved (approximately 2.8 times the pixel size). From a practical standpoint, however, a glacier 1 km^2 in area (1 mm^2 on a 1:1,000,000-scale Landsat multispectral scanner image) is about the smallest that can be unambiguously delineated under optimum contrast conditions.

TABLE 1.—*Areas of glaciers in the western conterminous United States*

[Glacier areas in the first column are taken from Meier (1961a); dashes mean not determined by Meier. Glacier areas in the second column are from Meier (1961a) where a more recent source is not available. The change in area between 1961 and the more recent source is normally due to a more complete data set rather than a true change. An asterisk indicates that the value is estimated. Glacier numbers correspond with those in figure 5]

Location	Area (square kilometers)	
	Meier (1961a)	More recent source, where available
Washington		
1. North Cascades[1] (northern Cascade Range)	251.7	[2]267.0
2. Olympic Mountains	33.0	[3]45.9
3. Mount Rainier	87.8	[4]92.1
4. Goat Rocks area	1.5	1.5
5. Mount Adams	*16.1	*16.1
6. Mount St. Helens	7.3	[5]5.92/2.16
Total	397.4	428.5/424.8
Oregon		
7. Mount Hood	9.9	[4]13.5
8. Mount Jefferson	3.2	3.2
9. Three Sisters area	7.6	[4]8.3
10. Wallowa Mountains	—	*.1
Total	20.7	25.1
California		
11. Mount Shasta	5.5	[4]6.9
12. Salmon-Trinity Mountains	.3	.3
13. Sierra Nevada	13.1	[6]50.0/63.0
Total	18.9	57.2/70.2
Montana		
14. Glacier National Park	13.8	[7]28.4
15. Cabinet Range	.5	[7].5
16. Flathead-Mission-Swan Ranges	*1.2	[7]*2.3
17. Crazy Mountains	*.5	[7]*.4
18. Beartooth Mountains	10.8	[7]10.9
Total	26.8	42.5
Wyoming		
19. Big Horn Mountains	.3	[7]1.0
20. Absaroka Range	*.7	[7]*.7
21. Teton Range	2.0	[7]1.7
22. Wind River Range	44.5	[7]31.6
Total	47.5	37.5
Colorado		
23. Rocky Mountain Park-Front Range, others	1.7	[7]1.5
Idaho		
24. Sawtooth Mountains	—	[8]*1.0
Utah		
25. Wasatch Mountains	—	[9].2
Nevada		
26. Wheeler Peak	.2	.2

[1] The region bounded by the Canadian border on the north, Snoqualmie Pass on the south, the Puget Lowlands on the west, and the Columbia and Okanogan Rivers on the east.

[2] Post and others, 1971.

[3] Spicer, 1986.

[4] Driedger and Kennard, 1986.

[5] Brugman and Meier, 1981. Before/after eruption of 18 May 1980.

[6] Raub and others, 1980; unpub. data. The 50-km^2 area includes glaciers plus moraine-covered ice; the 63-km^2 area includes glaciers, moraine-covered ice, and small ice bodies not large enough to be considered glaciers.

[7] Graf, 1977.

[8] Estimated; various observers have reported numerous small glaciers.

[9] Timpanogos Cave, Utah, USGS 1:24,000-scale topographic map.

glaciers because the residual snow cover is at a minimum and new snow has not started accumulating. The maps not only provide an accurate position of the glacier terminus but, even more important, give reliable ice elevations throughout the entire area. This third geometric dimension is especially valuable because, through the compilation of later maps from new vertical aerial photographic or ground surveys, volumetric change can be determined over a given time. Ice gain or loss is hydrologically important, and the distribution of the gain or loss over the glacier is vital to understanding the glacier's state of health and its relationship to climate.

In this chapter, no attempt is made to use Landsat multispectral scanner (MSS) or Landsat 3 return beam vidicon (RBV) images to define the shape or size of a glacier. In almost all cases, vertical aerial photographs are available that have spatial resolutions of one or two orders of magnitude better than the Landsat MSS images. With the exception of a few isolated cases, even the 1:125,000-scale topographic maps depict the glaciers more precisely than does Landsat. Occasionally though, misinterpretation of photographic data has resulted in map errors. Although numerous glaciers have undergone changes in terminus position of 100 m or more since the map compilations, no routine attempt has been made to correct the maps by using Landsat image data.

Landsat Images of the Glaciers of the Western United States

The spatial resolving power of the MSS of the Landsat 1, 2, and 3 systems is such that only glaciers in the States of Washington, Oregon, California, Montana, and Wyoming can be observed effectively. In the remaining States, the Landsat images commonly offer striking views of moraines from past glaciation and can also be useful in the study of glacial geology and variations in seasonal snowpack.

The effective spatial resolution of the Landsat MSS sensors is generally considered to be about 200 m under normal conditions of contrast. Under optimum conditions (high contrast) during the satellite pass and with careful image and photographic processing, MSS images can give glaciological information approaching 100 m in spatial resolution (Krimmel and Meier, 1975). The best possible analysis of Landsat imagery is achieved by using digital data rather than photographic prints. The Landsat MSS digital unit is a pixel, and each pixel has a reflectance (gray-scale) value, given as a digital number (DN), ranging from 1 to 127 (MSS bands 4–6) or 1 to 63 (MSS band 7) (1 is dark and 127 or 63 is bright). Manipulation of digital data not only allows simple analysis of single MSS bands but also permits the use of analytical techniques, such as band-to-band ratioing and date-to-date (temporal) comparisons of sequential images.

A very simple way to determine snow cover is by radiance threshold. A radiance value is picked above which it is assumed that all material is snow. A summation of these pixels with radiance values higher than the arbitrary value then represents the snow-covered area. However, in mountainous areas, some snow is always in shadow, which results in a reduced radiance. Also, most of the edge of the snow cover is irregular, and along that boundary, many pixels are only partially snow covered (mixed pixels) and normally may have reduced brightness. The radiance of any given pixel is an integration of the brightness values of all material within that pixel. Some subjectivity always exists in picking the radiance level for a given percent of snow cover, and the resulting regional snow-cover determination is a result of the selected radiance. Of course, other features in the image can also result in high radiance values, notably clouds.

The identification of ice is commonly more difficult than that of snow. Simple radiance thresholds do not identify ice because much of it is less bright than the surrounding rock, glacial outwash, or vegetation. Digital band-to-band ratios have been successfully used to identify both ice and snow under shadow conditions (Meier and Evans, 1975). On a regional scale, however, instead of digital data, it has proven to be more cost-effective to use analog photographic film combined with the subjective input of brightness variations in order to gain a knowledge of morainal landforms and trimlines.

Some digital-image processing has been used for selected glaciers. South Cascade Glacier in the State of Washington is about 3 km long and has an area of 2.5 km^2. It has been the site of remote sensing experiments since the 1960's (Meier and others, 1966). An exceptional Landsat image is required to obtain information about a glacier this small (Krimmel and Meier, 1975). Two cloud-free scenes, one from 11 August 1973 and one from 16 September 1973, were used to determine the change in snow-cover area. Figure 3 shows the August digital image compared to the September digital image, the pixels that are snow (DN>100 on MSS bands) in August, but not in September, being shown as heavy solid circles. Although such techniques may be useful in analyzing special cases in small areas, it has proven to be impractical for large areas

***Figure 4.**—(opposite page) Temporal color composite Landsat image (1420–18303, band 5; 16 September 1973; Path 50, Row 26; and 1258–18322, bands 5, 6, and 7; 7 April 1973; Path 50, Row 26) of two north Cascades (northern Cascade Range) images in Washington State and British Columbia, Canada. This image shows areas that were snow covered on 16 September 1973 as a brilliant red, areas that were snow covered on 7 April 1973 as a white, and healthy vegetation as a tan color (Deutsch, 1983, fig. 31–72, p. 1735) The southeast quadrant of the image includes most of the glaciers of the north Cascades. Relief in the north Cascades is extreme, the valley to summit difference being as high as 2,000 m. Mount Baker (image center), at 3,285 m, is the highest peak; many other peaks approach 2,500 m. Annual precipitation in the north Cascades increases rapidly from about 1 m in the Puget Lowlands to as high as 4.5 m at the crest of the Cascade Range. Precipitation diminishes rapidly east of the crest to less than 0.5 m (Phillips and Donaldson, 1972). The major glacier concentrations are on Mount Baker and on high peaks near the crest of the north Cascades.*

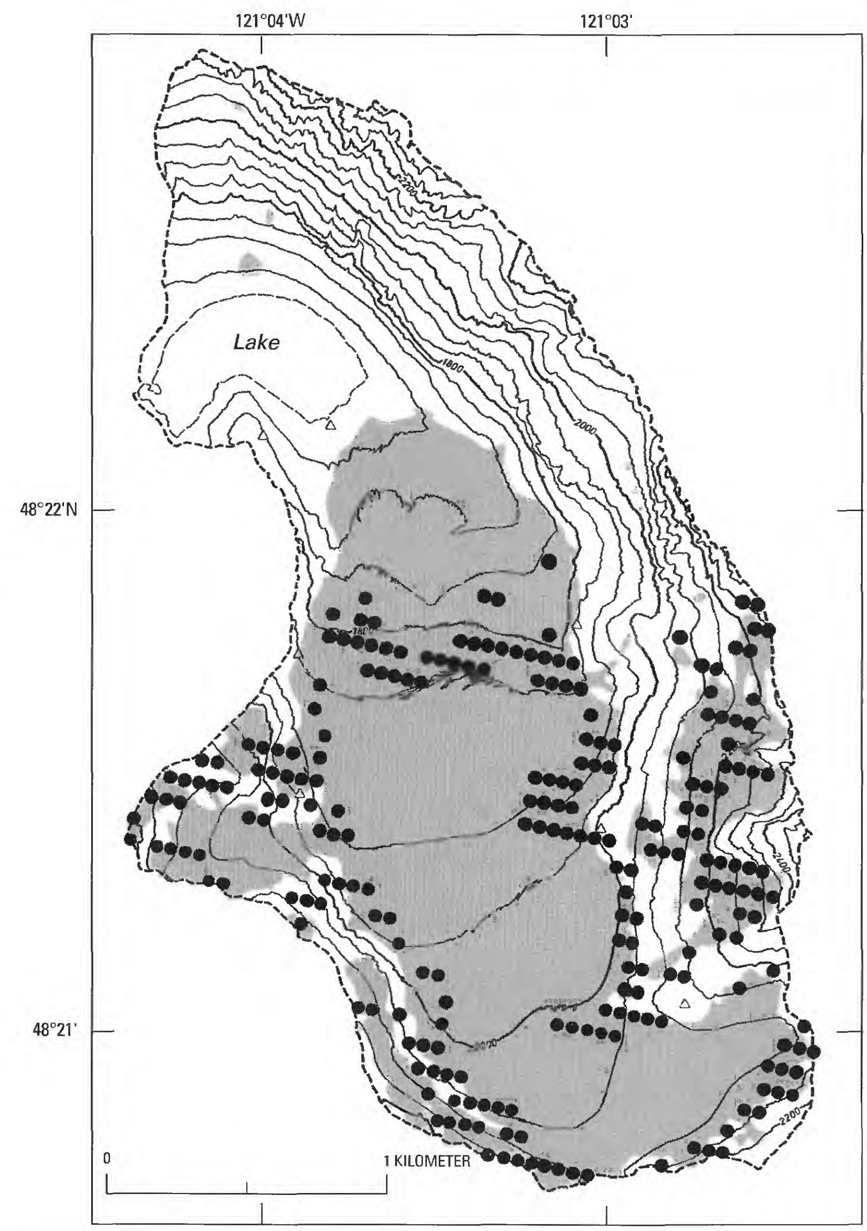

***Figure 3.**—Pixel-by-pixel temporal composite of two Landsat images of the South Cascade Glacier basin, Washington. All pixels having a radiance of 100 in MSS band 5 on images from 11 August 1973 (1384–18311) and 16 September 1973 (1420–18303) were considered to be snow. The heavy solid circles within the basin area show pixels that were snow on 11 August but not snow on 16 September. The shaded area within the basin represents areas of snow, firn, or ice cover at the end of the melt season in 1973, as determined from field observations. Most of the snow-cover loss between 11 August and 16 September was near the glacier edge, at high elevation, or on the lower glacier just below the equilibrium line (about 1,850 m). The small triangles indicate the positions of benchmarks.*

because of the high cost of digital data, and in addition, critical data needed from the end of the melt season commonly cannot be obtained because of cloud cover.

A similar date-to-date comparison of images can also be made optically. In figure 4, all the material having greater than a certain brightness level (assumed to be snow) is shown for a fall image (16 September 1973). This is then registered to a spring image (7 April 1973), which thereby produces a bitemporal color-composite image showing the location of perennial snow.

The RBV sensors carried on Landsats 1 and 2 offered no advantage over the MSS sensors for glacier observation. However, on Landsat 3, the RBV was modified to produce a panchromatic image having a pixel resolution of about 30 m (2.6 times better than the MSS image). Commonly the exposure of the photographic product was such that only some of the image was

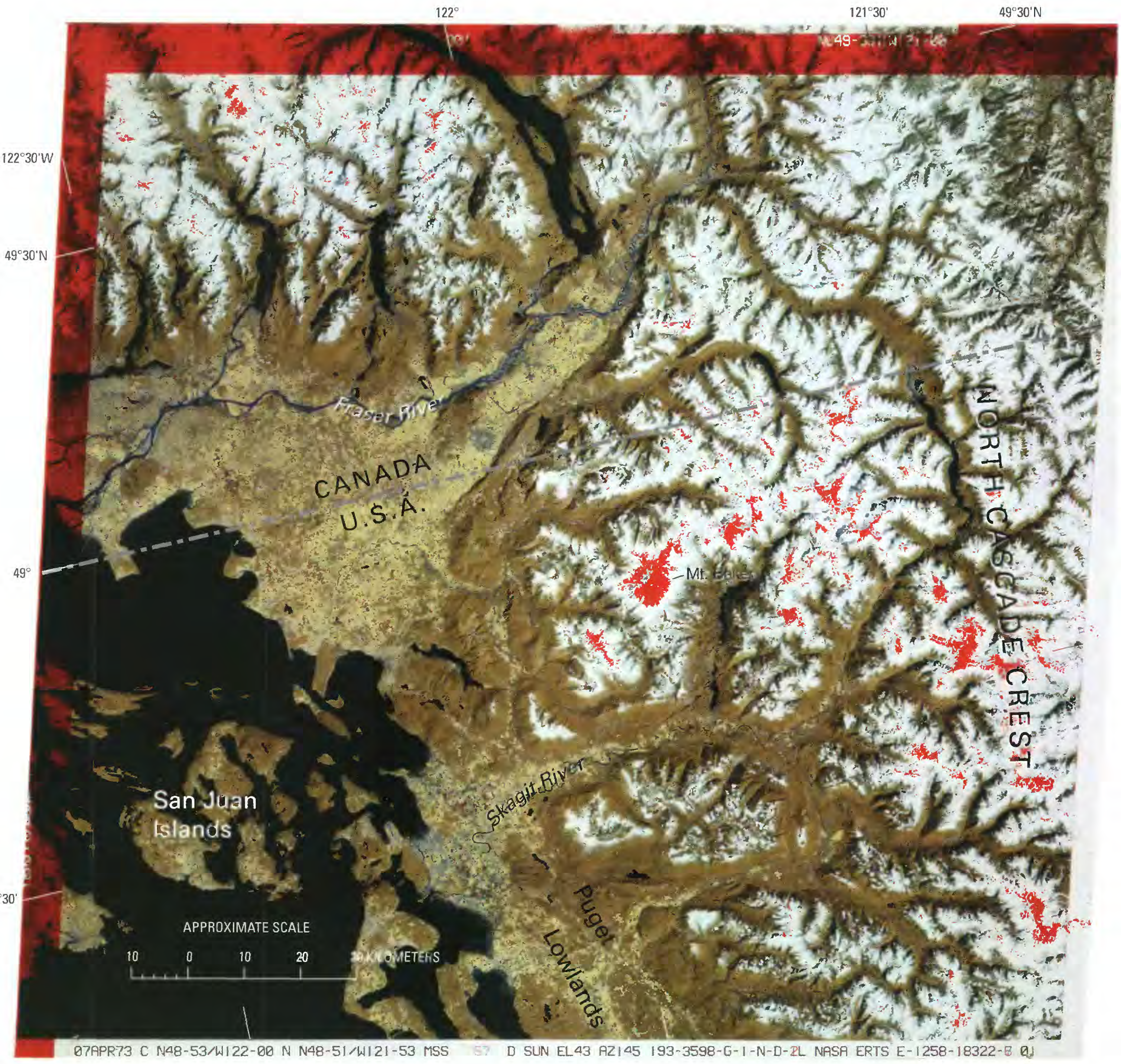

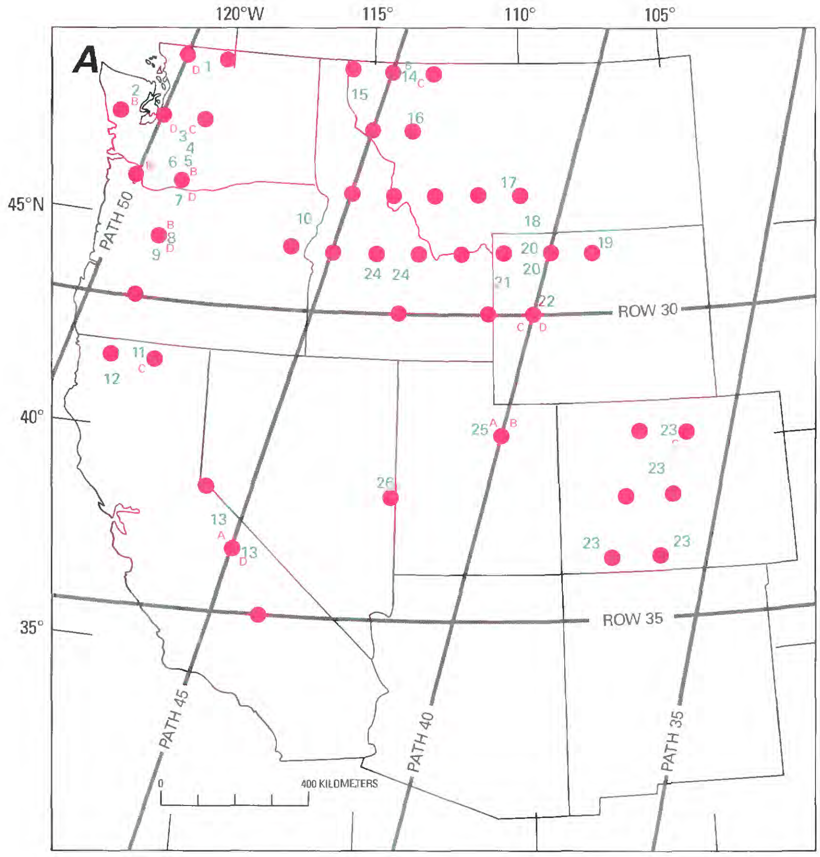

***Figure 5.**—Western conterminous United States showing Landsat nominal scene centers and optimum Landsat images of the glaciers. **A**, Landsat nominal scene centers, indicated by solid circles, are shown only for areas where glaciers exist. All except one of these nominal scene centers has an excellent image available. Red letters in the four quadrants around a scene center show that a usable Landsat 3 RBV subscene also exists. Scattered numerals indicate important glacier areas and are keyed to table 1. **B**, (opposite page) optimum Landsat 1, 2, and 3 MSS and Landsat 3 RBV images of the glaciers of the Western United States. See table 2 for detailed information.*

usable. Unfortunately, the data from this sensor are not now generally available. A few exceptional scenes of glacierized areas are in individual collections, but the available and usable Landsat 3 RBV images do not cover a sufficient area to allow glacier delineation over large regions.

Selection of Landsat Images

The optimum satellite image for the analysis of glacier cover would have no clouds, would have a high solar-elevation angle so that deep north-, northwest-, and west-facing valleys are not in shadow, and would have only perennial snow. Clouds commonly obscure the mountains where glaciers exist, although enough images have been processed of the United States so that cloudless scenes can normally be found. The high solar-elevation angle and minimum snow-cover factors are contradictory. The optimum Sun angle is in late spring and early summer, but the snowpack at this time of year is still heavy in the mountains. Because minimum snowpack is more important, the Sun-angle factor is rarely considered. In addition, the date of minimum snow cover changes from year to year. Optimum conditions, therefore, commonly are present on clear days in the fall before new snow falls.

In the western conterminous States, optimum conditions for satellite images typically fall between mid-September and mid-October. In addition to selecting imagery from the best time of year, it is also important to select a year that did not have an abnormally heavy snowpack or an uncommonly cool summer. Either of these conditions would leave excess snow in the fall and give an impression of greater snow (interpreted as glacier) coverage. With these factors in mind, the optimum images for all the glacierized areas in the western conterminous United States were selected and are listed in table 2. The locations of important glacierized areas are shown in figure 5, which keys these areas to table 1.

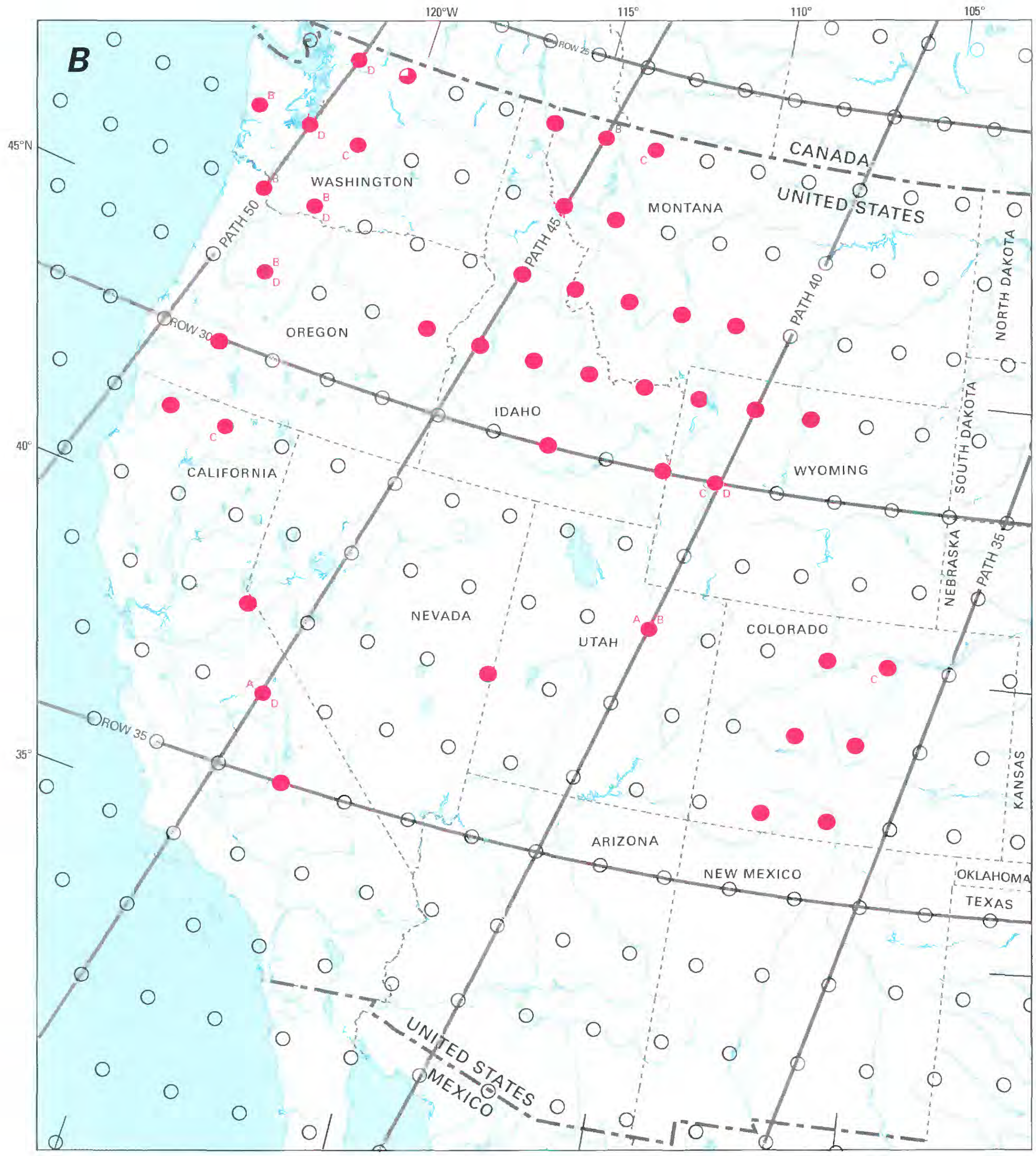

EXPLANATION OF SYMBOLS

Evaluation of image usability for glaciologic, geologic, and cartographic applications. Symbols defined as follows:

- Excellent image (0 to ≤5 percent cloud cover)
- Good image (>5 to ≤10 percent cloud cover)
- Nominal scene center for a Landsat image outside the area of glaciers
- A B C D Usable Landsat 3 return beam vidicon (RBV) scenes. A, B, C, and D refer to usable RBV subscenes

TABLE 2.—*Optimum Landsat 1, 2, and 3 MSS and RBV images of glaciers of the western conterminous United States*

[See fig. 5 for explanation of symbols used in "code" column]

Path-Row	Nominal scene center (lat-long)	Landsat identification number	Date	Solar elevation angle (degrees)	Code	Cloud cover (percent)	Remarks
36–32	105°02'W. 040°14'N.	2618–16525	01 Oct 76	38	●	0	Colorado Front Range. Some snow in the highlands
36–32	105°02'W. 040°14'N.	2222–17011	01 Sep 75	48	●	0	Entire Colorado Front Range
36–32	105°02'W. 040°14'N.	30929–16504– C	19 Sep 80	42	●	5	Superb Landsat 3 RBV of glaciers of Colorado Front Range (fig. 22). Archived by USGS–SGP[1]
36–33	105°31'W. 038°49'N.	21338–16451	21 Sep 78	41	●	0	Central Colorado. Considerable new snow in the highlands. No significant glaciers in the region
36–33	105°31'W. 038°49'N.	5843–15511	08 Sep 77	41	◐	30	Central Colorado. No significant glaciers in the region
36–34	105°59'W. 037°24'N.	30209–17041	30 Sep 78	42	●	0	South-central Colorado. No significant glaciers in the region
37–32	106°28'W. 040°14'N.	30516–17073	03 Aug 79	54	●	5	North-central Colorado. No significant glaciers in the region. Some previous winter snow in the highlands
37–32	106°28'W. 040°14'N.	21699–17025	17 Sep 79	43	●	0	Excellent image of north-central Colorado. No significant glaciers in the region
37–33	106°57'W. 038°49'N.	21699–17032	17 Sep 79	44	●	0	Excellent image of central Colorado Rocky Mountains. No significant glaciers in the region
37–33	106°57'W. 038°49'N.	21303–16491	17 Aug 78	49	●	0	Excellent image of central Colorado Rocky Mountains. No significant glaciers in the region
37–34	107°25'W. 037°24'N.	1425–17190	21 Sep 73	46	●	0	Southwestern Colorado. No significant glaciers in the region
37–34	107°25'W. 037°24'N.	30210–17095	01 Oct 78	42	●	0	Excellent image of southwestern Colorado. No significant glaciers in the region
39–29	107°46'W. 044°30'N.	1409–17285	05 Sep 73	46	●	0	Small glaciers in the Bighorn Mountains, Wyo. Snow in the highlands
39–29	107°46'W. 044°30'N.	5147–17022	13 Sep 75	40	●	0	Excellent image of Bighorn Mountains, Wyo.
40–29	109°12'W. 044°30'N.	5490–16444	21 Aug 76	43	●	0	Some snow in the highlands. Glaciers and moraines in the Beartooth Mountains, Absaroka Range, Wyo.
40–29	109°12'W. 044°30'N.	2244–17224	23 Sep 75	39	●	0	Small glaciers in the Beartooth Mountains, Wyo.
40–30	109°44'W. 043°05'N.	21720–17195	08 Oct 79	35	●	5	Excellent MSS image. Glaciers and moraines of the Wind River Range (fig. 18), Wyo.
40–30	109°44'W. 043°05'N.	30573–17231– C	29 Sep79	38	●	0	Good Landsat 3 RBV image of Wind River Range moraines, Wyo. Archived by USGS–SGP
40–30	109°44'W. 043°05'N.	30915–17131– D	05 Sep 80	44	●	0	Superb Landsat 3 RBV image of moraines and glaciers of the Wind River Range, Wyo. Archived by USGS–SGP
40–32	110°46'W. 040°14'N.	6000–16574	18 Oct 77	31	●	0	No significant glaciers in the region. Good image of moraines of Uinta Mountains, Utah (fig. 21)
40–32	110°46'W. 040°14'N.	30933–17133– A	23 Sep 80	40	●	0	Moraines and cirques in the western Uinta Mountains, Utah. Archived by USGS–SGP
40–32	110°46W. 040°14'N.	30933–17133– B	23 Sep 80	40	●	5	Moraines and cirques in the eastern Uinta Mountains, Utah. Archived by USGS–SGP
41–28	110°04'W. 045°55'N.	2965–17034	13 Sep 77	38	●	0	Crazy Mountains, Mont. No significant glaciers in the region
41–29	110°38'W. 044°30'N.	21685–17241	03 Sep 79	45	●	0	Northern part of Teton Range, Wyo. No significant glaciers in the region

TABLE 2.—*Optimum Landsat 1, 2, and 3 MSS and RBV images of glaciers of the western conterminous United States* —Continued

[See fig. 5 for explanation of symbols used in "code" column]

Path-Row	Nominal scene center (lat-long)	Landsat identification number	Date	Solar elevation angle (degrees)	Code	Cloud cover (percent)	Remarks
41–30	111°10'W. 043°05'N.	5509–16492	09 Sep 76	39	●	0	Central western Wyoming and eastern Idaho. No significant glaciers in the region
42–28	111°30'W. 045°55'N.	1790–17354	21 Sep 74	39	●	0	Southwestern Montana. No significant glaciers in the region
42–29	112°04'W. 044°30'N.	1790–17361	21 Sep 74	40	●	0	Southwestern Montana and northeastern Idaho. No significant glaciers in the region
42–33	114°08'W. 038°49'N.	22064–17363	16 Sep 80	45	●	0	Wheeler Peak, Nev. No significant glaciers in the region
43–28	112°56'W. 045°55'N.	30558–17395	14 Sep 79	41	●	0	Western Montana. Good image of moraines. No significant glaciers in the region
43–29	113°30'W. 044°30'N.	1791–17415	22 Sep 74	40	●	0	Eastern Sawtooth Range, Idaho. No significant glaciers in the region
43–30	114°02'W. 043°05'N.	22029–17405	12 Aug 80	51	●	0	Southern Sawtooth Range, Idaho. No significant glaciers in the region
44–26	113°09'W. 048°44'N.	30523–17452	10 Aug 79	49	●	5	Glacier National Park and Lewis Range, Mont. Some previous winter snow in the highlands (fig. 17)
44–26	113°09'W. 048°44'N.	30559–17445	15 Sep 79	39	●	0	Glacier National Park and Lewis Range, Mont.
44–26	113°09'W. 048°44'N.	30919–17342– C	09 Sep 80	39	●	0	Glacier National Park and Lewis Range, Mont. Archived by USGS–SGP
44–27	113°47'W. 047°20'N.	30523–17454	10 Aug 79	50	●	0	Flathead, Mission, and Swan Ranges, Mont. No significant glaciers in the region
44–28	114°22'W. 045°55'N.	2230–17452	09 Sep 75	43	●	0	Bitterroot Range, Idaho- Mont. No significant glaciers in the region
44–28	114°22'W. 045°55'N.	30559–17454	15 Sep 79	41	●	0	Bitterroot Range, Idaho- Mont. No significant glaciers in the region
44–29	114°56'W. 044°30'N.	2626–17371	09 Oct 76	33	●	0	Sawtooth Range, Idaho. Some snow in the highlands. No significant glaciers in the region (fig. 20)
44–29	114°56'W. 044°30'N.	30559–17460	15 Sep 79	42	●	0	Sawtooth Range, Idaho. No significant glaciers in the region
44–35	117°56'W. 035°58'N.	1396–18001	23 Aug 73	54	●	0	Southern Sierra Nevada, Calif. No significant glaciers in the region
45–26	114°36'W. 048°44'N.	22085–17505	07 Oct 80	31	●	0	Glacier National Park and Lewis Range. Cabinet Mountains, Mont.
45–26	114°36'W. 048°44'N.	30542–17505– B	29 Aug 79	44	●	5	Glacier National Park and Lewis Range, Mont.
45–27	115°13'W. 047°20'N.	21653–17452	02 Aug 79	51	●	5	Western Montana. No significant glaciers in the region
45–28	115°48'W. 045°55'N.	21293–17323	07 Aug 78	49	●	0	Western Sawtooth Range, Idaho. No significant glaciers in the region
45–29	116°22'W. 044°30'N.	21293–17325	07 Aug 78	49	●	0	Southwestern Sawtooth Range, Idaho. No significant glaciers in the region
45–34	118°54'W. 037°24'N.	30578–17532	04 Oct 79	40	●	0	Sierra Nevada, Calif. No significant glaciers in the region (fig. 13)
45–34	118°54'W. 037°24'N.	30578–17532– A	04 Oct 79	40	●	0	Northern Sierra Nevada, Calif. (fig. 14). Archived by USGS–SGP
45–34	118°54'W. 037°24'N.	30578–17532– D	04 Oct 79	40	●	0	Southern Sierra Nevada, Calif. (fig. 15). Archived by USGS–SGP
46–26	116°02'W. 048°44'N.	30561–17561	17 Sep 79	38	●	0	Cabinet Mountains, Idaho-Mont. No significant glaciers in the region

TABLE 2.—*Optimum Landsat 1, 2, and 3 MSS and RBV images of glaciers of the western conterminous United States* —Continued

[See fig. 5 for explanation of symbols used in "code" column]

Path-Row	Nominal scene center (lat-long)	Landsat identification number	Date	Solar elevation angle (degrees)	Code	Cloud cover (percent)	Remarks
46–29	116°39'W. 047°20'N.	1380–18093	07 Aug 73	53	●	0	Wallowa Mountains, Oreg. No significant glaciers in the region
46–33	119°52'W. 038°49'N.	30561–17591	17 Sep 79	45	●	0	Northern Sierra Nevada, Calif. No significant glaciers in the region
48–31	121°45'W. 041°40'N.	21710–18055	28 Sep 79	39	●	0	Mount Shasta, Calif.
48–31	121°45'W. 041°40'N.	30905–17595– C	26 Aug 80	47	◑	15	Mount Shasta, Calif. Archived by USGS–SGP
49–26	120°20'W. 048°44'N.	21657–18080	6 Aug 79	49	◕	10	Northern Cascade Range, Wash.
49–27	120°57'W. 047°20'N.	1419–18251	15 Sep 73	41	●	0	Northern Cascade Range, Mount Rainier, Wash.
49–27	120°57'W. 047°20'N.	30888–18043– C	09 Aug 80	49	●	0	Mount Rainier, Wash. (fig. 10). Archived by USGS–SGP
49–28	121°32'W. 045°55'N.	22053–18143	05 Sep 80	43	●	0	Mount St. Helens, Goat Rocks, Mount Adams, Mount Hood, Wash. (fig. 12)
49–28	121°32'W. 045°55'N.	30888–18050– B	09 Aug 80	49	●	0	Mount Adams, Wash. Archived by USGS–SGP
49–28	121°32'W. 045°55'N.	30942–18031– D	02 Oct 80	34	●	0	Mount Hood, Wash. Archived by USGS–SGP
49–29	122°06'W. 044°30'N.	21657–18091	06 Aug 79	51	●	0	Mount Jefferson, Three Sisters Range, Oreg. Some previous winter snow in the highlands.
49–29	122°06'W. 044°30'N.	30150–18160– B	02 Aug 78	53	●	0	Mount Jefferson, Oreg. Some previous winter snow in the highlands. Archived by USGS–SGP
49–29	122°06'W. 044°30'N.	30150–18160– D	02 Aug 78	53	●	0	Three Sisters Range, Oreg. Some previous winter snow in the highlands. Archived by USGS–SGP
49–30	122°39'W. 043°05'N.	1041–18271	02 Sep 72	48	●	0	Southern Oregon. No significant glaciers in the region. Some snow in the highlands
49–31	123°11'W. 041°40'N.	21693–18111	11 Sep 79	44	●	0	Salmon and Trinity Mountains, Mount Shasta, Calif.
50–26	121°46'W. 048°44'N.	1420–18303	16 Sep 73	39	●	0	Northern Cascade Range, Wash.
50–26	121°46'W. 048°44'N.	30223–18211– D	14 Oct 78	29	●	0	Northern Cascade Range, Wash. Archived by USGS–SGP
50–27	122°23'W. 047°20'N.	30583–18190	09 Oct 79	32	●	0	Northern Cascade Range, Olympic Mountains, Mount Rainier, Wash.
50–27	122°23'W. 047°20'N.	30889–18102– D	10 Aug 80	48	●	0	Mount Rainier, Wash. Archived by USGS–SGP
50–28	122°58'W. 045°55'N.	30889–18104– B	10 Aug 80	48	●	0	Mount St. Helens, Wash. (fig. 12C) Archived by USGS–SGP
51–27	123°50'W. 047°20'N.	2993–17590	11 Oct 77	28	●	0	Olympic Mountains, Wash. (fig. 9)
51–27	123°50'W. 047°20'N.	30926–18144– B	16 Sep 80	38	●	0	Olympic Mountains, Wash. Archived by USGS-SGP

[1] USGS-SGP is the U.S. Geological Survey-Satellite Glaciology Project (renamed the Glacier Studies Project).

Glaciers of the State of Washington

It has been estimated that 75 percent of the glaciers in the United States exclusive of Alaska are in the State of Washington (Meier, 1961a). The glaciers of Washington are conveniently grouped into six geographic divisions: (1) the north Cascades (northern Cascade Range), including the area from the Canadian border south to Snoqualmie Pass and from the Twin Sister Mountain area (about 15 km southwest of Mount Baker) in the west to long 120° W. in the east; (2) the Olympic Peninsula; (3) Mount Rainier; (4) the Goat Rocks area (about 50 km southeast of Mount Rainier); (5) Mount Adams; and (6) Mount St. Helens. Landsat images and other illustrations for each of the geographic divisions accompany the following discussions of each region.

Glaciers of the North Cascade Range

The most recent and comprehensive glacier inventory of the north Cascades, made in late 1969 by the USGS, shows that about one-half of the glaciers in Washington are in this region (Post and others, 1971). The source material for this inventory consisted of USGS large-scale (7.5-minute quadrangles, 1:24,000-scale) topographic map sheets and USGS oblique aerial photographs. The oblique aerial photography was used where maps were not available and also where the termini positions needed to be updated to the inventory date of 1970. This inventory counted 756 glaciers that had a total area of 267 km^2. Since that time, several additional small glaciers have been "discovered"; however, these small glaciers do not increase the total area significantly. The major concentrations of glaciers in the north Cascades are on Mount Baker, at the head of the Thunder Creek drainage, and on Glacier Peak. The largest glacier in this area is the Boston Glacier (lat 48°45' N., long 121°01' W.), which has an area of 7.0 km^2. The longest glacier, the Deming Glacier (lat 48°45' N., long 121°51' W.) on Mount Baker, is 4.8 km in length.

The north Cascades region is characterized by high relief; many of the valley floors are less than 500 m in elevation, whereas the nearby summits are in excess of 2,500 m. Precipitation is heavy; annual precipitation is commonly more than 4 m near the west side of the crest of the Cascade Range. On the east side of the crest, precipitation is considerably less.

The South Cascade Glacier is located within the north Cascades region at lat 48°22' N., long 121°03' W. Not necessarily representative of the glaciers of the north Cascades, it is a relatively flat glacier and has no major ice falls. However, it would be difficult to pick any one glacier that is typical of the north Cascades. This glacier has been studied in detail since 1957 (Meier and Tangborn, 1965; Meier and others, 1971; Fountain and Fulk, 1984). It is about 3 km long and 2.5 km^2 in area and has an equilibrium line altitude (ELA) of 1,860 m. Studies in the South Cascade Glacier basin have been directed toward glacier mass balance (Meier, 1961b; Meier and Post, 1962; Tangborn, 1965, 1968; Tangborn and others, 1975, 1977; Krimmel, 1989, 1993, 1994; Meier and others, 1980; Mayo, 1984; Walters and Meier, 1989), basin water balance (Tangborn, 1963; Krimmel and others, 1978; Sullivan, 1994; Krimmel, 1995, 1996, 1997, 1998, 1999, 2000, 2001) ice dynamics and subglacier and englacier water flow (Fountain, 1989, 1992a, b, 1993, 1994), and many other related topics (Meier, 1958, 1967; Tangborn, 1962).

The history of the South Cascade Glacier shows advances at about 3000 B.C. and during the 16th and 19th centuries. A sheared-off tree stump some 100 m above the 1970 ice level was dated by the radiocarbon method at about 5,000 years B.P. (before present). This suggests that the glacier had been at its present size or smaller for some centuries prior to 3000 B.C.

Figure 6.—Photographic record of South Cascade Glacier, Wash., from 1928 to 1996. **A**, *In 1928, the glacier had been retreating since the neoglaciation maximum length in the late 19th century. The average retreat rate from 1928 to 1980 was about 18 m a^{-1}; the maximum retreat rate took place from about 1950 to 1960 as the glacier retreated across the lake. The retreat rate during the 1970's was about 12 m a^{-1}. All the glaciers of the north Cascades experienced an overall retreat during the 20th century. Oblique aerial photograph by Wernstadt, U.S. Forest Service.* **B**, *South Cascade Glacier in 1939. Photograph taken by Watson.* **C**, *South Cascade Glacier in 1955. Photograph taken by Richard Hubley, University of Washington.* **D**, **E**, *see opposite page*

Sometime after 3000 B.C., the glacier made an advance that ended in the 16th century about 1.5 km downvalley from the 1970 position. The glacier retreated an unknown distance from the 16th century position and then readvanced to nearly the 16th century position near the end of the 19th century (Miller, 1969).

Since the late 19th century advance of the South Cascade Glacier, its terminus has been continuously receding. A 1928 oblique aerial photograph

Figure 6.—**D**, *South Cascade Glacier on 10 October 1983. Photograph number 83RI–188 taken by R.M. Krimmel, USGS.* **E**, *South Cascade Glacier on 9 October 1996. Black-and-white oblique aerial photograph from original 35-mm color slide taken by R.M. Krimmel, USGS.*

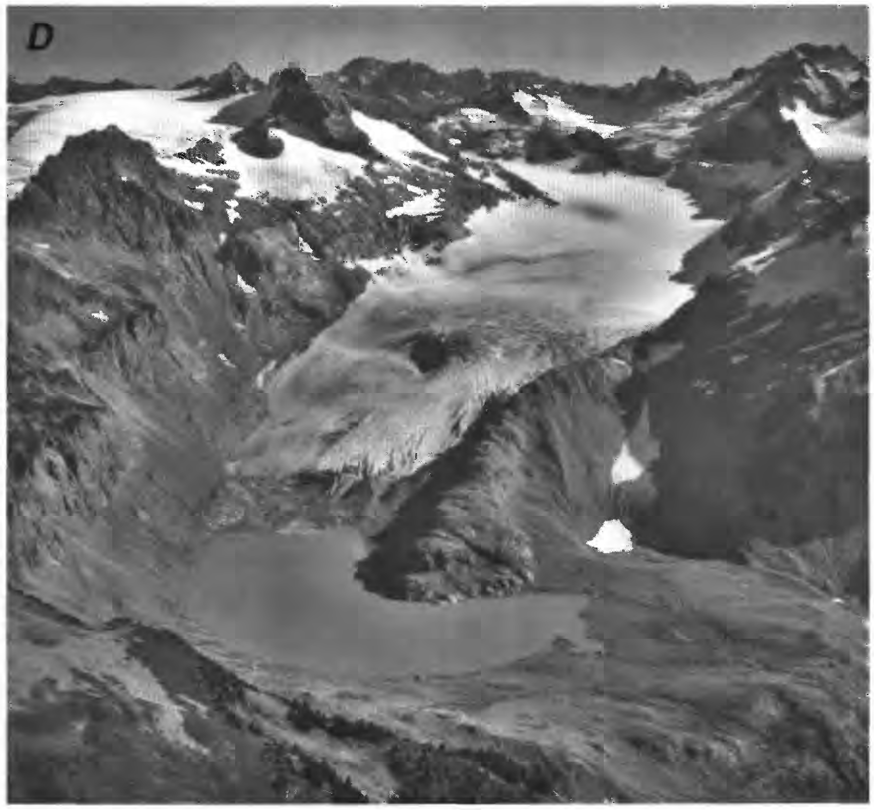

E

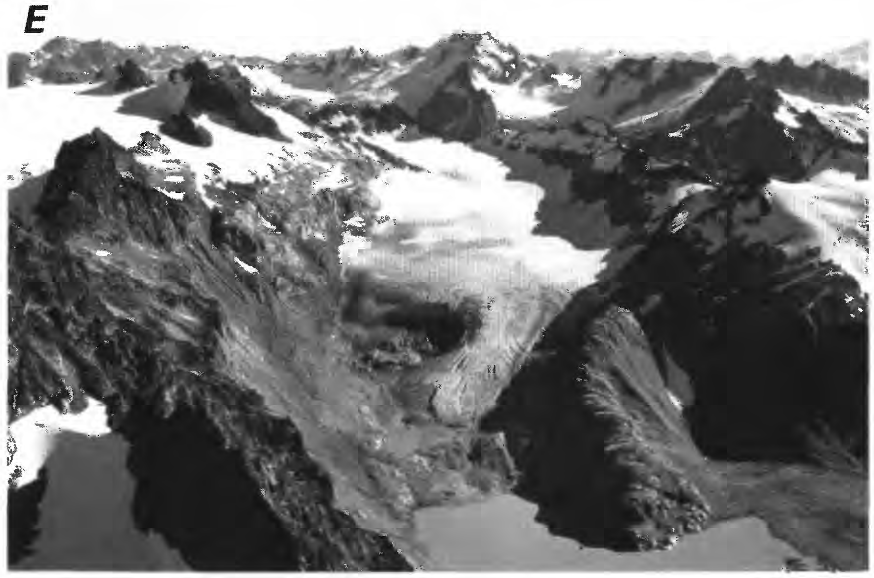

(fig. 6*A*) shows the terminus at today's west shore of South Cascade Lake. A photograph from 1939 (fig. 6*B*) shows about 100 m of lake opened, and the first vertical aerial photograph, from 1953, shows about one-half of the lake opened. By 1955, more of the lake was free of glacier ice (fig. 6*C*), and by 1968, the entire lake was clear of glacier ice. Since 1968, recession has continued, averaging about 12 m a^{-1}, although very minor advances have been recorded during this period. During the winter, ice motion continues but is not offset by ice ablation, and a seasonal advance takes place. In 1972, extremely heavy winter snowpack covered the terminus well into late summer. Because the snow protected the terminus from melting, it advanced a few meters. Figure 6*D*, showing the glacier in 1983, is an example from the collection of recent large-format oblique and vertical aerial photographs archived by the University of Alaska's Geophysical Institute in

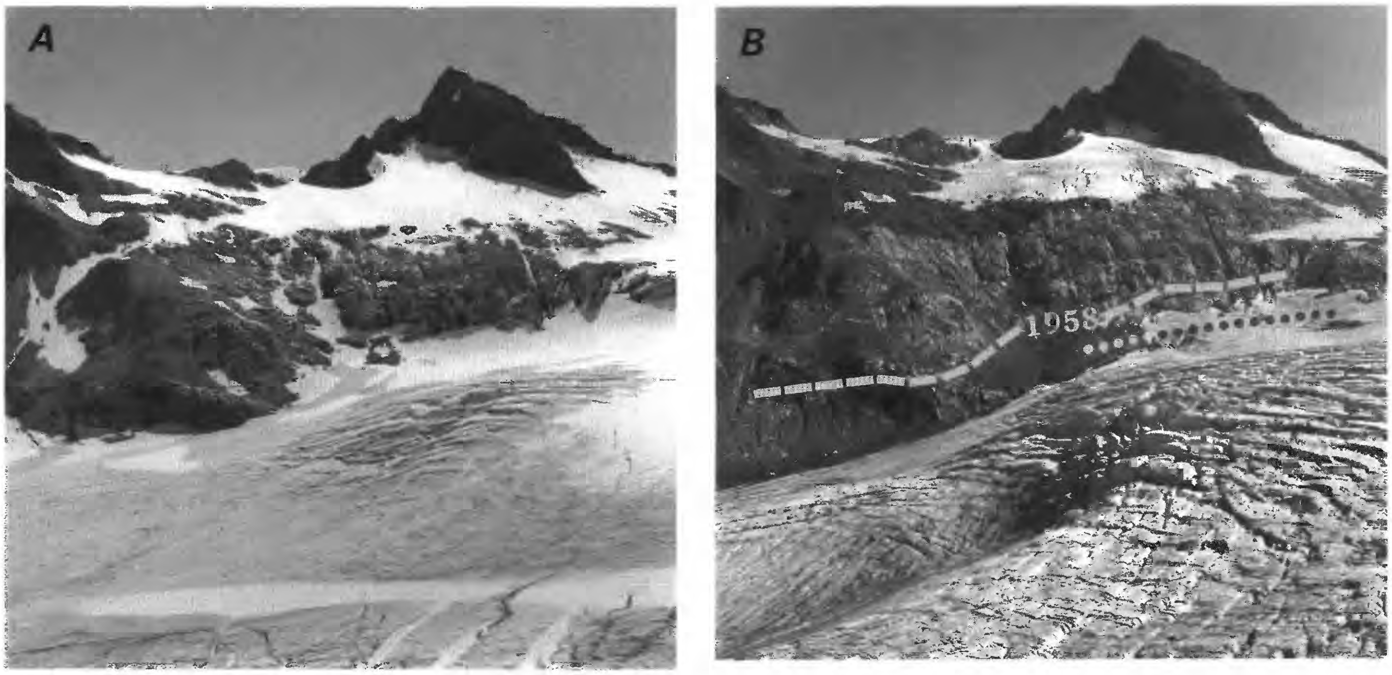

Fairbanks, Alaska. The University of Alaska archive includes most of the major glaciers in the United States. Figure 6*E* shows the position of the glacier terminus in 1996.

Figure 6 illustrates the exceptional photographic record for South Cascade Glacier. Figure 7 illustrates a time sequence of terrestrial photographs used for qualitative analysis of ice-level changes.

The annual mass balance of South Cascade Glacier has ranged from –2.6 m to +1.4 m and has had an average of –0.7 m from 1966 to 1995. Figure 8 shows the cumulative mass balance from 1884 to 1995. Annual runoff from the entire area of the basin (fig. 3) is normally about 4 m. Precipitation accounts for 93 percent of this total; the remainder is derived from loss of ice mass.

South Cascade Glacier has an average thickness of 100 m and a maximum thickness of 220 m (Krimmel, 1970). Its average velocity is about 10 m a^{-1}. The maximum velocity, about 30 m a^{-1}, is found near the center of the lower glacier. Maximum seasonal velocity takes place in the early summer and is 140 percent of the annual velocity; minimum velocity takes place during the fall and winter.

South Cascade Glacier is one of only a few glaciers worldwide that have been analyzed with regard to their dynamic response to change in climate. A hypothetical 1-m addition to the glacier surface for only 1 year would produce a thickening of the terminus that would amount to 5 m after 23 years. This would be followed by a slow return to normal, but it would have an excess of 0.6 m persisting at the terminus 100 years later. The actual glacier response is a combination of responses to weather events for each year of the last century or more, and thus it is complex and has a long "memory" (Nye, 1965).

Balance measurements have been made at numerous other north Cascades glaciers, and for the most part, these show trends similar to those at South Cascade Glacier. *Vesper Glacier* was measured during balance years 1974–75 (Dethier and Frederick, 1981); Pelto made measurements on Columbia, *Daniels*, *Foss*, *Ice Worm*, Lower Curtis, Yawing, Rainbow, *Spider*, and Lynch Glaciers from 1984 to 1994 (Pelto, 1996); and North Cascades National Park personnel measured North Klawatti, Silver, *Noisy*, and Sandelee Glaciers during 1992–96.

***Figure 7.**—Ice-level changes of South Cascade Glacier, Wash.* **A**, *South Cascade Glacier in July 1958. Photograph taken by Austin Post, USGS.* **B**, *South Cascade Glacier in August 1979. Photograph shows a loss of about 30 m near the equilibrium line since 1958. The dashed line is the 1958 position of the ice edge. The dotted line indicates the level of the active glacier ice. Photograph taken by R.M. Krimmel, USGS.* **C**, **D**, **E**, *see opposite page.*

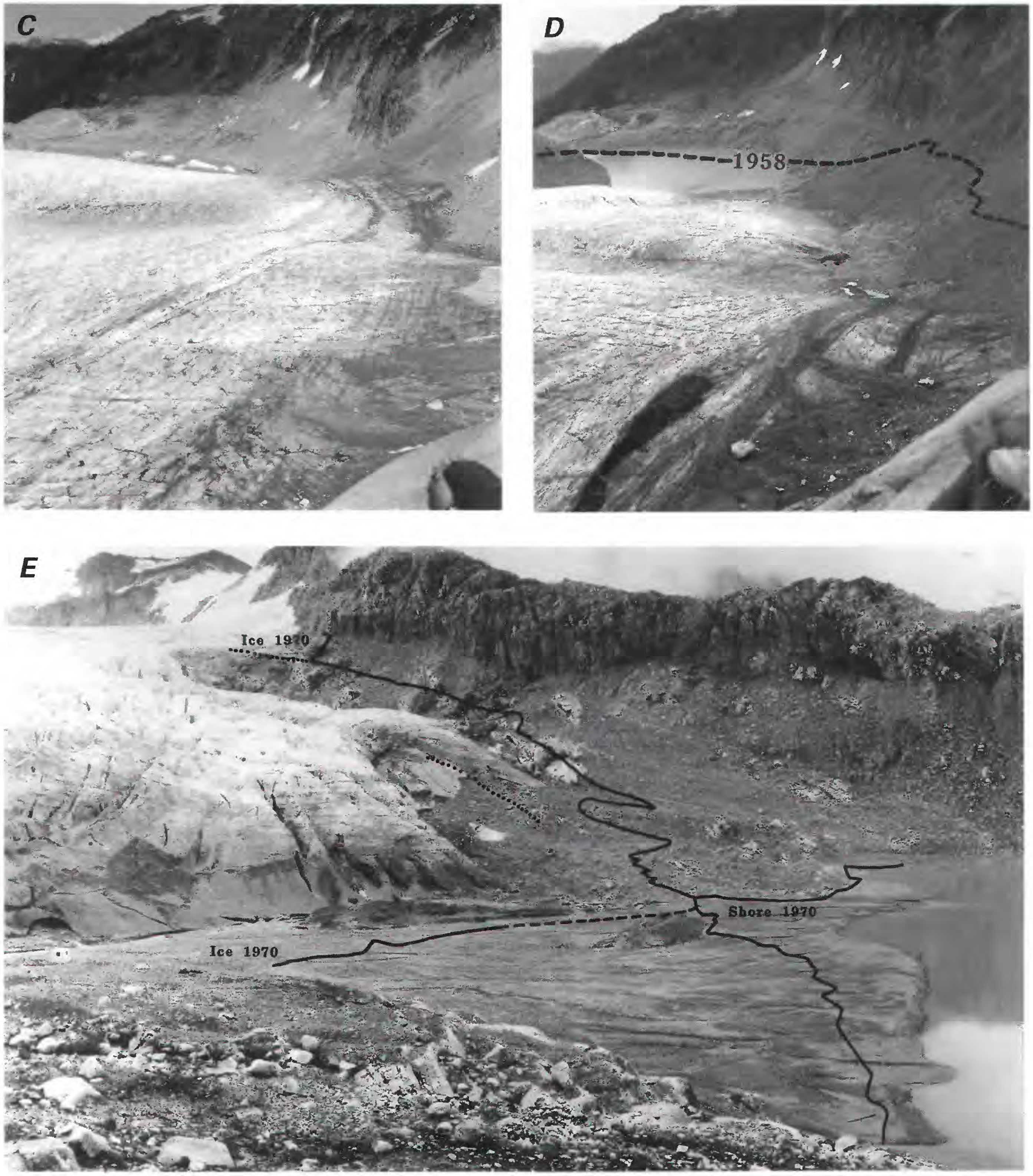

***Figure 7.*—C**, *Lower South Cascade Glacier in July 1958. Photograph taken by Austin Post, USGS.* **D**, *Lower South Cascade Glacier in August 1979. Photograph shows a loss of about 60 m since 1958. The dashed line is the 1958 position of the ice edge. Photograph taken by R.M. Krimmel, USGS.* **E**, *Lower South Cascade Glacier in August 1978. Ice loss on lower Cascade Glacier at the terminus from 1970 to 1978 was about 30 m, and recession during that period was about 90 m. The dashed line is the 1970 terminus position inferred from, but not visible in, a 1970 photograph. Dotted lines show 1970 levels of ice in areas between the photograph point and the far edge of the glacier. The inconspicuous building on the extreme left is 2 m high. Photograph taken by R.M. Krimmel, USGS.*

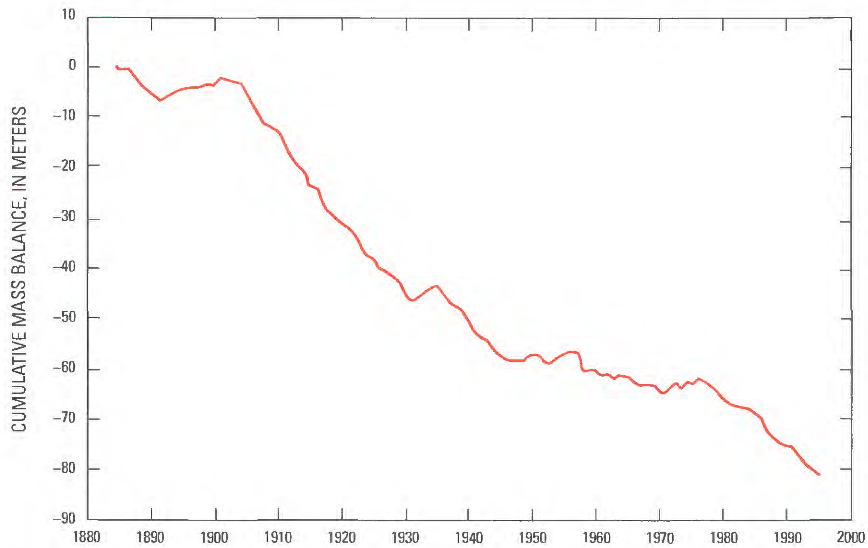

Figure 8.—Cumulative mass balance for South Cascade Glacier, Wash., for the years 1884–1995 (adapted from Tangborn, 1980). For the years 1884 to 1957, balance was calculated by a precipitation-temperature model; the balance was directly measured for the years 1958–95.

Glaciers of the Olympic Peninsula

Storm systems affecting the Olympic Peninsula tend to approach from the west and southwest. Because the Olympic Peninsula (fig. 9) forms a barrier to the moist clouds from the Pacific Ocean, strong precipitation gradients are found from the west to the east. Although most coastal stations receive 2 m of precipitation, about 3 m of precipitation is received 15 km inland, and at the crest of the Olympic Mountains 60 km inland, the annual precipitation is 6 m. Farther inland, to the northeast of the summits, the precipitation drops off rapidly to as low as 0.4 m. Because the freezing level during winter is often below 1,000 m, snow is heavy in the mountains, and glaciers exist on many of the higher peaks (Phillips and Donaldson, 1972).

The major glacier concentration is on the Mount Olympus massif, where three major glaciers, the Blue, Hoh, and White Glaciers, and numerous other smaller glaciers account for about 80 percent of the area of perennial snow and ice in the Olympic Mountains. Small glaciers are found on Mount Anderson at 2,233 m and on Mount Carrie at 2,133 m; numerous small glaciers or ice patches exist above 2,000 m in shaded areas on these and other peaks. The total area of perennial snow and ice on the Olympic Mountains is about 45.9 km^2 (Spicer, 1986).

The Blue Glacier is one of the most extensively studied glaciers in the United States. The variations of the Blue Glacier during recent centuries (Heusser, 1957) and its mass balance (LaChapelle, 1965), structure (Allen and others, 1960), internal deformation (Shreve and Sharp, 1970), and flow (Meier and others, 1974) have been the subjects of major research efforts.

Glaciers of Mount Rainier

Mount Rainier, a large stratovolcano, is 4,395 m high (fig. 10) and supports the largest concentration of glaciers in the United States, outside of Alaska (Dreidger, 1986, 1993). The largest glacier in the Western United States, the Emmons (11.2 km^2 in area), the longest glacier, the Carbon (8.2 km long), and the lowest glacier terminus, the Carbon (1,070 m), are all on Mount Rainier. The combined area of the 25 named and 50 or so unnamed glaciers on Mount Rainier and its satellite peaks is 92.1 km^2. The total volume of ice on Mount Rainier is 4.4 km^3 (Driedger

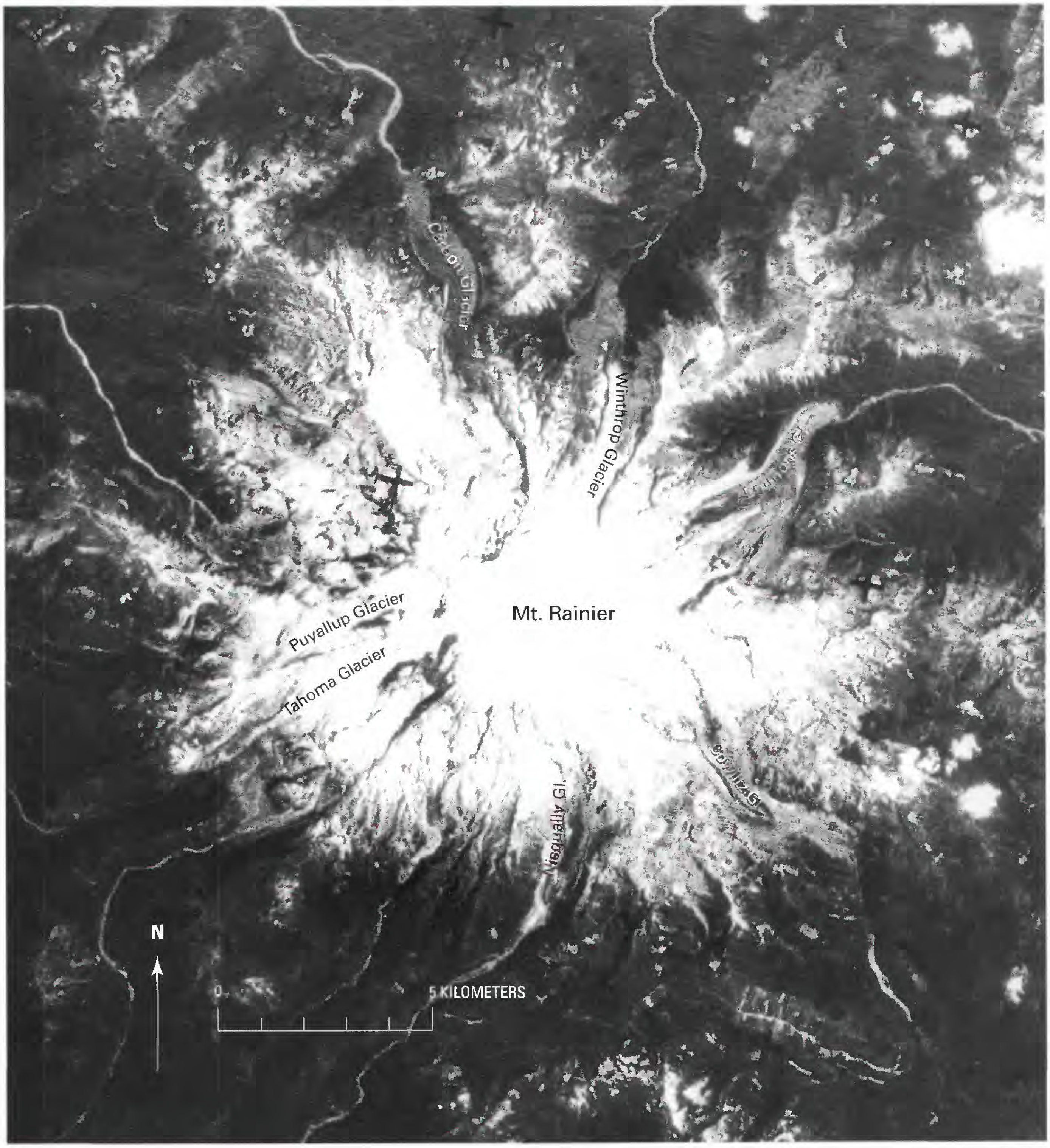

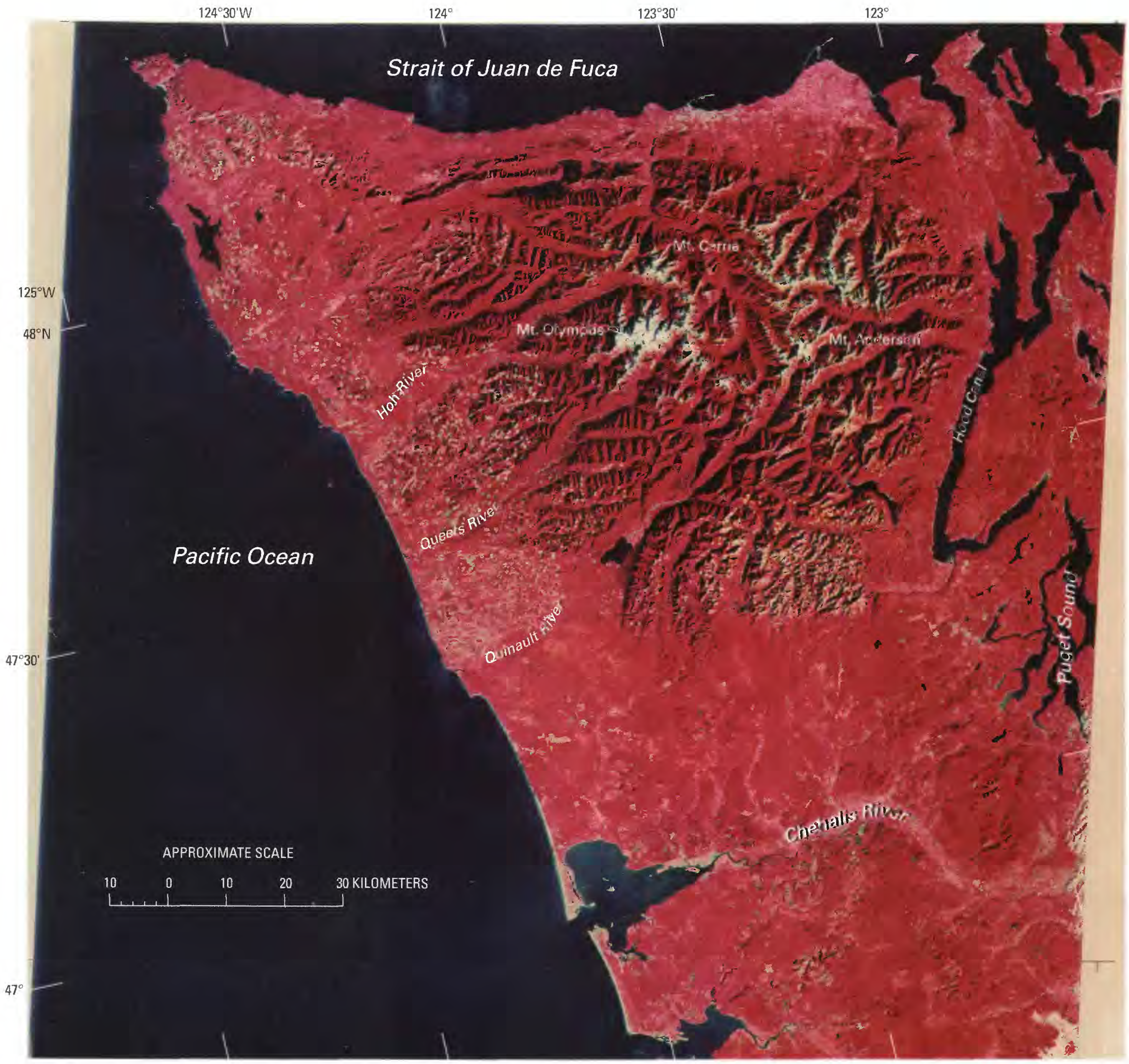

Figure 9.—*Landsat 2 MSS false-color composite image (2993–17590, bands 4, 5, and 7; 11 October 1977; Path 51, Row 27) of the Olympic Peninsula, Puget Sound, and vicinity, Wash. The Olympic Peninsula is a very distinct physiographic unit. To the west is the Pacific Ocean, to the north is the Strait of Juan de Fuca, to the east is the Hood Canal and Puget Sound, and to the south is the valley of the Chehalis River. Relief in the Olympic Mountains is extreme. Relatively low valleys extend into the interior, and the 300-m contour is within 8 km of the 2,429-m high Mount Olympus (north of image center). Other peaks greater than 2,000 m in elevation are numerous; all are east of the Mount Olympus massif. Evidence of the much greater extent of past glaciation is easily seen. The valleys of the Hoh, Queets, and Quinault Rivers, all draining to the west, have the classic broad, relatively straight shape that indicates erosional modification by glaciers. Glaciers from these valleys ended in piedmont lobes. Much smaller glaciers existed from the range toward the east because a precipitation pattern similar to the present probably existed during past glacials. Evidence of past glacier cover in Puget Sound is indicated by the small lakes and fjords.*

Figure 11.—Nisqually Glacier from the old Nisqually River bridge, Mount Rainier, Wash. The exact date and photographer of this photograph are unknown, but the date is approximately 1900. This is an example of a photograph that was presumably taken for nonscientific reasons but now provides valuable information on the position of the glacier terminus.

and Kennard, 1984, 1986). The potential for the interaction of volcanic activity and the glacier-ice cover makes Mount Rainier a very dangerous volcano that could produce, as it has in the geologic past, jökulhlaups (Driedger, 1988; Driedger and Fountain, 1989; Walder and Driedger, 1995) and lahars (Walder and Driedger, 1993). Richardson (1968) discussed jökulhlaups in the Pacific Northwest region.

Nisqually Glacier is the most accessible major glacier in the conterminous United States and offers numerous tourists their first closeup look at a glacier. This glacier also has the longest record of annual observations of the position of its terminus—since 1918—of any glacier in the Western Hemisphere. The history of the Nisqually Glacier is documented as well by numerous early photographs (Veatch, 1969). Figure 11 is an example of an early photograph of the glacier. The Nisqually Glacier has been the subject of several glaciological research projects (Hodge, 1972, 1976, 1979). Since 1931, annual measurements have been made of the change in thickness, and detailed topographic maps of the Nisqually Glacier were made by the USGS from vertical aerial photography at scales of 1:10,000 (see Heliker and others, 1984; U.S. Geological Survey, 1978) and 1:12,000 dated 16 August 1951, 4 September 1956, 19 August 1961, 25 August 1971, and 31 August 1976. The Nisqually Glacier 1976 map sheet (1:10,000 scale) (U.S. Geological Survey, 1978) was preceded by four earlier map sheets: Nisqually Glacier 1931, 1936, 1941, and 1946, published in 1960; Nisqually Glacier 1951, 1956, and 1961, published in 1963; Nisqually Glacier 1966, published in 1968; and Nisqually Glacier 1971, published in 1973. The terminus receded almost continuously from the first observation in 1857 through 1963 (Kautz, 1875; Heliker and others, 1984). In 1964, active ice advanced, and this advance continued to 1969 (Sigafoos and Hendricks, 1972). Advance began again in 1976 and was continued into 1982. Between 1983 and 1986, little change was noted in the terminus of Nisqually Glacier. From 1986 to 1990, a pronounced recession occurred, accompanied by thinning, and retreat was continuing in 2001 (Carolyn L. Driedger, oral commun., 2001). Since 1857, the total recession has been 1,945 m, and the total advance, 294 m (Heliker and others, 1984). An intensive study during the late 1960's and early 1970's showed speeds that varied from 60 to 160 mm d^{-1} near the terminus and from 200 to 700 mm d^{-1} near the equilibrium line. The speed was seasonably dependent, the early summer speed being generally about two times the late fall speed (Hodge, 1974).

Figure 10.—(opposite page) Mount Rainier, Wash., from a part of Landsat 3 RBV image 30888–18043–C on 9 August 1980 (Path 49, Row 27). The glacier termini are seen extending well beyond the snow-covered higher elevations in this Landsat image. Most of the glaciers terminate well above the vegetation trimlines, and the actual termini are in places identifiable by a darker perimeter where the steep glacier edge forms a shadow. Landsat 3 RBV images allow terminus fluctuations as small as 30 m to be observed under optimum conditions. Abbreviation: Gl., Glacier.

Glaciers of Southern Washington

Glaciers of southern Washington exist only in the Goat Rocks area, on Mount Adams, and on Mount St. Helens (fig. 12*A*). In the Goat Rocks area, numerous small glaciers (each less than 1 km^2 in area) are present on the north or west sides of the crest of the Cascade Range near Gilbert Peak (2,496 m). These glaciers form on slopes lee to the prevailing southwesterly storm winds.

Mount Adams (3,744 m) is the second highest summit in the State of Washington. The mountain has 10 major named glaciers, the largest of which is the Adams Glacier. Because most of the termini of Mount Adams' glaciers are completely covered with rock debris, it is difficult to define the precise glacier limits.

Most of the glaciers on the flanks of Mount St. Helens were either reduced in size or eliminated during the catastrophic explosive volcanic eruption of 18 May 1980 (fig. 12*B*) (Brugman and Post, 1981). The preeruption glacier area was approximately 5 km^2 and had a volume of 0.18 km^3. Seventy percent of this ice was removed on 18 May 1980, including all or virtually all of the Wishbone, Loowit, Leschi, and Forsyth Glaciers. The ice was removed either by the paroxysmal blast, which caused the displacement of

Figure 12.*—Glaciers of southern Washington.* **A**, *Landsat 2 MSS false-color composite image (22053–18143, bands 4, 5, and 7; 5 September 1980; Path 49, Row 28) showing part of southwestern Washington and northwestern Oregon. The ice remaining on Mount St. Helens (northwest part of image) 4 months after the 1980 eruptions, on Mount Adams (north-central part of image), and in the Goat Rocks area (extreme north-central part of image) is covered by tephra deposits and is not visible in this image. The ice in these three areas accounts for all the ice in Washington State south of Mount Rainier. Ice cover on Mount St. Helens previous to 18 May 1980 was 5.02 km^2, but it was only 2.16 km^2 after that date (Brugman and Meier, 1981). Ice cover on Mount Adams is about 16 km^2; in this image, summer snow is visible at higher elevations. Ice cover in the Goat Rocks area is 1.5 km^2 (Meier, 1961). Mount Hood, Oreg., (south-central part of image) has 13.5 km^2 of ice, the largest area of ice in that state.* **B**, **C**, *see opposite page.*

Figure 12.—**B**, *Oblique aerial photograph of Mount St. Helens, Wash., looking toward the northeast at about noon on 18 May 1980, approximately 3.5 hours after the beginning of the explosive eruption. Virtually all the glaciers were beheaded or destroyed by the collapse of the north slope of the volcano and the subsequent blast that removed approximately 2.6 km*^{3} *of volcanic material from the summit and northern part of the mountain (Foxworthy and Hill, 1982). Tephra blankets the remaining parts of the glaciers radiating from the now-missing summit region. The vertical, billowing eruption plume of tephra and other volatiles emanates from the 1.5-km-wide horseshoe-shaped crater (fig. 12*C*) and extends well into the stratosphere. A small base surge is also visible on the southeast edge of the crater. USGS photograph number 80–S3–137 by R.M. Krimmel, USGS.* **C**, *Landsat 3 RBV image 30889–18104–B taken of Mount St. Helens on 10 August 1980 (Path 50, Row 28), 3 months after the catastrophic explosive eruption (fig. 12*B*). The horseshoe-shaped crater is visible at the apex of a large fan-shaped area to the north, the region most devastated by the lateral "blast" (Tilling, [1984]). Light-colored tephra deposits blanket the slopes of the volcano, including the remnants of the surviving glaciers.*

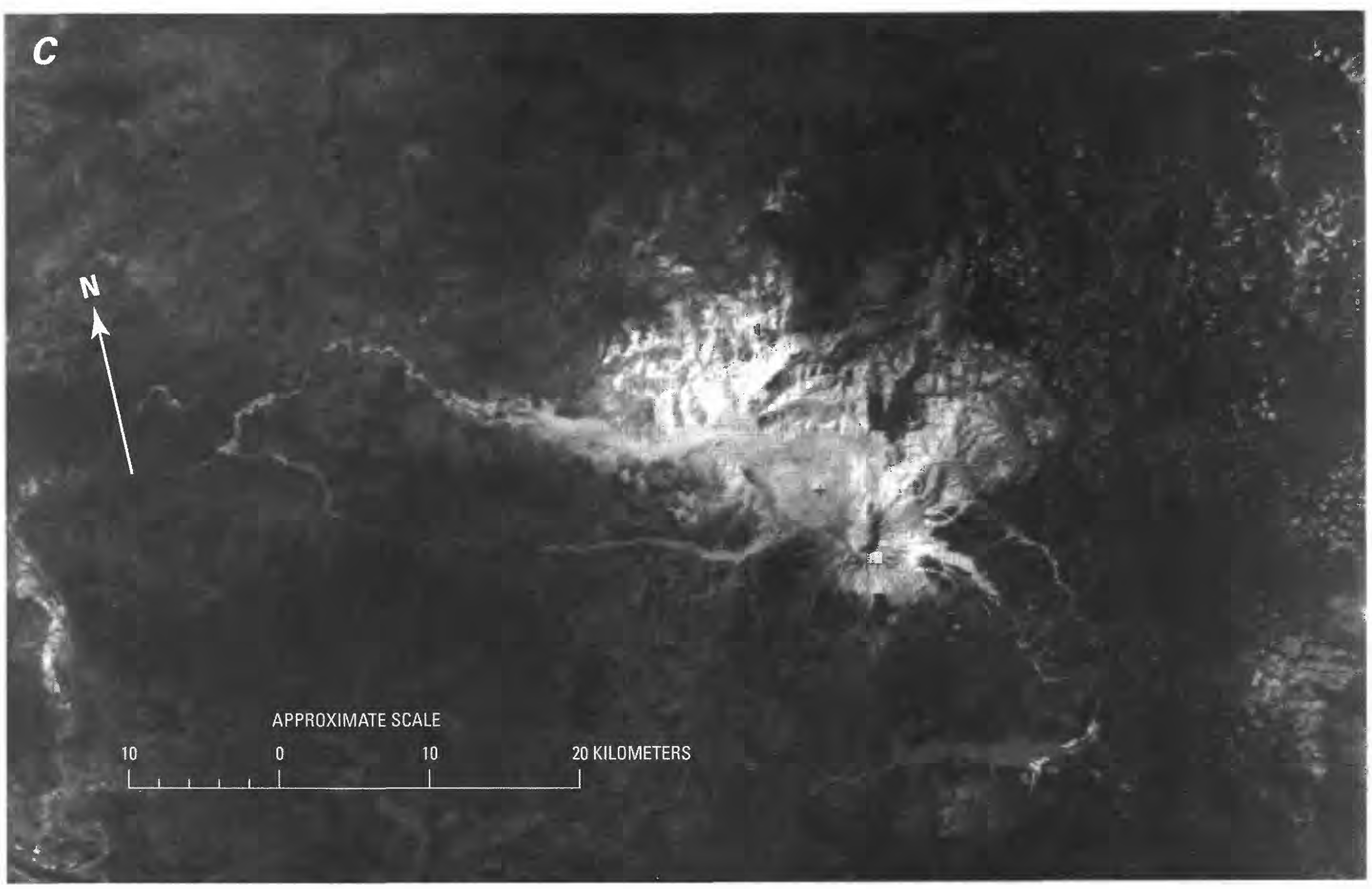

the underlying bedrock and the landslide process, or by melting from pyroclastic flows. The remaining snow and ice were covered with an average 1 m of tephra, which acted as in insulator against summer ablation (Driedger, 1981). The Shoestring Glacier was the site of an ongoing ice-dynamics study previous to the eruptions of 1980. During the 18 May 1980 eruption, however, 68 percent of this glacier, including the entire accumulation zone, was removed. Preeruption velocity was 20 to 50 cm d^{-1}; posteruption velocity was 10 to 20 cm d^{-1} (Brugman and Meier, 1981). The posteruption geometry of Mount St. Helens is such that a new glacier could form in the crater area (Jordan and Kieffer, 1982) (fig. 12*C*). The floor of the north-facing horseshoe-shaped crater is at 1,880 m in elevation, has steep-sided walls that enhance avalanche accumulation, is on the lee side of a steep ridge, so accumulation will be further enhanced, and has a northern exposure. In fact, snow from the previous winter was observed under rockfall debris in the crater in the late summer of 1983 (R.J. Janda, oral commun.). It is unlikely that a significant glacier will form in the crater, however, as long as the active lava-dome-building phase of Mount St. Helens continues.

Glaciers of the State of Oregon

Glaciers are found in Oregon on the Cascade Range volcanoes of Mount Hood (fig. 12*A*), Mount Jefferson, and Three Sisters Range, and in the Wallowa Mountains in eastern Oregon. Studies have been made to determine the ice volume on Mount Hood and the Three Sisters Range in response to requirements for a volcanic-hazards assessment. The total ice area on Mount Hood is 13.5 km^2; the total volume is 0.16 km^3 (Driedger and Kennard, 1986). The glaciers in the Wallowa Mountains may be locally significant, but they are less than 0.1 km^2 and are insignificant at the 79-m pixel resolution of Landsat MSS images.

A photographic study of the Collier Glacier on the North Sister Peak during the period 1934–60 showed general recession (Hopson, 1960). A topographic map of the Collier Glacier was compiled from aerial photographs acquired on 8 September 1958, on 8 September 1968, and on 29 September 1979. A longitudinal elevation profile from this map shows that no major change in the thickness of the glacier took place between 1959 and 1979. The extreme upper part of the glacier was about 16 m thicker in 1979 than in 1959; however, changes in the rest of the glacier were less than 5 m.

Glaciers of the State of California

Glaciers are present in California on Mount Shasta (4,319 m), in the Trinity Alps (approximately lat 41° N., long 123° W.), and in the high Sierra Nevada. The glaciers on Mount Shasta have a total area of 6.9 km^2 (Driedger and Kennard, 1984). The glaciers in the Trinity Alps are insignificant at the spatial resolution of the Landsat image.

A comprehensive glacier inventory of the Sierra Nevada has been completed (Raub and others, 1980; unpub. data). A major part of the area included in the Sierra Nevada glacier inventory is included in a single Landsat image (fig. 13), and part of the region is seen in more detail in Landsat 3 RBV images (figs. 14 and 15). In this inventory, glaciers and ice patches as small as 0.01 km^2 are counted. The total inventory counted 497 glaciers and 788 ice patches for a total area of 63 km^2. The largest glacier in the Sierra Nevada is the Palisade Glacier, which has an area of 1.6 km^2.

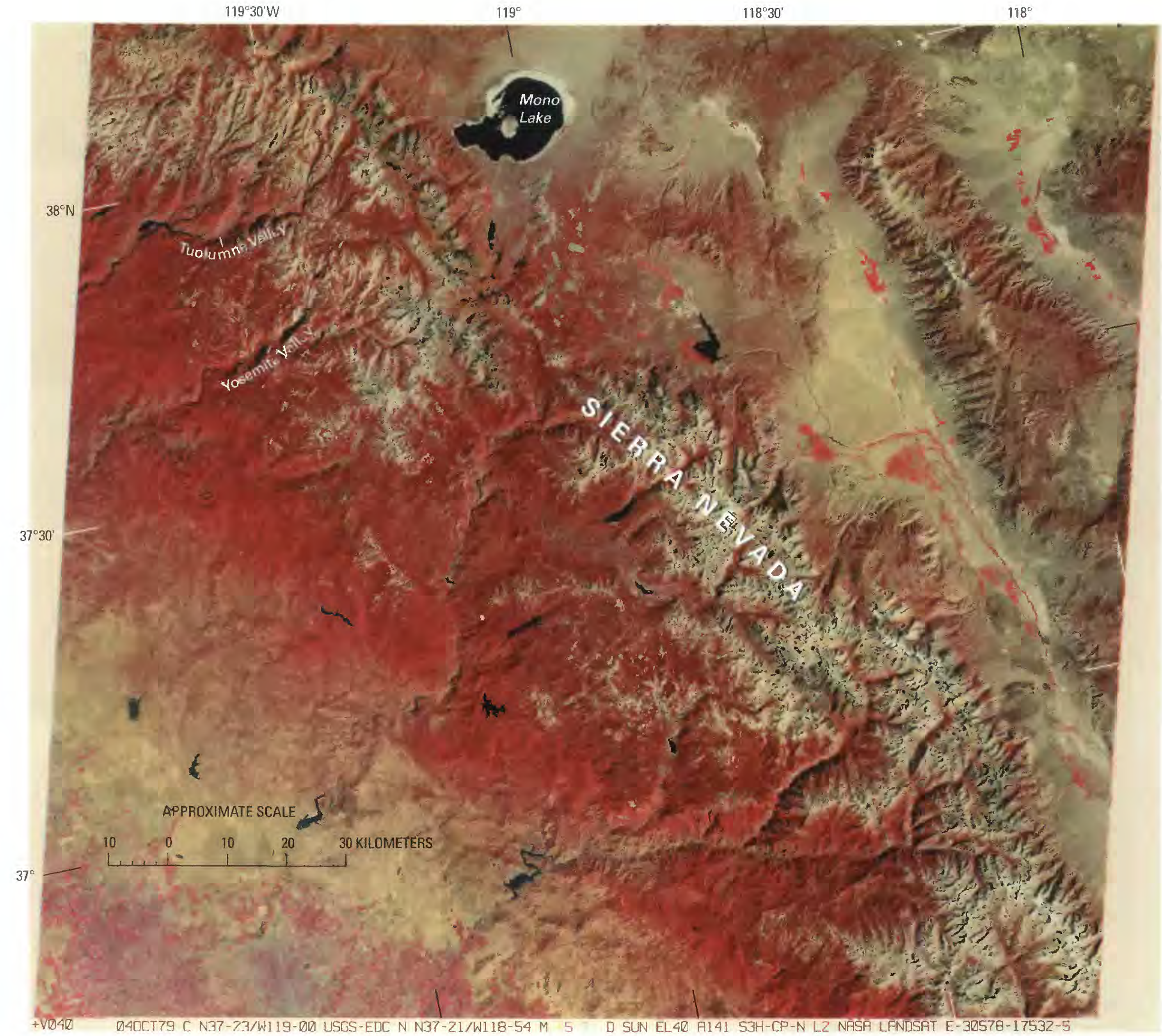

Figure 13.—*Landsat 3 MSS false-color composite image (30578–17532, bands 4, 5, and 7; 4 October 1979; Path 45, Row 34) of the Sierra Nevada of California. These mountains, extending from the northwest corner to the southeast corner of this image, have a total ice area of 63 km^2, as determined by a glacier inventory (Raub and others, 1980). This includes 497 glaciers and 788 ice patches too small to be counted as glaciers. None of these 1,285 ice bodies, the largest of which is Palisade Glacier (1.6 km^2), is significant at Landsat MSS resolution. The only significant glaciers in California not seen in this image cover 6.9 km^2 on Mount Shasta (Driedger and Kennard, 1986). Well-defined moraines extend eastward toward Mono Lake (north-central part of image) and westward in the glacier-carved Tuolumne and Yosemite Valleys (northwest corner of the image).*

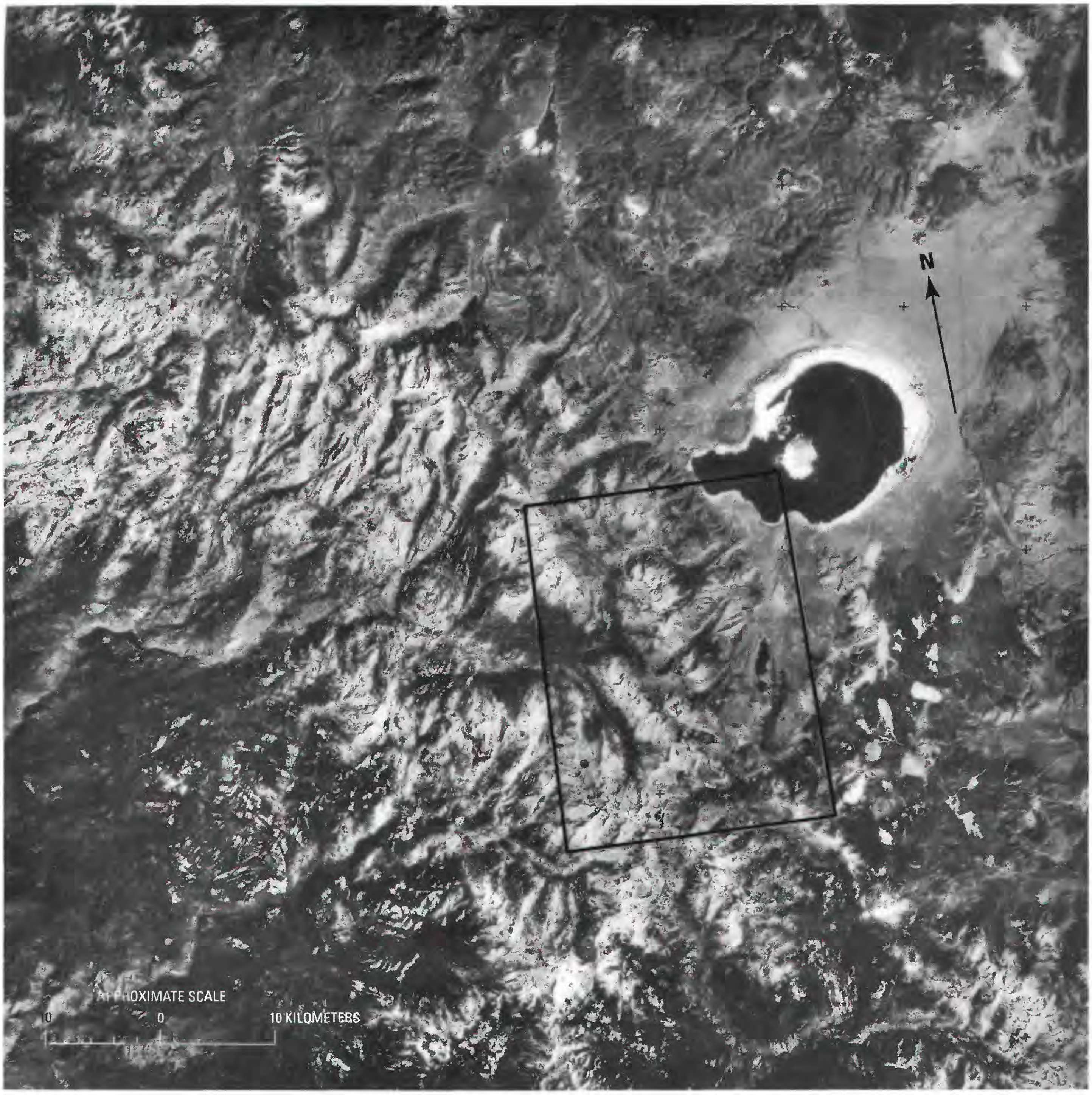

The glacier inventory and the high-quality Landsat MSS and Landsat 3 RBV images available for the Sierra Nevada provide the material needed for a direct comparison between an inventory that has been meticulously compiled from maps, conventional vertical and oblique aerial photographs, and direct observation and the synoptic view of glaciers offered by Landsat. Figure 16, an excerpt from a map in the Raub inventory (Raub and others, 1980; written commun.), correctly delineates each glacier. The Landsat 3 RBV image (fig. 15), having a 30-m pixel resolution, allows some glacier delineation, but areas in shade and areas of ice and moraine-covered ice are difficult to delineate. Landsat offers an excellent overall picture but must be supplemented with knowledge obtained by more conventional methods.

Figure 14.*—Landsat 3 RBV image (30578–17532–A; 4 October 1979; Path 45, Row 34) of the high central Sierra Nevada, centered at lat 37°57' N. and long 119°18' W., including Mono Lake (east-central part of image) and most of Yosemite National Park. The glaciers in this image are too small for any quantitative measurements. However, the extent of past glaciation can easily be mapped. The black rectangle, including the southwest part of Mono Lake, indicates the map area shown in figure 1.*

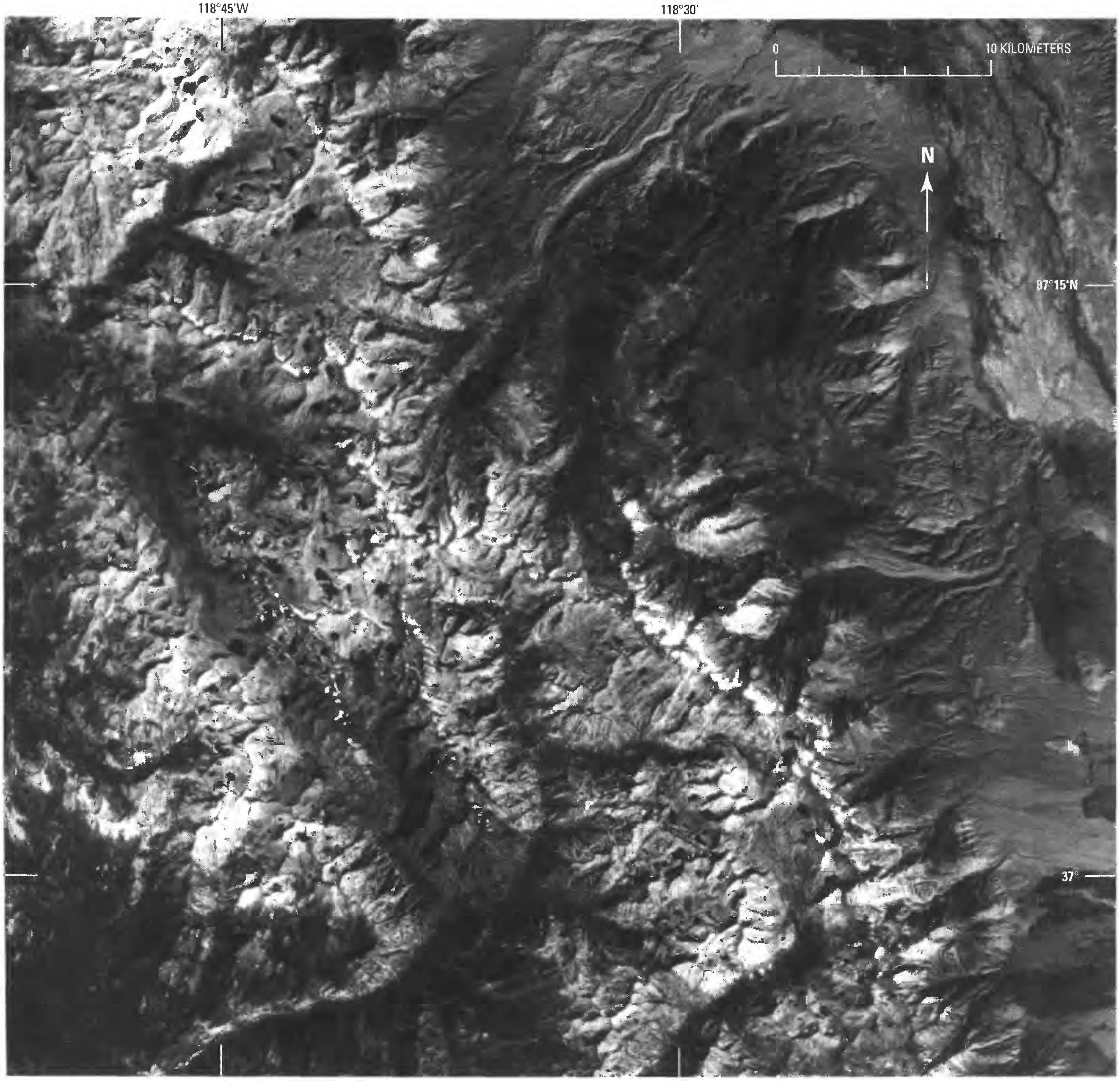

__Figure 15.__—Enlargement of part of Landsat 3 RBV image 30578–17532–D taken on 4 October 1979 (Path 45, Row 34) of the high central Sierra Nevada. This Landsat image is identical in location to figure 16 and demonstrates the difficulties of compiling a detailed glacier inventory from Landsat images. Whereas snow is easily seen on this panchromatic image, it is difficult to distinguish from light-colored rock. Where glacier ice is covered with debris, it is virtually impossible to distinguish. Areas in shade are also hard to delineate. On the other hand, the overall view offered by Landsat gives a good indication of the extent of present and past glaciation in a region.

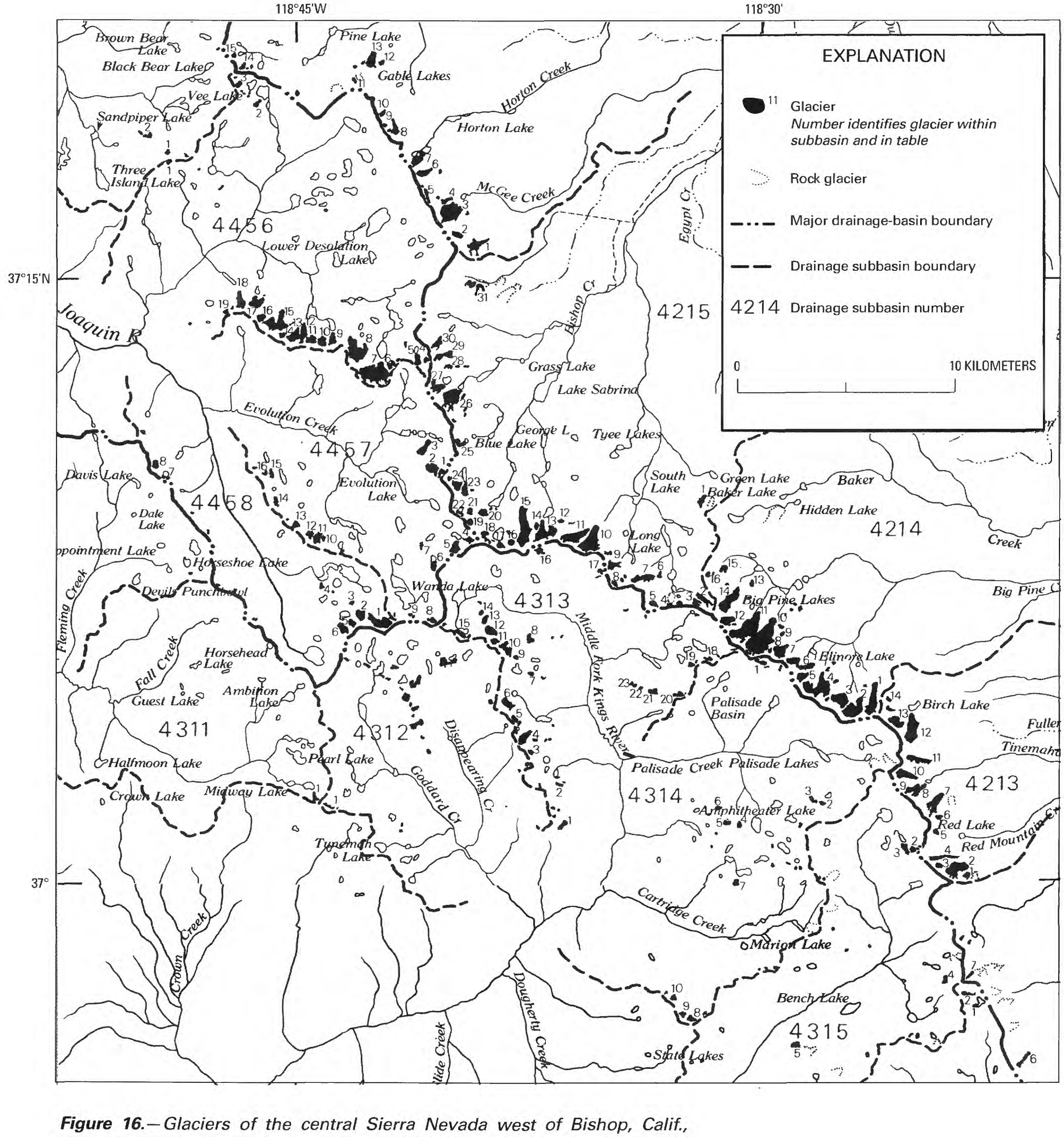

Figure 16.—*Glaciers of the central Sierra Nevada west of Bishop, Calif., delineated from vertical and oblique aerial photographs and direct field observation. This map excerpt is from the Sierra Nevada glacier inventory (Raub and others, 1980). Glaciers much too small to be identified on a Landsat image are shown. Compare this figure to figure 15, a Landsat 3 RBV image of the same area.*

Glaciers of the States of Montana, Wyoming, Colorado, Idaho, Utah, and Nevada

Glaciers in the inland states of the Western United States are significant at the resolution of the Landsat image only in Glacier National Park (fig. 17) and the Beartooth Mountains, Mont., and in the Wind River Range, Wyo. (figs. 18 and 19). Small glaciers, generally less than 1 km^2, are scattered throughout many of the high mountains of the Western States. These glaciers are discussed by Meier (1961a) and Field (1975) and are best identified on USGS topographic maps and (or) aerial photographs. Figures 20, 21, and 22 are selected images from these other mountain areas and show the geomorphic evidence of major past glaciation.

A long history of research is documented on glaciers in Glacier National Park, Mont. (Johnson, 1980), in the Wind River Range, Wyo. (Wentworth and Delo, 1931), and in Colorado (Waldrop, 1964). Glacier-ice cores from

__Figure 17.__—Landsat 3 MSS false-color composite image (30523–17452, bands 4, 5, and 7; 10 August 1979; Path 44, Row 26) of Glacier National Park, Mont. According to Graf (1977), the park contains 28.4 km^2 of glacier ice, about two-thirds of Montana's glacier cover. Moraines extend beyond lake-filled valleys into the plains to the east and into forested valleys to the west.

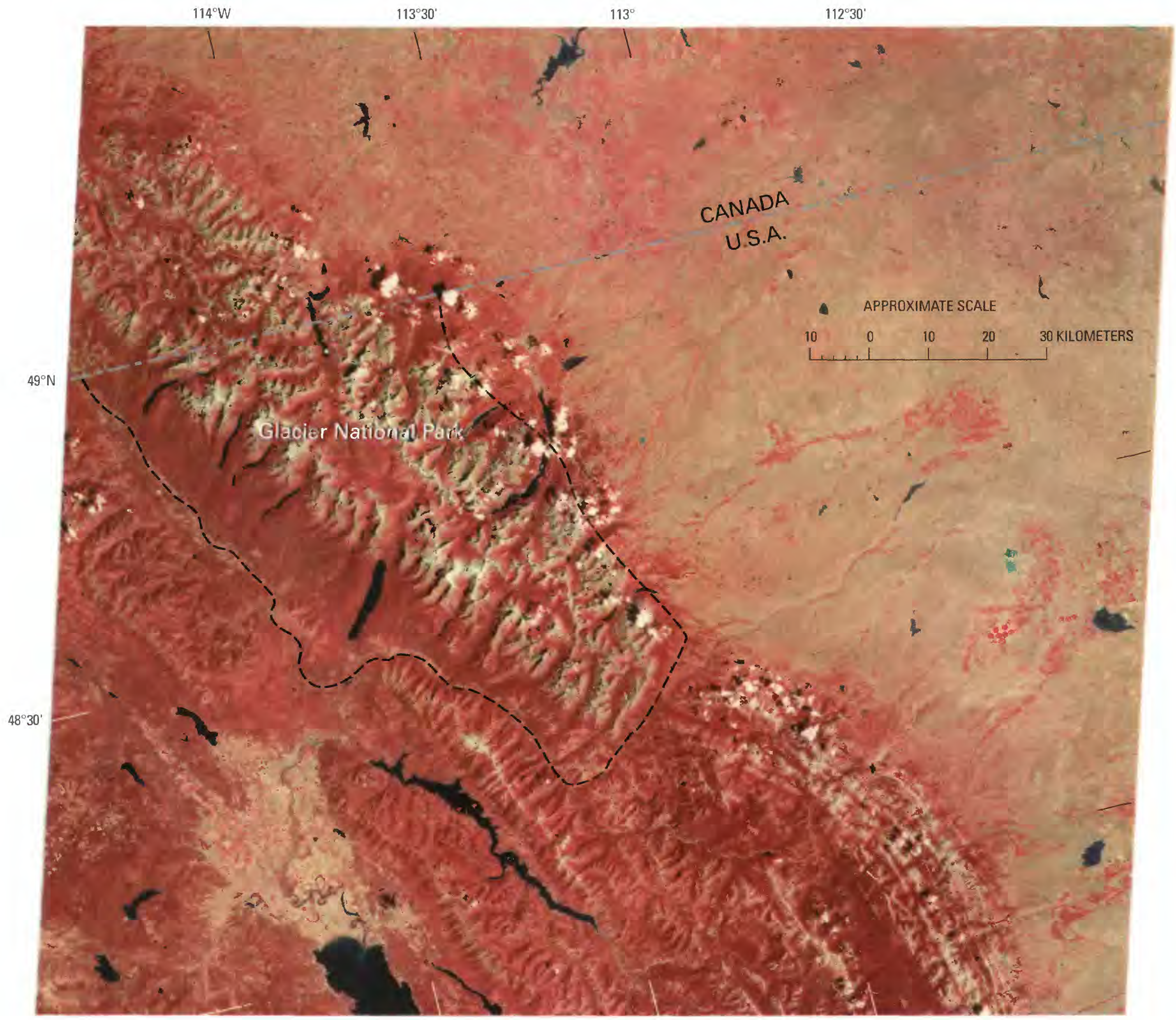

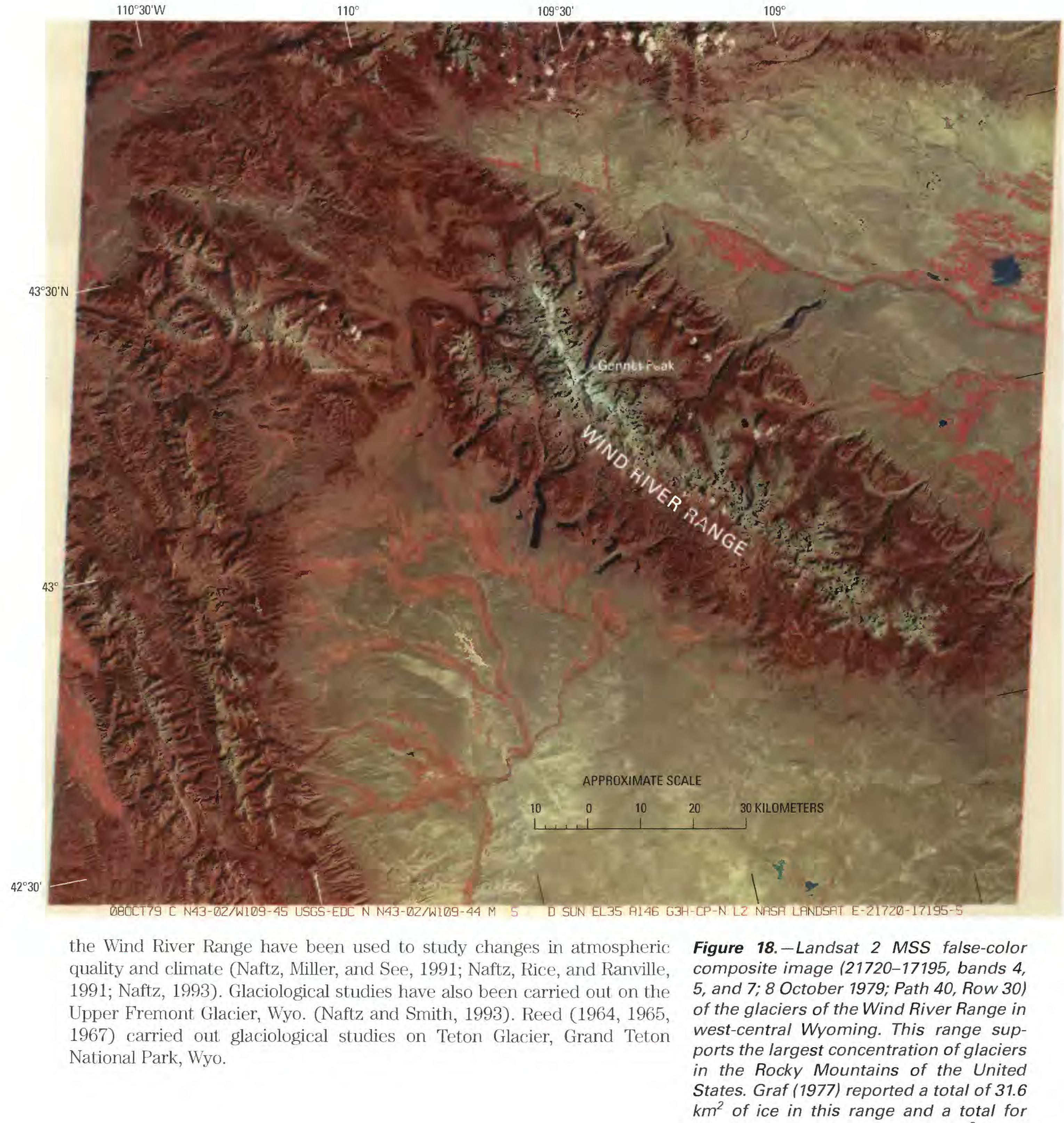

the Wind River Range have been used to study changes in atmospheric quality and climate (Naftz, Miller, and See, 1991; Naftz, Rice, and Ranville, 1991; Naftz, 1993). Glaciological studies have also been carried out on the Upper Fremont Glacier, Wyo. (Naftz and Smith, 1993). Reed (1964, 1965, 1967) carried out glaciological studies on Teton Glacier, Grand Teton National Park, Wyo.

***Figure 18.**—Landsat 2 MSS false-color composite image (21720–17195, bands 4, 5, and 7; 8 October 1979; Path 40, Row 30) of the glaciers of the Wind River Range in west-central Wyoming. This range supports the largest concentration of glaciers in the Rocky Mountains of the United States. Graf (1977) reported a total of 31.6 km^2 of ice in this range and a total for Wyoming glacier cover of 35 km^2. High peaks (up to 4,210 m) show negligible new snow. Moraines extend 50 km toward the northeast and 35 km toward the southwest from the crest of the range. Overdeepened valleys are now occupied by lakes.*

Figure 19.—Oblique aerial photograph taken on 6 August 1979 from above the Continental Divide in the Wind River Range, Wyo.; the view is toward the southeast. The Minor and Mammoth Glaciers are in the foreground. The glaciers flowing away from the viewer on the east side of the divide are, from left to right, Gannett, Dinwoody, Helen, and Fremont Glaciers.

Figure 20.—*Enlargement of part of a Landsat 3 RBV image (30929–16504–C; Path 36, Row 32) that includes most of the glaciers in the State of Colorado. It was taken on 19 September 1980 and is centered at about lat 40°12′ N. and 105°30′ W. The area shown extends from the city of Boulder on the east to Lake Granby on the west, to Rocky Mountain National Park on the north, and to near Berthod Pass on the south. The glaciers are only discernible as small snow patches in cirques in the Rocky Mountains along the east side of the Continental Divide. Moraines extend both east and west from the divide.*

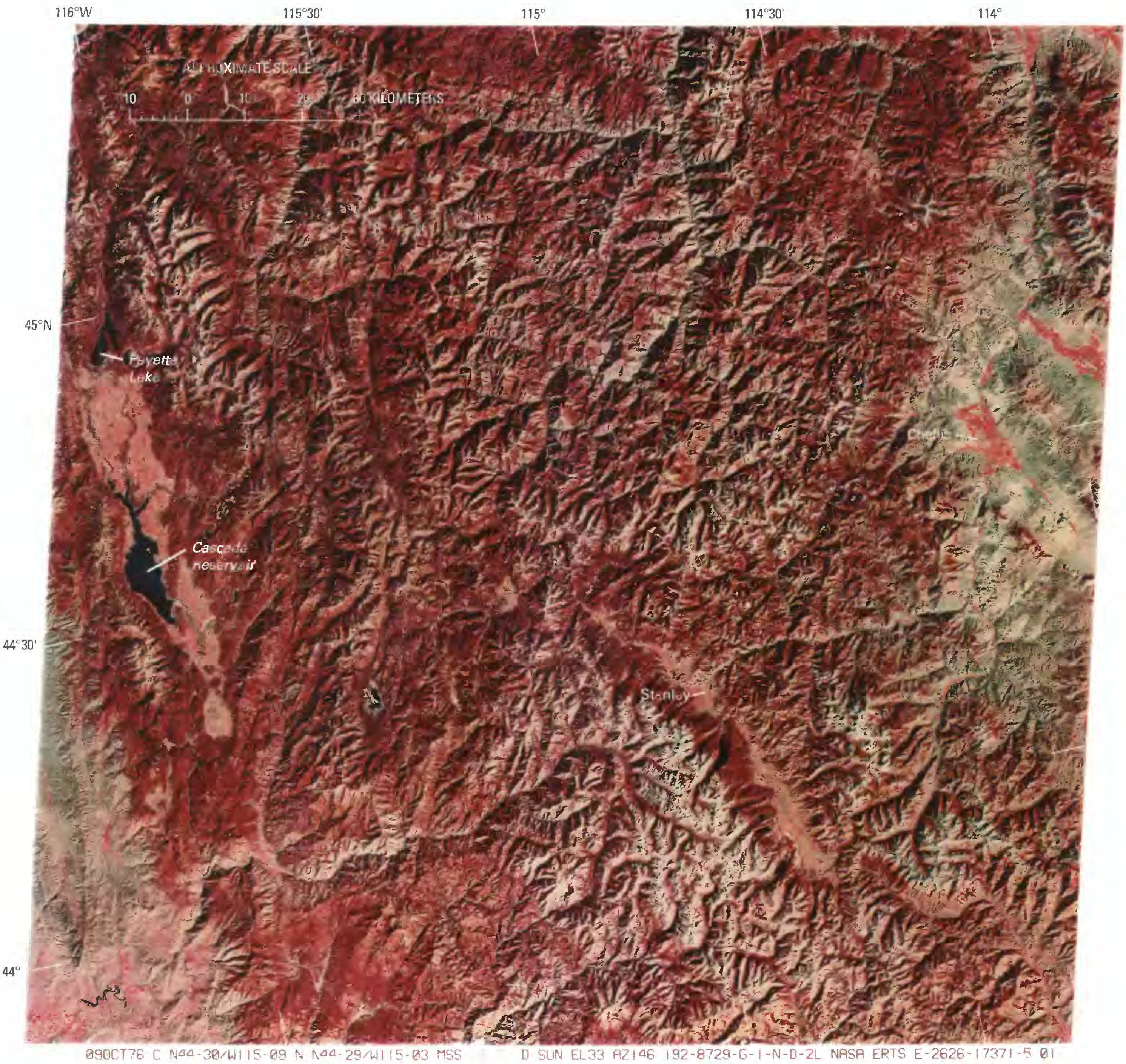

Figure 21.*—The Sawtooth Range of south-central Idaho covers an extensive area and has numerous peaks 3,500–3,800 m in elevation. Glacier cover in Idaho, all of it in the Sawtooth Range, is estimated to be 1 km^2, but it only exists as small ice patches in protected areas where the snowpack is locally increased by wind redeposition. This Landsat 2 MSS false-color composite image (2626–17371, bands 4, 5, and 7; 9 October 1976; Path 44, Row 29), its center about 140 km northeast of Boise, Idaho, shows new snow at higher elevations. Extensive moraines are seen in valleys in the southeast quadrant of the image.*

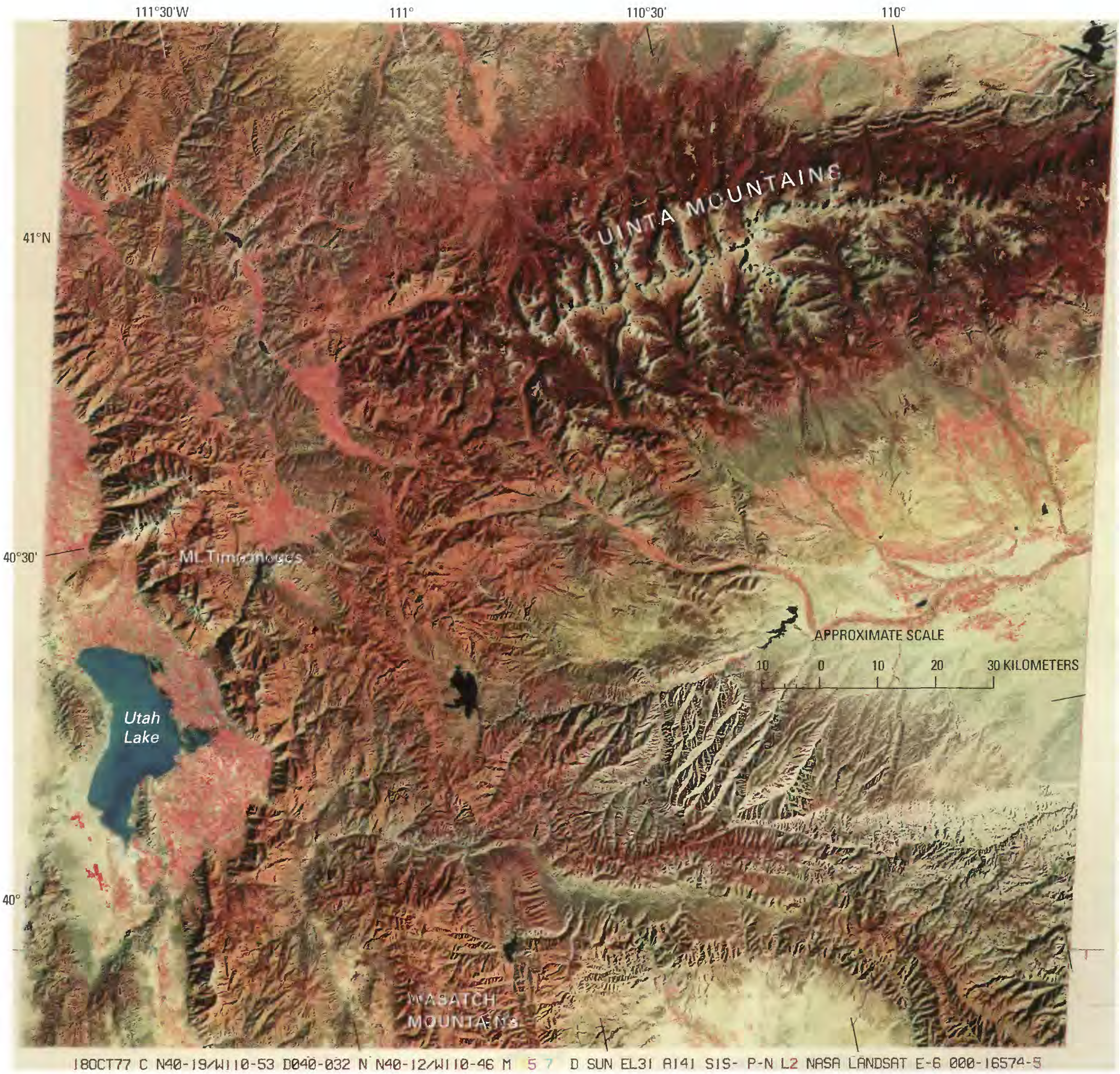

Figure 22.*—Excellent snowfree Landsat 2 MSS false-color composite image (6000–16574, bands 4, 5, and 7; 18 October 1977; Path 40, Row 32) covering an area in north-central Utah. The only glacier reported in Utah occupies a deep cirque on the east side of Mount Timpanogos (3,582 m) in the Wasatch Range (extreme west-central part of image) about 22 km north of Utah Lake. No glaciers are indicated on 1:24,000-scale USGS quadrangle maps in the Uinta Mountains (northeast quadrant of image), which are more extensive and higher (up to 4,100 m in elevation). Glacial moraines are clearly seen extending 40 km to the north and south of the crest of the Uinta Mountains.*

Glacier Retreat in Glacier National Park, Montana

By Carl H. Key,[6] Daniel B. Fagre[6], *and* Richard K. Menicke[7]

Glacier National Park encompasses a relatively large, mountainous region (4,080 km^2) of northwestern Montana that borders southern Alberta and British Columbia, Canada. It was established in 1910 because of its glaciers and unique, glacially carved topography located along the crest of the Rocky Mountains. In the 1990's, 37 named glaciers existed in Glacier National Park. All named glaciers within the park are mountain glaciers that have retreated dramatically since the middle 19th-century end of the Little Ice Age in the Western United States. All but one glacier are contained in the northern two-thirds of Glacier National Park between lat 48°30' and 49°00' N. and long 113°30' and 114°15' W. All head on the Continental Divide or near the divide on lateral connecting ridges. Mountain peaks in this glacierized region range from 2,560 m to 3,190 m in elevation at Mount Cleveland, the glacier-terminus elevations lying generally between 2,000 and 2,400 m.

Observations of the glaciers of Glacier National Park date from the second half of the 19th century. The earliest delineation of Glacier National Park glaciers is found on a map by Ayres (1898) that was made in conjunction with timber inventories of the former Flathead Forest Reserve. All of the present Glacier National Park was included in the map. The scale of Ayres' map is nominally 1:440,000, and some drainage features are incorrect, but it does provide clues to the areal extent of some of the first recognized glaciers in Glacier National Park. The first systematic mapping of the glaciers in the park is presented on the U.S. Geological Survey (USGS) 1:125,000-scale Chief Mountain and Kintla Lake quadrangle maps, published in 1904 and 1906, respectively. These maps resulted from planetable topographic surveys conducted between 1900 and 1904. It is important to note the number and relative sizes of named glaciers in these maps. Comparison with recent data shows that conspicuous changes have taken place during the 20th century. Unfortunately, the scale and horizontal control are such that quantitative measurements can only be crudely approximated to compare with contemporary map, photographic, and image sources.

In 1914, Alden published a description of Glacier National Park glaciers, which includes many oblique photographs of glaciers made from 1887 to 1913. Although not entirely complete, Alden's work remains the only monograph to describe characteristics of the park's glaciers at the start of the 20th century. In 1952, Dyson published an updated list of glaciers. However, it does not contain much descriptive material.

The most comprehensive and accurate depiction of Glacier National Park glaciers is obtained from USGS 1:24,000-scale quadrangle maps published in 1968 and compiled by the use of stereophotogrammetric techniques from aerial photographs made between 1963 and 1966. These maps provide an important benchmark for a parkwide assessment of glacier status. In addition, aerial photographs taken in 1950, 1960, 1968, and 1993 cover most of Glacier National Park's glaciers in late summer and provide additional data, both before and after the 1968 maps.

The USGS 1968 maps depict 83 ice-and-snow bodies having areas that exceed 0.1 km^2 within the boundary of Glacier National Park. Post and others (1971) use an area of 0.1 km^2 as a practical minimum size in order to indicate the presence of perennial ice-and-snow bodies in regional mapping and glacier-inventory surveys. Of these 83 ice-and-snow bodies, 34 are named glaciers. The three additional named glaciers within the park have areas less than 0.1 km^2 (table 3).

---

[6] U.S. Geological Survey, Glacier National Park, West Glacier, MT 59936.
[7] U.S. National Park Service, Glacier National Park, West Glacier, MT 59936.

TABLE 3.—*Named glaciers of Glacier National Park and vicinity, Montana*

[Glacier area at the end of the Little Ice Age is shown under "1850 area." "Most recent area" refers to the primary body of a glacier in the year displayed below "Source year." "Number of snow patches/glacierets" indicates the number of separate masses of perennial ice and snow in the cirque(s) associated with each glacier, based on 1:24,000-scale USGS quadrangle maps compiled from 1966 aerial photography. In most cases, the snow patches/glacierets are separate remnants of a glacier's former extent. Abbreviation: N., North. Leaders (–), not recorded; parentheses, estimated]

Number (fig. 23)	Named glacier	1850 area (square kilometers)	Most recent area (square kilometers)	Source year	Number of snow patches/ glacierets
3	Agassiz	4.06	1.02	1993	10
21	Ahern	–	.59	1966	10
4	Baby	–	.12	1966	1
33	Blackfoot	[1]7.59	1.74	1979	3
5	Boulder	–	.23	1966	1
14	Carter Glaciers	–	.47	1966	6
18	Chaney	–	.54	1966	10
13	Dixon	–	.29	1966	3
26	Gem	–	.02	1966	1
25	Grinnell	[2]2.33	.88	1993	6
1	Harris	–	.15	1966	1
31	Harrison	3.09	1.06	1993	18
10	Herbst	–	.14	1966	4
11	Hudson	–	.09	1966	4
19	Ipasha	–	.32	1966	8
32	Jackson	[1](3.44)	(1.02)	1979	23
2	Kintla	–	.66	1966	13
35	Logan	.92	[3].43	1993	1
37	Lupfer	–	.14	1966	1
15	Miche Wabun	–	.20	1966	3
22	N. Swiftcurrent	–	.07	1966	6
20	Old Sun	–	.42	1966	10
28	Piegan	–	.28	1966	1
34	Pumpelly	1.84	.72	1979	9
7	Rainbow	–	1.21	1966	6
36	Red Eagle	.49	[3].15	1993	2
29	Sexton	–	.40	1966	4
17	Shepard	–	.20	1966	5
27	Siyeh	–	.22	1966	3
30	Sperry	3.76	.87	1993	7
23	Swiftcurrent	.70	.14	1993	4
24	The Salamander	–	[2].23	1993	1
12	Thunderbird	–	.19	1966	6
8	Two Ocean	–	.43	1966	4
9	Vulture	.77	.21	1993	14
6	Weasel Collar	–	.56	1966	4
16	Whitecrow	–	.24	1966	10
39	[4]Gr ant	–	.34	1995	1
38	[4]Stanton	–	.37	1995	1
	Total	[5]25.55	[6]16.34		

[1] The area for Blackfoot Glacier encompasses Jackson Glacier. The area reported for Jackson Glacier is the estimated part of Blackfoot Glacier that yielded Jackson Glacier after the two became separate glaciers.

[2] The area for Grinnell Glacier encompasses what would later be called The Salamander, an ice apron.

[3] Considered to be stagnant or no longer active in 1979 by Carrara and McGimsey.

[4] Grant and Stanton Glaciers are located outside Glacier National Park.

[5] Total area includes 11 of 37 named glaciers in Glacier National Park.

[6] Total area from 1966, 1979, and 1993. Source material includes 37 named glaciers in Glacier National Park and 2 outside the park.

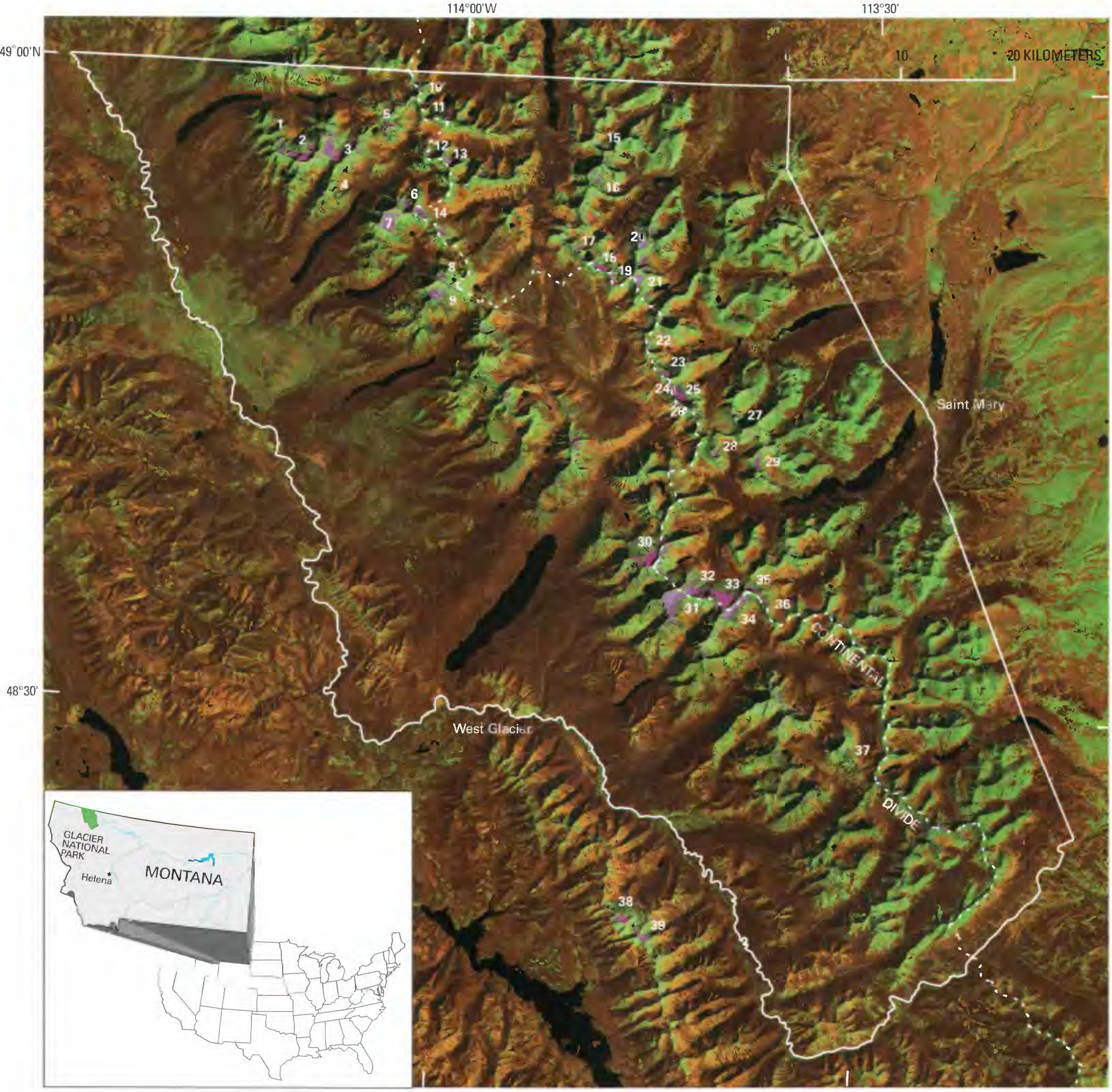

Figure 23.—*Computer-generated, unsupervised spectral classification of a Landsat TM scene (LT50410260095244, bands 3, 4, 5, Path 41, Row 26) of Glacier National Park and vicinity, Montana, collected on 1 September 1995. The image, which shows the boundary of Glacier National Park, has been rectified geometrically to (UTM) zone 12. Sixty multispectral clusters are represented in false color in order to approximate mean cluster reflectance in bands 4, 5, and 3 for red, green, and blue (RGB), respectively. Dark red to brown represents coniferous forest; light to dark orange includes herbaceous and shrub habitats; and yellow green to gray indicates dormant grass, rock, and nonvegetated terrain types. Areas of perennial ice and snow stand out in bright pink to dark purple and cover about 36 km^2 within Glacier National Park, including amounts estimated within dark shadow zones. The TM pixel resolution at 28.5 m (1 hectare=12.31 pixels) is about 6.6 times greater than that of Landsat multispectral scanner (MSS) data (1 hectare=1.86 pixels). Therefore, the TM pixel resolution is sufficient to resolve many of the smaller ice- and-snow patches that were present in 1995 from those that were mapped on USGS 1:24,000-scale quadrangle maps in 1968. Perennial ice and snow constitute a relatively small part of the entire region, and glaciers occupy even less area. Numbers 1–37 identify named glaciers (see table 3), some of which are now stagnant: 1, Harris; 2, Kintla; 3, Agassiz; 4, Baby; 5, Boulder; 6, Weasel Collar; 7, Rainbow; 8, Two Ocean; 9, Vulture; 10, Herbst; 11, Hudson; 12, Thunderbird; 13, Dixon; 14, Carter; 15, Miche Wabun; 16, Whitecrow; 17, Shepard; 18, Chaney; 19, Ipasha; 20, Old Sun; 21, Ahern; 22, North Swiftcurrent; 23, Swiftcurrent; 24, The Salamander; 25, Grinnell; 26, Gem; 27, Siyeh; 28, Piegan; 29, Sexton; 30, Sperry; 31, Harrison; 32, Jackson; 33, Blackfoot; 34, Pumpelly; 35, Logan; 36, Red Eagle; 37, Lupfer. Numbers 38 (Stanton Glacier) and 39 (Grant Glacier) are located outside Glacier National Park.*

A number of individual glaciers have been studied since the early 1930's. The most important work, which also provides reviews of previous investigations, includes that by Johnson (1980), Carrara and McGimsey (1981), and Carrara (1989).

An assessment by the authors of all available data shows that the area of existing ice-and- snow bodies in Glacier National Park totals approximately 36 km^2. Although the part that is glacier ice is difficult to determine, it is estimated to be less than 17 km^2 (table 3). This estimated cumulative area is based on a comparison of the size of the ice-and-snow bodies having areas greater than 0.1 km^2, as delineated in the 1968 quadrangle maps, with actual 1979–93 field measurements of 12 of these glaciers.

Analysis of a September 1995 Landsat thematic mapper (TM) image (fig. 23) indicates that almost all the discernible ice and snow is located in the northwestern (including Kintla, Agassiz, and Rainbow Glaciers) and south-central (including Sperry, Jackson, Blackfoot, Harrison, and Pumpelly Glaciers) regions of Glacier National Park. Current estimates of glacier size reveal that individual glaciers continue to shrink. Only five glaciers (Blackfoot, Jackson, Harrison, Agassiz, and Rainbow Glaciers) have areas larger than 1.0 km^2. Sperry and Grinnell Glaciers have areas of about 0.9 km^2. Five glaciers (Kintla, Weasel Collar, Chaney, Ahern, and Pumpelly Glaciers) have areas between 0.5 and 0.8 km^2.

On a regional scale, if one looks beyond Glacier National Park, perennial ice-and-snow accumulations of any size are scarce. In the 100 km examined north of Glacier National Park into Canada, only seven small ice-and-snow accumulations were noted. None approaches the 0.1 km^2 minimum glacier size. In the mountain ranges within 160 km of Glacier National Park to the south and west, Dyson (1952) identified only nine glaciers. Three are in the Cabinet Range, three in the Mission Range, two in the Flathead Range, and one in the Swan Range. Stanton and Grant Glaciers in the Flathead Range are nearest Glacier National Park and are the largest of the nine. In the 1995 Landsat image, Stanton Glacier has an area of approximately 0.37 km^2, whereas Grant Glacier has an area of 0.34 km^2 (fig. 23).

Today, the glaciers within Glacier National Park are an isolated group, the greatest accumulation of alpine glaciers within Montana. Where compared with their historical areal extent, they are an excellent example of the glacier retreat that is taking place throughout the Rocky Mountains. A variety of dynamics contribute to the health of the park's glaciers, including conditions that favor shelter from solar radiation, elevational temperature lapse rates, and catchment of winter precipitation. Glacier persistence in some cases may be due more to their orientation to storm tracks and wind-assisted depositional patterns (for example, drifting of snow across the Divide) than to thermal buffering. However, all these factors are integrated, and the topographic orientation and physiographic setting distinctly modify the primary drivers of climate.

Most Glacier National Park glaciers, especially the larger ones, are cirque glaciers having aspects that vary from northwest, through north and east, to southeast. The cirque morphologies range from deeply concave floors and high, nearly vertical headwalls to shallow, concave, nearly straight or undulating floors pitched on relatively steep slopes that have minimal headwalls. In addition, glaciers are found in niches in sloping gullies (Lupfer Glacier), near ridge-top saddles (Boulder Glacier), or in slight depressions (Gem Glacier, a dome-shaped mass near the apex of the Continental Divide). Other small glaciers (glacierets) and snow patches are situated in similar situations. After about 150 years of retreat, many glaciers have been reduced to ice aprons or stagnant ice masses plastered along steep slopes. The Salamander and parts of Kintla, Agassiz, and Harrison Glaciers have been separated from shrinking primary glacier-ice masses in recent decades.

Major cirque glaciers typically are hanging, are perched above cliffs, and in some cases, constitute a cascading series of glaciers or a "glacier staircase," like the former North Swiftcurrent Glaciers (fig. 24). Little Ice Age cirque glaciers that advanced over cliff margins pushed morainal material and ice off steep rock faces. This probably produced unconsolidated, reconstituted ice-and-sediment masses at the base of these slopes. Consequently, terminal moraines are absent below many cirques. This complicates the accurate mapping of the extent of many middle 19th-century glacier termini. Generally, well-defined lateral moraines do exist, and in the absence of additional evidence, the limit of Little Ice Age glaciers can be sufficiently well delineated, at least out to the cliff margins.

At several glaciers, terminal moraines exist where cliffs are absent or are sufficiently distant that they were not reached during Little Ice Age glacier expansion. Good examples exist at the Sperry and Red Eagle Glaciers, as well as in the deglacierized valleys below Heavens Peak and Mt. Clements (Demorest, 1938). In addition, at least two glaciers, Agassiz and Jackson Glaciers, extended far enough below bedrock slopes so that they created forest trimlines (krummholz), which provide explicit boundaries for the maximum extent of middle 19th- century advances.

Johnson (1980) describes the long series of observations on Grinnell and Sperry Glaciers, and he exhibits topographic maps that were compiled at a scale of 1:6,000 from 1960 aerial photographs. He also delineates profiles and terminus positions from 1887 through 1969. These maps complement another set of USGS topographic maps compiled at a scale of 1:4,800 from aerial photographs taken in 1950 for Sperry and Grinnell Glaciers. Carrara and McGimsey (1981) discuss the recession of Agassiz and Jackson Glaciers through 1979, the period of greatest retreat, and establish the age of most of the recent moraines as contemporary with the Little Ice Age that ended in the middle 1800's. This age (middle 1800's) had been hypothesized as early as 1939 (Matthes, 1939, 1940), similar to the age of moraines elsewhere in North America, Iceland, and Europe, but was not definitively dated in Glacier National Park until the work of Carrara and McGimsey in the late 1970's.

The moraines in Glacier National Park are significant because of their relatively young age and large size. They represent a long-standing glacial

Figure 24.—*Oblique photograph (taken about 1912) showing hanging cirque glaciers and the "glacier staircase" of North Swiftcurrent Glaciers (Alden, 1914). No terminal moraine exists on the upper part of the cliff, whereas a recognizable moraine is associated with the lower glacier.*

maximum (indeterminate age, but perhaps 40 to 150 years ago?) that overrode previous advances, which may have taken place during the preceding 9,000–10,000 years (Carrara, 1989). Because of the apparently long and relatively stable climatic interval preceding the Little Ice Age, it is believed that most of the glacier ice remaining in Glacier National Park was formed during the Little Ice Age and is not a relic from the Pleistocene Epoch (Matthes, 1939, 1940). In addition to his work on the moraines, Carrara (1989) presents details on the record of glacier fluctuations since the end of the Wisconsinan glacial stage. In 1988, Carrara and McGimsey published a map detailing neoglacial recession through 1979 in the Mount Jackson area, which includes Sperry, Jackson, Blackfoot, Harrison, Pumpelly, Logan, and Red Eagle Glaciers.

The Little Ice Age comprised a several-hundred-year-long cool period (about 1400 to about 1850 in North America), during which Glacier National Park glaciers formed and expanded. This continued until a warming climate initiated glacier retreat after the middle 1800's. Figure 25 illustrates the magnitude of that recession as of 1995 for the 11 glaciers where Little Ice Age moraines have been mapped. Because figure 25 displays both perennial ice and snow, the actual area covered by these glaciers in 1995 is only a subset of that shown. Glacier area would not include, for example, the small, separate snow patches nor the irregular, thin projections of ice along glacier margins. The overall reduction in area since the middle 19th century ranges between 77 percent and 46 percent on the six glaciers mapped from 1993 aerial photographs. At least two glaciers, Logan and Red Eagle Glaciers, have become stagnant ice masses. Parkwide, it is not known precisely how many named glaciers are now stagnant. The number probably includes many that had areas of less than 0.7 km^2 at the end of the Little Ice Age. Perennial ice-and (or)-snow patches likely remain at many of these locations.

Since the end of the Little Ice Age, small glaciers that were insulated or protected by the surrounding topography tended to lose proportionately less area to recession. Commonly, they changed rapidly to a stagnant condition. The larger glaciers generally experienced proportionately greater and more rapid reduction in area than the smaller glaciers, but they still continue to be active (fig. 25*A*). During the last 150 years, the larger glaciers, which had descended below cirque margins into subalpine terrain, would have had the greatest exposure to solar radiation and warmer temperatures for longer periods of time. As these large glaciers retreated and shrank in area, they regularly separated into discrete ice masses.

Earlier in the 20th century, Grinnell Glacier split into two ice masses (fig. 25*B*). The upper one, now called The Salamander, exists as an ice apron and has changed little since it separated sometime prior to 1929 (Dyson, 1941). In 1911, Blackfoot Glacier (fig. 25*C*) encompassed the current Jackson Glacier (Alden, 1914) but was distinctly separate from it by 1939 (Dyson, 1941). Sperry, Pumpelly, and Agassiz Glaciers each separated into smaller parts located in depressions within their cirques, so that each consisted of one primary mass and several smaller ice masses no longer connected to the main body of the glacier. The individual ice masses, like nearby remnant glaciers, generally became increasingly shielded by their surroundings and did not change much over time, so that they persisted as perennial ice-and- snow patches. These favored locations were protected from solar radiation and likely accumulated considerable wind-blown snow over a greater proportion of their surface area. These patterns are typical of most Glacier National Park glaciers and probably represent the condition of other nearby cirque glaciers undergoing prolonged recession throughout the Rocky Mountains of the U.S.

The glacial recession, though pervasive and continuous since the middle 1800's, progressed at variable rates over time and to varying degrees on different glaciers. Through the first decade of the 20th century, early

***Figure 25.**—(opposite page) Four enlargements of figure 23 (labeled* A, B, C, *and* D*) provide a comparison of the area covered by glacier ice in 1995 with that of the middle 19th century. Perennial ice and snow remaining on 1 September 1995 are shown in pink to purple colors. Yellow lines represent glacier-maximum margins during the Little Ice Age, as mapped from distinctive lateral and terminal moraines on 1993 aerial photographs and adapted from the work of Carrara and McGimsey (1988) and Johnson (1980).* **A**, *Glaciers in the vicinity of Agassiz Glacier. The unmapped Harris Glacier has essentially vanished and is today represented by just one glacieret. Only two separated parts of the unmapped Kintla Glacier remain active and have discernible crevasses; the eastern part (largest) is the primary fragment. During the middle 19th century, Boulder Glacier extended across Boulder Pass, where a prominent terminal moraine is visible. The small Baby Glacier, bounded by a conspicuous moraine, has lost proportionately less than has Agassiz Glacier.* **B**, *Grinnell and Swiftcurrent Glaciers. The bluish patch abutting Grinnell Glacier to the north is Upper Grinnell Lake, a proglacial lake that has formed since the 1930's.* **C**, *The complex of glaciers in the Mt. Jackson area.* **D**, *Vulture Glacier and environs. Rainbow Glacier is one of Glacier National Park's largest glaciers but has been little studied and has not yet been mapped. Weasel Collar remains active, as evidenced by crevassing, and sits in a dramatic, deep, fan-shaped cirque that narrows to the north over an extreme precipice. Today, Carter Glaciers are reduced to a series of stagnant ice aprons and patches. Vulture Glacier is one of Glacier National Park's highest and has an east-to-southeast aspect and a present terminus at about 2,440 m.*

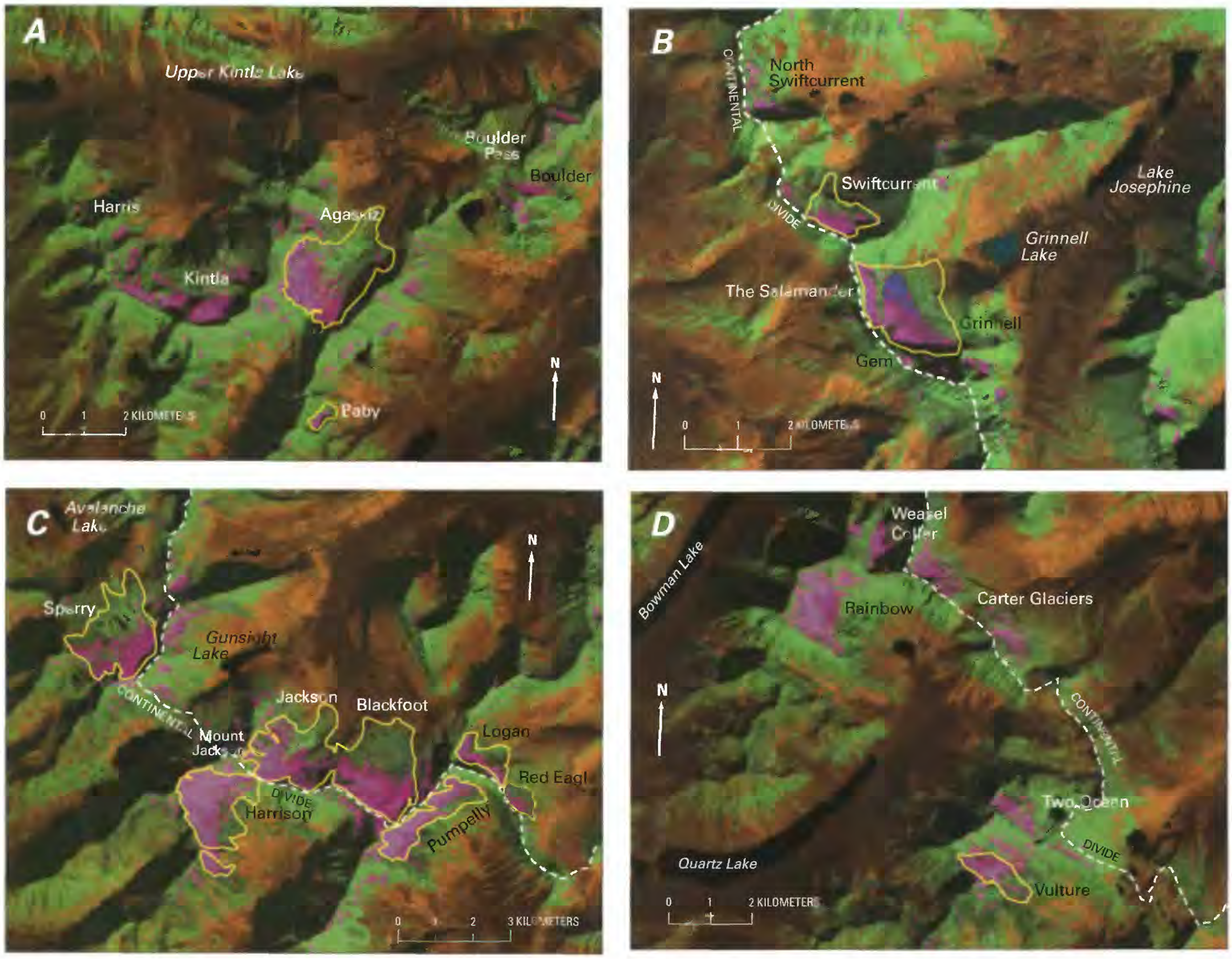

photographs and descriptions indicate that glaciers thinned but retreated little from the end moraines of the Little Ice Age (fig. 26) and that termini were still at -or- very near the inner margins of lateral and terminal moraines (Alden, 1914; Sperry, 1938; Dyson, 1941). In all cases, it must be noted that, although initially the distance of retreat was small, substantial thinning—and therefore appreciable volume loss—likely took place. This preceded the eventual retreat of termini. From 1910 onward, recession rates increased (Dyson, 1948; Johnson, 1980). This corresponded to a period of increased scientific interest in Glacier National Park glaciers, and many of the early investigators bore witness to dramatic instances of glacier recession. Following the middle 1940's, recession rates decreased, and glaciers became increasingly confined within cirque margins.

On Agassiz and Jackson Glaciers, retreat from 1850's trimlines below 1,800 m averaged less than 7 m a^{-1} until about 1911 (Carrara and McGimsey, 1981). Retreat rates increased steadily to 14–42 m a^{-1} by 1926 and to 112–117 m a^{-1} by 1932. At both glaciers, retreat exposed convex bedrock slopes. These slopes likely supported thinner ice and contributed to the rapid retreat during that interval.

By 1939, Jackson Glacier had separated from Blackfoot Glacier (fig. 25*C*) and rested within the confines of its present-day cirque. Its average rate of retreat decreased between 1932 and 1944 to about 10 m a^{-1}. Agassiz Glacier (fig. 25*A*), on the other hand, continued retreating up its valley slope at a rate of 90 m a^{-1} until 1942. From the middle 1940's until 1979, both

glaciers continued to retreat but at very low rates, less than 3 m a^{-1}. By 1979, Agassiz and Jackson Glaciers had been reduced to about 30 percent of their middle 19th- century area.

Sperry Glacier's retreat (fig. 25*C*) has a history similar to that of Agassiz and Jackson Glaciers, although variations in recession are not as dramatic. Figure 27 shows the changes in its size from 1850 to 1993. Until 1913, it retreated from its Little Ice Age moraine at a rate that varied between 1 and 5 m a^{-1}. From 1913 through 1945, retreat increased substantially to between 15 and 22 m a^{-1}. During this period, Sperry Glacier lost about 68 percent of its area. Since 1945, the rate of retreat has slowed to an average of 11 m a^{-1} between 1945 and 1950 and to about 5 m a^{-1} between 1950 and 1979. At that time, Sperry Glacier occupied only about 26 percent of its maximum area in the middle 19th century.

Grinnell Glacier (fig. 25*B*) displayed less overall variation and greater constancy in retreat than the glaciers already discussed. However, between the 1920's and middle 1940's, it experienced the largest amount of retreat of any Glacier National Park glacier (fig. 28). Through 1887, Grinnell receded an average of 2 m a^{-1}. Recession averaged 11 m a^{-1} from 1887 to 1911 but decreased to 5 m a^{-1} by 1920. During the period 1850 to 1920, the average recession was about 6 m a^{-1}. The rate of recession of Grinnell Glacier increased after 1920, averaging 15 m a^{-1}, for a total loss of 51 percent in glacier area by 1946. Between 1946 and 1979, recession averaged about 4 m a^{-1} and further reduced the glacier to 41 percent of its former area.

Figure 29 depicts the changes of Grinnell Glacier during the 43-year period from 1938 to 1981. Substantial changes are evident not only in the margin but also in the thickness of the glacier. Compared to the size and thickness of the glacier 50 years earlier (about 1887), when Grinnell Glacier included The Salamander ice apron, the magnitude of change is most noteworthy. Recession of Grinnell Glacier has been influenced by its deeply concave cirque, as well as by the formation of Upper Grinnell Lake in the early 1930's from meltwater that ponded in a concave basin exposed by the retreating glacier (fig. 29).

Between 1966 and 1979, small advances of parts of the glacier margins were noted at several glaciers, including Grinnell, Jackson, Blackfoot, and Harrison Glaciers (Carrara, 1989). Other parts of these glaciers did not advance, and overall sizes either remained essentially the same or receded slightly during the period.

Figure 26.*—Overlooking Blackfoot Glacier to the west in August 1914 by E.C. Stebinger, USGS. Mount Jackson is the highest peak in the center, and Reynolds Mountain is to the far right. Glacier ice remains on, or very near, the prominent lateral moraine, paralleling the glacier across the central-right part of the photograph. Rates of recession were comparatively slow from the end of the Little Ice Age through the early 20th century, in contrast to rapid recession in subsequent decades of the 1920's to 1940's. Early visitors had an opportunity to see Glacier National Park glaciers at or near their 19th century maximum extents. Today, most of the glacier ice visible in the right one-half of the photograph has melted away and exposed bedrock. From the same viewpoint, the current terminus would lie almost in a direct line with Mount Jackson (see fig. 25*C*).*

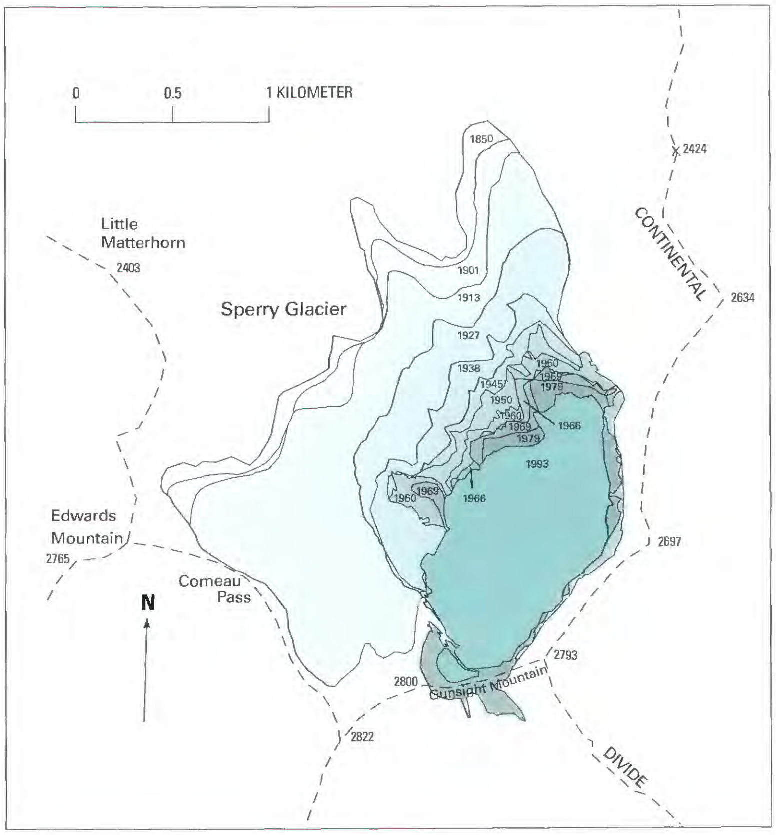

Figure 27.*—Neoglacial recession chronology of Sperry Glacier showing the series of termini mapped since the middle 19th century. This model was developed within a geographic information system (GIS) by incorporating data from previous glacier maps (Johnson, 1980; Carrara and McGimsey, 1988; P.E. Carrara, unpub. data), USGS 1:24,000-scale quadrangle maps (1968) (compiled from USGS 1966 1:40,000-scale aerial photographs), and aerial photographs [1945, 1950, 1960, 1968 (U.S. National Park Service 1:15,840-scale), and 1993]. Two challenges of using such models are, first, establishing a common geographic datum to rectify the various data sets spatially and, second, resolving discrepancies between sources. The latter often causes problems of scale and precision due to historical information's being generated from different, and sometimes rudimentary, types of technology available at the time of measurement.*

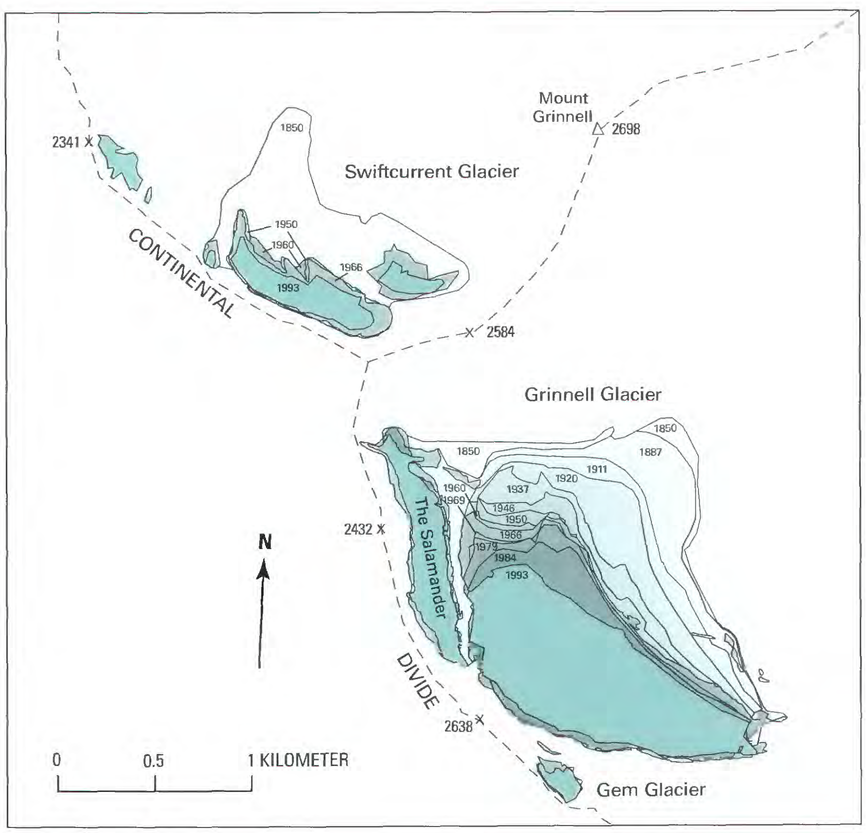

Figure 28.*—Neoglacial recession chronology of Grinnell and Swiftcurrent Glaciers showing the series of termini mapped since the middle 19th century. Grinnell Glacier, along with Sperry Glacier (fig. 27), is relatively accessible and has been frequently observed, so it has yielded a fairly complete record of recession. The first field measurement of the terminus position on Grinnell Glacier was recorded in 1931 (Johnson, 1958). By contrast, Swiftcurrent Glacier, with the exception of the moraine-defined 1850 perimeter, lacks positional delineations prior to 1950, the year of Glacier National Park's first aerial photographic survey. The value of an archived series of aerial photographs and satellite images is highlighted by the fact that mapping of the 1950 margin was not undertaken until 1993.*

Other Glacier National Park glaciers, because of their unique characteristics, have responded somewhat independently to changes in climate and show variations in recession. The magnitude of shrinkage in Grinnell Glacier (fig. 29) is most representative of the larger glaciers in the park. The smaller glaciers here, while experiencing increased rates of retreat from the 1920's through 1940's, did not recede nearly as far nor did they thin as much in magnitude, though most either disappeared completely or reached a steady state during that period. Collectively parkwide, such significant changes translate into dramatic losses of stored water, which result in concurrent variations in stream hydrology and sedimentation.

By the end of the 1970's, Glacier National Park glaciers had been confined mostly to high cirque basins for more than three decades. It is clear that retreat rates decreased in the three decades leading up to that time, but it is also evident that, even as glaciers became increasingly buffered at higher elevations, broad-scale recession continued as proportionately more surface area became sheltered by cirque walls. Between 1979 and 1993, Sperry Glacier retreated from 45 to 75 m (an average rate of 3 to 5 m a^{-1}) and lost about 11 percent of its surface area (fig. 27). During the same period, Grinnell Glacier retreated 117 to 130 m (an average rate of 8 to 9 m a^{-1}), receding about 26 percent (fig. 28). However, a significant amount of this retreat is due to icebergs' calving.

Between 1979 and 1993, Agassiz, Jackson, and Blackfoot Glaciers receded only about 50 m, but all exhibited signs of continued thinning, including newly exposed bedrock or increased bedrock outcrops within the perimeter of the glaciers. Harrison Glacier, which had lost 61 percent of its area by 1979, continued to retreat through 1993, when it had lost 12 percent of its 1979 area. Overall, it decreased to 35 percent of its

Figure 29.*—Paired 1938 (left) and 1981 (right) photographs of Grinnell Glacier and The Salamander. In the 1981 photograph, significant retreat and thinning are clearly evident on the lower level Grinnell Glacier; note comparative glacier-ice thickness indicated along the cliff below The Salamander. Formation of Upper Grinnell Lake, which began in the early 1930's, has resulted in icebergs' calving along the terminus of much of the Grinnell Glacier. This has significantly increased the rate of recession. Snow-and-firn lines on the glacier surface are relatively similar in the two photographs. Only a minor change is noted in the area of The Salamander, as compared to the large amount of area lost by Grinnell Glacier. In comparison, krummholz (dark treed patches of stunted conifers on slopes in the background showing the approximate location of the tree line) have been relatively stable over the same period. The 1938 photograph was taken by T.J. Hileman, probably in late summer; the 1981 photograph by C.H. Key in late summer.*

maximum area during the Little Ice Age (fig. 25*C*). Vulture Glacier, having a 1993 area of only 0.21 km^2, had receded about 18 percent since 1966. In 1993, it occupied only about 28 percent of its 1850 area (fig. 25*D*). Swiftcurrent Glacier, another small glacier (1993 area of 0.14 km^2), appears to be fairly stable. It had receded nearly to its 1993 size by 1966, and it has a relatively high terminus elevation of 2,200 m in a well-shaded, northeast-facing cirque (fig. 28).

The retreat of the glaciers observed in Glacier National Park in recent years is consistent with a trend observed in temperate glaciers in other regions during the last 150 years. Evidently, climate (temperature and precipitation) is the primary controlling factor. Two reasonable hypotheses warrant consideration. In the first, the temperature warmed quickly during the middle 1800's and then remained relatively stable, so that today's glaciers are still responding to that one change. In the second, the temperature has continued to warm since the Little Ice Age, although it has included some brief periods of cooling. In neither hypothesis has precipitation increased. Sigurðsson and Williams (1998) agreed with the second hypothesis with respect to Iceland's glaciers.

The hypothesis that temperature has continued to warm since the Little Ice Age implies that fluctuations of glacier termini are more closely coupled to temperature change and react within shorter time frames than would be implied by the hypothesis that temperature warmed quickly during the middle 1800's and then remained relatively stable. To address these issues specifically, the authors recommend the following be instituted: (1) intervals and magnitudes of climate variation be correlated more explicitly to the recession rates of glaciers in the park, (2) new long-term mass-balance measurements be carried out, and (3) complete thermodynamic budgets be determined that account, individually and over time, for glacier-bed morphology, elevation, and exposure to solar radiation. In any case, it is significant that, in spite of favorable topographic settings, Glacier National Park's larger glaciers are shrinking and have not reached an equilibrium with today's climate.

Recent Glacier Trends

An often asked question is, "How have glaciers changed in area, length, or volume with time?" The answer must be qualified. It is relatively simple to observe specific glaciers for several decades, as has been done at the Nisqually and South Cascade Glaciers, as well as at several other glaciers. In all cases, these long records have shown general recession. As the observation frequency is increased, however, some of these records have shown periods of advance within the general retreat, and these periods of advance do not always correlate from glacier to glacier. In fact, glaciers that are side by side geographically sometimes behave differently. These short advances in the overall trend are a result of the complex interaction between the effects of elevation, latitude, exposure, basin area-elevation distribution, the variables of climate, and the individual glacier's dynamic-response characteristics. A strategy for monitoring glaciers of the United States and other glacierized regions is discussed by Fountain and others (1996) and was the subject of a 1996 workshop on long-term monitoring of glaciers of North America and northwestern Europe (Williams and Ferrigno, 1997).

An apparent contradiction exists in this general long-term recession. Table 1 gives glacier areas from Meier (1961a) and from more recent sources, where available. Many of the recent sources show an increase in total ice during the last 10 to 20 years. An incorrect conclusion is that glacier cover has increased. The correct conclusion is that more glacier cover has been recorded as a result of better source material, mainly maps and vertical aerial photographs. Had the same quality of source material been available and the same methodology been applied for the earlier determinations of area, the apparent trend of glacier increase seen in table 1 would almost certainly be reversed.

References Cited

Alden, W.C., 1914, Glaciers of Glacier National Park: Washington, D.C., U.S. Government Printing Office, U.S. Department of the Interior, 48 p.

Allen, C.R., Kamb, W.B., Meier, M.F., and Sharp, R.P., 1960, Structure of the lower Blue Glacier, Washington: Journal of Geology, v. 68, no. 6, p. 601–625.

Ayres, H.B., 1898, Map of the Flathead Forest Reserve, Montana, *in* Ayres, H.B., 1900, The Flathead Forest Reserve: U.S. Geological Survey Annual Report 20, pt. 5, p. 246–316.

Brown, C.S., 1989, A description of the United States' contribution to the world glacier inventory, *in* Oerlemans, Johannes, ed., Glacier fluctuations and climate change: Dordrecht, Netherlands, Kluwer Academic Publishers, p. 103–108.

Brugman, M.M., and Post, Austin, 1981, Effects of volcanism on the glaciers of Mount St. Helens: U.S. Geological Survey Circular 850–D (Hydrologic effects of the eruptions of Mount St. Helens, Washington, 1980), p. D1–D11.

Brugman, M.M., and Meier, M.F., 1981, Response of glaciers to the eruptions of Mount St. Helens, *in* Lipman, P.W., and Mullineaux, D.R., eds., The 1980 eruptions of Mount St. Helens, Washington: U.S. Geological Survey Professional Paper 1250, p. 743–756.

Carrara, P.E., 1989, Late Quaternary glacial and vegetative history of the Glacier National Park region, Montana: U.S. Geological Survey Bulletin 1902, 64 p.

Carrara, P.E., and McGimsey, R.G., 1981, The late neoglacial histories of the Agassiz and Jackson Glaciers, Glacier National Park, Montana: Arctic and Alpine Research, v. 13, no. 2, p. 183–196.

———1988, Map showing distribution of moraines and extent of glaciers from the mid-19th century to 1979 in the Mount Jackson area, Glacier National Park, Montana: U.S. Geological Survey Miscellaneous Investigations Series Map I–1508–C, scale 1:24,000.

Demorest, Max, 1938, Ice flowage as revealed by glacial striae: Journal of Geology, v. 46, no. 5, p. 700–725.

Dethier, D.P., and Frederick, J.E., 1981, Mass balance of "Vesper" Glacier, Washington, U.S.A.: Journal of Glaciology, v. 27, no. 96, p. 271–282.

Deutsch, Morris, contributing author, 1983, Monitoring of snowline dynamics in the Cascade Mountains, United States and Canada, *in* Williams, R.S., Jr., Geological applications, chapter 31, *of* Colwell, R.N., editor-in-chief, Manual of remote sensing (2d ed.): Falls Church, Va., American Society of Photogrammetry, v. II, p. 1734–1735.

Driedger, C.L., 1981, Effect of ash thickness on snow ablation, *in* Lipman, P.W., and Mullineaux, D.R., eds., The 1980 eruptions of Mount St. Helens, Washington: U.S. Geological Survey Professional Paper 1250, p. 757–760.

———1986, A visitor's guide to Mount Rainier glaciers: Longmire, Wash., Northwest National Parks and Forest Association, 80 p.

———1988, Geology in action—jökulhlaups on Mount Rainier: U.S. Geological Survey Open-File Report 88–459, 2 p.

———1993, Glaciers on Mount Rainier: U.S. Geological Survey Open-File Report 92–474, 2 p.

Driedger, C.L., and Fountain, A.G., 1989, Glacier outburst floods at Mount Rainier, Washington State, U.S.A.: Annals of Glaciology, v. 13, p. 51–55.

Driedger, C.L., and Kennard, P.M., 1984, Glacier volume estimation on Cascade volcanoes—An analysis and comparison with other methods: Annals of Glaciology, v. 8, p. 59–64.

———1986, Ice volumes on Cascade volcanoes; Mount Rainier, Mount Hood, Three Sisters, and Mount Shasta, Washington, Oregon, and Washington: U.S. Geological Survey Professional Paper 1365, 28 p.

Dyson, J.L., 1941, Recent glacier recession in Glacier National Park: Journal of Geology, v. 49, no. 8, p. 815–824.

———1948, Shrinkage of Sperry and Grinnell Glaciers, Glacier National Park, Montana: Geographical Review, v. 38, no. 1, p. 96–103.

———1952, Glaciers of the American Rocky Mountains: American Geophysical Union, Committee on Glaciers, Subcommittee on the American Rocky Mountains Triennial Report 1950–52, 37 p.

Field, W.O., ed., 1975, Mountain glaciers of the Northern Hemisphere: Hanover, N.H., U.S. Army Corps of Engineers, Cold Regions Research and Engineering Laboratory, v. 1, 698 p.

Fountain, A.G., 1989, The storage of water in, and hydraulic characteristics of, the firn of South Cascade Glacier, Washington State, U.S.A.: Annals of Glaciology, v. 13, p. 69–75.

———1992a, Subglacial hydraulics of South Cascade Glacier: Seattle, Wash., University of Washington, unpublished Ph.D. dissertation, 265 p.

———1992b, Subglacial water flow inferred from stream measurements at South Cascade Glacier, Washington State, U.S.A.: Journal of Glaciology, v. 38, no. 128, p. 51–64.

———1993, Geometry and flow conditions of subglacial water at South Cascade Glacier, Washington State, U.S.A.—An analysis of tracer injections: Journal of Glaciology, v. 39, no. 131, p. 143–156.

———1994, Borehole water-level variations and implications for the subglacial hydraulics of South Cascade Glacier, Washington, U.S.A.: Journal of Glaciology, v. 40, no. 135, p. 293–304.

Fountain, A.G., and Fulk, M.A., 1984, South Cascade Glacier bibliography, Washington: U.S. Geological Survey Open-File Report 84–441, 13 p.

Fountain, A.G., Krimmel, R.M., and Trabant, D.C., 1996, A strategy for monitoring glaciers: U.S. Geological Survey Circular 1132, 20 p.

Fountain, A.G., and Tangborn, W.V., 1985a, Contemporary techniques for prediction of runoff from glacierized areas, *in* Report for the Working Group on Snow and Ice Hydrology of Glacierized Basins: International Commission on Snow and Ice, International Association of Hydrological Sciences Publication No. 149, p. 27–41.

———1985b, The effect of glaciers on streamflow variations: Water Resources Research, v. 21, no. 4, p. 579–586.

Fountain, A.G., Trabant, D.C., Brugman, M.M., Ommanney, C.S., and Monroe, D.S., 1991, Glacier mass balance standards: EOS (American Geophysical Union Transactions), v. 72, no. 46, p. 511–514.

Foxworthy, B.L, and Hill, Mary, 1982, Volcanic eruptions of 1980 at Mount St. Helens; the first 100 days: U.S. Geological Survey Professional Paper 1249, 125 p.

Graf, W.L., 1977, The distribution of glaciers in the Rocky Mountains of the United States: Journal of Glaciology, v. 18, no. 79, p. 325–328.

Haeberli, Wilfried, 1985, Fluctuations of glaciers 1975–1980: Paris, International Association of Hydrological Sciences and United Nations Educational, Scientific, and Cultural Organization (UNESCO), v. 4, 265 p., 13 special topographic maps of glaciers.

Haeberli, Wilfried, and Hoelzle, Martin, 1993, Fluctuations of glaciers, 1985–1990: Paris, International Association of Hydrological Sciences (International Commission on Snow and Ice), United Nations Environment Programme, Global Environmental Monitoring System (GEMS), International Hydrological Programme, and United Nations Educational, Scientific, and Cultural Organization (UNESCO), v. 6, 322 p.

Haeberli, Wilfried, and Müller, Peter, 1988, Fluctuations of glaciers 1980–1985: Paris, International Association of Hydrological Sciences (International Commission on Snow and Ice), United Nations Environment Programme, Global Environmental Monitoring System (GEMS), International Hydrological Programme, and United Nations Educational, Scientific, and Cultural Organization (UNESCO), v. 5, 290 p.

Haeberli, Wilfried, Hoelze, Martin, Suter, Stephan, and Frauenfelder, Regula, 1998, Fluctuations of glaciers 1990–1995: Paris, International Association of Hydrological Sciences (International Commission on Snow and Ice), United Nations Environment Programme, Global Environmental Monitoring Service (GEMS), International Hydrological Programme, and United Nations Educational, Scientific, and Cultural Organization (UNESCO), v. 7, 296 p.

Heliker, C.C., Johnson, Arthur, and Hodge, S.M., 1984, The Nisqually Glacier, Mount Rainier, Washington, 1857–1979: A summary of the long-term observations and a comprehensive bibliography: U.S. Geological Survey Open-File Report 83–541, 20 p.

Heusser, C.J., 1957, Variations of Blue, Hoh, and White Glaciers during recent centuries: Arctic (Journal of the Arctic Institute of North America), v. 10, no. 3, p., 139–150.

Hodge, S.M., 1972, The movement and basal sliding of the Nisqually Glacier, Mt. Rainier: Seattle, Wash., University of Washington, Department of Atmospheric Sciences, Science Report, (Ph. D. dissertation), 409 p.

———1974, Variations in the sliding of a temperate glacier: Journal of Glaciology, v. 13, no. 69, p. 349–369.

———1976, Direct measurements of basal water pressures—A pilot study: Journal of Glaciology, v. 16, no. 7, p. 205–218.

———1979, Direct measurement of basal water pressures—Progress and problems: Journal of Glaciology, v. 23, no. 89, p. 309–319.

Hopson, R.E., 1960, Collier Glacier—A photographic record: Mazama, v. 42, no. 13, p. 15–26.

Johnson, Arthur, 1958, Investigations on Grinnell and Sperry Glaciers, Glacier National Park, Montana: International Geodetic and Geophysical Union, International Association of Scientific Hydrology Assemblée Générale de Toronto, 1957, Gentbrugge, Belgium, 1958, Extrait des Comptes Rendus et Rapports, v. 4, p. 525–534. [In English.]

———1980, Grinnell and Sperry Glaciers, Glacier National Park, Montana—A record of vanishing ice: U.S. Geological Survey Professional Paper 1180, 29 p., topographic maps, scale 1:6,000.

Jordan, Raymond, and Kieffer H.H., 1982, Topographic map of Mount St. Helens, Washington, showing changes between April 11 and May 16, 1980: U.S. Geological Survey Miscellaneous Investigations Series I–1411, scale 1:10,000.

Kasser, Peter, 1967, Fluctuations of glaciers 1959–1965: Paris, International Association of Scientific Hydrology and United Nations Educational, Scientific, and Cultural Organization (UNESCO), v. 1, 52 p., 23 tables, 7 figs., 1:25,000-scale photogrammetric map of Aletschgletscher.

———1973, Fluctuations of glaciers 1965–1970: Paris, International Association of Hydrological Sciences and United Nations Educational, Scientific, and Cultural Organization (UNESCO), v. 2, 357 p., 5 special topographic maps of glaciers.

Kautz, A.V., 1875, Ascent of Mount Rainier: Overland Monthly, v. 14, no. 5, p. 393–403.

King, Clarence, 1871, On the discovery of actual glaciers on the mountains of the Pacific Slope: American Journal of Science, series 3, v. 1, p. 157–167.

Krimmel, R.M., 1970, Gravimetric ice thickness determination, South Cascade Glacier, Washington: Northwest Science, v. 44, no. 3, p. 147–153.

———1989, Mass balance and volume of South Cascade Glacier, Washington, 1958–1985, *in* Oerlemans, Johananes, ed., Glacier fluctuations and climatic change: Dordrecht, Netherlands, Kluwer Academic Publishers, p. 193–206.

———1993, Mass balance, meteorological, and runoff measurements at South Cascade Glacier, Washington, 1992 balance year: U.S. Geological Survey Open–File Report 93–640, 38 p.

———1994, Runoff, precipitation, mass balance, and ice velocity measurements at South Cascade Glacier, Washington, 1993 balance year: U.S. Geological Survey Water-Resources Investigations Report 94–4139, 34 p.

———1995, Water, ice, and meteorological measurements at South Cascade Glacier, Washington, 1994 balance year: U.S. Geological Survey Water-Resources Investigations Report 95–4162, 41 p.

———1996, Water, ice, and meteorological measurements at South Cascade Glacier, Washington, 1995 balance year: U.S. Geological Survey Water-Resources Investigations Report 96–4174, 37 p.

———1997, Water, ice, and meteorological measurements at South Cascade Glacier, Washington, 1996 balance year: U.S. Geological Survey Water-Resources Investigations Report 97–4143, 34 p.

———1998, Water, ice, and meteorological measurements at South Cascade Glacier, Washington, 1997 balance year: U.S. Geological Survey Water-Resources Investigations Report 98–4090, 30 p.

———1999, Water, ice, meteorological, and speed measurements at South Cascade Glacier, Washington, 1998 balance year: U.S. Geological Survey Water-Resources Investigations Report 99–4049, 36 p.

———2000, Water, ice, and meteorological measurements at South Cascade Glacier, Washington, 1986–1991 balance years: U.S. Geological Survey Water-Resources Investigations Report 2000–4006, 77 p.

———2001, Water, ice, meteorological, and speed measurements at South Cascade Glacier, Washington, 1999 balance year: U.S. Geological Survey Water-Resources Investigations Report 2000–4265, 36 p.

Krimmel, R.M., and Meier, M.F., 1975, Glacier application of ERTS images: Journal of Glaciology, v. 15, no. 73, p. 391–402.

Krimmel, R.M., Tangborn, W.V., Sikonia, W.G., and Meier, M.F., 1978, Ice and water balances, South Cascade Glacier, 1957–1977, *in* International Symposium on the Computation and Prediction of Runoff from Glacier and Glacial Area, Tbilisi, U.S.S.R., 1978: U.S.S.R. Academy of Sciences, Section of Glaciology, Data of Glaciological Studies, Publication 38, p. 143–147, 217–219.

LaChapelle, Edward, 1965, The mass budget of Blue Glacier, Washington: Journal of Glaciology, v. 5, no. 41, p. 609–623.

Matthes, F.E., 1931, Glacier measurements in the United States, *in* Reports and papers, Section of Hydrology: National Research Council, National Academy of Sciences, 12th annual meeting, Washington, D.C., American Geophysical Union Transactions, p. 211–215.

———1932, On glaciers, *in* Reports and papers, Section of Hydrology: National Research Council, National Academy of Sciences, 13th annual meeting, Washington, D.C., American Geophysical Union Transactions, p. 282–287.

———1933, On glaciers, *in* Reports and papers, Section of Hydrology: National Research Council, National Academy of Sciences, 14th annual meeting, Washington, D.C., American Geophysical Union Transactions, p. 345–350.

———1934, Report of the Committee on Glaciers, 1933–34, *in* Reports and papers, Section of Hydrology: National Research Council, National Academy of Sciences, 15th annual meeting, part 2, Washington, D.C., American Geophysical Union Transactions, p. 279–285.

———1935, Report of the Committee on Glaciers, 1934–35, *in* Reports and papers, Section of Hydrology: National Research Council, National Academy of Sciences, 16th annual meeting, part 2, Washington, D.C., American Geophysical Union Transactions, p. 387–392.

———1936, Report of the Committee on Glaciers, 1935–36, *in* Reports and papers, Section of Hydrology: National Research Council, National Academy of Sciences, 17th annual meeting, part 2, Washington, D.C., American Geophysical Union Transactions, p. 286–294.

———1937, Report of the Committee on Glaciers, 1936–37, *in* Reports and papers, Section of Hydrology: National Research Council, National Academy of Sciences, 18th annual meeting, part 2, Washington, D.C., American Geophysical Union Transactions, p. 293–299.

———1938, Report of the Committee on Glaciers, 1937–38, *in* Reports and papers, Section of Hydrology: National Research Council, National Academy of Sciences, 19th annual meeting, part 1, Washington, D.C., American Geophysical Union Transactions, p. 314–320.

———1939, Report of the Committee on Glaciers, April 1939, *in* Reports and papers, Section of Hydrology: National Research Council, National Academy of Sciences, 20th annual meeting, part 4, Washington, D.C., American Geophysical Union Transactions, p. 518–523.

———1940, Report of the Committee on Glaciers, 1939-40, *in* Reports and papers, Section of Hydrology: National Research Council, National Academy of Sciences, 21st annual meeting, part 2, Washington, D.C., American Geophysical Union Transactions, p. 396–406.

———1941, Report of the Committee on Glaciers, 1940-41, *in* Reports and papers, Section of Hydrology: National Research Council, National Academy of Sciences, 22d annual meeting, part 3, Washington, D.C., American Geophysical Union Transactions, p. 1006–1011.

——1942, Report of the Committee on Glaciers, 1941-42, *in* Reports and papers, Section of Hydrology: National Research Council, National Academy of Sciences, 23d annual meeting, part 2, Washington, D.C., American Geophysical Union Transactions, p. 374–392.

———1944, Report of the Committee on Glaciers, 1942-43, *in* Reports and papers, Section of Hydrology: National Research Council, National Academy of Sciences, 24th annual meeting, part 2, Washington, D.C., American Geophysical Union Transactions, p. 389–401.

———1945, Report of the Committee on Glaciers, 1943–44, *in* Reports, Section of Hydrology: National Research Council, National Academy of Sciences, 25th annual meeting, part 5, Washington, D.C., American Geophysical Union Transactions, p. 677–683.

Mayo, L.R., 1984, Glacier mass balance and runoff research in the U.S.A.: Geografiska Annaler, series A, v. 66, no. 3, p. 215–227.

Meier, M.F., 1958, Glacier observations in the Cascade Mountains, U.S.A., *in* American Geographical Society, Preliminary reports of the Antarctic and Northern Hemisphere glaciology programs: New York, International Geophysical Year Glaciological Report Series 1, p. IX–1–IX–6.

———1961a, Distribution and variations of glaciers in the United States exclusive of Alaska, *in* General Assembly of Helsinki, 1960: International Association of Scientific Hydrology Publication No. 54, p. 420–429.

———1961b, Mass budget of South Cascade Glacier, 1957–60: U.S. Geological Survey Professional Paper 424–B, p. B206–B211.

———1966, Some glaciological interpretations of remapping programs on South Cascade, Nisqually, and Klawatti Glaciers, Washington: Canadian Journal of Earth Sciences, v. 3, no. 6, p. 811–818.

———1967, South Cascade Glacier, Washington, *in* Annals of the International Geophysical Year: Glaciology, v. 41, p. 169–170.

Meier, M.F., Alexander, R.H., and Campbell, W.J., 1966, Multispectral sensing tests at South Cascade Glacier, Washington: Symposium on Remote Sensing of Environment, 4th, Ann Arbor, Mich., Proceedings, p. 145–159.

Meier, M.F., and Evans, W.E., 1975, Comparison of different methods for estimating snowcover in forested, mountainous basins using LANDSAT (ERTS) images, Washington and Santiam River, Oregon, *in* Rango, Al, ed., Workshop on Operational Applications of Satellite Snowcover Observations: National Aeronautics and Space Administration Special Publication–391, p. 215–234.

Meier, M.F., Kamb, W.B., Allen, C.R., and Sharp, R.P., 1974, Flow of Blue Glacier, Olympic Mountains, Washington, U.S.A.: Journal of Glaciology, v. 13, no. 68, p. 187–212.

Meier, M.F., Mayo, L.R., Trabant, D.C., and Krimmel, R.M., 1980, Comparison of mass balance and runoff at four glaciers in the United States, 1966 to 1977: U.S.S.R. Academy of Sciences, Section of Glaciology, Data of Glaciological Studies Publication 38, p. 138–147 (Russian text and figures), p. 214–219 (English text only).

Meier, M.F., and Post, A.S., 1962, Recent variations in mass net budgets of glaciers in western North America, *in* Ward, W., Variations of the regime of existing glaciers: International Union of Geodesy and Geophysics, International Association of Scientific Hydrology Publication No. 58, p. 63–77.

Meier, M.F., and Tangborn, W.V., 1965, Net budget and flow of South Cascade Glacier, Washington: Journal of Glaciology, v. 5, no. 41, p. 547–566.

Meier, M.F., Tangborn, W.V., Mayo, L.R., and Post, Austin, 1971, Combined ice and water balances of Gulkana and Wolverine Glaciers, Alaska, and South Cascade Glacier, Washington, 1965 and 1966 hydrologic years: U.S. Geological Survey Professional Paper 715–A, 23 p.

Miller, C.D., 1969, Chronology of neoglacial moraines in the dome peak area, North Cascade Range, Washington: Arctic and Alpine Research, v. 1, no. 1, p. 49–65.

Müller, Fritz, 1977, Fluctuations of glaciers 1970–1975: Paris, International Association of Hydrological Sciences and United Nations Educational, Scientific, and Cultural Organization (UNESCO), v. 3, 269 p., 12 special topographic maps of glaciers.

Müller, Fritz, Caflisch, T., and Muller, G., 1977, Instructions for compilation and assemblage of data for a world glacier inventory: Zürich, Swiss Federal Institute of Technology (ETH), Department of Geography, International Commission on Snow and Ice, Temporary Technical Secretariat for World Glacier Inventory, 28 p.

Naftz, D.L., 1993, Ice-core records of the chemical quality of atmospheric deposition and climate from mid-latitude glaciers, Wind River Range, Wyoming: Golden, Colo., Colorado School of Mines, unpublished Ph.D. dissertation, 204 p.

Naftz, D.L., Miller, K.A., and See, R.B., 1991, Using glacial ice cores from Wyoming as long-term records of atmospheric deposition quality and climate change—A progress report: American Water Resources Association Hydata Technote, v. 10, no. 4, p. 23–24.

Naftz, D.L., Rice, J.A., and Ranville, J.R., 1991, Glacial-ice composition—A potential long-term record of the chemistry of atmospheric deposition, Wind River Range, Wyoming: Water Resources Research, v. 27, no. 6, p. 1231–1238.

Naftz, D.L., and Smith, M.E., 1993, Ice thickness, ablation, and other glaciological measurements on Upper Fremont Glacier, Wyoming: Physical Geography, v. 14, no. 4, p. 404–414.

Nye, J.F., 1965, A numerical method of inferring the budget history of a glacier from its advance and retreat: Journal of Glaciology, v. 5, no. 41, p. 589–607.

Østrem, Gunnar, and Brugman, M., 1991, Glacier mass-balance measurements, a manual for field and office work: Saskatoon, Saskatchewan, Canada, Norwegian Water Resources and Energy Administration, and Environment Canada, National Hydrology Research Institute Science Report 4, 224 p.

Pelto, M.S., 1996, Annual net balance of North Cascade glaciers, 1984–1994: Glaciology, v. 42. no. 140, p. 3–9.

Phillips, E.L., and Donaldson, W.R., 1972, Washington climate for the counties Clallam, Grays Harbor, Jefferson, Pacific, Wahkiakum: Pullman, Wash., U.S. Department of Agriculture in cooperation with Cooperative Extension Service, Washington State University, p. 6.

Post, Austin, Richardson, Don, Tangborn, W.V., and Rosselot, F.L., 1971, Inventory of glaciers in the North Cascades, Washington: U.S. Geological Survey Professional Paper 705–A, 26 p.

Raub, W.B., Post, Austin, Brown, C.S., and Meier, M.F., 1980, Perennial ice masses of the Sierra Nevada, California, *in* World glacier inventory, Proceedings of the Riederalp (Switzerland) workshop: International Association of Hydrological Sciences-Association Internationale des Sciences Hydrologiques Publication No. 126, p. 33–34.

Reed, J.C., Jr., 1964, Recent retreat of the Teton Glacier, Grand Teton National Park, Wyo., *in* Geological Survey research 1964: U.S. Geological Survey Professional Paper 501–C, p. C147–C151.

———1965, Rate of ice movement and estimated ice thickness in part of the Teton Glacier, Grand Teton National Park, Wyo., *in* Geological Survey research 1965: U.S. Geological Survey Professional Paper 525–B, B137–B141.

———1967, Observations on the Teton Glacier, Grand Teton National Park, Wyo., 1965 and 1966, *in* Geological Survey research 1967: U.S. Geological Survey Professional Paper 575–C, p. C154–C159.

Richardson, Donald, 1968, Glacier outburst floods in the Pacific Northwest, *in* Geological Survey research 1968: U.S. Geological Survey Professional Paper 600–D, p. D79–D86.

Russell, I.C., 1885, Existing glaciers of the United States: U.S. Geological Survey Annual Report 5 (1883–84), p. 303–355.

———1898, Glaciers of Mount Rainier: U.S. Geological Survey Annual Report 18 (1896-97), pt. 2, p. 349-415.

Shreve, R.L., and Sharp, R.P., 1970, Internal deformation and thermal anomalies in lower Blue Glacier, Mount Olympus, Washington, U.S.A.: Journal of Glaciology, v. 9, no. 55, p. 65–86.

Sigafoos, R.S., and Hendricks, E.L., 1972, Recent activity of glaciers of Mount Rainier, Washington: U.S. Geological Survey Professional Paper 387–B, p. B1–B24.

Sigurðsson, Oddur, and Williams, R.S., Jr., 1998, Past, present, and future glacier fluctuations in Iceland: An environmental response to climatic variability in the North Atlantic [abs.]: *in* Abstracts and curriculum vitae of International Workshop on Environmental and Climatic Variations in the North Atlantic Region, Reykjavík, Iceland (23–26 September 1998), p. 29.

Snyder, E.F., 1996, Bibliography of glacier studies by the U.S. Geological Survey: U.S. Geological Survey Open-File Report 95–723, 35 p.

Sperry, A.L., 1938, Avalanche: Boston, Mass., Christopher Publishing House, 166 p.

Spicer, R.C., 1986, Glaciers in the Olympic Mountains, Washington: Present distribution and recent variations: Seattle, Wash., University of Washington, unpublished M.S. dissertation, 158 p.

Sullivan, M.E., 1994, South Cascade Glacier, Washington—Hydrologic and meteorological data, 1957–67: U.S. Geological Survey Open-File Report 94–77, 105 p. and diskette.

Tangborn, W.V., 1962, Glaciological investigations on South Cascade Glacier: Mountaineer, v. 55, no. 4, p. 9.

Tangborn, W.V., 1963, Instrumentation of a high altitude glacier basin to obtain continuous record for water budgets—A preliminary report, *in* General Assembly of Berkeley: International Association of Scientific Hydrology Publication No. 61, p. 131–137.

———1965, Net mass budget of South Cascade Glacier, Washington [abs.], *in* Geological Survey research 1965: U.S. Geological Survey Professional Paper 525A, p. A180–181.

———1968, Mass balances of some North Cascade glaciers as determined by hydrologic parameters, 1920–1965, in International Commission on Snow and Ice, Bern, Switzerland, 1967, Proceedings: International Association of Scientific Hydrology Publication No. 79, p. 267–274.

Tangborn, Wendell, 1980, Two models for estimating climate-glacier relationships in the North Cascades, Washington, U.S.A.: Journal of Glaciology, v. 25, no. 91, p. 3–21.

Tangborn, W.V., Fountain, A.G., and Sikonia, W.D., 1990, Effect of altitude-area distribution on glacier mass balance—A comparison of North and South Klawatti Glaciers, Washington State, U.S.A.: Annals of Glaciology, v. 14, p. 278–282.

Tangborn, W.V., Krimmel, R.M., and Meier, M.F., 1975, A comparison of glacier mass balance measurements by glaciologic, hydrologic and mapping methods, South Cascade Glacier, Washington, *in* International Association of Hydrological Sciences, General Assembly of Moscow, U.S.S.R., 1971 Proceedings: International Association of Hydrological Sciences-Association Internationale des Sciences Hydrologiques Publication No. 104, p. 185–196.

Tangborn, W.V., Mayo, L.R., Scully, D.R., and Krimmel, R. M., 1977, Combined ice and water balances of Maclure Glacier, California, South Cascade Glacier, Washington, and Wolverine and Gulkana Glaciers, Alaska, 1967 hydrologic year: U.S. Geological Survey Professional Paper 715–B, 20 p.

Tilling, R.I., n.d. [1984], Eruptions of Mount St. Helens: Past, present, and future: U.S. Geological Survey General Interest Publication, 52 p.

UNESCO (United Nations Educational, Scientific, and Cultural Organization), 1970, Perennial ice and snow masses; a guide for compilation and assemblage of data for a world inventory: Paris, UNESCO-International Association of Scientific Hydrology Technical Papers in Hydrology, 1, 19 p.

U.S. Geological Survey, 1978, Nisqually Glacier, Mount Rainier National Park, Washington: Reston, Va., U.S. Geological Survey, Nisqually Glacier, 1976 Plan, 1:10,000-scale topographic map based on aerial photographs taken on August 31, 1976.

Veatch, F.M., 1969, Analysis of a 24-year photographic record of Nisqually Glacier, Mount Rainier National Park, Washington: U.S. Geological Survey Professional Paper 631, 52 p.

Walder, J.S., and Driedger, C.L., 1993, Glacier-generated debris flows at Mount Rainier: U.S. Geological Survey Open-File Report 93–124, [Water Fact Sheet], 2 p.

———1995, Frequent outburst floods from South Tahoma Glacier, Mount Rainier, U.S.A.—Relation to debris flows, meteorological origin and implications for subglacial hydrology: Journal of Glaciology, v. 41, no. 137, p. 1–10.

Waldrop, H.A. 1964, Arapaho Glacier, a sixty-year record: University of Colorado Studies, Series in Geology, no. 3, 37 p.

Walters, R.A., and Meier, M.F., 1989, Variability of glacier mass balances in western North America, *in* Peterson, D.H., Aspects of climate variability in the Pacific and western Americas: American Geophysical Union Geophysical Monograph 55, p. 365–374.

Wentworth, C.K., and Delo, D.M., 1931, Dinwoody Glaciers, Wind River Mountains, Wyoming, with a brief survey of existing glaciers in the United States: Geological Society of America Bulletin, v. 42, no. 3, p. 605–620.

Glaciers of North America–

GLACIERS OF MÉXICO

By SIDNEY E. WHITE

SATELLITE IMAGE ATLAS OF GLACIERS OF THE WORLD

Edited by RICHARD S. WILLIAMS, Jr., *and* JANE G. FERRIGNO

U.S. GEOLOGICAL SURVEY PROFESSIONAL PAPER 1386–J–3

Glaciers in México are restricted to its three highest mountains, all stratovolcanoes. Of the two that have been active in historic time, Volcán Pico de Orizaba (Volcán Citlaltépetl) has nine named glaciers, and Popocatépetl has three named glaciers. The one dormant stratovolcano, Iztaccíhuatl, has 12 named glaciers. The total area of the 24 glaciers is 11.44 square kilometers. The glaciers on all three volcanoes have been receding during the 20th century. Since 1993, intermittent explosive and effusive volcanic activity at the summit of Popocatépetl has covered its glaciers with tephra and caused some melting

CONTENTS

SATELLITE IMAGE ATLAS OF GLACIERS OF THE WORLD

GLACIERS OF NORTH AMERICA–

GLACIERS OF MÉXICO

By SIDNEY E. WHITE[1]

Abstract

Glaciers in México are limited to its three highest mountains, all of which are volcanoes: Volcán Pico de Orizaba (Volcán Citlaltépetl), Volcán Iztaccíhuatl, and the active (since 1993) Volcán Popocatépetl, which have 9, 12, and 3 named glaciers, respectively. The total area of the 24 glaciers is 11.44 square kilometers. All of México's glaciers are small, with areas rarely exceeding a few tenths of a square kilometer, except for the ice cap and firn field of Gran Glaciar Norte on Citlaltépetl, which has an area of 9.08 square kilometers and from which seven outlet glaciers emanate. The small areal dimensions of México's glaciers severely restrict the usefulness of Landsat multispectral scanner images for delineating individual glaciers or for monitoring variations in terminus position. The nearly threefold improvement in spatial resolution of the Landsat 3 return beam vidicon images compared to multispectral scanner images (30-meter versus a 79-meter pixel), permits a more accurate delineation of the mountain glaciers of México.

Introduction

Under the present climatic conditions, three volcanoes in south-central México, all having highest elevations in excess of 5,000 m, support numerous small glaciers. (1) Volcán Pico de Orizaba (Volcán Citlaltépetl)[2], a 5,610-m-high (Simkin and Siebert, 1994; previous value was 5,675 m) stratovolcano in the State of Veracruz, supports nine named glaciers. Seven volcanic eruptions have been recorded there in historic time, the last in 1687 (Simkin and others, 1981). (2) Volcán Iztaccíhuatl, a 5,230-m-high (Simkin and Siebert, 1994; previous value was 5,286 m), dormant Holocene stratovolcano in the State of Puebla, has three summits and 12 named glaciers. (3) Volcán Popocatépetl, a 5,465-m-high (Simkin and Siebert, 1994; previous value was 5,452 m) stratovolcano in the State of Puebla, has three named glaciers. Since 1345, Popocatépetl has been the site of at least 25, and perhaps as many as 30, eruptions, the last at this writing in January 2001 (Simkin and Siebert, 1994; Smithsonian Institution, 1994, 1995, 1996, 1997, 1998, 1999, 2000; Roberto Quaas, written commun., 1997). The author also observed one gas-column eruption on 7 April 1953.

The equilibrium line altitude (ELA) of glaciers on Iztaccíhuatl and Popocatépetl is 4,880 m and 4,925 m, respectively; the ELA of glaciers on Citlaltépetl is not known. No other highland areas in México are sufficiently high to be above the present-day snowline. During the Illinoian age of the Pleistocene Epoch, however, the ELA was as low as 3,510 m on Iztaccíhuatl during the Tonicoxco (*Tomicoxco*) advance and was somewhat higher

Manuscript approved for publication 7 March 2002.

[1] Department of Geological Sciences, Ohio State University, 275 Mendenhall Laboratory, 125 South Oval Mall, Columbus, Ohio 43210–1398.

[2] Most of the geographic place-names used in this section are from the Gazetteer of Mexico (U.S. Board on Geographic Names, 1992). An exception is Citlaltépetl, where the Nahuatl place-name is used instead of the Spanish one (Volcán Pico de Orizaba). Throughout the text, references to Citlaltépetl, Iztaccíhuatl, and Popocatépetl are, after the first mention, without Volcán in the title. A few names not listed in the gazetteer are shown in italics.

during other advances. Cerro Ajusco, a 3,937 m-high volcanic mountain south of Mexico City in the Federal District (D.F., Distrito Federal), supported glaciers during times of lower ELA during the late Wisconsinan age and during the late Holocene Epoch (early neoglaciation and middle neoglaciation) (White, 1981a, 1984). The following discussion of the glaciers on Citlaltépetl, Iztaccíhuatl, and Popocatépetl emphasizes historic and modern observations.

Volcán Pico de Orizaba (Volcán Citlaltépetl)

At 5,610 m (Simkin and Siebert, 1994; previous value was 5,675 m, which is used as the reference elevation in the text for glacier elevations), Citlaltepétl is the highest mountain in México and the third highest on the North American Continent. It contains the largest ice cap and firn field in México (Gran Glaciar Norte) and has nine named glaciers (fig. 1 and table 1), including the ice cap, its seven outlet glaciers, and a mountain (niche) glacier. Its name is derived from the Nahuatl words Citlalli (star) and tépetl (mountain). However, its officially recognized name is Spanish, Pico de Orizaba. Situated at lat 19°02' N. and long 97°17' W., it is 210 km east of Mexico City and 120 km west of Veracruz and the Gulf of Mexico. Topographic maps of Citlaltépetl are sold by the Comisión Cartográfica Militar, Secretaría de la Defensa Nacional, México, D.F. Provisional maps by Estudios y Proyectos, Asociación Civil (A.C.), México, D.F., also may be purchased. Vertical aerial photos taken in 1955 by the Comisión del Papaloapan are in the Instituto de Geografía, Universidad de México, México, D.F. Oblique aerial photographs taken in 1942 are available from Compañía Mexicana Aerofoto, Sociedad Anónima (S.A.), México, D.F.

Because of its inaccessibility due to the 210-km distance from Mexico City and the 42-km journey from *Tlalchíchuca* or the 46-km trip from *San Andres Chalchícomula* by alternate third-class roads to trailheads from the northwest (fig. 2), Citlaltépetl rarely has been studied from any viewpoint. However, being the highest and the most esthetic mountain in México—a white shining star in the east—it caught the attention of Europeans early in the development of the country and was climbed several times from the mid-1800's to the early 1900's (Galeotti, 1850; Plowes and others, 1877; Angermann, 1904; Waitz, 1910). Glaciers and snowfields were mentioned in the description of these climbs because they were along the logical routes of ascent; unfortunately, scientific details are scarce in these works.

TABLE 1.—*Nine named glaciers of Citlaltépetl*
[Taken from Lorenzo, 1964, sketch III. Leaders (–), not known]

Glacier number	Glacier name	Glacier type	Area (square kilometers)
	Gran Glaciar Norte	Ice cap, firn field	9.08
I	Lengua del Chichimeco	Outlet	–
II	Glaciar de Jamapa	Outlet	–
III	Glaciar del Toro	Outlet	–
IV	Glaciar de la Barba	Outlet	–
V	Glaciar Noroccidental	Outlet	–
VI	Glaciar Occidental	Outlet	–
VII	Glaciar Suroccidental	Outlet	–
VIII	Glaciar Oriental	Mountain (niche)	.42
		Total	9.50

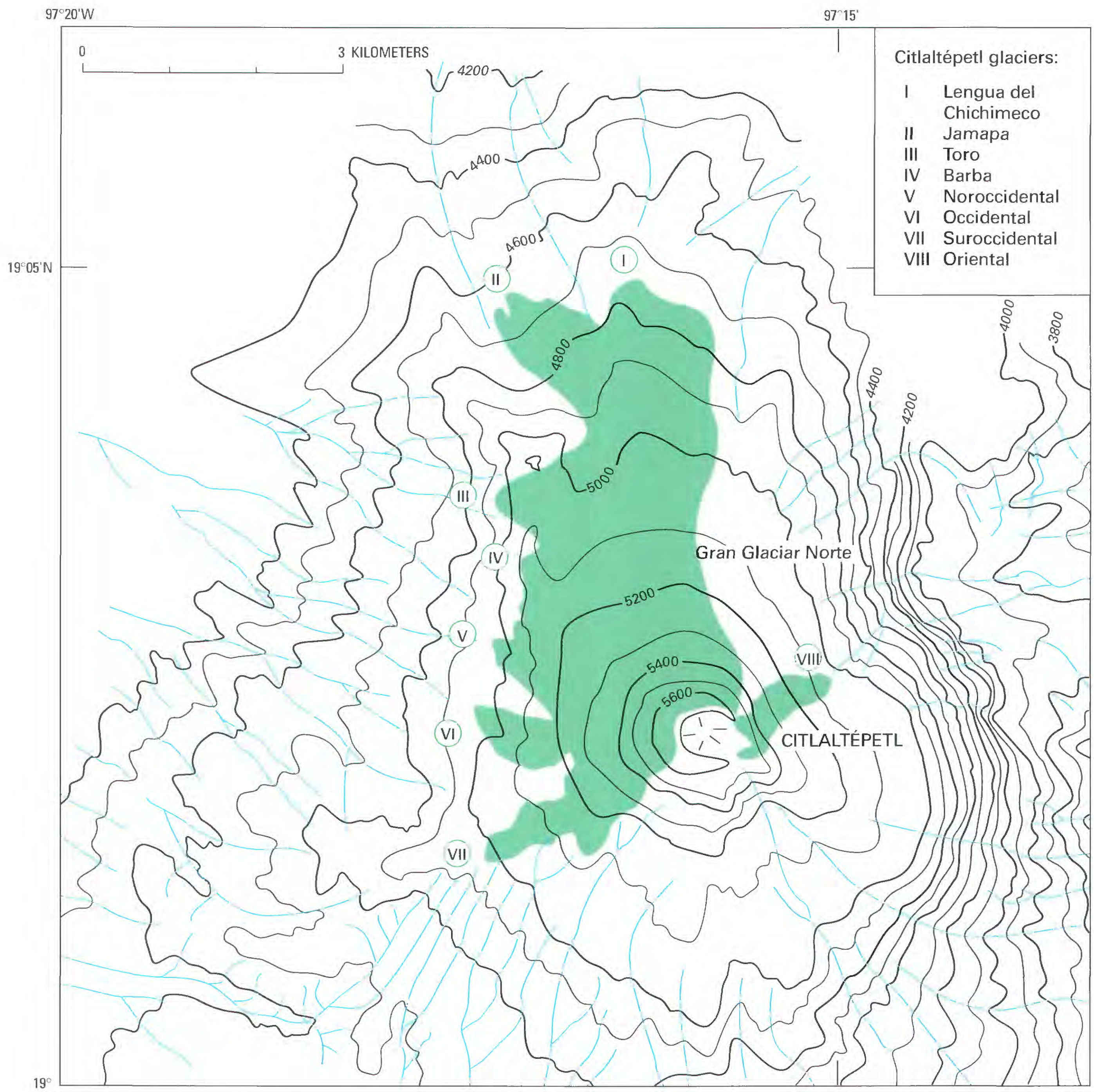

Figure 1.*—Glaciers (shown in green) on Citlaltépetl. The numbers refer to the named outlet and mountain glaciers listed in table 1. Contour interval, 100 m. Original map by Estudios y Proyectos, A.C., México, D.F. (Modified from Lorenzo, 1964, sketch III.)*

Blásquez (1957) may have been the first to study Citlaltépetl's glaciers from a glaciological viewpoint. He studied from a hydrogeological perspective the meltwater that is used locally. The most exacting study of Citlaltépetl's glaciers was by a team of mountaineering geophysicists led by José Luis Lorenzo in 1958, working under the auspices of the Comité Nacional de México for the International Geophysical Year (1957–58) through the Instituto de Geofísica. Despite hardships of elevation and unforeseen storms, the team measured glacier-surface slopes, accumulation areas, and elevations of glacier termini. In addition, they carried out topographic mapping of the nine glaciers and took scores of excellent photographs (Lorenzo, 1959, 1964). The retreat of the northernmost outlet glacier, Glaciar de Jamapa, is recorded by Palacios and Vázquez Selem (1996). No other scientific work on Citlaltépetl glaciers is known, except for an occasional mention in mountaineering journals.

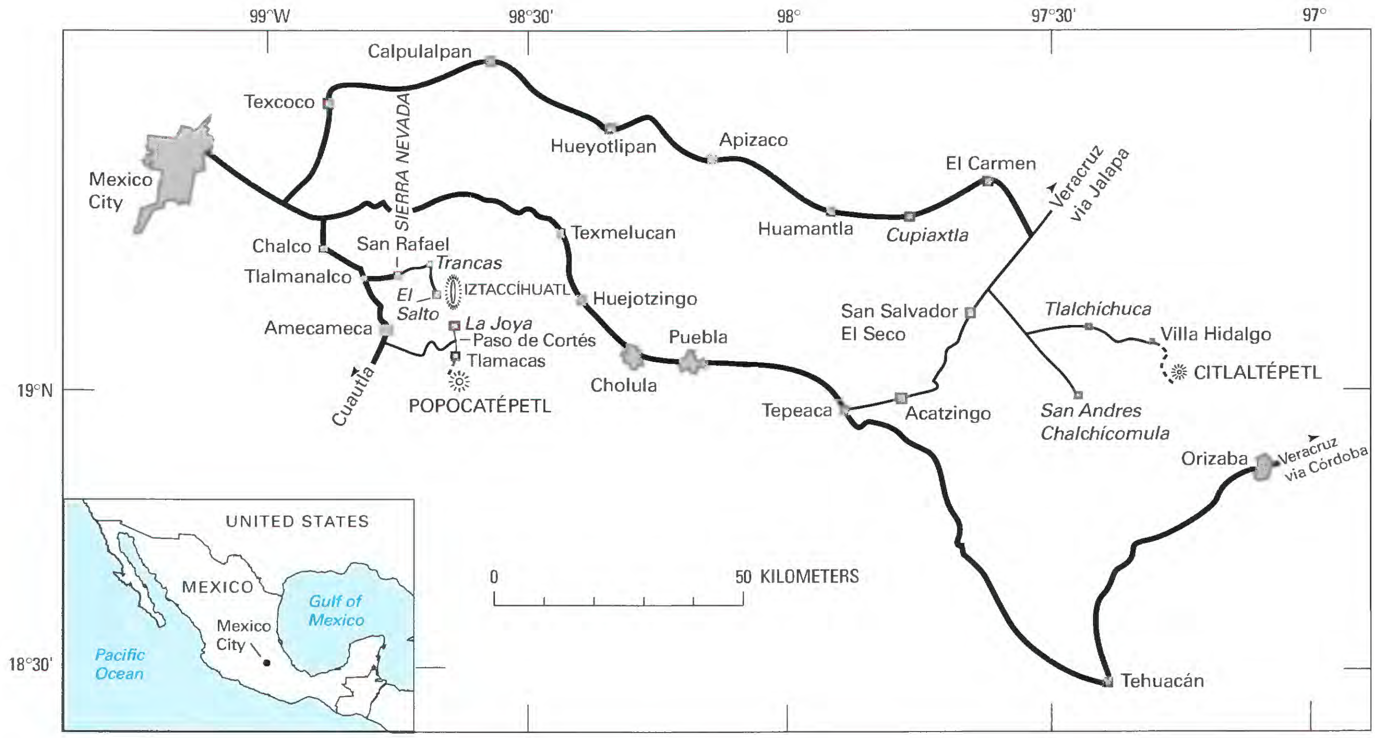

Figure 2.—*Principal overland routes to Citlaltépetl, Iztaccíhuatl, and Popocatépetl. Paved roads are shown in broadest lines; trails, in dashed lines. (Modified from Lorenzo, 1959, sketch II.)*

A temperate, humid climate with periodic rainy seasons, although drier in winter, surrounds Citlaltépetl up to about 4,300 m. Above this, tundra and ice-cap climates prevail to the summit. Heavy snowfall probably occurs both in winter and summer, as it does on the other high volcanoes. Snow falling on the south and southeast sides melts quickly because of solar radiation but persists on the northwest and north sides. Aided by the insolation angle and wind redeposition, the persistent snow cover develops into a huge accumulation area and firn field, which serves as a source for the outlet glaciers.

The entire north side of the upper Citlaltépetl cone is covered by the Gran Glaciar Norte of Lorenzo (1959), which fills an elongate highland basin with near-radial flow and is the source area for seven outlet glaciers (figs. 1 and 3). The main glacier extends 3.5 km north of the crater rim, has a surface area of about 9.08 km^2, and descends from 5,650 m to a little below 5,000 m (Lorenzo, 1964, fig. 12). It has a slightly irregular and stepped profile that is caused in part by the configuration of the bedrock. Most crevasses show an ice thickness of approximately 50 m.

Below the 5,000-m elevation on the north side of the volcano, the outlet glaciers Lengua del Chichimeco and Glaciar de Jamapa extend north and northwest another 1.5 km and 2 km, respectively. The terminal lobe of Lengua del Chichimeco at 4,740 m, having a gradient of only 140 m km^{-1}, is a low, broad ice fan that has a convex-upward profile (Lorenzo, 1964, fig. 10), a front typical of almost all Mexican glaciers. The most distinct glacier is Glaciar de Jamapa, which leaves Gran Glaciar Norte (figs. 1 and 3) at about 4,975 m and, after 2 km with a gradient of 145 m km^{-1}, divides into two small tongues that end at 4,650 m and 4,640 m. Both tongues terminate in broad convex-upward ice fans thinning along their edges (Lorenzo, 1964, figs. 14 and 15). The retreat of these tongues prior to 1994 produced much erosion downstream and buried their edges by ablation rock debris (Palacios and Vázquez Selem, 1996).

The west side of Gran Glaciar Norte generates five outlet glaciers (fig. 1). From north to south, the first two, Glaciar del Toro and Glaciar de la Barba (fig. 3), are hanging cliff or icefall glaciers, reaching the tops of giant lava steps (Lorenzo, 1964, fig. 18) at 4,930 m and 5,090 m, respectively. They then descend 200 to 300 m farther down into the heads of stream valleys as huge ice blocks but are not regenerated there. One kilometer farther south, Glaciar Noroccidental (fig. 3), a small outlet glacier 300 m long (Lorenzo, 1964, figs. 21 and 22), drains away from the side of Gran Glaciar Norte at about 5,100 m and draws down the ice surface a few tens of meters over a distance of 500 m, descending to 4,920 m with a gradient of 255 m km^{-1}. One kilometer still farther south, Glaciar Occidental (fig. 3) breaks away from Gran Glaciar Norte west of the summit crater at about 5,175 m as a steep, 1-km-long glacier (Lorenzo, 1964, figs. 22 and 23) having a gradient of 270 m km^{-1} that ends at 4,930 m. From the southwest corner of the mountain, another outlet glacier, Glaciar Suroccidental, 1.6 km long, flows from Gran Glaciar Norte at 5,250 m (Lorenzo, 1964, figs. 22 and 23) with a gradient of 200 m km^{-1}, which also ends at 4,930 m in a long smooth surface.

East of the summit cone, a separate steep niche glacier, Glaciar Oriental, 1.2 km long and having a gradient of 440 m km^{-1} (fig. 1), flows down the mountainside from about 5,600 m to 5,070 m; it contains many crevasses and seracs (Lorenzo, 1964, figs. 24 and 25) and is the most difficult glacier to climb.

Lorenzo (1964) calculated that Glacier Oriental had a surface area of about 420,000 m^2 in 1958, which makes the total area of glaciers and firn field on Citlaltépetl about 9.5 km^2. No earlier historical record of glacier tongue activity (advance or recession) is known for Citlaltépetl's glaciers.

Figure 4 is a Landsat 1 multispectral scanner (MSS) false-color composite image of Citlaltépetl and environs on 25 May 1973. Although the Gran Glaciar Norte ice cap is covered with snow, it is possible to see the seven outlet glaciers on the irregular west margin of the ice cap, especially Glaciar de Jamapa and Glaciar Occidental. The 79-m picture element (pixel) of the MSS image makes it difficult to delineate the termini of the seven outlet glaciers from the ice cap. Glacier Oriental, the niche glacier on the east, is not discernible in figure 4.

Figure 3.—*Citlaltépetl from the northwest. Gran Glaciar Norte is the high, white cone in the center. Glaciar de Jamapa, one of the seven outlet glaciers from Gran Glaciar Norte, is on the left skyline. The outlet glaciers Glaciar del Toro and Glaciar de la Barba are visible in the center; the outlet glaciers Glaciar Noroccidental and Glaciar Occidental are in the upper right. Oblique aerial photograph taken in February 1942, courtesy of Compañía Mexicana Aerofoto.*

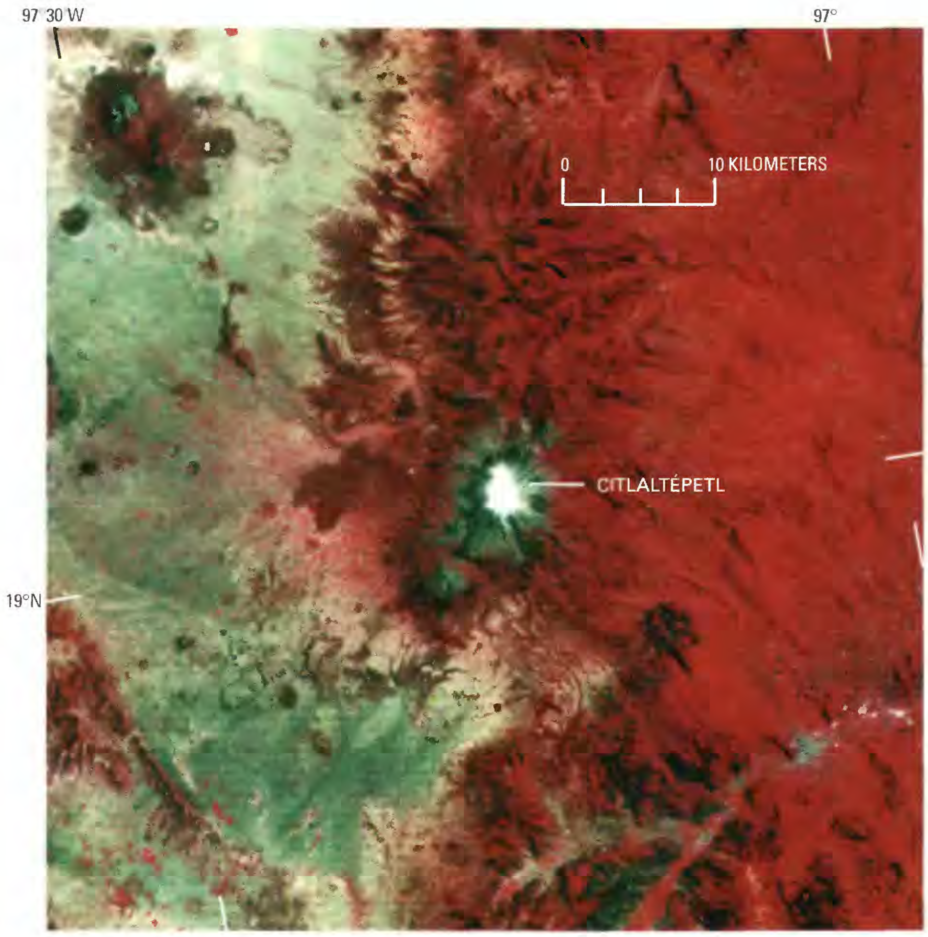

***Figure 4.**—Enlargement of part of a Landsat 1 MSS false-color composite image (1306–16231; 25 May 1973; Path 26, Row 47) of Citlaltépetl and environs. Landsat image from the EROS Data Center, Sioux Falls, S. Dak.*

TABLE 2.—*Twelve named glaciers of Iztaccíhuatl*

[Taken from Lorenzo, 1964, sketch VII]

Glacier number	Glacier name	Glacier type	Area (square kilometers)
I...........	Glaciar de la Cabeza	Mountain, ice cap	0.014
II	Glaciar del Cuello	Mountain, valley	0.050
III	Glaciar de Ayolotepito	Mountain, cirque, valley	0.213
IV	Glacier Norte	Mountain, niche, hanging, interrupted	0.046
V...........	Glaciar del Cráter	Mountain, crater, interrupted, cascading	0.180
VI	Glaciar Oestenoroeste	Mountain, ice cap, hanging	0.050
VII........	Glaciar Nororiental	Mountain, firn field,valley	0.025
VIII.......	Glaciar Centro Oriental	Mountain, firn field, valley	0.245
IX	Glaciar de Ayoloco	Mountain, cirque, valley	0.247
X	Glaciar Sudoriental	Mountain, firn field	0.078
XI	Glaciar Atzintli	Mountain, ice apron	0.058
XII........	Glaciar de San Agustín	Mountain, niche	0.011
		Total	1.217

Volcán Iztaccíhuatl

At 5,230 m (Simkin and Siebert, 1994; previous value was 5,286 m, which is still authoritative and is used as the reference elevation in the text for glacier elevations), Iztaccíhuatl is the third highest peak in México and the seventh highest on the continent. It has 2 firn fields and 12 named glaciers (fig. 5 and table 2). Its name is derived from the Nahuatl words Iztac (white) and cíhuatl (woman). When viewed from the west (fig. 6), the long profile from north to south conjures up the head, neck, chest, stomach, knees, and feet of a recumbent sleeping woman covered with a white shroud. Its name, often misspelled, is incorrectly translated in places. The highest of three summits, *El Pecho*, is situated at lat 19°10'30" N. and long 98°38'30" W. The 12 named glaciers are scattered along a north-south distance of approximately 3 km. Iztaccíhuatl can be seen from Mexico City, lying only 64 km to the southeast

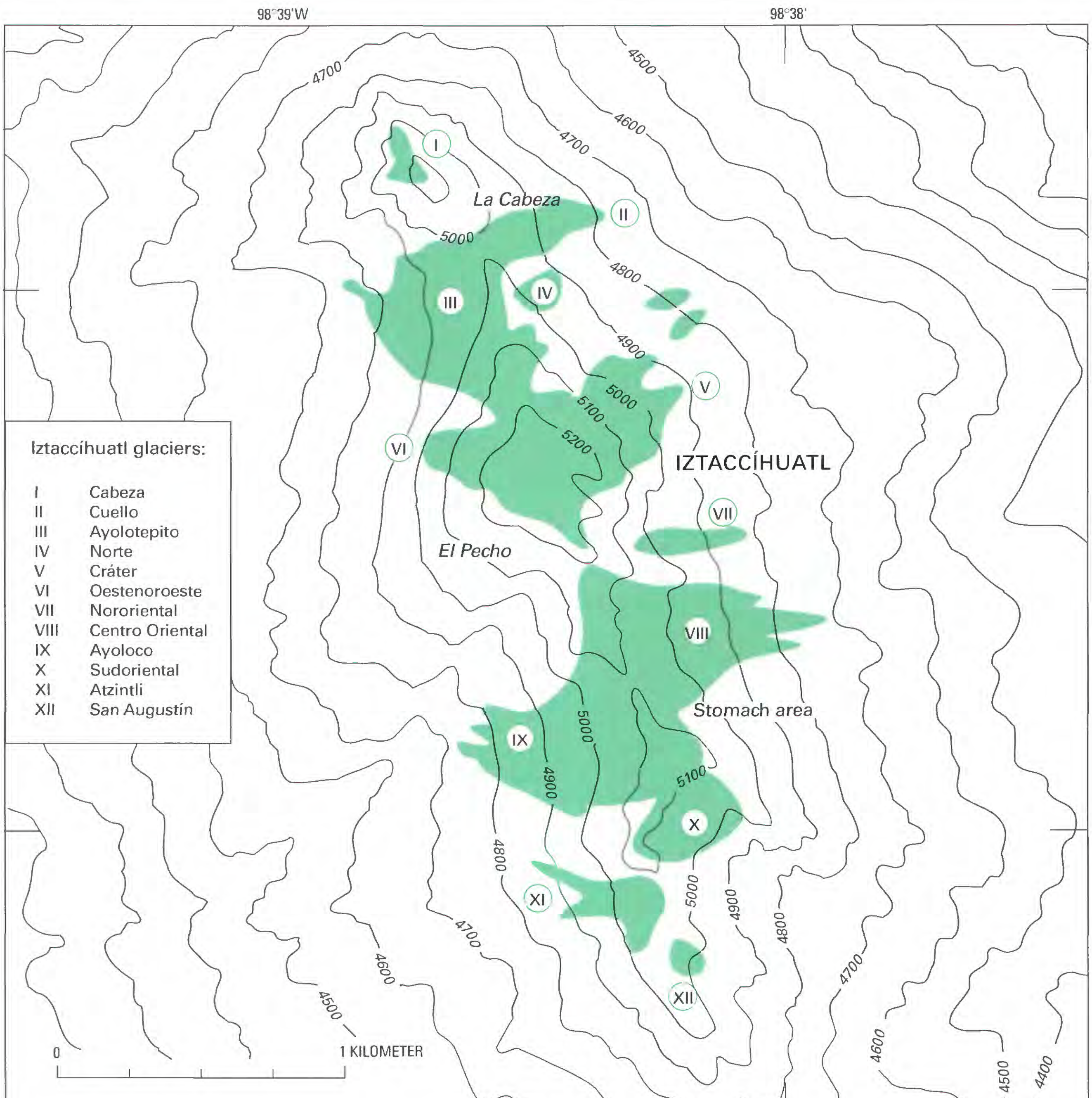

Figure 5.*—Glaciers on Iztaccíhuatl. The numbers refer to the named glaciers listed in table 2. Contour interval, 100 m. (Modified from Lorenzo, 1964, sketch VII.)*

near the southern end of the *Sierra Nevada* (fig. 2). Only one topographic map is needed, Iztaccíhuatl 14Q–h(107), which is sold by the Secretaría de la Defensa Nacional. Vertical aerial photos that have excellent quality and flight-line precision and were taken in 1945 by the Compañía Mexicana Aerofoto are easily purchased; these photographs were used by the company for the preparation of the maps by photogrammetric techniques. Oblique aerial photographs taken in 1942 and more recently are also available from Compañía Mexicana Aerofoto.

The proximity of Iztaccíhuatl to Mexico City and the relative ease in reaching the mountain from both the east and the west enticed many scientists and mountaineers to climb it and to observe the glaciers. Although not recommended, from the east side one may leave the old Mexico City—Puebla Highway at Texmelucan or at Huejotzingo (fig. 2) and drive 5 to 10 km onto the broad east slopes of the range. The field party should be accompanied by Spanish-speaking persons in order to explain its presence in the area. From Mexico City, however, a paved highway via Chalco and Tlalmanalco past the paper factory at San Rafael (fig. 2), a distance of about 50 km, allows access onto the northwestern and western slopes of the mountain by means of mountain roads and four-wheel-drive vehicles. From San Rafael, it is 7 km up to *Trancas* and 6 km more to the end of the road at *El Salto* at 3,750 m. From *El Salto*, the glaciers at 4,770 m and a mountain refuge are only 3 km distant. The route used most by climbers from Mexico City is about 65 km by Chalco and Amecameca up a paved mountain road to Paso de Cortés at 3,680 m, and then north on a poor road 3.5 km to its end at the south end of the mountain at *La Joya*, which is 4,000 m high (fig. 2). From here, the peaks above the glaciers and mountain refuges are reached in 3.5 km by a climber's route above 4,500 m along the crest of high peaks.

The oldest reference to glaciers on Iztaccíhuatl was made by José Antonio de Alzate y Ramírez sometime between 1781 and 1789 (Alzate y Ramírez, 1831; cited in Lorenzo, 1964). Not until 1890 did other reports on the glacier ice appear (Whitehouse, 1890; Heilprin, 1890, who briefly mentioned glaciers on Iztaccíhuatl, including a crevassed one he named the "Porfirio Diaz Glacier," probably Glaciar de Ayoloco). Several scientists discussed cirques on the west side, the glaciers in them, and meteorological factors responsible (Ordóñez, 1894; Farrington, 1897; Böse and Ordóñez, 1901; Brecker, 1908; Melgarejo, 1910; Freudenberg, 1911). The hydroelectric possibilities of glacier meltwater were studied by Paredes (1922), and glaciers and their

Figure 6.*—Iztaccíhuatl from the west. At the far left of the photograph, partly under clouds, is the separate, irregularly eroded Volcán Teyotl. Next is the higher, snow-covered, cliff-encircled peak, La Cabeza, with Glaciar de la Cabeza sloping to the left. The highest ice-covered peak is El Pecho (5,286 m), with the firn field in the "neck" between it and La Cabeza, source of Glaciar de Ayolotepito. The ice-covered peak of El Pecho is Glaciar Oestenoroeste. South of El Pecho (right) is the "stomach area" firn field, source of Glaciar de Ayoloco. Glaciar Atzintli is to the right of the "stomach area," but in the photograph, a recent snowfall joins all into one snowfield. La Joya (fig. 2) is at the right side of the photograph. Oblique aerial photograph taken in February 1942, courtesy of Compañía Mexicana Aerofoto.*

climatic situation, by Jaeger (1925, 1926) and Prister (1927). Robles Ramos (1944) conducted hydrologic and meteorologic studies in 1942 on the west side and related glacier melting to streamflow. De Terra (1947), De Terra and others (1949), White (1962, 1981a), and Vázquez-Selem and Phillips (1998), discussed the glaciers in relation to former glaciations.

According to Vázquez-Selem and Phillips (1998), the glacial deposits on Iztaccíhuatl volcano provide the "most complete record of [past] glaciation of central México." Their glacial chronology is based on dating moraines with the ^{36}Cl cosmogenic isotope and tephra from Popocatépetl. The Nexcoalango moraines at 3,100 m described by White (1962) are dated at between 151 and 126 Ka [marine isotope stage (MIS) 6]; the Hueyatlaco Moraines of White (1962), associated with the last global glacier maximum (LGGM), are dated at 20 to 14 Ka. A major deglaciation of Iztaccíhuatl started at 14–13 Ka; Little Ice Age (LIA) moraines are located at 4,300 to 4,700 m.

The elevations of 3 glacier termini in 1953 and 1955 appeared in White (1956), and the elevations of all 12 glaciers in 1959–60, in Lorenzo (1964). The best account by far of Iztaccíhuatl glaciers is that by Lorenzo and his colleagues.

A temperate-rainy climate with no conspicuous dry season encircles the lower slopes of the *Sierra Nevada* and the upper flanks of Iztaccíhuatl to about 4,000 m. Although rain falls every month, summer is the wettest and winter is the driest time of year. Snow falls as low as 4,000 m from November through January. Above 4,000 m are tundra and ice-cap climates. Snow accumulates on all slopes above 4,500 m not only in winter but also from June through middle-August. The volume of precipitation apparently decreases markedly above 4,000 m, but no record of rainfall and snowfall is known for the upper mountain slopes. The 5.8-km-long north-south axis of Iztaccíhuatl plus the location, orientation, and elevation of the highest peaks affect local wind directions during snowfall and provide protection from insolation. On the basis of all these factors, accumulation areas of firn develop above 5,000 m and serve as the source area for 8 of the 12 glaciers. Vázquez Selem (1989), however, in his study of periglacial features, discovered ice cores covered with detritus in the rock glaciers at about 4,400 m on the north side of the peak of Volcán Teyotl (fig. 6), a lower, much-eroded volcano north of Iztaccíhuatl. Small firn fields and ice glaciers existed there during the most recent neoglaciation, but they are now melted.

Most Iztaccíhuatl glaciers originate above the 5,000-m elevation in simple basins and become short, cascading mountain glaciers. Two on the west side, Glaciar de Ayolotepito and Glaciar de Ayoloco (fig. 6), are thickest in cirquelike valley heads. They are neoglacial remnants and have huge early neoglacial moraines and four small inner moraines in front of the ice (White, 1956), probably all built within the last 3,000 years. Three glaciers start from a high transection firn field that has flow both to the east and west (Glacier del Cuello, Glaciar de Ayolotepito, and Glaciar Norte), and two start from *El Pecho* (Glaciar del Cráter and Glaciar Oestenoroeste). Glaciar del Cráter on *El Pecho* occupies a now-dormant crater, although it was active as recently as post-early neoglaciation, possibly between 3,000 and 2,500 years ago. Because the early neoglacial moraines are covered with volcanic scoria from the now-dormant crater, scoria that has been verified petrographically, this suggests that the volcano should be considered to be dormant rather than extinct. The descriptions and measurements of Iztaccíhuatl glaciers that follow are from Lorenzo (1964), plus information added from White (1956) and White's unpublished fieldwork.

Glaciar de la Cabeza is a thin lens of ice of 14,400 m^2 on the northwest summit of *La Cabeza* and extends only 200 m northwest from about 5,145 m to slightly lower than 5,000 m (figs. 5 and 6; Lorenzo, 1964, fig. 48). It stops above cliffs, but during neoglaciation, it regenerated at the cliff bottom and built moraines north of *La Cabeza*.

Glacier del Cuello flows east from the transection firn field occupying the "neck" (Cuello). Beginning at 4,990 m, it extends 550 m to 4,760 m on a gradient of 420 m km^{-1} (Lorenzo, 1964, fig. 49), covers about 50,000 m^2, and enters a valley on the northeast side of Iztaccíhuatl. Glaciar de Ayolotepito originates from the same firn field, also at 4,990 m, and, in part, from a firn field on the north side of *El Pecho* at 5,250 m (figs. 5 and 6). It turns to the west 900 m from the summit area down into the cirquelike Ayolotepito valley head, where it has a gradient of 520 m km^{-1}. In 1959–60 it terminated at 4,760 m (Lorenzo, 1964, figs. 40 and 50) and occupied 212,500 m^2, but in 1953, it ended at about 4,670 m (White, 1956). Thus, it had retreated 90 m in elevation and about 125 m in distance in the 6 to 7 years, or about 19 m a^{-1}. If the accuracy of a barometer used by Böse and Ordóñez (1901) in November 1898 is reliable, then the terminus of Glaciar de Ayolotepito at 4,610 m had receded only 150 m in elevation or about 460 m distance in the 61 to 62 years since they visited the mountain. This is a rate of retreat of about 7 m a^{-1}, much slower than the retreat between 1953 and 1959–60. The third glacier developed from the Cuello firn field and north side of *El Pecho* is Glaciar Norte. It is a small hanging glacier totaling 46,200 m^2 that flows northeast from *El Pecho* at 5,250 m, down to cliff tops at 5,050 m, where it is interrupted. It regenerates below the cliffs at 5,010 m and, as a broad tongue, runs down to 4,910 m (Lorenzo, 1964, figs. 43, 51, 52).

Glaciar del Cráter starts on *El Pecho* at 5,286 m and cascades as a cliff glacier northeast, breaking into chaotic icefalls on a gradient of 755 m km^{-1} to 4,965 m, where it bifurcates into two lobes (Lorenzo, 1964, figs. 52 and 53). The longer northeast tongue continues to 4,890 m, where it is interrupted by cliffs and regenerates below in isolated masses extending to 4,750 m and 4,770 m. The shorter east tongue of accumulated ice blocks and great seracs ends above cliffs at 4,910 m. The whole Glaciar del Cráter covers about 179,500 m^2. On the northwest side of *El Pecho*, another cliff glacier, Glaciar Oestenoroeste (fig. 6), also descends from the mountaintop at 5,286 m to 5,010 m on a gradient of 835 m km^{-1} and covers about 50,000 m^2 (Lorenzo, 1964, fig. 54). The subdivision of this glacier system north of *El Pecho*, including the Cuello firn field and up to the top of *El Pecho*, is based on ice-surface topography and not on direction of ice movement. Southeast of *El Pecho* and separate from any other ice body is a small 400-m-long firn field of 25,000 m^2 sloping east from 5,060 m to 4,830 m, named Glaciar Nororiental (Lorenzo, 1964, fig 55).

A second high-transection firn field that produces a glacier system lies 0.5 to 1 km south of *El Pecho* above 5,000 m in the stomach area of Iztaccíhuatl (fig. 5). Glaciar Centro Oriental, which flows to the east, has as its source about 45,000 m^2 of firn on the ridge southeast of *El Pecho*. It drops from 5,190 m to 4,850 m, with a gradient of 550 m km^{-1} and is about 0.5 km wide and long. Its terminus divides into three lobes; the longest and lowest lobe ends at 4,715 m. The whole glacier covers about 245,000 m^2 (Lorenzo, 1964, fig. 56).

On the west side of the same ridge, and including about 50,000 m^2 of firn as its source, is the largest and best known glacier in México, Glaciar de Ayoloco, occupying in 1959–60 about 247,000 m^2. In almost all early reports of glacier ice on Iztaccíhuatl, it was Glaciar de Ayoloco that was observed (fig. 6). In 1959–60 it was approximately 0.5 km wide at its head between two high rock buttresses, *Peña Ordóñez* and *Peña Aguilera*, and had seracs, crevasses about 50 m deep, and an irregular bumpy surface (Lorenzo, 1964, fig. 57). Glaciar de Ayoloco descends a distance of 625 m from 5,190 m to 4,725 m on a gradient of 745 m km^{-1}. In 1955, the glacier ended at 4,668 m (White, 1956, table 1) and thus, to reach Lorenzo's 1959–60 position, had retreated 57 m in elevation and about 100 m in distance in the intervening 4 to 5 years, an average rate of about 22 m a^{-1}. However, comparison of the position of Glaciar de Ayoloco in a photograph taken 1 November 1898 (Böse and Ordóñez, 1901, fig. 2) with photographs taken at the same site by Lorenzo shows the terminus at White's 4,465-m (third) inner stadial moraine. This gives a retreat of about 260 m in elevation, about 810 m in distance, and an average rate of retreat about 13 m a^{-1} in the 61 to 62 years. A photograph in Melgarejo (1910, no. 8), presumably taken in the summer of 1910, shows the terminus of Glaciar de Ayoloco about at White's 4,540-m (fourth) inner stadial moraine (White, 1956, table 1). Vertical aerial photographs taken in November 1945 reveal a thin ice tongue at about 4,560 m, perhaps no longer active due to its tenuity in a protected position below a high rock ridge on the Ayoloco valley-head bottom, about 260 m downvalley from its 1955 position. On the other hand, Böse and Ordóñez (1901) obtained a November 1898 barometric elevation for Glaciar de Ayoloco of 4,545 m. If this elevation is accurate, then in 61 to 62 years, the glacier receded 180 m in elevation and about 475 m in distance compared to Lorenzo's position, or at an average rate of about 8 m a^{-1}. This is a much slower rate than that between 1955 and 1959–60, although it is quite consistent with the average rate of retreat of the Glaciar de Ayolotepito during the same period. From all these historic fluctuations, however disparate, it is evident that Glaciar de Ayoloco has been continuously retreating since the 1890's.

A third glacier also of this stomach-area system is Glaciar Sudoriental which has an area of about 77,500 m^2. It is moving toward the southeast, is only about 270 m long, and descends from about 5,110 m to 4,990 m (Lorenzo, 1964, fig. 58) on a gradient of 445 m km^{-1}.

Based on photographic documentation, Glaciar de Ayoloco and the next glacier 200 m to the south, prior to 1918, had been all one glacier, but in 1953, White realized that a name was needed for this small, separate, thin ice mass. Following the suggestion of José Luis Lorenzo, it was named Atzintli Glacier (White, 1956, p. 294). Glaciar Atzintli, now isolated south of the stomach area (figs. 5 and 6), was only 460 m long in 1959–60, starting at 5,085 m and ending at 4,855 m. It had an area of 57,500 m^2 (Lorenzo, 1964, figs. 40, 41, 59) and a gradient of 500 m km^{-1}. In 1953, its terminus had been at 4,785 m (White, 1956, table 1), which indicates a recession of 70 m in elevation over a 140 m distance, or about 21 m a^{-1} in the 6 to 7 years, similar to the retreat rate of 22 m a^{-1} for Glaciar de Ayoloco during the same period. As documented in a photograph that had Glaciar de Ayoloco in the foreground (Melgarejo, 1910, no. 1), glacier ice surrounding *Peña Aguilera* had not yet separated into two glaciers by the summer of 1910. In views from the same photographic site, glacier ice still surrounded *Peña Aguilera* by the summer of 1918 (Paredes, 1922, figs. 11, 17, and 18). Other long-distance photographs also show one large glacier on the west side of the stomach area in 1910 (Melgarejo, 1910, no. 5; after Hugo Brehme of Mexico City). A photograph taken in April 1946, before the ablation season began, shows the possible initiation of separation into two glaciers (De Terra and others, 1949, plate 20). Historic records of the elevations of Glaciar Atzintli are not known.

Glaciar de San Agustín, which has an area of about 11,250 m^2, is a remnant of a once much larger niche glacier on the southeast side of the stomach area. It begins about 80 m east of the 5,070 m ridgecrest at 5,030 m and ends about 100 m to the southeast at 4,980 m (Lorenzo, 1964, fig. 41). The total area covered by all 12 glaciers on Iztaccíhuatl in 1959–60 was 1,215,850 m^2, about one-eighth that of the glaciers on Citlaltépetl.

Figure 7 is an enlargement of a Landsat 1 MSS false-color composite image of Iztaccíhuatl and vicinity on 7 February 1973. Although not all of the 12 named glaciers on Iztaccíhuatl can be delineated because of the spatial resolution limitations of the MSS image and because of snow cover, the three largest glaciers, Glaciar de Ayolotepito, Glaciar Centro Oriental, and Glaciar de Ayoloco can be distinguished (table 2 and fig. 5).

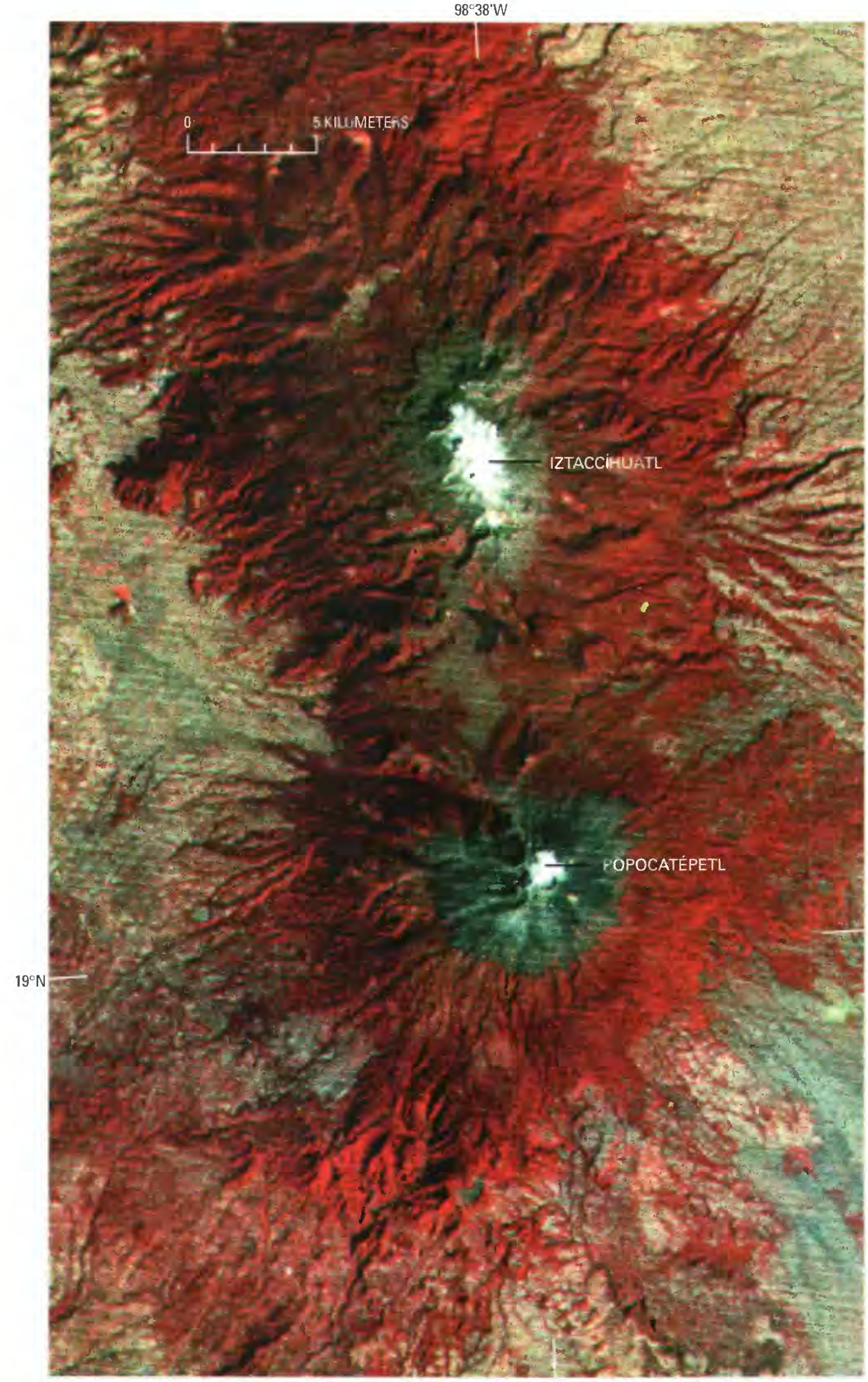

Figure 7.—*Enlargement of a Landsat 1 MSS false-color composite image (1199–16285; 7 February 1973; Path 27, Row 47) of Iztaccíhuatl and Popocatépetl and environs. Landsat image from the EROS Data Center, Sioux Falls, S. Dak.*

Volcán Popocatépetl

At 5,465 m (Simkin and Siebert, 1994; previous value was 5,452 m, which is used as the reference elevation in the text for glacier elevations), Popocatépetl is the second highest peak in México and the fifth highest on the continent. It is one of the Earth's highest active volcanoes and 20 million people live within a radius of 80 km from its summit (Williams, 1999). Since 1993, intermittent explosive and occasional effusive volcanic activity has occurred from the summit of Popocatépetl (Smithsonian Institution, 1994, 1995, 1996 1997, 1998, 1999, 2000). It has one firn field that has three small glaciers flowing to the north (figs. 8 and 9 and table 3). The name is derived from the Nahuatl words, Popoca (smoking) and tépetl (mountain). The west crater rim is the highest point and is situated at lat 19°01'15" N. and long 98°37'35" W. Only 72 km southeast of Mexico City and fully visible, Popocatépetl forms the southern end of the *Sierra Nevada* at the southern geologic boundary of the North American Continent. Two Secretaría de la Defensa Nacional topographic maps are needed to provide complete coverage: Popocatépetl 14Q–h(123) and Xalinatzintla 14Q–h(124). Vertical aerial photographs taken in 1945 by Compañía Mexicana Aerofoto are available, as are oblique aerial photographs taken in 1942 and more recently by the same company.

Figure 8.—Glaciers on Popocatépetl. The numbers refer to the named glaciers listed in table 3. Contour interval, 100 m. (Modified from Lorenzo, 1964, sketch V.)

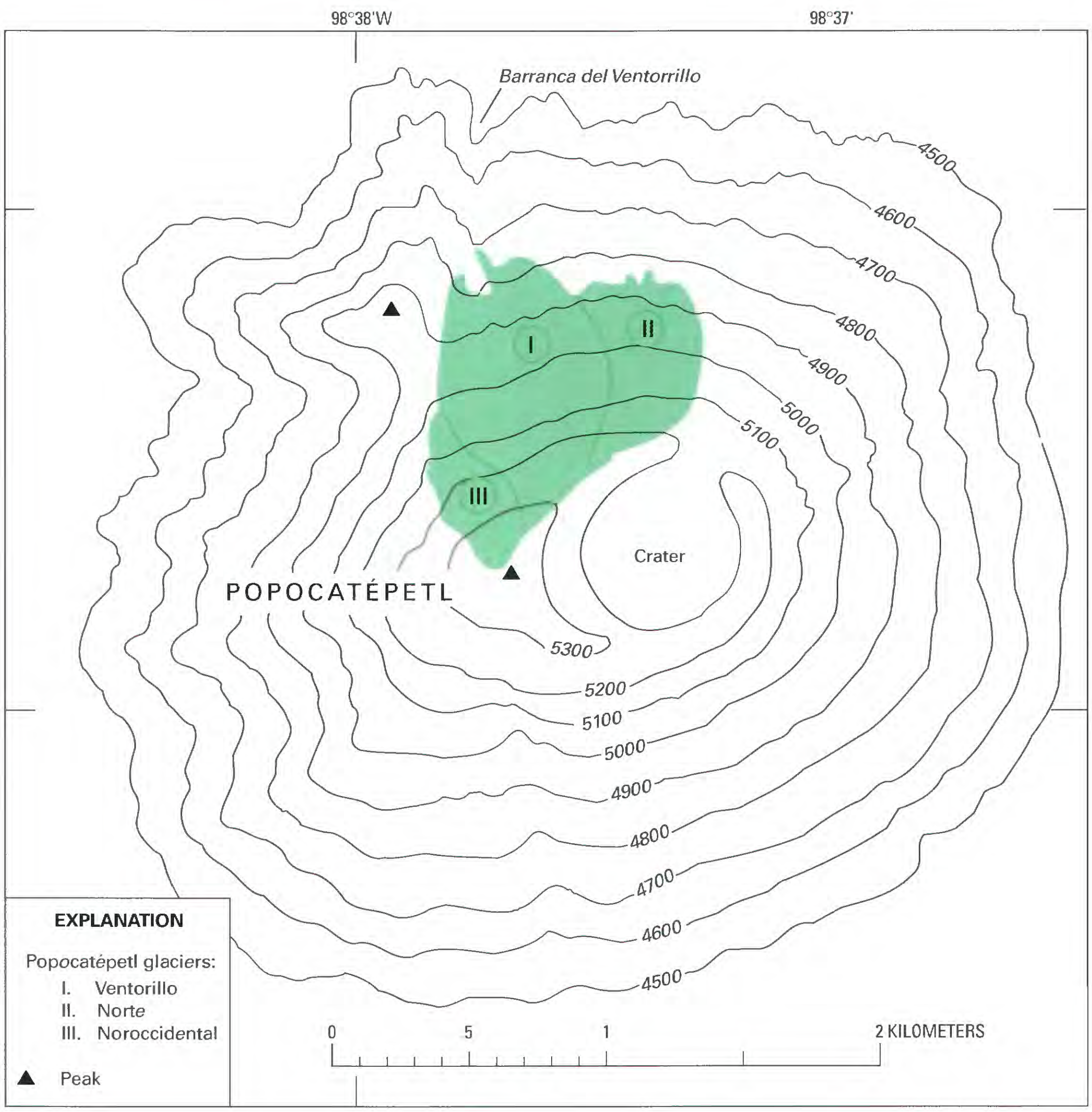

TABLE 3.—*Three named glaciers of Popocatépetl*
[Taken from Lorenzo, 1964, Sketch V]

Glacier number	Glacier name	Glacier type	Area (square kilometers)
I..................	Glaciar del Ventorrillo	Mountain, firn field, valley	0.400
II..................	Glaciar Norte	Mountain, firn field	0.200
III	Glaciar Noroccidental	Mountain, firn field	0.120
		Total	0.720

The relative ease with which one can reach a reasonable elevation on Popocatépetl in order to start the ascent to the summit crater has always made this active volcano readily accessible. The best route is 65 km from Mexico City by Chalco, Amecameca, and up the paved mountain road to Paso de Cortés [*Paso Cortés*] at 3,680 m and then south on an excellent road 4.5 km to end at Tlamacas at 3,882 m (fig. 2) and a luxurious mountain lodge that has all facilities. Several mountain refuges are located higher up along the climbing routes on the north side. The road south of *Paso Cortés* and the refuges are closed and off limits because of the potential danger of the intermittent explosive and effusive volcanic eruptions that have been occurring from the summit crater since 1993, after a long period of quiescence since the 1940's (Smithsonian Institution 1997, no. 10). An attempt to climb Popocatépetl from the west or south sides is very difficult because from south of Amecameca, one must climb 1,700 m up the west side to 200- to 300-m-high vertical lava cliffs, which are still 1,200 m below the summit. From the south side, the climb requires a vertical ascent of 4,400 m. Any ascent from the east side from Cholula or Puebla (fig. 2) involves an ascent of about 2,300 m to the east rim at 5,193 m that also is not recommended.

Observations on the firn field and glaciers on Popocatépetl did not appear in climber's reports until the last part of the 1800's (Dollfus and others, 1867; Packard, 1886; Aguilera and Ordóñez, 1895; and Farrington, 1897), although its existence was known as early as 1519 through the writing of the historian Prescott (1872–75). During eruptions in 1920–22, glacier ice did not completely disappear because it was in a protected position in *Barranca del Ventorrillo* on the north side of the cone (Waitz, 1921) (fig. 8). White (1954) described the firn field and the glacier ice and gave elevations of one small ice tongue for 1950 and 1953. Lorenzo (1959, 1964) and his team obtained data on glacier activity, areas, and elevations, took photographs, and named the three glaciers. Much of the information that follows is from White (1954, 1981b).

A warm temperate-rainy climate without any obvious dry season rings Popocatépetl to about 3,880 m. December through March is the driest time of year; summers are short and cool on the north and west sides. September is the rainiest month, but rain falls nightly in late June and July. Valleys leaving this area carry no perennial streams from the porous and permeable slopes above. A narrow band of tundra climate circles the volcano above 3,880 m up to the ice-cap climate of the firn field and glaciers. Winter accumulation added to that of summer enables the firn field to flourish on the upper cone. The loss of firn and new snow from melting increases from January through May, the greatest loss being in May. Greater cloudiness and new snow reduce melting in June through December, except for October, when skies are clearer and precipitation is less. Maximum evaporation on the upper cone takes place from March through May. Penitentes (conical or irregularly shaped pillars of snow and ice formed by differential ablation) appear all over the cone by May (White, 1954, fig. 5). Owing to summer cloudiness, the least evaporation takes place from July through September.

The firn field on the north, northwest, and west sides of the upper cone generates three glaciers downslope, Glaciar Norte above the north volcano flanks, Glaciar del Ventorrillo in *Barranca del Ventorrillo*, and Glaciar Noroccidental above the west side cliffs (fig. 8). In 1950, the lower limit of Glaciar Norte (not recognized then as a glacier) was estimated as about 4,800 m. Lorenzo in 1958 recorded it on the convex north cone from about 5,250 m down to 4,840 m (Lorenzo, 1964, figs. 26 and 27), but he noted that it was only the remnant of a glacier. From Lorenzo's map (fig. 8), Glaciar Norte, as he then subdivided the firn field, is about 600 m long, has a gradient of 600 m km^{-1}, and covers about 200,000 m^2 of the cone.

The fluctuation of Glaciar del Ventorrillo is more significant in determining the history of the Popocatépetl firn field and glaciers. The 1945 aerial photographs show no expansion of the Ventorrillo firn edge as glaciers, but by 1949, two conspicuous but small ice tongues extended into the head of *Barranca del Ventorrillo* (White, 1954, fig. 2). In 1950, the lower ice tongue was measured as 4,573 m; in 1953, it had melted back 4 m in elevation (White, 1954, fig. 4), and in 1958, Lorenzo (1964) found it at about 4,690 m. This is a recession of 117 m in elevation over a distance of about 270 m, an average rate of retreat of about 34 m a^{-1} in the 8-year interval. After 1958, the small ice tongue disappeared. In 1958, the glacier began below the north crater rim at about 5,200 m, was about 800 m long on a gradient of 640 m km^{-1}, and occupied about 400,000 m^2 of the cone (Lorenzo, 1964, figs. 26, 29, 30). This steep gradient pulls the ice apart to form huge crevasses (fig. 9). Ice on the cone above Glaciar del Ventorrillo above 5,030 m was about 40 m thick in 1951 and about 30 m thick in 1958.

Glaciar Noroccidental is the western counterpart of the other two glacier extensions of the firn field, becoming distinguished as a glacier at about 5,300 m. It ends above the lava cliffs at 5,015 m, is 440 m long on a gradient of 430 m km^{-1}, and occupies 120,000 m^2 of the cone (Lorenzo, 1964, figs. 29 and 31). In 1958, the Popocatépetl firn field and glaciers totaled only 720,000 m^2, about half that of Iztaccíhuatl glaciers. At the time of Lorenzo's measurements, all of Mexico's firn fields and glaciers covered about 11.4 km^2.

The firn field on Popocatépetl undoubtedly did not survive the "Hypsithermal Interval." Yet historic Toltec and Aztec sketches of the mountains depict much ice and snow on both Iztaccíhuatl and Popocatépetl. Cortes' captains had great difficulty crossing the perpetual snows of the Popocatépetl cone in 1519. Packard (1886) stated that in 1885 a stream flowing in the largest valley on the north side of the mountain was "fed by the snows

Figure 9.*—Popocatépetl from the north at Tlamacas (fig. 2). A permanent firn field exists above the arcuate crevasses and icefall. Glaciar Norte is on the cone under recent snowfall above the leftmost tree. The reactivated Glaciar del Ventorrillo is visible below the crevasses as a double-lobed glacier hanging down from the cone into Barranca del Ventorrillo. Glaciar Noroccidental is on the cone at the right edge of the firn field above a sloping, castellated rock crag. Photograph taken 23 March 1978 by M.L. White.*

of the peak." No stream flows there today, even with the huge firn field above, except on sunny days when it is melting. When Anderson (1917) climbed Popocatépetl in 1906, he found a glacier in *Barranca del Ventorrillo* down to nearly 4,335 m, as estimated from his photograph (Anderson, 1917, plate XXV). Because of the clarity of detail, photographs taken in 1910 by Hugo Brehme of Mexico City disclose the glacier in *Barranca del Ventorrillo* to be at a position estimated at 4,390 m. Melgarejo's photograph (1910, no. 2), taken from Brehme's photographic site, shows the glacier at this same elevation. Weitzberg (1923, photograph 8) pictures the glacier just before the 1920–21 eruptions at about 4,435 m. In addition, Brehme's other 1910 photographs reveal thick ice or firn on the west flanks of Popocatépetl below the lava cliffs beneath Glaciar Noroccidental at approximately 4,700 m, as well as at about 4,650 m on the flanks due west of the highest summit, places where no ice or firn exists at the time of this writing.

The 100-m recession in elevation of Glaciar del Ventorrillo from 1906 to 1920 agrees with field evidence of fresh striations and glacial polish on bedrock knobs down to 4,440 m and with weathered, disintegrated, striated bedrock below 4,335 m down to 4,236 m (White, 1954). Although quite speculative and without accurate dating control, the position where Anderson found the glacier in 1906 may match the retreat from the late-neoglacial Arapaho Peak advance (Benedict, 1973) of the southern and middle Rocky Mountains in the United States. Evidence of a still older advance, certainly prior to 1519 and possibly matching the middle-neoglacial Audubon advance of the Rocky Mountains, exists where *Barranca del Ventorrillo* emerges from the steeper part of the cone (fig. 9). Here, and 100 to 200 m beyond on the gentler north flanks to 4,150 m, are striated and polished but weathered surfaces on lava flows, an end moraine almost crossing the valley floor of *Barranca del Ventorrillo*, an inner lateral moraine on the east side of the valley, and striated blocks in the tephra of a dissected alluvial fan 10 to 100 m north of the end moraine (White, 1954).

When Waitz (1921) climbed Popocatépetl in early 1921 during an eruption, he saw the glacier still well preserved in *Barranca del Ventorrillo*. He attributed this preservation to the glacier's sheltered position and the thickness of volcanic deposits on this side of the cone. Waitz estimated that the glacier then reached to about 4,800 m. How much of the recession from the 4,435 m position in 1920, estimated from Weitzberg's (1923) pictures, is due to the 1920–21 volcanic activity is not known, but growth again since 1921 down to 4,573 m in 1950 attests to a healthy positive mass balance for those 30 years. The rapid recession of 117 m in elevation from 1950 to 1958 suggests a sudden change to a negative mass balance.

The activity of the firn field on the cone above Glaciar del Ventorrillo is revealed by a 37-year study of the appearance and disappearance of crevasses. No crevasses were visible on the oblique aerial photographs of the firn field in 1942. Vertical aerial photographs taken in November 1945 show only one crevasse about 225 m long. By July 1949, four crevasses about 300 to 400 m long had appeared and were accompanied by several smaller ones. By August 1950, all but two of the larger crevasses had disappeared because of snow infilling. By May 1953, no new crevasses had appeared, and all the old ones were nearly filled by snow. By April 1955, the small ice tongues of Glaciar del Ventorrillo had retreated high onto the cone, the old but unopened crevasses of 1950 still showed, and a new set of short, en echelon crevasses had opened between Glaciar Noroccidental and the west edge of upper Glaciar del Ventorrillo. By August 1956, one new crevasse above the healed 1950 crevasses and four new ones had opened up at the head of Glaciar del Ventorrillo, and the 1955 en echelon set was being filled by snow. The firn edge above the position where the small ice tongue had been since 1949 was so thin that many rocks showed through in 1956. The set of en echelon crevasses between Glaciar del Ventorrillo and Glaciar Noroccidental appears in Lorenzo's figure 31 that he prepared in 1958 (Lorenzo, 1964). By November 1968, three partially snow-filled crevasses on the north crater rim and one several hundred meters lower down had formed above the head of Glaciar del Ventorrillo. As a result of this crevasse study, no doubt exists as to the activity of the firn field and the importance of that gradient of 640 m km^{-1} on the northwest side of the cone.

The most significant change that took place in the 10 years between 1958 and 1968 was the growth of a thick bulge of ice down into *Barranca del Ventorrillo* in the same location as the small ice tongue of 1949–58. From the 1968 photos, its lower limit is estimated at about 4,700 m and its thickness at about 30 to 40 m. By March 1978, this large bulge of ice became a broad, lobed glacier (fig. 9), probably 70 to 100 m thick, extending from the former position of Glaciar Norte to a double-lobed glacier in *Barranca del Ventorrillo* at an estimated elevation of 4,600 m. Stratification, possibly annual, of the lobes of ice reveals at least 10 layers. In the 10 years following 1968, strong drawdown by this double-lobed glacier produced four or five deep, wide crevasses just above its head and a chaotic icefall of seracs on the cone. In August 1979, the sides of this double-lobed glacier appeared as 50-m-high vertical cliffs, except where the lowest lobe at 4,600 m projected as a steep ramp into *Barranca del Ventorrillo*. A few tens of meters below the crater rim, a new, long crevasse also cut across the cone. In 1984, French volcanologists recorded the continuing existence of this same double-lobed glacier and its vertical cliffs (Christian Boudal, letter dated 24 September 1984).

Glaciar del Ventorrillo has continued to retreat because of heating, sulfur dioxide gas flux, spasmodic fumarolic activity of the volcano, and tephra falls from the main crater. The area of glaciers on the north flanks already had diminished by 24 percent from 1958 to 1982 (Delgado and Brugman, 1995; Palacios, 1996; Smithsonian Institution, 1994, 1995, 1996, 1997). Estimations of the elevation of the glacier front made by Hugo Delgado are in Palacios (1996, table 1): in 1989 at 4,680 m, in 1992 at 4,694 m, and in 1993 at 4,702 m. Palacios (1996), on the basis of his field measurements, found the glacier front in February 1994 at 4,713 m and in November 1995 at 4,735 m, as is clearly shown on his map. Delgado and Brugman (1995) measured it in April 1995 at 4,879 m. Their rate of recession between 1982 and 1995 was 7.6 m a^{-1}. Palacios and Marcos (1998) noted that Pópocatépetl's glaciers had undergone significant retreat during the 1980's and early 1990's, a process that accelerated between 1994 and 1995.

In 1993, Popocatépetl awakened from a long period of quiescence. Since 1345, it has had 30 observed eruptions. In the 20th century, it has been active in 1920–1922, 1923–1924, 1933, 1942–1943, and 1947 (Smithsonian Institution, 1997, no. 10).

On 5 March 1996, tephra dropped over the north flank and covered the snow and glaciers there; this occurred also on 30 April and again on 28–29 October 1996 (Smithsonian Institution, 1996, no. 4, 10; 1997, no. 3).

In 1997, on 20 March and 24 and 29 April, tephra was blown to 4 km above the summit and fell on the glaciers on the north slopes; one of the most violent eruptions in the past three years threw tephra all over the volcano as well as far to the east on 11 May (Smithsonian Institution, 1997, no. 4). The amount of glacier recession and ice melted by hot tephra after such events is unknown. On June 1997, the largest tephra emission of the 1994-97 eruption occurred; several large tephra emissions had also taken place earlier during May and June.

Between June 1997 and June 1999, Popocatépetl experienced an increase in seismic activity and intermittent periods of explosive and occasional effusive volcanic activity from it steep-walled, 250 m-deep summit crater (Smithsonian Institution, 1998, nos. 1, 2, 5, 6, 8, 10, 12; 1999, nos. 1, 3, 4, 6). The Centro Nacional de Prevención de Desastres (CENAPRED), Universidad Nacional Autonoma de México (UNAM), sends periodic reports to the Smithsonian Institution that are published in the monthly bulletin of the Global Volcanism Network. Up-to-date information from CENAPRED about Popocatépetl volcanic activity can be obtained from their Web site [http://www.cenapred.unam.mx/] under the heading: Boletines and Boletin del Volcán Popocatépetl. The largest explosive event during this period occurred on 20 June 1997, when a 13-km-high column of tephra arose from the summit crater. This eruption had no observable effect on Popocatépetl's glaciers (Smithsonian Institution, 1997, no. 10). However, a closer inspection in January 1998 (Sheridan and others, 2001) revealed that "...the glaciers showed noticeable ablation and lacked marginal ice cliffs that had been observed in 1995." Sheridan and others (2001) also referenced floods that originated from the terminus of Glaciar Ventorillo on 1 July 1997, that must have resulted from melting of glacier ice. In late February and early March 1999, the glaciers were observed to be partially blanketed with tephra; impacts from the December 1998 activity were visible, and runoff from melting ice and snow was evident (Smithsonian Institution, 1999, no. 3). On 15 May 1999, the increase in activity was accompanied by runoff of meltwater (Smithsonian Institution, 1999, no. 5). Low-level activity continued during July into the first part of October 1999, including occasional low-magnitude microseismic and/or tectonic events and tephra plumes and falls on 1, 5, and 29 September, and a 4-km high tephra column on 3 October 1999 (Smithsonian Institution, 1999, no. 9). On 25 February 2000, a small block-lava dome was observed to be growing in the center of the summit crater (Smithsonian Institution, 2000, no. 1). In summer 2000, two small mudflows were noted on 23 and 24 June 2000, and tephra plumes and falls took place on 3, 4, and 14 July 2000, and on 4 and 10 August 2000. The 4 August 2000 explosive event was the largest, producing a 5-km high tephra column and tephra falls on several nearby towns (Smithsonian, 2000, no. 7). Additional explosive events were reported in October 2000 (Smithsonian, 2000, no. 10). In December 2000 and January 2001, additional tephra columns were reported; on 29 January 2001, flows of pyroclastics caused some melting of glacier ice (Smithsonian, 2000, no. 12). The long-term impact by the volcanic activity on the mass-balance of Popocatépetl's glaciers must await the cessation of its currently active phase. Research by Sheridan and others (2001) stated that the glacier ice on Popocatépetl covered an area of 0.559 km^2 in April 1995; radio-echo-sounding surveys showed a volume of 2.8×10^7 m^3 of glacier ice. They postulated that about one-third of the volume ($\sim 1 \times 10^7$ m^3) was available for melting, primarily by ablation from pyroclastic flows. Lorenzo (1964) calculated an area of 0.720 km^2 (Table 3), so the loss of area is 0.161 km^2 or about 22 percent.

Figure 7 is an enlargement of a Landsat 1 MSS false-color composite image of Popocatépetl and vicinity on 7 February 1973. The three named glaciers can be delineated on the northwest slope of the volcano, although they are just barely within the spatial resolution of the MSS image. Snow can also be seen in the 0.8-km-wide summit crater.

Landsat Images of the Glaciers of Citlaltépetl, Iztaccíhuatl, and Popocatépetl

Landsat MSS images are only marginally useful in delineating the termini of some of the larger individual glaciers at the summit areas of the Mexican volcanoes. The small area of these glaciers and the spatial resolution limitation (79-m pixels) of the MSS image are the limiting factors. A search of the Landsat image archive turned up two usable Landsat 3 return beam vidicon (RBV) images of the glaciers of Iztaccíhuatl and Popocatépetl; no Landsat 3 RBV images of Citlaltépetl were acquired. Unfortunately, however, the national Landsat 3 RBV archive has been destroyed. The only images that remain are in local archives, such as the Satellite Glaciology Project at the U.S. Geological Survey. Figure 10 is an enlargement of the December 1980 Landsat 3 RBV image of Iztaccíhuatl and Popocatépetl. When compared with figure 7, a Landsat 1 MSS false-color composite image of the same area, it is evident that the nearly threefold increase in spatial resolution of the Landsat 3 RBV image (30-m versus 79-m pixels) permits a more reliable delineation of the firn areas and termini of the 12 glaciers on Iztaccíhuatl and 3 glaciers on Popocatépetl. Table 4 provides a list of the optimum Landsat 1, 2, and 3 images of the glaciers of México; figure 11 is an index map showing the location and coverage of the optimum Landsat imagery.

TABLE 4.—*Optimum Landsat 1, 2, and 3 images of the glaciers of México*

[see fig. 11 for explanation of symbols used in "code" column]

Path-Row	Nominal scene center (lat-long)	Landsat identification number	Date	Solar elevation angle (degrees)	Code	Cloud Cover (percent)	Remarks
26–47	18°45'N. 96°53'W.	1180–16225	19 Jan 73	38	●	0	Citlaltépetl
26–47	18°45'N. 96°53'W.	1306–16231	25 May 73	61	●	0	Citlaltépetl, image used for figure 4
26–47	18°45'N. 96°53'W.	21508–16003	10 Mar 79	44	●	0	Citlaltépetl
27–47	18°45'N. 98°19'W.	1199–16285	07 Feb 73	41	●	0	Iztaccíhuatl and Popocatépetl, image used for figure 7
27–47	18°45'N. 98°19'W.	1235–16291	15 Mar 73	51	◕	10	Iztaccíhuatl and Popocatépetl
27–47	18°45'N. 98°19'W.	31028–16054-A	27 Dec 80	34	●	0	Iztaccíhuatl and Popocatépetl, image used for figure 10; Landsat 3 RBV image archived by the USGS Satellite Glaciology Project

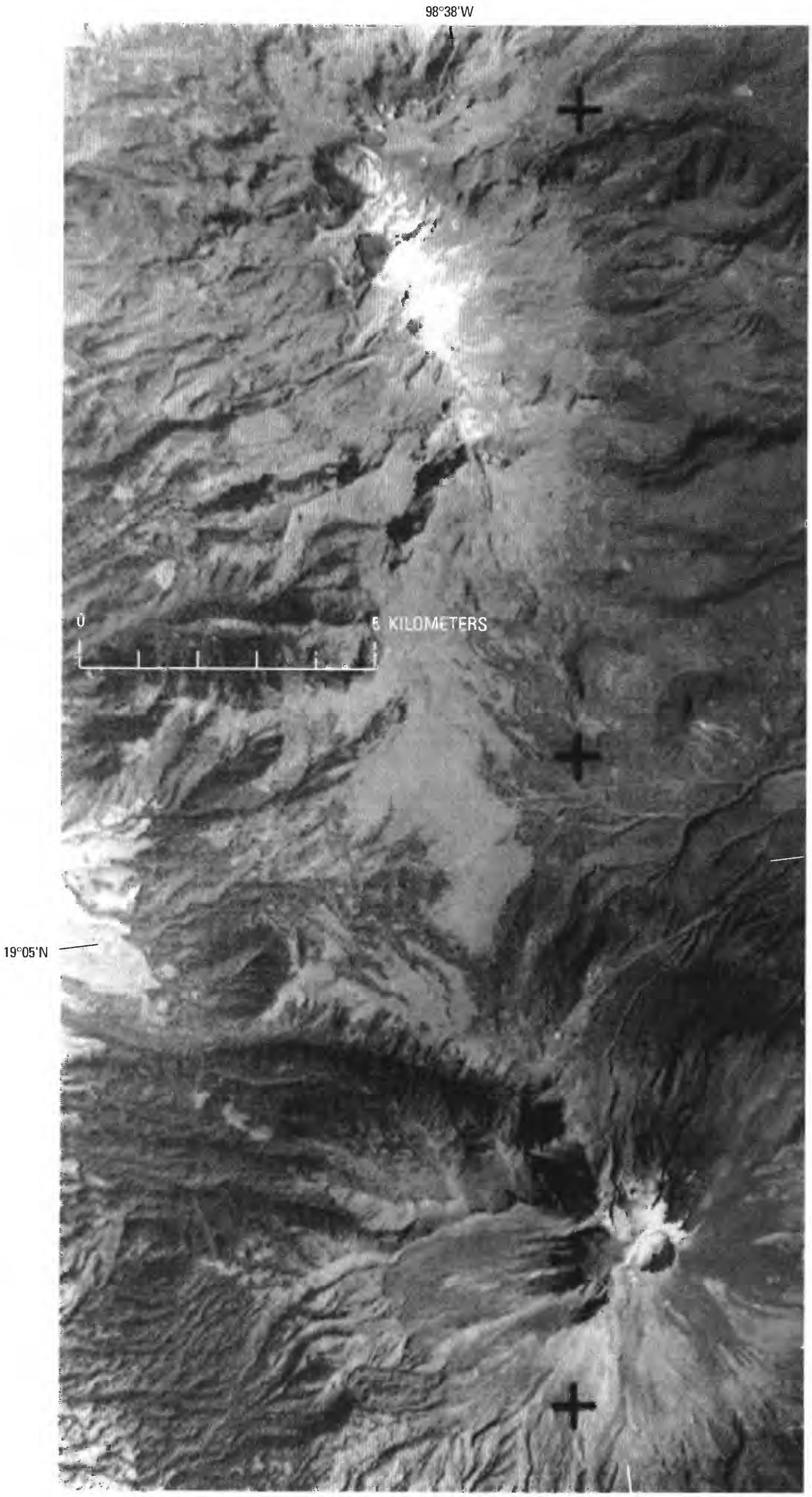

Figure 10.—*Enlargement of a Landsat 3 RBV image (31028–16054, subscene A; 27 December 1980; Path 27, Row 47) of the glaciers and firn on the summit areas of the Iztaccíhuatl (north) and Popocatépetl (south) volcanoes. Reproduced by permission of the Earth Observation Satellite Company (EOSAT).*

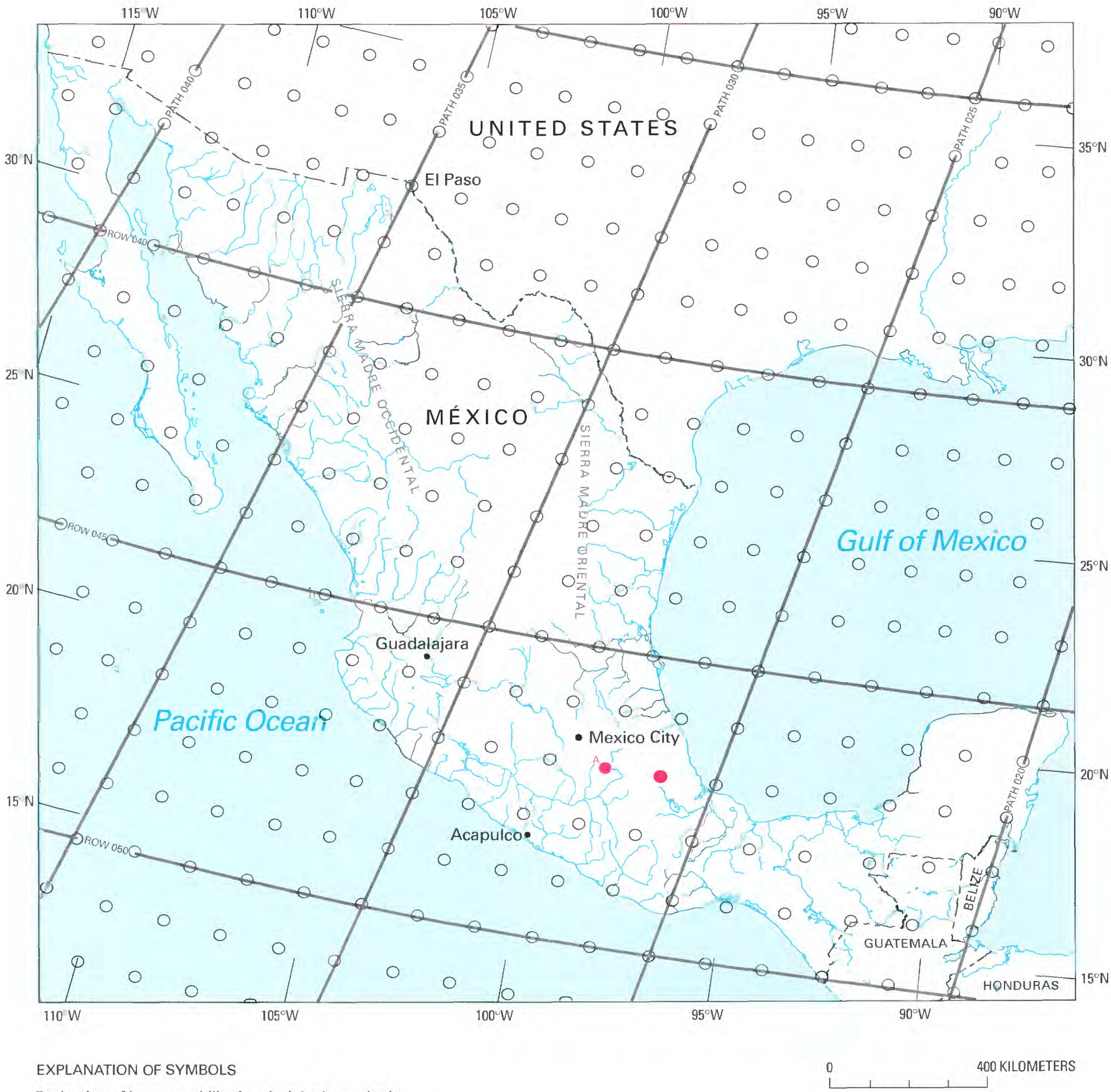

EXPLANATION OF SYMBOLS

Evaluation of image usability for glaciologic, geologic, and cartographic applications. Symbols defined as follows:

- Excellent image (0 to ≤5 percent cloud cover)
- Good image (>5 to ≤10 percent cloud cover)
- Nominal scene center for a Landsat image outside the area of glaciers
- A B C D Usable Landsat 3 RBV scenes. A, B, C and D refer to usable RBV subscenes

***Figure 11.**—Optimum Landsat 1, 2, and 3 images of the glaciers of México.*

References Cited

Aguilera, J.G., and Ordóñez, Ezequiel, 1895, Expedición científica al Popocatépetl [Scientific expedition to Popocatépetl]: México, Comisión Geológica Mexicana, 48 p.

Alzate y Ramírez, J.A., 1831, Observaciones físicas ejecutadas por D. José Antonio Alzate en la Sierra Nevada [Physical observations carried out by Don José Antonio Alzate in the Sierra Nevada], *in* Gacetas de literatura de México [Gazettes of Mexican literature]: Puebla, México, Reimpresas en la oficina del hospital de S. Pedro, á cargo del ciudadano M. Buen Abad, v. 1, p. 99–107.

Anderson, Tempest, 1917, Volcanic studies in many lands: London, John Murray, 2d series, 88 p.

Angermann, Ernesto, 1904, Observaciones geológicas en una ascensión al Citlaltépetl (Pico de Orizaba) [Geological observations on an ascent of Citlaltépetl (Pico de Orizaba)]: Sociedad Científica "Antonio Alzate," Memorias y revista, v. 21, p. 365–369.

Benedict, J.B., 1973, Chronology of cirque glaciation, Colorado Front Range: Quaternary Research, v. 3, no. 4, p. 584–599.

Blásquez, Luis, 1957, Hidrogeología de la cuenca superior de los ríos Jamapa, Atoyac y una parte del Blanco [Hydrogeology of the upper basin of the Río Jamapa, Río Atoyac, and a part of the Río Blanco], *in* Estudios hidrogeológicos: México Universidad Nacional, Instituto de Geología Anales, v. 12, p. 57–95.

Böse, Emil, and Ordóñez, Ezequiel, 1901, Der Ixtaccíhuatl (5280 m): Eine Berg und Gletscherfahrt in den Tropen [Iztaccíhuatl (5,280 m): A mountain and glacier expedition in the tropics]: Zeitschrift des Deutschen und Österreichischen Alpenvereins, v. 32, p. 138–158.

Brecker, C.S., 1908, Una ascensión al Iztaccíhuatl, por C. Gilchrist [An ascent of Iztaccíhuatl, by C. Gilchrist]: Sociedad Mexicana de Geografía y Estadística Boletín, 5a, Epoca 3, p. 222–229.

Delgado, H., and Brugman, M., 1995, Monitorio de los glaciares del Volcán Popocatépetl [Monitoring of the glaciers of the Popocatépetl Volcano], *in* Volcán Popocatépetl. Estudios realizados durante la crisis de 1994–1995: México, D.F., Comite Científico Asesor Centro Nacional de Prevención de Desastres - Universidad Nacional Autonama de México (CENAPRED - UNAM), p. 221-241.

De Terra, Helmut, 1947, Teoría de una cronología geológica para el Valle de Mexico [Theory of a geologic chronology for the Valley of Mexico]: Revista Mexicana Estudios Antropológicos, Sociedad Mexicana Antropología, v. 9, p. 11–26.

De Terra, Helmut, Romero, Javier, and Stewart, T.D., 1949, Tepexpan man [Mexico]: Viking Fund Publications in Anthropology, no. 11, 160 p.

Dollfus, Aguste de, Montserrat, E., and Pavie, P., 1867, Récit d'une ascension au Popocatepetl (23 Avril 1865) [Account of an ascent of Popocatépetl on 23 April 1865]: Paris, France, La commission scientifique de Mexique, Archives de la Commission Scientifique du Mexique, v. 2, p. 187–208.

Farrington, O.C., 1897, Observations on Popocatepetl and Ixtaccihuatl: Chicago, Field Columbian Museum, Publication 18, Geological series, v. 1, no. 2, p. 69–120.

Freudenberg, Wilhelm, 1911, The ascent of Iztaccihuatl from the south: Sociedad Científica "Antonio Alzate," Memorias y revista, v. 31, p. 73–75.

Galeotti, Enrique, 1850, Observaciones hechas en el volcán Pico de Orizaba en 1838 [Observations made on the Pico de Orizaba volcano in 1838]: Instituto Nacional de Geografía y Estadística de la Republica Mexicana Boletín, v. 1, no. 8, p. 199–202.

Heilprin, Angelo, 1890, Barometric observations among the high volcanoes of Mexico, with a consideration of the culminating point of the North American Continent: Academy of Natural Sciences of Philadelphia, Proceedings, v. 42, p. 251–265.

Jaeger, Fritz, 1925, Untersuchungen über das diluviale Klima in Mexiko [Investigations about the diluvial climate in Mexico]: Gesellschaft für Erdkunde zu Berlin, Zeitschrift, no. 9–10, p. 366–373.

———1926, Reisen und Forschungen in Mexiko im Sommer 1925 [Travels and research in Mexico during the summer of 1925]: Gesellschaft für Erdkunde zu Berlin, Zeitschrift, no. 7–8, p. 297–310.

Lorenzo, J.L., 1959, Los glaciares de México [The glaciers of México]: Universidad Nacional Autónoma de México, Instituto de Geofísica, Monografías 1, 114 p.

———1964, Los glaciares de México (segunda edición) [The glaciers of México (2d ed.)]: Universidad Nacional Autónoma de México, Instituto de Geofísica, Monografías 1, 124 p.

Melgarejo, A., 1910, The greatest volcanoes of Mexico: National Geographic Magazine, v. 21, no. 9, p. 741–760.

Ordóñez, Ezequiel, 1894, Observaciones relativas á los volcanes de México [Observations relative to the volcanoes of México]: Sociedad Científica "Antonio Alzate," Memorias y revista, v. 8, p. 183–196.

Packard, A.S., 1886, Ascent of the volcano of Popocatepetl: American Naturalist, v. 20, p. 109–123.

Palacios, David, 1996, Recent geomorphic evolution of a glaciovolcanic active stratovolcano: Popocatépetl (México): Geomorphology, v. 16, no. 4, p. 319–335.

Palacios, David, and Vázquez Selem, Lorenzo, 1996, Geomorphic effects of the retreat of Jamapa Glacier, Pico de Orizaba Volcano (México): Geografiska Annaler, v. 78A, no. 1, p. 19–34.

Palacios, David, and de Marcos, J., 1998, Glacial retreat and its geomorphological effects on Mexico's active volcanoes 1994–1995: Journal of Glaciology, v. 44, no. 146, p. 63–67.

Paredes, Trinidad, 1922, La circulación de las aguas en la falda occidental del Ixtaccihuatl [The circulation of water on the western slope of Iztaccíhautl]: Sociedad Científica "Antonio Alzate," Memorias y revista, v. 40, p. 1–40.

Plowes, Mateo, Rodríquez, Enrique, and Vigil, Pedro, 1877, Comisión del Citlaltepetl—Memoria de los trabajos ejecutados por los Ingenieros [Commission of Citlaltépetl—Memoir of the works carried out by the engineers]: Ministerio de Fomento de la República Mexicana Anales, v. 3, p. 79–113.

Prescott, W.H., 1872–75, History of the conquest of Mexico, *in* Kirk, J.F., ed., Complete works: Philadelphia, J.B. Lippincott, v. 4–6.

Prister, Augusto, 1927, Notas preliminares sobre vestigios glaciales en el Estado de Hidalgo y en el Valle de México [Preliminary notes about relict glaciers in the State of Hidalgo and in the Valley of México]: Sociedad Científica "Antonio Alzate," Memorias y revista, v. 48, p. 1–13.

Robles Ramos, Ramiro, 1944, Algunas ideas sobre la glaciología y morfología del Iztaccihuatl [Some ideas about the glaciology and morphology of Iztaccíhuatl]: Revista Geográfica del Instituto Panamericano de Geografía e Historia, v. 4, p. 65–75.

Sheridan, M.F., Hubbard, Bernard, Bursik, M.I, Abrams, Michael, Siebe, Claus, Macías, J.L., and Delgado, Hugo, 2001, Gauging short-term volcanic hazards of Popocatépetl: EOS, v. 82, no.16, p. 185 and p 188–189.

Simkin, Tom, and Siebert, Lee, 1994, Volcanoes of the world (2d ed.): Tucson, Ariz., Geoscience Press, Inc., in association with the Smithsonian Institution, 349 p.

Simkin, Tom, Siebert, Lee, McClelland, Lindsay, Bridge, David, Newhall, Christopher, and Latter, J.H., 1981, Volcanoes of the world, a regional directory, gazetteer, and chronology of volcanism during the last 10,000 years: Stroudsburg, Pa., Hutchinson Ross Publishing Company, 232 p.

Smithsonian Institution, 1994, Popocatépetl (México): Global Volcanism Network Bulletin (Smithsonian Institution), v. 19, nos. 11, 12.

———1995, Popocatépetl (México): Global Volcanism Network Bulletin (Smithsonian Institution), v. 20, nos. 1, 2, 3.

———1996, Popocatépetl (México): Global Volcanism Network Bulletin (Smithsonian Institution), v. 21, nos. 1, 4, 10, 12.

———1997, Popocatépetl (México): Global Volcanism Network Bulletin (Smithsonian Institution), v. 22, nos. 3, 4, 7, 10, 11, 12.

———1998, Popocatépetl (México): Global Volcanism Network Bulletin (Smithsonian Institution), v. 23, nos. 1, 2, 5, 6, 8, 10, 11, 12.

———1999, Popocatépetl (México): Global Volcanism Network Bulletin (Smithsonian Institution), v. 24, nos. 1, 3, 4, 6, 9.

———2000, Popocatépetl (México): Global Volcanism Network Bulletin (Smithsonian Institution), v. 25, nos. 1, 7, 10, 12.

U.S. Board on Geographic Names, 1992, Gazetteer of Mexico: Washington, D.C., Defense Mapping Agency, 3 v., 1,684 p.

Vázquez-Selem, Lorenzo, 1989, Geomorfología glacial y periglacial del Volcán Teyotl [Glacial and periglacial geomorphology of the Volcano Teyotl]: Universidad Nacional Autónoma de México, Colegio de Geografía, Unpublished Master's thesis, 155 p.

Vázquez-Selem, L., and Phillips, F.M., 1998, Glacial chronology of Iztaccíhuatl volcano, central Mexico, based on cosmogenic ^{36}Cl exposure ages and tephrochronology [abs.]: *in* Program and Abstracts of the 15th Biennial Meeting, American Quaternary Association, AMQUA 1998, Northern Hemisphere-Southern Hemisphere Interconnections (5–7 September 1998; Puerto Vallarta, México), p. 174.

Waitz, Paul, 1910, Observaciones geológicas acerca del Pico de Orizaba [Geological observations about the Pico de Orizaba]: Sociedad Geológica Mexicana Boletín, v. 7, p. 67–76.

———1921, Popocatepetl again in activity: American Journal of Science, 5th series, v. 1, no. 1, p. 81–85.

Weitzberg, Fritz, 1923, El ventisquero del Popocatépetl [The glacier of Popocatépetl]: Sociedad Científica "Antonio Alzate," Memorias y revista, v. 41, p. 65–90.

White, S.E., 1954, The firn field on the volcano Popocatépetl, Mexico: Journal of Glaciology, v. 2, no. 16, p. 389–392.

———1956, Probable substages of glaciation on Iztaccíhuatl, Mexico: Journal of Geology, v. 64, no. 3, p. 289–295.

———1962, Late Pleistocene glacial sequence for the west side of Iztaccíhuatl, México: Geological Society of America Bulletin, v. 73, no. 8, p. 935–958.

———1981a, Equilibrium line altitudes of late Pleistocene and Recent glaciers in central Mexico: Geografiska Annaler, v. 63A, no. 3–4, p. 241–249.

———1981b, Neoglacial to recent glacier fluctuations on the volcano Popocatépetl, México: Journal of Glaciology, v. 27, no. 96, p. 359–363.

———1984, Pleistocene glaciation of volcano Ajusco, central Mexico, and comparison with the Standard Mexican Glacial Sequence: Quaternary Research, v. 21, no. 1, p. 21–35.

Whitehouse, H.R., 1890, Ascent of 'Iztaccihuatl': Alpine Journal, v. 15, no. 110, p. 268–271.

Williams, A.R., 1999, Popocatépetl. Mexico's smoking mountain: National Geographic, v. 195, no. 1, p. 116–137.

☆ U.S. GOVERNMENT PRINTING OFFICE: 2002 — 773-049 / 30095 Region No. 8